



**This electronic thesis or dissertation has been
downloaded from Explore Bristol Research,
<http://research-information.bristol.ac.uk>**

Author:
Costil, Romain

Title:
Restricted rotation in sterically hindered diarylamines
Structural requirements, synthesis, and applications of a new class of atropisomers

General rights

Access to the thesis is subject to the Creative Commons Attribution - NonCommercial-No Derivatives 4.0 International Public License. A copy of this may be found at <https://creativecommons.org/licenses/by-nc-nd/4.0/legalcode>. This license sets out your rights and the restrictions that apply to your access to the thesis so it is important you read this before proceeding.

Take down policy

Some pages of this thesis may have been removed for copyright restrictions prior to having it been deposited in Explore Bristol Research. However, if you have discovered material within the thesis that you consider to be unlawful e.g. breaches of copyright (either yours or that of a third party) or any other law, including but not limited to those relating to patent, trademark, confidentiality, data protection, obscenity, defamation, libel, then please contact collections-metadata@bristol.ac.uk and include the following information in your message:

- Your contact details
- Bibliographic details for the item, including a URL
- An outline nature of the complaint

Your claim will be investigated and, where appropriate, the item in question will be removed from public view as soon as possible.

Restricted rotation in sterically congested diarylamines

Structural requirements, synthesis, and applications of a new
class of atropisomers

Romain Pierre Sébastien Costil

A dissertation submitted to the University of Bristol in accordance with the
requirements for award of the degree of Doctor of Philosophy in the Faculty of Science

—

School of Chemistry

—

September 2018

Word count: 86370

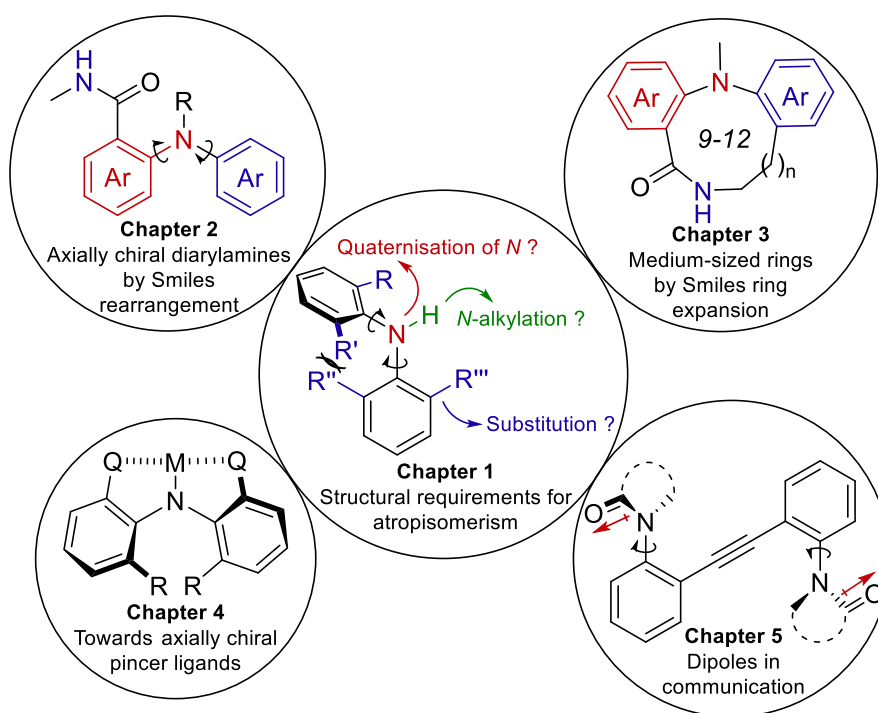
Abstract

Although the stereochemistry of most atropisomers arises from slow rotation about a C–C bond, the ability of the nitrogen atom to adopt a planar geometry promotes conformational rigidity in anilides and aryl ureas. Diarylamines are closely related in architecture to the conformationally stable diaryl ethers and sulfides. However, atropisomerism in this class of compounds had not been reported. Using Dynamic NMR and HPLC techniques, we investigated the factors determining the rates of bond rotation and established the requirements for atropisomerism in diarylamines (Chapter 1).

Common methods to synthesise diarylamines, namely metal-catalysed couplings and nucleophilic aromatic substitution reactions, lack tolerance of steric hindrance or generality in structures available, restricting the availability of poly-substituted diarylamines. We developed a *N*-to-*N'* Smiles rearrangement of anthranilamides affording atropisomeric diarylamines with exceptional steric demand (Chapter 2). Incorporating the amide nitrogen of the substrate into a ring allowed the synthesis of 9–12 membered heterocycles by ring expansion. The products adopted a chiral ground state with an intramolecular, transannular hydrogen bond. Their rate of interconversion was found to heavily depend on solvent polarity, ring size and proximate steric hindrance (Chapter 3).

Introducing axial chirality into diarylamine-based pincer ligands was attempted in order to study the possibility of atropisomerism to induce enantioselectivity in transition metal-catalysed reactions with this class of ligands (Chapter 4).

Finally, restricted rotation in the C–N bonds of anilides was used on rigid aromatic scaffolds to control the relative conformation of extended structures over long distances by dipole repulsion and gain insight on the impact of distance the communication of stereochemical information by dipoles (Chapter 5).



Acknowledgment

« Sait-on jamais où les vents nous mènent ? »

Les Ogres De Barback - *Contes, vents et marées*

First and foremost, I would like to thank Jonathan for opening his door to me, some four and a half years ago. Your guidance and your help throughout this time spent in Manchester and Bristol has transformed the student I was when I arrived into the researcher I am now. Your constant curiosity and excitement when something worked differently as planned taught me that the journey matters as much as the goal. I could not finish without thanking you for the garlic mayo prepared with care every year for the boat trip, surely one of the highlights of the year!

In four (and a bit) years in such a group, you get to meet a lot of memorable people. I have learned so much thanks to these colleagues, and I have had a lot of fun with these friends. I'll miss the lunchtime crosswords, the recurring nights at the pub, squash games, table tennis sessions, dinner parties... Mike, you've contributed to most of my knowledge about British craft beers, and after four years of denial I'm going to say it: English ales are better than Belgian beers. Dan, I missed your sick beats ever since I've stepped out of the house, and I doubt my next lab will have as great a DJ as you. Mo, your constant optimism is so inspiring! Jess, together, we've been through the ups and downs of the PhD. You've been a great colleague and friend, but also sometimes a bit of a mom by proxy ;) Dabs, I really hope to have you back soon, on the other side of the North Sea! Hoss, I hope one day you will forget this dreadful ping pong joke... Frank, first in, last out, but always up for a pint! Roman, as if life in a lab was not absurd enough, you manage make it crazier. Wojtek, you showed me what a Polish party was, and I'm still not recovered from it. Cath, your toad in the hole was probably the most significant discovery I ever made about British cuisine. Kathy, I will always remember that day, on your first Friday lunch, when you casually wondered: "Do you want to visit York tomorrow?". Samantha, I can now say that we both survived the team atropisomers! Rachel, you were my host in the group, thanks for helping me integrate in the group from day 1. I would also like to thank Francis, Matteo, John, Miriam, Johnno, Mary, Louise, Sam, Rakesh, Irene, Alex, Branca, Josep, Romy, Liam, Sarah, Fernando, Ana, Jenn, Edmund, Iñaki, Brian, Matej, Bryden, Hugo, Mish and Léa.

Une pensée spéciale va à la *French Connection* : Julien M, Julien B, Vincent, David et Quentin. C'est auprès de vous que j'ai appris le plus, autant sur le plan pratique, théorique ou en terme d'éthique de travail. Vous avez été des *role models*. Et puis, en tant qu'expat', être entouré de compatriotes (c'est-

à-dire des gens de bon goût!) a été un sacré soutien pour me sentir un petit peu plus à la maison en Angleterre.

I'd like to highlight the massive reviewing effort by my (great) team of experts. Mira, Quentin, Alex, the Hoss, Dan, Dabs and Jonathan, thank you for being so picky about my debatable English and so relevant in your corrections. Mary, Roman, Mo and Frank, thank you for your sense of detail, spotting typos and mistakes in a forest of data.

This PhD would not have gone so smoothly without the brilliant help from the University staff. Particularly, thank you Erzsebet and Himali for taking care of the instruments room. Paul and Tom, NMR and MS would not be so straightforward for us without your care, your reactivity and your skills. Finally, thank you Craig for your eagerness to find solutions to my NMR problems, and your patience when trying to teach me the science behind.

Maman, Papa, je ne pourrais bien évidemment pas en être arrivé là sans vous. Cette thèse, c'est la conclusion d'un loooooong périple qui a commencé il y a maintenant 10 ans. Merci pour votre patience et votre soutien sans faille aussi bien dans les hauts comme dans les moments de doute.

Und schließlich, Mira. Dein Beitrag zu dieser These, ob direkt oder indirekt, ist enorm. Du warst inspirierend (und du bist immer noch!), verständnisvoll, motivieren... Vielen Dank für deine Hilfe, deine Unterstützung und deine Liebe in diesem Abenteuer. Jetzt gehen wir zum nächsten in Groningen!

Author's declaration

I declare that the work in this dissertation was carried out in accordance with the requirements of the University's *Regulations and Code of Practice for Research Degree Programmes* and that it has not been submitted for any other academic award. Except where indicated by specific reference in the text, the work is the candidate's own work. Work done in collaboration with, or with the assistance of, others, is indicated as such. Any views expressed in the dissertation are those of the author.

SIGNED: ...Romain Costil..... DATE:.....07/09/2018.....

Table of Contents

Abbreviations.....	1
Chapter 1.....	3
I.1. Introduction	4
I.1.1. Atropisomerism: History and definition	4
I.1.2. Biaryl atropisomers.....	5
I.1.3. Non-biaryl atropisomers.....	6
I.1.4. C–N atropisomers	8
I.2. Results and discussion	13
I.2.1. Aim	13
I.2.2. Investigation of the barrier to interconversion of secondary diarylamines	14
I.2.3. External effectors on the barrier to rotation of secondary diarylamines.....	26
I.3. Conclusion.....	30
Chapter 2.....	31
II.1. Introduction	32
II.1.1. Synthesis of diarylamines by transition metal-catalysed reactions.....	32
II.1.2. Synthesis of diarylamines by Nucleophilic Aromatic Substitution.....	36
II.1.3. Synthesis of diarylamines by Smiles rearrangement	39
II.2. Results and Discussion	41
II.2.1. Initial discovery	41
II.2.2. Development of the rearrangement.....	42
II.2.3. Mechanism of the transformation.....	53
II.2.4. Atropisomeric diarylamines by Smiles rearrangement	54
II.3. Conclusion.....	57
Chapter 3.....	59
III.1. Introduction	60
III.1.1. 3D structures in drug discovery	60
III.1.2. Medium-rings heterocycles	61

III.1.3. Intramolecular hydrogen bonding in drug design	65
III.2. Results and discussion	69
III.2.1. Aim	69
III.2.2. Development of the rearrangement.....	70
III.2.3. Intramolecular hydrogen bonding in the medium-sized ring products.....	80
III.3. Conclusion	88
Chapter 4	89
IV.1. Introduction	90
IV.1.1. Diarylamines as pincer ligands	91
IV.1.2. Diarylamine pincer ligands in asymmetric catalysis	93
IV.1.3. Twisted conformation in pincer ligands	94
IV.2. Results and discussion	96
IV.2.1. Aim.....	96
IV.2.2. Towards axially chiral PNP ligands.....	97
IV.2.3. Towards an axially chiral analogue of Nickamine.....	107
IV.2.4. Towards an axially chiral NNN ligand by Smiles rearrangement.....	109
IV.3. Conclusion.....	112
Chapter 5.....	113
V.1. Introduction	114
V.1.1. Effect of dipolar interactions on conformation	114
V.1.2. Remote control of conformation by dipolar repulsion.....	118
V.1.3. C–N atropisomerism in anilides	120
V.2. Results and Discussion.....	121
V.2.1. Aim.....	121
V.2.2. Dipoles repulsion in a <i>meta</i> -oligo(phenylacetylene) scaffold	122
V.2.2. Influence of distance on dipolar repulsion	132
V.3. Conclusion.....	138
Experimental	139

General Information	139
Characterisation data.....	140
Chapter 1.....	140
Chapter 2.....	154
Chapter 3.....	180
Chapter 4.....	192
Chapter 5.....	201
Appendix	222
Chapter 1 - VT ¹ H NMR experiments.....	222
Chapter 1 - Chiral VT-HPLC experiments	227
Chapter 1 - Decay of enantiomeric excess.....	231
Chapter 2 - Decay of enantiomeric excess.....	233
Chapter 3 – EXSY experiments.....	234
Chapter 4 - Chiral VT-HPLC experiments	238
Chapter 5 - Chiral VT-HPLC experiments	239
Chapter 5 - determination of conformers distribution of 5.35	240
References	241

Abbreviations

18[C]6	18-crown-6
Ala	alanine
BINAP	2,2'-bis(diphenylphosphino)- 1,1'-binaphthyl
Boc	<i>tert</i> -butyloxycarbonyl
BPIn	(pinacolato)boron
br.	Broad
Bu	butyl
COD	1,5-cyclooctadiene
Conv	conversion
Cy	cyclo
dba	dibenzylideneacetone
DBU	1,8-Diazabicyclo[5.4.0]undec- 7-ene
DCE	dichloroethane
DIPEA	<i>N,N</i> -Diisopropylethylamine
DMA	dimethylacetamide
DMAP	4-dimethylaminopyridine
DMEDA	<i>N,N'</i> -dimethylethylene diamine
DMF	dimethylformamide
DMPU	1,3-Dimethyl-3,4,5,6- tetrahydro-2-pyrimidinone
DMSO	dimethyl sulfoxide
DPEPhos	(oxydi-2,1-phenylene) bis(diphenylphosphine)
dppf	1,1'-bis(diphenylphosphino) ferrocene
<i>ee</i>	enantiomeric excess
eq.	equivalent(s)

ESI	electospray ionisation
Et	ethyl
EWG	electron-withdrawing group
EXSY	exchange spectroscopy
HPLC	high performance liquid chromatography
HMDS	hexamethyldisilazide
<i>i</i>	<i>iso</i>
IR	infrared
L	ligand
LDA	lithium diisopropylamide
LG	leaving group
M	molar / molecular mass
maj	major
Me	methyl
MeCN	acetonitrile
MEM	2-methoxyethoxymethyl
min	minor
MOM	methoxymethyl
m.p.	melting point
MS	molecular sieves
MTBE	methyl <i>tert</i> -butyl ether
NBS	<i>N</i> -bromosuccinimide
NMR	nuclear magnetic resonance
NOE	nuclear overhauser effect
Np	neopentyl
Nu	nucleophile
P ₄ <i>t</i> Bu	CAS number: 111324-04-0
PE	petroleum ether
PG	protecting group

PMI	principal moment of inertia
Pr	propyl
PTSA	<i>para</i> -toluenesulfonic acid
rt	room temperature
<i>sec</i>	secondary
SEM	2-(trimethylsilyl)ethoxymethyl
S _N Ar	nucleophilic aromatic substitution
<i>t/tert</i>	<i>tertiary</i>
TBAF fluoride	tetra- <i>N</i> -butylammonium
TBHP	<i>tert</i> -butyl hydroperoxide
TDB	triazabicyclodecene
Tf	triflate
TFA	trifluoroacetic acid
TFAA	trifluoroacetic anhydride
THF	tetrahydrofuran
TIPS	triisopropyl silyl
TMEDA	tetramethylenediamine
TLC	thin layer chromatography
TMS	trimethyl silyl
TS	transition state
UV	ultraviolet
VT	variable temperature
μW	microwave heating

Chapter 1

Structural Requirements for Atropisomerism in Secondary Diarylamines

I.1. Introduction

I.1.1. Atropisomerism: History and definition

In 1922, Christie and Kenner reported the isolation of two optically active compounds from the co-crystallisation of biaryl **1.1** with brucine (Figure 1).^[1] As compound **1.1** does not have a chiral centre, the authors proposed a structure which allowed the existence of enantiomers, where the aryl rings lay perpendicular to each other. In this case, an axis of chirality is generated, and rotation by 180° of one aryl ring provides the opposite enantiomer.

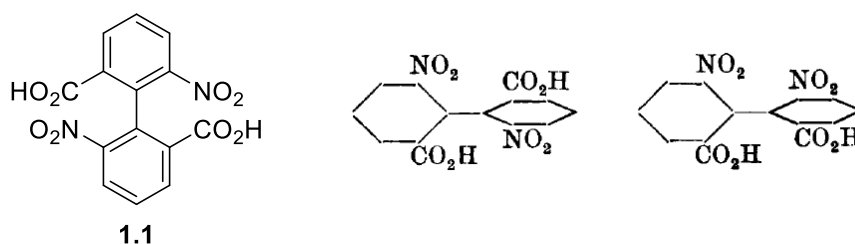
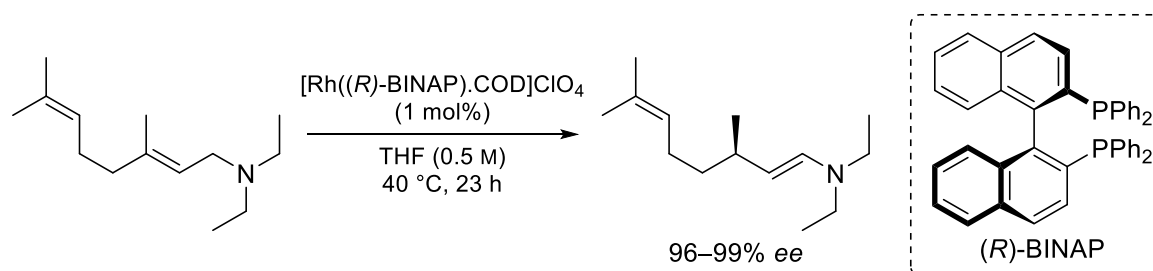


Figure 1: First representation of atropisomerism by Christie and Kenner (taken from ^[1])

These compounds were coined atropisomers by Kuhn,^[2] from the Greek *a* (not) and *tropos* (turn) and are stereoisomers which can be distinguished by the mean of rotation around an axis. Ōki defined atropisomers as ‘physically separable species when they interconvert with a half-life of more than 1000 seconds (about 17 min) at a given temperature’, corresponding to a Gibbs free energy of rotation of 93 kJ mol⁻¹ or more at room temperature.^[3]

A major field in which atropisomers have contributed in modern chemistry is asymmetric catalysis. The use of BINAP (Scheme 1) as a ligand in the asymmetric hydrogenation of C=C and C=O bonds, for example, was highlighted in the 2001 Nobel Prize to Ryōji Noyori ‘for [his] work on chirally catalysed hydrogenation reactions’.^[4] A powerful example of the use of BINAP is the industrial synthesis of (-)-menthol, where the key intermediate enamine is produced in 96–99% *ee* on large scale from diethylgeranylamine (Scheme 1), while extraction from natural resources only provides with an intermediate in 80% *ee*.^[4] This process was used to produce 1000 tons of (-)-menthol per year, corresponding to a third of the world demand in 2001.^[4]



Scheme 1: Key step in the synthesis of (-)-menthol by Takasago Internation^[4]

I.1.2. Biaryl atropisomers

Compound **1.1** is a member of the extensively studied class of biaryl atropisomers.^[5] Because of the planarity of aromatic rings and the relatively short length of the $C_{Ar}-C_{Ar}$ bond, it is not possible for biaryls to lie coplanar in the ground state.^[6] While conjugation favours coplanarity of the rings, steric interactions of the *ortho*-substituents destabilise this conformation. In the ground state of biphenyl, even the two aryl rings with only small hydrogen atoms at the *ortho*-positions, are estimated to be twisted by about 45° in the gas phase.^[7] While the main factor playing a role in the barrier to rotation of biaryls is steric hindrance *ortho* to the chirogenic axis, all three different positions on the ring have an influence on the half-life of the atropisomer, as described below. The impact of substitution on the barrier to rotation of several biaryls was observed by Sternhell and co-workers.^[8] By installing a *gem*-dimethyl group as a diastereotopic 1H and ^{13}C NMR probe in a series of biaryls **1.2**, the authors monitored the change in free energy of a series of compounds with different *ortho*-substituents by variable-temperature NMR. Systematic comparison of the barrier to rotation against the van der Waals radius of each *ortho*-substituent R showed a clear trend between the free energy and the steric demand at the *ortho*-position (Figure 2).

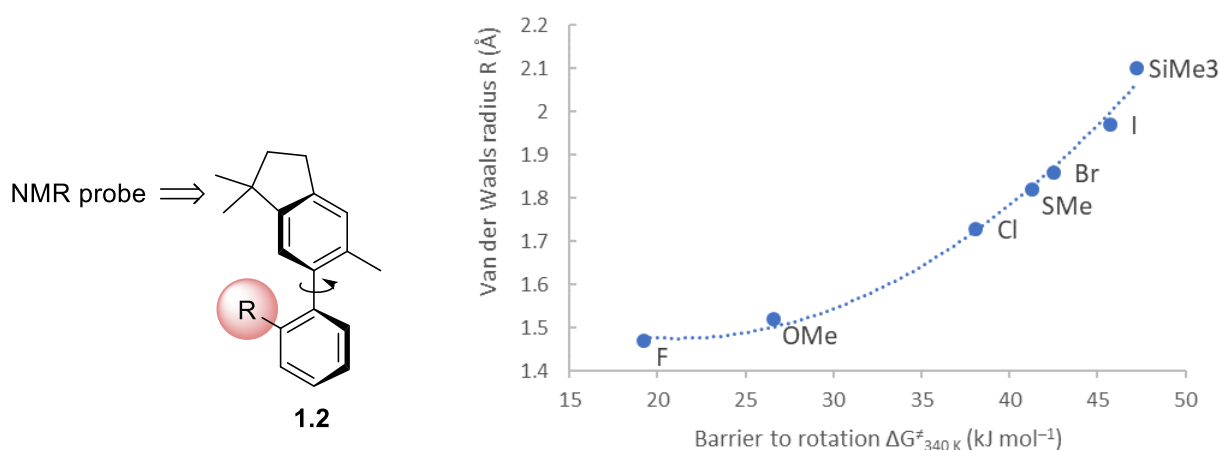
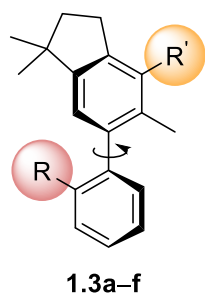


Figure 2: The barrier to rotation of **1.2** against the van der Waals radius of R^[8]

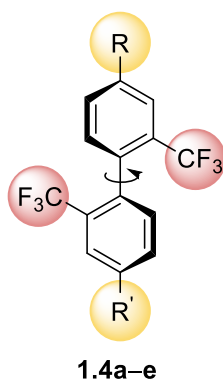
Inspired by Westheimer *et al.*,^[9] the authors also studied the outcome of a buttressing effect on similar compounds (Table 1). A bromine atom *meta* to the $C_{Ar}-C_{Ar}$ bond results in an increase in the barrier to rotation of biaryls **1.3b**, **1.3d** and **1.3f** (entries 2, 4 and 6). The increase of energy on the barrier to rotation appeared to be constant (around 8–9 kJ mol⁻¹) regardless of the biaryl.



Entry	Compound	R	R'	$\Delta G^\ddagger_{340\text{ K}}$ (kJ mol ⁻¹)
1	1.3a	F	H	59.6
2	1.3b	F	Br	67.9
3	1.3c	Cl	H	78.5
4	1.3d	Cl	Br	87.7
5	1.3e	NO ₂	H	72.8
6	1.3f	NO ₂	Br	81.2

Table 1 : Buttressing effect at the *meta*-position in biaryls^[8]

Although the steric demand of a group in *para*-position does not contribute to the barrier to rotation, the electronic properties of the substituent at this position have a significant effect. Roussel *et al.* showed the importance of the substitution at this position in a series of *para*-substituted biphenyls **1.4a–e** (Table 2).^[10] The addition of one or two electron-donating groups lowered the barrier to rotation by 6 and 8 kJ mol⁻¹, respectively (entries 2 and 3). This effect was thought to be due to the increase of the conjugation of both aryl rings by resonance, stabilising the coplanar transition state and increasing electron density at the carbon atoms in the pivot bond, thus enabling the out-of-plane bending in the transition state.



Entry	Compound	R	R'	ΔG^\ddagger_7 (kJ mol ⁻¹)
1	1.4a	H	H	109.2 (332 K)
2	1.4b	NH ₂	H	103.1 (320 K)
3	1.4c	NH ₂	NH ₂	101.0 (320 K)
4	1.4d	NO ₂	H	110.2 (334 K)
5	1.4e	NO ₂	NO ₂	113.2 (340 K)

Table 2: Electronic effect at the *para*-position in diarylamines^[10]

Electron-withdrawing groups have an opposite effect on the barrier to rotation by decreasing the electronic density at the pivot carbon as in biaryls **1.4d** and **1.4e**, although two nitro groups were needed for a significant change in the barrier to rotation (entries 4 and 5).

I.1.3. Non-biaryl atropisomers

Other classes of conformationally stable, axially chiral molecules have been described as well.^[11] Non-biaryl atropisomers have attracted much attention over the past twenty years, not only by virtue of restricted rotation around a C–C bond, as C–O,^[12] C–N^[13] or C–S^[14] atropisomers have also been described. Amongst non-biaryl atropisomers with a C–Heteroatom stereogenic bond, comprehensive

work has been done on the conformational restriction of biaryl ethers and thioethers.^[15] One of the most notable examples is the natural product Vancomycin (Figure 3). This macrocyclic peptide, used as an antibiotic against Gram-positive bacteria, is produced by the soil bacteria *Amycolatopsis orientalis*.^[16] With 18 stereocentres and 3 axis of chirality, Vancomycin has been fully synthesised in 1998 by the Evans and co-workers.^[17] Two atropisomeric diaryl ethers **A** and **B** and a biaryl **C** are embedded in the macrocycles. Rotation around these bonds is highly restricted, with barriers to rotation of up to 125 kJ mol⁻¹.

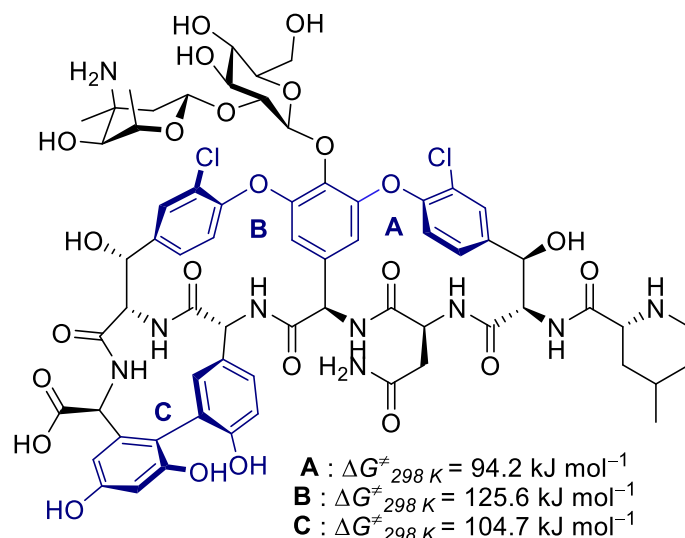
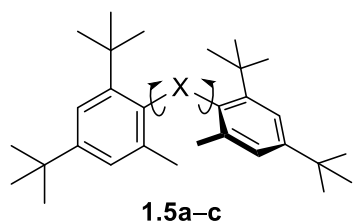


Figure 3: Structure of Vancomycin and barriers to rotation^[17]

The Clayden group has performed extensive research on the synthesis, conformational analysis and use of diaryls ethers and thioethers.^[12,14,18] Provided great steric hindrance was introduced at the *ortho*-positions, atropisomerism was observed in several series of diaryl ethers, sulfides and sulfones, although sulfur-based atropisomers have a rather low conformational stability (Table 3). The longest half-lives measured for sulfide **1.5a** and for sulfone **1.5c** were 14 h and 6 d, respectively. Sulfoxide **1.5b** showed a lower conformational stability, with a half-life of 70 s, presumably because of the longer C–S bond in sulfoxides.

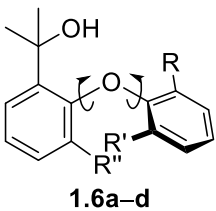


Entry	Compound	X	ΔG^\ddagger_T (kJ mol ⁻¹)
1	1.5a	S	100.8 (313 K)
2	1.5b	S(O)	86.3 (290 K)
3	1.5c	S(O) ₂	106.5 (323 K)

Table 3 : Influence of the nature of the sulfur atom on the barrier to rotation^[14]

Greater barriers to rotation were obtained in the diaryl ethers series, with half-lives of up to thousands of years. A selected series of compound is shown below for comparison of barrier to rotations (Table 4). In general, exchanging a sp³ carbon at the *ortho*-position for a trigonal planar atom lowered

the barrier to rotation (entries 1 vs. 2). Isopropyl groups were barely bulky enough to block rotation around the C_{Ar}–O bond such as in compound **1.6a**. However, substitution for a *tert*-butyl group in **1.6c** allowed the isolation of conformationally stable compounds. Interestingly, the barrier to rotation of diaryl ethers **1.6d** having one symmetrical ring could only be estimated with a value below 38 kJ mol⁻¹ (entry 4). Even two isopropyl groups were not enough to observe restricted rotation as the diastereotopic signals could not be resolved at low temperature by ¹H NMR. This drop in the energy of interconversion was thought to be due to the existence of a low-energy geared rotation in compounds with symmetrical rings, where none of the ring has to go through a very demanding, decoupled 180° rotation.



Entry	Compound	R	R'	R''	$\Delta G^\ddagger_{298\text{ K}}$ (kJ mol ⁻¹)
1	1.6a	<i>i</i> Pr	H	CH ₂ OH	90.9
2	1.6b	<i>i</i> Pr	H	CHO	78.5
3	1.6c	<i>t</i> Bu	H	CH ₂ OH	113.5
4	1.6d	<i>i</i> Pr	<i>i</i> Pr	CH ₂ OH	<38

Table 4 : Atropisomerism in some diaryl ethers^[12]

Atropisomerism around C–X bonds, as seen previously, has been largely studied in oxygen and sulfur-based compounds, both in natural products and synthetic molecules. Nevertheless, both cyclic and acyclic aromatic amines have demonstrated the existence of slow rotation in C–N bonds too.

I.1.4. C–N atropisomers

Restricted rotation around C–N bonds has been observed in heterobiaryl natural compounds. Ancisheynine (Figure 4, natural counter-anion unknown) was isolated as a racemate from the Congolese liana of the *Dioncophyllaceae* and *Ancistrocladaceae* families.^[19] Murrastifoline F (Figure 4), of which the absolute configuration is unknown, was first synthesised in 2001 by Bringmann *et al.*^[20] Although its two stereoisomers were never separated, its barrier to rotation was calculated to be around 165 kJ mol⁻¹.

Various groups have designed classes of synthetic C–N, bicyclic atropisomers such as *N*-aryl imides (Figure 4),^[21] or *N*-aryl tetrahydroquinolines.^[22] In the former, conjugation of the nitrogen lone pair with both carbonyl increases the rigidity of the ground state, thus increasing the barrier to rotation.

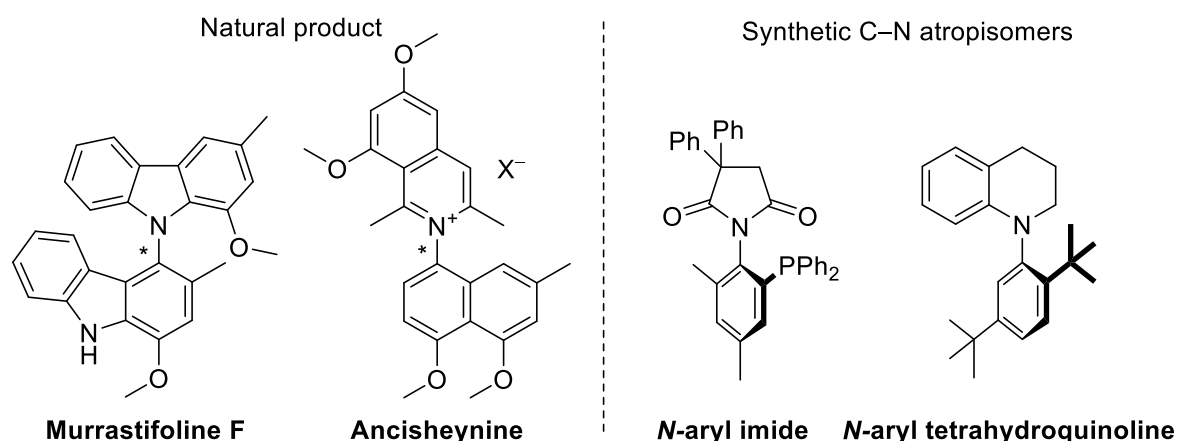


Figure 4: Structure of Murrastifoline F,^[20] Ancisheynine,^[19] and some synthetic C–N atropisomers^[21,22]

C–N bond atropisomerism in acyclic structures has been widely studied in *N*-aryl amides, or anilides. Seminal work by Sutherland *et al.*^[23] explored the impact of substitution of the nitrogen atom of anilines on restricted rotation. Both steric demand and pyramidalisation of the nitrogen played a role in barrier to rotation. While compounds **1.7** and **1.8**, of which the nitrogen possess some sp^3 character, had a relatively low barrier to rotation, the increase in conjugation of the nitrogen atom enhanced the ability to slow down interconversion, as shown in compounds **1.9** (Table 5).

Entry	Compound	$\Delta G^\ddagger_{273\text{ K}}$ (kJ mol ⁻¹)
1	1.7	62.0
2	1.8	65.3
3	1.9	80.8

Table 5 : Influence of the geometry of the nitrogen on atropisomerism in toluidine derivatives^[23]

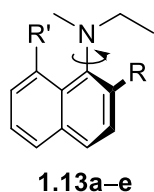
Stewart *et al.*^[24] demonstrated that atropisomerism in anilides could be achieved by introducing a bulky group at the *ortho*-position (Table 6). Later work by Curran and co-workers showed that a *tert*-butyl at this position significantly increased the barrier to rotation, obtaining atropisomers at room temperature.^[25,26]

Entry	Compound	$\Delta G^\ddagger_{298\text{ K}}$ (kJ mol ⁻¹)
1	1.10	93.4
2	1.11	106.3
3	1.12	121.4

Table 6 : Energy of C–N bond rotation in anilides^[24]

Origin of atropisomerism at the C–N bond in hindered anilines

During the second half of the 1980s, Lunazzi and co-workers described the conformational properties of several tertiary 1-naphthylamines. While the compounds studied at the time were not atropisomers, this series of papers shed light on the dynamic processes occurring both at the ground and transition states of such compounds and provided proof that atropisomerism could be achieved in anilines. Steric effects were observed in anilines **1.13a–e**, where an increase of the barrier to rotation resulted from an increase of the size of the alkyl group at the *ortho*-position (Table 7, entries 2 to 4).^[27] Substitution at the *peri* position has a larger contribution to the barrier to rotation, as a methyl group is sufficient to make compound **1.13e** an atropisomer with a barrier to rotation of 90.4 kJ mol^{−1} (entry 5). Unfortunately, the temperatures of calculation of the barriers to rotation were not reported, precluding comparison with other systems.



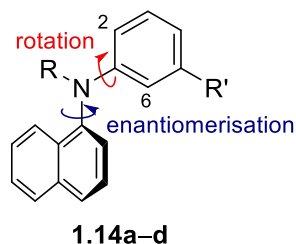
Entry	Compound	R	R'	ΔG^\ddagger_T (kJ mol ^{−1}) ^a
1	1.13a	H	H	34.7
2	1.13b	Me	H	65.7
3	1.13c	<i>i</i> Pr	H	72.0
4	1.13d	<i>t</i> Bu	H	82.1
5	1.13e	H	Me	90.4

^a: determined by coalescence of the diastereotopic signal for CH₂CH₃ by VT ¹H NMR.

Table 7 : Barrier to rotation of various *ortho*-substituted *N*-methyl-*N*-ethyl-1-naphthylamines^[27]

The stereomutation of tertiary diarylamines **1.14a–d** was also studied by Lunazzi *et al.* (Table 8).^[28] The energy of rotation around the *N*-phenyl bond (called 'rotation', in red) and the barrier to enantiomerisation, achieved by rotation around the N–C_{naphthyl} bond (in blue), were determined by variable-temperature ¹H NMR. Because of the low steric demand around the phenyl ring compared to the naphthyl group, it was expected that diarylamines **1.14a–d** adopt a ground state conformation in which the naphthyl ring lays perpendicular to the other two nitrogen substituents, and where the phenyl ring is in conjugation with the nitrogen lone pair.

Decrease of the barrier to rotation around the phenyl ring when replacing a methyl group for an ethyl (Table 8, entries 1 and 3) could be explained by the destabilisation of the ground state by disruption of the conjugation with the lone pair of the nitrogen atom, lowering the energy difference with the transition state. Increasing the steric bulk with an isopropyl group forces deconjugation of the phenyl ring in the ground state, leading to a twisted conformation of which the barrier to interconversion is raised due to steric demand (entry 5).



Entry	Compound	R	R'	Motion	ΔG^\ddagger_T (kJ mol ⁻¹)
1	1.14a	Me	H	Rotation ^a	29.7 (153 K)
2	1.14b	Me	Et	Enantiomerisation ^b	36.8 (186 K)
3	1.14c	Et	H	Rotation ^a	27.2 (142 K)
4	1.14c	Et	H	Enantiomerisation ^c	42.7 (215 K)
5	1.14d	<i>i</i> Pr	H	Rotation ^a	32.7 (169 K)
6	1.14d	<i>i</i> Pr	H	Enantiomerisation ^c	46.0 (234 K)

^a Calculated by coalescence of the diastereotopic ¹³C signals of carbons 2 and 6 in Me₂O. ^b Calculated by coalescence of the diastereotopic ¹H signals of Et in CD₂Cl₂. ^c Calculated by coalescence of the diastereotopic ¹H signals of R in CD₂Cl₂.

Table 8 : Barrier to rotation of various *N*-alkyl-*N*-phenyl-1-naphthylamines in dimethyl ether^[28]

Conversely, increase of the size of the nitrogen substituent leads to a growth of the barrier to rotation of the naphthyl ring in each example, in agreement with a twisted N–C_{naphthyl} bond in the ground state.

Atropisomerism in diarylamines was also observed by the Kawabata group in naphthylamine **1.15a–e** (Table 9).^[29] Half-lives to racemisation ranging from few seconds to a couple of years have been achieved by finely tuning the physicochemical properties of the compounds (Table 9). The steric demand around the C_{Ar}–N axis was increased by introducing a methyl group at the *peri* position of the naphthyl group (entry 2 vs. 6). The highest barriers to interconversion were obtained by strengthening the intramolecular hydrogen bond, as increasing the hydrogen bond donor ability of the amine by decreasing its electron density improved the barrier to rotation (entry 3 and 4). The electron-donating ability of the imine also influenced the strength of the hydrogen bond, and thus the barrier to rotation (entries 4 and 5). Half-lives to racemisation of up to 2 years at room temperature could then be reached with this design.

Chemical structure of 1.15a-e is shown. It features a naphthyl ring system with an imine group (N=C) and a diarylamine group (N-Ar). The imine nitrogen is bonded to an R' group, and the diarylamine nitrogen is bonded to an R'' group. The structure shows an intramolecular hydrogen bond between the imine nitrogen and the diarylamine nitrogen, forming a 6-membered pseudo-ring. The naphthyl ring has a substituent R at the 1-position and a methyl group at the 2-position. The structure is labeled 1.15a-e.

Entry	Compound	R	R'	R''	ΔG^\ddagger_T (kJ mol ⁻¹)	$t_{1/2}^a$
1	1.15a	H	<i>i</i> Pr	H	80.8 (365 K)	10 s
2	1.15b	NO ₂	<i>i</i> Pr	H	97.1 (295 K)	2.3 h
3	1.15c	Me	4-(MeO)Ph	Me	104.2 (295 K)	2.4 d
4	1.15d	NO ₂	4-(MeO)Ph	Me	113.9 (353 K)	133 d
5	1.15e	NO ₂	<i>i</i> Pr	Me	118.1 (353 K)	720 d

^a At 295 K

Table 9 : Barrier to rotation of various diarylamines with an intramolecular hydrogen bond^[29]

NOE experiments showed that, in solution, the imine nitrogen of compounds **1.15a–e** points towards the diarylamine nitrogen to form an intramolecular hydrogen bond in a 6-membered pseudo-ring (Figure 5, compound **1.15a**).^[30] However, blocking the possible interaction as in compound **1.15aMe**

resulted in a significant reduction of the barrier to rotation, as two C_{Ar}–N bonds freely rotate. By showing that the barrier to interconversion of most compounds present a large solvent dependency, the authors concluded that enantiomerisation of diarylamines with a small barrier to interconversion proceeded by rotation of the imine group followed by free C_{Ar}–N bonds rotation, with large negative activation entropy in polar solvents. However, as compounds **1.15d–e** did not undergo a similar high activation entropy process, it was inferred that the barrier to racemisation of these diarylamines was due to the slow rotation around a single C_{Ar}–N bond without disruption of the strong, intramolecular hydrogen bond (Figure 5).

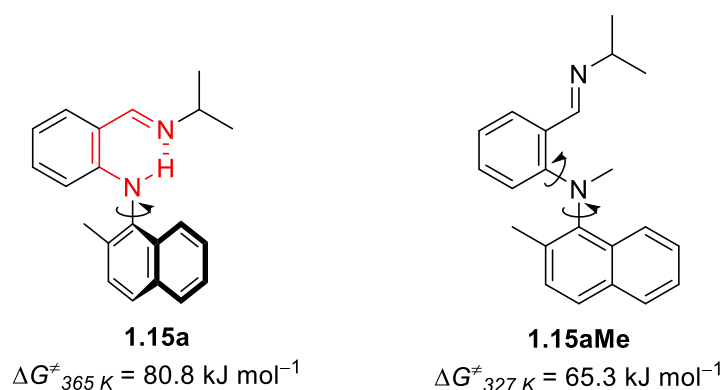
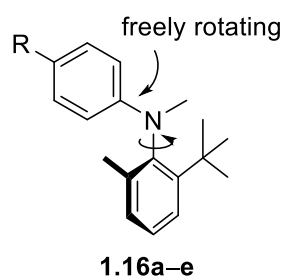


Figure 5: Mechanism of racemisation of anilido-aldimines with low barriers to racemisation^[30]

Although the compounds designed by Kawabata and co-workers were diarylamines, the strong intramolecular hydrogen bonding makes the aromatic nitrogen part of a pseudo-ring. It has been shown that enantiomerisation occurred without cleavage of the hydrogen bond in the highly conformationally stable examples. Thus, these diarylamines can be compared to bicyclic structures such as binaphthyls, with only one rotatable C–N bond.

During the course of the work described in this thesis, the Kitagawa group published their work on the conformational stability of some axially chiral, tertiary diarylamines.^[31] Building on their previous work on *N*-aryl tetrahydroquinolines (Figure 4), the authors were able to design and prepare atropisomeric diarylamines bearing a highly congested 2-*tert*-butyl-6-methylphenyl ring at the nitrogen by palladium-catalysed cross-coupling followed by *N*-methylation.^[31] The absence of sterically demanding functional group at the *para*-substituted aryl ring led to free rotation of the corresponding C_{Ar}–N bond, while the steric demand at the highly substituted ring, together with substitution of the nitrogen slowed down rotation of second C_{Ar}–N bond, permitting the elaboration of conformationally stable, atropisomeric diarylamines (Table 10).



Entry	Compound	R	$\Delta G^\ddagger_{298\text{ K}}$ (kJ mol ⁻¹)	$t_{1/2}$ (d) ^a
1	1.16a	NO ₂	123.0	2475
2	1.16b	CO ₂ Et	118.0	304
3	1.16c	H	110.9	19.0
4	1.16d	Me	109.2	9.2
5	1.16e	NH ₂	103.8	1.0

^a At 298 K

Table 10: Barrier to C–N rotation in *N*-aryl-2-*tert*-butyl-6-methyl anilines^[31]

While *N*-methyl-2-*tert*-butyl-6-methylaniline **1.16a** was conformationally stable at room temperature, with a half-life to racemisation of 19 days (entry 3), modification of the electronic properties of the phenyl ring displayed a great influence on the barrier to rotation, even-more-so than in the biaryl series (*cf.* Table 2). Electron-withdrawing groups significantly increased the barrier to rotation around the hindered C–N bond, while electron-donating groups gave the opposite effect, with the difference of the Gibbs free energy correlating with the substituent Hammett constant. Thorough calculations of the racemisation pathways and ground state conformation led the authors to postulate that in lower energy compounds, faster interconversion is possible with the *para*-substituted phenyl ring sitting in a twisted geometry in relation with the hindered ring. In the more stable examples, a stronger resonance in the phenyl ring forces it into a coplanar, more hindered conformation.

I.2. Results and discussion

I.2.1. Aim

Recent advances in Buchwald–Hartwig couplings allow the synthesis of severely congested diarylamines.^[32–34] However, when starting this project, no study had been done on the conformational properties of these highly hindered systems and their ability to retain a stable, chiral conformation. By analogy to the diaryl ethers and sulfides explored by our group, this work aimed to unravel the potential for atropisomerism in secondary diarylamines. Considering the importance of this scaffold in catalysis,^[35] life sciences^[36,37] and materials,^[38] we investigated in detail the factors which determine the rates of bond rotation, and hence the structural requirements for atropisomerism. This work focussed on the steric effects of simple, secondary diarylamines bearing only alkyl substituents, as previous work showed the extreme influence of electronic properties of the aromatic rings.

1.2.2. Investigation of the barrier to interconversion of secondary diarylamines

Simple diarylamines bearing different alkyl substituents at the *ortho*-positions were synthesised (Figure 6). Shaughnessy *et al.* reported the use of trineopentyl phosphine (PNp₃) as an efficient ligand for the Buchwald–Hartwig coupling of sterically hindered diarylamines.^[32,39] As this palladium-catalysed coupling between an aniline and aryl halides seemed the most powerful strategy for the synthesis of hindered diarylamine at the time, we envisaged the construction of a library of simple diarylamines by this method, with a systematic modification of the substitution pattern.

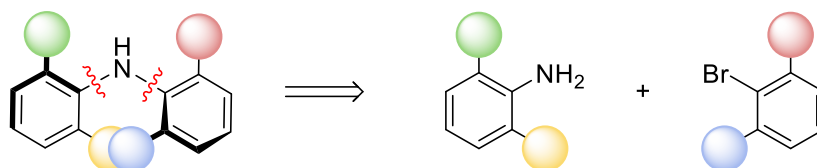
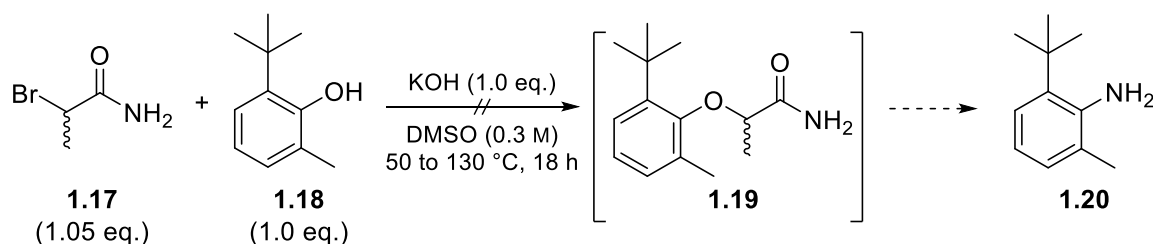


Figure 6: Synthesis of the target diarylamines

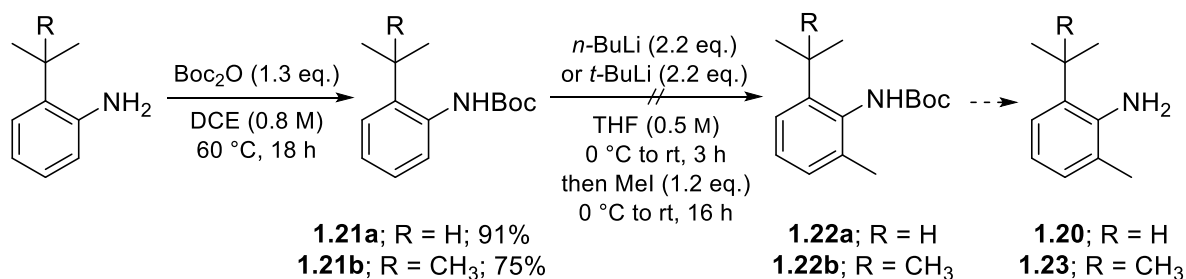
Synthesis of the substrates

Sterically hindered anilines still pose a synthetic challenge, and different routes were investigated for the synthesis of the highly hindered 2-*tert*-butyl-6-methylaniline **1.20**. Following recent reports,^[40,41] Smiles rearrangement of ether **1.19** to **1.20** was attempted in a one-pot procedure starting from amide **1.17** and phenol **1.18** (Scheme 2). However, even after prolonged reaction time at high temperature, no intermediate **1.19** was observed. Presumably, the high steric demand of the substrate prevented formation of the intermediate, suggesting that the *O*-to-*N* rearrangement would be even more challenging because of the unfavourable electron-density of the aryl ring.



Scheme 2 : Synthesis of highly hindered *ortho*-substituted anilines by Smiles rearrangement

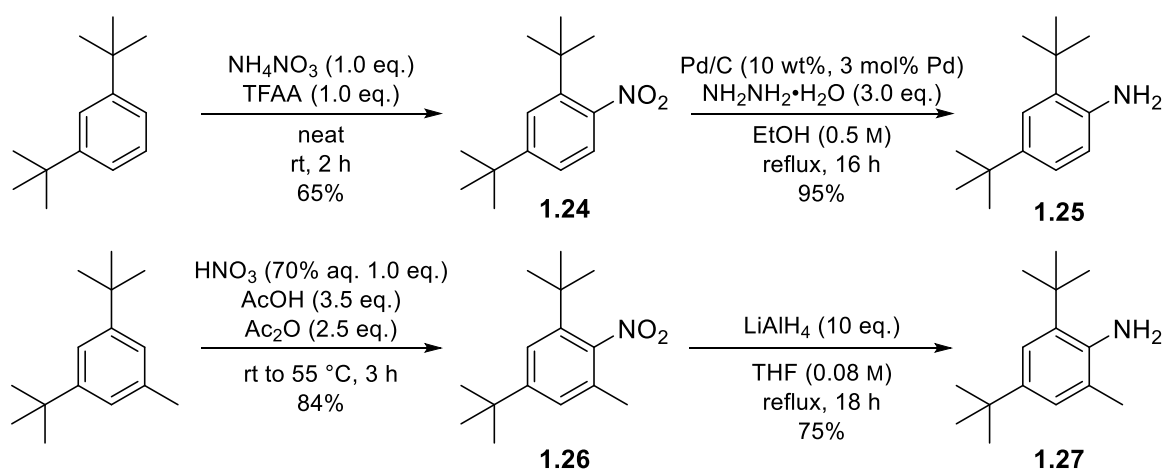
An alternative strategy was then followed using a Boc moiety as a directing group for a directed *ortho*-metalation, followed by quench with methyl iodide as reported by Zhu *et al.* with aniline (Scheme 3).^[42] Similar conditions were tried on *N*-Boc protected 2-isopropyl aniline **1.23b** and 2-*tert*-butyl aniline **1.20**.



Scheme 3 : Synthesis of highly hindered *ortho*-substituted anilines by *ortho*-lithiation

Following the reported procedure, using methyl iodide overnight at -20°C after addition of *tert*-butyl lithium unreacted starting material was fully recovered. Deprotonation at room temperature with *n*-butyl lithium and subsequent quench only provided a mixture of the *N*-methylated carbamate and unreacted substrate. Presumably, both isopropyl and *tert*-butyl groups at the *ortho*-position force the Boc group out of the plane of the aryl ring and restricts its rotation, therefore preventing the *ortho*-metalation step.^[43]

Alternatively, unsymmetrical anilines **1.25** and **1.27** bearing a *tert*-butyl groups in the *para*-position were synthesised in good yield by nitration of 3,5-di-*tert*-butylbenzene^[44] and 3,5-di-*tert*-butyl toluene^[45] followed by reduction of the nitro group into the corresponding amine, following reported procedures (Scheme 4).

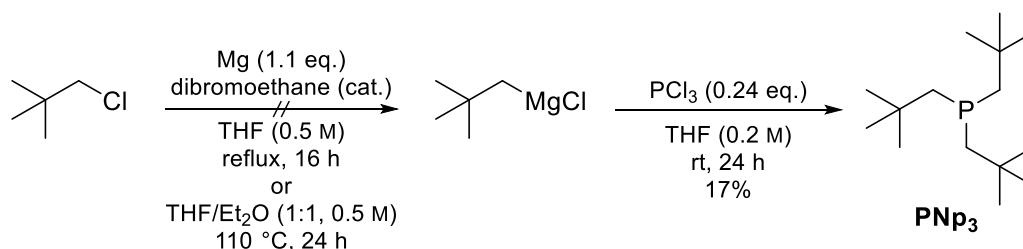


Scheme 4 : Synthesis of highly hindered *ortho*-substituted anilines by nitration of corresponding aryl

Synthesis of sterically hindered diarylamines

The synthesis of the ligand (PNp₃) proved to be tedious. While the use of neopentyl magnesium chloride has been described in the literature,^[46] reports of its synthesis are vague. Every attempt to prepare the Grignard reagent (under standard conditions, with dibromoethane as an activating agent, under pressure, or by using a freshly prepared magnesium anthracene THF complex^[47]) failed, and the commercially available – but expensive – solution in THF was used instead (Scheme 5). Although

described,^[48] the synthesis and separation of PNp_3 from its phosphine oxide by-product only succeeded in a poor yield, because of difficulties of purification.

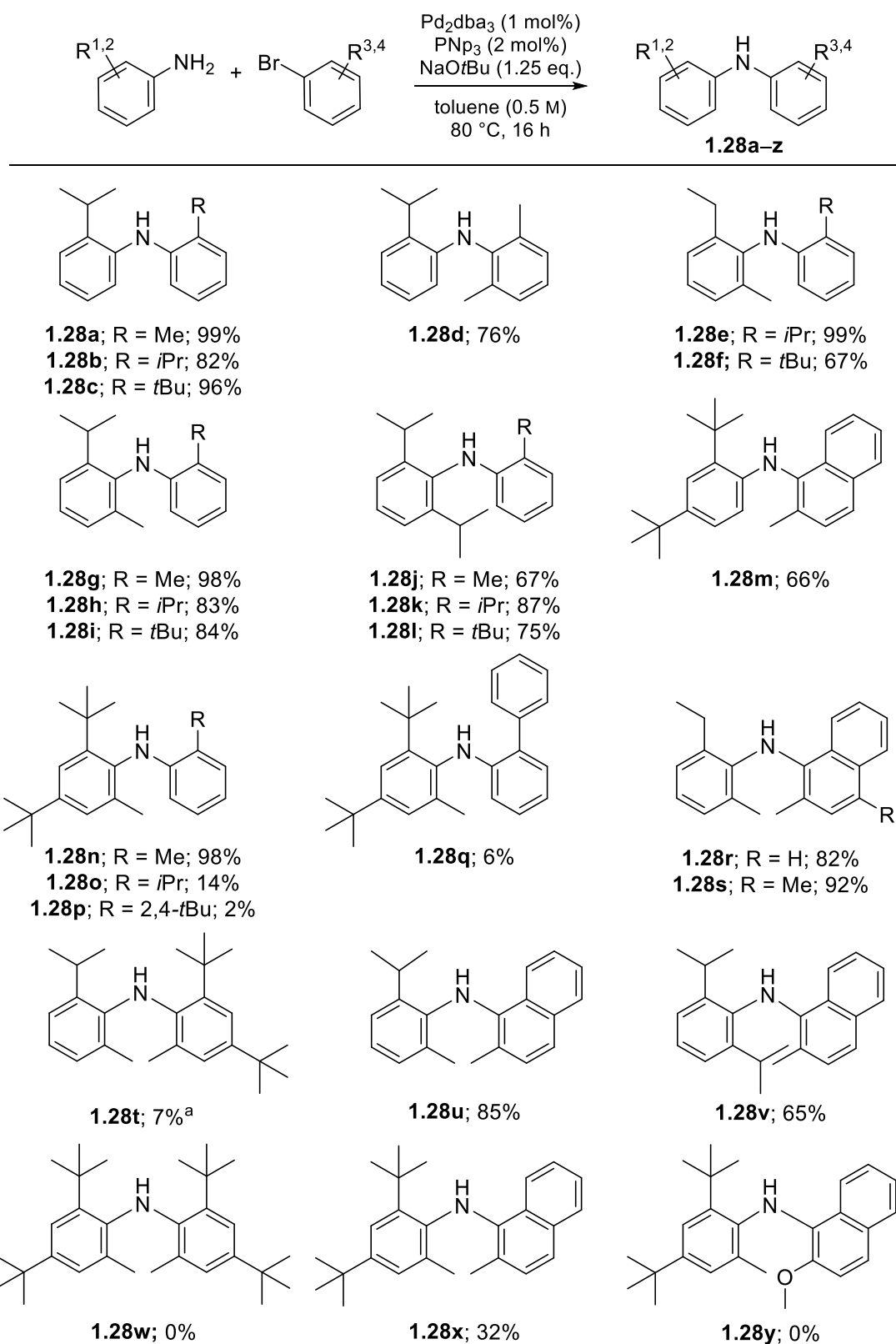


Scheme 5 : Synthesis of PNp_3

Although the reaction conditions for the Buchwald–Hartwig coupling of sterically hindered substrates were reported by Shaughnessy and co-workers,^[32] these had to be modified to obtain conversion in our case. The quality of the sodium *tert*-butoxide used in the reaction was critical for the reaction, as only Sigma-Aldrich ‘extra pure’ sodium *tert*-butoxide gave conversion. Furthermore, distillation of the solvent was necessary, as degassing toluene by freeze-pump-thaw did not yield any product. Failure to follow these conditions would yield protodehalogenation of the aryl bromide. The reaction time was also systematically changed to 16 h and the catalyst loading increased to 1 mol%. With these conditions, a series of hindered diarylamines was synthesised with gradual increase of the bulkiness of the *ortho*-substituents (Scheme 6).

The couplings produced diarylamines in good yield, and generally proceeded smoothly. When the yield of product was low, good recovery of the aniline and aryl bromide was usually observed. Couplings yielding di- and tri-*ortho*-substituted diarylamines gave the corresponding products in good to excellent yield (**1.28a–n**). Moderately hindered aryl bromides such as 1-bromo-2-methylnaphthalene were also tolerated (**1.28r–s** and **1.28u–v**), even when coupled to some di-*ortho*-substituted diarylamines.

Introduction of a *tert*-butyl motif proved to be more challenging. A drastic reduction of the yield was observed in the synthesis of tri-*ortho*-substituted diarylamines **1.28o–q**, **1.28t**, and **1.28w–y**. The near-quantitative yield obtained for **1.28n** dropped below 10% when substituting the methyl group for a bigger phenyl, isopropyl or *tert*-butyl group. Tetra-*ortho*-substituted diarylamines bearing at least one *tert*-butyl group proved even harder to obtain, as only **1.28t** and **1.28x** were obtained in poor yield. The non-reacted aniline could be retrieved and, in some cases, hindered aryl bromides could be isolated by column chromatography, indicating that no oxidative addition took place.



^a The reaction time was 48 h.

Scheme 6 : Synthesis of sterically hindered secondary diarylamines by Buchwald–Hartwig coupling

Investigation of the barrier to rotation of congested diarylamines

The barrier to rotation at a given temperature ΔG_T^\ddagger (kJ mol⁻¹) and the half-life of racemisation $t_{1/2}$ (s) can be calculated from the rate of enantiomerisation k_{enant} (s⁻¹, equals half the rate of racemisation k_{rac}) by using the Eyring equation (Equation 1), with R the gas constant, T the temperature, k_B the Boltzmann constant, and h the Planck constant:

$$\Delta G_T^\ddagger = R * T * \ln \left(\frac{k_B * T}{h * k_{\text{enant}}} \right)$$

Equation 1: The Eyring equation

$$t_{1/2} = \frac{\ln(2)}{2 * k_{\text{enant}}}$$

Equation 2: Half-life to enantiomerisation of the rate of enantiomerisation

In order to calculate barriers to rotation, dynamic analytical techniques are needed. Among the large choice available,^[49] three different methods were used for the determination of barrier to rotation of diarylamines: lineshape analysis of variable-temperature ¹H NMR spectra (VT-NMR), variable-temperature HPLC (VT-HPLC), and decay of enantiomeric excess of an enantioenriched sample. The barriers to rotation which can be calculated from these three techniques go from 20 kJ mol⁻¹ to a virtually infinite range.^[49]

Dynamic NMR is a technique which allows the study of bond rotation of events with a barrier to interconversion from 20 and up to 90 kJ mol⁻¹.^[49] While a mixture of enantiomers is impossible to distinguish by NMR without any external source of chirality, diastereotopic nuclei can act as an NMR probe to monitor stereodynamics in solution. Interconversion of one conformer or enantiomer can be observed by broadening and then coalescence of these diastereotopic signals by gradually increasing the temperature (Figure 7), as rotation around the axis becomes faster and the signals become equivalent by fast exchange on the NMR timescale.

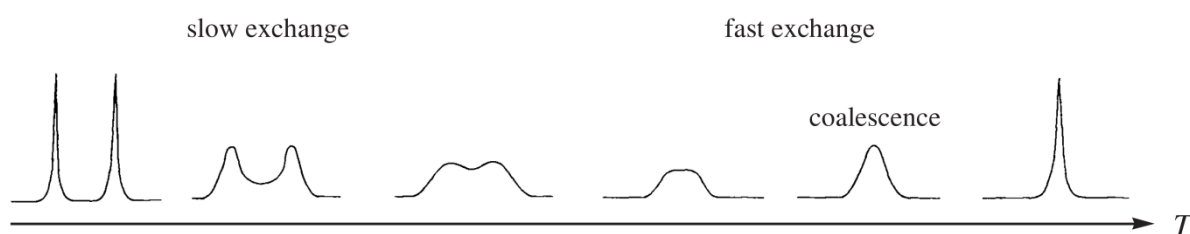


Figure 7 : Evolution of a diastereotopic signal in by VT NMR. Figure obtained from ^[49]

At the coalescence temperature T_c (Figure 7), the rate constant k of two exchanging singlets of equal intensity is defined as follow, where $\Delta\nu$ (Hz) is defined as the chemical shift separation:

$$k_{T_c} = \pi * \frac{\Delta\nu}{\sqrt{2}}$$

Equation 3: Calculation of the rate of enantiomerisation at the coalescence temperature

However, this value only provides information about the free energy at the coalescence temperature. To calculate a barrier to interconversion at any temperature, VT-NMR is needed. Lineshape analysis using a modelling software such as SpinWorks allows the determination of the rate constant k at a given temperature by comparison with the spectrum at slow exchange (Figure 7). The Eyring equation (Equation 1) is then used to calculate the barrier to rotation at any given temperature. Plotting $\ln(k/T)$ against $1/T$ (Eyring plot) gives a straight line from which the enthalpy of activation ΔH^\ddagger and entropy of activation ΔS^\ddagger can be calculated by regression as follows, where a is the slope of the linear regression and b its intercept:

$$\Delta H^\ddagger = -R * a$$

$$\Delta S^\ddagger = R * \left(b + \ln\left(\frac{h}{k_B}\right) \right)$$

Equation 4: Calculation of the enthalpy of activation and entropy of activation using an Eyring plot

Using the Gibbs equation ($\Delta G_T^\ddagger = \Delta H^\ddagger - T * \Delta S^\ddagger$), the barrier to rotation can then be calculated at any given temperature.

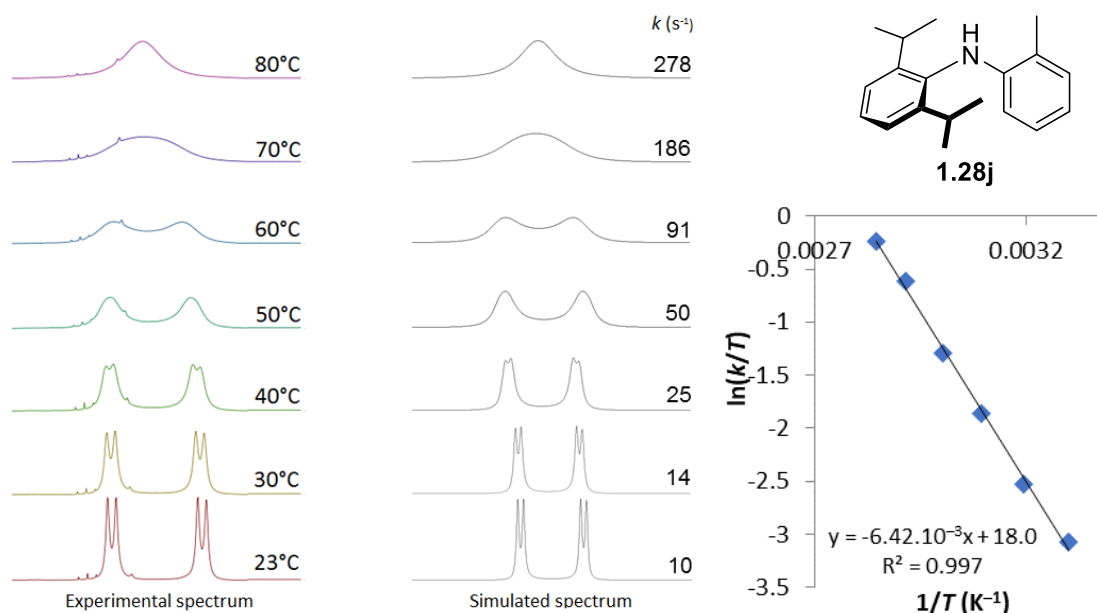
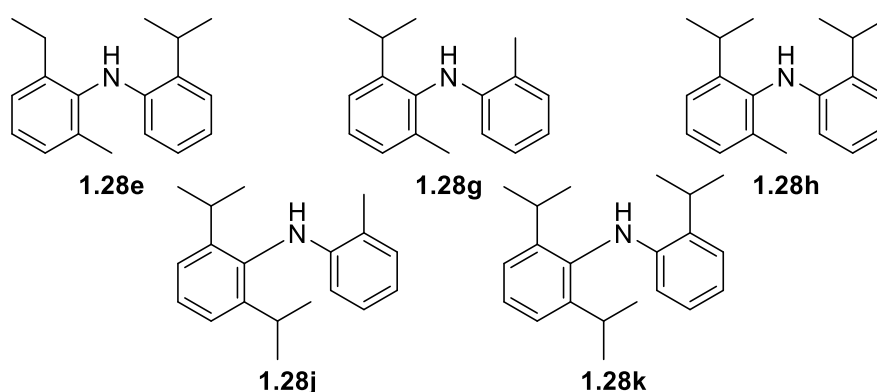


Figure 8: Lineshape analysis of the ¹H NMR (500 MHz) spectrum compound **1.28j** in DMSO-*d*₆

Appearance of diastereotopic signals into an AB system in the ¹H NMR spectra of **1.28g**, **1.28h** and **1.28j** (Figure 8) provided evidence that the congested diarylamines adopt a chiral ground state at room temperature. Calculation of the barrier to rotation of compounds rapidly interconverting was possible

using an ethyl or isopropyl group as a diastereotopic ^1H NMR probe. Lineshape analysis of the signal reaching coalescence allowed the calculation of the compounds rate of enantiomerisation at various temperatures. Using an Eyring plot (Figure 8), both enthalpy ΔH^\ddagger and entropy ΔS^\ddagger were calculated, and the corresponding Gibbs free energy ΔG^\ddagger and half-life to enantiomerisation $t_{1/2}$ were found at room temperature.

Dynamic ^1H NMR, though, is limited to substrates with a relatively low barrier to interconversion. These substrates were naturally the first prepared as their moderate steric hindrance made them easier to synthesise. Typical barriers to rotation determined in this series were in the 60–70 kJ mol^{-1} range (Table 11).



Entry	Compd.	ΔH^\ddagger (kJ mol^{-1})	ΔS^\ddagger ($\text{J mol}^{-1} \text{K}^{-1}$)	ΔG^\ddagger (kJ mol^{-1}) ^a	k_{enant} (s^{-1}) ^a	$t_{1/2}$ (ms) ^a
1 ^b	1.28e	58.3	−21.4	65.4	28.5	16.1
2 ^b	1.28g	65.0	7.5	62.8	62.2	5.6
3 ^b	1.28h	49.6	−53.7	65.7	19.2	18.0
4 ^c	1.28j	53.4	−47.7	67.3	9.9	35.0
5 ^b	1.28k	64.5	−21.0	70.7	2.5	137.8

^a At 298 K. ^b In toluene- d_8 . ^c in DMSO- d_6 .

Table 11 : Barriers to rotation, rates of exchange and half-lives of racemisation calculated by lineshape analysis

2,2'-Di-*ortho*-substituted diarylamines **1.28a–d** were insufficiently hindered for slow rotation around the C–N bonds to be evident by ^1H NMR. Even at low temperature (−40 °C), no diastereotopic signals could be observed, suggesting that the chiral ground state conformers interconvert rapidly on the NMR timescale. Interestingly, while a single *ortho-tert*-butyl group is enough to retain conformational stability in anilides,^[26] the lack of conformational restriction in **1.28c** demonstrates how much more flexible these diarylamines are in comparison. This may be due to an interconversion through geared rotation, which is of higher energy in anilides due to the conjugation of the carbonyl group with the nitrogen lone pair. While calculating the entropy of activation by dynamic NMR is notoriously unreliable,^[50] the strong, negative ΔS^\ddagger determined in Table 11 for **1.28h**, **1.28j** and, to some extent,

1.28e and **1.28k**, is indicative of a highly ordered transition state typical for the enantiomerisation of biaryls,^[49] possibly by alignment of the π system of one of the rotating aryl ring and participation of the nitrogen lone pair.

When coalescence could not be reached, VT-HPLC was used instead. It proved to be complementary to dynamic NMR, although its lower detection limit was attained by compound **1.28f**, for which routine VT-NMR could not reach temperature high enough for determination of its barrier to enantiomerisation. Molecules racemising within minutes can be difficult to study by VT-NMR due to their particularly high temperature of coalescence ($T > 373$ K). In addition, such near-atropisomers cannot be efficiently separated by preparative chromatography at room temperature. In this case, VT-HPLC is a suitable method to investigate their barrier to rotation. Specifically, variable-temperature – chiral – HPLC is a convenient tool for compounds with barriers to rotation of around 85 up to 100 kJ mol⁻¹. Elution of a compound partially interconverting within its retention time gives signals with a plateau between the two enantiomeric peaks (Figure 9).

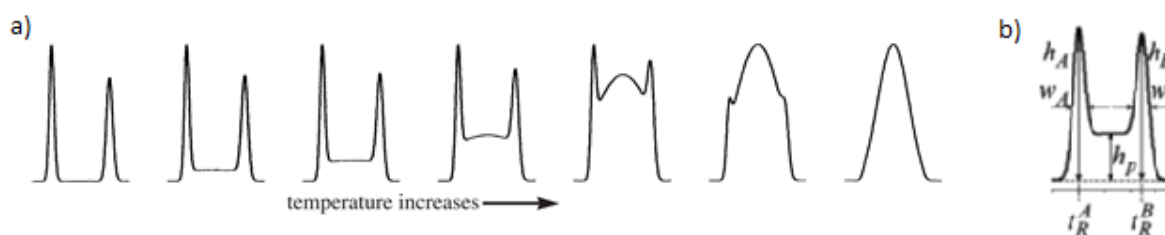


Figure 9: a) Temperature-dependant peak profiles b) Parameters for peak-shape analysis. Obtained from ref ^[49] and ^[51]

In 2006, Trapp demonstrated the use of a 'Unified Equation' for the calculation of rate constants by variable-temperature chromatography. By mathematically separating each non-interconverting peak from the plateau (of interconverting peaks), the rate of enantiomerisation can be calculated from the chromatograms at different temperatures. For racemic mixtures, the equation is the following with

$\sigma_X = \frac{\omega_X^h}{\sqrt{8 \cdot \ln(2)}}$, ω_X^h the peak width of X at half height (s), t_R^X the retention time of the peak of X (s), N the number of plateau and h_p the relative height of the plateau compared to the first peak:^[52]

$$k_{\text{enant}} = -\frac{1}{t_R^A} * \left(\ln \left(\frac{50 + 0.5 * \left(100 - h_p * \left(1 + \sqrt{\frac{2}{\pi}} * N \right) \right)}{t_R^B - t_R^A} \right) \right. \\ \left. - \ln \left(0.5 * \left(\frac{h_p * e^{-\frac{(t_R^A - t_R^B)^2}{2 * \sigma_B^2}} - 100 * e^{-\frac{(t_R^A - t_R^B)^2}{8 * \sigma_B^2}}}{\sigma_B * \sqrt{2 * \pi}} - \frac{100 * e^{-\frac{(t_R^B - t_R^A)^2}{8 * \sigma_A^2}}}{\sigma_A * \sqrt{2 * \pi}} - \frac{h_p * \left(1 + \sqrt{\frac{2}{\pi}} * N \right) - 200}{t_R^B - t_R^A} \right) \right) \right)$$

Equation 5: Calculation of the rate of enantiomerisation using the 'Unified Equation'

As for VT-NMR, calculation of the rate of enantiomerisation at different temperatures allows the use of an Eyring plot (Equation 4) and the calculation of ΔG^\ddagger_T at any temperature.

Generally, tri-*ortho*-substituted diarylamines with a *tert*-butyl group interconverted during the course of an HPLC run, with half-lives to enantiomerisation of a few minutes. These compounds displayed the typical ‘Batman’s hat’ peaks due to the apparition of an interconversion plateau between each enantiomer peak (Figure 10).

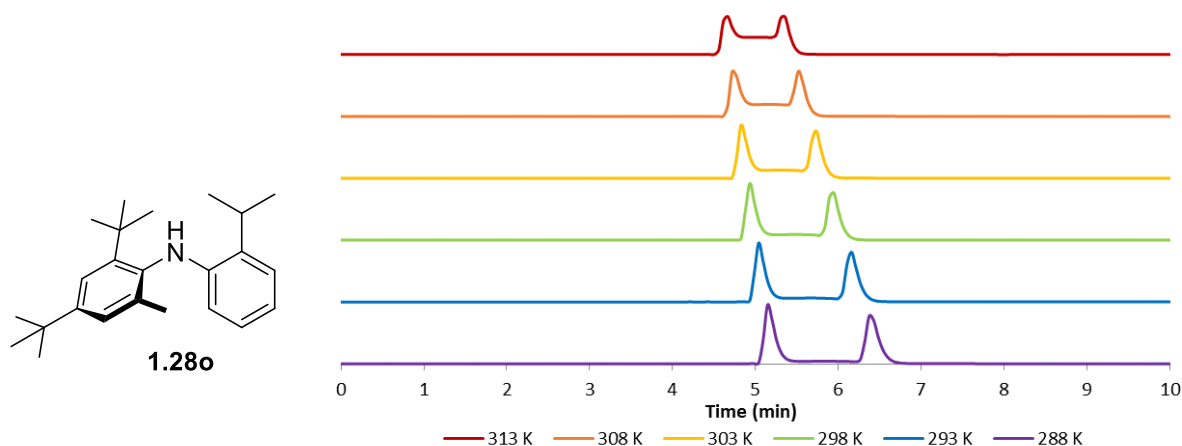
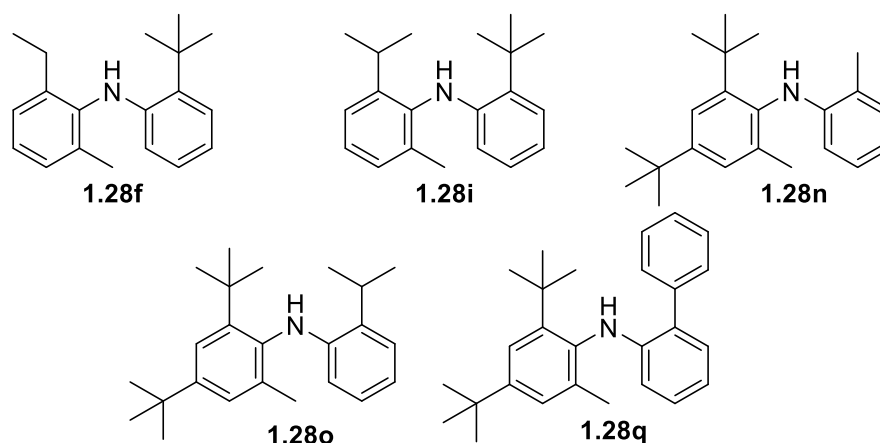


Figure 10: VT-HPLC profile of compound **1.28o**

While the enthalpy of activation of the compounds resolved by chiral HPLC is comparable to that of those determined by VT-NMR (Table 12), their entropy of activation is considerably larger, whilst still being negative, and accounts for most of the increase in the barrier to rotation.

Unless one of the substituents was a *tert*-butyl group, half-lives for interconversion of tri-*ortho*-substituted diarylamines were typically of the order of milliseconds (Table 11). While increasing the steric demand by replacing a methyl group for an isopropyl group led to a threefold increase of the half-life to enantiomerisation in **1.28g** and **1.28h**, replacement of an ethyl group for an isopropyl group only showed minor changes the barrier to rotation in **1.28e** and **1.28h**, with a maximum of a twofold difference in the rate of enantiomerisation in **1.28f** and **1.28i** (Table 12). The same order of magnitude was seen in symmetrical compounds **1.28j** and **1.28k** which, unlike diaryl ethers, did not seem affected by the symmetry of the aryl ring, as a tenfold difference in the half-life was observed between **1.28g–h** and symmetrically substituted **1.28j–k**. A great increase in the barrier to interconversion was found when exchanging an isopropyl group for a *tert*-butyl group, with a difference of more than 20 kJ mol⁻¹ in the barrier to rotation of **1.28e** and **1.28f** as well as **1.28h** and **1.28i**, making these compounds near-atropisomers. The relative position of each bulky substituent was also critical, as seen in the twofold increase of the rate of enantiomerisation of **1.28j** and **1.28n** compared to **1.28h** and **1.28i**, respectively.



Entry	Compound	ΔH^\ddagger (kJ mol ⁻¹)	ΔS^\ddagger (J mol ⁻¹ K ⁻¹)	ΔG^\ddagger (kJ mol ⁻¹) ^a	k_{enant} (s ⁻¹) ^a	$t_{1/2}$ (min) ^a
1 ^b	1.28f	53.2	-109.6	85.8	5.6 10 ⁻³	1.0
2 ^c	1.28i	51.8	-121.5	88.0	2.3 10 ⁻³	2.5
3 ^c	1.28n	37.9	-166.7	87.6	2.8 10 ⁻³	2.1
4 ^c	1.28o	40.8	-165.9	89.9	1.1 10 ⁻³	5.3
5 ^c	1.28q	45.0	-151.6	90.2	9.8 10 ⁻⁴	5.9

^a At 298 K. ^b In *n*-hexane/ethyl acetate. ^c In *n*-hexane/2-propanol.

Table 12 : Barriers to rotation, rates of exchange and half-lives of racemisation calculated by VT-HPLC

A single *tert*-butyl substituent on one of the rings allowed the separation of the enantiomers at room temperature, and racemisation could be observed with a moderately big isopropyl group on the second ring, such as in compounds **1.28i**, compared to **1.28h**. Similarly, compounds with a di-*ortho*-substituted ring and at least a *tert*-butyl group could also be resolved at room temperature, even with substituents as small as a methyl group on the other ring (compounds **1.28n**). A phenyl ring at the *ortho*-position gave a relatively high barrier to rotation, as its steric bulk seemed slightly greater than that of an isopropyl moiety (compounds **1.28q** and **1.28o**).

2,6-Disubstituted diarylamines containing one *tert*-butyl group had a significantly higher barrier to rotation. Even mono-substitution of the other ring as in compounds **1.28n**, **1.28o** and **1.28q**, although not sufficient to reach atropisomerism, allowed the racemisation to be observed at near-room temperatures by dynamic HPLC. However, more substituents were necessary to obtain conformationally stable diarylamines.

A conventional method to access the barrier to rotation of atropisomers is to follow the rate of racemisation of an enantioenriched sample. The quantification of decay of enantiomeric excess over time was done by chiral HPLC, but the concept can be extended to any chiral spectroscopic technique such as circular dichroism^[53] or optical rotation,^[54] for example. Plotting the natural logarithm of the enantiomeric excess (*ee*) against time gives a straight line from which linear regression determines

the rate of enantiomerisation with the equation $\ln(ee_t) = 2 * k_{\text{enant}} * t + ee_0$, for a first order decay. A major drawback in this technique is the need to prepare enantioenriched material. Also, the barrier to interconversion obtained is given for a specific temperature.

The only compounds which could be resolved with very high conformational stability were tetra-*ortho*-substituted diarylamines. Compound **1.28m** could regrettably not be separated by chiral HPLC. Compounds **1.28i** and **1.28p**, with a *tert*-butyl group on each ring, could be separated even at 40 °C, indicating high thermal stability. However, the poor resolution of their enantiomers prevented any isolation of an enantioenriched sample for calculation of barrier to rotation. Nevertheless, these results indicated that even moderately bulky groups such as an isopropyl can hinder bond rotation provided the other ring is highly congested and another group is present on the same ring. By repeated injections of a solution of **1.28x** on a chiral analytical column, an enantioenriched sample could be isolated and its decay of enantiomeric excess was followed (Figure 11).

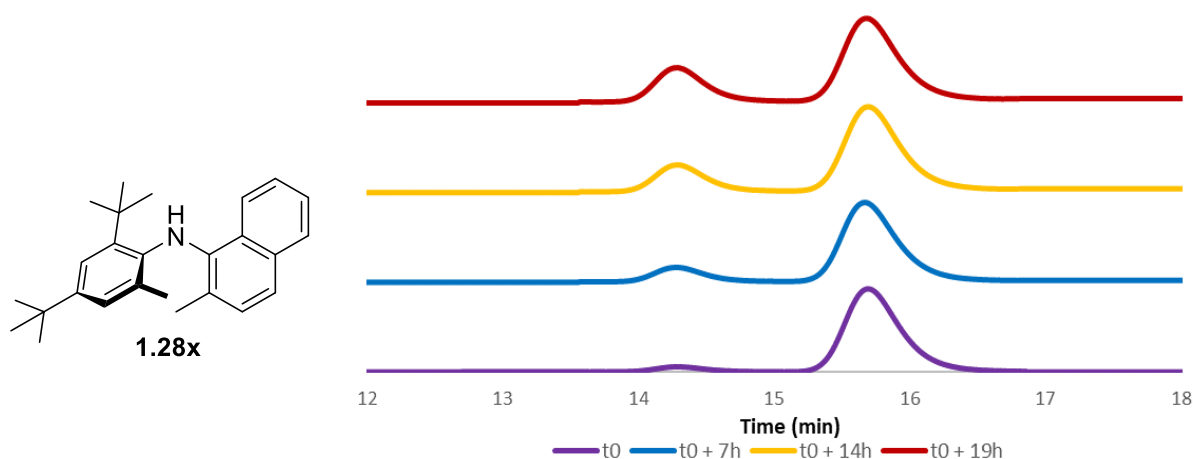
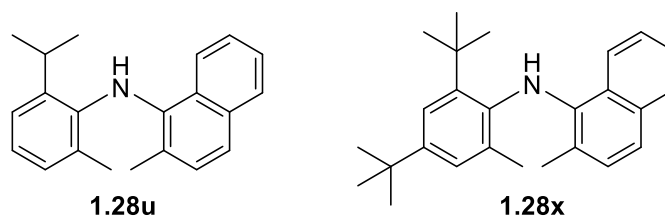


Figure 11: Part of the VT-HPLC traces used to determine the *ee* of **1.28x** during its racemisation

At 100 °C in toluene, compound **1.28x** racemised within 48 hours, allowing the calculation of its barrier to rotation at this temperature (Table 13). Similarly, enantio-enriched fractions of compound **1.28u** could be isolated and the decay of its enantiomeric excess was followed at 25 °C in toluene.

Compounds **1.28u** and **1.28x** proved once again the critical impact of the *tert*-butyl group. While compound **1.28u** was only conformationally stable enough at room temperature for its rate of enantiomerisation to be calculated, heating up diarylamine **1.28x** to 100 °C in toluene was required to observe racemisation, with a half-life of 20 hours at this temperature. Hence, compounds **1.28u** and **1.28x** demonstrate that secondary diarylamines can adopt a chiral ground state, with a conformational stability high enough for them to reach atropisomerism solely by the action of steric demand.



Entry	Compound	ΔG^\ddagger_r (kJ mol ⁻¹)	k_{enant} (s ⁻¹)	$t_{1/2}$
1 ^{a, b}	1.28u	93.9	$2.1 \cdot 10^{-4}$	27.3 min
2 ^{a, c}	1.28x	145.0	$4.3 \cdot 10^{-7}$	20.3 h

^a In toluene. ^b At 298 K. ^c At 373 K.

Table 13 : Barriers to rotation, rates of exchange and half-lives of racemisation of atropisomeric diarylamines

An X-ray crystal structure of compound **1.28u** was obtained by slow evaporation of a saturated solution of dichloromethane (Figure 12). The bond angles $\angle \text{C}_{\text{Ar}}\text{NH} = 116^\circ$ for each aromatic ring and $\angle \text{C}_{\text{Ar}}\text{NC}_{\text{Ar}} = 125^\circ$. The sum of these angles is 357° , indicating that the nitrogen adopts an almost planar conformation. The torsion angle between the naphthyl ring and the nitrogen plane is 45.4° , while it is 47.6° between the aryl ring and the nitrogen plane, suggesting that the nitrogen lone pair electrons are partially delocalised in both rings. While steric repulsion forces the aromatic rings out of the plane of the nitrogen atom, conjugation of the π system with the lone pair mitigates this phenomenon. The lone pair of the central nitrogen is distorted from its apical position and points towards a share in the π system of each ring.

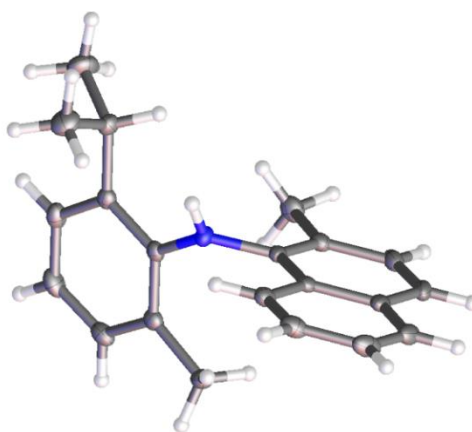


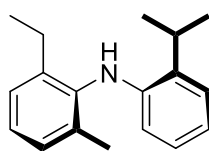
Figure 12: Crystal structure of 1.28u

Furthermore, the C–N bonds lengths are comprised between 1.40 and 1.41 Å, close to that of aniline (1.402 Å).^[55] This detail is critical as bond length plays an important role in the barrier to rotation (as seen in the case of diaryl sulfoxide **1.5b**) and shows that atropisomerism in diarylamines is not hampered by C–N bond lengths.

I.2.3. External effectors on the barrier to rotation of secondary diarylamines

Effect of the solvent on the barrier to interconversion

Because lineshape analysis, VT-HPLC and racemisation of enantioenriched samples were performed in different media, the effect of solvent polarity was investigated. Compound **1.28e** was selected as its barrier to rotation was easily calculated by lineshape analysis, for which a wide range of deuterated solvents can be used. Its rate of enantiomerisation was calculated in various polar and non-polar, protic and aprotic solvents (Table 14). The barrier to enantiomerisation was independent of the solvent, with errors of $\pm 2\%$, with a strong enthalpy/entropy compensation effect, even when using different signals of the same molecule. Large statistical errors can occur during the lineshape analysis which can lead to correlations between the errors in both enthalpy and entropy, then producing an artificial compensation. Although reported for the first time sixty years ago in the determination of the barrier to enantiomerisation of some biphenyls,^[56] the solvent-driven enthalpy/entropy compensation in rate of enantiomerisation is, to date, still largely unexplained.^[57]



1.28e

Entry	Solvent	Signal	ΔH^\ddagger (kJ mol ⁻¹)	ΔS^\ddagger (J mol ⁻¹ K ⁻¹)	ΔG^\ddagger (kJ mol ⁻¹) ^a
1	Toluene- <i>d</i> ₈	Isopropyl	41.5	-80.0	64.7
2	Toluene- <i>d</i> ₈	Ethyl	58.3	-21.4	65.7
3	C ₂ D ₅ OD	Isopropyl	31.7	-114.0	65.7
4	C ₂ D ₅ OD	Ethyl	35.8	-96.0	64.4
5	CD ₃ CN	Isopropyl	31.9	-112.1	65.3
6	CD ₃ CN	Ethyl	nd ^b	nd ^b	nd ^b

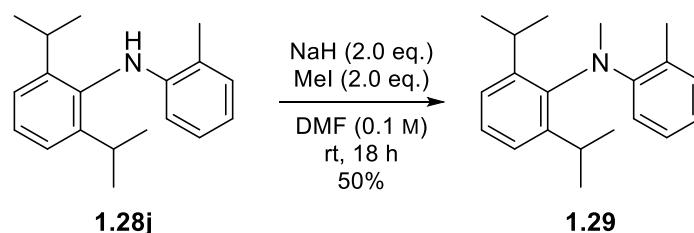
^a At 298 K. ^b Not determined due to peaks overlapping.

Table 14 : Solvent effect in barriers to rotation of 1.28e

Effect of N-methylation on the barrier to interconversion

Exploring the effect of increasing the steric demand on the nitrogen atom on conformational stability by addition of a third substituent proved to be more difficult than expected. Diarylamine **1.28j** could be *N*-methylated by treatment with sodium hydride and methyl iodide in 50% yield (Table 15) but was completely unreactive towards any other electrophile such as ethyl iodide, benzyl bromide, acetyl chloride or Boc anhydride. *N*-methylation of any other diarylamines prepared in the previous section

with an excess of base and alkylating agent in refluxing THF did not yield any product, showing that the nitrogen atom is buried within the sterically demanding groups at the *ortho*-positions.



Entry	Compound	ΔH^\ddagger (kJ mol ⁻¹)	ΔS^\ddagger (J mol ⁻¹ K ⁻¹)	ΔG^\ddagger (kJ mol ⁻¹) ^a	k (s ⁻¹) ^a	$t_{1/2}$ ^a
1	1.28j	53.4	-47.7	67.3	9.9	0.035 s
2	1.29	71.7	-7.80	74.0	6.7 10 ⁻¹	0.52 s

^a At 298 K.

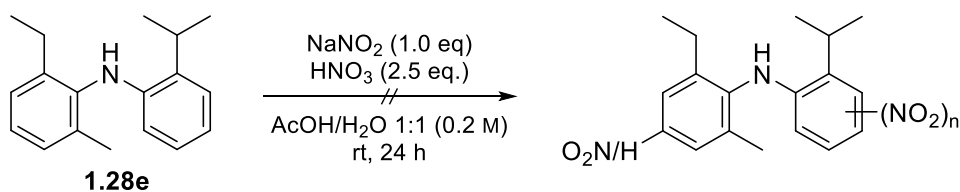
Table 15 : Effect of *N*-methylation

A methyl substituent on the nitrogen slows down the half-life to enantiomerisation by more than a tenfold (Table 15). The great increase of enthalpy of activation, together with the low, negative entropy of activation suggest that the transition state is destabilised by the strain caused by the methyl substituent in the vicinity of the aryl ring coplanar with the nitrogen.

Effect of electron-density on the barrier to interconversion

Similarly to the study by Kitagawa *et al.* on the effect of the electronic properties of the *para*-position on the barrier to C–N rotation of congested, tertiary diarylamines,^[31] we sought to introduce electron-withdrawing and -donating groups at one or multiple *para*-positions of the congested diarylamines previously prepared. We focussed on the introduction of a nitro group, as this can be hydrogenated and further derivatised to tune the electronic properties of the products.

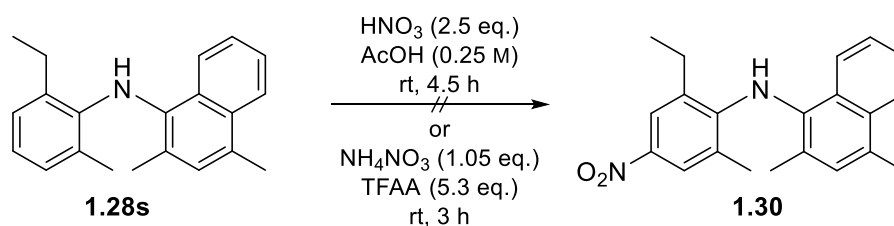
Introduction of a nitro group was first attempted by nitration of diarylamine **1.28e** by electrophilic aromatic substitution (Scheme 7). However, when using previously reported conditions for the nitration of electron-rich aromatics, a complex mixture of highly coloured compounds was formed.



Scheme 7 : Aromatic nitration of 1.28e

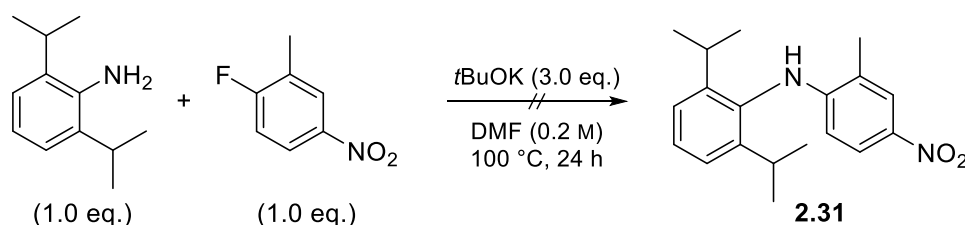
As **1.28e** possesses three electrophilic carbons available for nitration, our attention then moved on to compounds **1.28s** with four substituents to reach low rates of interconversion and a diastereotopic probes for potential use in lineshape analysis (Scheme 8). However, when subjecting aniline **1.28s** to

standard nitration conditions (fuming nitric acid in acetic acid),^[58] decomposition occurred rapidly. Milder condition with stoichiometric amounts of ammonium nitrate in trifluoroacetic anhydride resulted in the same complex mixture of products.^[45]



Scheme 8 : Aromatic nitration of 1.28s

The nitro group on the diarylamine products raises the possibility of using S_NAr reactions to synthesise these compounds. As the coupling was expected to be challenging, moderately hindered diarylamine **1.31** was the selected target (Scheme 9).



Scheme 9 : Attempt S_NAr toward nitrated diarylamine

However, using reported conditions for the synthesis of *para*-nitro diarylamines by S_NAr , with potassium *tert*-butoxide in DMF at elevated temperature gave no conversion, probably because of the consequent steric hindrance around the nucleophilic centre.

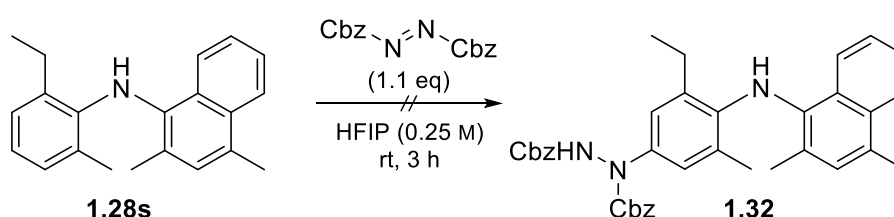
Instead, a new approach using the conditions used previously for the Buchwald–Hartwig coupling of sterically hindered substrates with PNP_3 as a ligand was attempted (Table 16).^[32] Coupling of electron-poor 2-isopropyl-4-nitroaniline with electron-rich aryl bromides did not yield any product under the standard conditions, with prolonged reaction times.

Entry	R ¹	R ²	R ³	R ⁴	Result
1	2- <i>i</i> Pr	4-NO ₂	2,3-benzo ^a	6-Me	No conversion
2	2- <i>i</i> Pr	4-NO ₂	2,4- <i>t</i> Bu	6-Me	No conversion
3	2,6- <i>i</i> Pr	—	2-Me	4-NO ₂	No conversion

Table 16 : Attempted Buchwald-Hartwig reactions on *para*-nitro substrates

The electronic properties of the substrates were then exchanged in order to optimise their reactivity (Table 16). When using electron-deficient 2-methyl-4-nitrobromo benzene and sterically hindered 2,6-diisopropylaniline, no coupling was observed either.

Eventually, a final attempt to *para*-aminate one of the congested diarylamines was performed using a procedure by Crousse *et al.* (Scheme 10),^[59] where treatment of diphenylamine with dibenzyl azodicarboxylate in hexafluoro-isopropanol (HFIP) results in a mild, *para*-selective amination in excellent yield. When **1.28s** was subjected to the reaction conditions, a bright green precipitate formed instantly, with full consumption of the starting material. The reaction gave a complex crude mixture, and no product **1.32** was obtained after purification by flash column chromatography.



Scheme 10 : Attempted amination with Benzyl-azodicarboxylate^[59]

Attempts to optimise the reaction by lowering the temperature to 0 °C, using a 1:1 mixture of HFIP and CH₂Cl₂, or performing a one-pot amination/hydrogenolysis of the resulting hydrazide with palladium over activated charcoal did not provide any product.

Thus, introduction of electron-donating and -withdrawing substituents at the *para*-position of hindered diarylamines proved to be unsuccessful. Nitration or amination by electrophilic aromatic substitution yielded mixtures of products, possibly arising from the formation of an iminoquinone intermediate. On the other hand, neither nucleophilic aromatic substitution and transition metal-catalysed reactions gave any conversion.

Effect of protonation on the barrier to interconversion

Sutherland *et al.* showed that the planarity of the nitrogen atom in anilides and conjugation of its lone pair with a delocalized π system is necessary for high conformational stability.^[23] This effect was also demonstrated by Kitagawa *et al.* with an axially chiral, enantiopure *N*-arylated tetrahydroquinoline which, upon protonation by trifluoroacetic acid, accelerates its rate of enantiomerisation significantly.^[22] To explore this feature in diarylamines, solutions of **1.28e** in different deuterated solvents were treated with a strong acid. Because of the low basicity of diarylamines ($pK_a \approx 1$ for diphenylamine), triflic acid was used.

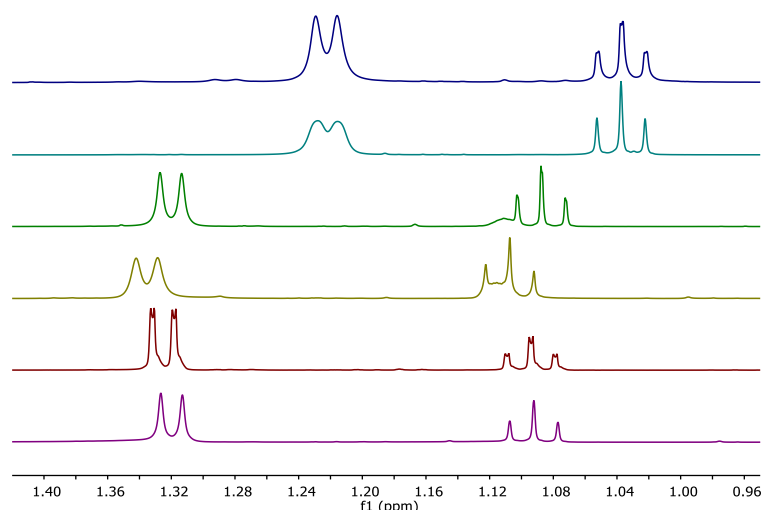


Figure 13 : Line sharpening of the diastereotopic signals (1.45-0.90 ppm) of **1.28e** upon protonation (500 MHz). From top to bottom: toluene- d_8 + TfOH; toluene- d_8 ; ethanol- d_6 + TfOH; ethanol- d_6 ; CD_3CN + TfOH; CD_3CN .

Excessive line broadening of the samples (probably due to precipitation) precluded lineshape analysis of protonated **1.28e** at low temperature. However, in all three solvents, the isopropyl $CHMe_2$ signals centred around 1.22 ppm in toluene- d_8 and 1.32 ppm in C_2D_5OD and CD_3CN became significantly sharper upon protonation, implying an acceleration of the rate of enantiomerisation. Thus, pyramidalization of the nitrogen by protonation leads to destabilization of the ground state and reduction of the barrier to rotation around the C–N bonds.

I.3. Conclusion

Atropisomerism can be achieved in sterically hindered, secondary diarylamines. While di-*ortho*-substituted diarylamines interconvert too rapidly for enantiomerisation to be observed at low temperature by 1H NMR, a third substituent slows down the rates of interconversion enough for the barriers to enantiomerisation to be calculated by lineshape analysis. Introduction of a *tert*-butyl group shows a critical effect on the rate of enantiomerisation. Tri-*ortho*-substituted diarylamines bearing such group can be separated by chiral HPLC at low temperature, although fast racemisation precludes their isolation as an enantiopure sample. Conformational stability was observed at room temperature when introducing four *ortho*-substituents, especially with one *tert*-butyl group. Diarylamine **1.28x** was the most congested molecule prepared and displayed a barrier to rotation of up to 145.0 kJ mol $^{-1}$ corresponding to a half-life of *circa* 20 hours at 100 °C. Additional work is currently performed by collaborators to understand the mechanism by which this compounds racemise.

However, the limits of the Buchwald–Hartwig coupling for the synthesis of congested diarylamines exhibiting atropisomerism were reached with highly hindered anilines and aryl bromides. As their post-functionalisation proved to be equally challenging, novel strategies to produce more complex diarylamines with diverse functionalities are necessary.

Chapter 2

Heavily Substituted Atropisomeric Diarylamines by Unactivated Smiles Rearrangement
of *N*-Aryl Anthranilamides

Part of the results presented in this chapter were published in:

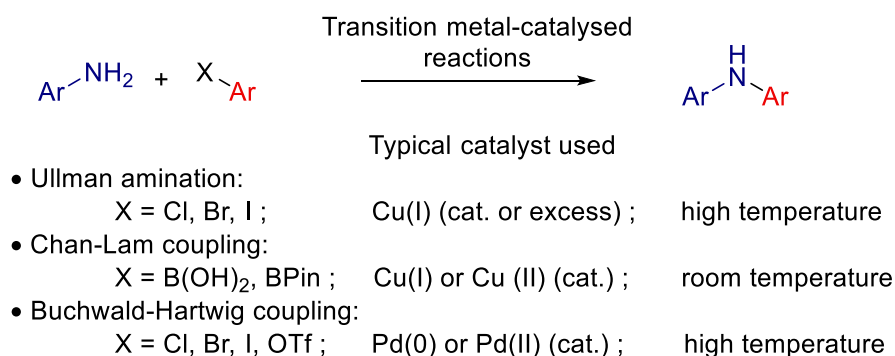
R. Costil, H. J. A. Dale, N. Fey, G. Whitcombe, J. V. Matlock, and J. Clayden, Angew. Chem. Int. Ed., **2017**, *56*, 12533–12537.

II.1. Introduction

The study of the conformational stability of sterically congested diarylamines presented in Chapter 2 was hampered by synthetic difficulties. The substrates of interest were not readily available, and the literature reports were insufficient for our needs. Consequently, we felt the need to develop new methodologies for the synthesis of this challenging class of molecules, aiming to develop an easily operated, efficient and robust protocol.

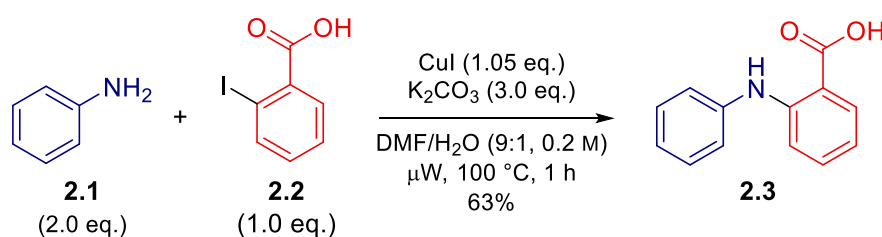
II.1.1. Synthesis of diarylamines by transition metal-catalysed reactions

The formation of C–N bonds using transition metal-catalysis has seen a significant progress since the pioneering work by Goldberg and Ullman more than a century ago.^[60] Ever since, formation of diarylamines with modern methods have been improved to greater functional group tolerance and lowered catalyst loading.^[61] The higher acidity of arylamines compared to alkylamines, together with a lack of unfavourable β -hydride elimination pathway make them an ideal coupling partner for this type of reactions.^[33]



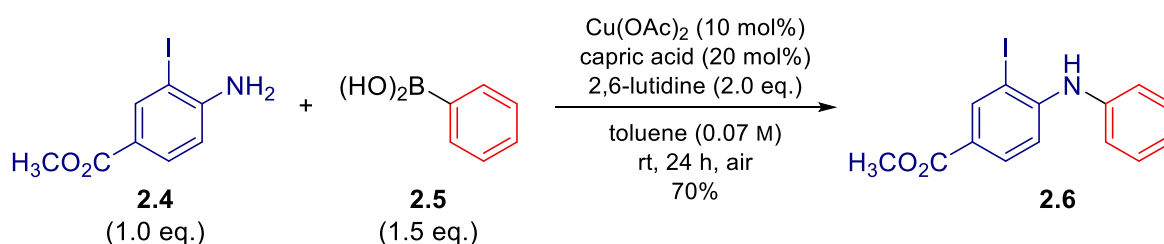
Scheme 11 : General overview of transition metal-catalysed methods for the synthesis of diarylamines

Historically, the most relevant transformation to access diarylamines is the Ullman condensation, later modified by Goldberg.^[60] In this reaction, a stoichiometric amount of copper(I) is used in combination with a base to achieve the coupling of an aryl halide **2.2** with an aniline **2.1** (Scheme 12) through the formation of an organocuprate.^[62] While this is a powerful reaction, the harsh conditions required for coupling, such as high temperature, the use of stoichiometric amount of copper, or the need for polar high boiling solvents limits its applicability.



Scheme 12: Ullman coupling^[62]

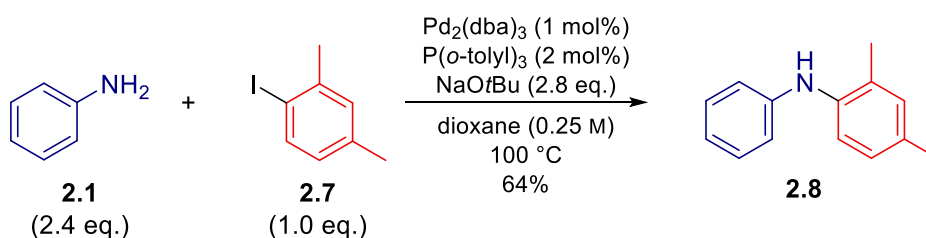
A modification of the Ullmann-conditions led to the development of the Chan–Lam reaction,^[63,64] where either copper(II) or copper(III) (generated *in situ*) catalyses the coupling of an aryl boronic acid **2.5** with an aniline **2.4**, an alkylamine or an amide (Scheme 13).^[65] This reaction has several advantages. It proceeds at room temperature, operates with low catalyst loading, and is performed in presence of air (to re-oxidise the catalyst).^[66] The conditions and relatively low cost and toxicity of copper, make this reaction valuable for process chemistry.



Scheme 13: Chan–Lam coupling^[65]

However, numerous side-reactions arise from the decomposition of the boronic acid starting material, such as protodeboronation, oxidation to the corresponding phenol or oxidative coupling to form diaryl ethers. Aryl–aryl homocoupling can also be observed.^[67] Furthermore, the challenge of steric hindrance has only been addressed for the arylation of highly reactive imidazoles by Wentzel *et al.*^[68]

Over the past decades, the use of palladium in transition metal-catalysed C–N bond formation in the Buchwald–Hartwig coupling of an aryl halide with an amine has emerged as a powerful method to synthesise diarylamines.^[69,70] The reaction takes place with low catalytic loading of palladium with a ligand and a base (Scheme 14).^[71] The wide use of this transformation makes this reaction widely studied, and various groups have developed strategies to design and fine-tune ligands to achieve the desired transformation efficiently. Amongst them are Buchwald’s 2-biaryl dialkylphosphines,^[34] but also trialkylphosphines,^[32,72,73] *N*-heterocyclic carbenes^[74] and bis-phosphines.^[75]

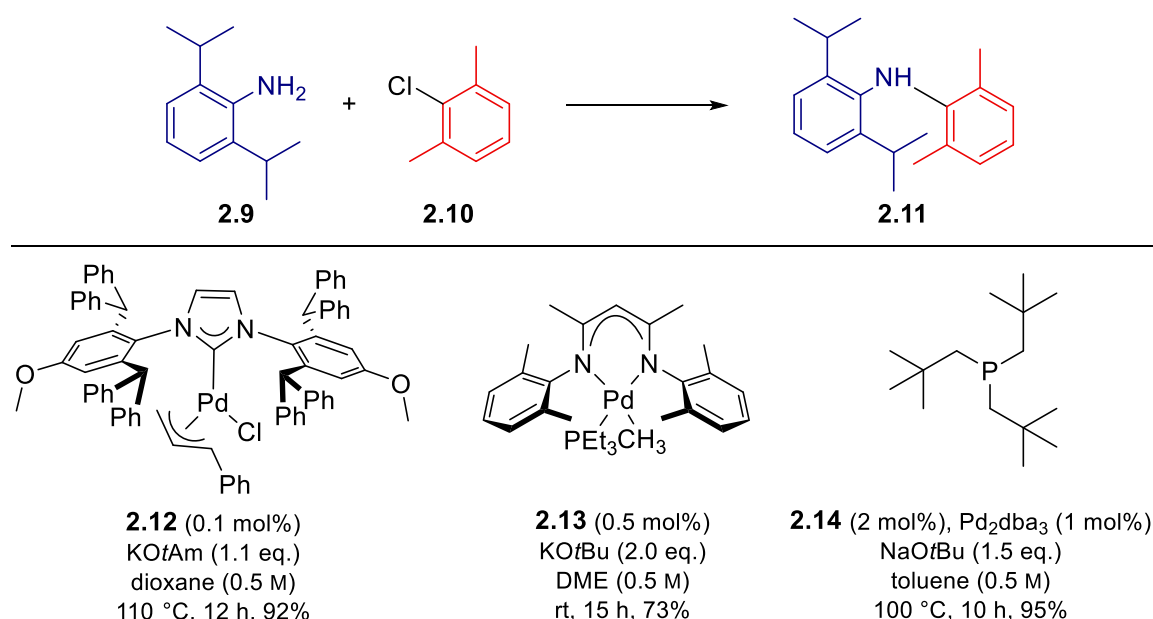


Scheme 14: Buchwald–Hartwig coupling^[71]

The major drawback of the previously discussed synthetic routes to diarylamines is that steric hindrance hampers the coupling.^[32] While sterically demanding ligands promote consecutive steps of palladium-catalysed coupling reactions, this decreases the reactivity of sterically congested substrates. Furthermore, as aromatic amines are relatively poor nucleophiles compared to other amines,^[76] ligand displacement on the palladium complex can be difficult.^[33] For these reasons,

oxidative addition of bulky aryl halides is problematic. However, provided oxidative addition is favoured, protodehalogenation or oxidation of the C–X bond can also easily compete with the desired coupling.^[77,78]

A handful of research groups have come up with finely tuned ligands allowing the coupling of sterically hindered anilines with sterically hindered aryl halides to provide congested diarylamines such as *N*-(2,6-diisopropylphenyl)-2,6-dimethylaniline **2.11**. The extensive work by Nolan *et al.* on the use of *N*-heterocyclic carbene-based precatalysts **2.12**^[74] (Scheme 15) unravelled the potential for this type of ligand to efficiently catalyse the Buchwald–Hartwig coupling of hindered starting materials at particularly low concentration of catalyst. Modularity of the scaffold permits fine tuning of the properties of the ligands, from steric bulk and flexibility to electronic properties or solubility.

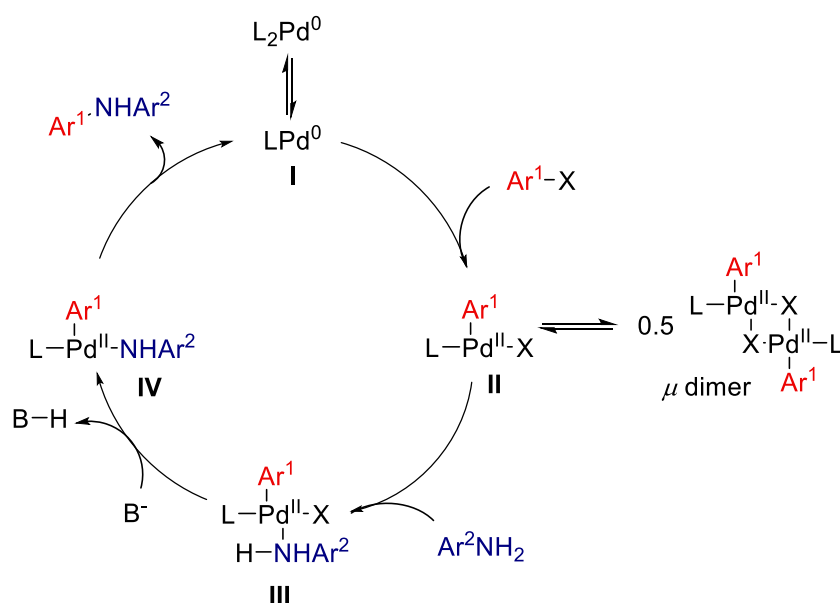


Scheme 15: Example of catalysts for the Buchwald–Hartwig coupling of hindered substrates^[32,74,79]

Jin reported a highly efficient β -diketiminato-palladium precatalyst **2.13**.^[79] Low catalyst loadings were achieved for the coupling of sterically hindered substrates, but the true highlight of their work is that coupling of aryl chlorides with anilines happens at room temperature in a few hours. However, this catalyst requires multistep synthesis, and work by Pörschke *et al.* suggests the complex might not be highly stable in solution.^[80] It is worth noting that ‘Verkade superbases’, namely proazaphosphatranes, also catalyse this coupling in good yield.^[81] However, their high price, difficult synthesis and moisture-sensitivity make them poor candidate for larger-scale applications.

Recently, Shaughnessy *et al.* reported a series of highly congested alkyl phosphines derived from the tri-*tert*-butylphosphine, for the synthesis of sterically hindered diarylamines such as **2.11**.^[32,72,73] Substituting the *tert*-butyl groups by neopentyl (methylene *tert*-butyl) groups afforded tri-neopentylphosphine **2.14** (PNp₃), a ligand of drastically increased the activity for the synthesis tetra-*ortho*-substituted diarylamines with previously unattained levels of steric hindrance.

The unique tolerance of the Buchwald–Hartwig reaction for steric congestion requires deep mechanistic investigation in order to further develop new ligands. The general mechanism using a monodentate ligand is shown in Scheme 16.^[33] First, ligand dissociation at the palladium to form mono-ligated complex LPd^0 **I** (with L the ligand) is necessary for palladium with bulky ligands. This allows oxidative addition of the aryl halide on the active species, a common intermediate in palladium catalysed methods.^[33] The palladium complex **II** thus formed is in fast exchange with a catalytically inactive dimeric species. Coordination of the amine decreases the $\text{p}K_{\text{a}}$ of the nitrogen^[82] and deprotonation of **III** triggers the displacement of the halide to form **IV**. Reductive elimination leads to the final arylated amine with regeneration of the active palladium(0) complex.



Scheme 16: General mechanism of the Buchwald–Hartwig coupling^[39]

The reaction relies on a fine balance of electronic and steric tuning of the active site by modification of the ligand. Ligand dissociation and oxidative addition are driven by the steric bulk of the ligands surrounding the palladium centre. Unhindered ligands such as triphenylphosphine lead to the formation of catalytically inactive $\text{L}_2\text{Pd}(\text{Ar})\text{X}$ (L = triphenylphosphine, X = halide).^[39] The other catalyst resting state μ is stabilised by the nature of the halide. While negligible when X = I or Br, this dimer is the major compound in solid state and in solution (benzene) when X = Cl.^[83,84]

Buchwald *et al.* showed the correlation between electron density at the ligand and the acidity of the amine-bound complex **III**.^[82] As electron-deficient phosphines gave better conversion, the authors concluded that the palladium species made more cationic by ligation with an electron-deficient phosphine increased the acidity of the bound amine, leading to higher catalyst turnover.

Reductive elimination requires a fine balance of steric hindrance. While reactivity is reduced with great steric hindrance around the nucleophilic atom, this step reduces strain at the metal centre, and thus is promoted by electron-deficient, bulky ligands.^[39]

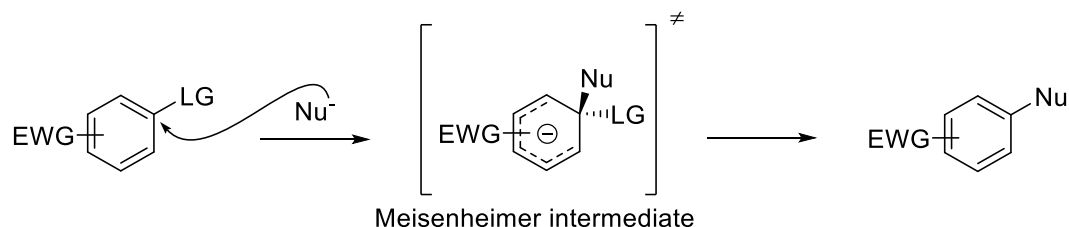
The uniqueness of PNP₃ **2.14** as a powerful ligand is due to its balance between highly bulky substituent and flexibility. The crystal structure of bis(PNP₃)palladium(0) showed that the steric bulk of the neopentyl group is directed towards the metal centre, achieving maximum steric hindrance and activating the complex for oxidative addition.^[32] The substituent flexibility allows for accommodation of bulky aryl groups by rotation of the CH₂ group, while keeping enough steric hindrance to prevent the formation of inactive dimer. Although the steric bulk prevents the formation of a stable coordination complex **III** with the aniline,^[39] its deprotonation is thermodynamically favoured by irreversible formation of a complex **IV** rapidly yielding the final product by reductive elimination.

While PNP₃ is probably the most powerful ligand for the Buchwald–Hartwig amination of hindered anilines, its use is far from trivial, as shown in Chapter 2. PNP₃ itself is a stable, crystalline solid, but its synthesis is expensive, low yielding, and the lack of reproducible procedure for the preparation of the Grignard starting material makes its synthesis poorly practical. Moreover, the coupling reaction itself seems to be extremely sensitive of parameters such as the quality of reagents used.

The coupling of secondary anilines is generally considered complicated due to steric constraints.^[61] In addition, *N*-alkyl anilines are prone to β-hydride elimination and are less acidic.^[33] Preparation of tertiary diarylamines using transition metal catalysis is therefore an undeveloped area of interest.

II.1.2. Synthesis of diarylamines by Nucleophilic Aromatic Substitution

Diarylamines can be made by nucleophilic aromatic substitution (S_NAr) of a deprotonated aniline nucleophile onto an electrophilic aryl. This nucleophilic attack of the nitrogen-centred anion can displace the leaving group of an electron-deficient aromatic ring (Scheme 17, Nu = nucleophile).^[61,85] Good leaving groups for S_NAr include halogens (by order of nucleofugality F > Cl > Br > I), alkyl and aryl ethers, as well as mesylates.



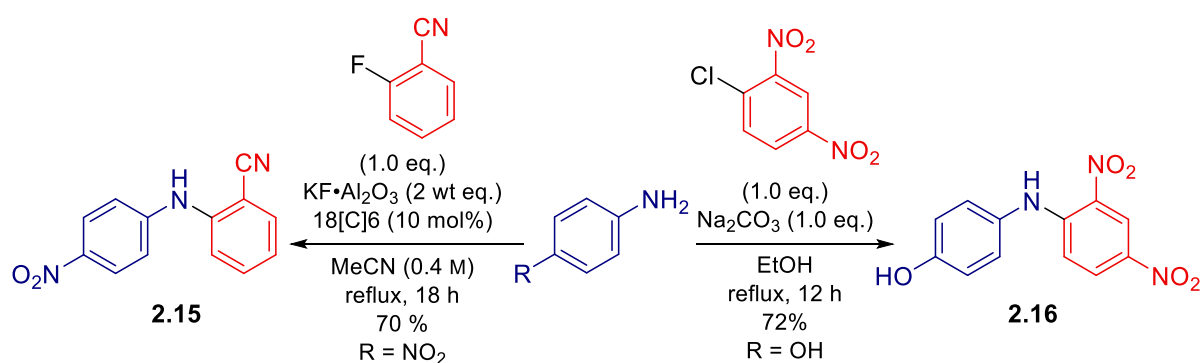
Scheme 17: General mechanism of the Nucleophilic Aromatic Substitution

The reaction generally proceeds through a stepwise addition of the nucleophile at the *ipso* position of the leaving group which results in a dearomatized intermediate, the Meisenheimer complex, carrying

a formal negative charge in a delocalised π -system.^[85] Rearomatisation of the intermediate by elimination of the leaving group at the newly formed sp^3 carbon yields the product of substitution. Thus, a common requirement for S_NAr to proceed is the activation of the electrophilic ring by strongly electron-withdrawing groups such as nitro at the *ortho*- and/or *para*-position to activate the electrophile, or through inherent electron-deficiency of certain heterocycles.^[85] However, recent work by Jacobsen *et al.* suggests that S_NAr reactions can go through a concerted mechanism depending on the nature of the leaving group, as well as the electron density of the electrophilic arene.^[86]

Anilines are common nucleophiles in S_NAr reactions, even though their low basicity results in relatively poor nucleophilicity, therefore limiting their application.^[61] Nevertheless, many groups have developed efficient methodologies to use deprotonated anilines in the synthesis of diarylamines by S_NAr , mostly involving primary anilines as a nucleophile. While secondary amines are more nucleophilic than related primary amines in the aliphatic series, *N*-substituted anilines have a tendency to be less nucleophilic and react with slower rate than comparable primary anilines, mostly because of increased steric hindrance around the nucleophilic nitrogen atom.^[87]

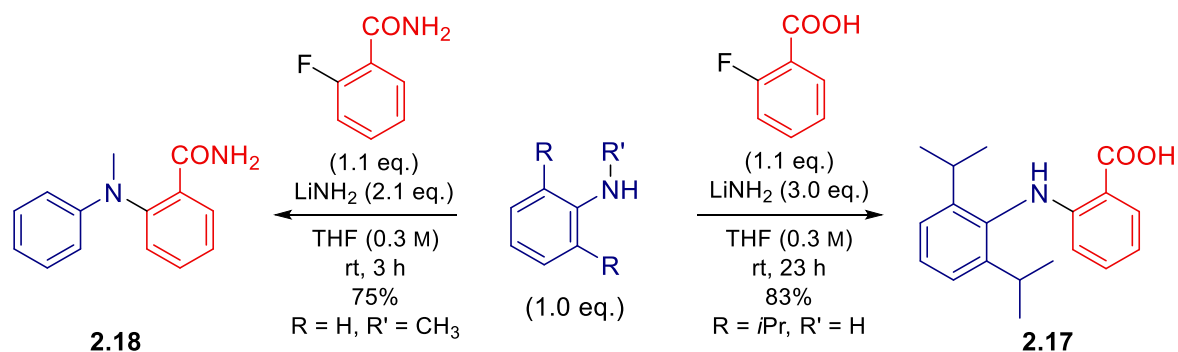
Various classes of synthetically relevant diarylamines were made by S_NAr of anilines on electrophilic arenes (Scheme 18). Addition of an electron-poor aniline to cyano-substituted aryl fluorides was possible under basic conditions, although the reaction was more sluggish than using phenol nucleophiles.^[88] Substitution on *ortho*-nitrated aryl rings allowed the formation of diarylamine **2.16**, an intermediate for the synthesis of carbazoles derived from natural products.^[89]



Scheme 18: Diarylamines made by S_NAr ^[88,89]

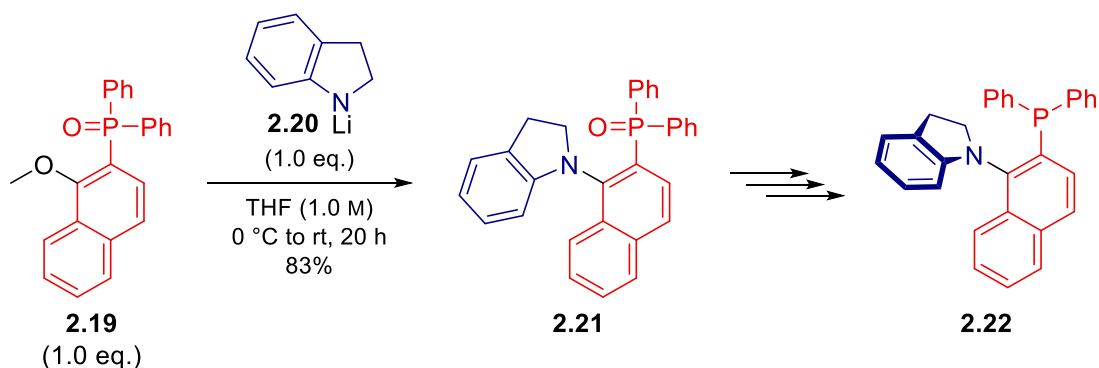
Researchers at Pfizer USA reported the coupling of anilines with 2-fluorobenzoic acid and amide derivatives. The reaction proceeded with the use of an excess of lithium amide ($LiNH_2$) as a base at room temperature (Scheme 19).^[90] The reaction tolerated primary anilines with a high degree of steric hindrance such as 2,6-diisopropylaniline, giving diarylamine **2.17** in good yield after 23 hours. While electron-rich anilines coupled smoothly, electron-withdrawing groups were detrimental to the

reaction. *N*-substitution, as well as the use of amide moiety was tolerated, although without any steric hindrance in the substrate.



Scheme 19: *N*-aryl anthranilamides made by S_NAr^[90]

Mino and co-workers demonstrated the applicability of S_NAr to the synthesis of axially chiral ligands such as **2.22** (Scheme 20). The ingenious use of an electron-withdrawing phosphine oxide as an activating group allows the attack of lithium indolate to aryl methyl ether **2.19**.^[91] Further reduction and resolution provided series of novel axially chiral ligands for palladium-catalysed asymmetric allylic alkylation.



Scheme 20: Chiral palladium ligand made by S_NAr^[91]

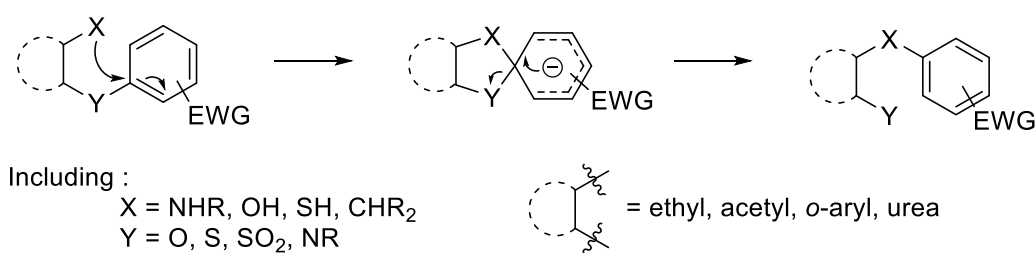
One feature of this last reaction is the relatively large steric hindrance of the product and substrates. The electrophile ring bears two *ortho*-substituents – a quaternary phosphine and an unsaturated ring – whereas the nucleophile is a secondary aniline with one *ortho*-substituent. Although S_NAr has not been widely applied in the synthesis of sterically hindered diarylamines, the relative tolerance for steric demand of this reaction makes it a good candidate for the development of novel, general methods.

After Zollinger's exploratory work on the influence of steric hindrance on the rate of addition of various anilines to activated electrophiles, the Crampton group thoroughly described the key steric parameters dictating their reactivity.^[87,92–94] Addition of aniline and *N*-methyl aniline to poly-nitro-substituted aryl chlorides showed great discrepancies in the rate of substitution depending on the

substituent on the nitrogen. As these two amines have similar pKa in water (4.60 and 4.84, respectively), Zollinger hypothesised the difference in rate of addition is mostly due to the increase of steric demand around the nucleophilic centre. Indeed, as the degree of substitution on the electrophile increases, the ratio of addition rate of aniline over *N*-methyl aniline increases drastically. However, as the entropy of activation was constant for all electrophiles tested, the authors demonstrated that steric hindrance at the electrophilic species was not interfering with the formation of the dearomatized intermediate. In fact, a more electron-withdrawing groups at the *ortho*-position of the reactive carbon increases the rate of addition by a fourfold.

II.1.3. Synthesis of diarylamines by Smiles rearrangement

The Smiles rearrangement is the intramolecular displacement of an aromatic ring by a nucleophilic species to deliver a 1,4- or a 1,5-migration (Scheme 21).^[95] The mechanism generally involves a Meisenheimer intermediate and the reaction is efficient for the migration of electron-deficient rings, and can be seen as an intramolecular S_NAr reaction. However, some examples in the literature suggested that conformational preorganization of the substrate may promote intramolecular S_NAr reactions of even neutral or electron-rich rings,^[96] making the Smiles rearrangement advantageous over intermolecular S_NAr reaction.

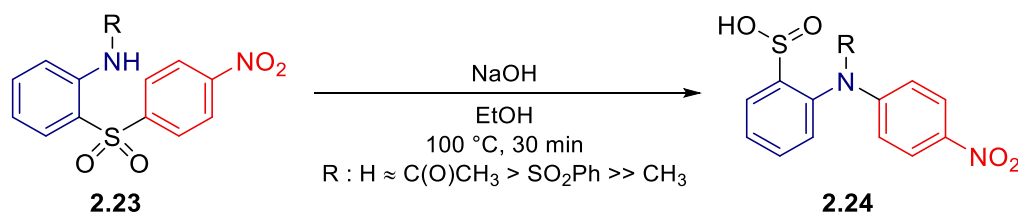


Scheme 21 : General overview of the Smiles rearrangement

The Smiles rearrangement has been used in the synthesis of both aryl amines and diarylamines by aryl transfer from easily prepared substrates, either by 1,4-migration of functionalised diaryl heteroatom-species with a free nitrogen at one *ortho* position (Schemes 22 and 23), or through a flexible linker (Scheme 24).

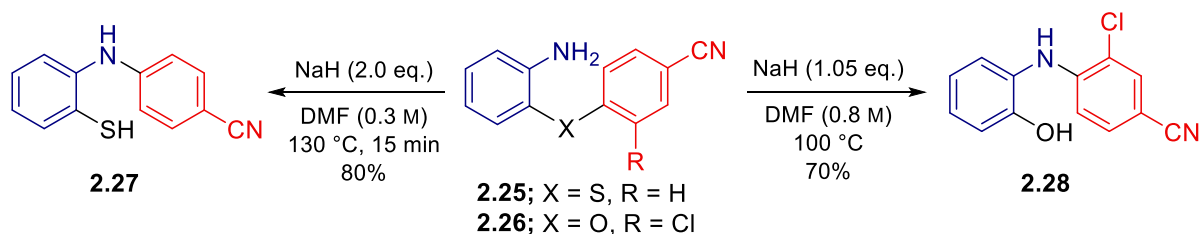
Smiles himself studied the formation of diarylamines by migration of 2-amino diarylsulfones **2.23** (Scheme 22).^[97] Although neither yields of pure products nor accurate protocols were reported, the important effect of the nucleophilicity of the nitrogen atoms was noted. While diarylsulfides did not undergo reaction under the reported conditions, diarylamine **2.24** was formed with a sulfinic acid group by migration of a nitro-substituted ring. By changing substitution pattern of the nucleophilic nitrogen, the author showed that acetylation of the nitrogen did not hamper rearrangement, while

sulfonylation slowed down the reaction, showing the impact of electron-density of the nucleophilic atom. *N*-methylation stopped the reaction and required increased concentration of base.



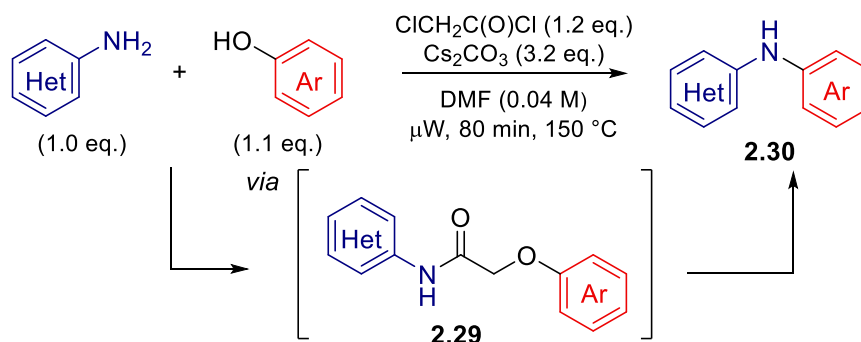
Scheme 22: 1,4-Smiles rearrangement of diaryl sulfones^[97]

Sulfones are not the only suitable leaving group. Vierfon *et al.* found that under basic treatment in DMF, diarylsulphide **2.25** rearranged to its related diarylamine,^[98] a substrate for the synthesis of phenothiazines (Scheme 23). Similarly, diaryl ethers such as **2.26** can be converted to their related diarylamine *en route* to medicinally relevant phenoxazines.^[99]



Scheme 23: Smiles rearrangement of diaryl ethers and diaryl sulfides^[98,99]

A recent method to synthesise diarylamines by Smiles rearrangement was developed by Wadia *et al.*, where deprotonated anilides with an electron-deficient α -aryloxy group such as **2.29** rearranged with displacement of the oxygen tethered aryl ring to the deprotonated nitrogen by *O*-to-*N* migration (Scheme 24).^[100] Zuo *et al.* improved this reaction by optimising a one-pot anilide formation/Smiles rearrangement /decarbonylation to form secondary diarylamines **2.30** from a phenol, an aniline and chloroacetyl chloride.^[101–103]



Scheme 24: Using a flexible, traceless for the Smiles rearrangement of diarylamines^[102]

Although the reaction requires microwave heating, this process is particularly efficient considering the number of single steps. The authors also developed the scope of the reaction to include electron-rich migrating rings, avoiding the need for an electronic activation of the substrate.

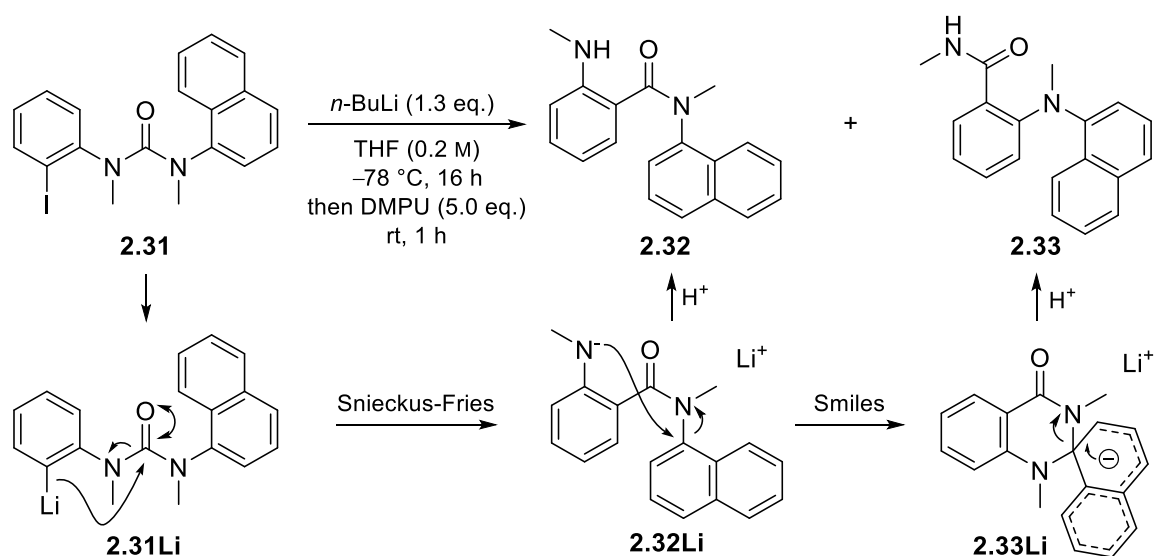
Insight on the particular effect of conformation on scope of ring migration was discussed by Bunnett and Maisey.^[104,105] Bulky substituents in proximity of the reactive species were found to accelerate Smiles rearrangement in phenols.^[104] Similarly, torsion of the starting material by Thorpe-Ingold effect can lead to migration of otherwise unreactive substrates.^[105]

While only a few examples of synthesis of diarylamines using the Smiles rearrangement can be found in the literature, the wide range of leaving groups tolerated makes this reaction promising (Schemes 22–24). Another attractive feature is the insensitivity to the steric hindrance of the coupling partners, suggesting that the Smiles rearrangement would be an ideal method for the synthesis of functionalised, sterically congested, atropisomeric diarylamines. In particular, recent progress has been made in the design of substrates allowing unconventional S_NAr -like reactivity on unactivated or even deactivated ring by conformational predisposition of the intermediate.^[106]

II.2. Results and Discussion

II.2.1. Initial discovery

An original *N*-to-*N'* aryl migration of anthranilamide **2.32** to the corresponding diarylamine **2.33** was discovered after the observation of co-workers Johnathan Matlock and George Whitcombe that *ortho*-lithiated *N,N'*-diarylurea **2.31** fully converts to a mixture of anthranilamide **2.32** and diarylamine **2.33** (Scheme 25). Two separate reactions were taking place. First, the carbanion generated by lithium-halogen exchange of the urea undergoes intramolecular attack of the urea carbonyl with cleavage of the related urea C–N bond to form anthranilamide **2.32Li** by an anionic Snieckus–Fries rearrangement.^[107] Then, the lithium amide generated through this rearrangement adds on the *ipso* carbon of the distal aryl ring by Smiles rearrangement, and forms diarylamine **2.33Li** after C–N bond cleavage. Conveniently, while the first step occurs at –78 °C, the *N*-to-*N'* aryl migration does not proceed at cryogenic temperatures, meaning that both steps can be optimised separately. Intriguingly, the reaction was discovered with a substrate that is not electronically set up favourably for a S_NAr reaction.



Scheme 25: Original discovery

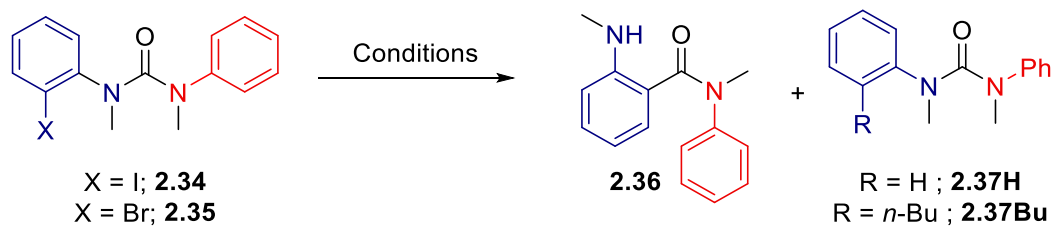
We therefore decided to investigate this reactivity, hoping that its lack of requisite for electronic bias would allow the synthesis of non-activated, bulky, and potentially atropisomeric diarylamines. Furthermore, this methodology would allow the transition metal-free synthesis of *N*-aryl anthranilic acid derivatives, a class of compounds marketed as anti-inflammatory agents for the treatment of rheumatic pain or dysmenorrhea^[108] which also showed positive results in the treatment of cancer and Alzheimer disease.^[109,110]

II.2.2. Development of the rearrangement

Optimisation of the Snieckus–Fries rearrangement

Optimisation of the first step, the anionic Snieckus–Fries rearrangement, was performed using electronically ureas **2.34** and **2.35** (Table 17). Their gram-scale synthesis was achieved by coupling of 2-halo-aniline with phenyl isocyanate followed by bis-methylation of the free nitrogen atoms with methyl iodide.

Two side-products arose from the common intermediate depending on the operating conditions. Quenching of the carbanion formed by lithium-halogen exchange before full conversion to the rearranged product led to the formation of *N,N'*-dimethyl-*N,N'*-diphenyl urea **2.37H**. When increasing the temperature to $-40\text{ }^{\circ}\text{C}$, alkylation of the lithiated starting material was observed, forming **2.37Bu**. Unfortunately, while the former side-product co-eluted during silica flash chromatography with the substrate, the later co-eluted with the product.



Entry	X	Base (eq.)	Solvent	<i>t</i> (h)	<i>T</i> (°C)	2.36 (%) ^a	2.37H (%) ^a
1	I	<i>n</i> -BuLi (1.1)	THF	16	−78	75	13
2	I	<i>n</i> -BuLi (1.3)	THF	16	−78	60	17
3	I	<i>n</i> -BuLi (1.5)	THF	16	−78	62	25
4	I	<i>n</i> -BuLi (1.1)	THF	2	−78	71	18
5	I	<i>n</i> -BuLi (1.1)	THF	24	−78	77	18
6	I	<i>n</i> -BuLi (1.1)	Et ₂ O	2	−78	10	73
7	I	<i>n</i> -BuLi (1.1)	MTBE	2	−78	12	73
8 ^b	I	<i>n</i> -BuLi (1.1)	THF	2	−40	36	26
9	I	<i>s</i> -BuLi (1.1)	THF	2	−78	63	18
10 ^c	I	<i>n</i> -BuLi (1.1)	THF	2	−78	67	22
11	Br	<i>n</i>-BuLi (1.1)	THF	2	−78	77	4
12 ^b	Br	<i>n</i> -BuLi (1.1)	THF	2	−40	56	8

To a solution of **2.34** or **2.35** (0.15 mmol, 1.0 eq.) in solvent (0.2 M) was slowly added *n*-BuLi (1.44 M in hexanes) or *s*-BuLi (1.06 M in cyclohexane) at −78 °C. The reaction was stirred at the stated temperature and quenched with MeOH.

^a ¹H NMR yields were calculated from the crude reaction mixture using 1,3,5-trimethoxybenzene as the internal standard.

^b Formation of **2.37Bu**. ^c LiCl (3.0 eq.) used as an additive.

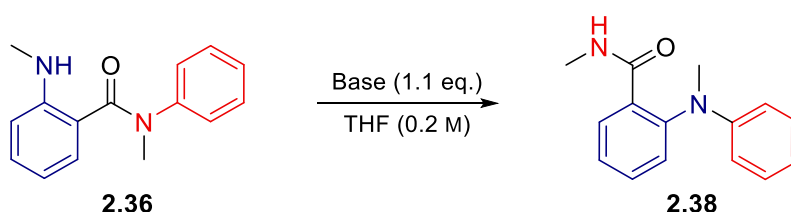
Table 17: Optimisation of the Snieckus-Fries rearrangement

Lower yield of **2.36** was observed when using an excess of the organometallic base after an overnight reaction (entries 2 and 3). When using only a slight excess of base, the reaction seemed to be complete within two hours (entry 4), but no decomposition was observed after prolonged exposure to the reaction conditions (entry 5). Apolar solvents such as diethyl ether and methyl *tert*-butyl ether (MTBE) drastically slowed down the reactivity and raising the temperature to −40 °C led to the formation of **2.37Bu**. Changing the base to *sec*-BuLi or using lithium chloride as an additive did not improve the reaction. Previous work by George Whitcombe and Johnathan Matlock also showed that addition of DMPU to the reaction mixture halts the rearrangement. Similar yields were obtained with bromo analogue **2.35**, and it was decided to pursue the scope with brominated ureas.

Optimisation of the Smiles rearrangement

Model substrate **2.36** was subjected to a range of conditions shown in Table 18. The Smiles rearrangement to form diarylamine **2.38** was confirmed by HMBC correlations, along with the appearance of the $^3J_{\text{NH-CH}}$ coupling in the amide group.

Following the reaction conditions used in the previous step, *n*-BuLi was first tested as a base to promote rearrangement. No conversion was observed after 3 hours at room temperature in the absence of additive. Addition of 5 equivalents of DMPU to the reaction mixture promoted the reaction at room temperature. However, in these conditions, reproducibility of the experiment was unreliable (entries 2 to 4) and another unidentified compound was produced.



Entry	Base	<i>t</i> (h)	<i>T</i> (°C)	Conversion (%) ^a	2.38 (%) ^a
1	<i>n</i> -BuLi ^b	3	0	0	0
2	<i>n</i> -BuLi ^b + DMPU (5.0 eq.) ^b	3	rt	54	37
3	<i>n</i> -BuLi ^b + DMPU (5.0 eq.) ^c	3	rt	79	62
4	<i>n</i> -BuLi ^b + DMPU (5.0 eq.) ^d	3	rt	85	48
5	KOtBu ^d	2.5	rt	86	21
6	Cs ₂ CO ₃ ^{d, e}	16	80	44	19
7	KHMDS ^c	2.5	rt	>95	57
8	NaHMDS ^c	2.5	rt	>95	71
9	NaHMDS^d	4	rt	>95	86^f
10	LiHMDS ^c	4	rt	25	6
11	LiHMDS ^c	16	reflux	>95	70
12	LiHMDS ^l + DMPU (5.0 eq.) ^d	4	rt	>95	83

To a solution of **2.36** (0.2 mmol, 1.0 eq.) in THF (0.2 M) was slowly added a base. The reaction was stirred at the stated temperature and quenched with MeOH. Bases : *n*-BuLi (1.44 M in hexanes), NaHMDS, KHMDS and LiHMDS (1.0 M in THF).

^a ¹H NMR yields were calculated from the crude reaction mixture using 1,3,5-trimethoxybenzene as the internal standard.

^b Added at –78 °C. ^c Added at 0 °C. ^d Added at rt. ^l The solvent was DMF. ^f Isolated yield.

Table 18: Optimisation of the Smiles rearrangement

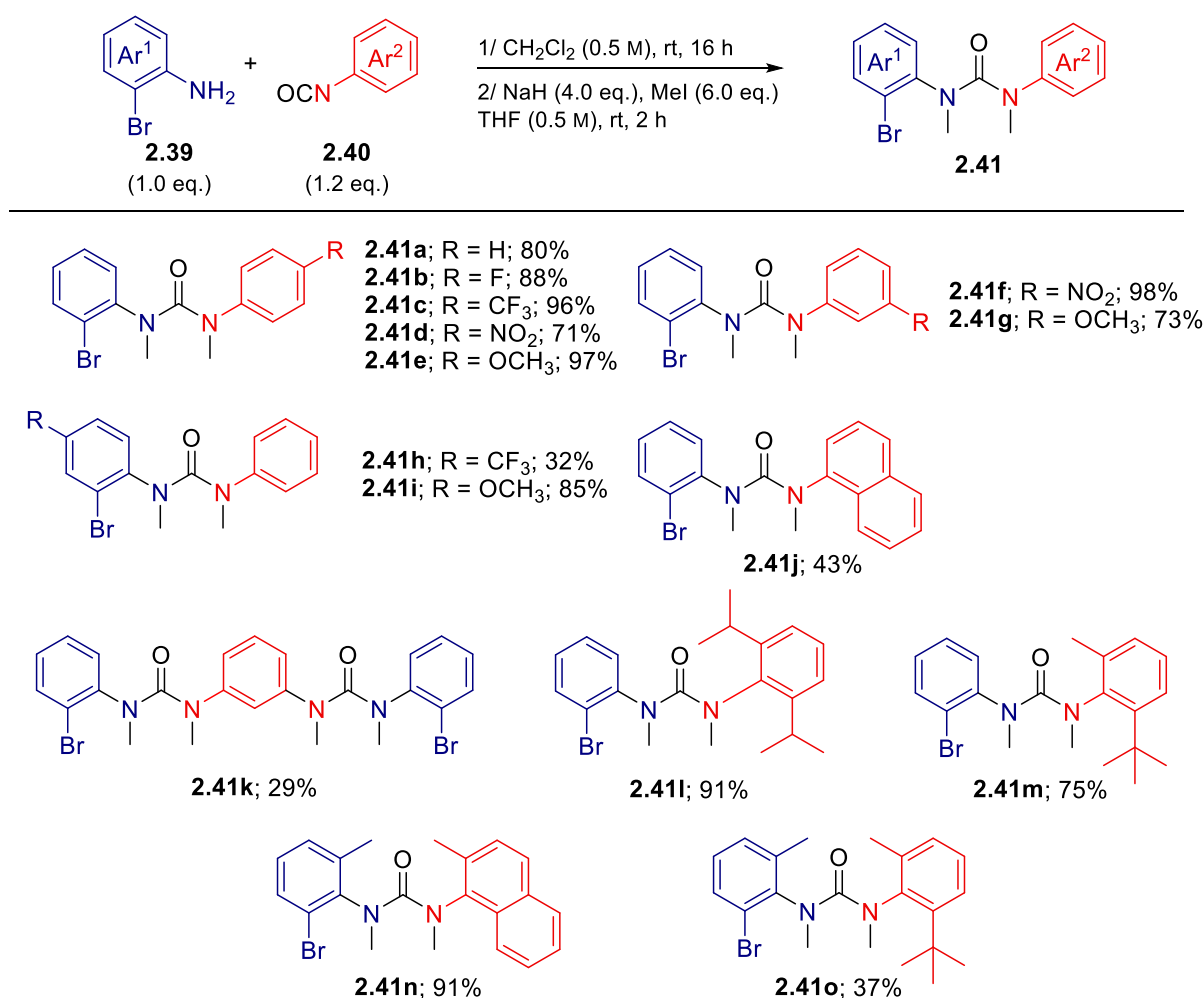
A change of the base and counter-cation proved to be critical for the reaction to proceed smoothly. The use of strong inorganic base KOtBu led to a complex mixture of products with decomposition of

the substrate (entry 5), and Cs_2CO_3 required DMF and heating to give conversion, although slow and low yielding (entry 6). Smiles rearrangement to diarylamine **2.38** was possible in good to excellent yields under several different sets of conditions, with sodium and potassium hexamethyldisilazide at room temperature providing the best yields of 86% (entry 4). The reaction proved to be reproducible with an excellent isolated yield of product upon scaling up to 6.0 mmol of substrate. LiHMDS required heating to reflux overnight or the addition of DMPU to promote the reaction at room temperature, showing the great impact of the nature of the counter-cation in this rearrangement (entries 10–12).

With conditions optimised, a set of diaryl ureas with electronically and sterically diverse rings were synthesised to probe the scope and limitations of both the Snieckus-Fries and Smiles rearrangement.

Synthesis of the starting materials

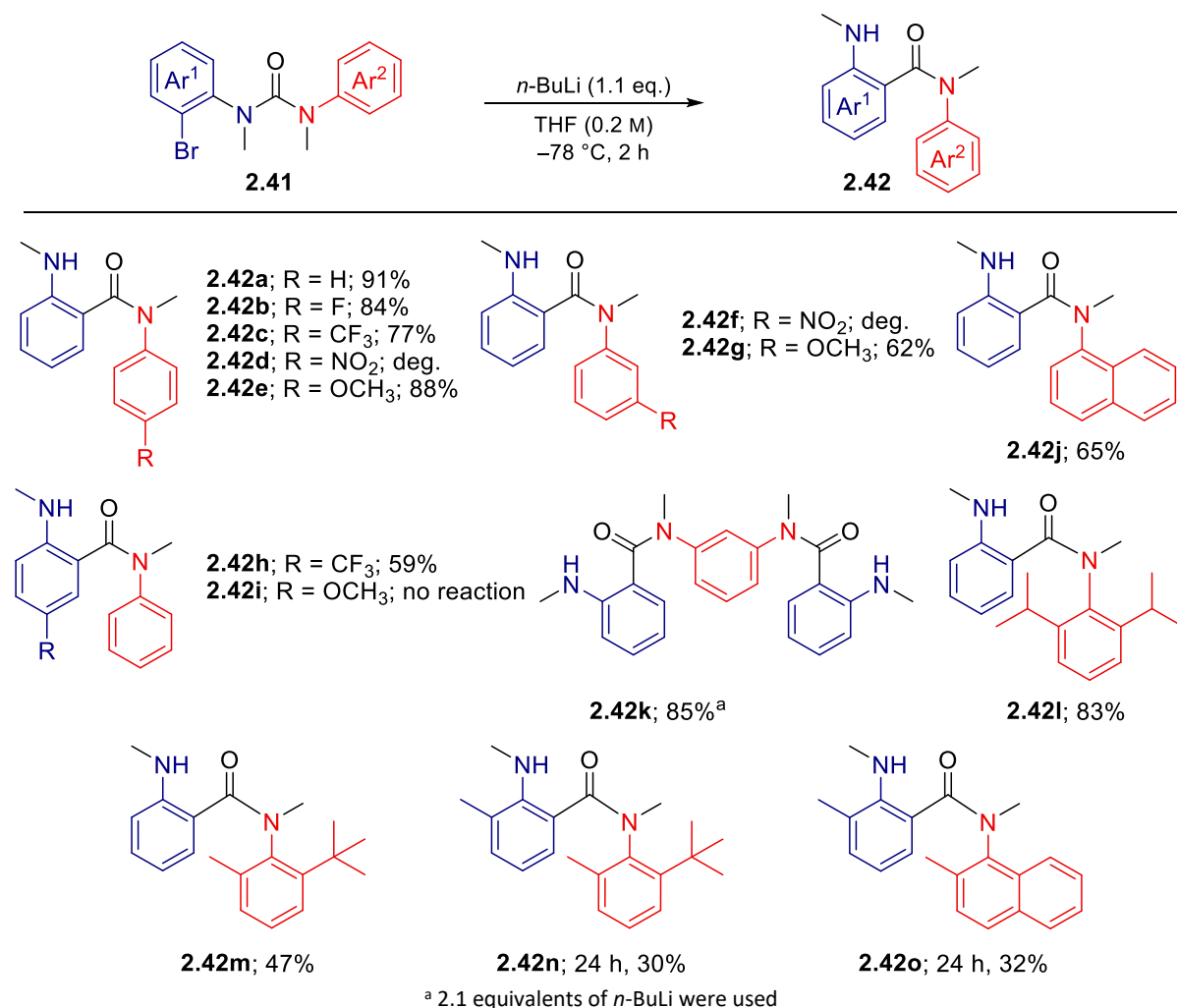
The various diaryl ureas were synthesised according to previously described procedures (Scheme 26).^[111] Condensation of 2-bromoaniline derivatives **2.39** with aryl isocyanates **2.40** in CH_2Cl_2 led to the precipitation of the corresponding urea. Filtration followed by bis-methylation of the crude product afforded diaryl ureas **2.41a–o** in moderate to excellent yield over two steps.



Scheme 26: Scope of the urea formation/methylation

The transformation was particularly robust, as excellent yields are obtained with electronically varied isocyanates (**2.41c** and **2.41e**). The nucleophilicity of the aniline, though, was critical for the urea formation, as addition of electron-deficient 2-bromo-4-trifluoromethylaniline formed urea **2.41h** in poor yield. The urea intermediate in the synthesis of **2.41k** was not alkylated under the standard conditions. Instead, the use of sodium hydroxide was a suitable alternative to obtain tetra-methylated urea **2.41k**. However, stability of either the substrate or the product in these conditions was not optimal, and the product obtained in poor yield despite full conversion of the substrate. Poly-*ortho*-substituted ureas **2.41l–n** with particularly hindered aryl rings reacted smoothly in excellent yields, while the formation **2.41o** proved to be more sluggish. The ^1H NMR spectra of these products showed significant line broadening presumably due to slow rotation of the $\text{C}_{\text{Ar}}\text{--N}$ bond.

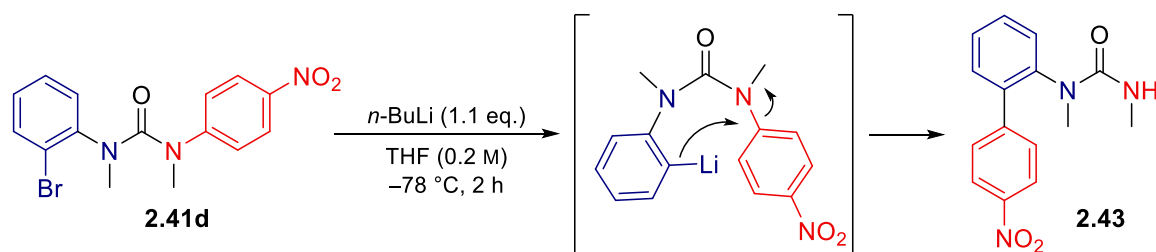
Using the previously optimised conditions for the Snieckus–Fries rearrangement, ureas **2.41** rearranged to their corresponding anthranilamide (Scheme 27). The Snieckus–Fries rearrangement proceeded with good functional group tolerance for both electron-withdrawing and -donating groups on the distal aryl ring.



Scheme 27: Scope of the Snieckus–Fries rearrangement

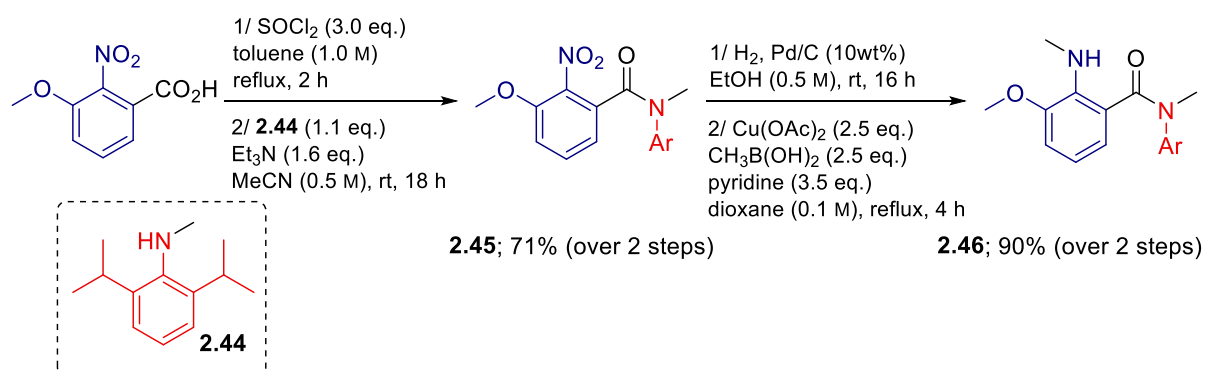
Substitution at the *meta*-position of this ring was tolerated for a methoxy group, but a nitro group led to decomposition of the starting material (**2.42f** and **2.42g**). Surprisingly, while decreasing electron density on the migrating ring with a CF₃ group did not influence rearrangement of **2.41h**, an electron-donating group at the same position halted the rearrangement to **2.42i**, yielding its protodehalogenated derivative quantitatively. Double migration of **2.41k** was tolerated as well, and moderate to excellent yields were observed for particularly sterically hindered substrates **2.42l–o**, with the need for longer reaction time.

While no anthranilamide was formed in the reaction of urea **2.41d**, biphenyl **2.43** was isolated (Scheme 28). This compound probably arises from an intramolecular S_NAr reaction of the carbanion on the *ipso* carbon of the distal ring, through a 6-membered intermediate. Surprisingly, no trace of biphenyl product was observed during the rearrangement of electron-deficient urea **2.41c**, showing the peculiar reactivity of the nitro derivative.



Scheme 28: Unexpected reactivity of the nitro-derived urea

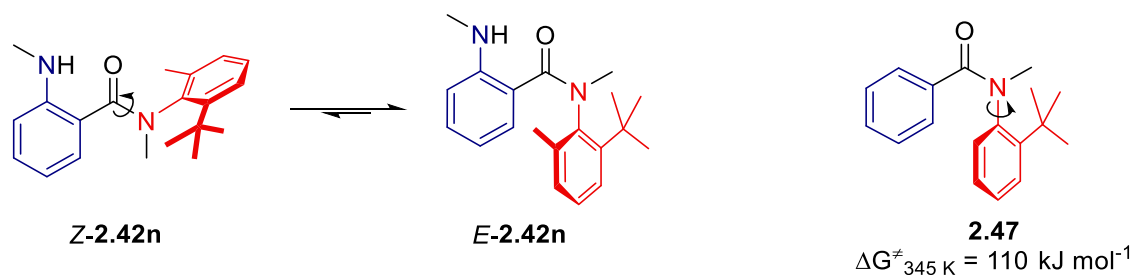
Poly-substituted anthranilamide **2.46**, bearing both sterically demanding substituents and an electron-donating methoxy group on the anthranilamide ring, was made from the corresponding anthranilic acid by an a less elegant but successful sequence composed of acyl chloride formation, amide coupling, hydrogenation of the nitro group and methylation of the aniline by Chan–Lam coupling with methyl boronic acid (Scheme 29).



Scheme 29: Synthesis of sterically congested anthranilamide **2.47**. Ar = 2,6-*i*PrPh

The ¹H NMR spectra of anthranilamides **2.42l–o** showed two sets of sharp, well resolved peaks. Steric demand on the amide aryl ring destabilises the preferred *E* amide conformer, and these substrates

exist as a pair of slowly interconverting conformers (Scheme 30). Anilides have been known to exhibit axial chirality, and a single *ortho-tert*-butyl group in related benzanilide **2.47** is sufficient to obtain atropisomerism, with a barrier to rotation around the C_{Ar}–N bond of 110 kJ mol^{–1} at 72 °C (Scheme 30).^[26] However, to the best of our knowledge, the barrier to rotation of the N–C(O) bond in tertiary benzanilides has not been reported yet. When triturating of **2.42n** in pentane, a white solid of the enriched Z rotamers (assigned by the downfield shift of the N–CH₃ singlet by ¹H NMR) was isolated and used to study to rate of N–C(O) bond rotation (Scheme 30).



Scheme 30 : Slow bond rotation in benzanilides

Following the interconversion of the rotamers at room temperature by ¹H NMR (Figure 14) in various solvents allowed the calculation of the forward and reverse rate of interconversion using the Equation 6, where R_0 , r_t and R_{eq} are the ratio of isomers at $t = 0$, at t , and at the equilibrium, respectively. Gibbs free energies of isomerisation were found using the Eyring equation (Equation 1) at 25 °C.^[112]

$$\ln\left(\frac{R_t - R_{eq}}{R_0 - R_{eq}}\right) = (k_{E \rightarrow Z} + k_{Z \rightarrow E}) * t$$

Equation 6: Calculation of the rates of exchange of diastereomers

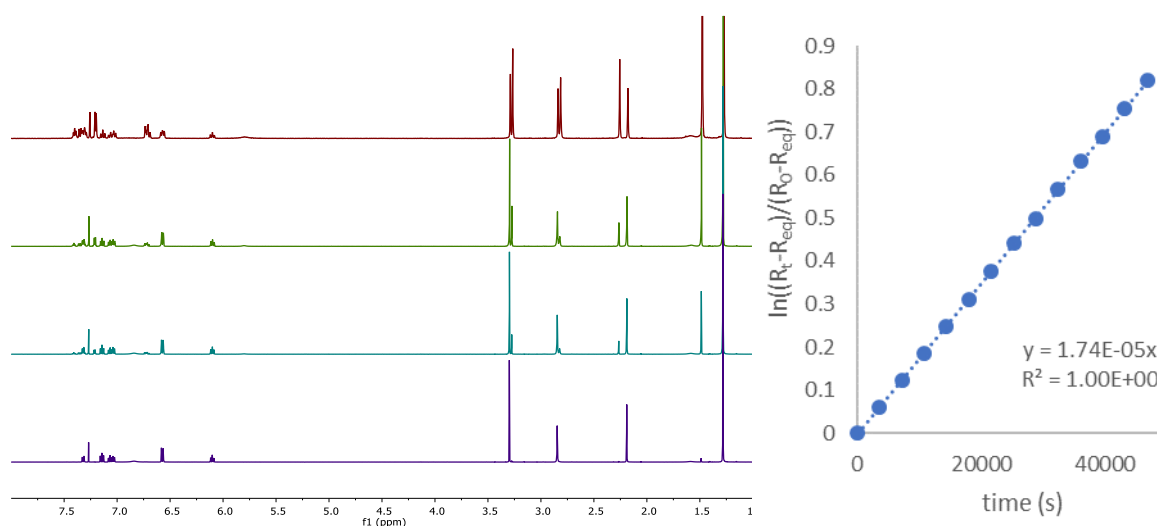


Figure 14 : Isomerisation of **2.42n** by ¹H NMR (bottom to top: t_0 , 5 h, 10 h, t_{eq}) and plot of its equilibration over the time

The C_{Ar}–N bond of **2.42n** was estimated to be stable enough not to interconvert at room temperature over the course of the experiment, as it is bulkier than in **2.47**. Also, the C_{Ar}–C(O) bond in mono-*ortho*-

substituted benzamides rotate at rates too high to be observed by this method.^[113] Hence, only rotation around the N–C(O) bond would be in the adequate range to be observed.

Over the course of 24 h, equilibrium was not reached. However, after only one hour, signals for the *E* isomer could be observed. Interestingly, while the *E* isomer was predominant in chloroform and methanol after equilibrium, the *Z* isomer was slightly in excess in toluene-*d*₈. Barriers to rotation around 100 kJ mol^{−1} were found in all solvents, making the amide bond of **2.42n** conformationally stable at room temperature. (Table 19)

Solvent	<i>E/Z</i> ratio	<i>k</i> _{Z-to-E} (s ^{−1})	<i>k</i> _{E-to-Z} (s ^{−1})	Δ <i>G</i> [‡] _{Z-to-E} (kJ mol ^{−1}) ^a	Δ <i>G</i> [‡] _{E-to-Z} (kJ mol ^{−1}) ^a
<i>CD</i> ₃ <i>OD</i>	1.7:1	5.22 10 ^{−6}	2.92 10 ^{−6}	102.1	102.8
<i>CDCl</i> ₃	1.7:1	1.02 10 ^{−5}	7.10 10 ^{−6}	101.4	102.3
<i>Toluene-d</i> ₈	1:1.1	2.94 10 ^{−5}	2.35 10 ^{−5}	98.8	98.5

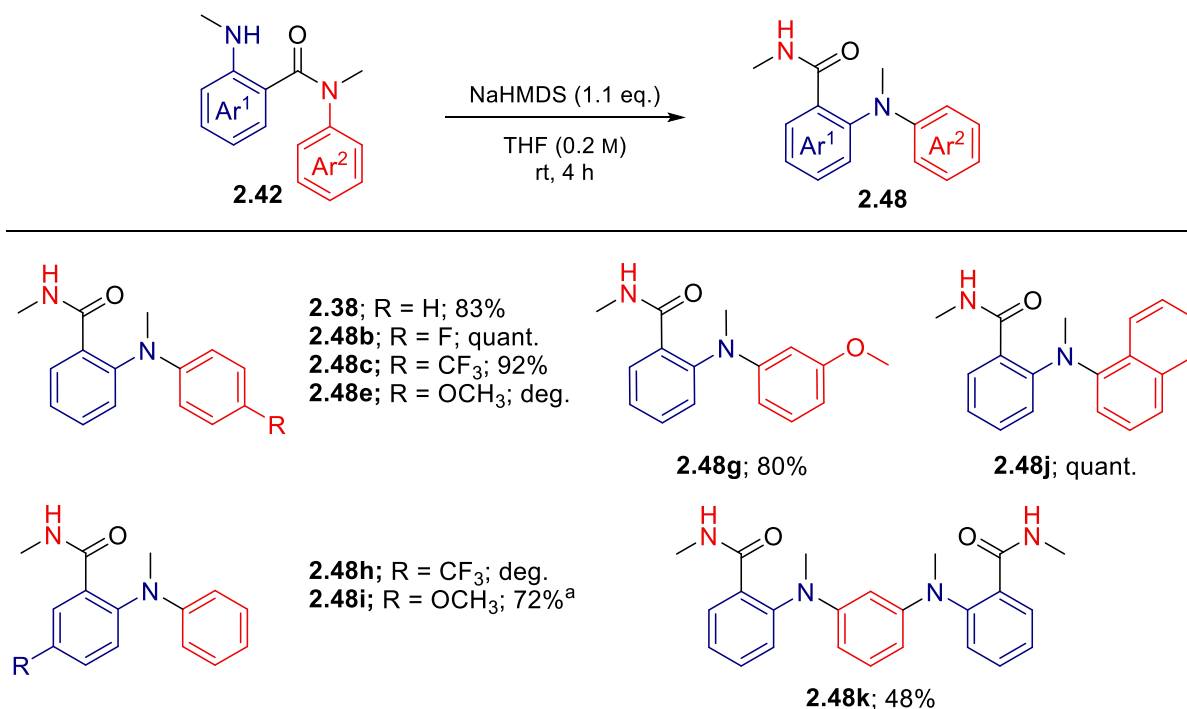
^a At 298 K.

Table 19 : Kinetic parameters of the *E/Z* isomerisation of **2.42n**

Scope of the Smiles rearrangement

The Smiles rearrangement of anthranilamides is notable by the nature of its amide leaving group. Typical Smiles rearrangement occur with an oxygen- or sulfur-based leaving group.^[85,95] Also, the insensitivity of this reaction to the electronic nature of the migrating ring turned out to be general (Scheme 31). This might be because of the preferred *cis* conformation of *N*-methylated benzanilides,^[114–117] where torsion of the C_{Ar}–N bond forces deconjugation with the amide group and places the aryl ring into close proximity with the nucleophile.

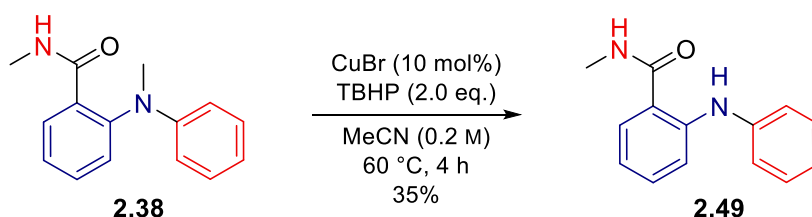
Excellent to quantitative yields of diarylamines were obtained for a range of substrates **2.48a–k** whether the migrating ring was electron-deficient such as **2.48c** or electron-rich such as **2.48l**. When migrating the *para*-methoxyphenyl ring of anthranilamide **2.42e**, hydrolysis of the amide group yielded decomposition products. Of more importance were the electronic properties of the nitrogen nucleophile. While the rearrangement proceeded in excellent yield with electron-rich aniline **2.42i**, decreasing its electron-density with a *para*-trifluoromethyl group led to decomposition of the starting material to multiple unidentified side-products. Double Smiles rearrangement of **2.42k** was used to prepare **2.48k** in good yield.



^a Compound prepared by Johnathan Matlock.

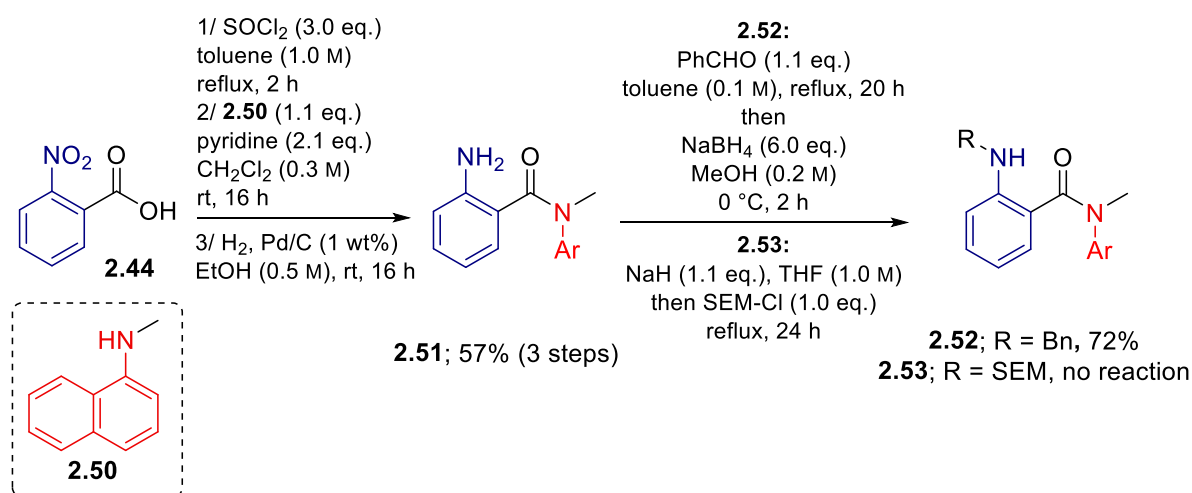
Scheme 31: Scope of the Smiles rearrangement

The anthranilamides studied had a methyl group at the nucleophilic nitrogen and were therefore only applicable to preparing tertiary amines. Synthetic methodologies for the *N*-demethylation of aniline are scarce,^[118–120] and even more so for diarylamines. Test reactions to ‘deprotect’ compound **2.48a** were not promising, and the best results were obtained using a procedure by Tang and Jiao^[121] for the demethylation of *N*-methyl-*N,N*-diphenylamine under oxidative conditions. Using their conditions on substrate **2.48a** led to the isolation of secondary diarylamine **2.49** in moderate yield (Scheme 32). Optimization did not succeed, as the results were difficult to reproduce.



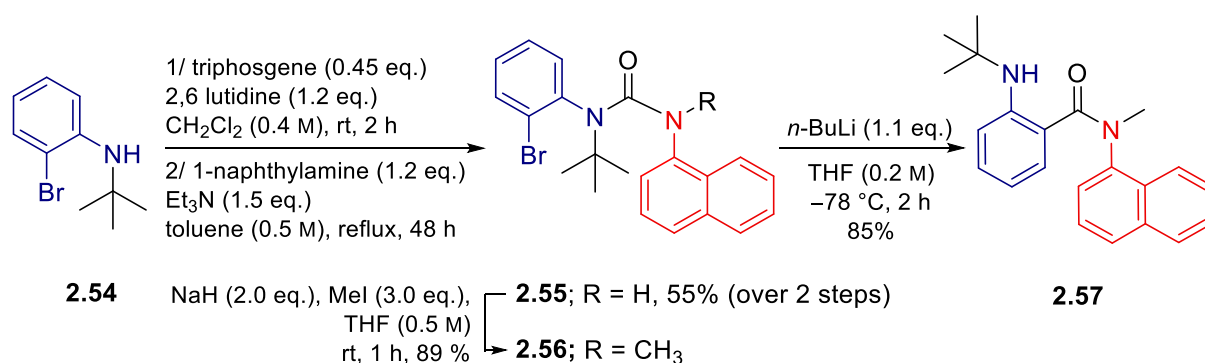
Scheme 32: Demethylation of the Smiles product

The scope of substituents on the nucleophilic nitrogen was then investigated. Condensation of the acyl chloride with *N*-methyl-1-naphthylamine **2.50** followed by hydrogenation gave anthranilamide **2.51** in good yield over three steps. Installation of a benzyl group was possible by reductive amination of benzaldehyde, while introduction of a protecting SEM (2-(trimethylsilyl)ethoxymethyl) group to form **2.53** through alkylation under basic conditions proved unsuccessful (Scheme 33).



Scheme 33: Introducing protecting groups in the anthranilamide starting material. Ar = 1-naphthyl

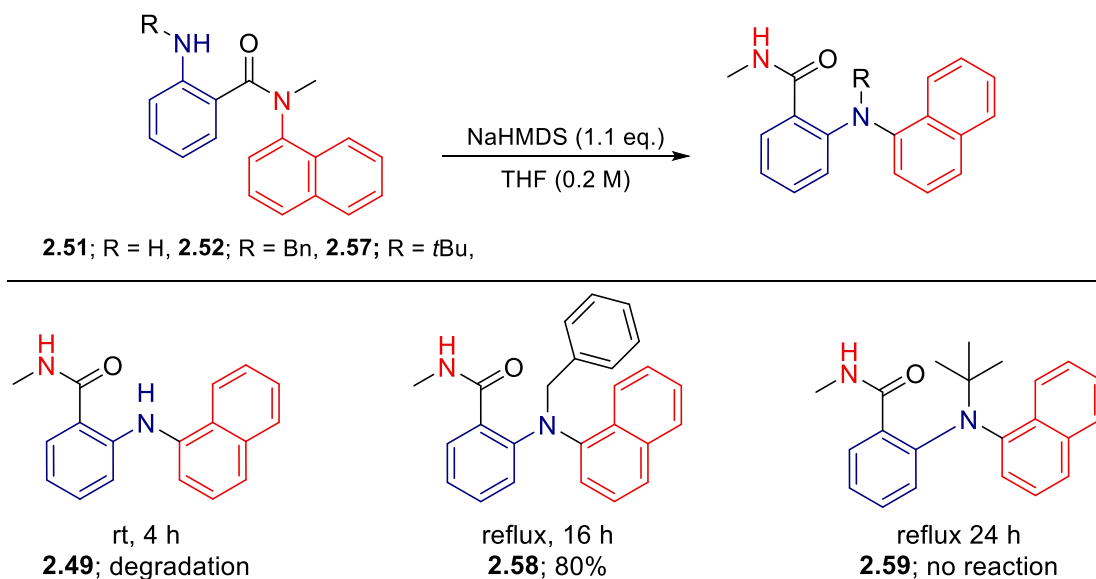
Introduction of highly bulky *tert*-butyl group on the nucleophilic nitrogen was also possible, although another route had to be used. Addition of *tert*-butyl amine nucleophile on an *ortho*-fluorinated benzanilide gave complex reaction mixtures, while amide bond formation on the acyl chloride of *N*-*tert*-butyl anthranilic acid did not provide any conversion. Instead, unsymmetrically substituted urea **2.56** was prepared by condensation of the carbamoyl chloride of aniline **2.54** with 1-naphthylamine, followed by *N*-methylation (Scheme 34). This three-step procedure was necessary as coupling of the same carbamoyl chloride with *N*-methyl-1-naphthylamine **2.50** was unsuccessful. Snieckus–Fries rearrangement of urea **2.56** cleanly afforded anthranilamide **2.57** in excellent yield.



Scheme 34: Route to the *N*-*tert*-butyl anthranilamide starting material

The primary aniline **2.51** did not rearrange to product **2.49** (Scheme 35). Instead, an intermolecular transamidation product was formed in approximately 50% conversion of the substrate, and no improvement was observed when using an excess of base or increasing reaction time. Attempt to *in situ* protect the nitrogen with trimethylsilyl chloride, followed by a second deprotonation and an acidic workup did not yield any product. Changing the nitrogen substituent to a benzyl group in **2.52** required longer reaction time and heating to reflux but resulted **2.58** in excellent yield. Hydrogenolysis of **2.58** afforded secondary amine **2.49** in good yield. Increasing the steric hindrance further hampered the

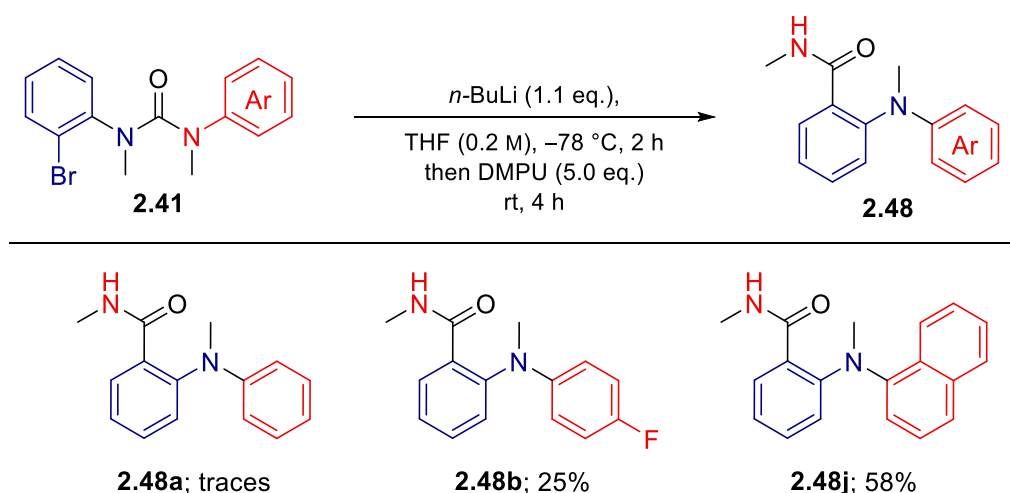
reaction, as subjecting **2.57** to the reaction conditions at reflux temperature for 24 hours left the substrate untouched.



Scheme 35: Scope of *N*-substitution for the Smiles rearrangement

One-pot reaction

The conversion of anthranilamide **2.37** to diarylamine **2.38** using *n*-BuLi with DMPU raised the possibility of using both the anionic Snieckus–Fries and Smiles rearrangements in tandem to form diarylamines from *N,N'*-diaryl ureas (Scheme 36). However, this approach was not optimal: **2.48j** was synthesised in 58% yield upon treatment of **2.41j** with *n*-BuLi at $-78\text{ }^{\circ}\text{C}$ followed by addition of DMPU (5 equivalents, warming to room temperature), while under similar conditions, **2.48b** was formed in 25% yield and **2.48a** only in trace quantities.



Scheme 36: One-pot Snieckus-Fries/Smiles of 2-bromo-*N,N'*-diaryl ureas

II.2.3. Mechanism of the transformation

While the rearrangement proceeded smoothly with sodium and potassium bases, optimisation of the reaction showed that the use of lithium as a counter-cation halted the reaction. The need for a non-coordinative additive such as DMPU or increased temperature for the rearrangement to take place indicated that the nature of the cation plays a role in the aryl migration. Work was conducted by Harvey Dale and Natalie Fey at the University of Bristol to explore possible reaction pathways computationally, using density functional theory (DFT), by comparison of the computed pathways for the rearrangement of deprotonated **2.42a** to **2.48a** mediated by either a lithium or sodium counter-cation coordinated to molecules of THF solvent.

For a lithium counter-cation, a stable complex was found for the deprotonated substrate, with chelation of lithium by the carbonyl and the deprotonated nitrogen (Figure 15). In comparison, the final product was thermodynamically less favourable by around 5 kJ mol⁻¹. The reaction proceeds by concerted migration of the aryl group with a high energy of the single transition state of around 121 kJ mol⁻¹ relative to the deprotonated starting material, where the *ipso* carbon gains a strong tetrahedral character. The typical Meisenheimer complex observed in usual Smiles rearrangement was not found for this pathway.^[86,96,122]

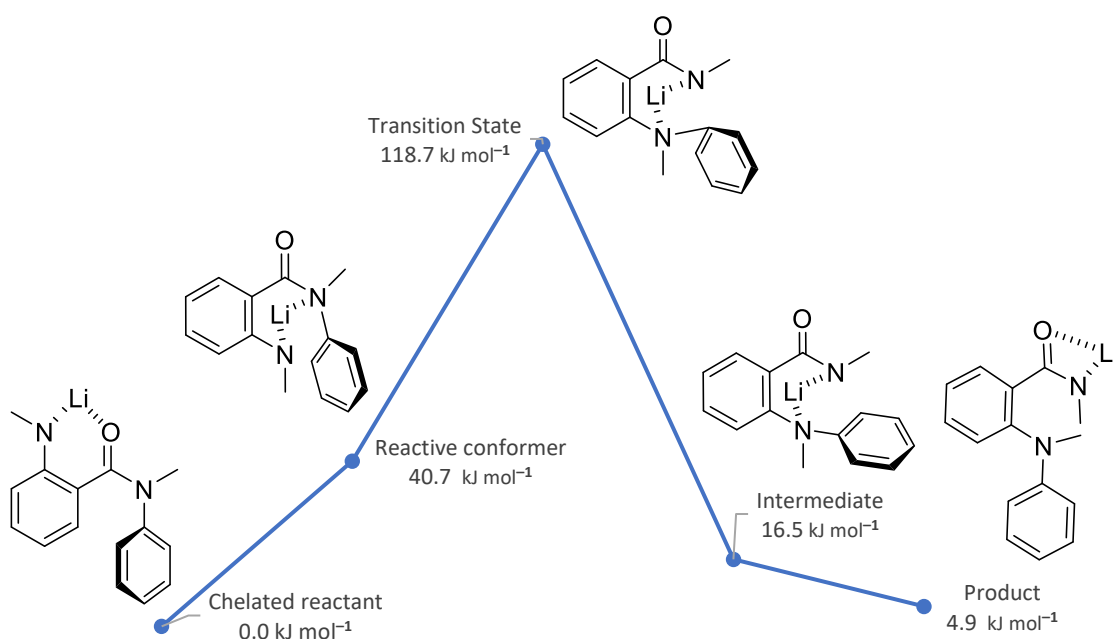


Figure 15 : Mechanism with a lithium counter-cation. DFT calculations performed by Harvey Dale and Natalie Fey

Using a sodium counter-cation, a different reaction pathway was observed (Figure 16). The product was now thermodynamically favoured by around 17 kJ mol⁻¹. Coordination of the starting material to Na⁺ was weaker. The reaction proceeds in two steps, with an intermediate showing some characteristics of a Meisenheimer complex such as a delocalised negative charge on the migrating

ring. Despite the lack of anion-stabilising substituents, this intermediate is typical of a classical S_NAr reaction, with localized single bonds on the formed, tetrahedral sp^3 -carbon.

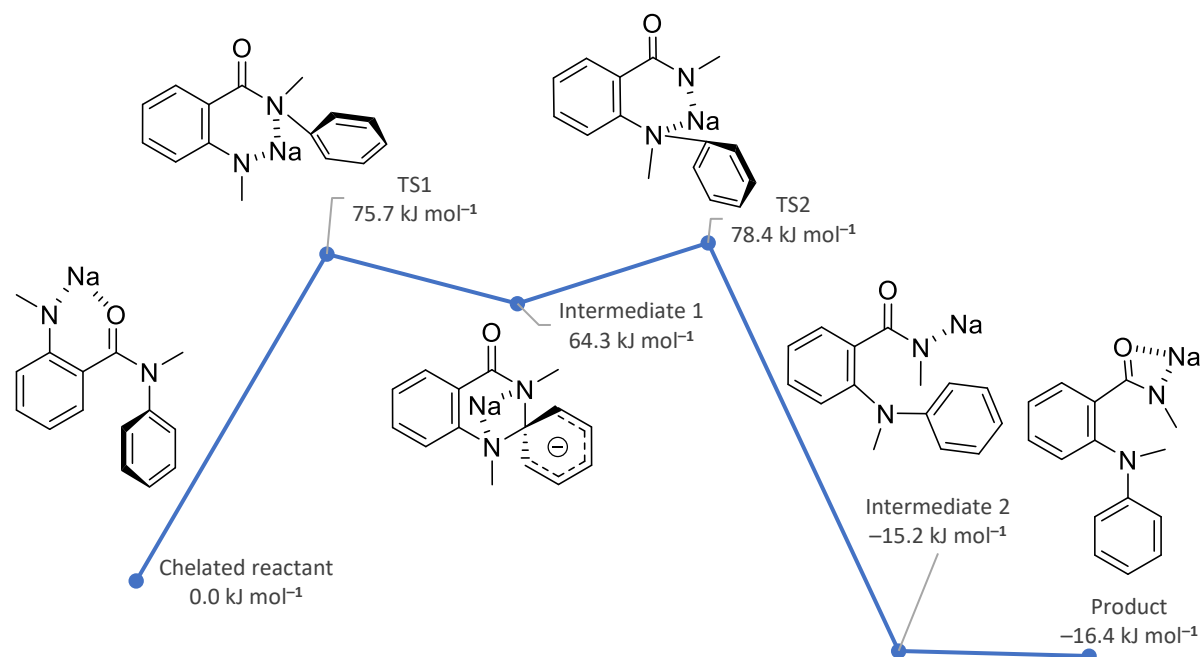
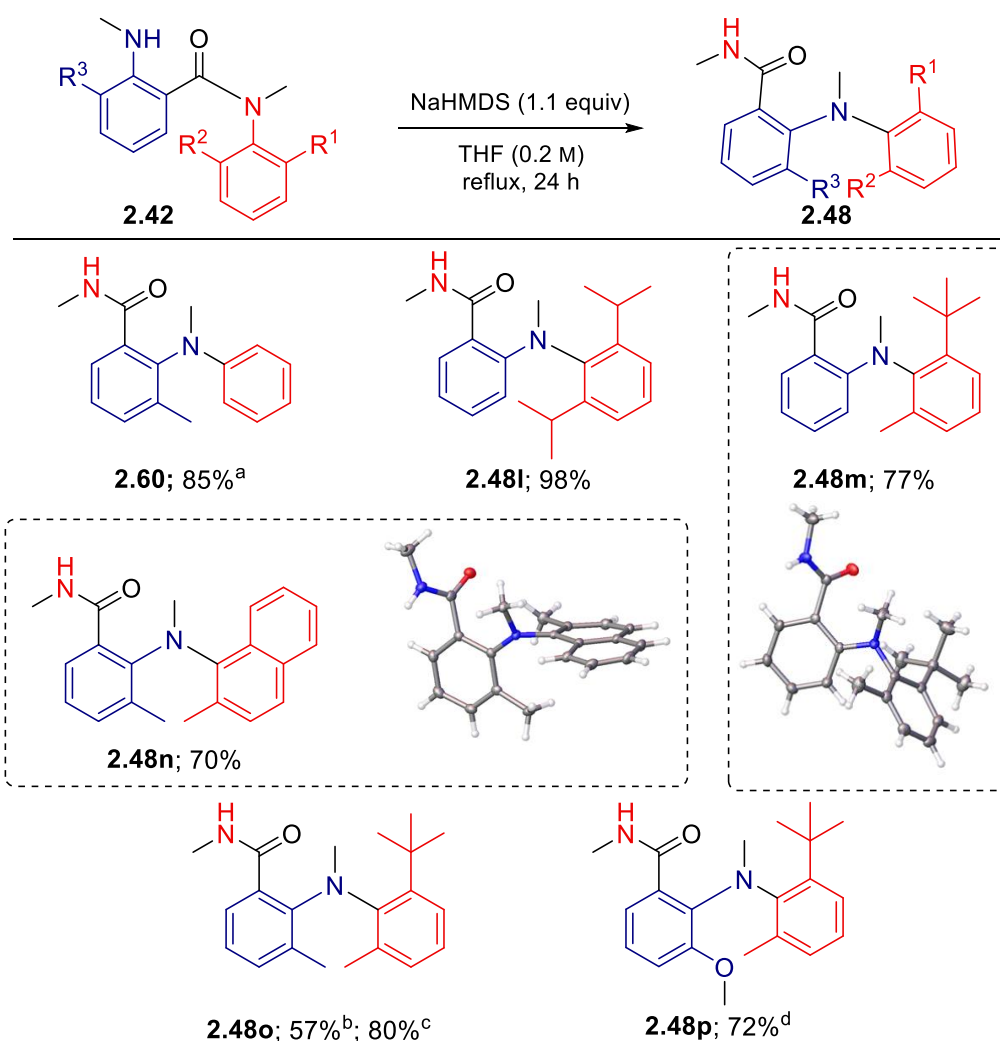


Figure 16 : Mechanism with a sodium counter-cation. DFT calculations performed by Harvey Dale and Natalie Fey

The lower stability of the chelated reactant, together with the existence of a low-energy intermediate explains the difference in reactivity observed for the rearrangement using NaHMDS, as opposed to the use of lithium bases.

II.2.4. Atropisomeric diarylamines by Smiles rearrangement

One key feature of the transformation was that sterically encumbered anthranilamides **2.42l–p** readily rearranged to diarylamines **2.48l–p** (Scheme 37) with high levels of steric demand around the central nitrogen atom. The reactions were slower and required heating (sometimes in a sealed tube) for extended period but provided the products in good to excellent yields. X-ray crystal structures of **2.48m** and **2.48n** showed bond angles around the central nitrogen atom of around 360°, indicating a planar nitrogen atom with its lone pair delocalized into the anthranilamide ring, as the other bulky aryl ring is perpendicular to the plane.



^a Compound prepared by Johnathan Matlock. ^b The reaction time was 96 h. ^c Based on recovered starting material.

^d Reaction performed in a microwave oven at 150 °C. The reaction time was 16 h.

Scheme 37: Scope of sterically hindered substrate for the Smiles rearrangement

The steric bulk around the central nitrogen atom of **2.48l–p** is comparable to that of related atropisomeric diarylamines described in Chapter 1 (with an additional substituent on the nitrogen), making these compounds potentially atropisomeric. At room temperature, ¹H NMR spectrum of amine **2.48l** showed two well-resolved CHMe₂ doublets which did not coalesce even at 100 °C in toluene-*d*₈. The barrier to rotation of compound **2.48l** was calculated using EXchange Spectroscopy (EXSY) at 25 °C in toluene-*d*₈ (Figure 17). Irradiation of the signal centred around 1.48 ppm gave a cross-peak of same sign centred around 1.62 ppm, corresponding to partial interconversion of the irradiated nuclei during the mixing time. Extrapolation using the Eyring equation (Equation 1) allowed the calculation of kinetic parameters for the interconversion of **2.48l**, showing its rapid racemisation.

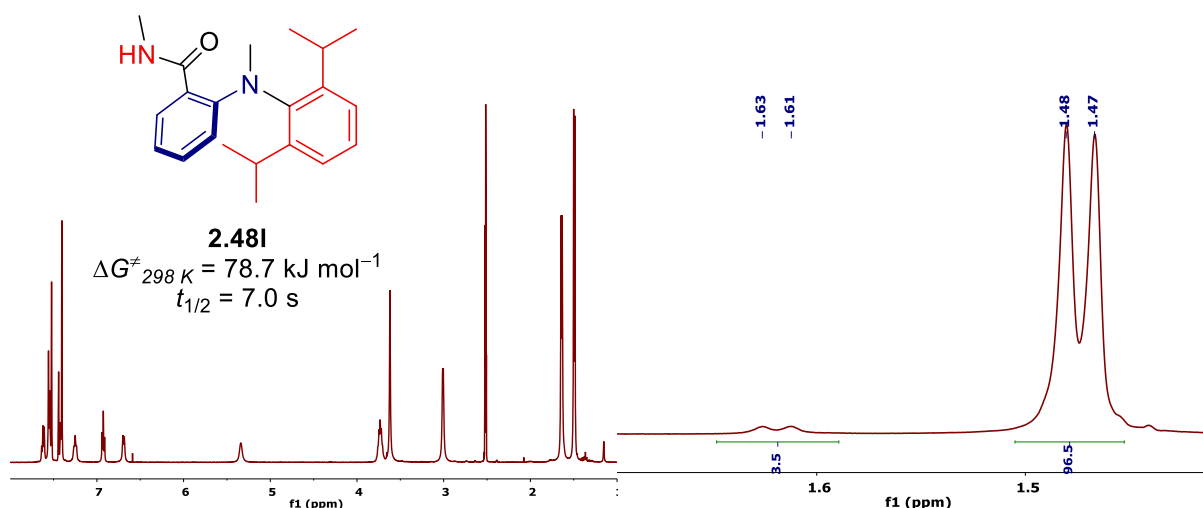
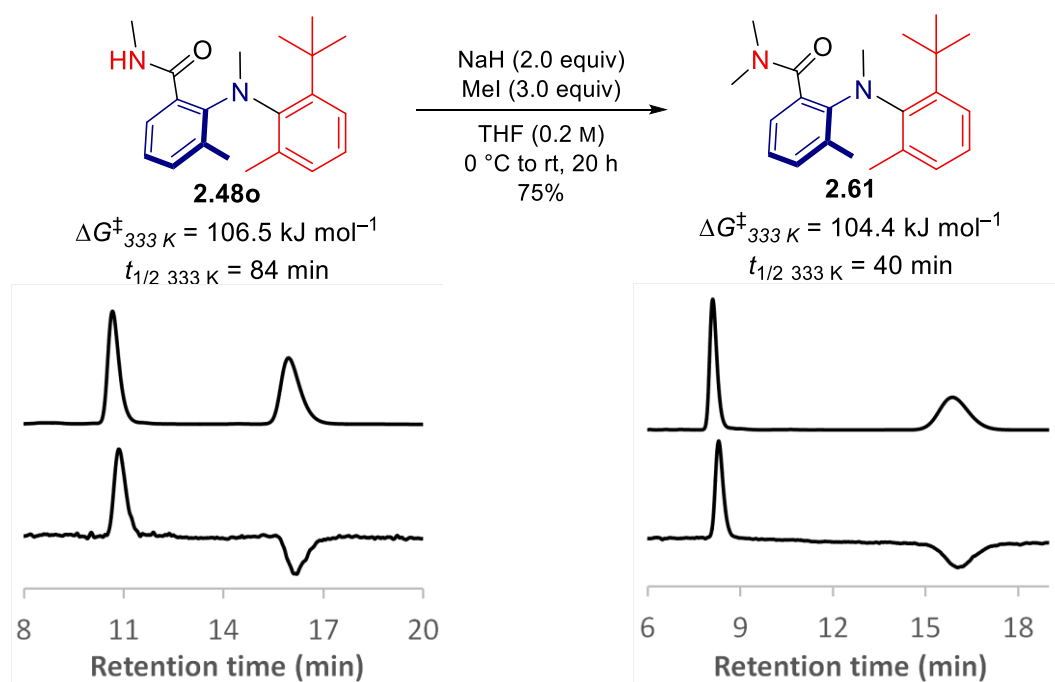


Figure 17 : ^1H NMR spectrum and ^1H EXSY NMR spectrum of **2.48l** (500 MHz, mixing time: 500 ms)

Bulkier diarylamines bearing four *ortho*-substituent and/or a *tert*-butyl group were analysed by chiral HPLC. Compounds **2.48n** and **2.48p** could not be resolved. HPLC of **2.48m** showed two resolved enantiomers using a chiral stationary phase at 0 °C. However, the broadness and poor resolution of the peaks prevented any calculation of a barrier to rotation.

Both enantiomers of diarylamine **2.48o** were resolved by HPLC. Following the first order decay of enantiomeric excess of an enantioenriched sample isolated by semi-preparative chiral HPLC (See Chapter 2), its barrier to C–N rotation was calculated at 333 K, with $\Delta G^\ddagger_{333\text{ K}} = 106.5\text{ kJ mol}^{-1}$ in toluene, corresponding to a half-life to racemisation of 84 min (Scheme 38). Thus, diarylamines **2.48o**, formed by the Smiles rearrangement of anthranilamide **2.47o** is an atropisomer up to 60 °C.



Scheme 38: Barrier to rotation of **2.48o** and **2.61**. HPLC traces of UV and optical rotation detectors (above and below)

Previous examples of atropisomeric diarylamines by Kawabata *et al.* featured an intramolecular hydrogen bond, locking rotation about one of the C_{Ar}–N bonds (see Chapter 1).^[29,30] To confirm that the atropisomerism of **2.48o** was only owed to steric hindrance, the potentially hydrogen bonding amide of **2.48o** was alkylated to form compound **2.61**. The barrier to rotation decreased only marginally to 104.4 kJ mol^{–1} at the same temperature, while disruption of the intramolecular hydrogen bonding in Kawabata's examples reduced the barrier to rotation by 15.5 kJ mol^{–1}.

II.3. Conclusion

In conclusion, both sterically hindered and unhindered diarylamines can be accessed in two steps from diaryl ureas using a novel, versatile Smiles rearrangement. No electronic activation of the migrating ring is required owing to the conformational preorganisation of the substrate. This transition metal-free route to diarylamines derived of anthranilic acid is particularly notable for its functional-group tolerance and its compatibility with extremely hindered aryl rings. It provides a valuable alternative to metal-catalysed coupling for the synthesis of challenging compounds. This rearrangement allows the facile synthesis of sterically hindered diarylamines displaying atropisomerism owing to restricted rotation around highly encumbered C_{Ar}–N bonds.

Chapter 3

Medium-Sized-Ring Analogues of Dibenzodiazepinones by Smiles Ring Expansion

Part of the results presented in this chapter were published in:

*R. Costil, Q. Lefebvre, and J. Clayden, Angew. Chem. Int. Ed., **2017**, 56, 14602–14606.*

III.1. Introduction

III.1.1. 3D structures in drug discovery

Modern approaches to drug design have recently focussed on shape-based three-dimensional molecular descriptors in an effort to ‘escape from flatland’,^[123,124] with good success in the prediction of the likeliness of clinical success.^[125,126] Since the introduction by Lipinski of the ‘Rule of 5’ physicochemical properties to follow in order to develop drug-like molecules from hit to lead,^[127,128] the community has been constantly surveying the properties of drug candidates during lead development. Among the properties considered are molecular weight, number of hydrogen bond donors and acceptors, number of rotatable bonds, or lipophilicity (as proposed by Lipinski), but also the polar surface area.^[129] These properties are now benchmarks for the development of drug-like scaffolds and are scrutinised on preclinical candidates for the prediction of their absorption, distribution, metabolism, excretion and toxicity (ADME-Tox) profile.

Due to the considerable increase in methods for the formation of $C_{sp^2}-C_{sp^2}$ bonds over the past decades, most notably by transition metal-catalysed reactions,^[130] the pharmaceutical industry has focussed on creating libraries of easily assembled, highly aromatic compounds from commercially available substrates.^[123,124] This trend has continued further with the development of high-throughput practice, allowing the rapid formation of libraries containing hundreds of thousands of compounds using robust procedures.^[123] While these methods allow the facile introduction of chemical diversity on a given scaffold, the functional groups introduced this way are usually planar and aromatic, with a rod-like or discoid shape.^[131] Hence, the chemical space which can be explored by such products is fairly restricted.

Recently, it has been demonstrated that increasing the structural complexity of drug candidates – and driving them towards natural product-like scaffolds – correlates with successfully advancing from the hit discovery stage to a marketed drug.^[125,132] Different descriptors defining the important physicochemical properties of the scaffold shape have been proposed, such as the radius of gyration.^[125] Another popular metric is the quantification of the fraction of sp^3 carbons in a molecule,^[123] as saturation of a scaffold increases its topological complexity without compromising the molecular weight.

Furthermore, various groups have shown that scaffolds exhibiting a higher degree of three-dimensionality tend to have better solubility, as planarity of a substrate can lead to solid state crystal lattice packing.^[133] Shape complexity also improves the selectivity towards the selected target, and

side-effects of highly three-dimensional molecules are considerably reduced as off-target binding by promiscuity is less favourable.^[124]

III.1.2. Medium-rings heterocycles

Medium-sized rings in drug discovery

Medium-sized rings – cyclic compounds comprising 8 to 12 atoms within a ring – are promising scaffolds for the development of small-molecule drugs with an extended three-dimensional shape.^[134–136] While their relative flexibility is beneficial for enhanced binding affinity by induced fit compared to smaller rings, their well-defined conformation allows the organisation and finely-tuned orientation of key pharmacophores for improved interactions with the target, preventing the major entropic loss of binding of linear, flexible systems.^[137] Furthermore, the restricted conformations of these substrates can ameliorate physicochemical properties such as bioavailability or cell permeability.^[138] However, it is well recognised that unfavourable transannular interactions increase the enthalpy of transition states of reactions leading to medium-rings.^[139] This makes their synthesis difficult, and consequently medium-rings are under-represented in screening libraries.^[140,141]

The potential of medium-size rings in drug development was recently highlighted by the drug candidate Lorlatinib, which was recently submitted to Phase 3 clinical trials for the treatment of lung cancer (Figure 18).^[142] Its cyclic structure containing a reduced number of rotatable bonds as well as a shielded polar surface area was found to be particularly relevant for further development of central nervous system (CNS) penetrant drugs.^[142] Other 8-, 9- and 12-membered benzannulated medium-sized lactams have been discovered for the treatment of breast cancer,^[143] as antibacterial agent^[144] or against leukaemia,^[145] respectively.

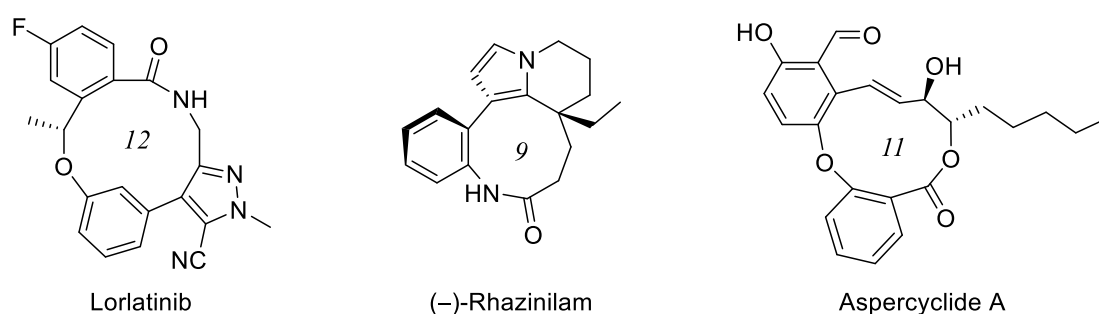


Figure 18: Bioactive medium -rings

Medium-size rings are also found in a plethora of natural products. Rhazinilam, a benzannulated lactam isolated from flowering plants from the Apocynaceae family,^[146] is a lead compound for the development of new antitumor compounds. Its unusual heterobiaryl moiety embedded in a 9-membered lactam ring procures rigidity, making the axially chiral $C_{sp^2}-C_{sp^2}$ bond configurationally stable. Aspercyclide A is an 11-membered diphenyl ether lactone isolated from *Aspergillus sp.*

inhibiting the binding of immunoglobulin E antibodies (IgE) to the human IgE receptor, therefore having potential application in the treatment of allergic disorders.^[147]

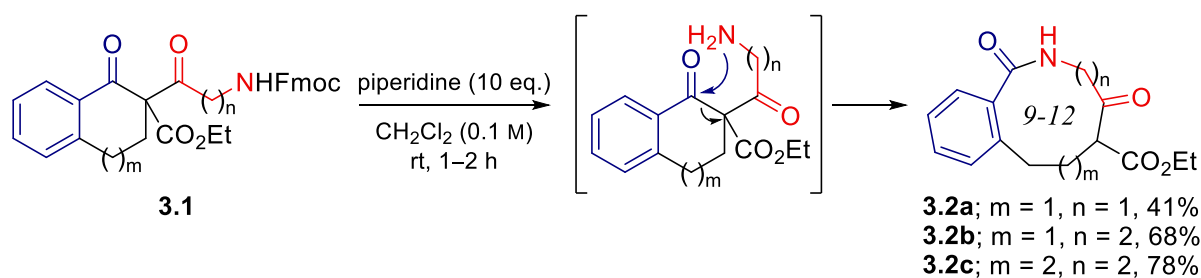
Synthesis of benzannulated medium-sized lactams by ring expansion

Benzannulated medium-sized lactams such as Lorlatinib are an emergent class of drug-like scaffolds which can be accessed by new synthetic methods. Their higher stability towards hydrolysis compared to the related linear or 5- or 6-membered cyclic amides is an asset, as amide bond cleavage is a common pathway for drug metabolism.^[148]

Cyclisation reactions are common strategies for the formations of lactams and lactones. The use of intramolecular reactivity offers advantages over reactions such as cycloadditions, as only one bond forming step is key to the reaction.^[149] Cyclisations to form 5- and 6-membered rings are generally more trivial than smaller rings, whose formation is impaired by significant enthalpic penalties due to the high strain of the product. While this is not a problem in cyclisations to generate macrocyclic structures, the long, flexible linker between the two reactive sites generally creates an unfavourable entropic cost upon ring formation. This leads to the possibility of intermolecular couplings, for which the main method of prevention is high dilution, limiting the application of macrocyclisations.

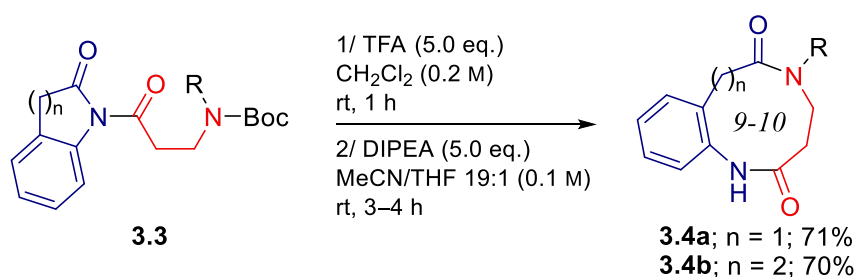
Medium-ring synthesis suffers from both these limitations.^[134] Illuminati *et al.* have found that the rate of lactonisation of various aliphatic bromo-carboxylic acids suffer from up to a millionfold decrease in the formation of 8- to 12-membered products compared to the cyclisation of the 5-membered γ -butyrolactone.^[139] It has been determined that torsional strain due to forced eclipsed conformations, as well as repulsive interactions between atoms across the scaffold leading to transannular strains are the major enthalpic penalties in the formation of medium-rings. Ring expansion provides an appealing alternative to access these heterocyclic rings, as not only is the transannular strain lessened in the transition state,^[149] but also because smaller heterocycles are readily available. Consequently, various groups have developed methods for the synthesis of benzannulated medium-sized lactams by ring expansion.

The Unsworth group reported the two-step synthesis of highly three-dimensional scaffolds **3.2** made through a 2-steps process *via* ring expansion (Scheme 39).^[150] Tricarbonyl **3.1** was formed by magnesium-promoted C-alkylation of an amino acid derived acyl chloride with a cyclic β -keto ester. Deprotection of the pendant nitrogen under basic conditions triggers nucleophilic attack at the ketone which initiates ring expansion to yield lactams **3.2** by 'stapling' of the amino acid moiety within the main core. This method provides scaffolds with methylene chains of modifiable length allowing fine tuning of their structural complexity, as demonstrated by extensive calculations of the lead-like properties of the scaffolds.^[150]



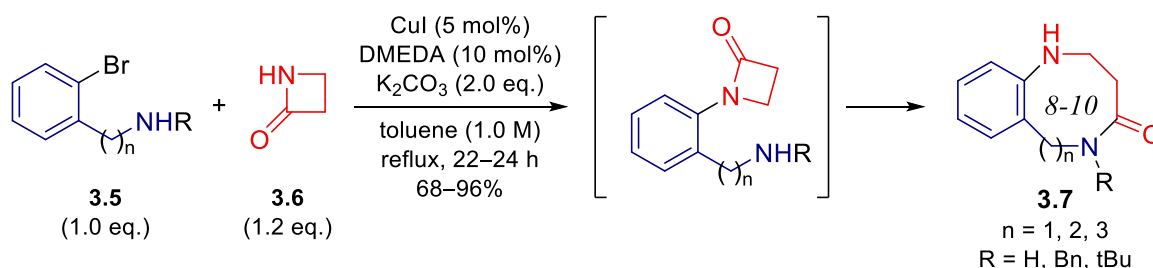
Scheme 39: Ring expansion of tricarbonyl compounds^[150]

Ring expansion by transamidation is also a popular alternative to macrocyclisations. Imides **3.3** were easily prepared by the acylation of the corresponding cyclic amide with *para*-nitrobenzyl-capped amino acid pentafluorophenol esters as coupling partners.^[151] Upon acidic cleavage of the Boc group followed by treatment with DIPEA in one-pot, the pendant nitrogen atom adds to the carbonyl position *via* a favoured 6-membered transition state similar to the previous example, this time on an imide moiety (Scheme 40). The imidic C–N bond cleavage then yields medium-sized anilides **3.4** with modulable ring size by tuning the methylene chain on the benzolactam substrate.



Scheme 40: Ring expansion of cyclic imides (R = *p*-NO₂Bn)^[151]

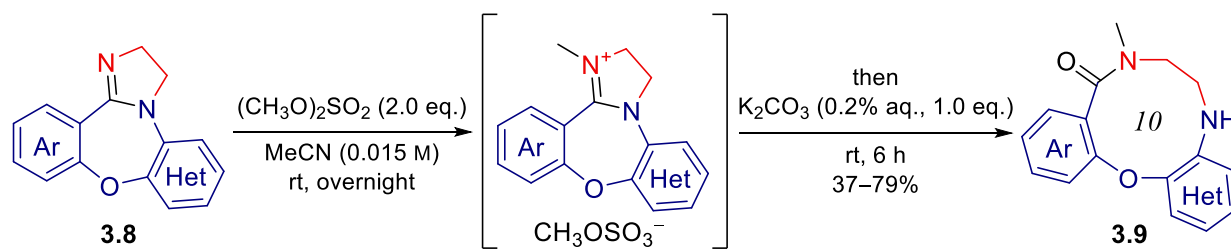
The Buchwald group developed their copper(I) methodology towards the synthesis of benzolactams by a one-pot transamidation/ring expansion strategy.^[152] When attempting the copper-catalysed coupling of azetidinone **3.6** with 2-halobenzylamines **3.5**, 8-membered lactam **3.7** was isolated in almost quantitative yield (Scheme 41, n = 1).



Scheme 41: Copper-catalysed ring expansion of *N*-aryl azetidinones^[152]

Another strategy for the formation of medium-sized lactams by strain-relief was proposed by the Krasavin lab (Scheme 42).^[153] 10-Membered lactams (**3.9**) with an embedded diaryl ether scaffold were made by ring expansion of easily prepared imidazoline-fused oxazepines **3.8** by hydrolytic ring

expansion. A one-pot procedure was devised to *N*-alkylate/ring expand in good to excellent yield, accessing heteroatom-rich structures **3.9**.

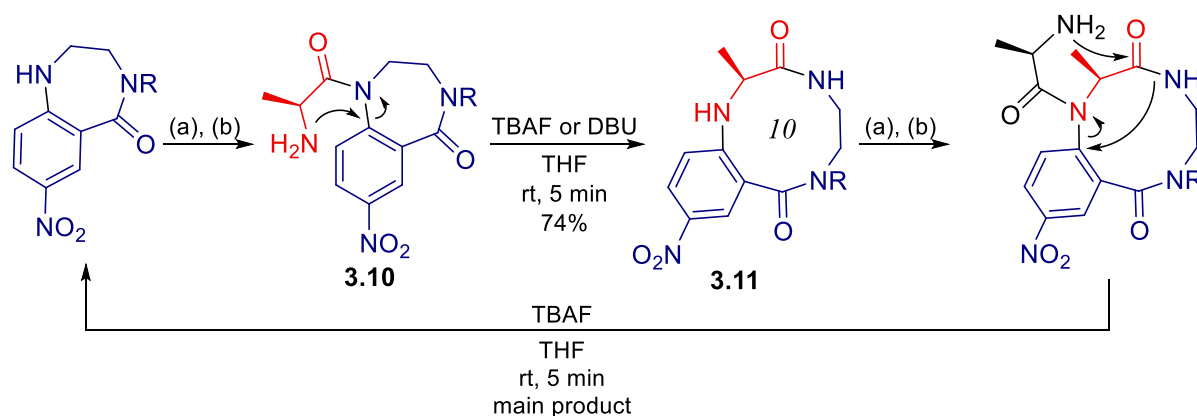


Scheme 42: Medium-rings by hydrolytic ring expansion^[153]

Although the substrate scope provided suggests that the reaction proceeds smoothly irrespective of the substitution pattern, even tolerating heteroaromatic rings, the oxazepine ring itself is formed by a complex cascade reaction involving two S_NAr steps and a Smiles rearrangement, limiting the scope of compounds amenable to the ring-expansion step.

Smiles reaction in ring expansions

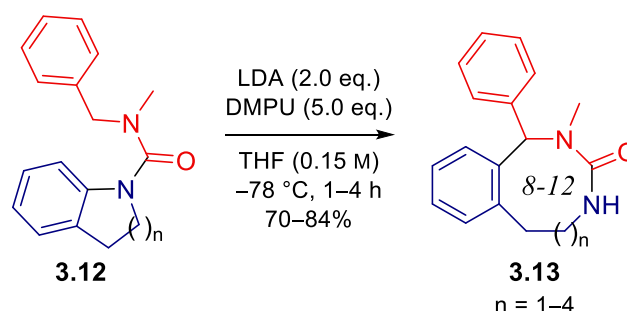
The Smiles rearrangement was applied by Still and co-workers for the ring expansion of 7-membered dibenzazepinone **3.10** to form medium-ring heterocycle **3.11** (Scheme 43).^[154] Upon deprotonation, incorporation of the amino acid into the core structure proceeded by nucleophilic attack at the *ipso* position of the aromatic amine. The reaction necessitates electronic activation and requires one or more nitro group on the aromatic ring. Additionally, only a 7-to-10-membered ring expansion proceeded. Indeed, acylation of the product **3.11** with alanine and iterative ring-expansion resulted in the reverse-Smiles rearrangement to the former 7-membered substrate.



Scheme 43: Ring expansion by Smiles rearrangement,^[154] R = $\text{CH}_2\text{CO}_2t\text{Bu}$. (a) NaH, THF, DMF, then BocAlaO(*p*-NO₂Ph). (b) TFA, CH₂Cl₂, Toluene

Recently, our group described the use of the Smiles rearrangement of lithiated ureas in the ring expansion of common *N*-heterocycles (Scheme 44).^[155] Upon deprotonation of the benzylic position of urea **3.12**, an unconventional S_NAr reaction occurs with attack at the *ipso* position of the

heterocycle. After collapse of the Meisenheimer intermediate, C–N bond cleavage provides 8- to 12-membered medium-sized ureas **3.13** in excellent yields, constituting a formal *N*-to-*C* aryl migration.



Scheme 44: Unactivated Smiles ring expansion of ureas^[155]

In comparison to the anthranilamide rearrangement presented in Chapter 3, this Smiles rearrangement is insensitive to electron-donating groups on the migrating aryl ring, suggesting that Smiles ring expansions do not necessarily require electronic activation of the substrate.

III.1.3. Intramolecular hydrogen bonding in drug design

Hydrogen bonding is a crucial concept in drug discovery, and a major phenomenon dictating the folding of proteins, mainly through bonding of the amidic N–H with carbonyls.^[156] Consequently, binding of a drug-like small molecule to its target is strongly affected by its hydrogen bonding properties, which must be manipulated to offer strong, directed interactions. Thus, the introduction of polar groups with defined orientations is a key challenge in drug design.

Controlling the active conformation with intramolecular hydrogen bonding

More recently, the medicinal chemistry community identified the use of intramolecular hydrogen bonding as a way to introduce conformational bias to obtain a desired functional group arrangement without the need for a covalently bonded, rigid scaffold. Researchers from Novartis, for example, designed a mimic of PD166285,^[157] a broadly active tyrosine kinase inhibitor developed by Pfizer (Figure 19); by moving the nitrogen atoms in the pyrimidine ring, and replacing the pyrimidone ring with a urea, a particularly stable, planar and conjugated pseudo six-membered ring was formed by intramolecular hydrogen bonding. Although less potent than PD166285, compound **3.14** retained a submicromolar activity against a wide range of tyrosine kinases.^[158]

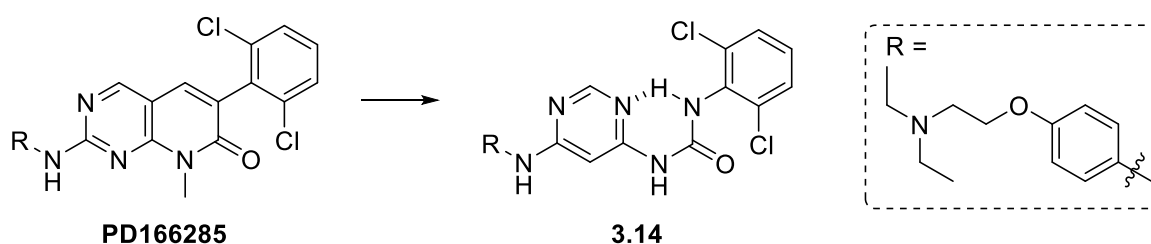


Figure 19: Bioactive compound mimic by intramolecular hydrogen bonding^[158]

New classes of biologically active chemotypes can thus be obtained by locking the active conformation as a molecular mimic, offering potentially different ADME-Tox profiles, easier methods of synthesis as well as new patentability.

Hidden hydrophilicity

When designing a new drug scaffold, one must pay attention to the polarity of the target compound. The ADME-Tox profile of a molecule is directly related to its polarity and ionizability. Polar and/or ionised molecules struggle to penetrate the cells lipid bilayer by passive diffusion and require active transporters to be absorbed.^[159] This limits their design and introduces more challenges to their development. Furthermore, lipophilic compounds are metabolised and excreted at a significantly slower rather than their polar counterparts.^[137] Yet, polarity is necessary to increase the solubility of the active ingredient in physiological media (*i.e.* aqueous solutions), and high lipophilic compounds have their own drawbacks, including poor bioavailability due to plasma protein binding, as well as unfavourable entropic costs to bind deeply solvated enzyme pockets.^[129,138] Hence, the polarity of a drug molecule must be finely balanced to optimise its ADME-Tox properties.

Polarity, however, can be a dynamic property. Trapoxins and Apicidins, two classes of cyclotetrapeptides metabolites isolated from fungi (Figure 20), have found application as anti-protozoal agents by irreversible inhibition of histone deacetylase through their α -epoxyketone and alkyl ketone warheads, respectively.^[160,161] Variable-temperature NMR analysis revealed that Apicidins possess a highly rigid 12-membered scaffold containing several intramolecular hydrogen bonds (designated by the red arrows in Figure 3-3).^[161] This array of intramolecular hydrogen bonds is made possible by the D-Pip amino acid in the chain. Indeed, cyclotetrapeptides made from all-L-amino acids are known to be sensitive to hydrolysis and have multiple conformations in water because of the unfavourable strain induced by homochiral amino acids in the major all-*trans* conformation.^[162]

Cyclisation of small peptides generally improves lipid bilayer penetration by removing the charge at each terminus, thus making the peptides neutral at physiological pH.^[132] Restricting the number of rotatable bonds also lowers the entropic costs of desolvation and can allow the formation of more stable, internal hydrogen bond-containing conformations.

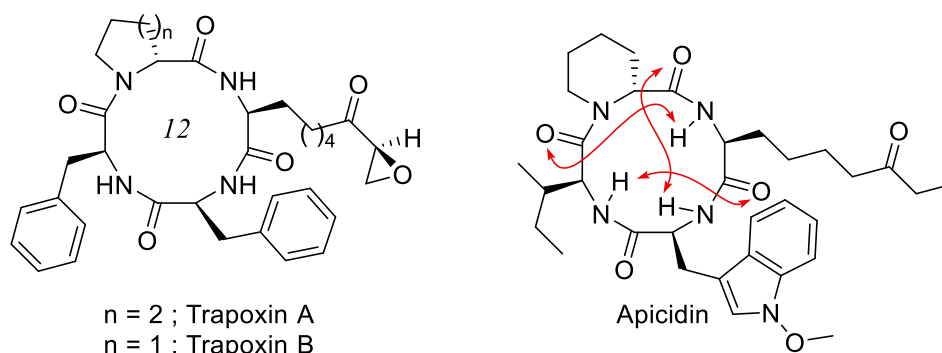


Figure 20: Bioactive cyclic tetrapeptides. Intramolecular hydrogen bonds are highlighted by the red arrows

Furthermore, evidence of the positive impact of intramolecular hydrogen bonding on cell wall permeation was observed by Lokey and co-workers.^[132,163] Cyclic hexapeptide **3.15**, containing both D- and L-amino acids crosses lipid bilayers with a ten-fold increase in its diffusion coefficient compared to its homochiral analogue.^[163] This ratio increases to a hundred-fold when compared to a linear homologue. Careful investigation of the conformation of **3.15** in solution by ^1H NMR analysis led to the conclusion that the absolute configuration of the amino acids and the cyclised nature of the scaffold allow the folding of the peptide into a tight structure comprising of four hydrogen bonds. In this conformation, the overall lipophilicity of the compound is increased by ‘hiding’ the polar moieties from the medium (Figure 21).

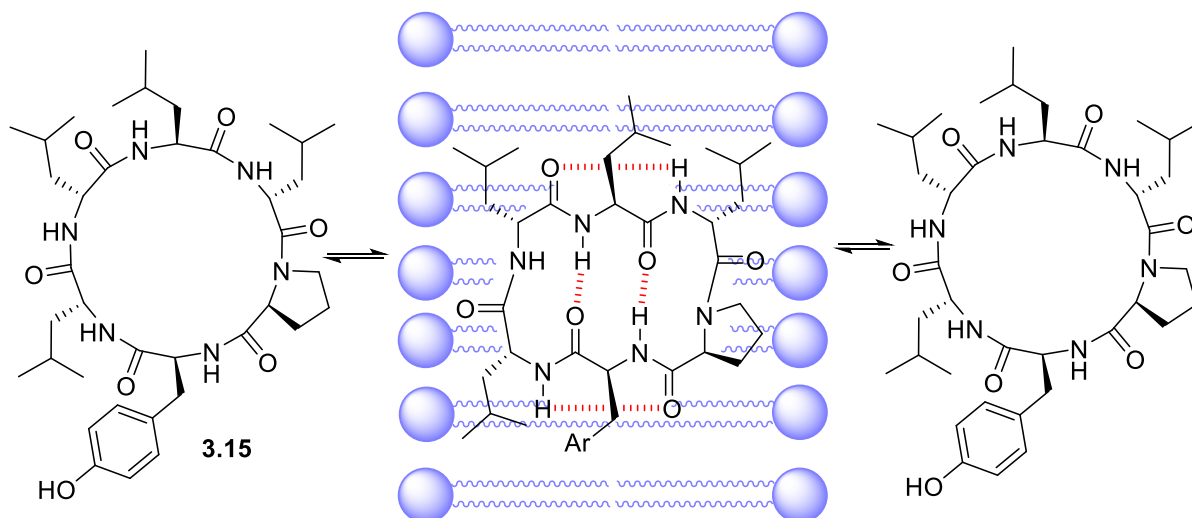


Figure 21: Schematic representation of lipid bilayer permeation by hidden hydrophilicity in cyclic peptides

Consequently, while the highly polar peptide is easily solvated by water molecules, the entropic cost of desolvation to cross the lipidic membrane is reduced by this intramolecular hydrogen bonding. The polarity of the compound is then easily modulated to adapt to the medium, rendering it dynamic.^[163] The hundred-fold difference in membrane-crossing compared to the linear analogue highlights the importance of the structural preorganisation brought by cyclisation, while the homochiral, cyclic

analogue can only fold into a structure comprising of three intramolecular hydrogen bond, not as lipophilic as **3.15**.^[132]

This particular ‘chameleonic behaviour’ was applied to design new transmembrane vectors to improve the ADME profile of small bioactive molecules.^[164,165] Aminocoumarin **3.16** is a fluorescent, cytotoxic compound inducing reactive oxygen species in *Cryptococcus*. Its poor cell permeability, however, restricts its application as an antiproliferative.^[164] Conjugation of the molecule with a non-toxic tetrapeptide inspired from Trapoxins and Apicidins through a click reaction forms the bioconjugate molecule **3.16** (Figure 22).^[165] Although its large molecular weight exceeds the limits defined by Lipinski’s ‘Rule of 5’, compound **3.16** crossed the lipid bilayer and is highly active against *P. falciparum*, as visualised by fluorescence spectroscopy.

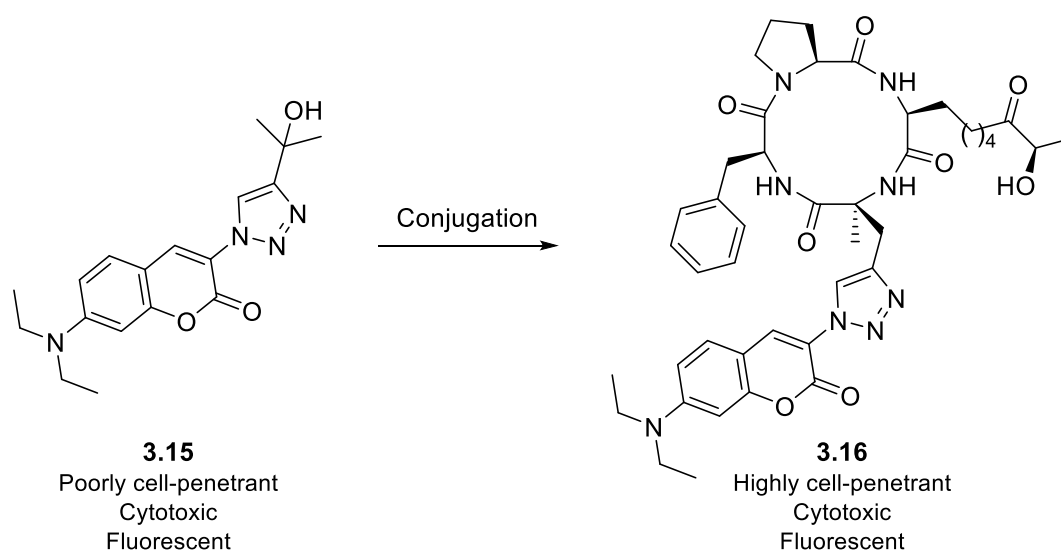


Figure 22: Application of the hidden hydrophilicity to molecular shuttling^[165]

Introducing intramolecular hydrogen bonds to improve the physicochemical properties of a bioactive substance is not limited to large, cyclic peptides. CI1021 is a carbamate-capped quaternary amino acid derivative with low nanomolar activities against the human neurokinin-1 receptor, a G protein-coupled receptor found in the central nervous system.^[166] This receptor is considered an attractive drug target as it mediates many biological processes such as pain transmission, activation of the immune system, as well as proliferation and migration of tumour cells.^[167] However, as CI1021 is poorly soluble in aqueous media and barely crosses the blood-brain barrier, researchers at Pfizer have worked on improving its ADME profile while keeping activity by modifying the substitution pattern at the quaternary carbon.^[168] This led to the discovery of the closely related derivative, **3.16** (Figure 23), which forms an intramolecular hydrogen bond between the new tertiary amine and the amidic proton, as evidenced by variable temperature ¹H NMR analysis, together with computational modelling and X-ray crystal structure determination. This compound presented similar *in vitro* activity, the

protonable amine increased its solubility. Furthermore, the formation of this intramolecular hydrogen bond decreases the compounds apparent lipophilicity, resulting in noticeable improvement in CNS penetration.

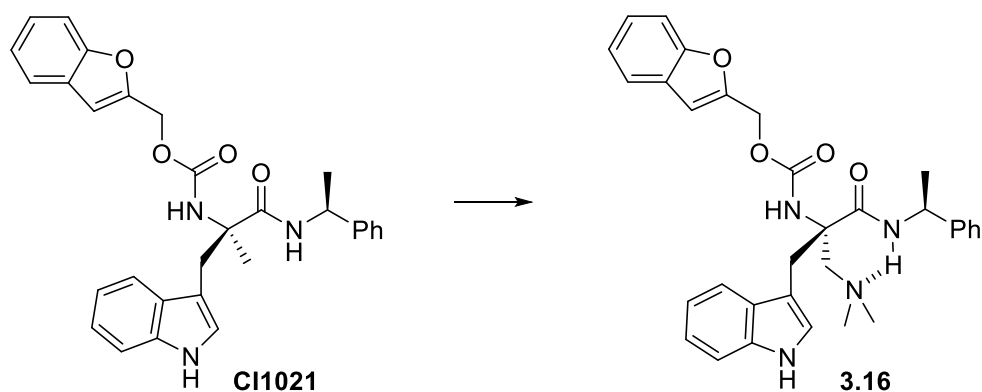


Figure 23: Improving ADME profile of a drug by intramolecular hydrogen bonding^[168]

It is clear that the design of flexible yet structurally defined pharmacophores which can accommodate one or many intramolecular hydrogen bonds can successfully lead to the improvement of the physicochemical properties of drug-like molecules.^[137] The combination of this approach together with further emphasis on the three-dimensional shape of molecules has allowed medicinal chemists to go beyond the ‘Rule of 5’.^[169] This permits the design of non-canonical drug chemotypes at a time where targeted diseases are harder to address, as only half of the pool of targets are estimated to be druggable within the ‘Rule of 5’ today.^[138]

III.2. Results and discussion

III.2.1. Aim

Tricyclic antidepressants (TCA) such as Imipramine and Dibenzipin (Figure 24) are broadly prescribed for the treatment of depression and schizophrenia.^[170,171] Dibenzodiazepines possess a pair of rigid, rapidly interconverting enantiomeric ‘butterfly’ conformations, arising from the strain in the dibenzofused 7-membered heterocycle.^[172,173] This interconversion is locked in telenzepine, of which one of the two atropisomers is 500 times more active than the other.^[174]

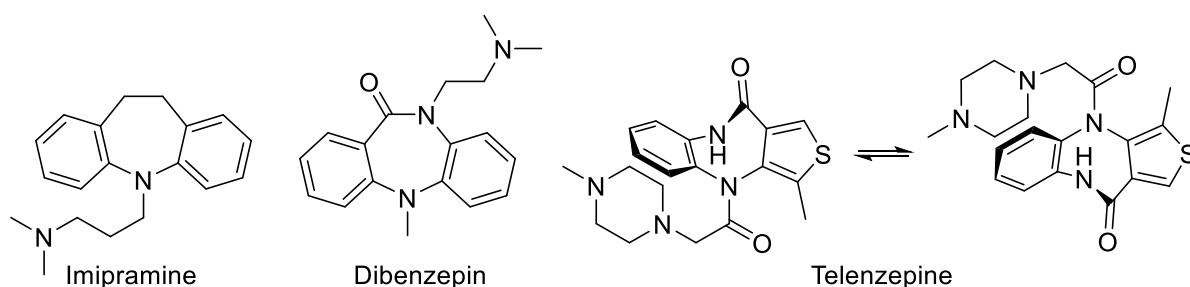
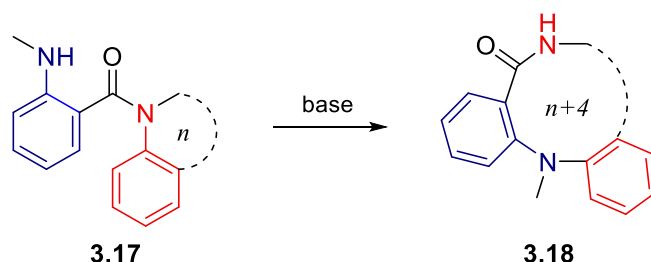


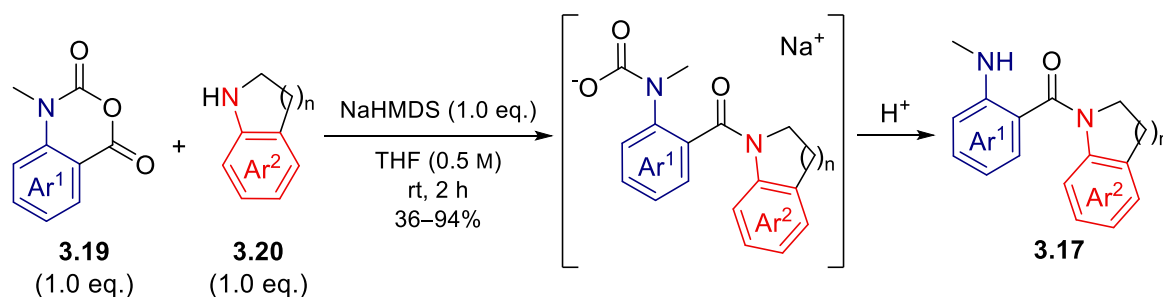
Figure 24: Examples of tricyclic antidepressants (TCA) approved by the FDA

Building on the work described in Chapter 3, we envisaged the rearrangement of anthranilamides where the amide nitrogen is tethered to its closest aryl ring (**3.17**, Scheme 45). Smiles rearrangement of such compounds would lead to $n \rightarrow n+4$ ring expansion of the heterocyclic amide to generate medium-rings from simpler benzo-fused nitrogen heterocycles. The resulting heterocycle would also possess a hydrogen bond donor/acceptor pair in its core scaffold, making it a potential candidate for intramolecular hydrogen bonding, with different conformations accessible by modulating ring size.



Scheme 45: Concept of the Smiles ring expansion of anthranilamides

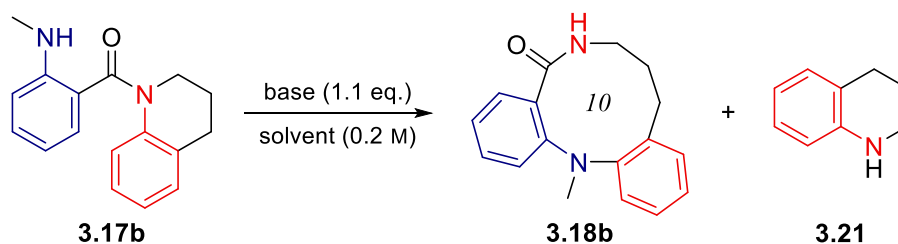
The anthranilamide substrates were all synthesised by Quentin Lefebvre, and their synthesis will only be briefly discussed. The Snieckus–Fries rearrangement reported in Chapter 3 unfortunately provided anthranilamides **3.17** in low yields and required long reaction times. In contrast, treatment of nitrogen-heterocycles **3.20** with NaHMDS in the presence of isatoic anhydrides **3.19** results in the addition of the deprotonated nitrogen to the carbonyl directly bonded to the aromatic ring, subsequently initiating ring opening (Scheme 46). Acidic workup of the resulting carbamic acid leads to decarboxylation to form anthranilamide **3.17** in poor to excellent yield, in one step. The reaction usually proceeds at room temperature and is typically complete within two hours. When not commercially available, isatoic anhydrides were made by reaction of triphosgene with the corresponding anthranilic acid followed by *N*-methylation.



Scheme 46: Synthesis of the anthranilamides starting materials as performed by Quentin Lefebvre

III.2.2. Development of the rearrangement

Optimisation of the Smiles ring expansion was carried out on anthranilamide **3.17b** (Table 20), made in one step from cheap, commercially available substrates.



Entry	Base	Solvent	<i>T</i> (°C)	<i>t</i>	Conv. (%)	3.18b (%)	3.21 (%)
1	NaHMDS	THF	rt	16 h	66	<5	43
2	NaHMDS	THF	66	2 h	>95	55	27
3 ^a	NaHMDS	THF	100	15 min	>95	66	22
4^b	NaHMDS	THF	100	15 min	>95	72^c	<5
5 ^b	NaHMDS	2-MeTHF	100	15 min	>95	67	<5
6 ^b	NaHMDS	MTBE	100	15 min	91	28	43
7 ^b	NaHMDS	Toluene	100	15 min	86	18	44
8 ^b	LiHMDS	THF	100	15 min	8	<5	<5
9 ^b	KHMDS	THF	100	15 min	89	62	<5
10 ^b	KHMDS	THF	100	30 min	>95	45	29
11 ^b	P4- <i>t</i> Bu	THF	100	15 min	28	0	0
12 ^b	TDB	THF	100	15 min	18	0	0
13 ^b	KOtBu	THF	100	15 min	>95	0	73

Reaction procedure: To a solution of **3.17b** (0.2 mmol) in solvent (0.2 M) was added a base (0.22 mmol, 1.1 eq.). The reaction mixture was stirred at the given temperature and quenched with MeOH.

¹H NMR yields were calculated from the crude reaction mixture using 1,3,5-trimethoxybenzene as internal standard.

^a Reaction performed in a sealed tube. ^b Reaction performed in a microwave oven. ^c Isolated yield.

Table 20: Optimisation of the Smiles ring expansion

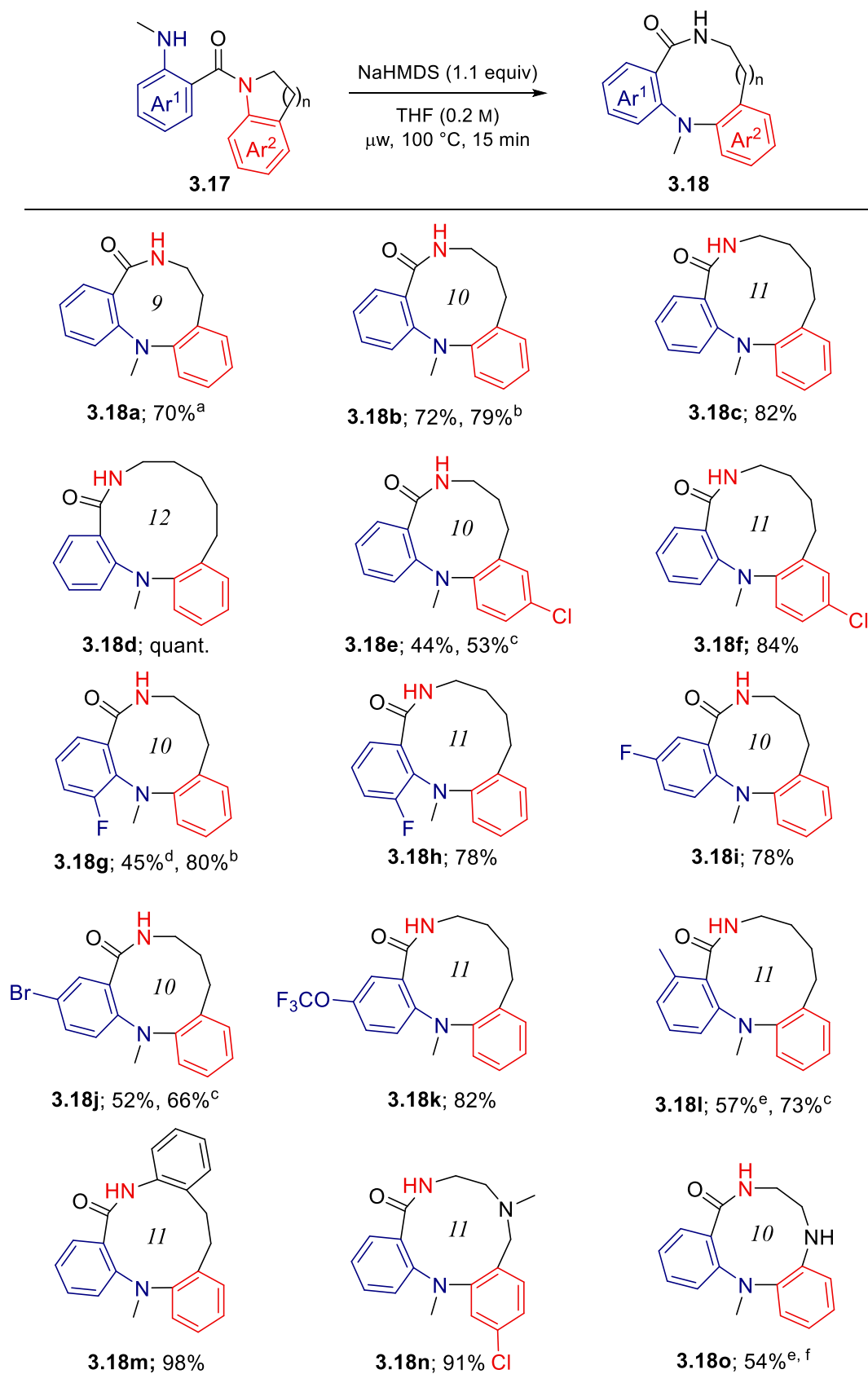
On treatment with NaHMDS in refluxing THF, **3.17b** rearranged to the 10-membered lactam **3.18b** in 55% yield (entry 2). However, decomposition of the starting material to the corresponding *N*-methyl anthranilic acid (usually removed during work up) and tetrahydroquinoline (THQ, **3.21**, Table 20) was also observed. Increasing the temperature to 100 °C in a sealed tube reduced the reaction time and improved the yield (entry 3). Microwave heating yielded a cleaner reaction, giving the product in 72% yield with only trace amounts of THQ (entry 4).

KHMDS gave comparable results, albeit proceeding at a slower rate, and decomposition of the product was observed over prolonged reaction time (entries 9 and 10). As mentioned in the previous chapter, the conversion was negligible when LiHMDS was used as the base (entry 8). Other bases investigated were either too weak, leaving the starting material untouched (entries 11 and 12), or too nucleophilic,

leading to decomposition (entry 13). Renewably-sourced 2-Methyl THF provided a good alternative solvent, with only a slight decrease in yield (entry 5), whereas toluene and MTBE led to decomposition (entries 6 and 7).

Scope and limitations

Ring expansion of 5- to 8-membered heterocycles was possible, providing 9- to 12-membered lactams (Scheme 47). Rearrangement of the smallest ring, the 5-membered indoline derivative **3.17a** required more forcing conditions (4 hours at 120 °C) but yielded the corresponding 9-membered product **3.18a** in excellent yield. Rearrangements of larger rings also proceeding smoothly and were cleaner, providing the corresponding 10- to 12-membered compounds **3.18b–d** in excellent yields after short reaction times. In contrast to the organolithium bases, NaHMDS allowed good tolerance to halogen substituents at various positions of the aryl ring, with fluoro-, bromo-, and chloro-substituted products **3.18e–j** formed without decomposition. The reaction conditions were also compatible with a lipophilic trifluoromethoxy group (**3.18k**). In some examples, full conversion could not be reached despite heating at higher temperature or extending the reaction times. Moderate steric hindrance was somewhat tolerated. Fluorine atoms *ortho* to the nucleophilic nitrogen decreased the reactivity, as **3.18g** needed prolonged reaction time and did not go to full conversion. Its 7-membered ring analogue, **3.17h**, though, reacted cleanly to give **3.18h** in excellent yield. Steric demand *ortho* to the amide group, for example a methyl group (**3.18l**), had a dramatic effect, requiring a longer reaction time, and full conversion was not reached, whilst its 6-membered derivative did not rearrange at all and degraded under the reaction conditions.



^a The reaction time was 4 h at 120 °C. ^b 3 mmol scale. ^c Based on recovered starting material. ^d The reaction time was 45 min. ^e The reaction time was 1 h. ^f From the Boc-protected starting material, using 2.0 eq. NaHMDS followed by 6.0 M HCl.

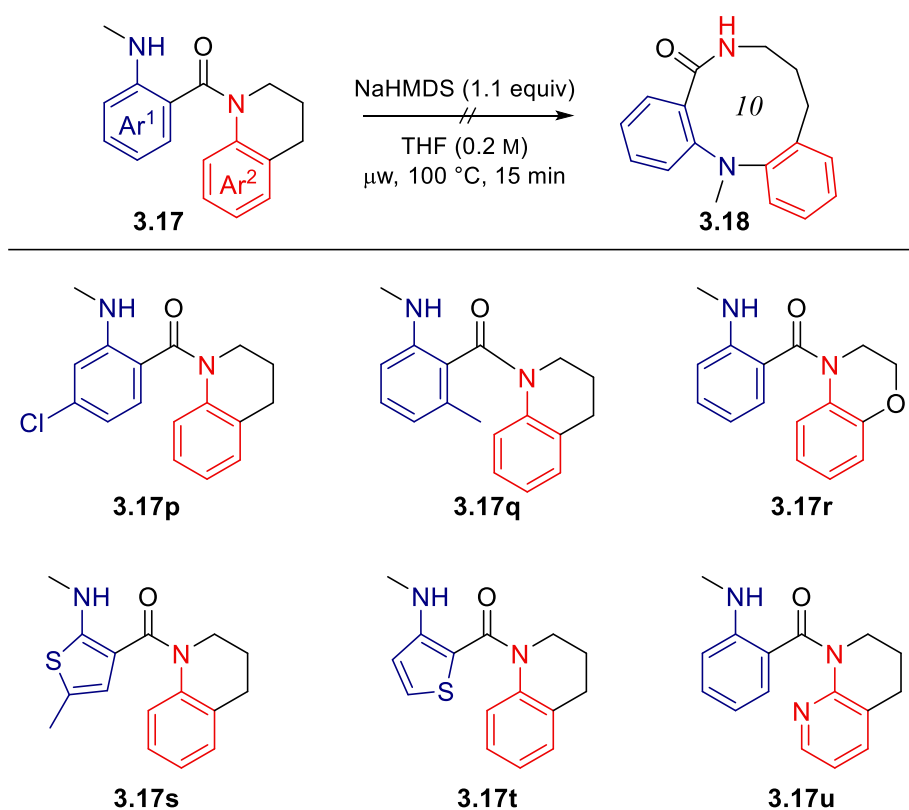
Scheme 47 : Scope of the Smiles ring expansion

More complex products with functional groups on the contiguous methylenes chain were made by ring opening of various heterocycles. Ring opening of dibenzazepine afforded anilide **3.18m**, containing an arylated side chain, in near-quantitative yield. Ring opening of a benzodiazepane – made by condensation of isatoic anhydride and *N*-methyl glycine, followed by reduction – yielded another nitrogen-rich medium-ring **3.18n** in excellent yield. Ring opening of *N*-Boc protected quinoxaline was possible with longer reaction time. However, slow bond rotation of the Boc protecting group, together with interconversion of conformers by ring-flipping complicated analysis of the product. One-pot ring opening followed by Boc deprotection was then conducted, affording nitrogen-rich compound **3.18o** in good yield.

This reaction, however, showed some limitations. First, the solubility of the substrates for the formation of anthranilamide **3.17** sometimes proved to be a limitation to the extension of the scope. In general, benzo-fused or methoxylated isatoic anhydrides were insoluble in THF and DMF, the two solvents used for the *N*-methylation and anthranilamide condensation. This problem was also faced when trying to introduce a nitrogen atom in the isatoic anhydride ring to provide pyridyl derivatives. Insolubility of the anthranilamide substrate was also an issue when trying to add an amide *N*-heterocycle to isatoic anhydride (indolinone, isatin or quinolinone) or a nitro-substituted heterocycle.

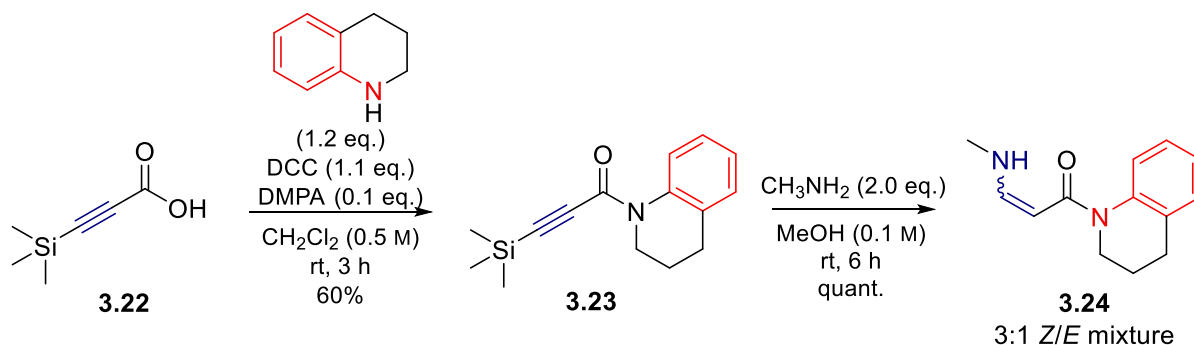
Introducing heterocyclic structure in the isatoic anhydride substrate was possible with thiophene rings. However, compounds **3.17s** and **3.17t** were unreactive under the ring expansion conditions. Heating up the reaction mixture to 150 °C for 2 hours left anthranilamide **3.17s** untouched (Scheme 48), while amide bond cleavage was observed in **3.17t** under the same conditions.

This side-reaction appeared to be common. When solubility was not an issue, poor conversion or decomposition of the starting material was occasionally observed. A chlorine atom *para* to the amide moiety leads to no conversion of the starting material **3.17p**, even at higher temperature and with longer reaction times. As stated earlier, a methyl group *ortho* to the amide moiety drastically slows down the conversion of the ring expansion of the 6-membered heterocycle **3.17q**, to the advantage of the amide bond cleavage and formation of tetrahydroquinoline **3.21**. Similarly, electron-rich benzoxazine, and pyridine-derived anthranilamides **3.17r** and **3.17u** were not stable under the reaction conditions, similarly resulting in amide cleavage.



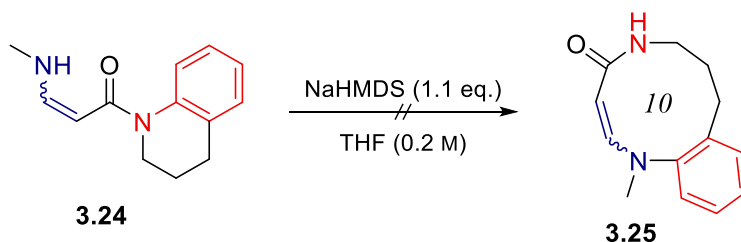
Scheme 48 : Unsuccessful scaffolds for the Smiles ring expansion

Although rearrangement of heterocyclic substrates seemed troublesome, we turned our attention to extending the scope to different core structures. Enamine **3.24** was accessed by modifying a previously reported procedure for the formation of enamines from trimethylsilyl acetylene derivative (Scheme 49).^[175,176] Formation of the acyl chloride of carboxylic acid **3.22** followed by condensation with THQ proved unfeasible. Instead, peptide coupling using DCC and DMPA furnished protected trimethylsilyl acetylene amide **3.23** (Scheme 49) in good yield. Stirring the alkyne with methylamine gave the corresponding enamine in quantitative yield, in a 3:1 ratio of *cis/trans* isomers, as determined by ¹H NMR analysis of the product mixture.



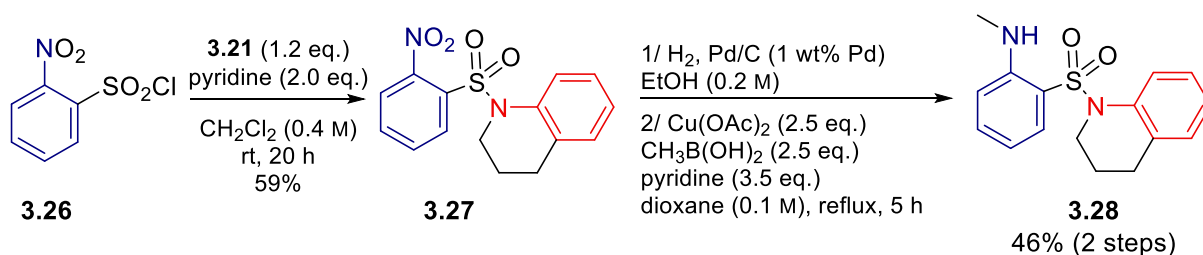
Scheme 49 : Synthesis of enamine **3.24**

Submitting the resulting enamine to the reaction conditions, however, did not show any conversion (Scheme 50). As previously seen, increasing the temperature to 120 °C and extending the reaction time to 30 minutes led to the decomposition to tetrahydroquinoline.



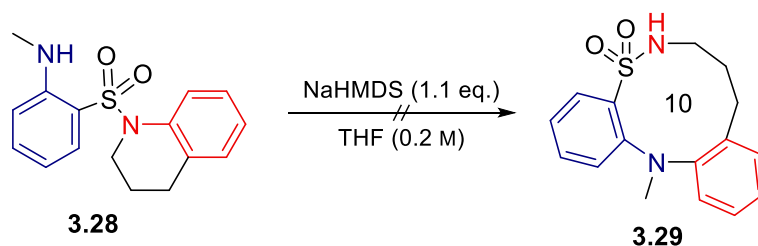
Scheme 50 : Attempted ring expansion of enamine **3.24**

Amide groups can be metabolically labile in physiological medium. A common isostere to the amide functionality is the sulfonamide group.^[177] Modification of the anthranilamide substrates to replace the amide moiety for a sulfonamide could be achieved following a similar strategy to that described in Chapter 3. Coupling of the commercially available *ortho*-nitrobenzene sulfonyl chloride **3.26** with THQ under basic condition afforded sulfonamide **3.27** in good yield (Scheme 51). Sequential hydrogenation of the nitro group followed by Chan–Lam coupling with methylboronic acid afforded sulfonamide **3.28** in good yield after two steps.



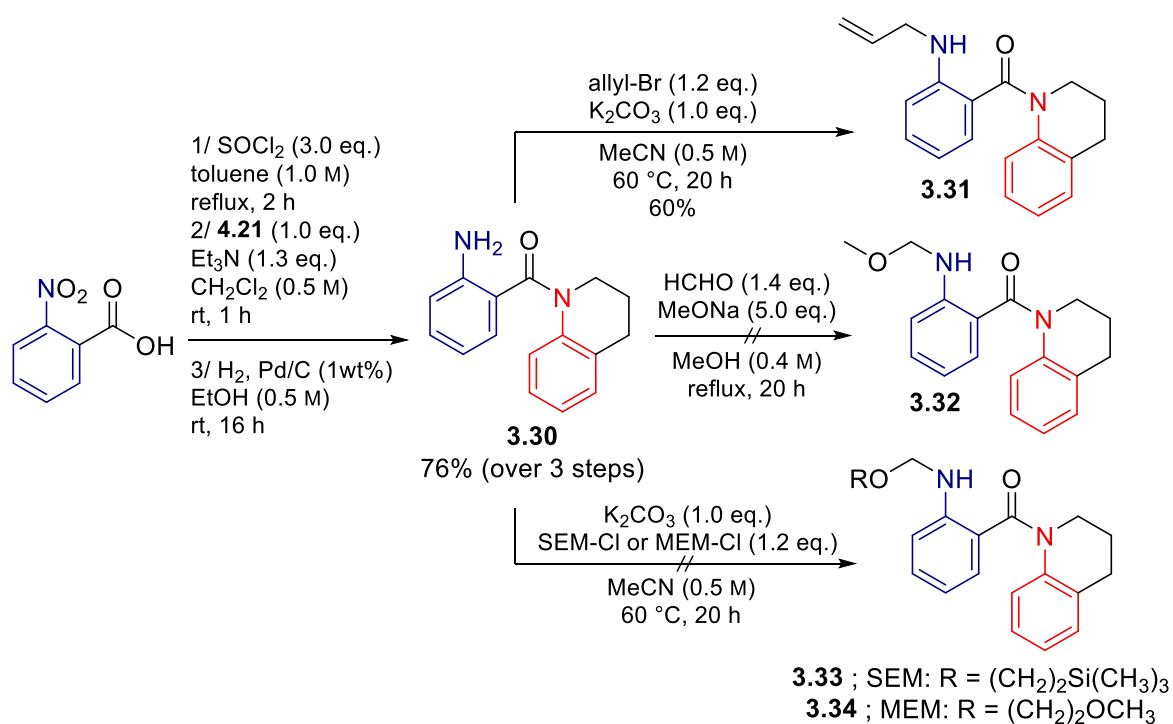
Scheme 51 : Synthesis of sulfonamide **3.28**

When subjecting sulfonamide **3.28** to the reaction conditions, no conversion was observed (Scheme 52). Raising the temperature to 120 °C and the reaction time to 2 hours offered no improvements. Modification of the amide moiety presumably changes the substrate conformation.^[177] The sulfur atom is sp^3 hybridised, in contrast to the sp^2 hybridised carbon atom of the amide carbonyl. Consequently, the aryl ring of benzenesulfonamides (here in blue) lacks the conjugation as in benzamides in the solid state, highlighting the importance of the amide group on the rearrangement.



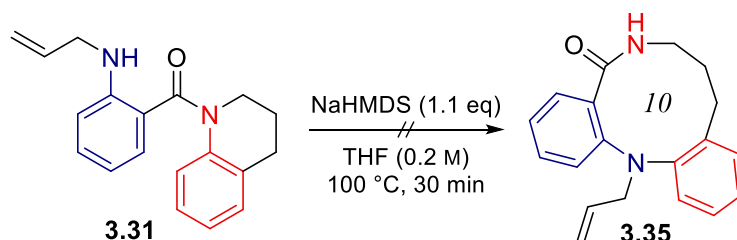
Scheme 52 : Attempted ring expansion of sulfonamide **3.28**

Following a similar approach to the previous chapter, it was decided to improve the scope of the reaction by introduction of protecting groups at the nucleophilic nitrogen atom (*i.e.* replacing the methyl group). Although it was initially decided to use a benzyl group, this use of this group was rejected for two reasons: a) the benzyl group required drastic changes to the conditions for the acyclic Smiles rearrangement to happen, b) it was anticipated that the benzyl group would be too bulky to allow ring expansion. Instead, the moderately hindered allyl was selected for investigation. The allyl group was introduced in good yield by substitution of allyl bromide on primary aniline **3.30**, which itself was made following a previously reported protocol (Scheme 53).^[178] Heteroatom-containing protecting groups were also considered, including the MOM (methoxymethyl ether), SEM (2-(trimethylsilyl)ethoxymethyl ether), and MEM (2-methoxyethoxy-methyl ether) protecting groups. Protection of the aniline nitrogen by a MOM group under basic conditions with sodium methoxide did not provide any product **3.32**, with decomposition to THQ occurring instead. Introduction of a SEM or a MEM protecting group to yield **3.33** and **3.34**, respectively, also proved difficult, with no conversion observed in both cases.



Scheme 53 : Route to *N*-protected anthranilamides

The ring expansion was initially explored on the unprotected aniline **3.30**. Whilst no reaction took place under the standard condition, increasing the temperature and reaction time led to a transamidation reaction, even at concentrations as low as 0.01 M. Subjecting the allyl-protected substrate **3.31** to the standard reaction conditions in 30 minutes, decomposition to tetrahydroquinoline was observed in 50% conversion (Table 21, entry 1).



Entry	Change in conditions	Conversion ^a
1	None	50%, 3.31 /THQ 1:1
2	DMPU (5.0 eq.)	50%, 3.31 /THQ 1:1
3	18-crown-6 (5.0 eq.)	50%, 3.31 /THQ 1:1
4	150 °C	85%, 3.31 /THQ 1:6
5	150 °C, in DMF (0.2 M)	90%, 3.31 /THQ 1:9

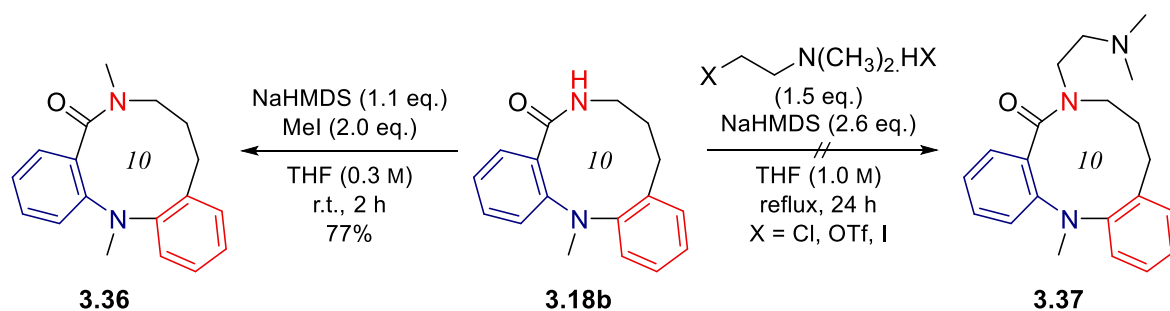
^a ¹H NMR yields were calculated from the crude reaction mixture using 1,3,5-trimethoxybenzene as internal standard.

Table 21 : Ring expansion of *N*-allyl anthranilamide

Modification of the conditions, including the use of additives such as DMPU as a decoordinating agent (entry 2) or 18-crown-6 as a potassium cation chelator (entry 3), raising the temperature to 150 °C and exchanging the solvent to DMF (entries 4 and 5). However, none of these conditions yielded any product.

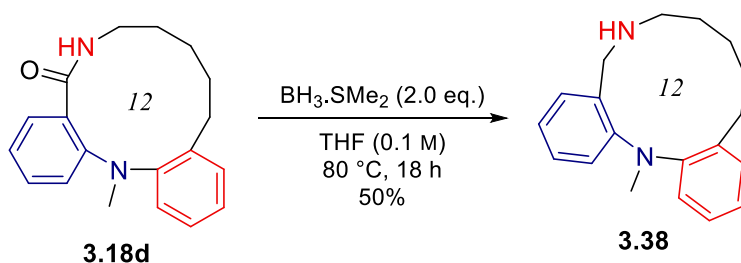
Post-functionalisation

To demonstrate the versatility of the medium-ring products obtained by Smiles ring expansion in a drug discovery context, further transformations of the amide function were investigated. Alkylation of the amide nitrogen with methyl iodide proceeded in excellent yield to form tertiary amide **3.36** (Scheme 54). However, attempts to functionalise the same medium-ring product to introduce a dimethylamino ethyl chain, as present in Dibenzepin, proved unsuccessful. The use of a chloro or triflate derivative of the alkylating agent led to no conversion to **3.37**, and the alkylating agent was recovered. When using the more activated alkyl iodide derivative (made by Finkelstein halogen exchange), no substrate was recovered, presumably because elimination of the iodine by the strong base occurred instead. Switching to a weaker base such as potassium carbonate did not improve, and instead initiated a reverse-Smiles ring contraction to anthranilamide **3.17b**.



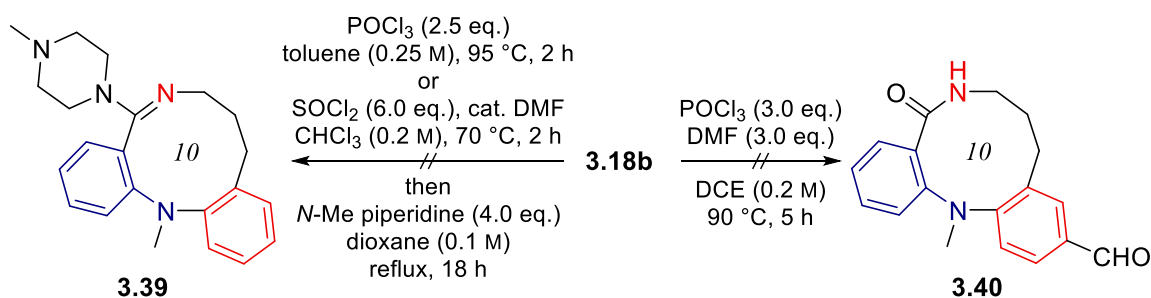
Scheme 54 : Alkylation of the medium-ring product amide

Reduction of the amide of **3.18d** to the respective amine did not proceed even under refluxing conditions with a large excess of lithium aluminium hydride in THF, but diamine **3.38** was obtained in good yield by reduction with borane dimethylsulfide while heating the reaction mixture in a sealed vial (Scheme 55). This reaction was optimised by Quentin Lefebvre.



Scheme 55 : Reduction of the medium-ring product amide

Introduction of an *N*-methyl piperazine amidine moiety to give **3.39**, as encountered in TCA, was attempted by nucleophilic attack of the amine at both the chlorimine, formed by treatment of **3.18b** with POCl₃, and by a thionyl chloride mediated formation of the nitrile (Scheme 56).



Scheme 56 : Diverse post-functionalisation of the medium-ring product

However, in both conditions, the reverse-Smiles ring contraction gave anthranilamide **3.17b** with full conversion. Similarly, attempted introduction of an aldehyde group on the aromatic ring by Vilsmeier–Haack reaction only yielded anthranilamide **3.17b**.

III.2.3. Intramolecular hydrogen bonding in the medium-sized ring products

Conformation of the medium-ring products in the solid state and in solution

Crystals of the medium-sized products suitable for X-ray analysis were obtained by either slow evaporation of a saturated solution of the corresponding compound in toluene, or by slow diffusion of pentane into a solution of the material in dichloromethane. A solid-state structure was obtained for each ring size, revealing the solid-state conformation of compounds **3.18a–d**, as well as **3.18l** and **3.18m** (Figure 25).

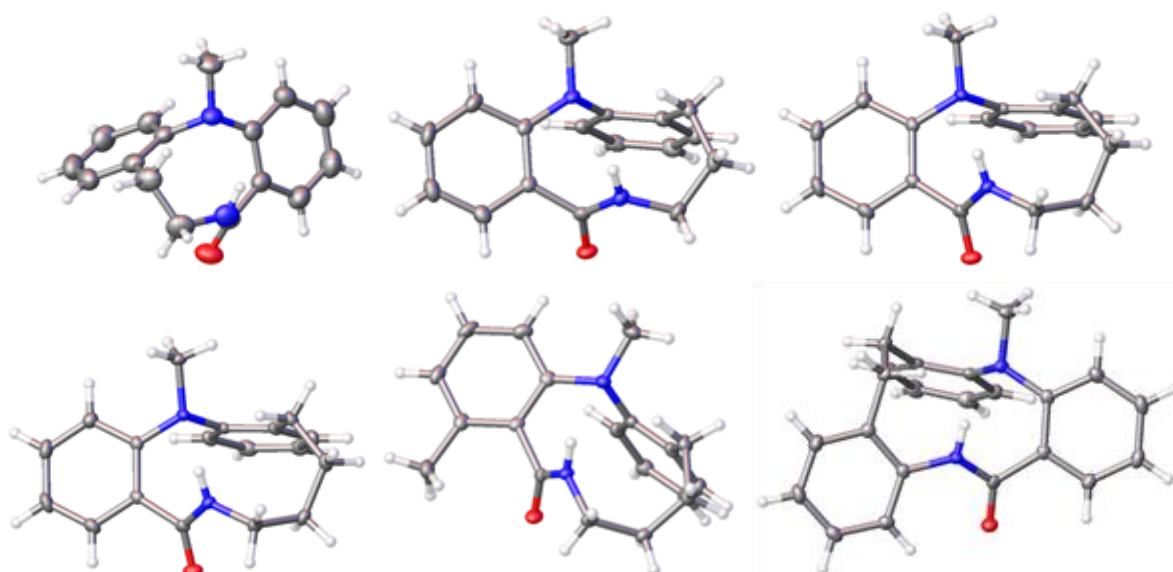


Figure 25 : Top left to bottom right: crystal structure of **3.18a**, **3.18b**, **3.18c**, **3.18d**, **3.18l**, and **3.18m**

The solid-state structures of the 9- to 12-membered compounds revealed great conformational intricacy, with the various substituents projected in all directions. Although not immediately obvious when represented by their structural formula, the medium-rings synthesised by this Smiles ring expansion have a complex, highly three-dimensional shape. Using the open-access computational tool ‘Lead-Likeness and Molecular Analysis’ (LLAMA) provided by the University of Leeds,^[179] the Principal Moment of Inertia (PMI) of each synthesised medium-sized heterocycle was plotted against the stripped down dibenzodiazepinone scaffold **3.41** (Figure 26). This descriptor measures the extent to which the scaffold has a rod-, disc- or sphere-shape, thereby indicating the three-dimensionality of a molecule. It is drawn as a ternary plot, with each vertex representing a model rod, disc or sphere (using butadiyne, benzene and adamantane, in the top-left, bottom and top-right corner, respectively). The closer to the ‘adamantane vertex’, the more spherical a molecule is. While natural products are usually spread all over the plot, with shapes often accumulating near the spherical vertex, synthetic drug-like molecules, often made by C_{sp^2} – C_{sp^2} coupling or amide bond formation, usually lie in the ‘rod’ or ‘discoid’ region, close to the axis.^[133] Dibenzodiazepinones themselves are not planar, as their central 7-membered ring is twisted, forcing the flanking aromatic ring outside of the plane in a typical

‘butterfly’ conformation. However, all medium-rings performed better than the reference scaffold, with a wide shape space coverage over the graph and shorter distances to the spherical vertex.^[125]

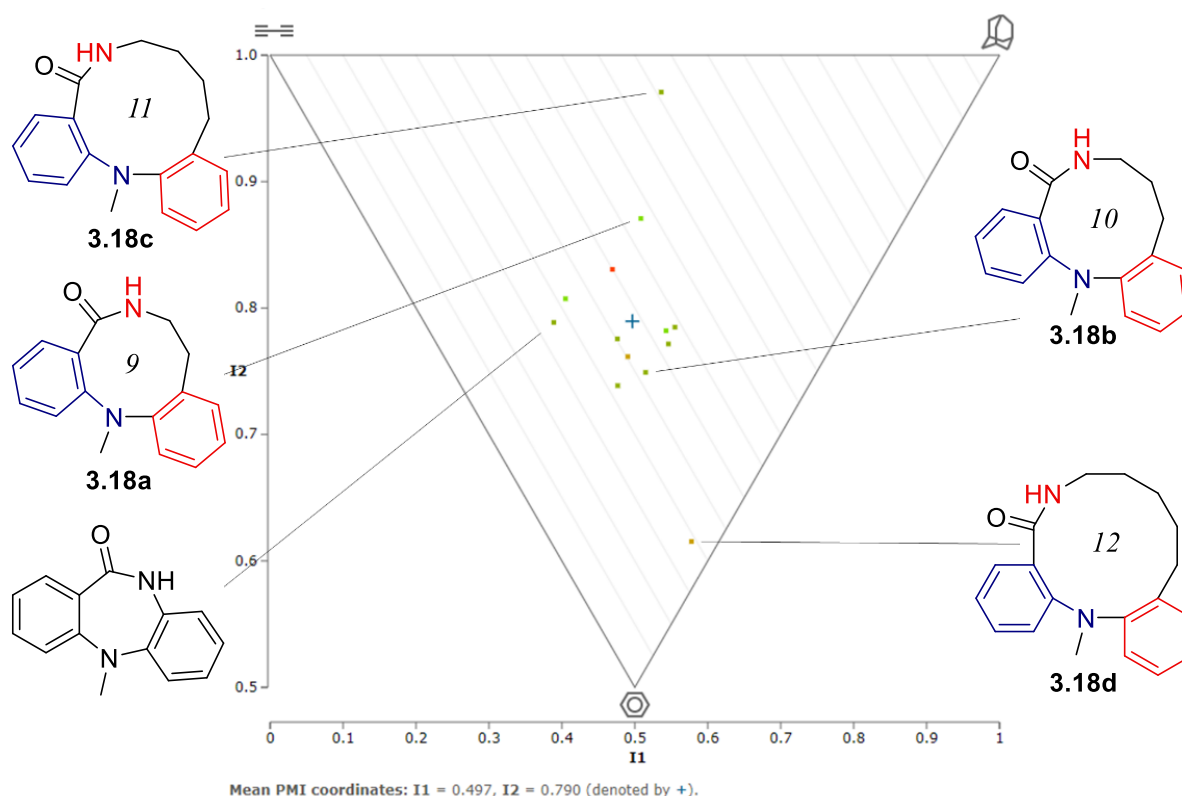
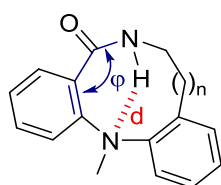


Figure 26: PMI plot of compounds 3.18a–d

The forcing conditions required to synthesise compound **3.18a**, which contains a 9-membered ring, can be explained by the deviation from planarity of its amide group. Its nitrogen atom possesses significant sp^3 character, evidenced by its pyramidalization constant being $\chi_N = 47.8^\circ$ and given that the sum of its bond angles is 343.4° .^[180,181] Moreover, while the C(O)–N bond torsion angle is moderate ($\tau = 23.4^\circ$), the dihedral angle between the amide group and the adjacent aromatic ring ($\vartheta_{Ar-C(O)} = 54^\circ$) prevents delocalisation. As depicted in the crystal structures, this behaviour seemed to ease in the larger rings, where the length of the methylene bridge has been increased (Table 22).



Entry	Compound	d_{N-H-N} (Å)	$\vartheta_{Ar-C(O)}$ (°)	δ_{N-H} (ppm)
1	3.18a	2.42	54	5.87
2	3.18b	2.72	58	6.46
3	3.18c	2.47	42	7.72
4	3.18d	1.95	1.3	9.10
5	3.18l	2.73	116	6.16

Table 22 : Some conformation parameters of the solid-state structure of 3.18a–d and 3.18l

Larger rings have a sharper angle between the amide and its adjacent aryl ring. Indeed, coplanarity is achieved in the 12-membered ring containing compound, **3.18d**. The amide hydrogen comes closer to the diarylamine nitrogen lone pair, suggesting the presence of a transannular hydrogen bond of varying strength depending of the ring size. Finally, the downfield shift of the N–H signal in the ^1H NMR spectra of the products **3.18a–d** in CDCl_3 from 6.46 to 9.10 ppm when increasing ring size also indicated a progressively stronger hydrogen bond.

DMSO titration

The intramolecular hydrogen bonding can be measured by ^1H NMR by titration with $\text{DMSO-}d_6$ of a solution of the compound in a non-hydrogen-bonding solvent such as CDCl_3 . Increasing the proportion of $\text{DMSO-}d_6$ in solution leads to interaction between the sulfoxide oxygen and the amide hydrogen, resulting in deshielding. However, if the amide is already participating in an intramolecular hydrogen bonding network, little to no change should be observed. ^1H NMR spectra of solutions of 10 to 15 mg of compounds **3.18a–d** in 600 μL CDCl_3 were recorded after addition of known amounts of $\text{DMSO-}d_6$ (%v/v) (Figure 27). The chemical shift of the N–H signal was monitored, and its variation was plotted against the percentage of $\text{DMSO-}d_6$ in the sample.

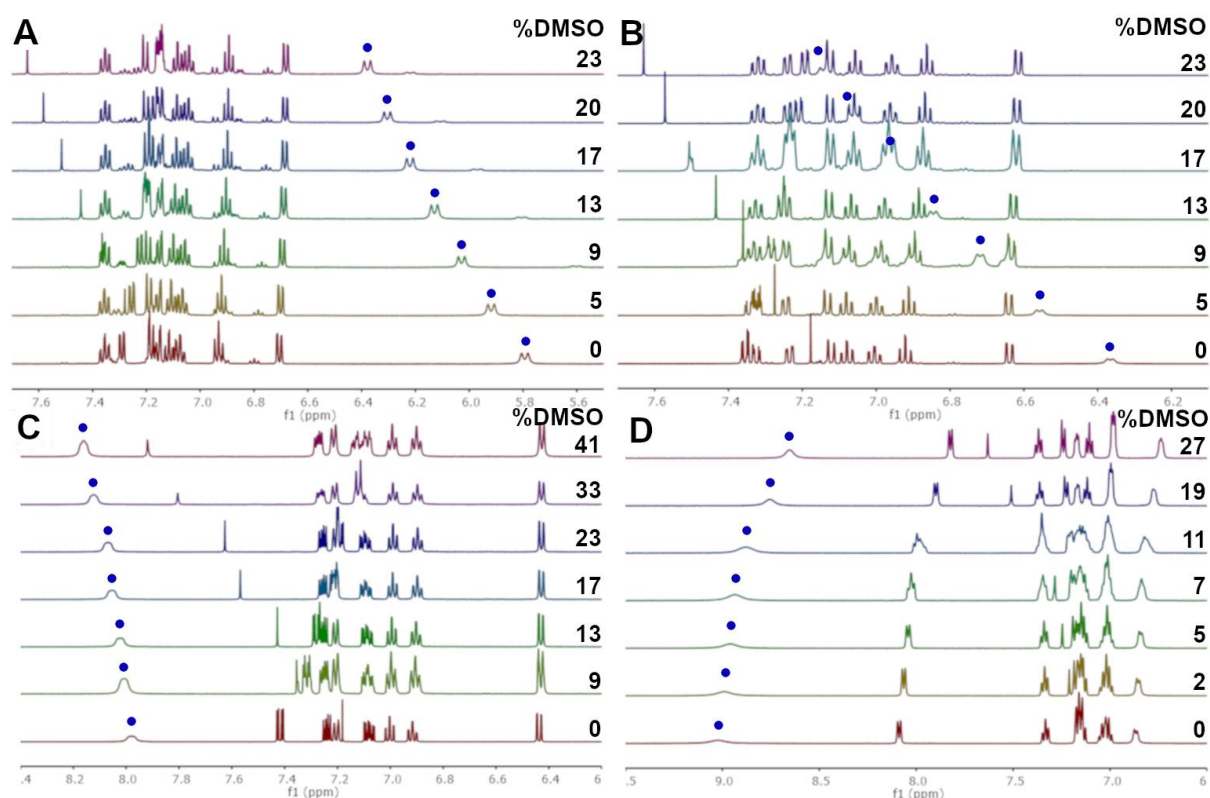


Figure 27 : $\text{DMSO-}d_6$ titration of CDCl_3 solutions of A: **3.18a**, B: **3.18b**, C: **3.18c** and D: **3.18d**. The amide proton is denoted by a blue spot.

Addition of DMSO- d_6 resulted in a strong downfield shift of the N–H signal of 9-membered **3.18a** and 10-membered **3.18b** (Figure 3-10), while hardly any shift was observed for 11-membered compound **3.18c**, and compound **3.18d** exhibited a moderate upfield shift.

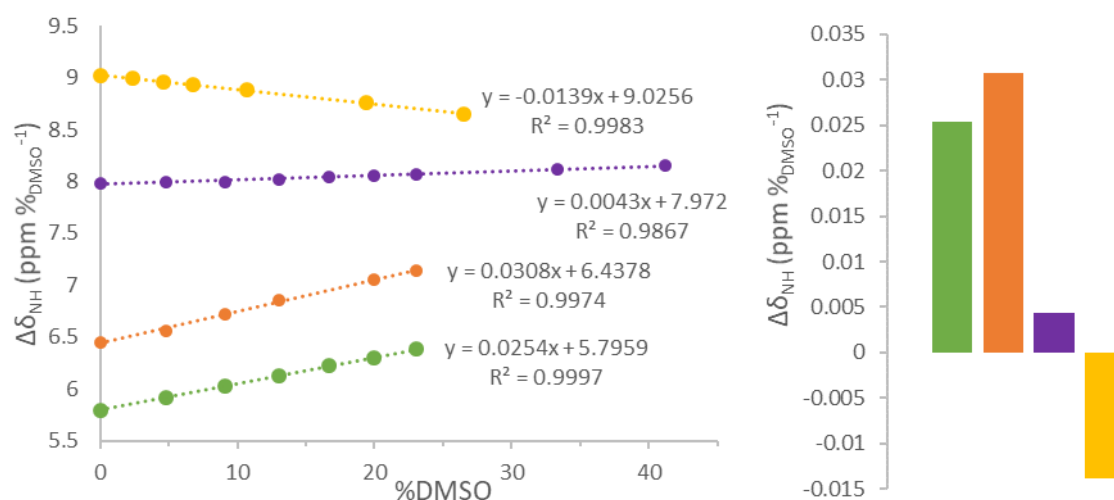


Figure 28 : N–H chemical shift drift of compounds **3.18a**–**d**. Green: **3.18a** ; Orange: **3.18b** ; Purple: **3.18c** ; Yellow: **3.18d**

These results suggest the persistence of an intramolecular hydrogen bond in solution in some medium-ring products. Flexible substrates **3.18c** and **3.18d**, in which the ^1H NMR N–H signal was not affected by DMSO- d_6 , are involved in a strong intramolecular hydrogen bond. However, the smaller rings in **3.18a** and **3.18b** are presumably too strained to accommodate this bond, as seen by the large dihedral angle of the amide group and the long distance between the amide hydrogen and the diarylamine nitrogen lone pair.

Quantifying rates of enantiomerisation by dynamic ^1H NMR

^1H NMR of all medium-ring products **3.18** showed diastereotopic signals for the methylenes chain within the ring, indicating that these heterocycles adopt chiral ground states whose enantiomeric conformations interconvert slowly on the NMR time scale. Variable-temperature ^1H NMR analysis of compounds **3.18b** and **3.18c** in DMSO- d_6 resulted in significant broadening of these signals (Figure 29). But without coalescence even at 100 °C, calculation of the barrier to enantiomerisation by line-shape analysis was precluded.

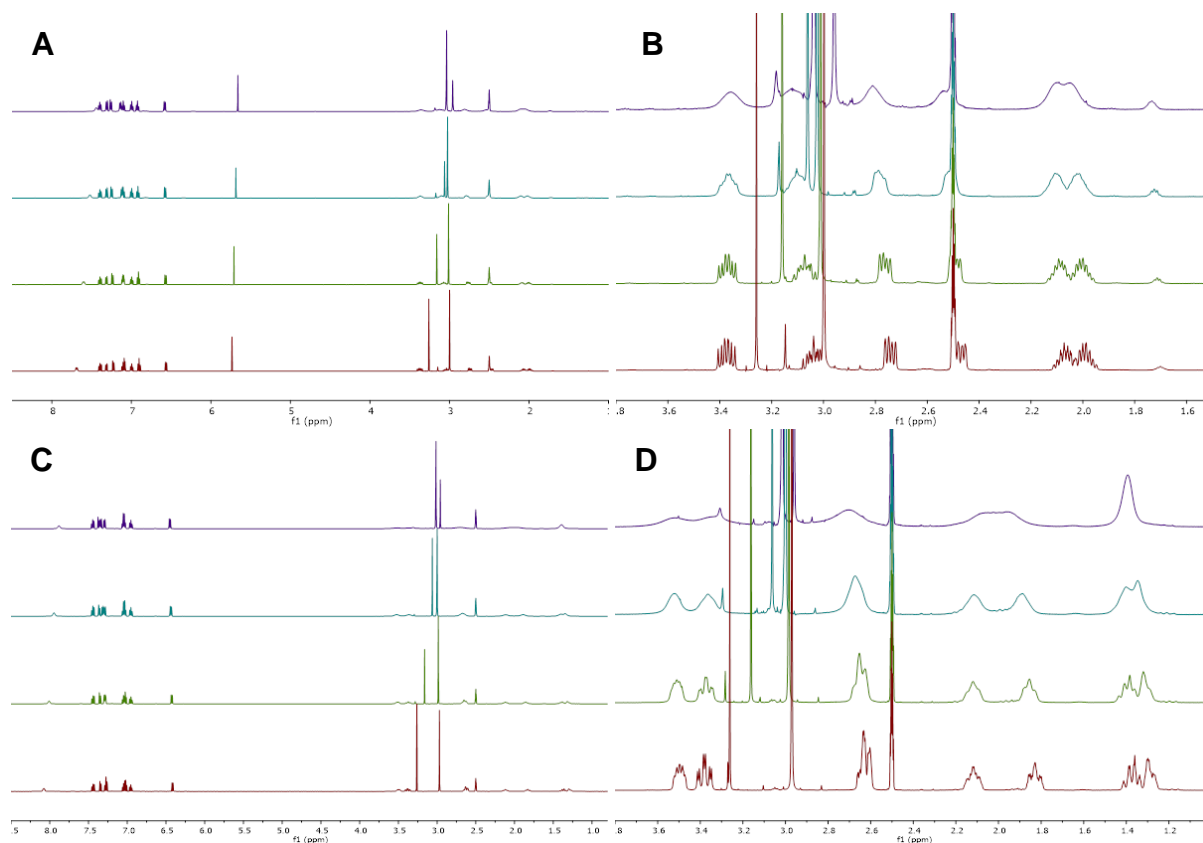


Figure 29 : ^1H NMR (500 MHz) at 100 °C of A: **3.18b** and C: **3.18c** and zoom in the alkyl region of C: **3.18b** and D: **3.18c** respectively, in $\text{DMSO-}d_6$.

However, rate constants of enantiomerisation of compounds **3.18a–d** and **3.18l** could be determined by variable-temperature exchange spectroscopy (VT-EXSY), a 2D-NOE experiment commonly used to calculate rates of conformational exchange. After excitation by a ^1H pulse, the sample is left to stand for a given mixing time before the ^1H spectrum is recorded. During this period, if interconversion occurs, a cross peak will appear for the exchanging protons (Figure 30), proportional to the mixing time and the rate of exchange (in this case, the rate of exchange equals the rate of enantiomerisation). For two equally populated sites with equal spin-lattice relaxation times, the rate of exchange k is calculated using the Equation 7, with τ the mixing time and r the ratio of the cross-peak integral to the diagonal peak integral:^[182]

$$e^{-\tau/2*k} = \frac{1-r}{1+r}$$

Equation 7: Calculation of the rate of exchange by ^1H EXSY NMR

For unequal populations such as in diastereomerisation processes, the equation becomes too complex to manually calculate rates of interconversion. For convenience, the software EXSYCalc by MestreLab was used to calculate these kinetic parameters.

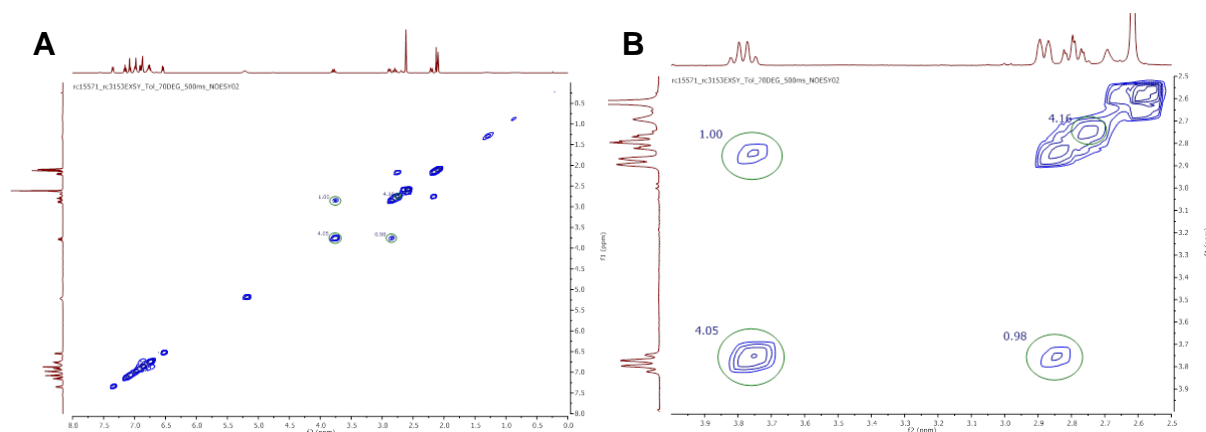


Figure 30 : A: ^1H NMR EXSY spectrum of **3.18a** in toluene- d_8 at 60 °C, 0.5 s mixing time, B: 2.5-4.0 ppm region.

Once suitable temperature T and mixing time were identified, two additional experiments at $(T + 5)$ K and $(T - 5)$ K were performed, and the rate of enantiomerisation at room temperature was calculated from an Eyring plot (Equation 4, Table 23).

Entry	Compound	Solvent	k_{enant} (s^{-1})	$\Delta G^\ddagger_{298\text{ K}}$ (kJ mol^{-1})	$t_{1/2\ 298\text{ K}}$ (s^{-1})
1	3.18a	DMSO- d_6 /CD $_3$ OD	—	—	—
2		Toluene- d_8	8.2×10^{-3}	84.9	42.3
3	3.18b	DMSO- d_6	7.4×10^{-3}	85.1	47.1
4		CDCl $_3$	1.9×10^{-3}	88.5	180.9
5	3.18c	DMSO- d_6	1.6×10^{-1}	77.5	2.1
6		CDCl $_3$	1.6×10^{-2}	83.2	21.6
7	3.18d	CD $_3$ OD	30.7	63.5	0.011
8		CDCl $_3$	3.6	69.2	0.076
9	3.18l	DMSO- d_6	4.9×10^{-2}	80.4	7.0
10		CDCl $_3$	3.1×10^{-2}	81.6	11.1

Table 23 : Barrier to enantiomerisation of **3.18a–d** and **3.18l** in different solvents

Large differences in the rate of enantiomerisation arise when varying the medium-ring size. In CDCl $_3$, the largest 12-membered ring **3.18d** inverts almost 300 times faster than 11-membered **3.18c** and more than 2000 times faster than 10-membered **3.18b**. This trend changes with **3.18a**, which presumably inverts faster than **3.18b** because of the raised ground-state energy of its non-planar amide. Interestingly, 11-membered rings **3.18l** and its analogue **3.18c** have similar rate of enantiomerisation despite the increase in steric hindrance provided by the *ortho*-methyl group in **3.18l**. The latter is the only compound to see its barrier to enantiomerisation hardly affected by solvent polarity.

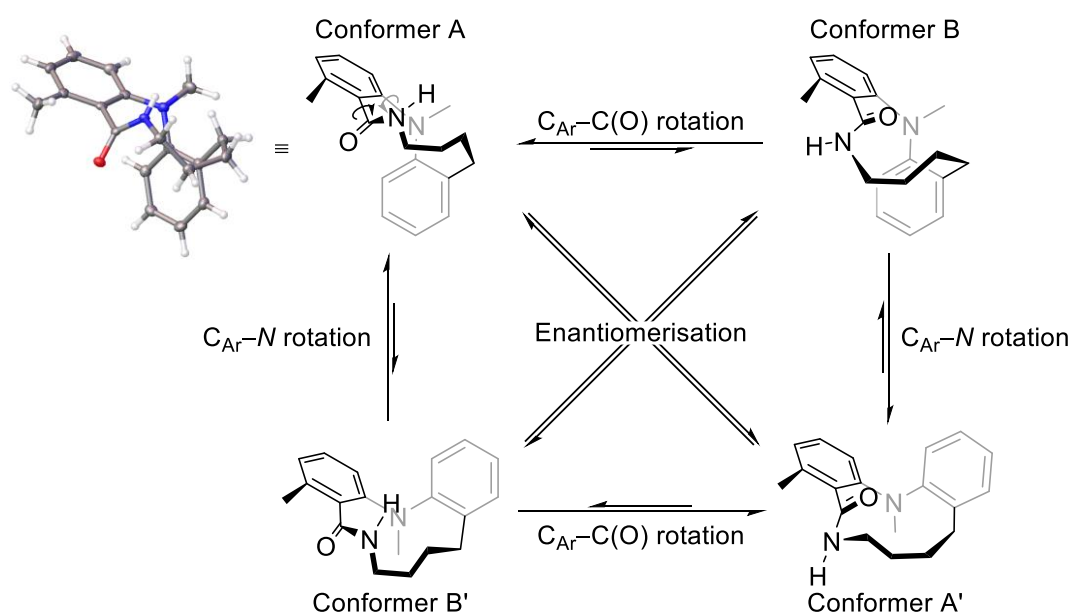
For **3.18b–d**, a strong dependence on the nature of the solvent can be seen on the rates to enantiomerisation. The rate of enantiomerisation of 11-membered compound **3.18c** is decreased tenfold in the hydrogen bond donating solvent DMSO-*d*₆, suggesting that the intramolecular hydrogen bond governs the conformational stability of this compounds. These dramatic changes in the rate of conformational exchange correlate with the data on hydrogen-bonding deduced from the crystal structures and DMSO titrations, as barriers to enantiomerisation in larger rings **3.18c** and **3.18d** are more sensitive to solvent polarity than in **3.18b**. Unfortunately, cross-peak overlaps precluded the calculation of barriers to rotation of compound **3.18a** in polar solvents.

Compound **3.18a** also showed another interesting feature in its ¹H NMR spectrum. Another set of peaks, attributed to a minor diastereoisomeric conformers, can be observed in different ratios when varying the solvent. This minor conformer is less abundant in toluene-*d*₈ or CDCl₃ (ratios of 7:1 and 6:1, respectively) than in CD₃OD and DMSO-*d*₆ (ratios of 3:1), indicating that the major conformer of **418a** is somewhat stabilised by an intramolecular hydrogen bond.

Similarly, **3.18l** exists as a pair of inequivalent conformers in ratios of 3:1 in toluene-*d*₈, 4:1 in CDCl₃ and 10:1 in CD₃OD, displaying contrasting behaviour to **3.18a**. This trend shows that while the *ortho*-methyl group forces a perpendicular twist in the amide of **3.18l**, the central 11-membered ring is flexible enough to allow an intramolecular hydrogen bond in solution, although only in the minor conformer. While the existence of two pairs of diastereoisomeric conformers in **3.18a** may be due to the rigidity of the scaffold, an *ortho*-methyl group in the flexible 11-membered scaffold probably slows down bond rotation of the adjacent amide.

Quantifying rates of diastereoisomerisation by dynamic ¹H NMR

These interconverting diastereomers presumably exist from the two relative orientations of the C_{Ar}–C(O) and C_{Ar}–N bonds highlighted in Scheme 57. The crystal structure of compound **3.18l** (Figure 25) shows that the amide moiety is almost perpendicular to the aryl ring, and a strong downfield shift of the N–H signal from 6.12 ppm in CDCl₃ to 7.84 ppm in DMSO-*d*₆ indicates that the intramolecular hydrogen bond in **3.18l** is weaker than in **3.18c**.



Scheme 57 : Interconversion of **3.18I**

However, **3.18I** possesses a similar barrier to enantiomerisation as compound **3.18c** (Table 23). As cross-peaks for the interconversion of the diastereomeric conformers of **3.18a** and **3.18I** were visible by EXSY NMR, their barriers to diastereomerisation in solvents with both low and high dielectric constant were calculated at room temperature (Table 24). As exchange is no longer equally populated, a short mixing time was selected to obtain an EXSY spectrum containing no cross-peaks, and diastereomeric ratio at slow exchange was compared to cross-peaks as fast exchange at various temperature. The data obtained from EXSYCalc was used to calculate the free energies of activation at room temperature using an Eyring plot (Equation 4).

Compd.	Solvent	$k_{\text{min-maj}} (\text{s}^{-1})^{\text{a}}$	$k_{\text{maj-min}} (\text{s}^{-1})^{\text{b}}$	$\Delta G^{\ddagger}_{\text{min-maj}} (\text{kJ mol}^{-1})^{\text{a}}$	$\Delta G^{\ddagger}_{\text{maj-min}} (\text{kJ mol}^{-1})^{\text{b}}$
3.18a	CD ₃ OD	$3.3 \cdot 10^{-1}$	$9.9 \cdot 10^{-2}$	75.8	78.7
	Toluene- <i>d</i> ₈	$3.1 \cdot 10^{-1}$	$3.5 \cdot 10^{-2}$	75.9	81.3
3.18I	DMSO- <i>d</i> ₆	$5.2 \cdot 10^{-4}$	$2.2 \cdot 10^{-4}$	91.7	93.9
	CDCl ₃	$8.3 \cdot 10^{-3}$	$2.6 \cdot 10^{-3}$	84.8	87.8

Rates and free energies of activation for conversion of the ^a minor-to-major and ^b major-to-minor conformer, at 298 K.

Table 24 : Barrier to diastereomerisation of **3.18a** and **3.18I** in different solvents

While the rate at which the minor diastereomer of **3.18a** converts to the major shows no dependence on the solvent, the rate of the reverse process is three times as fast in CD₃OD. This suggests that the major conformer can accommodate some interaction by intramolecular hydrogen bonding, stabilising its ground state.

Unlike compound **3.18a**, diastereomerisation of compound **3.18I** is slower than enantiomerisation by a factor of almost four in CDCl₃ and up to a hundred in DMSO-*d*₆. The rates of diastereomerisation of

compound **3.18I** (unlike those of enantiomerisation) are strongly solvent-dependent. Both the forward and reverse rate of enantiomerisation is decreased in DMSO-*d*₆ relative to CDCl₃. Because of the perpendicularity of the amide group and the adjacent aryl ring, diastereomerisation must occur through a transition state in which these two groups are coplanar. In non-hydrogen bonding solvents such as CDCl₃, the barrier to diastereomerisation is lowered by a transient transannular hydrogen bond between the amide proton and the diarylamine nitrogen. In DMSO-*d*₆, the relative energy of transition state becomes less favourable, decreasing the rate of enantiomerisation by more than a tenfold. Unlike compound **3.18a**, for which enantiomerisation occurs through stepwise bond rotation, these higher values for diastereomerisation compared to enantiomerisation suggest that racemisation of compound **3.18I** occurs through geared rotation of the C_{Ar}–C(O) and the C_{Ar}–N bonds.

III.3. Conclusion

Smiles ring expansion of anthranilamides provides medium-size heterocyclic analogues of pharmacologically-relevant dibenzodiazepinones. The use of microwave heating reduces reaction time to 15 minutes and decreases the amount of side-product formed, delivering 9- to 12-membered rings in good to excellent yields. The reaction tolerates sensitive functional groups and can be performed in a renewable solvent. However, no heterocycle could be introduced in the scaffold, and the nucleophilic nitrogen substitution could not be altered. Furthermore, post-functionalisation of the motif was difficult due to either underactivity or decomposition in a reverse-Smiles ring contraction.

The product thus formed possess a transannular hydrogen bond resulting in ‘hidden hydrophilicity’ properties. Ring size or steric hindrance close to the amide group can modulate the strength of this hydrogen bond to control the stereodynamic properties of the medium-sized heterocycles, making this class of compounds a versatile tool of drug development. Furthermore, conformational diastereomers were observed in smaller structures or with bulky substituents. Two different diastereomerisation pathways were found, depending on the nature of the medium-ring.

Chapter 4

Towards Axially Chiral Diarylamine Pincer Ligands

IV.1. Introduction

Careful ligand design in transition metal-mediated catalysis can ameliorate the performance of a catalytic system by improving the activity of a complex, resulting in higher turnover number or lower catalyst loading.^[183] Catalyst stability and selectivity, however, should not be impaired. Pincer ligands are tridentate ligands with a well-defined bonding to the metal centre, discovered by Shaw *et al.* more than forty years ago.^[184] Their donors occupy adjacent binding sites in a metal centre, with a preference for a meridional geometry.^[185] Compounds such as **4.1** (Figure 31),^[184] comprising of an aryl carbanion flanked by two side arms bearing soft donors, are a common class of pincer ligands. These compounds are termed PCP in reference to the three chelating atoms. The strong σ metal-carbon bond, together with the structural rigidity brought to the structure by the chelating side arms make these complexes particularly stable, as dissociation of the metal and further decomposition of the complex is reduced.^[186] Hence, while these complexes can react with external ligands to catalyse various reactions, coordination of the ligand is retained even at high temperatures. This results in better performances in reactions requiring notoriously harsh conditions in which catalyst stability might be compromised, such as Heck couplings or alkane dehydrogenation.^[187]

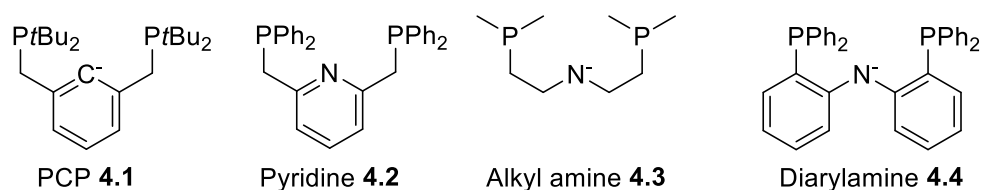


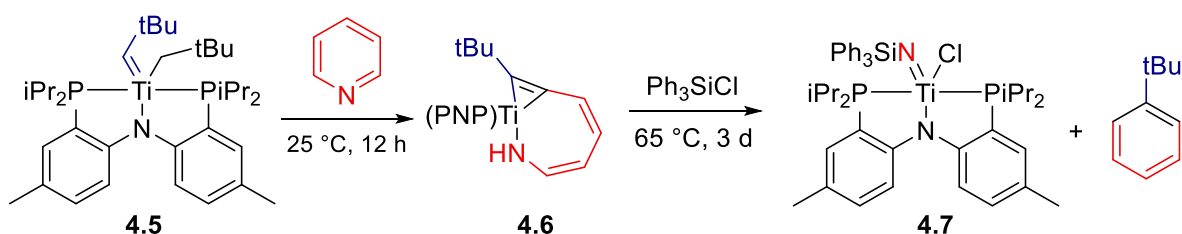
Figure 31: Some selected phosphine-based pincer ligands^[183]

Variation of the nature of the donor atoms leads to modification of the properties of the pincer complex. PNP ligands, with a central amine donor, are much stronger σ -bond donors than PCP ligands, leading to a weaker *trans* influence on the free binding site of the metal.^[186] The nitrogen atom can be neutral in the case of pyridines,^[188] or anionic for dialkyl^[189] and diarylamines.^[190,191] The conjugated system in **4.1**, **4.2** and **4.4** allows dearomatisation of the pincer complex by delocalisation, meaning these compounds can participate in redox reactions.^[192] The hard amine-based donor, together with the soft phosphine donors, allow PNP ligands to bind both hard (early) and soft (late) transition metal centres.^[183] Phosphine donors are not the only functionalities which can be introduced on the wingtips, and the catalytic properties of the metal centre can be fine-tuned by modification of these moieties. Design alteration of the ligand permits versatility in the modification of the electronic properties of the complexes and of the σ -bond donation ability of the chelating groups, as well as adjustment of the local steric demand.^[193]

IV.1.1. Diarylamines as pincer ligands

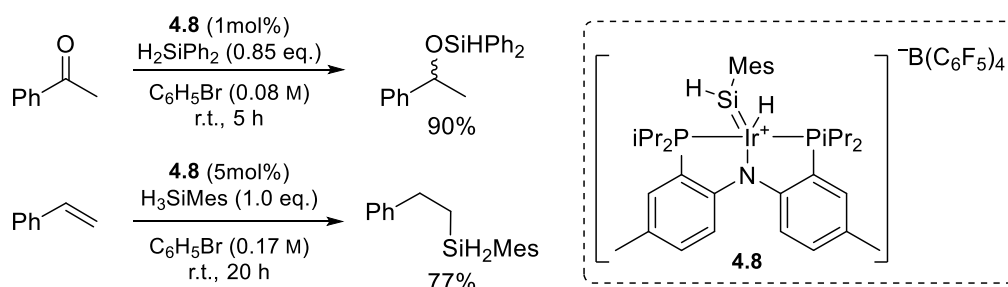
Problems arise from the use of amido ligand **4.3**; the high flexibility of the scaffold allows rapid association/dissociation of the phosphine groups to the metal centre and exchange between a *mer* and *fac* arrangement, leading to poor definition of the complex.^[191] Furthermore, the β -hydrogens makes the ligand more prone to decomposition at high temperatures. To overcome these issues, diarylamine PNP ligand **4.4** was independently introduced by Mayer, Kaska,^[190] and Liang.^[191] This novel scaffold confers rigidity to the planar complex, with the sp^2 nitrogen π -donating electrons to the aromatic system.^[191]

Bisphosphines such as **4.4** were the first diarylamines reported as pincer ligands and are probably the most studied. Complexes of these substrates with transition metals have been observed for group 8 (Ru^[194] and Fe^[195]), group 9 (Rh,^[196] Ir,^[197] and Co^[195]), and group 10 elements (Ni,^[191] Pd,^[198] and Pt^[199]), but also with main group elements such as P(III).^[200] Unusual alkylidene complexes of group 4 elements such as Hf,^[201] Ti^[202] or Zr^[203] (Schrock carbenes) can be prepared with these ligands. The particular reactivity of these complexes was demonstrated by Mindiola.^[202,204] In pyridine, titanium alkylidene **4.5** extrudes neopentane to generate a transient titanium alkylidyne which reacts with pyridine by ring opening metathesis (Scheme 58). Treatment of metallazaabicyclo **4.6** with a silyl monochloride results in denitrogenation and formation of *tert*-butyl benzene by insertion of the corresponding olefin group.



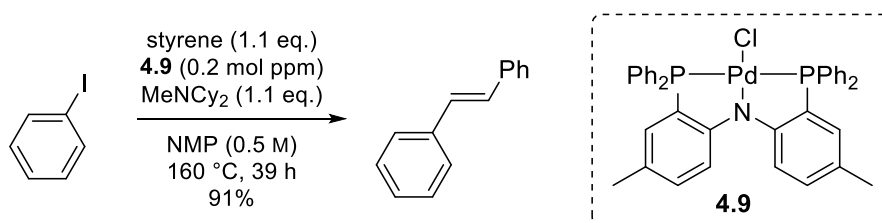
Scheme 58: Ring opening metathesis of pyridine by a diarylamine-based titanium alkylidyne^[204]

Despite thorough investigation of diarylamine-based PNP complexes, only a few catalytic applications have been described thus far. The cationic, PNP-supported iridium complex **4.8** is a precatalyst for the hydrosilylation of alkenes^[205] and ketones^[206] (Scheme 59). The addition to the alkene occurs with full anti-Markovnikov selectivity by direct insertion of a Si-H bond, in an analogous manner to that in hydroboration. The authors also suggest that the complete regioselectivity is owed to the large steric demand of the complex.^[197] The reactivity of complex **4.8** is also unique for the hydrosilylation of ketones as this reaction usually require high oxidation states and coordination numbers at the iridium centre.^[206] This can be attributed to both a Lewis acidic silylene ligand and a Lewis base amido nitrogen participating in the delivery of the reactive hydride species.



Scheme 59: Hydrosilylation of alkenes and ketones by a PNP supported iridium complex^[205,206]

The superior stability and activity of pincer ligands was demonstrated by Liang and co-workers with diarylamine based PNP palladium ligand **4.9** in the Heck reaction of styrene with aryl iodides and aryl bromides (Scheme 60).^[207] The high activity of this complex allowed the use of catalyst loadings as low as 0.2 mol ppm in the synthesis of 1,2-diphenylethene, with catalyst turn-over number (TON) as high as 4,500,000 – one of the highest reported to date.^[208]

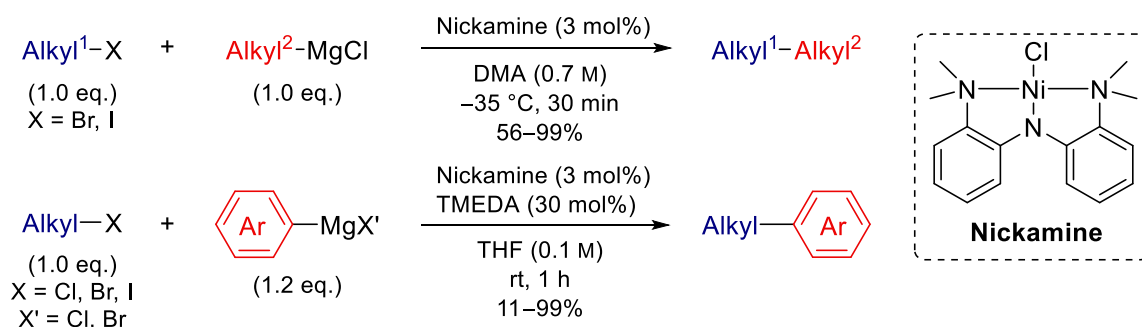


Scheme 60: Heck reaction using sub-ppm level of pincer complex^[207]

Nickel complexes of PNP ligands have been used in the cross-coupling of alkyl and aryl halides with Grignard reagents (Kumada coupling). The reaction, catalysed by nickel-pincer complexes, proceeded at ambient temperature, preventing decomposition of the catalyst.^[209] The particular strength of the pincer complex is the absence of β -hydrogen elimination in the reaction conditions, which was kinetically allowed but thermodynamically disfavoured, allowing the coupling of saturated substrates.^[210] However, while PNP ligands catalyse the cross coupling of aryl Grignard reagents with aryl iodides in excellent yield, the use of alkyl Grignard reagents leads to a significant formation of homocoupling by-products.^[211] Investigation of the reaction mechanism suggested the existence of a Ni(III)/Ni(IV) redox cycle.^[212] Stabilisation of the highly reactive Ni(IV) intermediate was thought to be improved by replacement of the phosphine wingtips with harder donors. Diarylamines are also redox active, non-innocent ligands, providing access to otherwise unstable oxidation states at the metal centre.^[212] Following this concept, a NNN nickel pincer complex coined Nickamine by Hu and co-workers, was developed and found to be particularly active for the Kumada reaction.^[213,214]

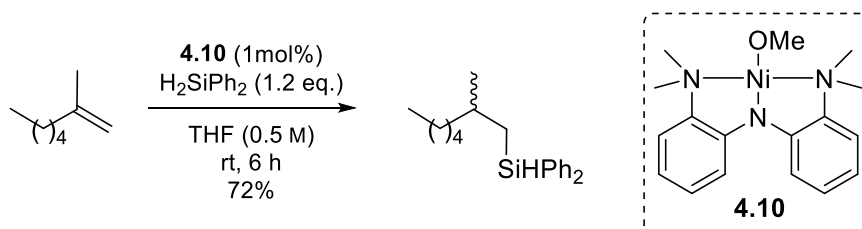
Replacing phosphine donors with dimethylamino groups proved to be beneficial for the development of a highly tolerant Kumada coupling, even on substrates containing β -hydrogens (Scheme 61). The coupling of non-activated alkyl halides with alkyl Grignard reagents occurred at low temperature and in short reaction time,^[214] while the use of aryl Grignard reagents necessitated the use of an additive

and warming the reaction mixture to room temperature.^[213] The reaction tolerated a large variety of functional groups, even those which are prone to side reaction with the highly nucleophilic and basic Grignard reagents. Functionalized aryl and heteroaryl Grignard reagents were also tolerated, a feature which previously necessitated cross coupling with organozinc, boron, or silicon compounds, most of which to be prepared from the related Grignard reagent.^[215]



Scheme 61: A NNN nickel pincer complex active for the Kumada reaction^[213,214]

The marked activity of Nickamine was also demonstrated in the coupling of alkyl halides with terminal alkynes^[216] (Sonogashira coupling) as well as with alkynyl Grignard reagents,^[217] and for the alkylation of heterocyclic C–H bonds with alkyl halides.^[218] A diarylamine precatalyst **4.10**, analogous to Nickamine, was also found to be active in the highly selective, anti-Markovnikov hydrosilylation of *gem* alkenes (Scheme 62).^[219]



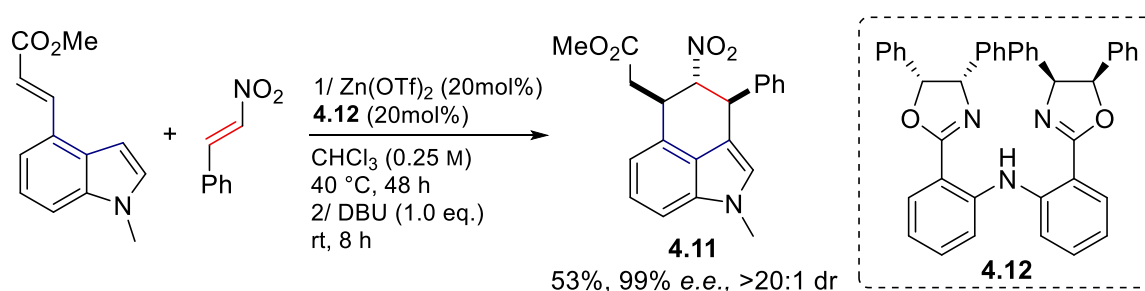
Scheme 62: A NNN nickel pincer complex active for the hydrosilylation of alkenes^[219]

IV.1.2. Diarylamine pincer ligands in asymmetric catalysis

The side arms of pincer complexes are not free to rotate.^[193] This means that substituents on sp^3 atoms in the vicinity of the wingtips will be projected into geometrically defined quadrants, offering a well-defined conformation at the catalytic centre.^[192] Many approaches have used other classes of pincer compounds to introduce enantiodifferentiation by incorporating chirality in the bridging units,^[220] namely P-stereogenic compounds^[221] or pendant chiral units.^[222] However, only one class of diarylamine-based chiral pincer ligands have emerged so far, using chiral oxazoline side arms as two flanking lone-pair donors (BOPA).^[223] Conveniently, BOPA derivatives can be easily assembled by Buchwald–Hartwig coupling,^[224] or modular synthesis can be performed from the corresponding

carboxylic acid by amide coupling with an amino alcohol, followed by zinc-promoted cyclisation to obtain a vast collection of BOPA derivatives with various chiral groups.^[225]

Zinc complexes of BOPA ligands have been widely applied in the asymmetric Friedel–Craft alkylation of heterocycles with Michael acceptors such as nitroalkenes. The Du group reported the highly enantioselective alkylation of pyrroles,^[226] indoles,^[227] and 2-methoxyfurans,^[222] and developed a reusable catalyst supported on dendrimers.^[228] The Guiry group developed a highly enantioselective one-pot Friedel–Craft alkylation/Michael addition of functionalised indoles with nitroalkenes *en route* to ergoline derivatives (Scheme 63), obtaining heterocyclic structure **4.11** containing three contiguous chiral centres in perfect diastereocontrol and enantioselectivity.^[229]



Scheme 63: Highly enantioselective one-pot Friedel–Craft alkylation/Michael addition of indoles^[229]

BOPA ligands have been used for asymmetric catalysis using a variety of transition metal centres as catalysts. The enantioselective hydrosilylation of ketones was performed using either iron or cobalt complexes with BOPA ligands, providing enantioenriched secondary benzyl alcohol after work-up.^[230] The Ward group used BOPA ligands in the calcium-catalysed enantioselective hydroamination of amino-olefins. While the enantiomeric excesses reported were moderate, BOPA ligands provided a significantly higher degree of selectivity compared to other reported calcium systems.^[231] Guiry *et al.* disclosed a chromium(III)-catalysed homoallenylation of aldehydes (also known as the Nozaki–Hiyama–Kishi reaction) proceeding in excellent regio- and enantioselectivity, using a diarylamine–chromium complex.^[232] Interestingly, the use of a pincer ligand improved the regioselectivity compared to TMEDA.

IV.1.3. Twisted conformation in pincer ligands

It has largely been accepted that the particular stability and activity of pincer ligands is due to the rigidity of their backbone, forming a tightly bound complex with the metal centre and preventing ligand dissociation.^[185] However, the planarity associated with pincer ligands can sometimes be plagued with poor solubility.^[233] Examples involving a twisted conformation in diarylamine-based pincer ligands have been scarce. In fact, to the best of our knowledge, only one C_2 -symmetric diarylamine ligand has been reported by Ozerov *et al.*^[234] Building on the superior results of tied pincer

ligands **4.13** over diarylamine **4.14** in the rhodium-catalysed dimerization of alkynes,^[235] the authors tested the effect of steric constraint over a non-fused scaffold (Table 25).

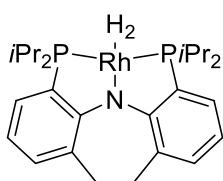
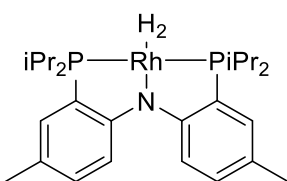
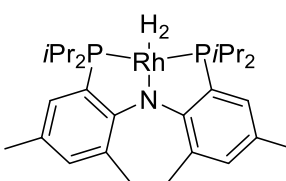
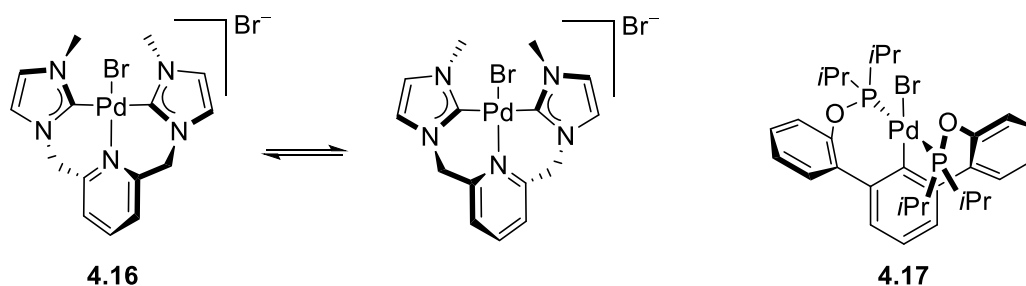
$\text{pTol}-\text{C}\equiv\text{C}-\text{H} \xrightarrow[\text{C}_6\text{D}_6]{\text{Catalyst}} \text{pTol}-\text{C}(\text{CH}_3)=\text{C}(\text{C}\equiv\text{C}-\text{pTol}) + \text{pTol}-\text{C}(\text{CH}_3)=\text{C}(\text{C}\equiv\text{C}-\text{C}(\text{CH}_3)=\text{C}(\text{CH}_3)-\text{pTol}) + \text{oligomers}$ <div style="display: flex; justify-content: space-around; align-items: center;"> <div style="text-align: center;">  <p>4.13</p> </div> <div style="text-align: center;">  <p>4.14</p> </div> <div style="text-align: center;">  <p>4.15</p> </div> </div>					
Entry	Catalyst	<i>T</i> (°C)	<i>t</i> (h)	Conversion	Ratio A:B:C
1	4.13 (0.5 mol%)	100	7	98%	2:98:0
2	4.14 (0.5 mol%)	100	120	85%	2:98:0
3	4.15 (1.0 mol%)	80	70	74%	2:73:25

Table 25: Influence of conformation of PNP pincer ligands on alkyne dimerization

Unfortunately, this hypothesis did not prove to be valid. While tied ligand **4.13** provides full conversion to a single *E* alkene product in a short reaction time, **4.15** is as sluggish as **4.14**. The authors showed that, using **4.15**, a similar degree of conversion could be achieved in a shorter reaction time versus **4.14**, albeit with double the catalyst loading. But **4.15** suffers from poor selectivity, as oligomers **C** arise from the formation and further reactivity of *gem* alkene **A**.

Crabtree *et al.* designed CNC ligand **4.16** which supports a methylene linker between the NHC side arms and the pyridine core (Scheme 64).^[233] As a consequence of the fused ring/metallacycle system, the methylene bridges sit outside of the plane while the ligands still tightly bind palladium(II) in a square-planar fashion. The resulting ligand is chiral, rapidly interconverting, with a barrier to interconversion $\Delta G^\ddagger_{278\text{ K}} = 52.9\text{ kJ mol}^{-1}$ in CDCl_3 .^[233] The interconversion was reported to take place through a stepwise mechanism where no planar transition state was found.^[236] As compound **4.16** was still extremely active for the Heck coupling of aryl chlorides, achieving full conversion using only 0.2 mol% of catalyst, the authors demonstrated that planarity is not necessary in the design of pincer ligands with high activity.^[233]



Scheme 64: Interconversion of a fluxional pincer complex

Compound **4.16** forms two six-membered palladacycles, more likely to be fluxional due to their higher flexibility, but others also described pyridine-based PNP ligands of which a twisted, chiral iridium complex forms two fused, rapidly interconverting puckered 5-membered metallacycles.^[237] Similarly, compound **4.17** is a highly twisted pincer complex forming two fused 7-membered metallacycles.^[238] Complex **4.17** was highly active for the Suzuki-Miyaura coupling of sterically hindered aryl chlorides under mild conditions.^[238]

Hence, this lack of prerequisite for planarity of pincer ligands supports investigation of axial chirality in the scaffolds. No work has been reported on stable, atropisomeric axially chiral in pincer ligands and their application to asymmetric catalysis.

IV.2. Results and discussion

IV.2.1. Aim

Based on the results presented in Chapter 2, it is now known that large steric hindrance can produce conformationally stable, axially chiral diarylamines. Induction of enantioselectivity with diarylamine-based pincer ligands has only been performed using pendant oxazolines as a chiral unit for enantiodifferentiation. Axial chirality in diarylamines has been overlooked thus far and understanding the conformational properties of such ligands in transition metal-complexes may provide insight into ligand design. As Crabtree *et al.* proved that twisted geometry in the ligand is not detrimental for activity (see section IV.1.3.), the potential for introducing a stable chirogenic axis in the core scaffold of pincer ligands should be addressed. Diarylamines have been used in several reactions yielding chiral, racemic products which have the potential to be made enantioselectively using axially chiral ligands.

Hence, bulky *ortho*-functional groups necessary for the design of pincer ligands, such as diarylphosphines or tertiary amines, can be used to promote conformational stability in novel, axially chiral ligands. The introduction of such bulky groups can be achieved by the use of a handle for post-

functionalisation (or before, provided the steric bulk and electronic effects do not hinder the reactivity), or potentially by introducing the functional groups directly in the substrates, using methods which are less sensitive to steric hindrance, such as S_NAr reactions.

IV.2.2. Towards axially chiral PNP ligands

Phosphine-based PNP diarylamines ligands have been widely applied to reactions with a potential for asymmetric induction (see section IV.1.1.). Inspired by Tilley's phosphines for the hydrosilylation of ketones^[206] and alkenes,^[205] we decided to focus on the synthesis of congested diarylamines bearing pendant phosphine groups at one *ortho*-position of each ring. Following the results on the conformational stability of diarylamine presented in Chapter 2, tetra-*ortho*-substituted diarylamines **4.18** and **4.19** were chosen as model substrates for the introduction of axial chirality in diarylamines pincer ligands, as a *para*-substituent would simplify their synthesis (Figure 32). The first design focussed on the use of triarylphosphines ligands, but diversification of the targets was also considered.

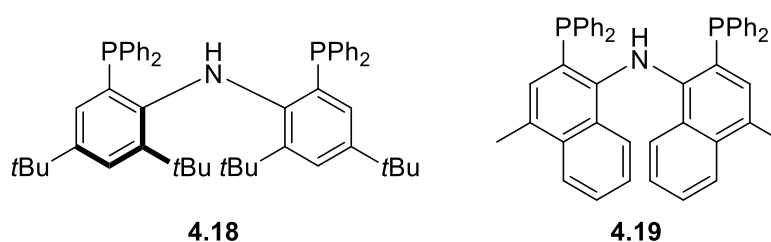
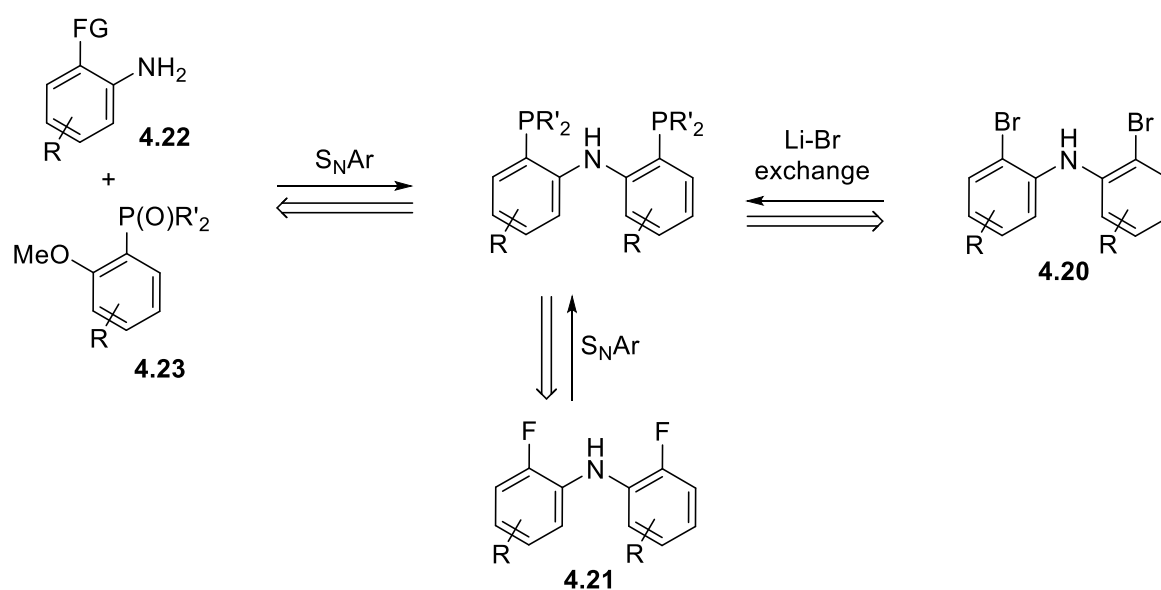


Figure 32: Targets for the preparation of axially chiral PNP ligands

Three different routes were envisaged to prepare these targets. Di-*ortho*-bromination of diarylamines prepared by Buchwald–Hartwig coupling would allow the introduction of phosphine moieties on **4.20** by a lithiation/electrophilic quench sequence (Scheme 65).^[190]



Scheme 65: Retrosynthetic routes towards axially chiral PNP ligands

The advantage of this route is the possibility of a late-stage addition of a wide range of phosphines on a specific scaffold to tune the properties of the resulting ligand, but also the relatively modest steric demand of the substrate prior to halogenation, simplifying the preparation of the starting materials. Furthermore, other reactivities of the C–Br bond can be envisaged, such as transition metal-catalysed reactions, to access different type of side-arm functionalities.^[239]

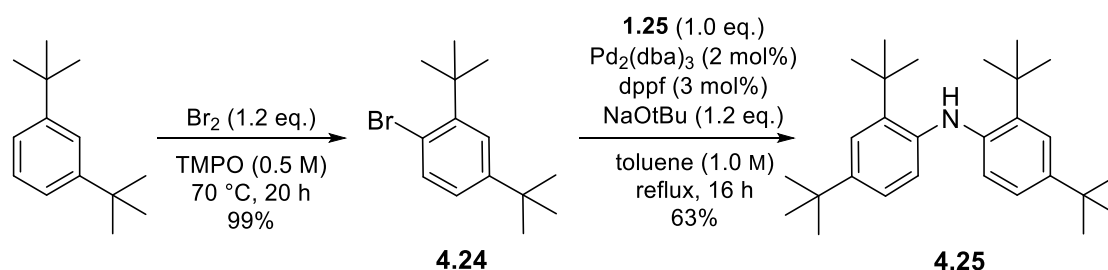
Nucleophilic aromatic substitution reactions were also envisaged for the synthesis of diarylamines **4.18** and **4.19**. Synthesis of *ortho*-fluorinated diarylamines **4.21** would allow the late-stage introduction of phosphine ligands by microwave-assisted S_NAr with a secondary phosphine.^[240] Alternatively, a phosphine oxide moiety can be used as an electron-withdrawing group allowing the formation of a C–N bond by S_NAr of **4.22** on anisole **4.23**.^[241]

By *ortho*-bromination

The bromination of diarylamines with subsequent functionalisation by lithium–halogen exchange and electrophilic quench is a key strategy for the introduction of functional groups in XNX pincers.^[242] These *ortho*-brominated diarylamines can then be functionalised by various groups such as phosphines,^[190] but diversity can be obtained from the same substrate as electrophilic species allowing the introduction of moieties such as alcohols^[243] or heteroaryls.^[239]

As *tert*-butyl groups showed a significant impact of the barrier to rotation of atropisomeric diarylamines, compound **4.25** was prepared as an intermediate in the synthesis of **4.18** (Scheme 66). To facilitate the synthesis, both *para*-positions were substituted with *tert*-butyl groups.

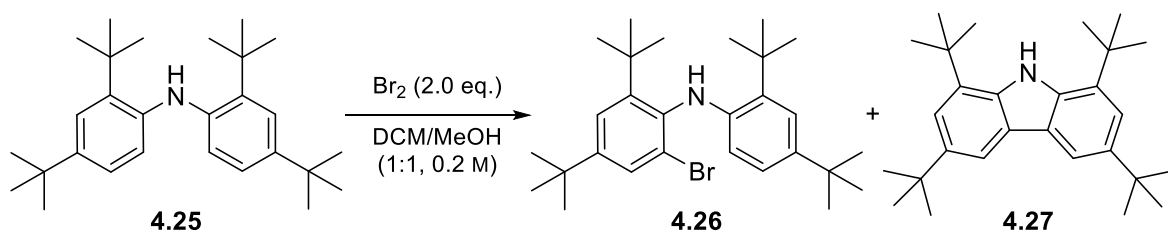
Synthesis of bis(2,4-di-*tert*-butylphenyl)amine **4.25** was achieved by a convergent palladium-catalysed cross-coupling reaction between aryl bromide **4.24** and the previously made aniline **1.25**, both synthesised from the same precursor according to reported procedures (Scheme 66). Pleasingly, the Buchwald–Hartwig coupling of sterically hindered **4.24** and **1.25** on gram scale proceeded in good yield with the commercially available phosphine ligand 1,1'-bis(diphenylphosphino)ferrocene (dppf).



Scheme 66: Synthesis of bis(2,4-di-*tert*-butylphenyl)amine **4.25**

Diarylamine **4.25** was then subjected to different brominating conditions (Table 26). Although different sources of bromine were tested (Br₂, *N*-bromosuccinimide, or copper(II) bromide), none of

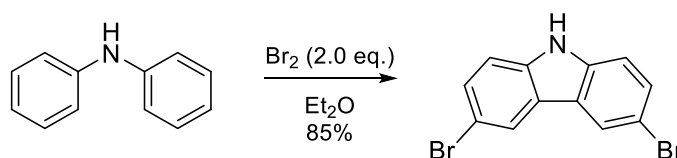
the conditions yielded the desired product **4.18**. Instead, carbazole **4.27** was formed by oxidative cyclisation in most cases.



Entry	Conditions	Results
1	Br ₂ (2.0 eq.), DCM/MeOH (1:1, 0.1 M), rt, 2 h	4.26 (18%) + 4.27 (55%)
2	Br ₂ (2.0 eq.), P(O)(OMe) ₃ (0.1 M), 70 °C, 3 h	Complex mixture
3	CuBr ₂ (2.5 eq.), Oxone (6.0 eq.), MeCN (0.1 M), rt, 16 h	4.27 (60%)
4	NBS (2.1 eq.), acetone (0.1 M), 0 °C, 3 h	Complex mixture

Table 26: *Ortho*-bromination of **4.25**

The use of bromine in a mixture of DCM and methanol reacted quickly to form a mixture of the product of mono-bromination **4.26** and carbazole **4.27**. Exchanging the solvent to trimethyl phosphate made the reaction more sluggish and heating the mixture to 70 °C gave a complex mixture of products which could not be separated. While using copper(II) bromide only gave the carbazole product, reaction with NBS in acetone produced a mixture of inseparable by-product including the mono-brominated derivative. In a short communication, Polivin *et al.* described the oxidative cyclisation of diphenylamine with bromine (Scheme 67).^[244]

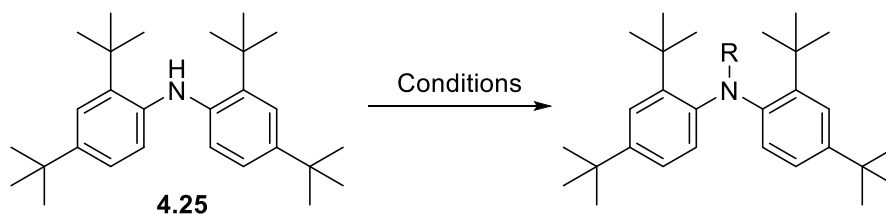


Scheme 67: Cyclisation of diphenylamine with bromine^[244]

Others have reported the formation of carbazoles from the cyclisation of *N*-centred radicals,^[245] but also from radical dianions *via* radical-nucleophilic aromatic substitution,^[246] as well as from diphenyl nitrenium ions through Nazarov-like cyclisation, followed by rearomatisation.^[247] However, no example of formation of such reactive species with a halogen source has been reported to date. This reaction likely proceeds because of the proximity of the reactive positions due to steric repulsion of the two *ortho-tert*-butyl groups. To overcome this issue, the nature of the diarylamine nitrogen was altered. Reaction of diarylamine **4.26** in acetic acid with bromine was attempted in order to prevent the nitrogen lone pair to participate in the diarylamines π system.^[248] Unfortunately, compound **4.25**

was not soluble in the reaction conditions, and thus bromination of tertiary diarylamines was explored as an alternative approach.

Installation of a third substituent on the nitrogen of compound **4.25** was tried with various groups (Table 27).

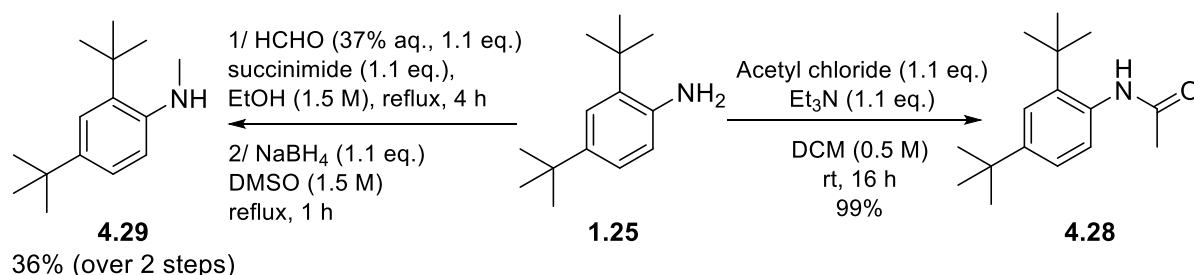


Entry	Conditions	R	Results
1	Boc ₂ O (1.5 eq.), DMAP (0.1 eq.), THF (0.05 M), rt, 24 h	Boc	No conversion
2	(4-Cl)PhNCO (3.0 eq.), DCM (0.5 M), rt, 18 h	4-chlorophenyl urea	No conversion
3	NaH (1.1 eq.), THF (0.1 M), 0 °C, 30 min then AcCl (1.1 eq.), rt, 18 h	Ac	No conversion
4	AcCl (0.1 M), reflux, 18 h	Ac	No conversion
5	NaH (4.0 eq.), THF (0.2 M), reflux, 30 min then MeI (3.5 eq.), reflux, 18 h	CH ₃	No conversion
6	NaH (4.0 eq.), THF (0.2 M), reflux, 30 min then SO ₂ (OMe) ₂ (3.5 eq.), reflux, 18 h	CH ₃	No conversion
7	<i>n</i> -BuLi (1.2 eq.), THF (0.2 M), 0 °C, 15 min then MeI (1.5 eq.), rt, 1 h	CH ₃	Complex mixture
8	LiHMDS (1.2 eq.), THF (0.5 M), rt, 15 min then MeI (1.5 eq.), rt, 1 h	CH ₃	Complex mixture

Table 27: Attempts at the *N*-methylation of the unprotected nitrogen of **4.25**

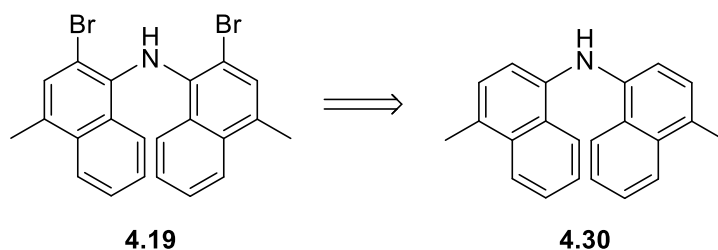
Highly reactive electrophiles such as anhydrides or isocyanates did not yield any reaction with **4.25** at room temperature (entries 1 and 2). Amide bond formation using neat acetyl chloride at high temperature over a prolonged time did not give any conversion, and neither did using a strong base to promote addition (entries 3 and 4). As diarylamine **4.25** proved to be unreactive towards highly electrophilic reagents, even in relatively drastic conditions, efforts were concentrated on a smaller electrophile by *N*-methylation. However, this strategy did not prove successful either. Deprotonation by sodium hydride, followed by methylation over extended periods of time with both methyl iodide and dimethyl sulfate also failed (entries 5 and 6). Only the use of stronger organometallic bases such as butyl lithium and lithium hexamethyldisilazide, afforded conversion, though providing complex, inseparable mixtures of by-products (entries 7 and 8).

Alternatively, the Buchwald–Hartwig coupling of protected aniline substrates was envisaged. *N*-acylated and *N*-methylated 2,4-di-*tert*-butylaniline **1.25** derivatives **4.28** and **4.29** were made in quantitative and moderate yield, respectively (Scheme 68).



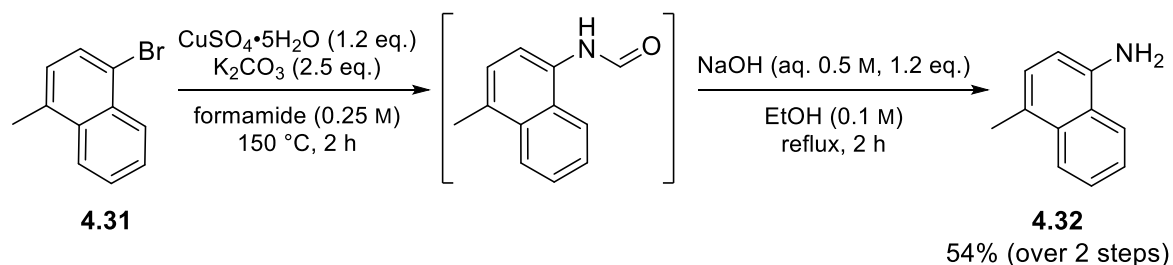
Scheme 68: Functionalisation of **1.25**

These two compounds were subjected to the typical coupling conditions for the synthesis of diarylamines **1.28a–z** with PNP_3 (see Chapter 2), as well as with the commercially available ligand dppf. Unfortunately, both procedures failed to yield any product for the substrates tested. The total lack of reactivity of bis(2,4-di-*tert*-butylphenyl)amine **4.25** derivatives necessitated the selection of alternative targets. As naphthalene rings provide high barriers to rotation (see Chapter 1), the *ortho*-bromination strategy was brought towards dinaphthylamine **4.19** (Scheme 69).



Scheme 69: Diarylamines **5.19** by *ortho*-bromination of **4.30**

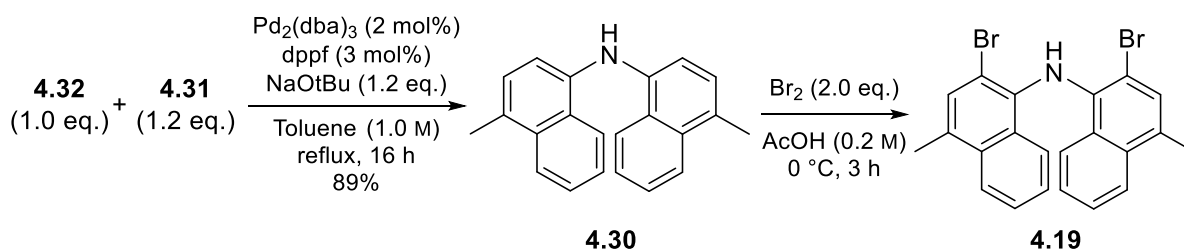
Aniline **4.32** was prepared in good yield by a one-pot sequence comprising the copper-catalysed Ullman amination of aryl bromide **4.31** with formamide and subsequent hydrolysis (Scheme 70).



Scheme 70: Synthesis of aniline **4.32**

Buchwald–Hartwig coupling of aniline **4.32** with aryl bromide **4.31** using a commercially available phosphine ligand then afforded diarylamine **4.30** in excellent yield (Scheme 71). Bis-brominated diarylamine **4.19** was then obtained in excellent yield by treatment of its precursor **4.30** with bromine in acetic acid. Interestingly, bromination of **4.30** under oxidative conditions, using stoichiometric

amounts of copper(II) bromide and Oxone in acetonitrile led to decomposition, while using NBS in acetone afforded only the mono-brominated analogue in low yield, possibly because of the poor solubility of the product.

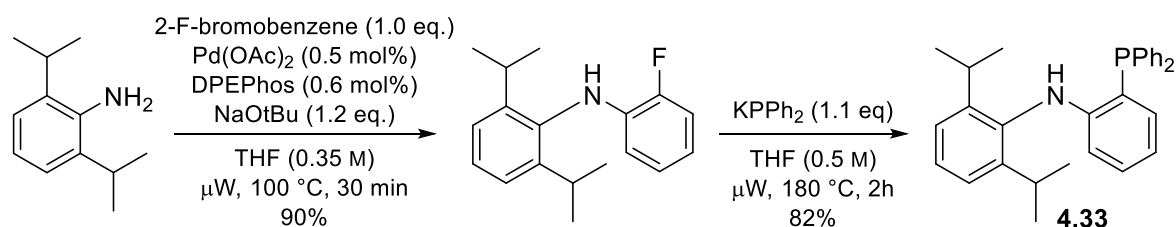


Scheme 71: Synthesis of **4.19**

The insolubility of compound **4.19** turned out to be a general feature hampering further work. Consequently, investigation of its barrier to enantiomerisation by chiral HPLC analysis proved to be difficult. While enantiomerical peaks of compound **4.19** could be observed, its poor solubility in the mobile phase, together with poor resolution, precluded any investigation of its barrier to rotation. Furthermore, any attempt to functionalise diarylamine **4.19** failed, as lithium–halogen exchange led to decomposition and both copper- and palladium-catalysed reactions did not yield any conversion.

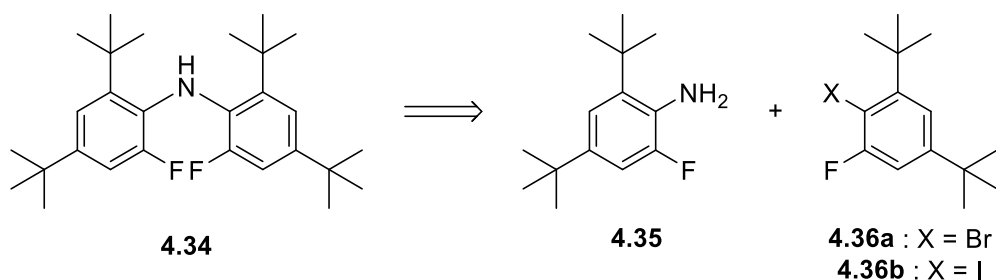
By functionalisation of ortho-fluorinated diarylamines

As the use of di-*ortho*-brominated diarylamines seemed to be a tedious strategy for the introduction of phosphines at the desired position, another approach in which a functional handle is introduced at the beginning of the synthesis was attempted. Due to its low steric hindrance and high reactivity towards S_NAr , the fluorine atom seemed to be an ideal functional handle. Previous work by Seipel *et al.* demonstrated that the introduction of a phosphine group at the *ortho*-position of a diarylamine was possible in excellent yield by a microwave-assisted displacement of a fluorine atom by S_NAr (Scheme 72).^[240] Due to its substitution pattern, ligand **4.33** is not chiral but the good reactivity of this relatively hindered molecule was encouraging.



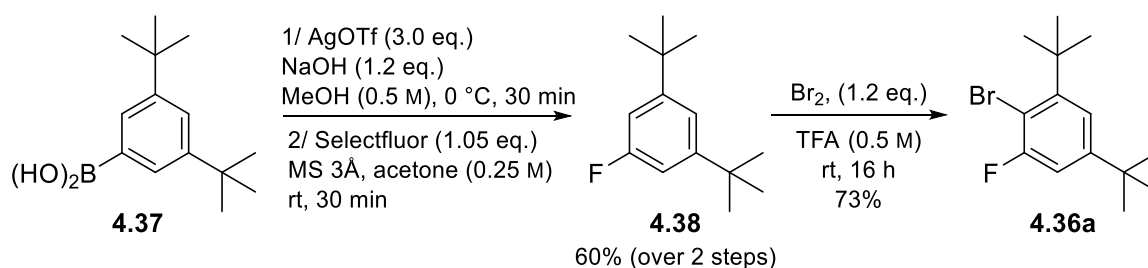
Scheme 72: Previous work on microwave-assisted S_NAr ^[240]

As with earlier attempts at *ortho*-bromination, it was decided to attempt the functionalisation of bis(2,4-di-*tert*-butyl-6-fluorophenyl)amine **4.34** (Scheme 73). Again, for ease of synthesis of the substrates, the target molecule **4.34** contained *tert*-butyl groups at the *para*-positions. The coupling of fluoroaniline **4.35** and aryl fluorides **4.36a** and **4.36b** was envisaged.



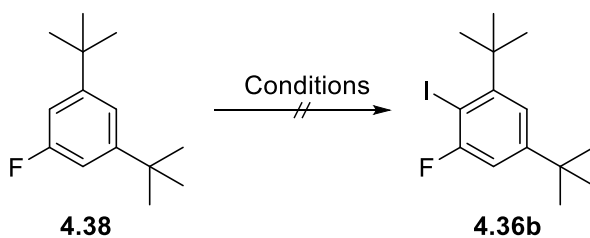
Scheme 73: Retrosynthetic analysis of compound 4.34

The precursor to both starting materials, 1,3-di-*tert*-butyl-5-fluorobenzene **4.38**, was prepared using a procedure described by Ritter *et al.* (Scheme 74).^[249] Boronic acid **4.37** was prepared in excellent yield by addition of the related Grignard reagent to trimethylborate, followed by hydrolysis.^[250] Fluorination of its silver complex with Selectfluor then allowed isolation of **4.38** in good yield, which was converted to aryl bromide **4.36a** in excellent yield using bromine.



Scheme 74: Synthesis of compound 4.36a

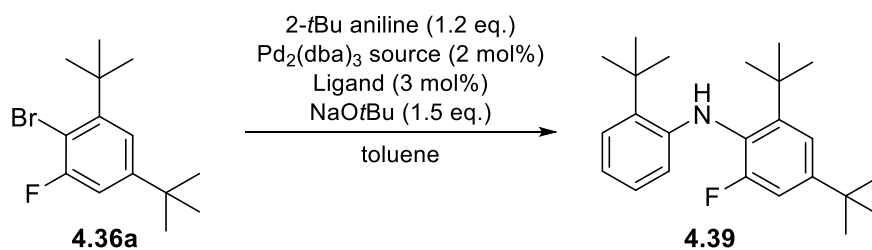
The synthesis of aryl iodide **4.36b** was also envisaged following reported procedures for the iodination of similar compounds (Table 28). Electrophilic iodination with NIS did not yield any conversion. Forcing conditions using a concentrated solution of iodine in DMF at high temperature for 4 days was not effective either. Generation of the aryl anion and quench with molecular iodine gave a mixture of starting material as well as multiple compounds which could not be separated.



Entry	Conditions	Results
1	<i>N</i> -Iodosuccinimide (1.0 eq.), MeCN (0.5 M), rt, 48 h	No conversion
2	I ₂ (1.2 eq.), K ₃ PO ₄ (1.25 eq.), DMF (1 M), 130 °C, 96 h	No conversion
3	<i>n</i> -BuLi (1.1 eq.), THF (0.5 M), –78 °C, 1.5 h then I ₂ (1.1 eq.), rt, 16 h	Complex mixture

Table 28: Iodination of 4.38

A series of test reactions for the Buchwald–Hartwig of **4.36a** were performed with 2-*tert*-butylaniline, a substrate with a similar steric demand as **4.35** (Table 29). The coupling was first attempted using the standard conditions used before for the synthesis of sterically hindered diarylamines, both with dppf and PNP₃ (entries 1 and 2).



Entry	Ligand	Concentration	<i>T</i> (°C)	<i>t</i> (h)	Results
1	dppf	0.65 M	80	40	No conversion
2	PNP ₃	0.65 M	80	40	No conversion
5	dppf	1 M	100	168	No conversion
6	PNP ₃	1 M	100	168	No conversion
7	DPEPhos	1 M	100	168	No conversion
8 ^a	DPEPhos	1.6 M	100 ^b	2.5	No conversion
9 ^{a,c}	DPEPhos	1.6 M	100 ^b	2.5	No conversion

^a Pd(OAc)₂ (2 mol%), DPEPhos (2.4 mol%), NaOtBu (1.2 eq.), THF (1.6 M) ^b Reaction performed under microwave heating

^c Aniline used as ArNH₂

Table 29: Attempt at coupling fluorinated aryl bromide **4.36a with 2-*tert*-butylaniline**

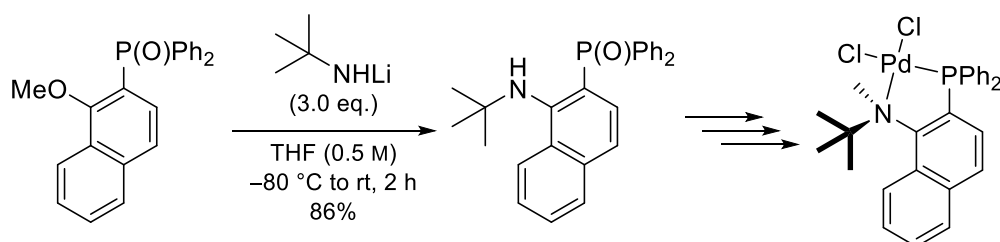
Similar conditions were used at higher temperature and in higher concentration for up to seven days. DPEPhos was also screened as a potential ligand, but neither condition gave any conversion (entries 3, 4, and 5). As these gave no conversion, the conditions reported by Seipel were tried,^[240] using both 2-*tert*-butylaniline and aniline (entries 8 and 9), without success. Starting material **4.36a** was always distinguishable in the ¹H NMR spectrum of the crude mixture, indicating that oxidative addition does not happen. The lack of reactivity in this step prevents any subsequent coupling from occurring.

As fluorinated aryls yielded no reaction, this strategy appeared unfeasible. Results in Chapter 1 showed the limits of transition metal-catalysed reactions, and the synthesis of these hindered functionalised substrates may be not possible by this route. However, the potential for making C–N bonds in hindered diarylamines by nucleophilic aromatic substitution reactions was still encouraging.

Using the phosphine oxide moiety as an activating group for S_NAr

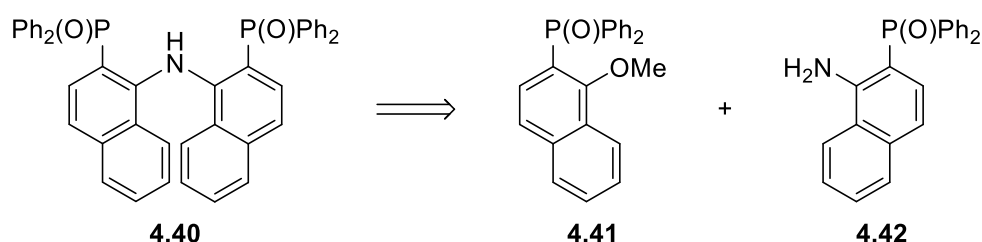
Whilst investigating the preparation of atropisomeric ligands based on *N,N*-dialkylanilines, the Mino group prepared various congested, *ortho*-phosphorylated anilines by addition of lithiated amines on

electron-poor anisoles (Scheme 75).^[13,91,251,252] The reaction, first disclosed by Hattori *et al.*,^[241] ingeniously uses the inherent electron-deficiency of the phosphine oxide group to improve the reactivity of the substrate towards S_NAr , allowing the facile formation of novel *P,N*-ligands.



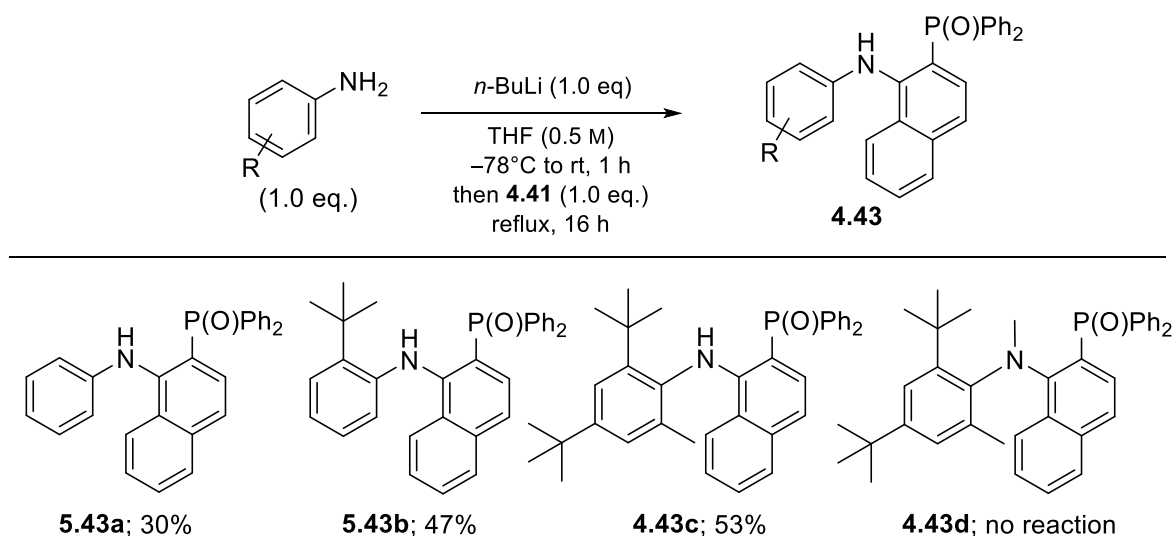
Scheme 75: Synthesis of *P,N*-ligand by S_NAr ^[252]

The authors were able to prepare configurationally stable, axially chiral ligands capable of inducing enantioselectivity in the palladium catalysed allylic alkylation by addition of a hindered alkyl amines on anisole derivatives. Considering the high steric demand of the substrates made this way, the high reactivity of *ortho*-phosphorylated anisole derivatives towards S_NAr reactions was employed for the synthesis of atropisomeric diarylamines. Thus, formation of target diarylamine **4.40** by S_NAr reaction of aniline **4.42** and anisole **4.41** was envisaged (Scheme 76). Conveniently, aniline **4.42** can be accessed from anisole **4.41** by S_NAr reaction of a protected amine followed by deprotection.



Scheme 76: Retrosynthetic analysis of **4.40**

First, commercially available, hindered anilines were reacted with **4.41** following the procedure reported by Hattori *et al.*^[13,241] As anilines were less reactive than alkylamines, the coupling was performed at reflux. While the reaction was sluggish with aniline, high steric demand at the *ortho*-positions was tolerated, as diarylamines **4.43b** and **4.43c** were synthesised in moderate yield (Scheme 77). Interestingly, augmentation of the steric demand around the reactive atom by a second substituent at the nucleophilic nitrogen leads to no observable conversion to compound **4.43d**.



Scheme 77: Synthesis of *ortho*-phosphorylated diarylamines by S_NAr

The ^{13}C NMR spectra of **4.43b** and **4.43c** showed diastereotopic signals for the phosphine phenyl carbons, indicating a chiral ground state slowly interconverting over the NMR timescale at room temperature. Enantiomers of **4.43b** could be resolved by chiral HPLC and displayed an interconversion plateau typical of dynamic compound with a half-life to enantiomerisation of a few minutes (Figure 33). VT-HPLC was used to calculate the barrier to rotation and compound **4.43b** was atropisomer with a barrier to interconversion of 93.3 kJ mol^{-1} . Unfortunately, enantiomers of **4.43c** could not be separated.

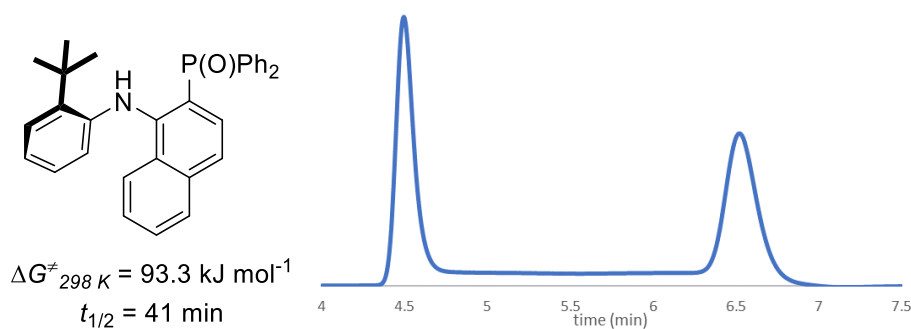
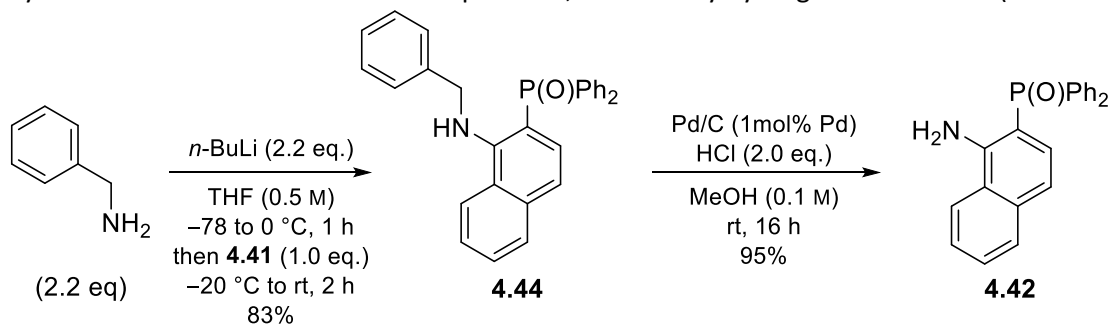


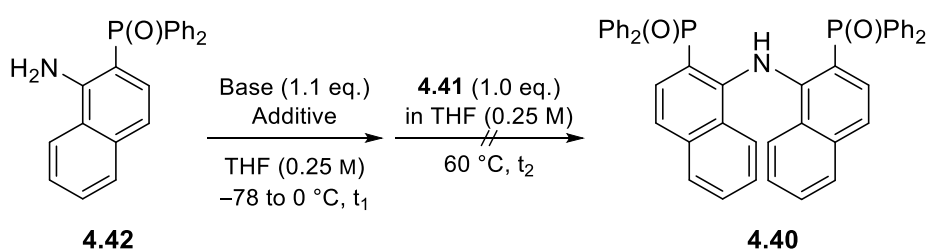
Figure 33: Portion of the HPLC chromatogram of **4.43b** at 40°C

With these promising results, aniline **4.42** was prepared in excellent yield by addition of lithiated benzylamine on anisole **4.41** at room temperature, followed by hydrogenation of **4.44** (Scheme 78).



Scheme 78: Synthesis of aniline **4.42**

Coupling of **4.41** and **4.42** was then attempted using the modified procedure (Table 30, entry 1). However, as no reaction occurred, the use of different additives and bases was explored. Following a report by Bappert *et al.*,^[253] TMEDA was used as an additive, as well as DMPU. However, neither of these gave any conversion (Entries 2 and 3). As Hellwinkel *et al.*^[254] suggested the chelation of a lithium cation between the deprotonated nitrogen and the phosphine oxide oxygen, we speculated that the anion was stabilised and thus less reactive. However, exchanging the counter-cation using KHMDS or NaHMDS as a base did not affect any change (entries 4 and 5). Using 18-crown-6 as a chelator of the potassium cation to increase the nucleophilicity of the aniline yielded some conversion, although a complex mixture of side products was obtained after work-up, mostly containing starting materials **4.41** and **4.42** (entry 6). This lower reactivity of aniline is probably due to the electron-withdrawing phosphine oxide, making the nitrogen a poor nucleophile.



Entry	Base	Additive	t_1 (h)	t_2 (h)	Results
1	<i>n</i> -BuLi	–	1	16	No conversion
2	<i>n</i> -BuLi	TMEDA (1.0 eq.)	1	16	No conversion
3	<i>n</i> -BuLi	DMPU (1.1 eq.),	1	16	No conversion
4	KHMDS	–	1	4	No conversion
5	NaHMDS	–	1	4	No conversion
6	KHMDS	18-crown-6 (2.0 eq.)	0.25	16	Complex mixture

Bases: *n*-BuLi (1.4 M in hexanes), NaHMDS and KHMDS (1.0 M in THF).

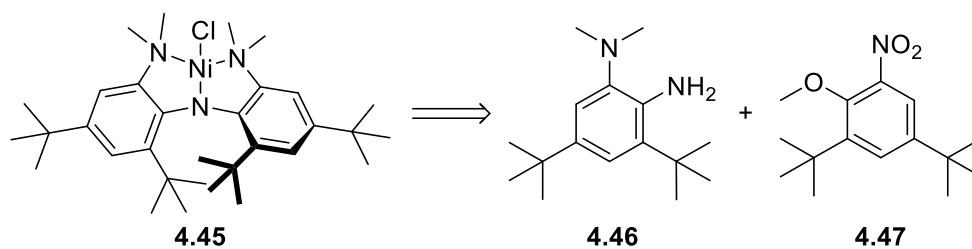
Table 30: Coupling of **4.41** and **4.42**

As the strategies applied to the synthesis of axially chiral, diarylamine-based PNP ligands proved unsuccessful, our efforts focussed on diarylamines with different functionalities at the *ortho*-position.

IV.2.3. Towards an axially chiral analogue of Nickamine

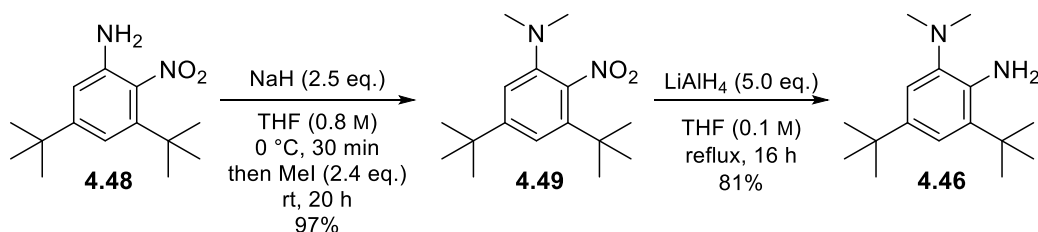
Nickamine and its analogues have been used as catalysts for reaction with potential for asymmetry, such as alkene hydrosilylation (see IV.1.1.). Hence, an axially chiral analogue of Nickamine was designed by adding bulky groups at the two free *ortho*-positions (Scheme 79, diarylamine **4.45**). In this case, it was possible to design the synthesis of **4.45** so that the electronic properties of both substrates are optimised towards S_NAr . Electron-deficient anisole **4.47**, with a functional handle for the formation

of the desired dimethylamino group, was synthesised by methylation of the corresponding phenol according to reported protocols.^[255]



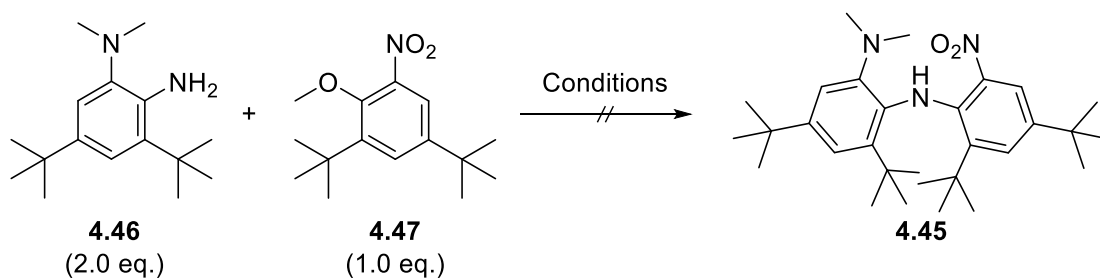
Scheme 79: An axially chiral analogue of Nickamine

Musk **4.48**, obtained in three steps from 3,5-di-*tert*-butylaniline,^[58] was used to produce aniline **4.49** in excellent yield by bismethylation of the aniline, followed by reduction of the nitro group (Scheme 80). Aniline **4.46**, already containing the dimethylamino moiety as an electron-donating group, was thought to be activated for S_NAr .



Scheme 80: Synthesis of aniline **4.46**

Different coupling conditions were tested, using microwave irradiation or by stepwise deprotonation of aniline **4.46** followed by addition to anisole **4.47** (Table 31). Forcing conditions reaching high temperature by microwave irradiation, with a strong base, did not afford any conversion (entry 1). Treatment of the starting materials with a procedure similar to the one of Bappert *et al.*^[253] only afforded decomposition of **4.46** as well as full recovery of **4.47** (entry 2). Changing the base and the counter-cation did not affect the reaction either, as both starting materials were recovered (entries 3 and 4). Thus, as S_NAr reactions did not yield any encouraging results, it was decided at this point to focus our efforts on another target.



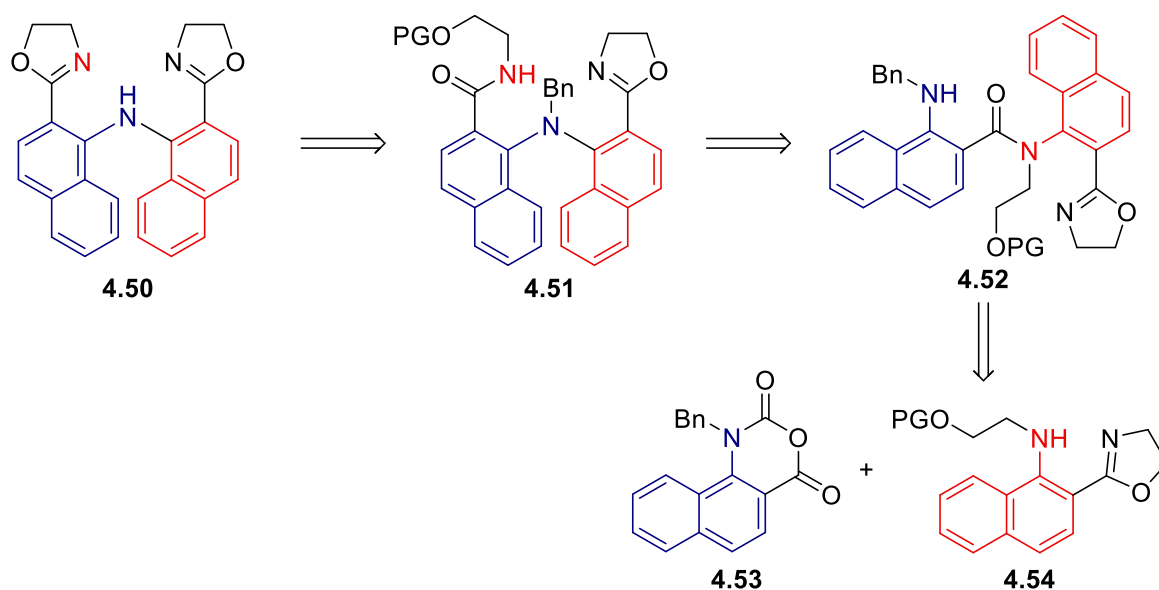
Entry	Conditions	Results
1 ^a	KOtBu (1.1 eq.), DMF (0.6 M), 170 °C, 2 h	No conversion
2	4.46 , <i>n</i> -BuLi (2.0 eq.), TMEDA (4.0 eq.), THF (0.5 M), –20 °C, 30 min then 4.47 , 60 °C, 16 h	Decomposition of 4.46
3	4.46 , KHMDS (2.0 eq.), TMEDA (4.0 eq.), THF (0.5 M), –20 °C, 30 min then 4.47 , 60 °C, 16 h	No conversion
4	4.46 , NaHMDS (2.0 eq.), TMEDA (4.0 eq.), THF (0.5 M), –20 °C, 30 min then 4.47 , 60 °C, 16 h	No conversion

^a Reaction performed under microwave heating

Table 31: Coupling of **4.46** and **4.47**

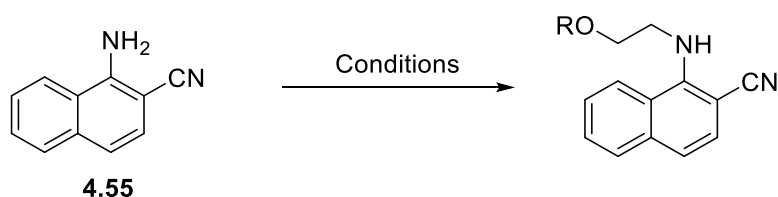
IV.2.4. Towards an axially chiral NNN ligand by Smiles rearrangement

The Smiles rearrangement of anthranilamides presented in Chapter 2 is particularly tolerant of steric demand on the product, and the reaction yields diarylamines with a pendant amide group. While only *N*-methyl amides were investigated (as well as the ring expansion of heterocycles in Chapter 3), we sought to exploit the possibility of using the resulting amide moiety as a functional handle to prepare axially chiral diarylamine pincer ligands. Diarylamines bearing pendant oxazoline rings at their *ortho*-positions had been used successfully in asymmetric catalysis, with the source of chirality coming from the functionalised oxazolines (see IV.1.2.). We therefore aimed at preparing diarylamine **4.50**, with achiral oxazoline rings (Scheme 81). This compound was expected to be made from diarylamine **4.41** by protecting group removal and cyclisation of the resulting alcohol to produce the corresponding oxazoline, followed by hydrogenolysis of the benzyl group. This diarylamine would be the product of the Smiles rearrangement of anthranilamide **4.52**. While the large steric demand of the product and the unknown reactivity of the amide side chain were identified as key challenges to overcome, we thought that the inherent electron-deficiency of the migrating ring would favour rearrangement. Finally, building blocks **4.53** and **4.54** were expected to react to form anthranilamide **4.52** in a similar strategy to that used in Chapter 3.



Scheme 81: Retrosynthetic analysis of diarylamine 4.48. PG = Protecting group.

Isatoic anhydride **4.53** is known,^[256] and alkylation of *ortho*-cyano naphthylamine **4.55**^[257] was attempted with 2-ethoxy chains with various protecting groups (Table 32).



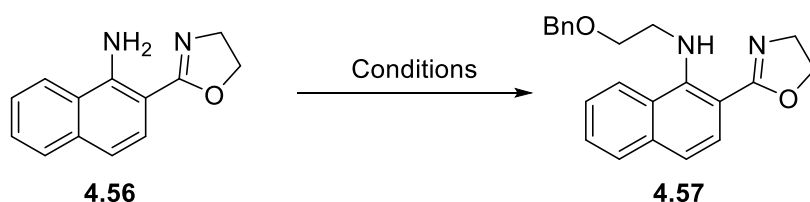
Entry	R	Conditions	Results
1 ^a	H	HOCH ₂ CH ₂ OTf (10 eq.), Et ₃ N (1.5 eq.), neat, 150 °C, 24 h	No conversion
2 ^a	H	Ethylene glycol (10 eq.), Pd/C (10mol% Pd), ZnO (3.0 eq.) H ₂ O (0.15 M), 150 °C, 24 h	No conversion
3	Bn	Benzyloxy acetaldehyde (1.5 eq.), THF (0.5 M), rt, 72 h then Hantzsch dihydropyridine ^b (1.0 eq.), PTSA (0.1 eq.), 24 h, reflux	Decomposition
4	MOM	MOMOCH ₂ CH ₂ Br (1.0 eq.), Et ₃ N (1.0 eq.), toluene (0.5 M), reflux, 48 h	No conversion
5 ^b	MOM	MOMOCH ₂ CH ₂ Br (2.0 eq.), K ₃ PO ₄ (2.0 eq.), toluene (0.5 M), 150 °C, 4 h	No conversion
6 ^b	MOM	MOMOCH ₂ CH ₂ Br (2.0 eq.), K ₃ PO ₄ (2.0 eq.), DMF (0.5 M), 150 °C, 4 h	Decomposition
7	MOM	MOMOCH ₂ CH ₂ Br (2.0 eq.), NaH (1.1 eq.), THF (0.5 M), rt, 72 h	No conversion

^a Reaction performed in a sealed vial ^b Reaction performed under microwave irradiation ^b Diethyl 1,4-dihydro-2,6-dimethyl-3,5-pyridinedicarboxylate

Table 32: Alkylation of naphthylamine 4.55

Attempted substitution of an alkyl triflate,^[258] neat, at high temperature did not yield any conversion (entry 1). A hydrogen borrowing reaction was tried with ethylene glycol and a heterogeneous catalyst mixture of palladium on charcoal and ZnO₂ in water^[259] left the substrate untouched (entry 2). Reductive amination using a mild reducing agent^[260] led to the formation of multiple compounds by reaction of the nitrile group (entry 3). While substitution of a protected alkyl bromide using a weak base and high temperature did not yield any product in toluene (entries 4 and 5), the use of DMF as a solvent led to a side reaction on the substrate, presumably by reaction with the solvent at high temperature (entry 6). Upon exchanging solvent to THF and using a strong organometallic base, no reaction was observed either (entry 7).

The nitrile group *ortho* to the reactive nitrogen likely decreases its nucleophilicity. To overcome this, oxazoline-substituted naphthylamine **4.56** was made in good yield by treating naphthylamine **4.55** with ethanolamine and zinc(II) chloride in chlorobenzene. Its *N*-alkylation was expected to be easier due to the lower electron-withdrawing character of the oxazoline group compared to that of the nitrile moiety (Table 33).^[261]



Entry	Conditions	Results
1	BnOCH ₂ CHO (2.0 eq.), AcOH (2.0 eq.), NaHB(OAc) ₃ (2.0 eq.), DCE (0.5 M), rt, 3 h	No conversion
2 ^a	BnOCH ₂ CH ₂ I (2.0 eq.), KOtBu (1.5 eq.), THF (0.3 M), 150 °C, 18 h	Decomposition
3 ^a	BnOCH ₂ CH ₂ I (2.0 eq.), <i>n</i> -BuLi ^b (1.1 eq.), THF (0.3 M), 150 °C, 18 h	No conversion
4 ^a	BnOCH ₂ CH ₂ I (2.0 eq.), NaHMDS ^c (1.1 eq.), THF (0.3 M), 150 °C, 18 h	No conversion
5 ^a	BnOCH ₂ CH ₂ I (2.0 eq.), DIPEA (1.5 eq.), toluene (0.5 M), 150 °C, 18 h	No conversion
6 ^a	BnOCH ₂ CH ₂ I (2.0 eq.), DIPEA (1.5 eq.), DMF (0.5 M), 150 °C, 4 h	20 %
7 ^a	BnOCH ₂ CH ₂ I (2.0 eq.), DIPEA (1.5 eq.), DMAc (0.5 M), 150 °C, 4 h	14 %

^a Reaction performed under microwave irradiation ^b *n*-BuLi (1.4 M in hexanes) ^c NaHMDS (1.0 M in THF)

Table 33: Alkylation of naphthylamine **4.56**

Reductive amination using sodium borohydride led to the reduction of the oxazoline ring. Decreasing the reactivity of the reducing agent, using sodium triacetoxyborohydride, though, did not give any conversion (entry 1). As using alkyl bromides gave no alkylation, benzyloxyethyl iodide was prepared from benzyl-protected ethylene glycol using the imidazole-triphenylphosphine-iodine reagent.^[262,263]

Screening of strong bases in THF under microwave heating was not successful, as potassium *tert*-butoxide gave decomposition of the substrates (entry 2) and *n*-butyl lithium and sodium hexamethyldisilazide did not yield any conversion (entries 3 and 4). When using a weaker base, no reaction was observed in toluene, but *N*-alkylated aniline **4.57** was isolated in poor yield after reaction in DMF (entries 5 and 6). In order to avoid side reaction with DMF, dimethyl acetamide was used as a solvent, although the product was isolated in lower yield (entry 7). As this yield could not be improved, the project was halted.

IV.3. Conclusion

The synthesis of sterically congested diarylamines containing functional group at the *ortho*-positions was attempted in order to study the impact of axial chirality in pincer ligands. Unfortunately, attempts to introduce steric demand large enough to obtain atropisomerism in the desired diarylamines were hampered by a lack of reactivity.

Introduction of *ortho*-functional groups by reaction on *ortho*-halogenated diarylamines was unsuccessful due to either side reaction preventing the bromination step or because of the poor solubility of the brominated diarylamines. When *ortho-tert*-butyl groups were present, an unexpected intramolecular cyclisation to the corresponding carbazole proceeded cleanly.

Attempts to introduce fluorine atoms at the *ortho*-positions were hampered by the lack of reactivity of the substrate towards Buchwald–Hartwig coupling. Further attempts to increase reactivity by iodination failed. While the S_NAr reaction of anilines on *ortho*-phosphorylated anisole derivative **4.41** proceeded with good tolerance towards steric hindrance, the lack of reactivity of the electron-deficient phosphorylated aniline **4.42** prevented the synthesis of axially chiral PNP ligands.

Attempts to synthesise NNN ligands were not successful either. The synthesis of a Nickamine analogue **4.45** by S_NAr reaction of substrates seemingly matched the right electronic properties yet did not provide any observable reaction. Finally, the strategic use of the newly discovered Smiles rearrangement of anthranilamides could not be applied in this case as the synthesis of the required *N*-alkylated aniline substrate was prevented by a lack of reactivity of the starting material.

Chapter 5

Remote control of conformation using anilides

V.1. Introduction

The ‘rise of the molecular machines’ over the past decades has demonstrated the fundamental role of dynamic stereochemistry in the recent applications of chemical sciences.^[264] The “original” molecular machines, namely biomacromolecules, have implications in a large number of biological processes – from carrying substrates around cells to synthesising or replicating proteins – and have inspired chemists to design synthetic, functional compounds.^[265] The use of chirality to control molecular motion in technomimetic systems such as molecular gears,^[266] propellers,^[267] or motors^[268] results in translocation of the classical, Euclidean chirality to topological chirality.^[269] These advances are further eased by the advances of analytical techniques such as dynamic NMR analysis or dynamic chromatography (see Chapter 1).

Molecules hold information in their stereochemistry.^[270] For example, the stereochemical environment of a chiral catalyst defines the asymmetric induction in a reaction.^[271] Organic molecules rarely have a single, fixed topology, as they usually fluctuate into stereoisomeric structures, depending on the relative stability of the resulting conformers.^[269] Many non-covalent interactions define the distribution of conformations in a given compound due to adjacent functionalities. The steric and electronic interactions between these functionalities can be exploited to reduce the conformational space available, thus controlling the overall topology of a molecule.^[270] To this end, stereochemical relays and thermodynamic control can permit the remote control of conformation over nanometre distances.^[272]

V.1.1. Effect of dipolar interactions on conformation

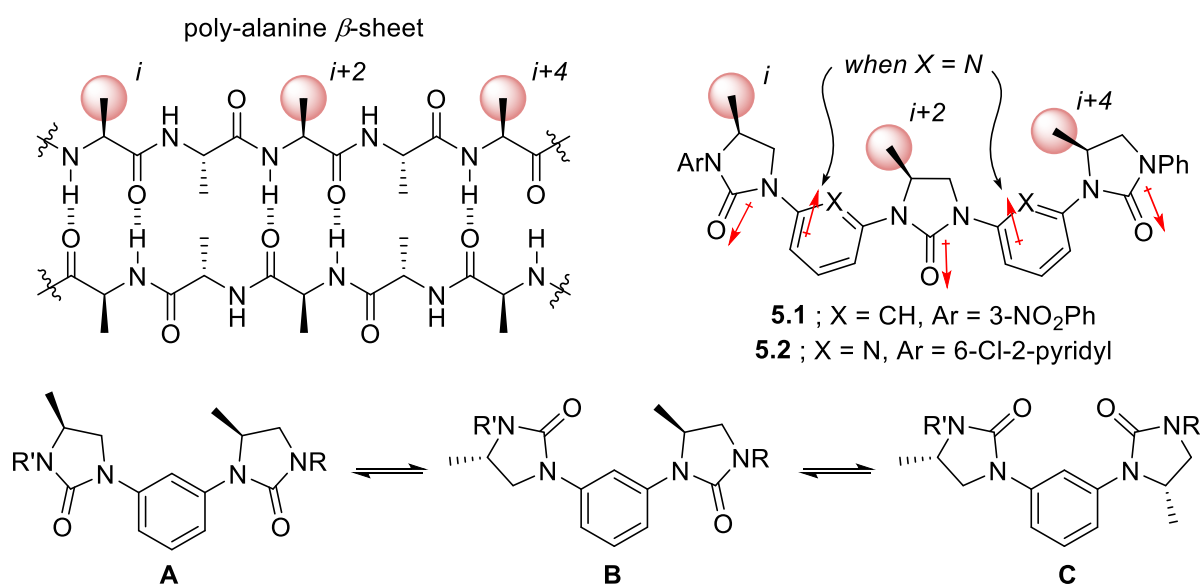
Non-covalent interactions form the basis of conformational preferences from natural peptides to synthetic foldamers.^[273] Hydrogen bonding, dipolar and electrostatic interactions are used to generate a conformational bias in foldamers, producing structural complexity through weak interactions.^[274] The rigidity and large dipole moment of carbonyl groups make them attractive for conformation-imparting interactions.^[274]

Electrostatic and dipolar interactions are commonly found in the solid-state structure of organic molecules, particularly planar, aromatic compounds.^[275] In crystallographic databases, three types of dipole-dipole interactions have been observed: the antiparallel arrangement of carbonyls is the most prevalent, but parallel orientations and orthogonal relationships also exist.^[275] In solution, provided a scaffold offers enough flexibility to give rise to multiple conformations, dipole-dipole interactions of carbonyl groups result in a parallel, coplanar, ‘head-to-tail’ orientation, or an antiparallel, stacked arrangement of the carbonyls, termed ‘side-by-side’.^[276,277] This feature was used by various groups

to bias the conformational equilibrium of organic molecules, allowing the use of dipolar repulsion for conformational control,^[278] ligand sensing^[279] or remotely relaying chiral information.^[272]

Coplanar alignment of the dipoles

In an effort to address the challenge of targeting protein-protein interactions, the Hamilton group developed non-peptidic molecules mimicking protein β -strands.^[278,280,281] β -sheets are an extended secondary structure of proteins where hydrogen bonding aligns the amide groups in a plane (Scheme 82, top left corner).^[282] Each amino acid residue is projected perpendicularly to the amide backbone, alternating between protruding upwards and downwards. The synthetic design of Hamilton and co-workers alternates *meta*-substituted (hetero)aryl rings with imidazolidinones mimicking only one side of the strand (*i.e.* the *i*, *i*+2, *i*+4... residues).^[278,280,281] First-generation compound **5.1**, connected through *meta*-substituted phenyl group, exist as a mixture of conformers that rapidly interconverted at room temperature because of unrestricted rotation around the C–N bond, giving rise to different relative arrangements of the imidazolidinone carbonyls.^[280] While conformer **C** was highly unfavourable due to dipolar repulsion, conformers **A** and **B** were energetically equivalent. However, only conformer **A** is reminiscent of the geometry of β -strands, and foldamer **5.1** would presumably bind protein targets in an energy-demanding, induced-fit manner.



Scheme 82: Using dipoles repulsion to control the conformation of a β -strand mimic

Conformational homogeneity was achieved by linking the imidazolidinone rings through a 2,6-disubstituted pyridine in compound **5.2**. Dipolar repulsion between the carbonyl groups and the pyridine linkers was found to be the determinant for attaining a single conformation of oligomer **5.2** in solution (Scheme 82).^[278] This dipole obviates the existence of conformer **B**, as conformer **A** accounted for 98% of the populated conformations in **5.2**. The solid-state structure of **5.2** was

approximately planar, with side-chains projecting on one face, and with inter-residue distances similar to those in peptidic β -strands. The conformation in solution was confirmed by NOESY analysis.

Stacked alignment of the dipoles

The work by Hamilton and co-workers on β -strand mimetic **5.1** demonstrated that dipolar repulsion across an arene rapidly decreases with distance if the dipoles are coplanar. Bulky tertiary benzamides are known to adopt an approximately perpendicular arrangement with regards to the arene.^[113] Clayden *et al.* have found that *meta*-related bis-benzamides such as **5.3** existed almost exclusively as the *anti* conformer in CDCl_3 , where both amides pointed in opposite directions, perpendicular to the plane of the aryl ring, because of dipolar repulsion (Figure 34).^[283] When a third dipole was introduced as in ester **5.4**, predomination of the *syn* conformer (relative the two amido carbonyls) was observed as a result of the relay of the relative *anti* orientation of the adjacent dipoles.

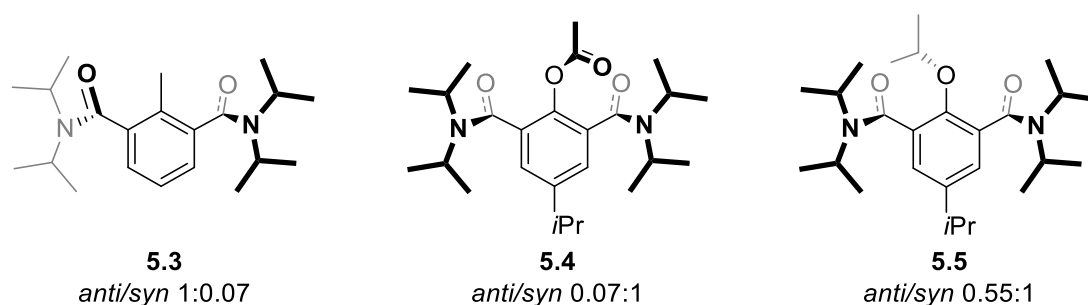
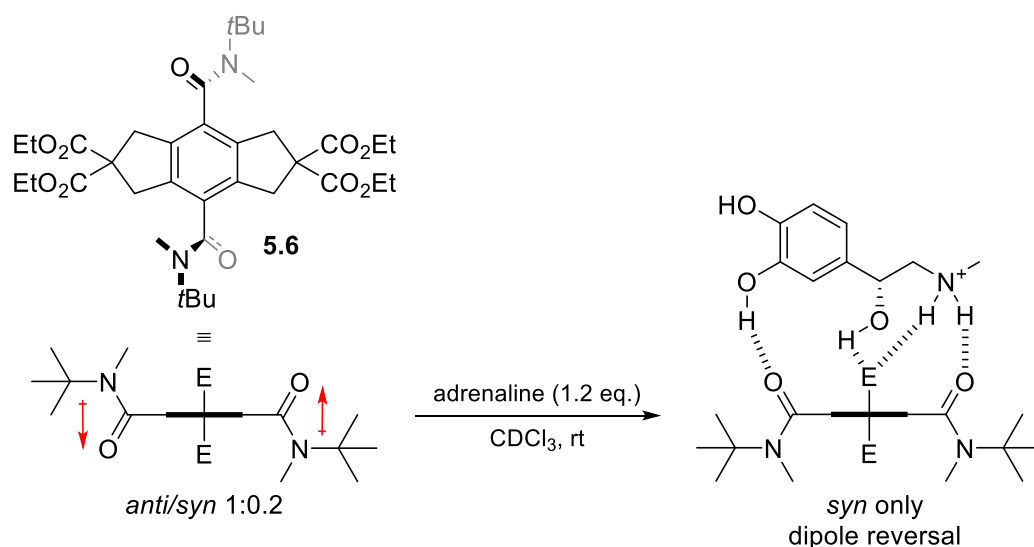


Figure 34: The influence of steric and electronic parameters on the conformation of *meta*-related amides in CDCl_3

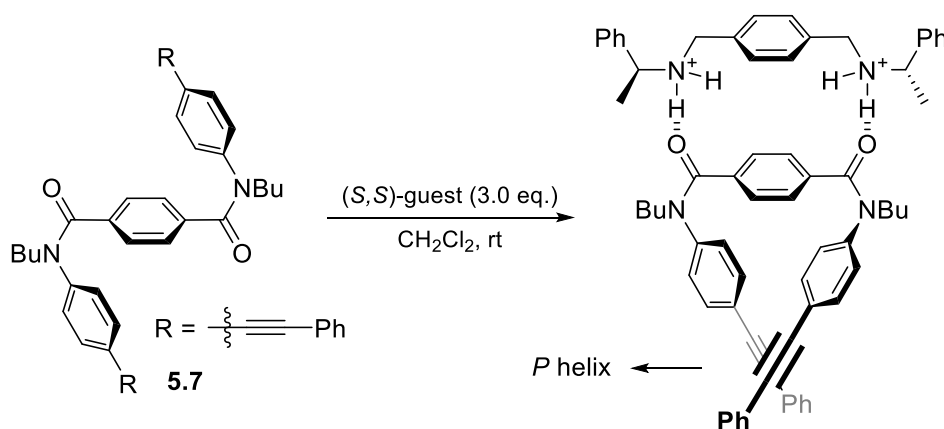
When steric hindrance between the two dipoles was introduced as in compound **5.5**, the *syn* conformation was favoured, albeit with poorer control than in **5.3**, indicating that dipolar repulsion played a major role in the conformer distribution.

Kawai *et al.* built on this phenomenon to design a sensor for catecholamines such as adrenaline.^[279] Hydrindacene **5.6** possessed a pair of chiral axes due to the perpendicular arrangement of the benzamide groups (Scheme 83). Following a similar trend to compound **5.3**, bis-benzamide **5.6** existed as a pair of *syn* and *anti* conformers, slowly interconverting relative to the NMR timescale. In CDCl_3 , dipolar repulsion induced a conformational bias towards the *anti* conformer, as observed by ^1H NMR analysis. However, portion-wise addition of an excess of adrenaline resulted in the progressive disappearance of the peaks corresponding to the *anti* conformer in the ^1H NMR spectrum of **5.6** to achieve full conversion to the *syn* conformer. In this orientation, compound **5.6** adopted an ideal conformation for binding adrenaline by forming hydrogen bonds between the amide carbonyls and the phenol and ammonium cation. The esters also augmented the interaction by providing additional hydrogen bonding interactions.



Scheme 83: Adrenaline-induced conformational change in a bis-benzamide

Signal transduction was created by modulation of the conformation of the receptor by an external effector molecule, making this compound mimetic of adrenergic receptors. However, ¹H NMR analysis of this compound can become difficult due to the complexity of the spectra and/or partial overlap of the conformers signals, which results in the output being difficult to decipher. Furthermore, this design only gave an “on/off” signal for the presence or absence of a given analyte, and chirality was not sensed. These problems were addressed by the same group, using circular dichroism as a reporter of the guest chirality (Scheme 84).^[284] The two chiral axes of compound **5.7** rapidly interconverted to form a mixture of *anti* and *syn* conformers, with a preference for the former. Upon complexation with the chiral diammonium salt, the *syn* conformation of **5.7** was favoured. Steric hindrance of the two stiff diphenylacetylene units rendered the molecule helical – and therefore chiral – with arms serving as a chromophore for the dynamic recognition of the absolute chirality of the analyte by circular dichroism.



Scheme 84: Conformational changes for the determination of absolute configuration of an ammonium salt

V.1.2. Remote control of conformation by dipolar repulsion

Clayden *et al.* observed that the relative conformation of amides installed on a scaffold made of non-rigidly interconnected aromatic rings such as 2,2'-disubstituted biphenyl **5.8** was biased. While the synthesis of **5.8** by introduction of the benzylic methyl groups by double *ortho*-lithiation solely produced the centrosymmetric *syn* conformer, thermal equilibration in toluene led to a mixture of stereoisomers in which the C_2 -symmetric *anti* compound predominated.^[285] Despite the fast rotation of the $C_{Ar}-C_{Ar}$ bond, the two dipoles interacted with each other, resulting in a preferred conformer due to dipolar repulsion. This communication could be extended to longer distances as in terphenyl **5.9**. Chiral HPLC analysis showed that the single compound obtained after thermal equilibration was chiral and racemic, therefore adopting the conformation depicted in Figure 35 in which a C_2 axis features in the central aromatic ring, perpendicular to its plane.

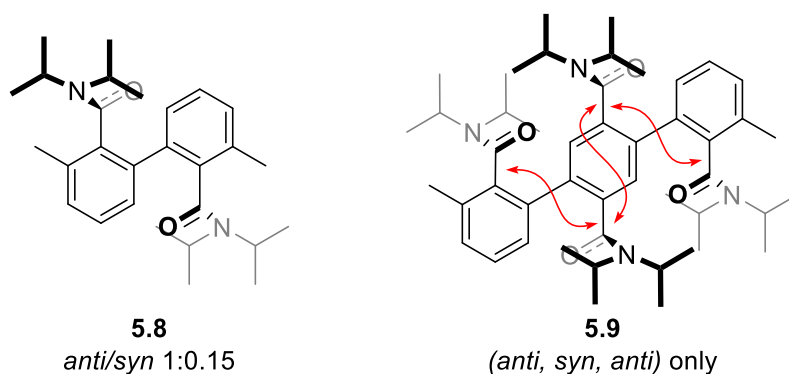
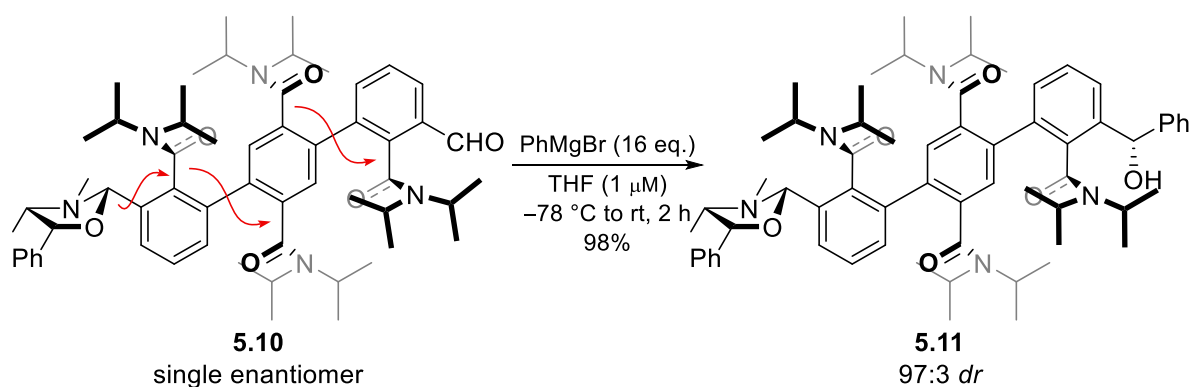


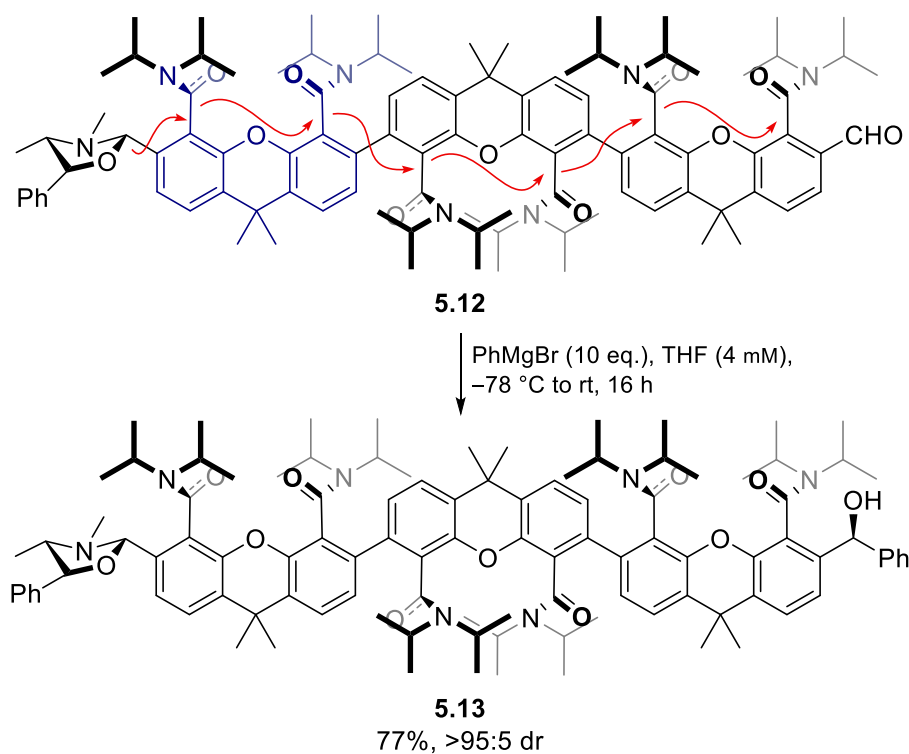
Figure 35: Relay of conformation by dipolar repulsion in biphenyls and terphenyls (the red arrows denote the relative relationships used to describe the conformation)

The same group demonstrated that the orientation of an axially chiral amide was sensitive to the local chiral environment.^[286] By introduction of a chiral centre in the vicinity of one of the terminal amides, steric and electronic interactions reorientated the proximal dipole and set the absolute configuration of the related chiral axis (Scheme 85).^[270] Consequently, the overall absolute configuration of a dynamic compound can be set by a single chiral centre. After formation of the enantiopure oxazolidine **5.10** from (–)-ephedrine, one diastereoisomeric form was relayed along the scaffold to the terminal amide to form exclusively one enantiomer.^[287] Upon treatment with phenylmagnesium bromide, formation of alcohol **5.11** occurred with excellent diastereoselectivity as governed by the orientation of the adjacent amide.^[271] The stereoselective outcome of the Grignard addition hence came from the chiral oxazolidine ring placed 11 bonds away, remotely relaying asymmetry to a locally achiral site.



Scheme 85: 1,11-Relay of chirality in a terphenyl

1,8-Xanthene dicarboxamides (Scheme 86, highlighted in blue) arrange their amide groups outside of the xanthene plane, creating two chiral axes.^[288] The relative orientation of the amide groups originates from the steric demand of the nitrogen substituents, and a single C_2 -symmetric *anti* diastereomer was observed by ^1H NMR analysis with diisopropyl amides.^[288] Combining this conformational bias with their biphenyl relay, Clayden *et al.* were able to control the stereoselective outcome of the Grignard addition on the aldehyde moiety of **5.12**, achieving full diastereocontrol by the remote relay of the configuration by a (–)-ephedrine-derived oxazolidine.^[272] This “ultra-remote” control allowed the formation of a chiral centre by relaying chiral information along 22 bonds. This corresponded to a distance of approximately 2.5 nm, the order of thickness of a cell membrane.



Scheme 86: 1,22-Relay of chirality in 1,8-xanthene dicarboxamides

V.1.3. C–N atropisomerism in anilides

Various C–N atropisomers were presented in Chapter 1. While secondary amides usually exist predominantly as the less hindered *E* isomer, *N,N*-disubstituted amides exist as a mixture in a ratio greatly dependent on factors such as steric demand.^[289,290] Steric demand forces the aryl ring to twist out of the plane of the amide, breaking conjugation. The *E* isomer is then favoured as it prevents unfavourable interactions between the lone pair of electrons of the oxygen lone pair and the aryl ring π -electrons.^[26] Axial chirality arises at the C_{Ar}–N bond as a consequence of this twisting. Curran and co-workers have described atropisomeric anilides with a single *ortho*-*tert*-butyl group, such as in compound **5.14** (Figure 36).^[26] *N*-aryl lactams such as **5.16** retained their conformation at room temperature, with a fixed amide bond geometry.^[291] 5-Membered *N*-aryl lactams such as **5.17** were also found to be axially chiral at room temperature, albeit with a significantly lower barrier to rotation.^[292]

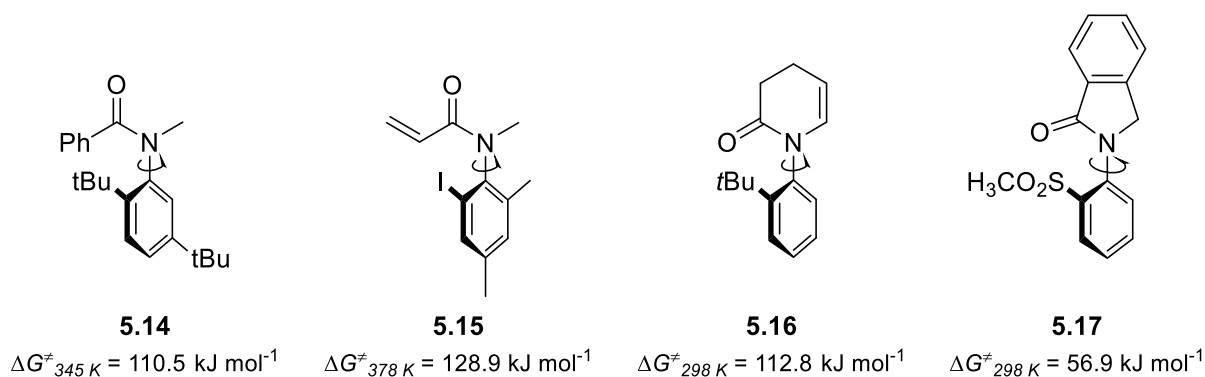
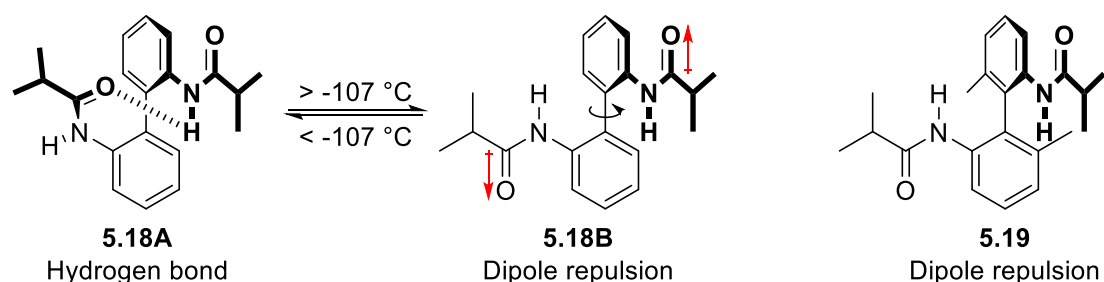


Figure 36: Selected atropisomeric anilides and their barrier to enantiomerisation

Dipolar repulsion in 2,2'-bis-anilides

Mazzanti *et al.* thoroughly studied the conformation of 2,2'-bis-anilides such as **5.18** (Scheme 87).^[293] Although facile bond rotation allowed for the rapid interconversion of different stereoisomers at room temperature, apolar mixtures of chlorofluorocarbons gave a major conformer by ¹H NMR analysis at cryogenic temperatures. This conformer was attributed to the formation of an intramolecular hydrogen bond (**5.18A**) and was also observed in the solid-state. However, above these temperatures, bis-anilide **5.18** exists as a mixture of two conformers in fast exchange, of which the major compound was C₂-symmetric. Further computational work highlighted the existence of conformer **5.18B** in which the amide groups were in conjugation with the aryl rings, allowing dipolar repulsion to dictate the conformation. When the steric demand around the C_{Ar}–C_{Ar} bond was increased, conformational flexibility was decreased and so compound **5.19** was observed as a single conformer resulting from dipolar repulsion, as it could not accommodate an intramolecular hydrogen bond.



Scheme 87: Dipolar repulsion in 2,2'-bis-anilides

To gain insight into the influence of this intramolecular hydrogen bond on conformation, the authors prepared a tertiary analogue of **5.18** by methylation of the amide groups. However, the ^1H NMR spectrum of the resulting compound became particularly complex. The hindered amides were expected to be disposed perpendicularly to the aryl rings, creating two stereogenic axes, in addition to *E/Z* isomerisation. Dynamic exchange between several conformers hence precluded detailed analysis.

V.2. Results and Discussion

V.2.1. Aim

The use of dynamic molecules in relaying information over long distances has led to communication of chirality over nanometre distances in rigid, aromatic scaffolds. A major limitation for the development of a longer structures for the remote communication of chirality comes from problems arising from the tedious, work-intensive synthesis of the substrates and their poor solubility.^[272,288,294] Furthermore, while dipolar interactions clearly play a major role in the relative orientation of the amides of compound **5.12**, the great steric bulk of these groups is also critical in the high selectivity. New scaffolds purely based on dipolar repulsion are needed to gain a greater understanding of the requisites to develop efficient conformational relays with a high stereocontrol.

Mazzanti *et al.* determined the various conformations of 2,2'-bis-anilides in solution, showing the potential for axially chiral amides to create conformational control by dipolar repulsion. The diphenylacetylene scaffold (Figure 37, in blue), offering a rigid structure over extended distances, is easily assembled by Sonogashira coupling.^[295] In the design of functional groups for dipolar interactions, isoindolinones (Figure 37, in red) offer advantages such as planarity and rigidity, limiting the number of interconverting ground state conformations, while the inclusion of the amide nitrogen in a ring eliminates *E/Z* isomerisation. Bates *et al.* showed that *N*-aryl isoindolinones with a single functionality at the *ortho*-position adopt a chiral ground state at room temperature with barriers to rotation small enough to allow fast equilibration.^[292]

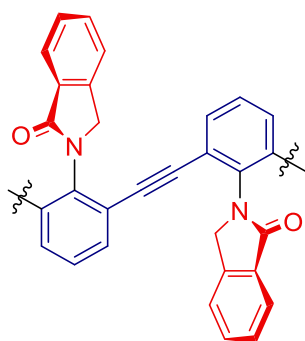
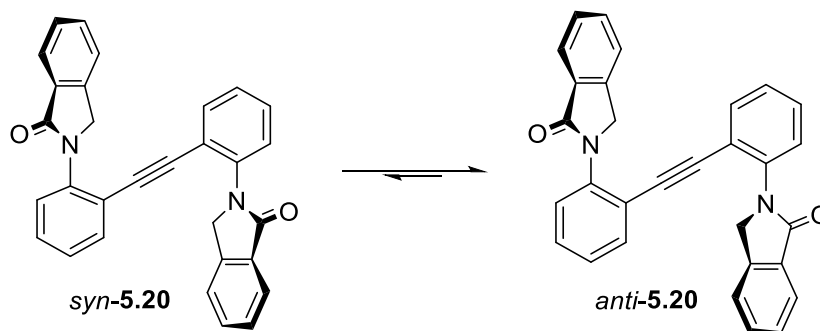


Figure 37: Model for the long-distance dipolar repulsion of isoindolinones

V.2.2. Dipoles repulsion in a *meta*-oligo(phenylacetylene) scaffold

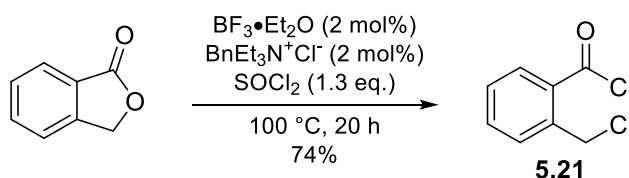
Conformational control by isoindolinones

To probe the influence of dipolar repulsion in isoindolinones through a diphenyl acetylene scaffold, dimer **5.20** was designed (Scheme 88). The only two chiral axes reduces the number of possible conformations. While the ground state of the diphenyl acetylene core is expected to be planar and rapidly rotating, it was anticipated that dipolar repulsion and steric hindrance would force the amide ground out of the plane of the aryl ring, creating a bias towards one conformer (presumably with an *anti* relationship).



Scheme 88: Model dimer **5.20**

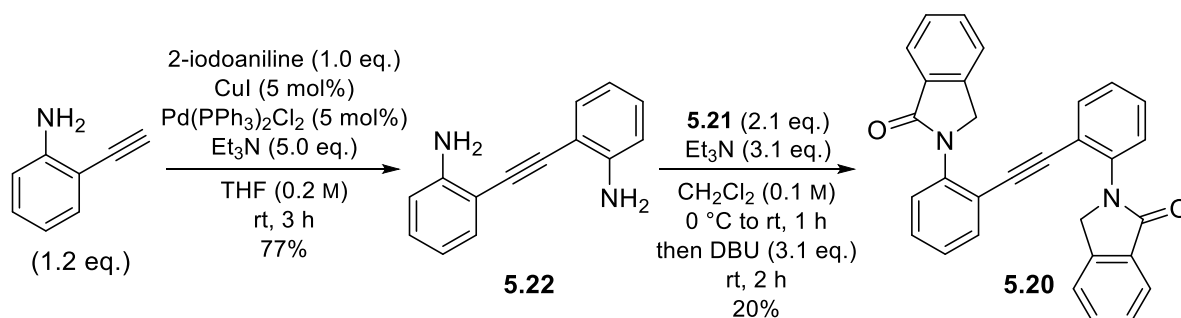
To access isoindolinone **5.20**, a two-step, one-pot procedure for the synthesis of *N*-aryl isoindolinones from the corresponding aniline with acyl chloride **5.21** (Scheme 89) was devised as a key step. Compound **5.21** was prepared in high yield on multigram scale according to a reported protocol.^[296]



Scheme 89: Preparation of **5.21**

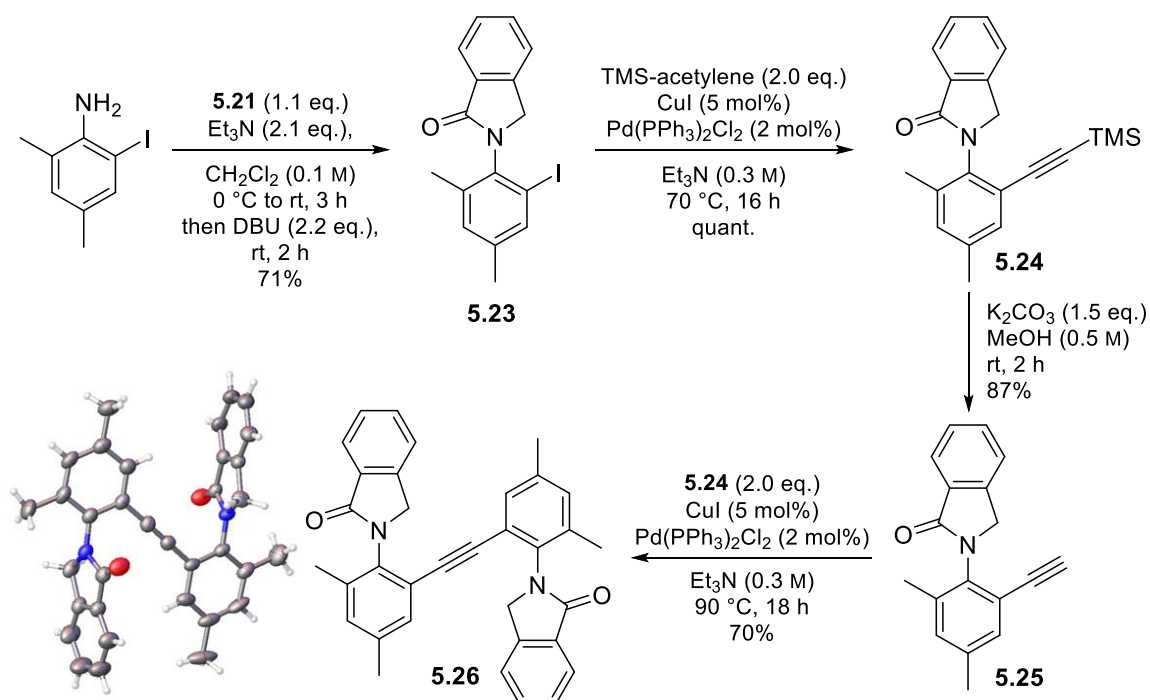
Dianiline **5.22** was made in good yield by Sonogashira coupling of commercially available 2-iodoaniline and 2-ethynyl aniline (Scheme 90). Model dimer **5.20** was then made in poor yield by amide bond

formation, followed by DBU-promoted intramolecular cyclisation to form the corresponding *N*-arylisindolinone.



Scheme 90: Synthesis of dimer **5.20**

Dimer **5.20** displayed a sharp singlet in its ^1H NMR spectrum for the benzylic proton, implying that at room temperature, the ground state conformation of **5.20** adopts a planar, achiral conformation interconverting too rapidly to be observed on the NMR timescale. To slow down C–N bond rotation and enforce a chiral, three-dimensional geometry of the amide group at room temperature, additional steric hindrance near the C–N bond was necessary, and dimer **5.26** was designed (Scheme 91). Due to the low yield of the isoindolinone formation, compound **5.26** was made through a step-intensive route from 2-iodo-4,6-dimethyl aniline. Isoindolinone ring formation on this substrate allowed the preparation of anilide **5.23** in good yield and on large scale. Sonogashira coupling with trimethylsilyl (TMS) acetylene, followed by desilylation using potassium carbonate in methanol produced terminal alkyne **5.25** in excellent yield. Finally, cross-coupling with **5.23** afforded dimer **5.26**. Although longer, this sequence was found to be more robust than the previous strategy used for **5.20**.



Scheme 91: Synthesis of dimer **5.26**

The isoindolinone benzylic protons of **5.26** displayed sharp signals corresponding to AB systems in the ^1H NMR spectrum, characteristic of a chiral compound slowly interconverting on the NMR timescale (Figure 38). In CDCl_3 , splitting of most signals suggested the existence of a minor conformer. Crystals of **5.26** suitable for X-ray diffraction were grown by slow evaporation of a saturated solution of **5.26** in toluene. The solid-state structure showed a near-perpendicular arrangement of the amide moiety with a torsion angle of 89.1° , while the diphenylacetylene core was approximately planar, as the average torsion angle was 4.7° .

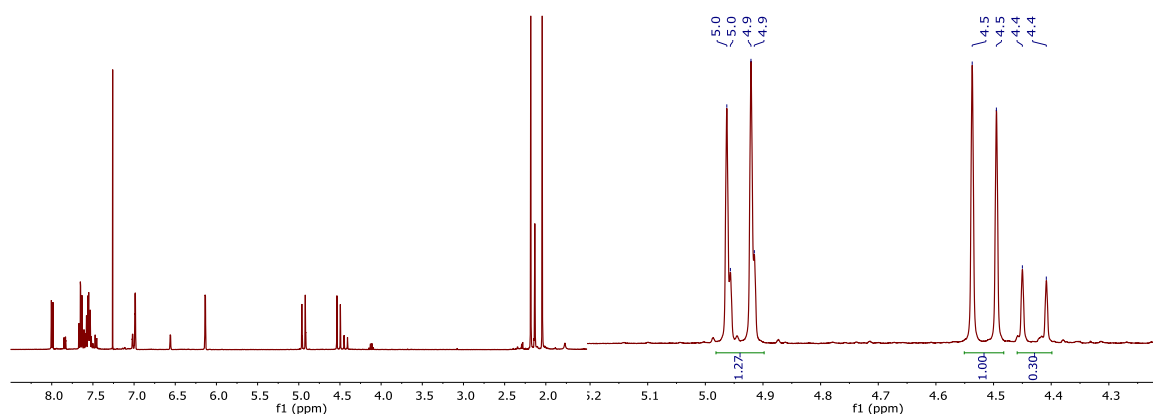


Figure 38: ^1H NMR spectrum of **5.26** and zoom of the isoindolinone benzylic methylene region

The conformer distribution was solvent-dependent (Table 34), as determined by the relative integration of well-resolved signals of each stereoisomer. From earlier work using bis-benzamides (see section V.1.2.), and from the solid-state structure of **5.26**, it was assumed that the *anti* conformer was the major stereoisomer. In polar solvents such as $\text{DMSO}-d_6$ and CD_3CN , the proportion of minor conformer increased, with the major conformer being present only in a slight excess in $\text{DMSO}-d_6$. The trend was similar, although less significant in CD_3OD . Dipolar interactions with the solvent presumably decreased the intramolecular repulsion, stabilising the *syn* conformer. The largest ratio was in toluene- d_8 , where the amount of major conformer was fivefold larger than the minor.

Solvent	toluene- d_8	CDCl_3	$\text{DMSO}-d_6$	CD_3OD	CD_3CN
Ratio (<i>anti</i>:<i>syn</i>)^a	1:0.20	1:0.30	1:0.75	1:0.55	1:0.67

^a Determined by integration of the ^1H NMR signals.

Table 34: Conformer distribution of **5.26** in various solvents

Dimer **5.26** exists as a pair of racemic, inequivalent stereoisomers. To gain insight into the kinetic parameters of conformer interconversion in **5.26**, enantiomers of its starting material **5.24**, bearing only one stereogenic axis, were resolved by chiral HPLC (Figure 39).

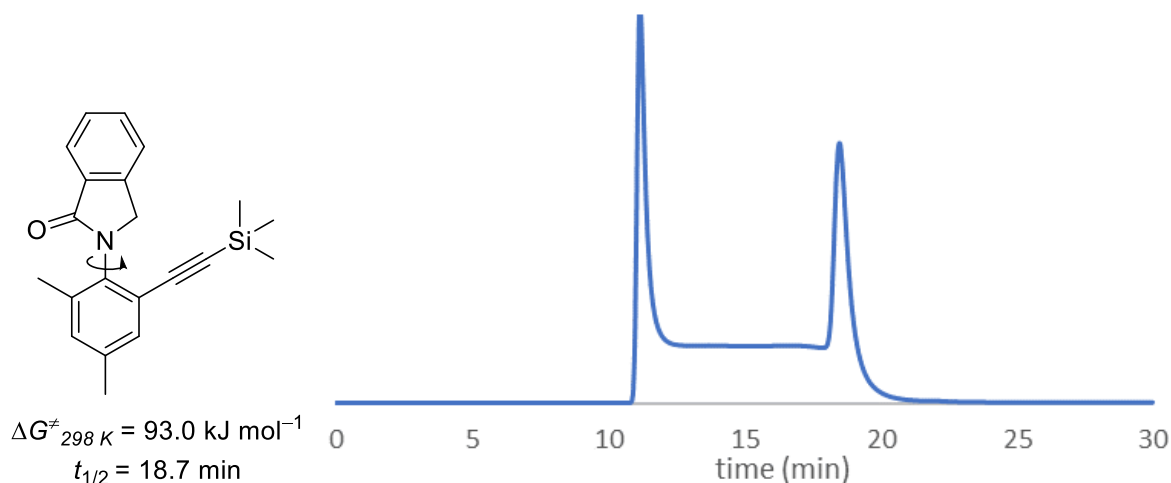
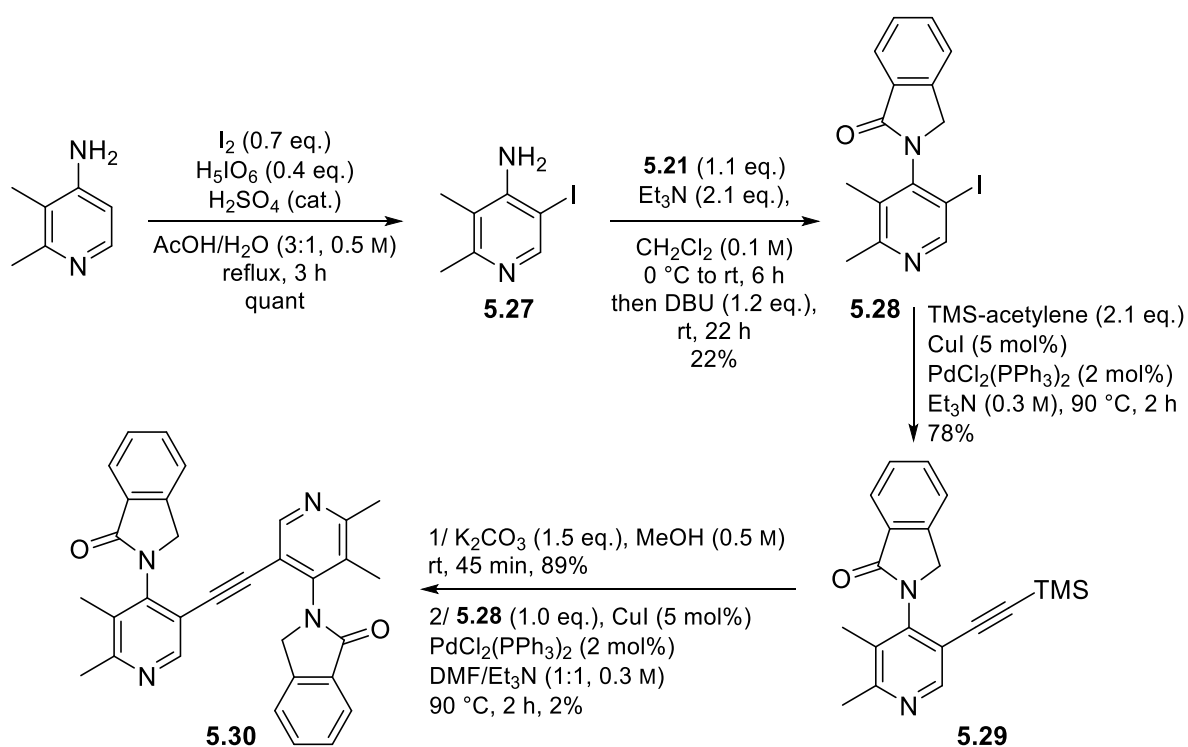


Figure 39: HPLC trace of **5.24** at 40 °C

Above room temperature, substrate **5.24** displayed a plateau typical of an atropisomer with a low barrier to enantiomerisation. VT-HPLC, followed by Eyring analysis allowed the calculation of the barrier to rotation about the C_{Ar}–N bond of **5.24** (See Chapter 1). Anilide **5.24** was found to be an atropisomer with a barrier to enantiomerisation of 93.0 kJ mol^{−1} at room temperature, corresponding to a half-life of 19 minutes under these conditions. Hence, enough time had to be left for samples of compounds derived from **5.26** to allow them to thermally equilibrate.

Towards stimuli-responsive dipolar repulsion

Modification of the electron density of the *N*-aryl ring of dimer **5.26** was thought to have an impact on the electronic properties of the amide electronic properties, and hence lead to a change of the conformational bias. Furthermore, direct modification of the electronic properties of the scaffold would offer the possibility to switch conformer preference with an external stimulus. *Para*-substituted pyridines were thought to bring electronic modification and potential for a property switch by treatment with an appropriate acid. Model compound **5.30** was synthesised to test this hypothesis (Scheme 92). Isoindolinone formation on the iodinated DMAP derivative **5.27**, though, performed in poor yield. While Sonogashira coupling with trimethylsilyl acetylene proceeded in good yield, the two steps deprotection/cross-coupling to form dimer **5.30** only provided trace amounts of products. Presumably, poor solubility of both the substrates and the product in the reaction solvents, together with a strong affinity of the product for silica during purification led to the isolation of **5.30** in very low yield.



Scheme 92: Synthesis of dimer **5.30**

Nevertheless, sufficient material was isolated to observe the two conformers by ^1H NMR, in a similar ratio to that of dimer **5.26**. Treatment of pyridine **5.30** with five equivalents of trifluoroacetic acid and overnight equilibration of the sample at room temperature resulted in a modification of the conformer distribution (Table 35), with almost no preference for one stereoisomer over the other.

Compound	5.26	5.30	[5.30·TFA₂]²⁺
Ratio (<i>anti/syn</i>) ^a	1:0.30	1:0.40	1:0.90 ^b

^a Determined by integration of the ^1H signals in CDCl_3 ^b After treatment of **5.30** with 5 equivalents of TFA

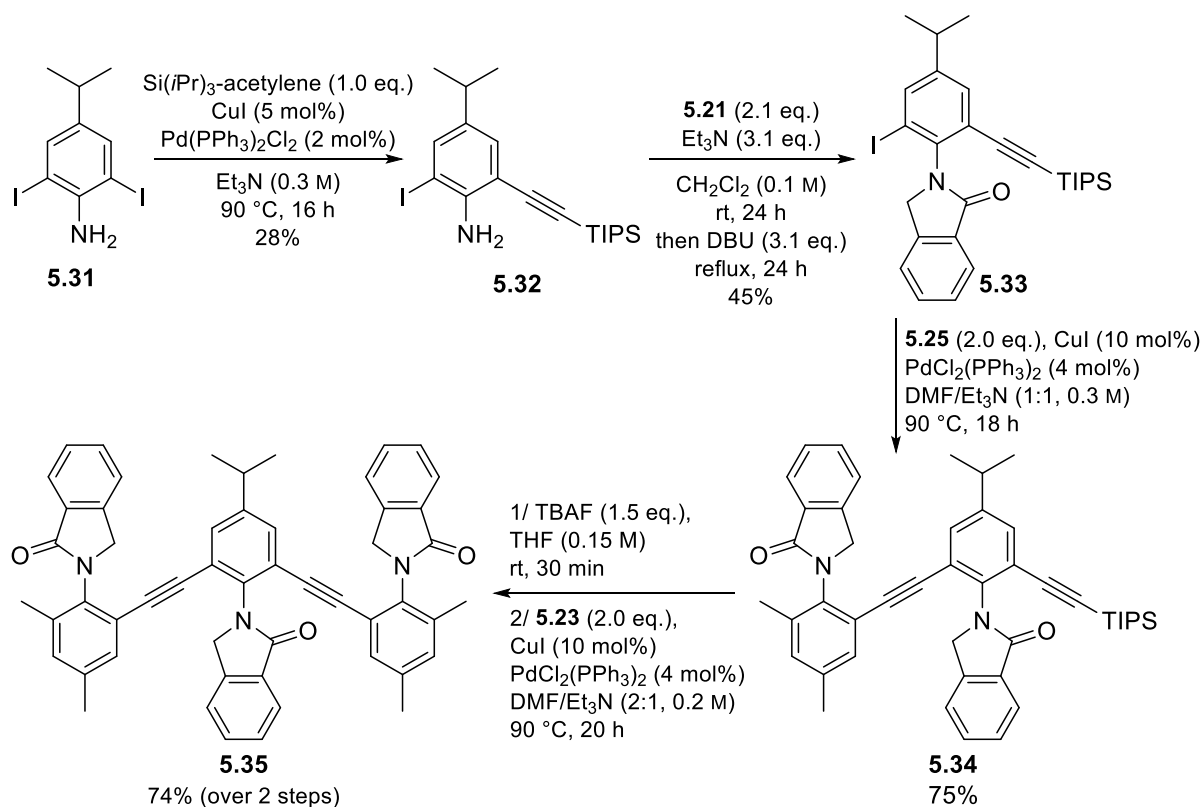
Table 35 : Conformer ratio of **5.30**

Addition of trifluoroacetic acid to the solution to protonate the pyridine rings possibly changes the medium polarity. Furthermore, the various ionic species formed can interact with the amido carbonyl groups to disrupt intramolecular interactions and lead to no conformational preference.

Conformational relay through a meta-oligo(phenylacetylene) scaffold

While dimer **5.26** did not display exclusive conformational control, we focused our efforts on understanding the strength of the repulsive interaction between the amide dipoles over longer distances with trimer **5.35** (Scheme 93). Initial attempts to directly form the isoindolinone ring on aniline **5.31** did not yield any product, while using the same conditions to its dibrominated derivative led to decomposition of the amide intermediate after addition of DBU. As steric hindrance seemed to

impart reactivity for the synthesis of the starting materials, a step-intensive, iterative approach was attempted.



Scheme 93 : Synthesis of trimer **5.35**

An isopropyl group was introduced at the *para*-position of **5.32** in the hope it would provide information on the compound symmetry, and hence be used to deduce its relative conformation. Mono-alkynylation of aniline **5.31** was performed following standard conditions forming aniline **5.32** in poor yield. Isoindolinone formation was then used to obtain **5.33** in moderate yield. The use of a triisopropylsilyl (TIPS) protecting group was necessary, as formation of the isoindolinone ring on the TMS-protected analogue of **5.32** led to decomposition, with disappearance of the alkynyl peaks by ^{13}C NMR. Silyl-protected compound **5.33** was then coupled to terminal alkyne **5.25** in good yield, and a two steps deprotection/coupling allowed the isolation of trimer **5.35** in excellent yield.

Analysis of trimer **5.35** proved to be difficult. The existence of three stereogenic axes gave rise to three diastereomeric compounds **A**, **B** and **C**, with a (*syn, syn*), (*anti, anti*), and (*syn, anti*) relative orientation respectively, as illustrated by the portion of the ^1H NMR spectrum corresponding to the isoindolinone benzylic protons of **5.35** (Figure 40).

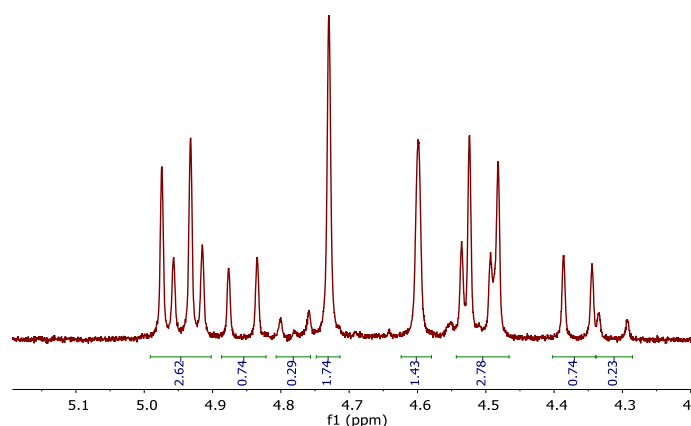
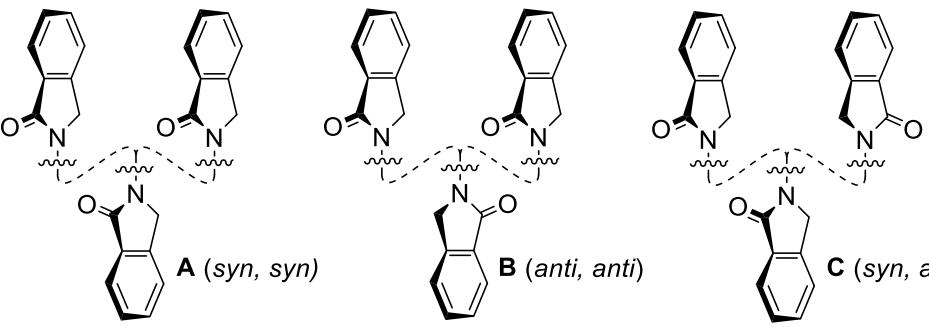


Figure 40: Portion of the ^1H NMR spectrum of **5.35** used to determine the conformer distribution

The conformer distribution of trimer **5.35** varied in different solvents, although with a general trend (Table 36). The relative conformation was deduced from the signal multiplicity of the ^1H NMR signals for the benzylic protons as well as the number of signals for the carbonyl and the alkyne groups by ^{13}C NMR analysis. The ^{13}C NMR spectrum of the minor conformer **A** displayed two carbonyl resonances in a 2:1 ratio and two alkynic resonances, showing a plane of symmetry. The same features were observed in the ^{13}C NMR spectrum of conformer **B**, the major isomer in CDCl_3 and toluene- d_8 . Its ^1H NMR spectrum also unambiguously displayed one AB system and one singlet in a 2:1 ratio for the benzylic protons of the isoindolinone rings, also due to a plane of symmetry. Eventually, neither the ^1H nor ^{13}C NMR spectra of isomer **C** displayed characteristics of a symmetrical molecule. Based on these pieces of evidence, and on the crystal structure of dimer **5.26**, isomer **C** was assigned as the (*anti*, *syn*) conformer, while **A** and **B** were assigned as (*syn*, *syn*) and (*anti*, *anti*), respectively (Table 36).

			
Ratio ^a	toluene- d_8	CDCl_3	CD_3OD
A (<i>syn</i> , <i>syn</i>)	4%	8%	16%
B (<i>anti</i> , <i>anti</i>)	55%	49%	35%
C (<i>syn</i> , <i>anti</i>)	41%	43%	49%

^a Determined by averaged integration of the carbonyl and alkyne ^{13}C signals

Table 36: Schematic representation of the conformer of **5.35** and their distribution in various solvents

The conformer distribution of trimer **5.35** showed the same trend in its solvent-dependence as for dimer **5.26**, with a marginal amount of conformer **A** in toluene-*d*₈ gradually increasing in CDCl₃ and CD₃OD, respectively. The stability of the preferred (*anti*, *anti*) conformer was also imparted by the change of solvent as it became minor compared to the doubly degenerate (*syn*, *anti*) conformer in CD₃OD. This mixture of conformers resulted in a heterogeneously-defined scaffold, making it a poor candidate for relaying conformational changes over long distances.

Influence of dipole moment on dipolar repulsion

The ability of other dipoles to provide conformational control on a diphenylacetylene scaffold was investigated. Oxazolidinone **5.37**, sulfonamide **5.38** and imidazolone **5.39** were selected as dipolar groups because of their potential access from the same aniline substrates. Their respective dipole moments were calculated using the software Spartan, after optimisation of their ground state geometry using the 6-31G* basis in a vacuum (Table 37).

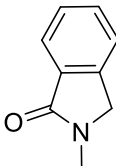
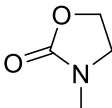
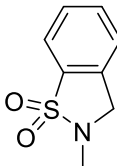
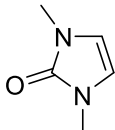
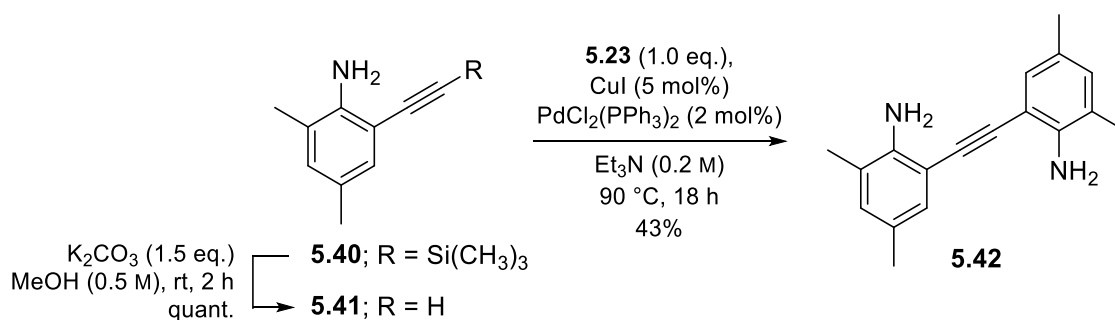
				
5.36	5.37	5.38	5.39	
Compound	5.36	5.37	5.38	5.39
Dipole moment (D)	4.26	5.71	6.19	3.93

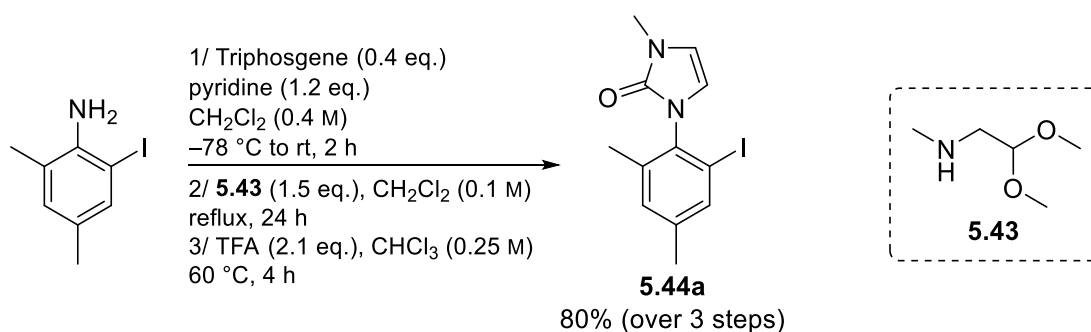
Table 37: Calculated dipole moment of selected molecules

Oxazolidinone **5.37** and sulfonamide **5.38** were found to have the largest dipoles, and thus were expected to provide more control of the topology of the diphenylacetylene scaffold, while imidazolone **5.39** had a slightly lower dipole than isoindolinone **5.36**. These three moieties were deemed to be easily amenable to the synthesis of derivatives of dimer **5.26**. Dianiline **5.42** was made in moderate yield by cross-coupling of the respective *ortho*-iodoaniline and *ortho*-ethynylaniline (Scheme 94). However, treatment of this compound with the substrates used for the formation of the sulfonamide, oxazolidinone and imidazolone rings did not yield any product. Therefore, a step-intensive approach was necessary.



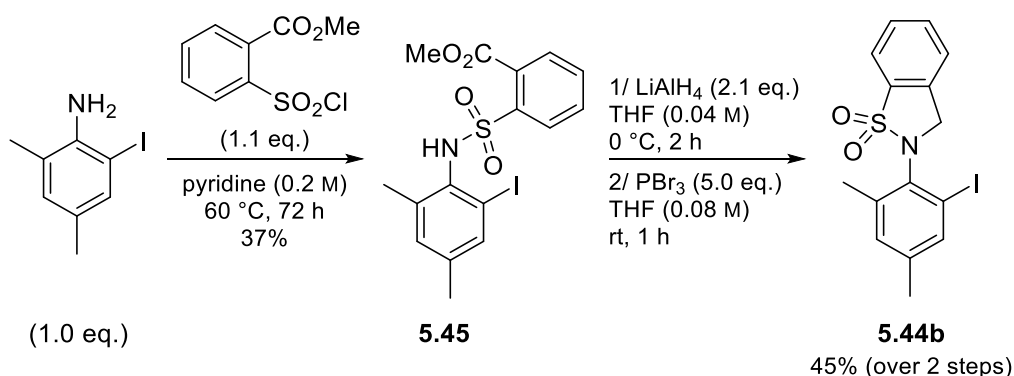
Scheme 94 : Synthesis of substrate 5.42

Synthesis of imidazolone **5.44a** was initially attempted by coupling 2-iodo-4,6-dimethylaniline with the carbamoyl chloride derived from **5.43**, but gave no reaction. 2-Iodo-4,6-dimethyl aniline was then transformed into the corresponding isocyanate by treatment with triphosgene, followed by coupling with secondary amine **5.43** (Scheme 95). Eventually, deprotection of the acetal group under acidic conditions^[297] yielded the cyclised product in excellent yield over three steps.



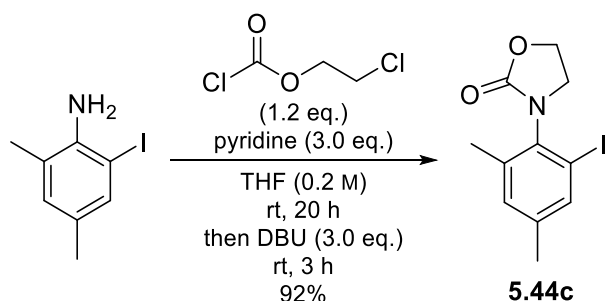
Scheme 95: Synthesis of imidazolone substrate 5.44a

Preparation of sulfonamide **5.44b** was undertaken following a procedure by Ulven *et al.* (Scheme 96).^[298] Condensation of 2-iodo-4,6-dimethylaniline with the corresponding sulfonyl chloride gave sulfonamide **5.45** in moderate yield. Cyclic compound **5.44b** was obtained in good yield over two steps by reduction of the ester group of **5.45**, followed by displacement of the resulting alcohol using phosphorus tribromide and spontaneous cyclisation.



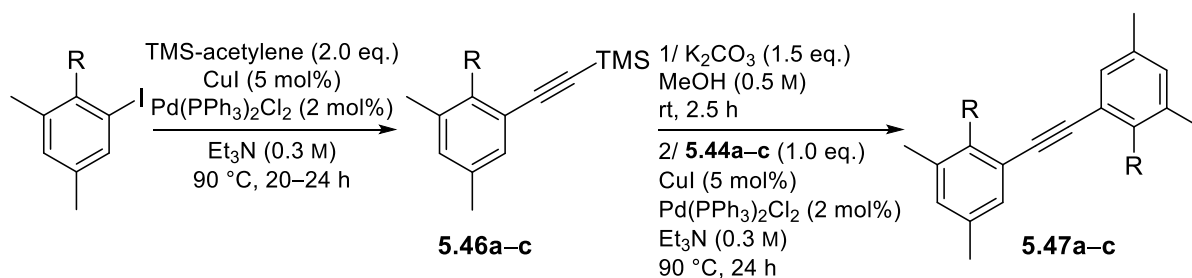
Scheme 96: Synthesis of sulfonamide substrate 5.44c

With a similar strategy to that employed for the formation of the isoindolinone ring, oxazolidinone **5.44c** was prepared by a one-pot sequence from 2-chloroethyl chloroformate involving carbamate formation followed by cyclisation to the corresponding oxazolidinone upon treatment with DBU to afford **5.44c** in excellent yield (Scheme 97).

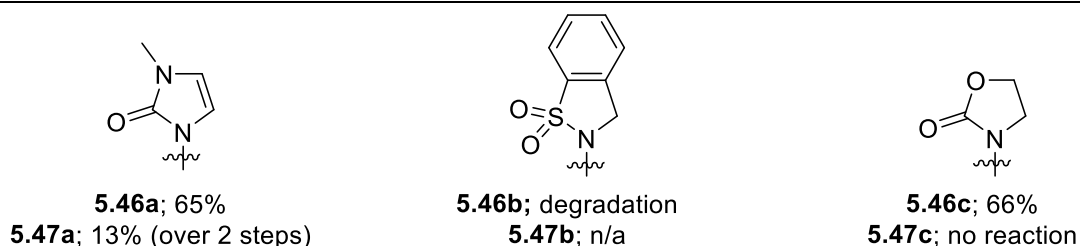


Scheme 97: Synthesis of carbamate substrate **5.44c**

These three derivatives were then subjected to Sonogashira coupling with TMS-acetylene following the procedure previously described (Scheme 98). While imidazolone **5.44a** and oxazolidinone **5.44c** readily reacted to form the corresponding phenyl acetylene product, decomposition of sulfonamide **5.44b** occurred under the reaction conditions.



R =



Scheme 98: Synthesis of dimers with various dipoles

Removal of the silyl protecting group followed by Sonogashira coupling with the corresponding aryl iodide did not yield any oxazolidinone dimer, and imidazolone **5.47a** was only formed in poor yield.

The ^1H and ^{13}C NMR spectra of dimer **5.47a** displayed two stereoisomers, as demonstrated in the change of their distribution in various solvents. Unfortunately, compound **5.47a** was poorly soluble in most organic solvents, limiting its applicability. Nonetheless, a similar trend to that of dimer **5.26** was observed relative to the solvent polarity (Table 38). While the major conformer of **5.47a** was present in more than a twofold ratio in CDCl_3 and toluene- d_8 , the distribution dropped significantly in CD_3OD .

Solvent	toluene- d_8	$CDCl_3$	CD_3OD
Ratio (anti/syn)^a	1:0.40	1:0.45	1:0.70

^a Determined by integration of the 1H signals

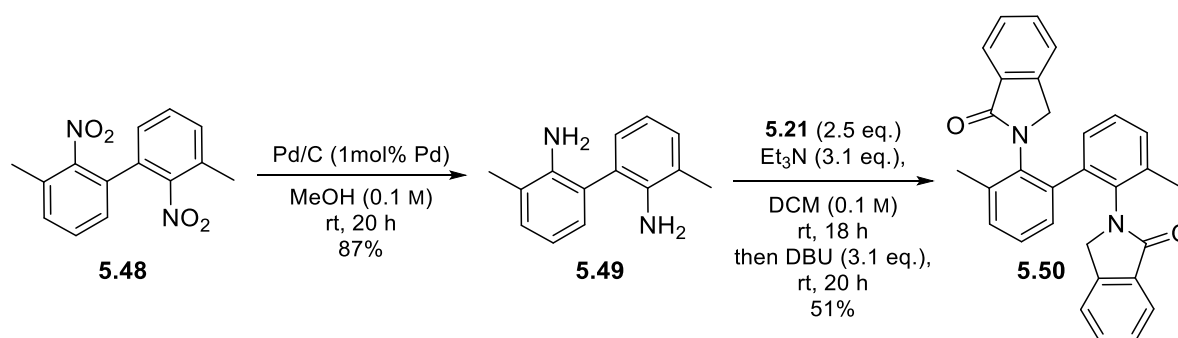
Table 38: Conformers distribution of **5.47a** in various solvents

Imidazolone dimer **5.47a** offered poorer conformational control than its analogous compound **5.26**, as expected from its lower dipole moment. This, together with the poor yields obtained during its synthesis and the poor solubility of compound **5.47a**, shows that the *N*-aryl isoindolinone scaffold is the most versatile and easily amenable to a variety of conformational relays.

V.2.2. Influence of distance on dipolar repulsion

While dimer **5.26** does not exist as a single conformer, it is still remarkable, considering the distance by which these dipoles are separated, that conformation is remotely influenced solely by dipolar repulsion. We sought to gain more insight into the distance at which dipoles can be separated and still be 'in communication' by modification of the core scaffold.

Biphenyl **5.50** did not bear an acetylene spacer, bringing the two dipoles in closer proximity (Scheme 99). Symmetrical biphenyl **5.48** was prepared by palladium-catalysed decarboxylative homocoupling of the corresponding benzoic acid.^[299] Reduction of the nitro groups followed by the key isoindolinone formation allowed the preparation of biphenyl **5.50** in good yield.



Scheme 99: Synthesis of 2,2'-substituted biphenyl **5.50**

Despite the proximity of the two dipoles, two conformers were in an approximately 1:1 ratio in CD_2Cl_2 as well as in toluene- d_8 (Figure 41). Upon cooling to $-80\text{ }^{\circ}C$ in both solvents, line-broadening was followed by appearance of more resonances. The ratio of conformers reached 2:1 in both solvents at this temperature, and complexity arose from the isoindolinone benzylic protons signal. The splitting of each methyl signal into two resonances upon cooling suggested that the conformer did not hold a plane or centre of symmetry. Possibly, the $C_{Ar}-C_{Ar}$ bond sits in a skewed arrangement of the two aryl rings of the biphenyl moiety, leading to asymmetry of the molecule regardless of the relative orientation of the amide groups.

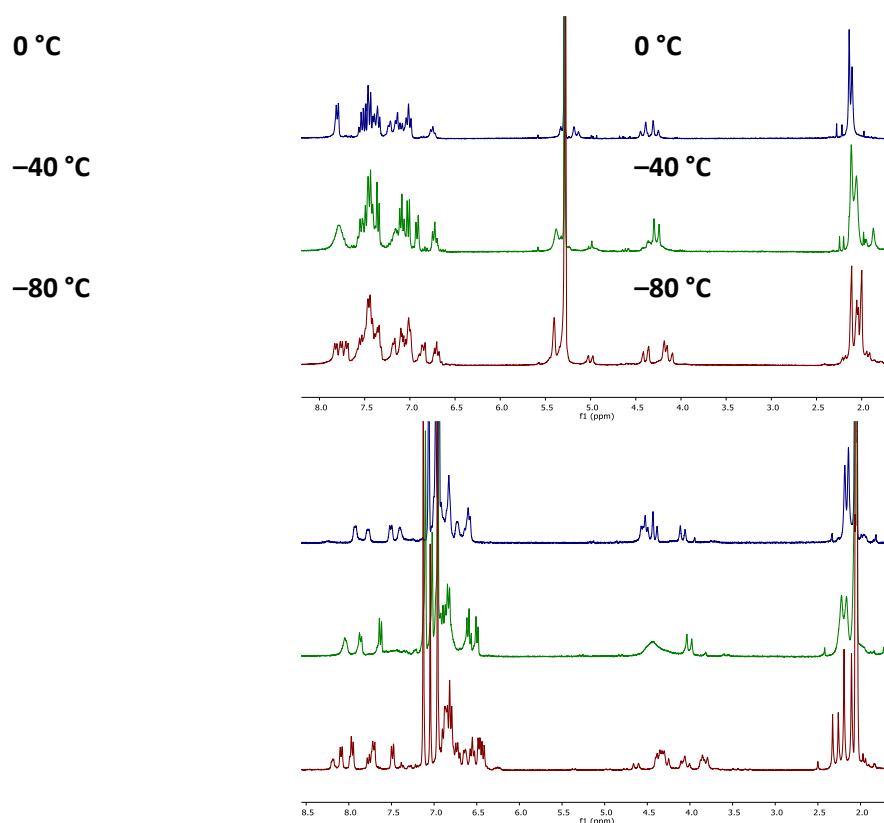


Figure 41: VT ^1H NMR spectrum (300 MHz) of **5.50** in CD_2Cl_2 (left) and toluene- d_8 (right).

Upon warming a sample of **5.50** in toluene- d_8 up to 100 °C, one of the benzylic AB systems coalesced, together with line broadening of some aromatic signals (Figure 42). Interestingly, the two singlets of the methyl groups merged into one signal.

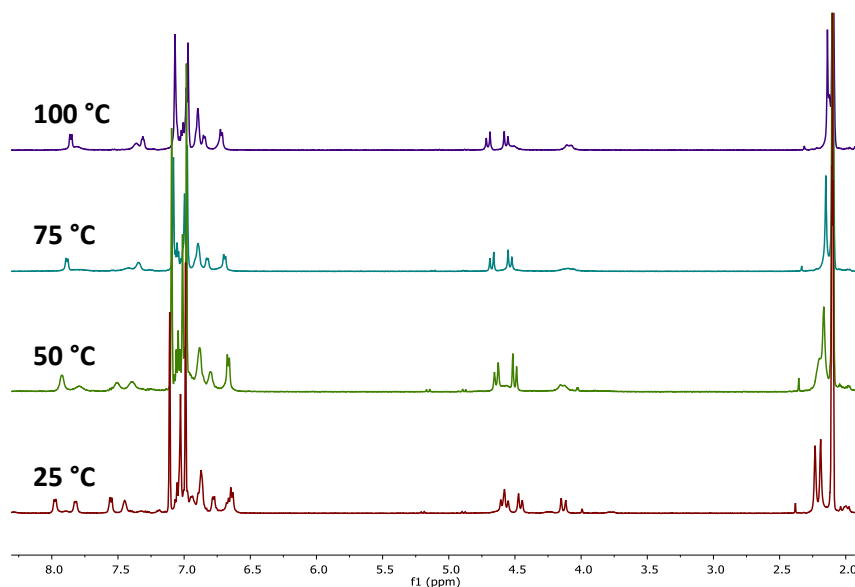
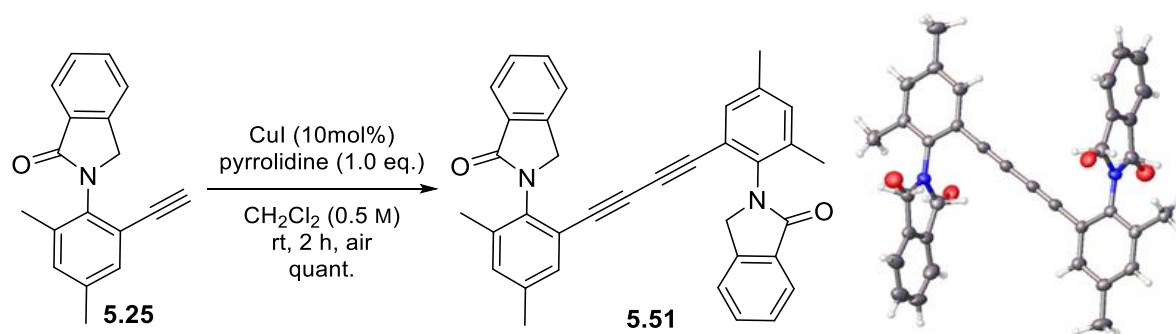


Figure 42: VT ^1H NMR spectrum (500 MHz) of **5.50** toluene- d_8 .

Bringing the dipoles to close proximity did not result in the formation of a single conformer at room temperature. Instead, the complexity of the NMR spectra of biphenyl **5.50** arising from another slowly rotating $\text{C}_{\text{Ar}}\text{--}\text{C}_{\text{Ar}}$ chirogenic bond made its analysis more complex as many conformers interconverted

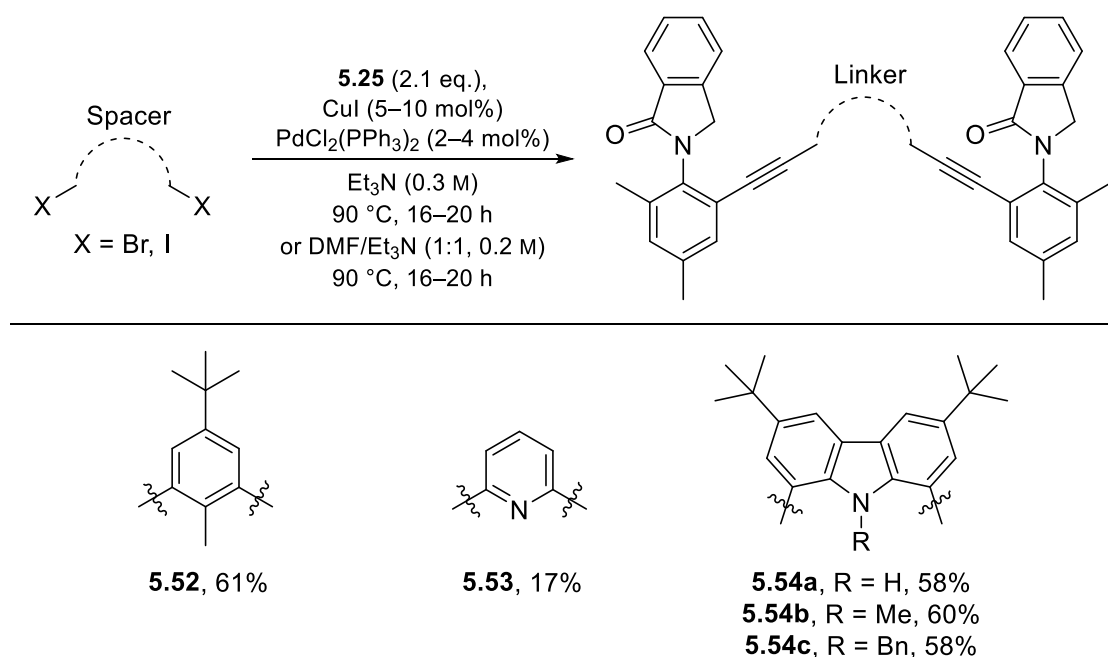
slowly in solution. Snieckus *et al.* found the barrier to rotation around the $C_{Ar}-C_{Ar}$ bond in similar biphenyls to be high enough to observe slow rotation on the NMR timescale at low temperature.^[300] Hence, at cryogenic and room temperatures, multiple atropdiastereomers of different ground state energies arose from this third chiral axis. Upon warming to high temperature, coalescence of the benzylic proton resonances suggested that rapid rotation around the $C_{Ar}-C_{Ar}$ bond revealed the existence of only one relative arrangement of the dipoles due to their close proximity.

While shorter dipole-dipole distances lead to complete control of the relative orientation of the amide groups, the effect of separating dipoles to longer distances was investigated to gain insight into the maximum distance at which dipoles can still be in communication. Diyne **5.51** was made in quantitative yield by oxidative homocoupling of monomer **5.25** (Scheme 100). Crystals of **5.51** suitable for X-ray diffraction were grown by slow evaporation of a saturated solution of **5.51** in methanol. While no preferred relative orientation of the dipoles was observed in the solid-state, the amide groups still lay perpendicular to the central core, with torsion angles of 98.0 and 95.8°. Remarkably, despite the high degree of flexibility offered by the diyne moiety, the diphenylacetylene scaffold was still planar, with an average torsion angle of 1.2°.



Scheme 100: Synthesis of diyne **5.51**

The 1H NMR spectrum of diyne **5.51** in $CDCl_3$ showed a mixture of conformers in a 1:0.7 ratio. While this ratio showed that the difference in energy between the *anti* and *syn* stereoisomers was low, it was remarkable that despite the increased distance between the dipole ($d_{N-N'} = 8.62$ Å in the crystal structure), dipolar repulsion was still strong enough to impart a conformational bias. Larger distances were then covered by (hetero)aromatic groups connecting both monomer through an alkyne bond (Scheme 101). While compound **5.52** did not contain a polarised linker, carbazoles **5.54a–c** and pyridine **5.53** would potentially contribute to the overall dipole moment of the molecule, and bias one conformer over the other.



Scheme 101: Introduction of various linkers between the dipoles

In CDCl₃, the aryl spacer in **5.52** yielded a 1:1 mixture of conformers (Table 39). Consequently, communication of information was prevented by the particularly long linker bridging the two dipoles, as the distance between both nitrogen atoms was calculated to be $d_{N-N'} = 10.5 \text{ \AA}$ in the optimised geometry of **5.52** using semi-empirical methods in a vacuum (PM3). While only poor, the influence of the pyridine dipole **5.53** on conformer distribution was apparent in the ¹H NMR spectrum. Despite the similar distance separating the dipoles compared to **5.52**, one conformer was in slight excess. However, should the oligo(phenylacetylene) scaffold be planar, the pyridine and isoindolinone dipoles would be orthogonal. Possibly, the ground state conformation of the core scaffold is twisted, allowing alignment of the various dipoles to a certain extent. Unfortunately, attempts to optimise the geometry of **5.53** using computational methods did not provide any clear major conformer. Upon protonation of the pyridine using trifluoroacetic acid, a 1:1 mixture of conformers was obtained after equilibration. No significant change on the chemical shift and resonance of the signals in the ¹H NMR spectrum of **[5.53·TFA]⁺** supported the hypothesis of a similar overall conformation of the core scaffold. In water, the dipole moment of pyridinium ion is lower than that of pyridine,^[301] and probably is not strong enough to participate in long-distance communication in **[5.53·TFA]⁺**. As with dimer **5.30**, the equal energy of the two conformers might also be due to the change in solvent polarity, or to intermolecular interactions with the resulting ion pair.

Compound	5.52	5.53	[5.53·TFA]⁺ ^a	5.54a	5.54b	5.54c
Ratio ^b (<i>anti/syn</i>)	1:1 ^c	1:0.85 ^c	1:1 ^c	1:0.35 ^c	1:0.80 ^c	1:0.90 ^d

^a After treatment of **5.53** with 5 eq. of TFA. ^b In CDCl₃. ^c Determined by ¹H NMR analysis. ^d Determined by ¹³C NMR analysis.

Table 39: Influence of the linker on conformer ratio

Although unsubstituted pyridine and carbazole have a similar dipole moment (respectively 2.15^[302] and 2.09 D^[303]), the proportion of the major conformer of dimer **5.54a** was greater than that of **5.53**. In fact, this ratio was close to the one for the shorter isoindolinone dimer **5.26**, despite the longer linker between the two dipoles. However, *N*-substitution significantly changed the conformer distribution. *N*-alkylated carbazoles have a smaller dipole moment compared to carbazole itself (the dipole moment of *N*-ethyl carbazole, for example, is 1.74 D^[303]), which led to a drop in the conformer ratio to reach a near-equivalent mixture. The effect was even more dramatic when a benzyl group was introduced on the carbazole nitrogen as in **5.54c**. However, while the ¹H NMR spectra of **5.54a** and **5.54b** displayed sharp signals, significant line broadening was observed for **5.54c** (Figure 43).

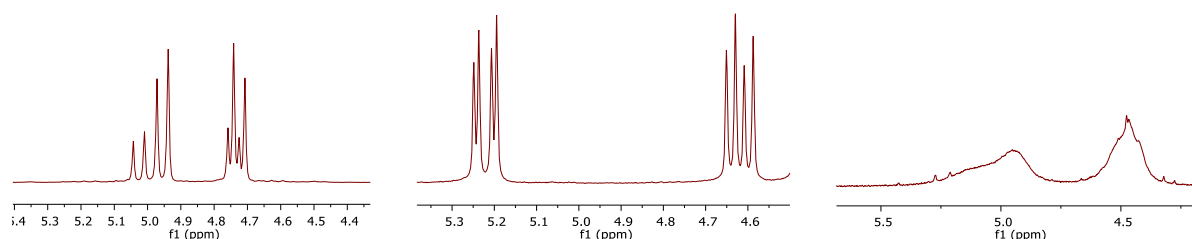


Figure 43: The ¹H NMR signals of the isoindolinone benzylic protons in carbazoles **5.54a**, **5.54b** and **5.54c** respectively

Upon cooling in CD₂Cl₂, the broad isoindolinone benzylic signals de-coalesced into two sets of peaks, in the same ratio as observed by ¹³C NMR at room temperature, indicating two conformers (Figure 44). One conformer possesses a plane of symmetry, as revealed by the existence of a single AB system for its isoindolinone benzylic protons, while the other pair of AB systems showed that the second conformer does not hold any element of symmetry.

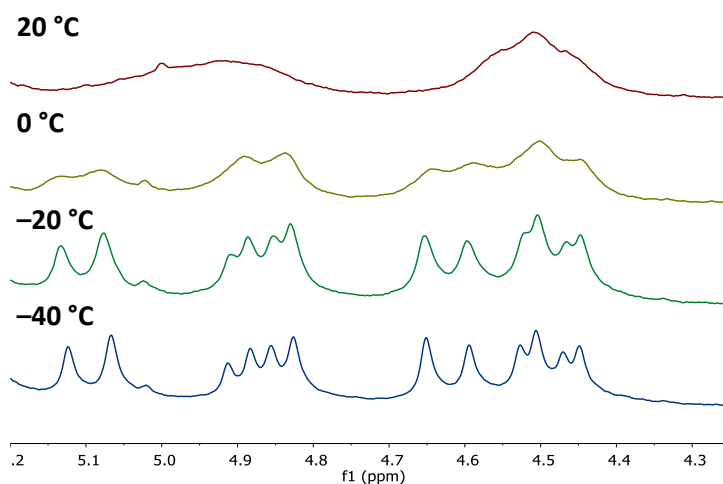


Figure 44: VT ¹H NMR (300 MHz) of **5.54c** in CD₂Cl₂, isoindolinone benzylic protons.

Oligo(phenylacetylene)s linked by carbazole derivatives are known to form helices by π -stacking.^[304] While the geometry of the amide group, forced out of the plane of the aryl group by the adjacent hindering methyl group, was expected to prevent this behaviour, ground state conformations of

carbazole derivatives **5.54a–c** were modelled using semi-empirical methods in a vacuum (PM3) with the software Spartan (Figure 45). While this level of theory was too basic to elucidate the energy difference of conformers arising from dipolar repulsion, this method gave insight towards the change in ground state conformation brought about by steric hindrance around the carbazole nitrogen atom.

In carbazole dimer **5.54a**, the core scaffold sits in an approximately planar, extended fashion, with the two aryl rings lying at 10.6° and 14.0° with respect to the carbazole group. The isoindolinones rings sat on the outer side of the carbazole moiety, perpendicular to the rest of the scaffold at 73.9°, with planar nitrogen atoms. Due to the long distance between the isoindolinone rings ($d_{N-N'} = 11.6 \text{ \AA}$), the dipole of the carbazole group must play a role in the communication of information as $d_{N-N'H} = 6.5 \text{ \AA}$ on average, similar to that in the crystal of dimer **5.26**. A similar structure was found after methylation of the carbazole, although twisting of the aryl rings through the alkyne bonds in **5.54b** was more pronounced at 9.5° and 33.5°, resulting in longer inter-dipolar distances $d_{N-N'} = 12.4 \text{ \AA}$ and $d_{N-N'Me} = 6.7 \text{ \AA}$. Hence, an alkyl substituent not only reduced the dipole moment of the carbazole ring, disrupting the dipolar repulsion, but the added steric hindrance presumably hampered bond rotation and prevented the optimisation of an ideal conformation for dipolar interaction.

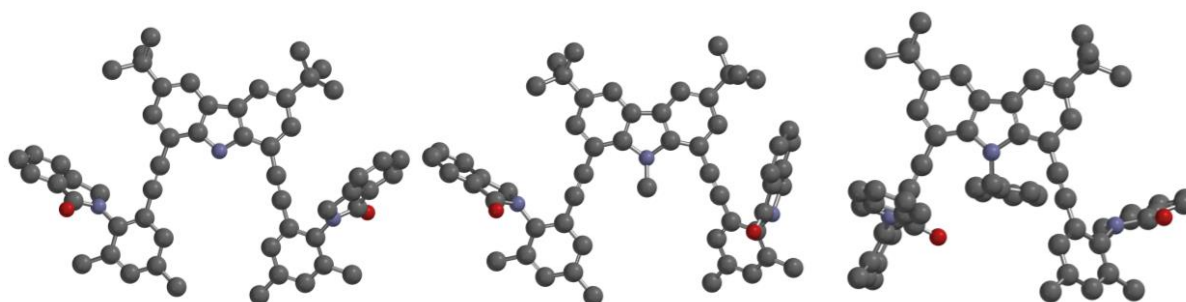


Figure 45: Ground state conformations of **5.54a**, **5.54b**, and **5.54c**, respectively, at the PM3 level of theory, in vacuum

A more significant change in the ground state conformation was observed for **5.54c**. Benzylation of the carbazole provided too much steric encumbrance about the side arms to allow coplanarity and conjugation through the alkyne. In this case, the aryl rings sit perpendicularly to the carbazole, at angles of 57.5° and 84.2°, giving rise to an *anti* arrangement of the *N*-aryl rings relative to the plane of the carbazole, slowly interconverting at the NMR timescale. The distance between the dipole and the carbazole was shortened, $d_{N-N'Bn} = 5.9 \text{ \AA}$, but the substrate was not able to arrange for dipole alignment because of steric bulk. Furthermore, the inter-dipolar distance was too large ($d_{N-N'} = 10.0 \text{ \AA}$) to give rise to a preferred conformation.

V.3. Conclusion

Remote control of conformation was previously achieved by using both steric and electronic interactions to bias the relative conformation of dipoles along a rigid scaffold. We found that conformational control can be attained in a rigid, rapidly rotating diphenylacetylene scaffold. Isoindolinones can serve as non-sterically demanding dipoles, and dipolar interactions alone impact the relative conformation of molecules at distances of up to 8.6 Å. However, dipolar interactions alone do not seem to be sufficient to relay a major relative conformation over multiple dipoles, as the conformational analysis of trimer **5.35** suggested.

While other dipoles were expected to act similarly, only imidazolone containing models could be synthesised. The poorer control over the relative orientation correlated with the lower calculated dipole moment of this scaffold.

The use of longer linking units to study the impact of long distance on dipolar repulsion showed that at distances higher than 10.5 Å, no intramolecular interactions were observed. Compound **5.52** also demonstrated the intramolecular nature of the conformational bias in shorter substrates. Eventually, introducing additional dipoles within the rigid scaffold have an impact on the peripheral dipoles relative conformation, as demonstrated by pyridine **5.53** and carbazoles **5.54a–c**. Insight into the conformation of the various carbazole scaffolds suggested that freedom of rotation was required for dipole-dipole interactions to be optimised.

Experimental

General Information

Reactions requiring anhydrous conditions were performed under nitrogen atmosphere in glassware which was flame-dried. Air- and moisture-sensitive liquids and solutions were transferred by syringe or cannula into the reaction vessels through rubber septa. Reactions run in a microwave oven were completed on a Biotage Initiator+. All reagents were purchased at highest commercial quality and used as received. Non-anhydrous solvents were purchased (unless specified) at the highest commercial quality and used as received. All solvents were removed *in vacuo* using a rotary evaporator. Petroleum ether indicates fractions of PE boiling at 40-60 °C. Acetone/dry ice cooling baths were used to obtain -78 °C. Anhydrous THF, Et₂O, CH₂Cl₂, and toluene were purified by filtration over a column of activated alumina (A-2).

Nuclear Magnetic Resonance (NMR) spectra (¹H and ¹³C) were recorded on either Bruker Avance III 400 or 500 MHz, Jeol ECS 300 or 400 MHz or Varian VNMRs 400 or 500 MHz spectrometers. The residual solvent peak was used as internal standards when assigning NMR spectra.^[305] Chemical shifts (δ) are quoted in Parts per million (ppm) downfield of trimethylsilane. Coupling constants (J) are reported to the nearest 0.1 Hz. The splitting patterns for the spectra assignment are abbreviated to singlet (s), doublet (d), triplet (t), quartet (q), septet (sept.), multiplet (m), broad (br.) and some as a combination of these. When possible, each signal was assigned to the corresponding atom.

IR spectra were recorded on neat compounds using a Perkin Elmer (Spectrum One) FT-IR spectrometer. Only strong and selected absorbance's (ν_{max} expressed in cm⁻¹) are reported.

High resolution mass spectra were recorded on a Bruker Daltonics MicroTOF 2 (ESI), a Bruker Daltonics ultrafleXtreme (MALDI) or a Thermo ORBITRAP Exactive Plus (APCI) mass spectrometers.

Capillary melting points were determined on a Stuart Scientific melting point SMP 10 apparatus.

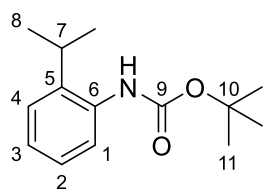
Thin layer chromatography (TLC) was performed using commercially available pre-coated plates (Macherey-Nagel alugram SIL G/UV₂₅₄). Visualisation was by UV light (at 254 nm) or by staining with phosphomolybdic acid or 'Seebach' dip (2.50 g phosphomolybdic acid hydrate, 1.00 g Cerium (IV) sulfate tetrahydrate, 3.2 mL conc. H₂SO₄, 90 mL H₂O) then heating. Flash column chromatography used chromatography grade silica, 60 Å particle size from Aldrich or was performed on an automated Biotage Isolera™ Spektra Four using gradient elution on pre-packed silica gel Biotage® SNAP Ultra columns. Compounds were loaded as saturated solutions.

Characterisation data

Chapter 1

General Procedure 1.1 (GP1.1), Buchwald–Hartwig coupling: A flame-dried microwave vial was allowed to cool to rt *in vacuo* and refilled with nitrogen. To this was added the required aniline (1.2 eq.), aryl bromide (1.0 eq.), NaOtBu (1.25 eq.), Pd₂dba₃ (1 mol%), PNP₃ (2 mol%) and distilled toluene (1.0 M). The reaction was allowed to stir at 80 °C for 16 h, cooled down to rt, filtered over Celite and concentrated *in vacuo* to yield the crude diarylamine. Purification by column chromatography yielded the desired product.

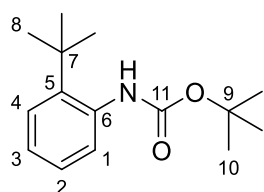
Tert-butyl (2-isopropylphenyl)carbamate – 1.21a



To a solution of 2-isopropylaniline (4.6 mL, 32.8 mmol, 1.0 eq.) in DCE (40 mL) was added di-*tert*-butylcarbonate (9.0 g, 41.0 mmol, 1.25 eq.). The reaction mixture was stirred for 16 h at 40 °C, concentrated *in vacuo*, and dissolved in CH₂Cl₂. The solution was washed with an aqueous solution of 1M HCl, a

saturated aqueous solution of NaHCO₃, brine, dried over Na₂SO₄ and concentrated *in vacuo*. Purification by flash column chromatography (SiO₂, petroleum ether /EtOAc, 99:1) yielded the title compound as a red oil (8.6 g, 29.9 mmol, 91%). Mixture of conformers in a 1:0.25 ratio. **$\delta^1\text{H}$ (400 MHz, CDCl₃)** 7.70 (1 H, d, *J* = 5.5 Hz, H-1), 7.25 (1 H, d, *J* = 7.8 Hz, H-4), 7.18 (1 H, t, *J* = 7.6 Hz, H-2), 7.10 (1 H, t, *J* = 7.5 Hz, H-3), 6.31 (1 H, s, NH), 3.03 (1 H, sept., *J* = 5.8 Hz, H-7), 1.53 (9 H^{min}, s, H-11), 1.52 (9 H^{maj}, s, H-11), 1.25 (6 H, d, *J* = 5.8 Hz, H-8). **$\delta^{13}\text{C}$ (101 MHz, CDCl₃)** 153.7 (C-9^{maj}), 146.9 (C-9^{min}), 139.0 (broad, C-6), 134.8 (C-5), 126.4 (C-2), 125.5 (C-4), 124.8 (C-3), 123.0 (C-1), 85.3 (C-10^{min}), 80.4 (C-10^{maj}), 28.5 (C-11^{maj}), 27.8 (C-7), 27.5 (C-11^{min}), 23.1 (C-8). Data consistent with that reported.^[306]

Tert-butyl (2-(tert-butyl)phenyl)carbamate – 1.21b

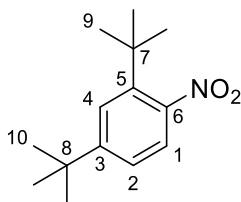


To a solution of 2-*tert*-butylaniline (3.1 mL, 19.9 mmol, 1.0 eq.) in DCE (25 mL) was added di-*tert*-butylcarbonate (5.7 g, 26.0 mmol, 1.3 eq.). The reaction mixture was stirred for 16 h at 60 °C. As the reaction did not go to full conversion, extra di-*tert*-butylcarbonate (2.5 g, 11.4 mmol, 0.6 eq.) was added

and the reaction mixture was heated for 96 h at 70 °C. The solution was concentrated *in vacuo*, taken up in CH₂Cl₂, washed with an aqueous solution of 1M HCl, a saturated aqueous solution of NaHCO₃, brine, dried over Na₂SO₄ and concentrated *in vacuo*. Purification by flash column chromatography (SiO₂, petroleum ether /EtOAc, 99:1) yielded the title compound as a white solid (4.5 g, 14.9 mmol, 75%). **$\delta^1\text{H}$ (400 MHz, CDCl₃)** 7.56 (1 H, d, *J* = 7.0 Hz, H-1), 7.36 (1 H, d, *J* = 7.9 Hz, H-4),

7.21 (1 H, t, J = 7.6 Hz, H-2), 7.11 (1 H, t, J = 7.6 Hz, H-3), 6.35 (1 H, s, NH), 1.51 (9 H, s, H-8), 1.41 (9 H, s, H-10). $\delta^{13}\text{C}$ (101 MHz, CDCl_3) 153.8 (C-11), 141.9 (C-5), 135.8 (C-6), 127.0 (C-1), 126.9 (C-2), 126.5 (C-4), 125.3 (C-3), 80.3 (C-9), 34.6 (C-7), 30.8 (C-10), 28.6 (C-8). Data consistent with that reported.^[307]

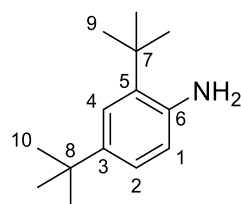
2,4-Di-*tert*-butyl-1-nitrobenzene – 1.24



To a solution of 1,3-di-*tert*-butylbenzene (7.9 g, 41.8 mmol, 1.0 eq.) in trifluoroacetic acid (32 mL) was added NH_4NO_3 (3.43 g, 42.8 mmol, 1.02 eq.). The reaction mixture was stirred for 2 h, poured in water and extracted with CH_2Cl_2 . The organic phases were combined, washed with brine, dried over

MgSO_4 and concentrated *in vacuo*. Recrystallization in isopropanol yielded the title compound as an off-white solid (6.4 g, 27.2 mmol, 65%). $\delta^1\text{H}$ (400 MHz, CDCl_3) 7.55 (1 H, d, J = 1.5 Hz, H-4), 7.29 (1 H, dd, J = 8.4, 1.7 Hz, H-2), 7.26 (1 H, d, J = 8.2 Hz, H-1), 1.41 (9 H, s, H-9), 1.33 (9 H, s, H-10). $\delta^{13}\text{C}$ (101 MHz, CDCl_3) 154.1 (C-3), 149.1 (C-6), 140.9 (C-5), 125.5 (C-4), 123.9 (C-1), 123.8 (C-2), 35.9 (C-7), 35.3 (C-8), 31.3 (C-10), 30.8 (C-9). Data consistent with that reported.^[44]

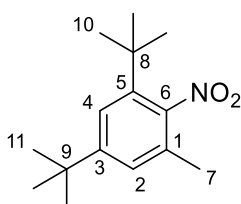
2,4-Di-*tert*-butyl-aniline – 1.25



2,4-di-*tert*-butyl-1-nitrobenzene **1.24** (4.1 g, 17.6 mmol, 1.0 eq.) and palladium on activated charcoal (10%, 0.5 g, 0.5 mmol, 3 mol%) were suspended in a mixture of ethanol (35 mL) and hydrazine hydrate (25 mL). The reaction mixture was heated under reflux for 16 h, concentrated *in vacuo*, taken up in a

solution of 5M NaOH and extracted with ethyl acetate. The organic phases were combined, washed with brine, dried over Na_2SO_4 , filtered and concentrated *in vacuo* to yield the title compound as a yellow oil (3.4 g, 16.7 mmol, 95%) $\delta^1\text{H}$ (400 MHz, CDCl_3) 7.28 (1 H, d, J = 2.3 Hz, H-4), 7.06 (1 H, dd, J = 8.2, 2.3 Hz, H-2), 6.61 (1 H, d, J = 8.2 Hz, H-1), 3.72 (2 H, br. s, NH), 1.43 (9 H, s, H-9), 1.28 (9 H, s, H-10). $\delta^{13}\text{C}$ (101 MHz, CDCl_3) 142.1 (C-3), 141.2 (C-6), 133.3 (C-5), 123.8 (C-2), 123.7 (C-4), 117.6 (C-1), 34.7 (C-7), 34.3 (C-8), 31.7 (C-10), 29.8 (C-9). IR (film, cm^{-1}) ν_{max} 3502 (N–H), 3407 (N–H), 2956 (C–H), 1621 (N–H), 1484 (C–C), 874 (N–H); HRMS (ESI⁺) m/z calcd for $\text{C}_{15}\text{H}_{26}\text{N}$ $[\text{M}+\text{H}]^+$ 220.2065, found 220.6068.

1,5-Di-*tert*-butyl-3-methyl-2-nitrobenzene – 1.26

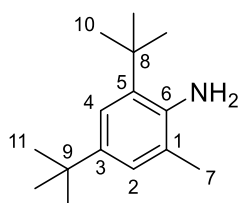


To a solution of 3,5-di-*tert*-butyltoluene (5.2 g, 25.4 mmol, 1.0 eq.) in acetic anhydride (4.3 mL) was added dropwise a mixture of aq. HNO_3 (70%, 1.6 mL, 101 mmol, 4 eq.), AcOH (1.5 mL) and acetic anhydride (1.5 mL) while keeping the internal temperature below 20 °C. The solution was stirred at rt for 3 h and

at 55 °C for 10 min. The reaction mixture was poured on ice, filtered and recrystallized in ethanol,

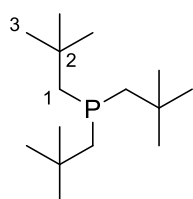
yielding the title compound as a pale yellow solid (3.1 g, 12.2 mmol, 49%). $\delta^1\text{H}$ (400 MHz, CDCl_3) 7.37 (1 H, d, J = 1.9 Hz, H-4), 7.13 (1 H, d, J = 1.7 Hz, H-2), 2.23 (3 H, s, H-7), 1.38 (9 H, s, H-10), 1.31 (9 H, s, J = 1.8, H-11). $\delta^{13}\text{C}$ (101 MHz, CDCl_3) 152.3 (C-3), 149.1 (C-6), 139.6 (C-5), 129.2 (C-1), 126.1 (C-2), 122.9 (C-4), 36.0 (C-8), 35.0 (C-9), 31.3 (C-11), 31.1 (C-10), 17.8 (C-7). Data consistent with that reported in the literature.^[308]

2,4-Di-*tert*-butyl-6-methylaniline – 1.27



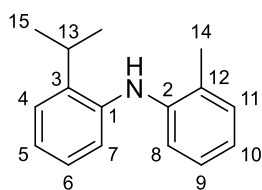
To a solution of **1.26** (1.0 g, 4.05 mmol, 1.0 eq.) in THF (50 mL) was added portionwise LiAlH_4 (1.5 g, 40.5 mmol, 10.0 eq.). The reaction mixture was cautiously heated to reflux and stirred for 16 h, then quenched with a saturated aqueous solution of $\text{Na}_2\text{S}_2\text{O}_3$. After filtration, the reaction mixture was extracted with Et_2O and concentrated *in vacuo*. The resulting oil was dissolved in a solution of HCl in MeOH, concentrated *in vacuo* and triturated in Et_2O . The pink solid was suspended in an aqueous solution of 2M NaOH and extracted with Et_2O . Organic phases were combined, dried over Na_2SO_4 , filtered and concentrated *in vacuo*, and filtration over a small plug of silica (petroleum ether/ CH_2Cl_2 60:40) yielded the title compound as a colourless oil (660 mg, 3.0 mmol, 75%). $\delta^1\text{H}$ (400 MHz, CDCl_3) 7.19 (1 H, d, J = 1.6 Hz, H-4), 7.01 (1 H, d, J = 1.6 Hz, H-2), 3.75 (2 H, br. s.), 2.20 (3 H, s, H-7), 1.45 (9 H, s, H-11), 1.29 (9 H, s, H-10). $\delta^{13}\text{C}$ (101 MHz, CDCl_3) 140.36 (C-6), 140.23 (C-5), 132.7 (C-3), 125.5 (C-2), 122.9 (C-1), 121.7 (C-4), 34.6 (C-9), 34.2 (C-8), 31.8 (C-10), 30.0 (C-11), 18.8 (C-7). Data consistent with that reported in the literature.^[308]

Trineopentyl phosphine – PNp_3



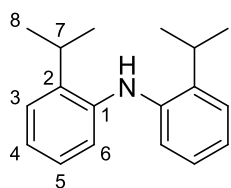
To a solution of neopentyl magnesium chloride in THF (1.0 M, 24 mL, 24 mmol, 4.5 eq.) at 0 °C was added phosphorus trichloride (0.46 mL, 5.27 mmol, 1.0 eq.) dropwise. The solution was heated under reflux for 5 h, allowed to cool to rt and stirred for 14 h. The reaction mixture was concentrated *in vacuo*, and degassed Et_2O was added, as well as a saturated aqueous solution of NH_4Cl . The aqueous phase was extracted with Et_2O . The organic phases were combined, dried over MgSO_4 and concentrated *in vacuo*. The resulting brown oil was distilled *in vacuo* (15 mbar, 150 °C) and recrystallized in ethanol to yield PNp_3 as white crystalline needles (222 mg, 0.91 mmol, 17%), m.p.: 59 °C. $\delta^1\text{H}$ (400 MHz, CDCl_3) 1.35 (6 H, d, J = 3.7 Hz, H-1), 0.98 (27 H, s, H-3). $\delta^{13}\text{C}$ (101 MHz, CDCl_3) 47.7 (d, J = 14.8 Hz, C-1), 32.0 (d, J = 13.8 Hz, C-2), 31.1 (d, J = 8.3 Hz, C-3). Data consistent with that reported.^[48]

2-Isopropyl-N-(o-tolyl)aniline – 1.28a



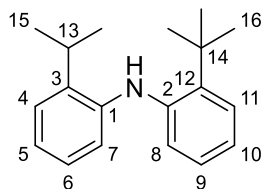
Following **GP1.1** with 2-bromotoluene (180 μ L, 1.5 mmol, 1.0 eq.), 2-isopropylaniline (263 μ L, 1.87 mmol, 1.25 eq.), NaOtBu (159 mg, 1.65 mmol, 1.5 eq.), Pd₂(dba)₃ (13.7 mg, 0.015 mmol, 1 mol%), PNp₃ (7.3 mg, 0.03 mmol, 2 mol%) and toluene (3 mL). Filtration over a plug of silica (SiO₂, petroleum ether) yielded the title compound as a yellow oil (341 mg, 1.5 mmol, quant.). **$\delta^1\text{H}$ (400 MHz, CDCl₃)** 7.33 (1 H, dd, J = 7.5, 1.5 Hz, H-4), 7.21 (1 H, d, J = 7.4 Hz, H-11), 7.14 (2 H, m, H-6 + H-9), 7.08 (1 H, m, H-7), 7.05 (1 H, m, H-5), 6.93 (1 H, d, J = 8.0 Hz, H-8), 6.88 (1 H, td, J = 7.4, 1.1 Hz, H-10), 5.25 (1 H, s, NH), 3.16 (1 H, sept, J = 5.8 Hz, H-13), 2.30 (3 H, s, H-14), 1.29 (6 H, d, J = 5.9 Hz, H-15). **$\delta^{13}\text{C}$ (101 MHz, CDCl₃)** 143.2 (C-2), 140.4 (C-3), 139.5 (C-1), 130.8 (C-11), 127.0 (C-7), 126.6 (C-6), 126.5 (C-12), 126.1 (C-4), 122.8 (C-9), 121.0 (C-5), 120.7 (C-10), 117.0 (C-8), 27.9 (C-13), 23.1 (C-15), 18.0 (C-14). **IR (film, cm⁻¹)** ν_{max} 3405 (N–H), 3033 (C–H), 2960 (C–H), 1584 (N–H), 1491; **HRMS (APCI⁺)** m/z calcd for C₁₆H₂₀N [M+H]⁺ 226.1596, found 226.1599.

Bis(2-isopropylphenyl)amine – 1.28b



Following **GP1.1** with 1-bromo-2-isopropylbenzene (230 μ L, 1.5 mmol, 1.0 eq.), 2-isopropylaniline (263 μ L, 1.87 mmol, 1.25 eq.), NaOtBu (159 mg, 1.65 mmol, 1.5 eq.), Pd₂(dba)₃ (13.7 mg, 0.015 mmol, 1 mol%), PNp₃ (7.3 mg, 0.03 mmol, 2 mol%) in distilled toluene (3 mL). Filtration over a plug of silica (SiO₂, petroleum ether) yielded the title compound as a yellow oil (312 mg, 1.2 mmol, 82%). **$\delta^1\text{H}$ (400 MHz, CDCl₃)** 7.32 (2 H, d, J = 7.9 Hz, H-3), 7.13 (2 H, td, J = 7.6, 1.4 Hz, H-5), 7.01 (2 H, t, J = 7.8 Hz, H-4), 7.00 (2 H, d, J = 7.9 Hz, H-6), 5.36 (1 H, s, NH), 3.15 (2 H, sept., J = 5.8 Hz, H-7), 1.32 (12 H, d, J = 5.8 Hz, H-8). **$\delta^{13}\text{C}$ (101 MHz, CDCl₃)** 141.5 (C-2), 138.3 (C-1), 126.6 (C-5), 125.9 (C-3), 121.9 (C-4), 119.5 (C-6), 27.9 (C-7), 22.9 (C-8). **IR (film, cm⁻¹)** ν_{max} 3412 (N–H), 3034 (C–H), 2960 (C–H), 1583 (N–H), 1502, 1489, 1449; **HRMS (APCI⁺)** m/z calcd for C₁₈H₂₄N [M+H]⁺ 254.1909, found 253.1897.

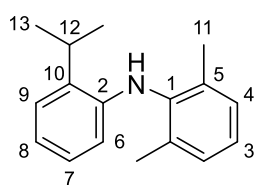
2-(Tert-butyl)-N-(2-isopropylphenyl)aniline – 1.28c



Following **GP1.1** with 1-bromo-2-*tert*-butylbenzene^[309] (180 μ L, 1.5 mmol, 1.0 eq.), 2-isopropylaniline (263 μ L, 1.87 mmol, 1.25 eq.), NaOtBu (159 mg, 1.65 mmol, 1.5 eq.), Pd₂(dba)₃ (13.7 mg, 0.015 mmol, 1 mol%), PNp₃ (7.3 mg, 0.03 mmol, 2 mol%) in distilled toluene (3 mL). Filtration over a plug of silica (SiO₂, petroleum ether) yielded the title compound as an orange oil (388 mg, 1.4 mmol, 96%). **$\delta^1\text{H}$ (400 MHz, CDCl₃)** 7.43 (1 H, dd, J = 7.9, 1.2 Hz, H-11), 7.32 (1 H, dd, J = 7.6, 1.0 Hz, H-4), 7.15 (1 H, m, H-9), 7.11 (1 H, m, H-6), 7.08 (1 H, d, J = 5.8 Hz, H-8), 7.01 (1 H, m, H-10), 6.99 (1 H, m, H-5), 6.96 (1 H, d, J = 7.9 Hz, H-7), 5.47 (1 H, br. s, NH), 3.12 (1 H, sept, J = 5.8 Hz, H-13), 1.50 (9 H, s,

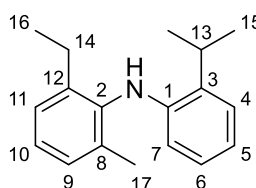
H-16), 1.33 (6 H, d, J = 5.8 Hz, H-15). $\delta^{13}\text{C}$ (101 MHz, CDCl_3) 142.9 (C-2), 141.9 (C-1), 140.4 (C-12), 137.6 (C-3), 127.02 (C-11), 126.99 (C-9), 126.6 (C-6), 125.8 (C-4), 122.7 (C-8), 122.1 (C-10), 121.3 (C-5), 119.0 (C-7), 34.8 (C-14), 30.5 (C-16), 27.8 (C-13), 23.0 (C-15). IR (film, cm^{-1}) ν_{max} 3479 (N–H), 2959 (C–H), 1580 (N–H), 1499, 1443; HRMS (APCI⁺) m/z calcd for $\text{C}_{19}\text{H}_{26}\text{N}$ $[\text{M}+\text{H}]^+$ 268.2065, found 268.2061.

N-(2-Isopropylphenyl)-2,6-dimethylaniline – 1.28d



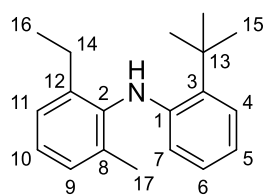
Following **GP1.1** with 2-bromo-1,3-dimethylbenzene (200 μL , 1.5 mmol, 1.0 eq.), 2-isopropylaniline (263 μL , 1.87 mmol, 1.25 eq), NaOtBu (159 mg, 1.65 mmol, 1.5 eq.), $\text{Pd}_2(\text{dba})_3$ (13.7 mg, 0.015 mmol, 1 mol%), PNp_3 (7.3 mg, 0.03 mmol, 2 mol%) in distilled toluene (3 mL). Filtration over a plug of silica (SiO_2 , petroleum ether) yielded the title compound as an off-white solid (274 mg, 1.1 mmol, 76%), **m.p.**: 116 – 119 $^\circ\text{C}$ (degradation). $\delta^1\text{H}$ (400 MHz, CDCl_3) 7.25 (1 H, d, J = 7.2 Hz, H-9), 7.14 (2 H, d, J = 7.2 Hz, H-4), 7.09 (1 H, dd, J = 8.5, 6.2 Hz, H-3), 6.97 (1 H, t, J = 7.6 Hz, H-7), 6.81 (1 H, t, J = 7.2 Hz, H-8), 6.20 (1 H, d, J = 8.0 Hz, H-6), 5.14 (1 H, br. s, NH), 3.17 (1 H, sept, J = 5.8 Hz, H-12), 2.20 (6 H, s, H-11), 1.40 (6 H, d, J = 5.8 Hz, H-13) $\delta^{13}\text{C}$ (101 MHz, CDCl_3) 142.9 (C-2), 139.0 (C-1), 135.5 (C-5), 133.0 (C-10), 128.7 (C-4), 126.6 (C-7), 125.43 (C-3), 125.34 (C-9), 118.7 (C-8), 112.7 (C-6), 27.8 (C-8), 22.5 (C-13), 18.5 (C-11). IR (film, cm^{-1}) ν_{max} 3407 (N–H), 3033 (C–H), 2956 (C–H), 1604 (N–H), 1581 (N–H), 1498, 1453; HRMS (APCI⁺) m/z calcd for $\text{C}_{17}\text{H}_{22}\text{N}$ $[\text{M}+\text{H}]^+$ 240.1752, found 240.1753. Supplementary crystallographic data can be obtained free of charge from The Cambridge Crystallographic Data Centre (CCDC 1842708).

2-Ethyl-*N*-(2-isopropylphenyl)-6-methylaniline – 1.28e



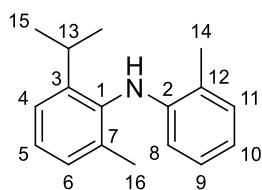
Following **GP1.1** with 1-bromo-2-isopropylbenzene (230 μL , 1.5 mmol, 1.0 eq.), 2-ethyl-6-methylaniline (260 μL , 1.87 mmol, 1.25 eq), NaOtBu (159 mg, 1.65 mmol, 1.5 eq.), $\text{Pd}_2(\text{dba})_3$ (13.7 mg, 0.015 mmol, 1 mol%), PNp_3 (7.3 mg, 0.03 mmol, 2 mol%) in distilled toluene (3 mL). Filtration over a plug of silica (SiO_2 , petroleum ether) yielded the title compound as a yellow oil (348 mg, 1.4 mmol, 91%). $\delta^1\text{H}$ (400 MHz, CDCl_3) 7.25 (1 H, d, J = 7.5 Hz, H-4), 7.18 (3 H, m, H-9 + H-10 + H-11), 6.97 (1 H, t, J = 7.7 Hz, H-6), 6.80 (1 H, t, J = 7.4 Hz, H-5), 6.18 (1 H, dd, J = 8.0, 0.9 Hz, H-1), 5.17 (1 H, s, NH), 3.15 (1 H, sept., J = 5.7 Hz, H-13), 2.58 (2 H, m, H-14), 2.18 (3 H, s, H-17), 1.40 (6 H, d, J = 5.8 Hz, H-15), 1.17 (3 H, t, J = 7.6 Hz, H-16). $\delta^{13}\text{C}$ (101 MHz, CDCl_3) 143.3 (C-3), 141.5 (C-12), 138.2 (C-2), 136.0 (C-8), 132.6 (C-1), 128.7 (C-9), 126.9 (C-10), 126.6 (C-6), 125.8 (C-11), 125.3 (C-4), 118.5 (C-5), 112.5 (C-7), 27.7 (C-13), 24.9, (C-14) 22.5 (C-15), 22.5 (C-15), 18.6 (C-17), 14.9 (C-16). IR (film, cm^{-1}) ν_{max} 3420 (N–H), 2961 (C–H), 2871 (C–H), 1604 (N–H), 1581 (N–H), 1498, 1454; HRMS (APCI⁺) m/z calcd for $\text{C}_{18}\text{H}_{24}\text{N}$ $[\text{M}+\text{H}]^+$ 254.1909, found 254.1910.

N-(2-(*Tert*-butyl)phenyl)-2-ethyl-6-methylaniline – 1.28f



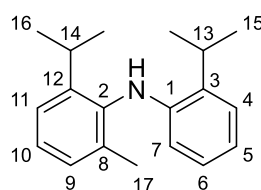
Following **GP1.1** with 1-bromo-2-*tert*-butylbenzene^[309] (476 mg, 2.2 mmol, 1.0 eq.), 2-ethyl-6-methylaniline (0.39 mL, 2.8 mmol, 1.25 eq), NaOtBu (0.24 g, 2.5 mmol, 1.1 eq.), Pd₂(dba)₃ (20.6 mg, 0.022 mmol, 1 mol%), PNp₃ (11.0 mg, 0.045 mmol, 2 mol%) in distilled toluene (4.5 mL). Filtration over a plug of silica (SiO₂, petroleum ether) yielded the title compound as an off-white solid (425 mg, 1.6 mmol, 72%), **m.p.:** 67 – 68 °C. **$\delta^1\text{H}$ (400 MHz, CDCl₃)** 7.34 (1 H, dd, J = 7.8, 1.2 Hz, H-4), 7.17 (1 H, dd, J = 8.9, 4.7 Hz, H-10), 7.14 (2 H, m, H-9 + H-11), 6.96 (1 H, t, J = 7.6 Hz, H-6), 6.75 (1 H, t, J = 7.5 Hz, H-5), 6.20 (1 H, dd, J = 8.0, 0.8 Hz, H-7), 5.36 (1 H, s, br.s, NH), 2.60 (CH_AH_B, 1 H, sept., J = 7.6 Hz, H-14), 2.57 (CH_AH_B, 1 H, sept., J = 7.6 Hz, H-14), 2.16 (3 H, s, H-17), 1.56 (9 H, s, H-15), 1.16 (3 H, t, J = 7.6 Hz, H-16). **$\delta^{13}\text{C}$ (101 MHz, CDCl₃)** 144.5 (C-3), 141.3 (C-12), 138.4 (C-2), 135.9 (C-6), 133.9 (C-1), 128.8 (C-9), 127.1 (C-6), 126.9 (C-10), 126.5 (C-4), 125.7 (C-11), 118.3 (C-5), 113.8 (C-7), 34.6 (C-13), 30.0 (C-15), 25.0 (C-14), 18.8 (C-17), 15.0 (C-16). **IR (film, cm⁻¹)** ν_{max} 3458 (N–H), 2963, (C–H), 1600 (N–H), 1591 (N–H), 1576; **HRMS (APCI⁺)** m/z calcd for C₁₉H₂₆N [M+H]⁺ 268.2065, found 268.2053.

2-Isopropyl-6-methyl-*N*-(*o*-tolyl)aniline – 1.28g



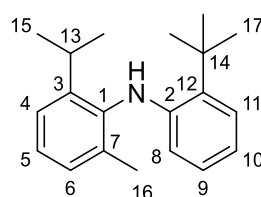
Following **GP1.1** with 2-bromotoluene (42 μL , 0.35 mmol, 1.0 eq.), 2-isopropyl-6-methylaniline (68 μL , 0.44 mmol, 1.25 eq), NaOtBu (50 mg, 0.52 mmol, 1.5 eq.), Pd₂(dba)₃ (3.2 mg, 3.5 μmol , 1 mol%), PNp₃ (1.7 mg, 7 μmol , 2 mol%) in distilled toluene (0.7 mL). Filtration over a plug of silica (SiO₂, petroleum ether) yielded the title compound as a colourless oil (82 mg, 0.34 mmol, 98%). **$\delta^1\text{H}$ (400 MHz, CDCl₃)** 7.34 (1 H, d, J = 7.2 Hz, H-4), 7.29 (1 H, t, J = 7.5 Hz, H-5), 7.23 (2 H, d, J = 7.0 Hz, H-6 + H-8), 7.06 (1 H, t, J = 7.6 Hz, H-10), 6.79 (1 H, t, J = 7.3 Hz, H-9), 6.23 (1 H, d, J = 8.0 Hz, H-11), 5.05 (1 H, br. s, NH), 3.26 (1 H, sept., J = 5.8 Hz, H-13), 2.44 (3 H, s, H-14), 2.26 (3 H, s, H-16), 1.27 (6 H, br. s, H-15). **$\delta^{13}\text{C}$ (101 MHz, CDCl₃)** 146.7 (C-3), 145.1 (C-7), 137.3 (C-1), 136.5 (C-2), 130.3 (C-8), 128.4 (C-6), 127.1 (C-10), 126.5 (C-5), 124.0 (C-4), 122.0 (C-12), 117.8 (C-9), 111.5 (C-11), 28.2 (C-13), 24.6 (C-15), 23.2 (C-15), 18.6 (C-16), 17.8 (C-14). **IR (film, cm⁻¹)** ν_{max} 3412 (N–H), 3034 (C–H), 2961 (C–H), 2867 (C–H), 1606 (N–H), 1584 (N–H), 1500, 1462; **HRMS (APCI⁺)** m/z calcd for C₁₇H₂₂N [M+H]⁺ 240.1752, found 240.1753.

2-Isopropyl-N-(2-isopropylphenyl)-6-methylaniline – 1.28h



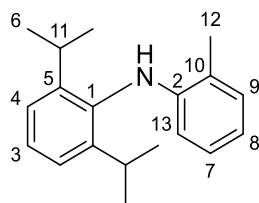
Following **GP1.1** with 2-bromotoluene (230 μ L, 1.5 mmol, 1.0 eq.), 2-isopropyl-6-methylaniline (0.29 mL, 1.87 mmol, 1.25 eq), NaOtBu (159 mg, 1.65 mmol, 1.5 eq.), Pd₂(dba)₃ (13.7 mg, 0.015 mmol, 1 mol%), PNp₃ (7.3 mg, 0.03 mmol, 2 mol%) in distilled toluene (3 mL). Filtration over a plug of silica (SiO₂, petroleum ether) yielded the title compound as a yellow oil (334 mg, 1.2 mmol, 83%). **$\delta^1\text{H}$ (400 MHz, CDCl₃)** 7.26 (2 H, d, J = 7.5 Hz, H-4 + H-11), 7.21 (1 H, t, J = 7.5 Hz, H-10), 7.16 (1 H, d, J = 7.2 Hz, H-9), 6.97 (1 H, t, J = 7.7 Hz, H-6), 6.80 (1 H, t, J = 7.4 Hz, H-5), 6.18 (1 H, dd, J = 8.0, 0.8 Hz, H-7), 5.17 (1 H, s, NH), 3.16 (1 H, m, H-14), 3.15 (1 H, m, H-13), 2.19 (3 H, s, H-17), 1.41 (6 H, d, J = 5.8 Hz, H-15), 1.20 (CH_AH_B, 3 H, d, J = 5.8 Hz, H-16), 1.18 (CH_AH_B, 3 H, d, J = 5.9 Hz, H-16). **$\delta^{13}\text{C}$ (101 MHz, CDCl₃)** 146.5 (C-12), 143.7 (C-2), 137.4 (C-3), 136.3 (C-8), 132.3 (C-1), 128.5 (C-5), 126.7 (C-6), 126.3 (C-10), 125.2 (C-4), 124.0 (C-11), 118.3 (C-5), 112.2 (C-7), 28.2 (C-14), 27.8 (C-13), 24.6 (C-16), 23.1 (C-16), 22.48 (C-15), 22.43 (C-15), 18.8 (C-17). **IR (film, cm⁻¹)** ν_{max} 3423 (N–H), 3035 (C–H), 2960 (C–H), 2868 (C–H), 1604 (N–H), 1581 (N–H), 1497, 1454; **HRMS (APCI⁺)** m/z calcd for C₁₉H₂₆N [M+H]⁺ 268.2065 found 268.2056.

N-(2-(Tert-butyl)phenyl)-2-isopropyl-6-methylaniline – 1.28i



Following **GP1.1** with 1-bromo-2-*tert*-butylbenzene^[309] (73 mg, 0.35 mmol, 1.0 eq.), 2-isopropyl-6-methylaniline (68 μ L, 0.44 mmol, 1.25 eq), NaOtBu (50 mg, 0.52 mmol, 1.5 eq.), Pd₂(dba)₃ (3.2 mg, 3.5 μ mol, 1 mol%), PNp₃ (1.7 mg, 7 μ mol, 2 mol%) in distilled toluene (0.7 mL). The reaction time was 48 h, after which filtration over a plug of silica (SiO₂, petroleum ether) yielded the title compound as a yellow oil (34 mg, 0.12 mmol, 34%). **$\delta^1\text{H}$ (400 MHz, CDCl₃)** 7.38 (1 H, dd, J = 7.8, 1.0, H-8), 7.28 (1 H, d, J = 7.4 Hz, H-4), 7.22 (1 H, t, J = 7.5 Hz, H-5), 7.18 (1 H, d, J = 7.0 Hz, H-6), 6.99 (1 H, t, J = 7.2 Hz, H-9), 6.78 (1 H, t, J = 7.4 Hz, H-10), 6.24 (1 H, d, J = 8.0 Hz, H-11), 5.39 (1 H, s, NH), 3.15 (1 H, sept, J = 5.8 Hz, H-13), 2.20 (3 H, s, H-16), 1.60 (9 H, s, H-17), 1.23 (3 H, d, J = 5.9 Hz, H-15), 1.19 (3 H, d, J = 5.9 Hz, H-15). **$\delta^{13}\text{C}$ (101 MHz, CDCl₃)** 146.3 (C-1), 144.9 (C-2), 137.6 (C-3), 136.1 (C-7), 133.5 (C-12), 128.6 (C-6), 127.1 (C-2), 126.5 (C-8), 126.1 (C-5), 124.0 (C-4), 118.1 (C-3), 113.6 (C-11), 34.5 (C-14), 30.0 (C-17), 28.3 (C-13), 24.7 (C-15), 22.9 (C-15), 19.0 (C-16). **IR (film, cm⁻¹)** ν_{max} 3463 (N–H), 3049 (C–H), 2963 (C–H), 2871 (C–H), 1600 (N–H), 1576 (N–H), 1497, 1443; **HRMS (APCI⁺)** m/z calcd for C₂₀H₂₈N [M+H]⁺ 282.2222, found 282.2236.

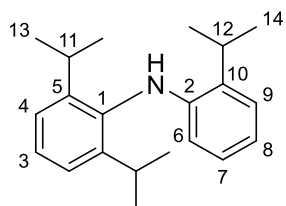
2,6-Diisopropyl-N-(*o*-tolyl)aniline – 1.28j



Following **GP1.1** with 2-bromotoluene (230 μ L, 1.5 mmol, 1.0 eq.), 2,6-diisopropyl aniline (260 μ L, 1.87 mmol, 1.25 eq), NaOtBu (159 mg, 1.65 mmol, 1.5 eq.), Pd₂(dba)₃ (13.7 mg, 0.015 mmol, 1 mol%), PNP₃ (7.3 mg, 0.03 mmol, 2 mol%) in distilled toluene (3 mL). Filtration over a plug of silica (SiO₂, petroleum ether) yielded the title compound as a colourless oil (348 mg,

1.3 mmol, 87%). **$\delta^1\text{H}$ (500 MHz, CDCl₃)** 7.31 (1 H, m, H-3), 7.25 (2 H, m, H-4), 7.16 (1 H, d, J = 7.3 Hz, H-13), 6.97 (1 H, t, J = 7.7 Hz, H-7), 6.69 (1 H, t, J = 7.3 Hz, H-8), 6.14 (1 H, d, J = 8.0 Hz, H-9), 4.93 (1 H, br. s, NH), 3.13 (2 H, sept, J = 5.8 Hz, H-11), 2.37 (3 H, s, H-12), 1.18 (CH_AH_B, 6 H, t, J = 7.5 Hz, H-6), 1.14 (CH_AH_B, 6 H, d, J = 5., H-6). **$\delta^{13}\text{C}$ (126 MHz, CDCl₃)** 147.4 (C-1), 146.2 (C-2), 135.9 (C-5), 130.2 (C-9), 127.2 (C-3), 127.1 (C-7), 123.9 (C-4), 121.4 (C-10), 117.6 (C-8), 111.6 (C-13), 28.4 (C-11), 24.9 (C-6), 23.1 (C-6), 17.8 (C-12). **IR (film, cm⁻¹)** ν_{max} 3425 (N–H), 2961 (C–H), 1606 (N–H), 1585 (N–H), 1500; **HRMS (APCI⁺)** m/z calcd for C₁₉H₂₆N [M+H]⁺ 268.2065, found 268.2066.

2,6-Diisopropyl-N-(2-isopropylphenyl)aniline – 1.28k

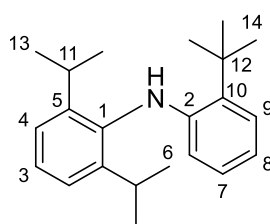


Following **GP1.1** with 1-bromo-2-isopropylbenzene (54 μ L, 0.35 mmol, 1.0 eq.), 2,6-diisopropylaniline (83 μ L, 0.44 mmol, 1.25 eq), NaOtBu (50 mg, 0.52 mmol, 1.5 eq.), Pd₂(dba)₃ (3.2 mg, 3.5 μ mol, 1 mol%), PNP₃ (1.7 mg, 7 μ mol, 2 mol%) in distilled toluene (0.7 mL). Filtration over a plug of silica

(SiO₂, petroleum ether) yielded the title compound as a yellow oil (90 mg, 0.23 mmol, 65%).

$\delta^1\text{H}$ (400 MHz, CDCl₃) 7.31 (1 H, dd, J = 8.6, 6.4 Hz, H-3), 7.26 (2 H, m, H-4), 7.24 (1 H, br. d, H-6), 6.95 (1 H, t, J = 7.3 Hz, H-8), 6.77 (1 H, t, J = 7.4 Hz, H-7), 6.16 (1 H, d, J = 8.0 Hz, H-9), 5.11 (1 H, s, NH), 3.12 (3 H, m, H-12 + H-11), 1.41 (6 H, d, J = 5.8 Hz, H-14), 1.18 (CH_AH_B, 6 H, d, J = 5.9 Hz, H-13), 1.13 (CH_AH_B, 6 H, d, J = 5.9 Hz, H-13). **$\delta^{13}\text{C}$ (101 MHz, CDCl₃)** 147.2 (C-5), 144.7 (C-2), 135.8 (C-1), 131.6 (C-10), 127.0 (C-3), 126.6 (C-8), 125.1 (C-6), 124.0 (C-4), 117.9 (C-7), 112.1 (C-9), 28.3 (C-11), 27.8 (C-12), 24.9 (C-13), 23.0 (C-13), 22.4 (C-14). **IR (film, cm⁻¹)** ν_{max} 3432 (N–H), 3034 (C–H), 2961 (C–H), 1605 (N–H), 1581 (N–H), 1498, 1445; **HRMS (APCI⁺)** m/z calcd for C₂₁H₃₀N [M+H]⁺ 296.2378, found 296.2364.

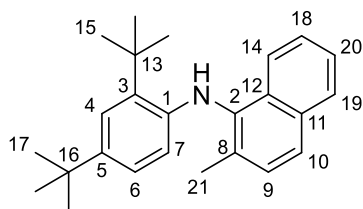
N-(2-(*Tert*-butyl)phenyl)-2,6-diisopropylaniline – 1.28l



Following **GP1.1** with 1-bromo-2-*tert*-butylbenzene^[309] (75 mg, 0.35 mmol, 1.0 eq.), 2,6-diisopropylaniline (83 μ L, 0.44 mmol, 1.25 eq), NaOtBu (50 mg, 0.52 mmol, 1.5 eq.), Pd₂(dba)₃ (3.2 mg, 3.5 μ mol, 1 mol%), PNP₃ (1.7 mg, 7 μ mol, 2 mol%) in distilled toluene (0.7 mL). Filtration over a plug of silica (SiO₂, petroleum ether) yielded the title compound as a yellow oil (80 mg,

0.26 mmol, 76%). **$\delta^1\text{H}$ (400 MHz, CDCl₃)** 7.34 (1 H, dd, J = 7.9, 1.0 Hz, H-9), 7.30 (1 H, m, H-3), 7.25 (2 H, m, H-4), 6.95 (1 H, t, J = 7.6 Hz, H-7), 6.73 (1 H, t, J = 7.5 Hz, H-8), 6.19 (1 H, d, J = 8.0 Hz, H-6), 5.28 (1 H, s, NH), 3.09 (2 H, sept, J = 5.8 Hz, H-11), 1.57 (9 H, s, H-14), 1.18 (CH_AH_B, 6 H, d, J = 5.9 Hz, H-13), 1.12 (CH_AH_B, 6 H, d, J = 5.9 Hz, H-13). **$\delta^{13}\text{C}$ (101 MHz, CDCl₃)** 147.1 (C-5), 146.0 (C-2), 136.0 (C-1), 132.9 (C-10), 127.1 (C-7), 126.9 (C-3), 126.4 (C-9), 124.1 (C-4), 117.8 (C-8), 113.6 (C-6), 34.4 (C-12), 29.9 (C-14), 28.4 (C-11), 25.0 (C-13), 22.9 (C-13). **IR (film, cm⁻¹)** ν_{max} 3468 (N–H), 2961 (C–H), 2869 (C–H), 1601 (N–H), 1576 (N–H), 1497, 1443; **HRMS (APCI⁺)** m/z calcd for C₂₂H₃₂N [M+H]⁺ 310.2535, found 310.2520.

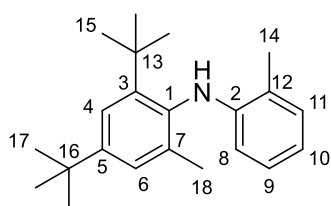
N-(2,4-Di-*tert*-butylphenyl)-2-methylnaphthalen-1-amine – 1.28m



Following **GP1.1** with 1-bromo-2-methylnaphthalene (63 μ L, 0.41 mmol, 1.0 eq.), aniline **1.25** (104 mg, 0.51 mmol, 1.25 eq), NaOtBu (58 mg, 0.61 mmol, 1.5 eq.), Pd₂(dba)₃ (3.7 mg, 4.1 μ mol, 1 mol%), PNP₃ (2.0 mg, 8.2 μ mol, 2 mol%) in distilled toluene

(0.8 mL). Filtration over a plug of silica (SiO₂, petroleum ether) yielded the title compound as a yellow oil (93 mg, 0.27 mmol, 66%). **$\delta^1\text{H}$ (400 MHz, CDCl₃)** 7.91 (1 H, d, J = 8.1 Hz, H-14), 7.85 (1 H, d, J = 7.5 Hz, H-19), 7.68 (1 H, d, J = 8.4 Hz, H-9), 7.41 (4 H, m, H-4 + H-10 + H-18 + H-20), 6.88 (1 H, dd, J = 8.4, 2.3 Hz, H-6), 6.09 (1 H, d, J = 8.4 Hz, H-7), 5.63 (1 H, br. s, NH), 2.38 (3 H, s, H-21), 1.68 (9 H, s, H-15), 1.29 (9 H, s, H-17). **$\delta^{13}\text{C}$ (101 MHz, CDCl₃)** 142.2 (C-5), 140.9 (C-3), 135.9 (C-2), 133.6 (ArC), 133.5 (ArC), 131.4 (ArC), 131.2 (ArC), 129.5 (C-4), 128.3 (C-19), 126.2 (C-18 or C-20), 125.24 (C-18 or C-20), 125.21 (C-9), 123.7 (C-14), 123.6 (C-6 + C-10), 114.8 (C-7), 35.0 (C-13), 34.3 (C-16), 31.7 (C-17), 30.3 (C-15), 19.0 (C-21). **IR (film, cm⁻¹)** ν_{max} 3450 (N–H), 3052 (C–H), 2959 (C–H), 2868 (C–H), 1608 (N–H), 1571 (N–H), 1491, 1391; **HRMS (APCI⁺)** m/z calcd for C₂₅H₃₂N [M+H]⁺ 346.2535, found 346.2541.

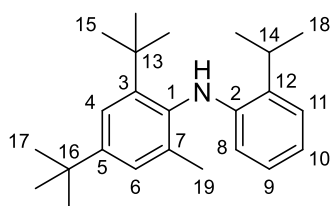
2,4-Di-*tert*-butyl-6-methyl-*N*-(*o*-tolyl)aniline – 1.28n



Following **GP1.1** with 2-bromotoluene (49 μ L, 0.41 mmol, 1.0 eq.), aniline **1.27** (111 mg, 0.51 mmol, 1.25 eq), NaOtBu (58 mg, 0.61 mmol, 1.5 eq.), Pd₂(dba)₃ (3.7 mg, 4.1 μ mol, 1 mol%), PNp₃ (2.0 mg, 8.2 μ mol, 2 mol%) in distilled toluene (0.8 mL). Filtration over a plug of silica (SiO₂, petroleum ether) yielded the title compound as a colourless oil (123 mg, 0.40 mmol, 97%).

$\delta^1\text{H}$ (400 MHz, CDCl₃) 7.36 (1 H, d, J = 2.1 Hz, H-4), 7.16 (1 H, d, J = 2.0 Hz, H-6), 7.13 (1 H, d, J = 7.3 Hz, H-11), 6.97 (1 H, t, J = 7.6 Hz, H-9), 6.66 (1 H, t, J = 7.1 Hz, H-10), 6.09 (1 H, d, J = 8.0 Hz, H-8), 5.06 (1 H, br. s, NH), 2.31 (3 H, s, H-14), 2.06 (3 H, s, H-18), 1.38 (9 H, s, H-15), 1.35 (9 H, s, H-17). **$\delta^{13}\text{C}$ (101 MHz, CDCl₃)** 148.4 (C-5), 147.0 (C-3), 145.2 (C-2), 137.6 (C-1), 135.9 (C-7), 130.2 (C-11), 127.0 (C-9), 126.3 (C-6), 122.0 (C-4), 121.4 (C-12), 117.3 (C-6), 112.1 (C-8), 35.7 (C-13), 34.7 (C-16), 31.6 (C-17), 31.4 (C-15), 19.3 (C-18), 17.9 (C-14). **IR (film, cm⁻¹)** ν_{max} 3457 (N–H), 2961 (C–H), 2867 (C–H), 1607 (N–H), 1586 (N–H), 1492, 1471; **HRMS (APCI⁺)** m/z calcd for C₂₂H₃₂N [M+H]⁺ 310.2535, found 310.2531.

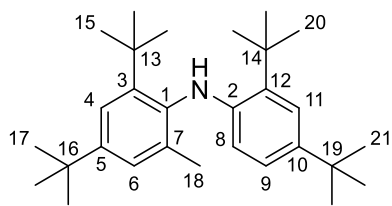
2,4-Di-*tert*-butyl-*N*-(2-isopropylphenyl)-6-methylaniline – 1.28o



Following **GP1.1** with 1-bromo-2-isopropylbenzene (62 μ L, 0.41 mmol, 1.0 eq.), aniline **1.27** (111 mg, 0.51 mmol, 1.25 eq), NaOtBu (58 mg, 0.61 mmol, 1.5 eq.), Pd₂(dba)₃ (3.7 mg, 4.1 μ mol, 1 mol%), PNp₃ (2.0 mg, 8.2 μ mol, 2 mol%) in distilled toluene (0.8 mL). Filtration over a plug of silica (SiO₂, petroleum ether) yielded the title compound as a colourless oil (20 mg, 0.06 mmol, 14%).

$\delta^1\text{H}$ (400 MHz, CDCl₃) 7.37 (1 H, d, J = 2.0 Hz, H-4), 7.23 (1 H, d, J = 7.6 Hz, H-11), 7.16 (1 H, d, J = 1.8 Hz, H-6), 6.95 (1 H, t, J = 7.6 Hz, H-9), 6.75 (1 H, t, J = 7.4 Hz, H-10), 6.12 (1 H, d, J = 8.0 Hz, H-8), 5.25 (1 H, s, NH), 3.07 (1 H, sept., J = 5.7 Hz, H-14), 2.06 (3 H, s, H-19), 1.39 (9 H, s, H-17), 1.37 (6 H, m, C-18), 1.35 (9 H, s, H-15). **$\delta^{13}\text{C}$ (101 MHz, CDCl₃)** 148.2 (C-3), 146.9 (C-5), 143.9 (C-12), 137.4 (C-1), 136.1 (C-7), 132.0 (C-12), 126.5 (C-9), 126.5 (C-4), 125.1 (C-8), 122.0 (C-6), 117.8 (C-10), 113.1 (C-8), 35.7 (C-13), 34.7 (C-16), 31.7 (C-17), 31.4 (C-15), 27.7 (C-14), 22.8 (C-18), 22.4 (C-18), 19.5 (C-19). **IR (film, cm⁻¹)** ν_{max} 2961 (C–H), 2869 (C–H), 1605 (N–H), 1582 (N–H), 1498, 1456, 1362; **HRMS (APCI⁺)** m/z calcd for C₂₄H₃₆N [M+H]⁺ 338.2848, found 338.2833.

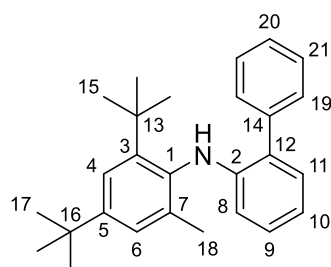
2,4-Di-*tert*-butyl-*N*-(2,4-di-*tert*-butylphenyl)-6-methylaniline – 1.28p



Following **GP1.1** with aniline **1.25** (109 mg, 0.41 mmol, 1.0 eq.), 2,4-di-*tert*-butyl-1-bromobenzene^[310] (111 mg, 0.51 mmol, 1.25 eq), NaOtBu (58 mg, 0.61 mmol, 1.5 eq.), Pd₂(dba)₃ (3.7 mg, 4.1 μ mol, 1 mol%), PNp₃ (2.0 mg, 8.2 μ mol, 2 mol%) in distilled

toluene (0.8 mL). Filtration over a plug of silica (SiO₂, petroleum ether) yielded the title compound as a colourless oil (3 mg, 0.0074 mmol, 2%). **¹H (400 MHz, CDCl₃)** 7.35 (1 H, d, *J* = 2.1 Hz, H-4), 7.30 (1 H, d, *J* = 2.2 Hz, H-8), 7.12 (1 H, d, *J* = 1.8 Hz, H-6), 6.91 (1 H, dd, *J* = 8.4, 2.1 Hz, H-9), 6.08 (1 H, d, *J* = 8.4 Hz, H-8), 5.30 (1 H, br. s, NH), 2.00 (3 H, s, H-18), 1.54 (9 H, s, C(CH₃)₃), 1.39 (9 H, s, C(CH₃)₃), 1.33 (9 H, s, C(CH₃)₃), 1.26 (9 H, s, C(CH₃)₃). **IR (film, cm⁻¹)** ν_{\max} 2958 (C–H), 2855 (C–H), 1610 (N–H), 1500, 1480, 1393; **HRMS (APCI⁺)** *m/z* calcd for C₂₉H₆N [M+H]⁺ 408.3630, found 408.3646. Too little material was isolated for the measurement of a ¹³C NMR spectrum.

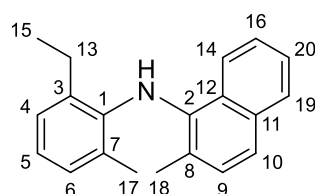
N-(2,4-Di-*tert*-butyl-6-methylphenyl)-[1,1'-biphenyl]-2-amine – 1.28q



Following **GP1.1** with 2-bromo-1,1'-biphenyl (70 μ L, 0.41 mmol, 1.0 eq.), aniline **1.27** (111 mg, 0.51 mmol, 1.25 eq.), NaOtBu (58 mg, 0.61 mmol, 1.5 eq.), Pd₂(dba)₃ (3.7 mg, 4.1 μ mol, 1 mol%), PNP₃ (2.0 mg, 8.2 μ mol, 2 mol%) in distilled toluene (0.8 mL). Filtration over a plug of silica (SiO₂, petroleum ether) yielded the title compound as a colourless

oil (9 mg, 0.024 mmol, 6%). **¹H (400 MHz, CDCl₃)** 7.52 (2 H, d, *J* = 7.1 Hz, H-19), 7.46 (2 H, t, *J* = 7.6 Hz, H-21), 7.36 (1 H, t, *J* = 7.3 Hz, H-20), 7.30 (1 H, d, *J* = 1.9 Hz, H-4), 7.17 (1 H, d, *J* = 7.4 Hz, H-11), 7.13 (1 H, d, *J* = 1.8 Hz, H-6), 7.09 (1 H, t, *J* = 7.7 Hz, H-9), 6.76 (1 H, t, *J* = 7.3 Hz, H-10), 6.18 (1 H, d, *J* = 8.1 Hz, H-8), 5.32 (1 H, br. s, NH), 2.09 (3 H, s, H-18), 1.32 (9 H, s, H-17), 1.28 (9 H, s, H-15). **¹³C (101 MHz, CDCl₃)** 148.6 (C-5), 147.5 (C-3), 144.3 (C-2), 139.6 (C-14), 137.7 (C-1), 135.6 (C-7), 130.0 (C-11), 129.7 (C-19), 129.0 (C-21), 128.6 (C-9), 127.5 (C-20), 127.4 (C-12), 126.4 (C-6), 122.0 (C-4), 117.1 (C-10), 112.3 (C-8), 35.7 (C-13), 34.7 (C-16), 31.6 (C-17), 31.2 (C-15), 19.6 (C-18). **IR (film, cm⁻¹)** ν_{\max} 3480 (N–H), 2959 (C–H), 2867 (C–H), 1592 (N–H), 1466; **HRMS (APCI⁺)** *m/z* calcd for C₂₇H₃₄N [M+H]⁺ 372.2691, found 372.2692.

N-(2-Ethyl-6-methylphenyl)-2-methylnaphthalen-1-amine – 1.28r

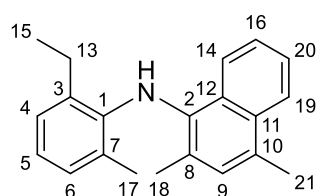


Following **GP1.1** with 1-bromo-2-methylnaphthalene (0.31 mL, 2.0 mmol, 1.0 eq.), 2-ethyl-6-methylaniline (0.36 mL, 2.5 mmol, 1.25 eq.), NaOtBu (0.24 g, 2.5 mmol, 1.25 eq.), Pd₂(dba)₃ (9.1 mg, 0.01 mmol, 0.5 mol%), PNP₃ (4.9 mg, 0.02 mmol, 1 mol%) in distilled toluene (4 mL).

The reaction time was 48 h, after which filtration over a plug of silica (SiO₂, petroleum ether) yielded the title compound as a green oil (548 mg, 2.0 mmol, quant.). **¹H (400 MHz, CDCl₃)** 7.95 (1 H, d, *J* = 8.2 Hz, H-14), 7.80 (1 H, d, *J* = 7.7 Hz, H-19), 7.48 (1 H, d, *J* = 8.3 Hz, H-10), 7.39 (2 H, m, H-16 + H-20), 7.24 (1 H, d, *J* = 8.3 Hz, H-9), 7.10 (1 H, d, *J* = 7.4 Hz, H-6), 6.98 (1 H, d, *J* = 7.4 Hz, H-4), 6.93 (1 H, t, *J* = 7.4 Hz, H-5), 2.54 (2 H, q, *J* = 7.5 Hz, H-13), 2.07 (3 H, s, H-18), 1.86 (3 H, s, H-17), 1.17 (3 H, t, *J* = 7.5 Hz, H-15). **¹³C (101 MHz, CDCl₃)** 141.9 (C-13), 137.7 (C-2), 134.5 (C-1), 133.4 (C-11), 129.9 (C-9), 129.3 (C-7), 129.2 (C-4), 128.9 (C-12), 128.3 (C-19),

126.7 (C-6), 125.7 (C-8), 125.6 (C-16 or C-20), 125.1 (C-16 or C-20), 122.6 (C-14), 122.4 (C-10), 121.9 (C-5), 25.1 (C-13), 19.44 (C-17 or C-18), 19.39 (C-17 or C-18), 14.0 (C-15). IR (film, cm^{-1}) ν_{max} 3416 (N–H), 3049 (C–H), 2965 (C–H), 1593 (N–H), 1569, 1468. HRMS (APCI⁺) m/z calcd for $\text{C}_{20}\text{H}_{22}\text{N}$ $[\text{M}+\text{H}]^+$ 276.1747, found 276.1767.

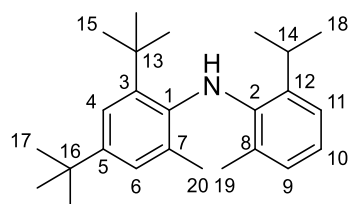
N-(2-Ethyl-6-methylphenyl)-2,4-methylnaphthalen-1-amine – 1.28s



Following **GP1.1** with 1-bromo-2,4-di-methylnaphthalene (0.80 g, 3.4 mmol, 1.2 eq.), 2-ethyl-6-methylaniline (0.39 mL, 2.8 mmol, 1.0 eq.), NaOtBu (0.34 g, 0.52 mmol, 1.25 eq.), $\text{Pd}_2(\text{dba})_3$ (51 mg, 0.056 mmol, 2 mol%), PNp_3 (47 mg, 0.084 mmol, 3 mol%) in distilled toluene (0.7 mL).

Filtration over a plug of silica (SiO_2 , petroleum ether) yielded the title compound as a yellow oil (0.74 mg, 92%). $\delta^1\text{H}$ (400 MHz, CDCl_3) 8.24 – 8.07 (1 H, dd, J = 8.6, 1.3 Hz, H-14), 8.08 – 7.93 (1 H, dd, J = 8.6, 1.3 Hz, H-19), 7.50 (1 H, ddd, J = 8.3, 6.7, 1.5 Hz, H-20), 7.45 (1 H, ddd, J = 8.2, 6.7, 1.5 Hz, H-16), 7.12 (2 H, dd, J = 7.4, 1.5 Hz, H-4 + H-9), 7.01 (1 H, dd, J = 7.6, 1.7 Hz, H-6), 6.92 (1 H, t, J = 7.5 Hz, H-5), 5.38 (1 H, br. s, NH), 2.68 (3 H, s, H-21), 2.57 (2 H, q, J = 7.5 Hz, H-13), 2.08 (3 H, s, H-18), 1.89 (3 H, s, H-17), 1.22 (3 H, t, J = 7.5 Hz, H-15). $\delta^{13}\text{C}$ (101 MHz, CDCl_3) 142.4 (C-1), 135.9 (C-2), 133.5 (C-3), 132.2 (C-11), 130.6 (C-9), 129.9 (C-12), 129.3 (C-6), 129.0 (C-10), 128.3 (C-7), 126.7 (C-4), 126.6 (C-8), 125.4 (C-16), 124.9 (C-20), 124.6 (C-19), 123.3 (C-14), 121.2 (C-5), 25.1 (C-13), 19.4 (C-17), 19.2 (C-18 + C-21), 13.9 (C-15). IR (film, cm^{-1}) ν_{max} 3465 (N–H), 2865 (C–H), 1583 (N–H), 1569, 1463.

2,4-Di-*tert*-butyl-*N*-(2-isopropyl-6-methylphenyl)-6-methylaniline – 1.28t

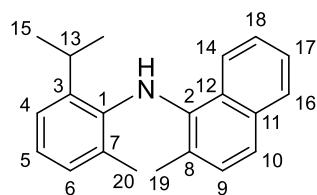


Following **GP1.1** with 2-bromo-1,5-di-*tert*-butyl-3-methylbenzene^[14] (115 mg, 0.41 mmol, 1.0 eq.), 2-isopropyl-6-methylaniline (79 μL , 0.51 mmol, 1.25 eq.), NaOtBu (58 mg, 0.61 mmol, 1.5 eq.), $\text{Pd}_2(\text{dba})_3$ (3.7 mg, 4.1 μmol , 1 mol%), PNp_3 (2.0 mg, 8.2 μmol , 2 mol%) in distilled

toluene (0.8 mL). Filtration over a plug of silica (SiO_2 , petroleum ether) yielded the title compound as a colourless oil (11 mg, 0.03 mmol, 7%). $\delta^1\text{H}$ (400 MHz, CDCl_3) 7.28 (1 H, d, J = 2.1 Hz, H-4), 7.11 (1 H, d, J = 7.5 Hz, H-11), 6.95 (1 H, d, J = 1.9 Hz, H-6), 6.92 (1 H, d, J = 5.7 Hz, H-9), 6.85 (1 H, t, J = 7.5 Hz, H-10), 5.34 (1 H, br. s, NH), 3.02 (1 H, dt, J = 13.6, 6.8 Hz, H-14), 1.86 (3 H, s, H-19), 1.72 (3 H, s, H-20), 1.51 (9 H, s, H-15), 1.31 (9 H, s, H-17), 1.18 ($\text{CH}_\text{A}\text{H}_\text{B}$, 3 H, d, J = 5.8 Hz, H-18), 1.14 ($\text{CH}_\text{A}\text{H}_\text{B}$, 3 H, d, J = 5.8, H-18). $\delta^{13}\text{C}$ (101 MHz, CDCl_3) 144.8 (C-5), 140.7 (C-2), 139.8 (C-3), 139.3 (C-1), 137.6 (C-12), 131.5 (C-7), 129.1 (C-9), 127.5 (C-8), 126.5 (C-6), 124.1 (C-11), 121.7 (C-4), 120.6 (C-10), 35.6 (C-13), 34.5 (C-16), 31.7 (C-17), 31.0 (C-15), 27.8 (C-14), 24.7 (C-18), 22.3 (C-18), 20.4 (C-20), 19.9 (C-19). IR (film, cm^{-1}) ν_{max} 3439 (N–H), 2955 (C–H), 2925 (C–H), 2867 (C–H),

1605 (N–H), 1580 (N–H), 1503, 1486, 1458; **HRMS (APCI⁺)** m/z calcd for C₂₅H₃₈N [M+H]⁺ 352.3004, found 352.3021.

N-(2-Isopropyl-6-methylphenyl)-2-methylnaphthalen-1-amine – 1.28u

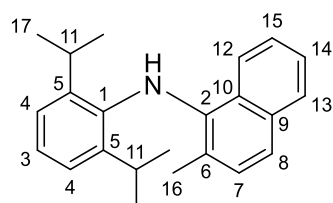


Following **GP1.1** with 1-bromo-2-methylnaphthalene (55 μ L, 0.35 mmol, 1.0 eq.), 2-isopropyl-6-methylaniline (68 μ L, 0.44 mmol, 1.25 eq), NaOtBu (50 mg, 0.52 mmol, 1.5 eq.), Pd₂(dba)₃ (3.2 mg, 3.5 μ mol, 1 mol%), PNp₃ (1.7 mg, 7 μ mol, 2 mol%) in distilled toluene (0.7 mL). Filtration over a

plug of silica (SiO₂, petroleum ether) yielded the title compound as a pink oil (86 mg, 0.30 mmol, 85%).

$\delta^1\text{H}$ (400 MHz, CDCl₃) 7.94 (1 H, d, J = 8.3 Hz, H-14), 7.82 (1 H, d, J = 8.2 Hz, H-16), 7.47 (1 H, d, J = 8.3 Hz, H-10), 7.42 (1 H, t, J = 7.9 Hz, H-17), 7.37 (1 H, m, H-18), 7.25 (1 H, d, J = 8.2 Hz, H-9), 7.21 (1 H, d, J = 7.4 Hz, H-4), 7.02 (1 H, t, J = 7.4 Hz, H-5), 6.99 (1 H, d, J = 7.3 Hz, H-6), 5.49 (1 H, s, NH), 3.27 (1 H, sept, J = 5.8 Hz, H-13), 2.10 (3 H, s, H-19), 1.85 (3 H, s, H-20), 1.24 (CH_AH_B, 3 H, d, J = 5.8 Hz, H-15), 1.20 (CH_AH_B, 3 H, d, J = 5.8 Hz, H-15). **$\delta^{13}\text{C}$ (101 MHz, CDCl₃)** 141.0 (C-7), 140.0 (C-3), 138.1 (C-2), 133.5 (C-12), 130.5 (C-1), 130.1 (C-9), 128.9 (C-6), 128.4 (C-16), 128.3 (C-12), 125.4 (C-18), 125.1 (C-17), 124.6 (C-8), 123.9 (C-4), 122.7 (C-5), 122.5 (C-14), 121.9 (C-10), 28.1 (C-13), 23.8 (C-15), 23.0 (C-15), 19.63 (C-20), 19.46 (C-19). **IR (film, cm⁻¹)** ν_{max} 3423 (N–H), 3051 (C–H), 2960 (C–H), 2866 (C–H), 1593 (N–H), 1568, 1465; **HRMS (APCI⁺)** m/z calcd for C₂₁H₂₄N [M+H]⁺ 290.1909, found 290.1895. Supplementary crystallographic data can be obtained free of charge from The Cambridge Crystallographic Data Centre (CCDC 1842707).

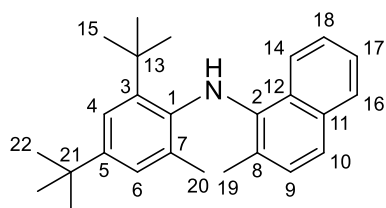
N-(2,6-Diisopropylphenyl)-2-methylnaphthalen-1-amine – 1.28v



Following **GP1.1** with 1-bromo-2-methylnaphthalene (55 μ L, 0.35 mmol, 1.0 eq.), 2,6-diisopropylaniline (83 μ L, 0.44 mmol, 1.25 eq), NaOtBu (50 mg, 0.52 mmol, 1.5 eq.), Pd₂(dba)₃ (3.2 mg, 3.5 μ mol, 1 mol%), PNp₃ (1.7 mg, 7 μ mol, 2 mol%) in distilled toluene (0.7 mL).

Filtration over a plug of silica (SiO₂, petroleum ether) yielded the title compound as a yellow oil (72 mg, 0.23 mmol, 65%). **$\delta^1\text{H}$ (400 MHz, CDCl₃)** 7.86 (1 H, d, J = 8.5 Hz, H-12), 7.80 (1 H, d, J = 8.1 Hz, H-13), 7.41 (1 H, d, J = 8.0 Hz, H-8), 7.39 (1 H, d, J = 7.9 Hz, H-14), 7.32 (1 H, t, J = 7.6 Hz, H-15), 7.24 (1 H, d, J = 8.3 Hz, H-7), 7.18 (3 H, s, H-3 + H-4), 5.41 (1 H, s, NH), 3.15 (2 H, sept., J = 5.8 Hz, H-11), 2.13 (3 H, s, H-16), 1.14 (CH_AH_B, 6 H, d, J = 5.8 Hz, H-17), 1.04 (CH_AH_B, 6 H, d, J = 5.8 Hz, H-17). **$\delta^{13}\text{C}$ (101 MHz, CDCl₃)** 142.8 (C-5), 139.5 (C-1), 139.2 (C-2), 133.8 (C-9), 130.5 (C-7), 128.4 (C-13), 127.0 (C-10), 125.04 (C-15), 124.96 (C-14), 124.4 (C-3), 123.8 (C-4), 122.5 (C-12), 122.1 (C-6), 120.7 (C-8), 28.2 (C-11), 23.9 (C-17), 23.2 (C-17), 19.6 (C-16). **IR (film, cm⁻¹)** ν_{max} 3430 (N–H), 3054 (C–H), 2960 (C–H), 2867 (C–H), 1567, 1465, 1384; **HRMS (APCI⁺)** m/z calcd for C₂₃H₂₈N [M+H]⁺ 318.2222, found 318.2208.

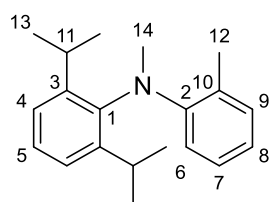
N-(2-(*Tert*-butyl)-6-methylphenyl)-2-methylnaphthalen-1-amine – 1.28x



Following **GP1.1** with 1-bromo-2-methylnaphthalene (55 μ L, 0.35 mmol, 1.0 eq.), aniline **1.27** (96 mg, 0.44 mmol, 1.25 eq), NaOtBu (50 mg, 0.52 mmol, 1.5 eq.), Pd₂(dba)₃ (3.2 mg, 3.5 μ mol, 1 mol%), PNP₃ (1.7 mg, 7 μ mol, 2 mol%) in distilled toluene (0.7 mL).

Filtration over a plug of silica (SiO₂, petroleum ether) yielded the title compound as a yellow oil (38 mg, 0.11 mmol, 30%). **$\delta^1\text{H}$ (500 MHz, CDCl₃)** 7.80 (1 H, d, J = 8.1 Hz, H-14), 7.76 (1 H, d, J = 8.6 Hz, H-16), 7.40 (1 H, d, J = 2.2 Hz, H-4), 7.39 (2 H, m, H-18 + H-10), 7.27 (2 H, m, H-17 + H-9), 7.02 (1 H, d, J = 2.1 Hz, H-6), 5.82 (1 H, s, NH), 2.14 (3 H, s, H-19), 1.69 (3 H, s, H-20), 1.58 (9 H, s, H-15), 1.38 (9 H, s, H-22). **$\delta^{13}\text{C}$ (126 MHz, CDCl₃)** 145.6 (C-5), 140.6 (C-3), 139.3 (C-1), 138.1 (C-2), 133.7 (C-11), 132.5 (C-12), 130.4 (C-9), 128.5 (C-14), 126.7 (C-7), 126.5 (C-6), 124.9 (C-18), 124.8 (C-17), 122.4 (C-14), 121.8 (C-4), 121.1 (C-8), 120.2 (C-10), 35.5 (C-15), 34.6 (C-21), 31.7 (C-22), 31.2 (C-15), 20.0 (C-20), 19.5 (C-19). **IR (film, cm⁻¹)** ν_{max} 3465 (N–H), 2953 (C–H), 2867 (C–H), 1567, 1481; **HRMS (APCI⁺)** m/z calcd for C₂₆H₃₄N [M+H]⁺ 360.2691, found 360.2682.

2,6-Diisopropyl-*N*-methyl-*N*-(*o*-tolyl)aniline – 1.29



To a solution of compound **1.28j** (53 mg, 0.20 mmol, 1.0 eq.) in DMF (2.0 mL, 0.1 M) at 0 °C was added NaH (60% suspension in mineral oil, 16 mg, 0.40 mmol, 2.0 eq.) followed by iodomethane (33 μ L, 0.40 mmol, 2.0 eq.).

The reaction mixture was allowed to warm up to rt, stirred for 18h, then quenched with an aqueous solution of saturated NaHCO₃ and extracted with ethyl acetate. The organic phases were combined, washed with brine, dried over MgSO₄ and concentrated *in vacuo*. Purification by flash column chromatography (SiO₂, petroleum ether) yielded the title compound as a colourless oil (28 mg, 50%). **$\delta^1\text{H}$ (400 MHz, DMSO-*d*₆)** 7.28 – 7.20 (1 H, m, ArCH), 7.20 – 7.06 (3 H, m, ArCH), 7.02 – 6.76 (2 H, m, ArCH), 6.67 (1 H, td, J = 7.3, 1.2 Hz, ArCH), 3.16 (3 H, s, NCH₃), 3.08 (2 H, hept, J = 5.9 Hz, CH(CH₃)₂), 1.47 (3 H, br. s, CCH₃), 1.14 (CH_AH_B, 6 H, d, J = 5.9 Hz, CH(CH₃)₂), 0.93 (CH_AH_B, 6 H, d, J = 5.8 Hz, CH(CH₃)₂). **$\delta^{13}\text{C}$ (126 MHz, CDCl₃)** 147.2 (C-1), 144.6 (C-2), 132.5 (C-5 + C-9), 126.9 (C-3), 126.7 (C-7), 125.5 (C-4), 124.3 (C-10), 118.6 (C-8), 111.4 (C-13), 42.9 (C-14), 27.9 (C-11), 25.4 (C-6), 22.8 (C-6), 21.2 (C-12). **IR (film, cm⁻¹)** ν_{max} 2966 (C–H), 1697, 1514, 1156 (C–N); **HRMS (APCI⁺)**: m/z calcd for C₂₀H₂₈N [M+H]⁺ 282.2222, found 282.2212.

Chapter 2

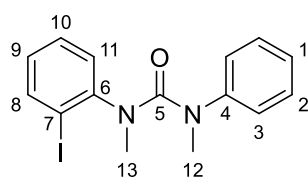
General Procedure 2.1 (GP2.1), formation of N,N'-diarylureas: **Part 1:** A flame-dried round bottom flask was allowed to cool to rt *in vacuo* and refilled with nitrogen. To this was added the required 2-bromoaniline (1.0 eq.) and anhydrous CH₂Cl₂ (0.55 M). The required isocyanate (1.2 eq.) was added dropwise and the reaction allowed to stir at rt until consumption of the urea was observed by TLC. The reaction mixture was filtered, and the residue was rinsed with a small amount of cold CH₂Cl₂ to give the desired urea which was directly used in the next step without further purification.

Part 2: A flame-dried round bottom flask was allowed to cool to rt *in vacuo* and refilled with nitrogen. To this was added the required urea (1.0 eq.) and anhydrous THF (0.5 M) and the reaction mixture was cooled to 0 °C. NaH (4.0 eq.) was added portion wise, followed by dropwise addition of methyl iodide (6.0 eq.). The reaction mixture was allowed to stir at rt until consumption of the urea was observed by TLC. The reaction mixture was quenched with sat. Na₂S₂O₃ (aq.) and extracted with Et₂O. The combined organic phases were washed with brine, dried over MgSO₄, filtered and concentrated *in vacuo* to yield the crude methylated urea. Purification by flash column chromatography yielded the desired product.

General Procedure 2.2 (GP2.2), anionic ortho-Fries rearrangement of ureas: A flame-dried round bottom flask was allowed to cool to rt *in vacuo* and refilled with nitrogen. To this was added the required methylated urea (1.0 eq.) and anhydrous THF (0.2 M) and the reaction mixture was cooled to -78 °C. *n*-BuLi (1.44 M in hexanes, 1.1 eq.) was added dropwise and the reaction was left to stir at -78 °C for 2 h. The reaction mixture was quenched with MeOH and concentrated *in vacuo* to yield the crude benzamide. Purification by flash column chromatography yielded the desired product.

General Procedure 2.3 (GP2.3), Diarylamine formation by Smiles Rearrangement: A flame-dried round bottom flask was allowed to cool to rt *in vacuo*. To this was added the required aniline (1.0 eq.) and anhydrous THF (0.2 M) and the reaction mixture was cooled to 0 °C. NaHMDS (1.0 M in THF, 1.1 eq.) was added dropwise and the reaction was allowed to stir at rt for 4 h. The reaction mixture was quenched with MeOH and concentrated *in vacuo* to yield the crude diarylamine. Purification by column chromatography yielded the desired product. (N.B. reactions heated under reflux (66 °C) were performed in flame-dried sealed Biotage microwave vials)

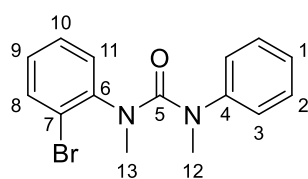
1-(2-Iodophenyl)-1,3-dimethyl-3-phenylurea – 2.34



Following **GP2.1 (Part 1)** 2-iodoaniline (5.0 g, 23 mmol, 1 eq.), phenyl isocyanate (3.0 mL, 27 mmol, 1.2 eq.) in CH_2Cl_2 (40 mL, 0.55 M) were stirred at rt for 3 h. Filtration yielded the urea as a white solid (6.1 g, 79%) which was used directly in the next step. Following **GP2.1 (Part 2)**

The required urea (6.0 g, 18 mmol, 1 eq.), NaH (1.7 g, 72 mmol, 4.0 eq., 60% in mineral oil), MeI (6.6 mL, 107 mmol, 6.0 eq.) in THF (36 mL, 0.5 M) were stirred at rt overnight. Purification by flash column chromatography eluting with (10% to 60% EtOAc/Petrol) yielded the *title compound* as an off-white solid (5.4 g, 83%). R_f 0.12 (40% Et₂O/Petrol). **m.p.:** 74 – 77 °C. $\delta^1\text{H}$ (400 MHz, CDCl_3) 7.59 (1 H, dd, J = 8.3, 1.4 Hz, H-8), 7.03 (2 H, t, J = 7.5 Hz, H-2), 6.98 – 6.90 (2 H, m, H-1 + H-9), 6.76 (2 H, d, J = 9.4 Hz, H-2), 6.66 (2 H, d, J = 7.9 Hz, H-10 + H-11), 3.19 (3 H, s, H-12), 3.15 (3 H, s, H-13). $\delta^{13}\text{C}$ (101 MHz, CDCl_3) 160.4 (C-5), 147.2 (C-6), 145.4 (C-4), 139.7 (C-8), 129.6 (C-11), 129.0 (C-2), 128.8 (C-1), 127.4 (C-10), 126.3 (C-3), 125.5 (C-9), 98.5 (C-7), 40.4 (C-12), 39.0 (C-13). **IR (film, cm^{-1})** ν_{max} 1655 (C=O), 749 (C-I). **HRMS (ESI⁺)** m/z calcd for $\text{C}_{15}\text{H}_{16}\text{IN}_2\text{O}$ $[\text{M}+\text{H}]^+$ 367.0302; found: 367.0310.

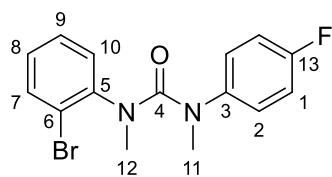
1-(2-Bromophenyl)-1,3-dimethyl-3-phenylurea – 2.35



Following **GP2.1 (Part 1)** 2-bromoaniline (1.2 mL g, 11 mmol, 1 eq.), phenyl isocyanate (1.4 mL, 13 mmol, 1.2 eq.) in CH_2Cl_2 (22 mL, 0.55 M) were stirred at rt overnight. Filtration yielded the urea as a white solid (2.7 g, 84%) which was used directly in the next step. Following **GP2.1**

(Part 2) The required urea (2.7 g, 9.2 mmol, 1 eq.), NaH (1.5 g, 37 mmol, 4.0 eq., 60% in mineral oil), MeI (3.5 mL, 55 mmol, 6.0 eq.) in THF (18 mL, 0.5 M) were stirred at rt for 2 h. Purification by flash column chromatography eluting with (10% to 60% EtOAc/Petrol) yielded the *title compound* as an off-white solid (2.8 g, 95%). R_f 0.32 (25% EtOAc/Petrol). **m.p.:** 100 – 101 °C. $\delta^1\text{H}$ (400 MHz, CDCl_3) 7.30 (1 H, dd, J = 7.9, 1.4 Hz, H-8), 7.02 (2 H, t, J = 7.5 Hz, H-2), 6.94 (1 H, br. t, J = 7.5 Hz, H-1), 6.92 (1 H, td, J = 7.9, 1.4 Hz, H-10), 6.82 (1 H, td, J = 7.9, 1.7 Hz, H-9), 6.77 (2 H, dd, J = 7.5, 1.7 Hz, H-3), 6.71 (1 H, dd, J = 7.9, 1.7 Hz, H-11), 3.19 (3 H, s, H-13), 3.15 (3 H, s, H-12). $\delta^{13}\text{C}$ (101 MHz, CDCl_3) 160.7 (C-5), 145.3 (C-4), 144.0 (C-6), 133.3 (C-8), 130.1 (C-11), 128.9 (C-2), 128.0 (C-10), 127.4 (C-9), 126.1 (C-3), 125.4 (C-1), 122.8 (C-7), 40.1 (C-13), 38.6 (C-12). **IR (film, cm^{-1})** ν_{max} 1645 (C=O), 723 (C-Br). **HRMS (ESI⁺)** m/z calcd for $\text{C}_{17}\text{H}_{19}\text{N}_2\text{O}^+$ $[\text{M}+\text{H}]^+$ 267.1492; found: 267.1491.

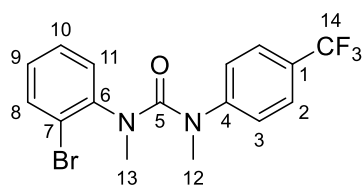
1-(2-Bromophenyl)-3-(4-fluorophenyl)-1,3-dimethylurea – 2.41b



Following **GP2.1 (Part 1)** 2-bromoaniline (0.50 mL, 4.4 mmol, 1 eq.), 4-fluorophenyl isocyanate (0.60 mL, 5.3 mmol, 1.2 eq.) in CH_2Cl_2 (8.0 mL, 0.55 M) were stirred at rt overnight. Filtration yielded the urea as a white solid (1.26 g, 93%) which was used directly in the next step.

Following **GP2.1 (Part 2)** the required urea (1.25 g, 4.05 mmol, 1 eq.), NaH (0.64 g, 16.1 mmol, 4.0 eq., 60% in mineral oil), MeI (1.5 mL, 24 mmol, 6.0 eq.) in THF (8.1 mL, 0.5 M) were stirred at rt overnight. Purification by flash column chromatography eluting with (5% to 50% EtOAc/Petrol) yielded the *title compound* as a colourless oil (1.44 g, 95%). R_f 0.15 (25% EtOAc/Petrol). $\delta^1\text{H}$ (400 MHz, CDCl_3) 7.33 (1 H, dd, J = 7.8, 1.6 Hz, H-7), 6.98 (1 H, td, J = 7.8, 1.6 Hz, H-9), 6.87 (1 H, td, J = 7.8, 1.6 Hz, H-8), 6.72 (1 H, dd, J = 7.8, 1.6 Hz, H-10), 6.73 – 6.69 (4 H, m, H-1 + H-2), 3.15 (3 H, s, H-11), 3.14 (3 H, s, H-12). $\delta^{13}\text{C}$ (101 MHz, CDCl_3) 160.6 (C-4), 160.3 (d, J = 245 Hz, C-13), 144.0 (C-5), 141.3 (d, J = 3.1 Hz, C-3), 133.4 (C-7), 130.0 (C-10), 128.1 (C-9), 127.9 (d, J = 8.5 Hz, C-2), 127.6 (C-8), 122.8 (C-6), 115.7 (d, J = 22.5 Hz, C-1), 40.3 (C-11), 38.7 (C-12). $\delta^{19}\text{F}$ NMR (376 MHz, CDCl_3) -116.5 (p, J = 5.7 Hz, C-F). IR (film, cm^{-1}) ν_{max} 1658 (C=O), 1508, 1351 (C-N). HRMS (ESI⁺) m/z calcd for $\text{C}_{15}\text{H}_{14}\text{BrFN}_2\text{ONa}^+ [\text{M}+\text{Na}]^+$ 359.0166; found: 359.0179.

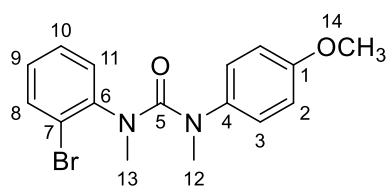
1-(2-Bromophenyl)-1,3-dimethyl-3-(4-(trifluoromethyl)phenyl)urea 2.41c



Following **GP2.1 (Part 1)** 2-bromoaniline (0.50 mL, 4.4 mmol, 1.4 eq.), 4-trifluoromethylphenyl isocyanate (0.46 mL, 3.2 mmol, 1.0 eq.) in CH_2Cl_2 (8.0 mL, 0.55 M) were stirred at rt for 3 h. Filtration yielded the urea as a white solid (1.15 g, quant.) which was used directly in the next step.

Following **GP2.1 (Part 2)** the required urea (1.15 g, 3.2 mmol, 1 eq.), NaH (0.51 g, 13 mmol, 4.0 eq., 60% in mineral oil), MeI (1.2 mL, 19 mmol, 6.0 eq.) in THF (6.4 mL, 0.5 M) were stirred at rt overnight. Purification by flash column chromatography eluting with (5% to 50% EtOAc/Petrol) yielded the *title compound* as a white solid (1.19 g, 96%). R_f 0.31 (25% EtOAc/Petrol). $m.p.$: 94 – 95 °C. $\delta^1\text{H}$ (400 MHz, CDCl_3) 7.27 (1 H, dd, J = 8.1, 1.5 Hz, H-8), 7.25 (2 H, d, J = 8.1 Hz, H-2), 6.90 (1 H, td, J = 7.6, 1.5 Hz, H-10), 6.86 (2 H, d, J = 8.3 Hz, H-3), 6.81 (1 H, td, J = 7.7, 1.7 Hz, H-9), 6.68 (1 H, dd, J = 7.9, 1.7 Hz, H-11), 3.17 (3 H, s, H-12), 3.13 (3 H, s, H-13). $\delta^{13}\text{C}$ (101 MHz, CDCl_3) 160.2 (C-5), 148.4 (q, J = 1.5 Hz, C-4), 143.5 (C-6), 133.4 (C-7), 129.9 (C-11), 128.1 (C-10), 127.8 (C-9), 127.1 (q, J = 32.7 Hz, C-1), 126.0 (q, J = 3.8 Hz, C-2), 125.7 (C-3), 124.0 (q, J = 271.8 Hz, C-14), 122.7 (C-7), 39.5 (C-12), 38.6 (C-13). $\delta^{19}\text{F}$ (376 MHz, CDCl_3) -62.40 (s, CF_3). IR (film, cm^{-1}) ν_{max} 1663 (C=O), 1322 (C-N) 1110. HRMS (ESI⁺) m/z calcd for $\text{C}_{16}\text{H}_{14}\text{BrN}_2\text{ONa}^+ [\text{M}+\text{Na}]^+$ 409.0134; found: 409.0133.

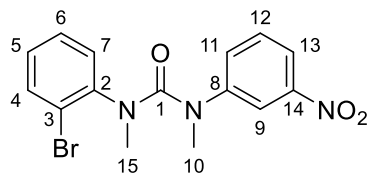
1-(2-Bromophenyl)-1,3-dimethyl-3-(4-(methoxy)phenyl)urea 2.41e



Following **GP2.1 (Part 1)** 2-bromoaniline (0.50 mL, 4.4 mmol, 1 eq.), 4-methoxyphenyl isocyanate (0.69 mL, 5.3 mmol, 1.2 eq.) in CH₂Cl₂ (8.0 mL, 0.55 M) were stirred at rt overnight. Filtration yielded the *title compound* as a white solid (1.15 g, 81%) which was used

directly in the next step. Following **GP2.1 (Part 2)**, the required urea (1.14 mg, 3.55 mmol, 1 eq.), NaH (567 mg, 14.2 mmol, 4.0 eq., 60% in mineral oil), MeI (1.3 mL, 21.3 mmol, 6.0 eq) in THF (10.1 mL, 0.35 M) were stirred at rt overnight. Purification by flash column chromatography eluting with (5% to 50% EtOAc/Petrol) yielded the *title compound* as colourless oil (1.22 g, 98%). *R_f* 0.15 (25% EtOAc/Petrol); **$\delta^1\text{H}$ (400 MHz, CDCl₃)** 7.32 (1 H, dd, *J* = 8.0, 1.5 Hz, H-8), 6.96 (1 H, td, *J* = 7.6, 1.5 Hz, H-10), 6.84 (1 H, td, *J* = 7.7, 1.6 Hz, H-9), 6.72 (1 H, dd, *J* = 7.9, 1.7 Hz, H-11), 6.66 (2 H, d, *J* = 8.7 Hz, H-3), 6.54 (2 H, d, *J* = 8.9 Hz, H-2), 3.70 (3 H, s, H-14), 3.14 (3 H, s, H-12), 3.13 (3 H, s, H-13). **$\delta^{13}\text{C}$ (101 MHz, CDCl₃)** 160.8 (C-5), 157.3 (C-1), 144.2 (C-6), 138.4 (C-4), 133.3 (C-8), 130.00 (C-11), 127.96 (C-10), 127.5 (C-3), 127.4 (C-9), 122.8 (C-7), 114.2 (C-2), 55.6 (C-14), 40.3 (C-12), 38.7 (C-13). **IR (film, cm⁻¹)** ν_{max} 1654 (C=O), 1510, 1354 (C-N), 1245 (C-O). **HRMS (ESI⁺)** *m/z* calcd for C₁₆H₁₇BrN₂ONa⁺ [M+Na]⁺ 37.0366; found 371.0377.

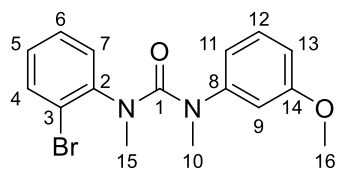
1-(2-Bromophenyl)-3-(3-nitrophenyl)-1,3-dimethylurea 2.41f



Following **GP2.1 (Part 1)** 2-bromoaniline (0.50 mL, 4.4 mmol, 1 eq.), 3-nitrophenyl isocyanate (0.87 g, 5.3 mmol, 1.2 eq.) in CH₂Cl₂ (8.0 mL, 0.55 M) were stirred at rt overnight. Filtration yielded the *title compound* as a yellow solid (1.48 g, quant.) which was used directly

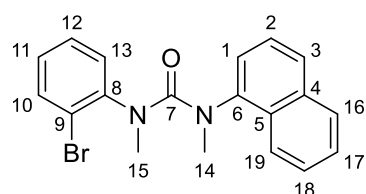
in the next step. Following **GP2.1 (Part 2)** the required urea (1.52 g, 4.4 mmol, 1 eq.), NaH (0.70 g, 17.6 mmol, 4.0 eq. 60% in mineral oil), MeI (1.6 mL, 26.4 mmol, 6.0 eq) in THF (13.8 mL, 0.32 M) were stirred at rt overnight. Purification by flash column chromatography eluting with (5% to 55% EtOAc/Petrol) yielded the *title compound* as a yellow solid (1.45 g, 98%). *R_f* 0.21 (25% EtOAc/Petrol). **m.p.:** 106 °C. **$\delta^1\text{H}$ (400 MHz, CDCl₃)** 7.80 (1 H, ddd, *J* = 8.1, 2.2, 1.1 Hz, H-3), 7.62 (1 H, t, *J* = 2.2 Hz, H-5), 7.29 (1 H, ddd, *J* = 7.9, 1.6, 0.6 Hz, H-10), 7.23 (1 H, t, *J* = 8.0 Hz, H-2), 7.15 (1 H, ddd, *J* = 8.0, 2.1, 1.1 Hz, H-1), 7.00 (1 H, td, *J* = 7.6, 1.5 Hz, H-12), 6.84 (2 H, m, H-11 + H-13), 3.22 (3 H, s, H-14), 3.19 (3 H, s, H-15). **$\delta^{13}\text{C}$ (101 MHz, CDCl₃)** 159.9 (C-7), 148.5 (C-4), 146.2 (C-6), 142.4 (C-8), 133.6 (C-10), 131.8 (C-1), 129.7 (C-2 + C-13), 128.2 (C-12), 128.0 (C-11), 122.6 (C-9), 120.9 (C-5), 120.1 (C-3), 39.7 (C-14), 38.6 (C-15). **IR (film, cm⁻¹)** ν_{max} 1665 (C=O), 1527 (N-O), 1346 (C-N). **HRMS (ESI⁺)** *m/z* calcd for C₁₅H₁₄N₃O₃BrNa⁺ [M+Na]⁺ 386.0111; found 386.0132.

1-(2-Bromophenyl)-3-(3-methoxyphenyl)-1,3-dimethylurea 2.41g



Following **GP2.1 (Part 1)** 2-bromoaniline (0.50 mL, 4.4 mmol, 1 eq.), 3-methoxyphenyl isocyanate (0.69 mL, 5.3 mmol, 1.2 eq.) in CH₂Cl₂ (8.0 mL, 0.55 M) were stirred at rt overnight. Filtration yielded the urea as a white solid (1.21 g, 86%) which was used directly in the next step. Following **GP2.1 (Part 2)** the required urea (1.21 g, 3.76 mmol, 1 eq.), NaH (0.60 g, 15 mmol, 4.0 eq., 60% in mineral oil), MeI (1.4 mL, 23 mmol, 6.0 eq.) in THF (6.9 mL, 0.5 M) were stirred at rt for 2 h. Purification by flash column chromatography eluting with (5% to 60% EtOAc/Petrol) yielded the *title compound* as colourless oil (1.12 g, 85%). *R_f* 0.17 (25% EtOAc/Petrol). **¹H (400 MHz, CDCl₃)** 7.31 (1 H, dd, *J* = 8.0, 1.5 Hz, H-4), 6.98 – 6.89 (2 H, m, H-6 + H-9), 6.85 (1 H, ddd, *J* = 8.0, 7.4, 1.7 Hz, H-5), 6.75 (1 H, dd, *J* = 7.8, 1.7 Hz, H-7), 6.50 (1 H, ddd, *J* = 8.3, 2.5, 0.9 Hz, H-12), 6.37 (1 H, ddd, *J* = 7.8, 2.0, 0.9 Hz, H-11), 6.27 (1 H, t, *J* = 2.2 Hz, H-13), 3.64 (3 H, s, H-16), 3.17 (3 H, s, H-10), 3.14 (3 H, s, H-15). **¹³C (101 MHz, CDCl₃)** 160.6 (C-1), 159.9 (C-14), 146.4 (C-8), 143.9 (C-2), 133.2 (C-4), 130.1 (C-7), 129.5 (C-9), 127.9 (C-6), 127.4 (C-5), 122.8 (C-3), 118.6 (C-11), 111.64 (C-12 or C-13), 111.59 (C-12 or C-13), 55.3 (d, *J* = 5.3 Hz, C-16), 40.0 (C-10), 38.6 (C-15). **IR (film, cm⁻¹)** *v*_{max} 1655 (C=O), 1597, 1352 (C–N), 1043 (O–CH₃), 755 (C–Br). **HRMS (ESI⁺)** *m/z* calcd for C₁₆H₁₇N₂OBrNa⁺ [M+Na]⁺ 371.0366; found: 371.0367.

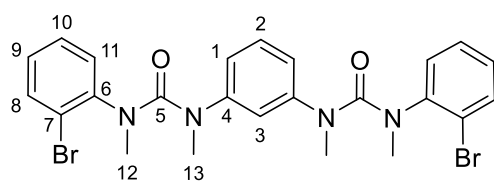
1-(2-Bromophenyl)-1,3-dimethyl-3-(naphthalen-1-yl)urea – 2.41j



Following **GP2.1 (Part 1)** 2-bromoaniline (0.50 mL, 4.4 mmol, 1 eq.), 1-isocyanatonaphthalene (0.76 mL, 5.3 mmol, 1.2 eq.) in CH₂Cl₂ (8.0 mL, 0.55 M) were stirred at rt overnight. Filtration yielded the urea as a white solid (0.79 g, 49%) which was used directly in the next

step. Following **GP2.1 (Part 2)** the required urea (0.74 g, 2.2 mmol, 1 eq.), NaH (0.34 g, 8.6 mmol, 4.0 eq., 60% in mineral oil), MeI (0.80 mL, 12.9 mmol, 6.0 eq.) in THF (8.3 mL, 0.26 M) were stirred at rt for 3 h. Purification by flash column chromatography eluting with (5% to 50% EtOAc/Petrol) yielded the *title compound* as an off-white solid (0.70 g, 87%). *R_f* 0.30 (25% EtOAc/Petrol). **m.p.:** 109 – 110 °C. **¹H (400 MHz, CDCl₃)** 7.73 – 7.68 (1 H, m, H-19), 7.68 – 7.65 (1 H, m, H-16), 7.51 (1 H, d, *J* = 8.2 Hz, H-3), 7.40 – 7.31 (2 H, m, H-17 + H-18), 7.16 (1 H, t, *J* = 7.7 Hz, H-2), 7.06 (1 H, d, *J* = 7.7 Hz, H-10), 6.99 (1 H, d, *J* = 7.3 Hz, H-1), 6.51 (1 H, td, *J* = 7.5, 1.7 Hz, H-12), 6.46 (1 H, td, *J* = 7.7, 1.8 Hz, H-11), 6.26 (1 H, d, *J* = 7.8 Hz, H-13), 3.31 (3 H, s, H-14), 3.11 (3 H, s, H-15). **¹³C (101 MHz, CDCl₃)** 161.3 (C-7), 143.2 (C-8), 141.7 (C-6), 134.4 (C-4), 133.1 (C-10), 129.8 (C-13), 129.7 (C-5), 128.1 (C-16), 127.6 (C-12), 126.93 (C-11), 126.88 (C-3), 126.1 (C-17 or C-18), 126.0 (C-17 or C-18), 125.7 (C-2), 124.8 (C-1), 123.1 (C-19), 122.9 (C-9), 40.1 (C-14), 38.8 (C-15). **IR (film, cm⁻¹)** *v*_{max} 1653 (C=O), 1356 (C–N). **HRMS (ESI⁺)** *m/z* calcd for C₁₉H₁₇BrN₂ONa⁺ [M+Na]⁺ 391.0416; found: 391.0415.

1,1'-(1,3-Phenylene)bis(3-(2-bromophenyl)-1,3-dimethylurea) – 2.41k

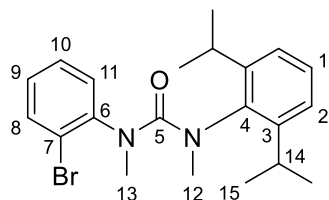


Following the procedure reported by Clayden *et al.*^[2]

2-bromoaniline (0.82 mL, 7.2 mmol, 2.3 eq.), 1,3-phenylene diisocyanate (0.50 g, 3.1 mmol, 1.0 eq.) in THF (15.0 mL, 0.2 M) were stirred at rt for 3 h. Volatiles were

evaporated *in vacuo* and the residue was suspended in Et₂O. Filtration yielded the urea as a white solid (1.3 g, 86%) which was used directly in the next step. The required urea (1.3 g, 2.6 mmol, 1 eq.), NaOH (0.51 g, 12 mmol, 4.8 eq.), MeI (0.81 mL, 13 mmol, 5.0 eq) in THF (43 mL, 0.06 M) were stirred at rt overnight. Purification by flash column chromatography eluting with (10% to 60% EtOAc/Petrol) yielded the *title compound* as an off-white solid (0.50 g, 34%). **¹H (400 MHz, CDCl₃)** 7.28 (2 H, dd, *J* = 8.0, 1.5 Hz, H-8), 6.89 (2 H, td, *J* = 7.6, 1.5 Hz, H-10), 6.80 (2 H, td, *J* = 8.0, 1.6 Hz, H-9), 6.75 (1 H, t, *J* = 8.0 Hz, H-2), 6.65 (2 H, dd, *J* = 7.9, 1.6 Hz, H-11), 6.45 (2 H, dd, *J* = 8.0, 2.0 Hz, H-1), 6.10 (1 H, t, *J* = 2.0 Hz, H-3), 3.09 (6 H, s, H-12), 2.98 (6 H, s, H-13). **¹³C (101 MHz, CDCl₃)** 160.3 (C-5), 145.7 (C-4), 143.8 (C-6), 133.2 (C-8), 130.0 (C-11), 129.2 (C-2), 127.9 (C-10), 127.5 (C-9), 123.0 (C-2), 123.0 (C-3), 122.7 (C-7), 39.8 (C-13), 38.7 (C-12). Spectroscopic data were consistent with those reported in the literature.^[2]

1-(2-Bromophenyl)-3-(2,6-diisopropylphenyl)-1,3-dimethylurea 2.41l

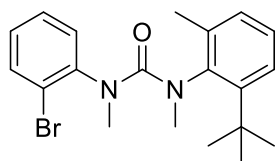


Following **GP2.1 (Part 1)** 2-bromoaniline (0.50 mL, 4.4 mmol, 1 eq.), 2,6-diisopropylphenyl isocyanate (1.1 mL, 5.3 mmol, 1.2 eq.) in CH₂Cl₂ (8.0 mL, 0.55 M) were heated to reflux for 72h. Volatiles were evaporated *in vacuo*, and the residue was suspended in Et₂O. Filtration

yielded the urea as a white solid (1.6 g, 97%) which was used directly in the next step. Following **GP2.1 (Part 2)** the required urea (1.55 g, 4.1 mmol, 1 eq.), NaH (0.66 g, 16 mmol, 4.0 eq., 60% in mineral oil), MeI (1.5 mL, 25 mmol, 6.0 eq) in THF (8.2 mL, 0.5 M) were stirred at rt overnight. Purification by flash column chromatography eluting with (10% to 50% Et₂O/Petrol) yielded the *title compound* as a white solid (1.56 g, 94%). *R_f* 0.58 (25% EtOAc/Petrol). **m.p.:** 94 – 95 °C. Mixture of conformers in a 1.0:0.3 ratio. **¹H (400 MHz, CDCl₃)** 7.71 (1 H^{min}, br. s), 7.44 (1 H^{maj}, d, *J* = 7.8 Hz, H-8^{maj}), 7.35 (1 H^{min}, br. s), 7.21 – 7.05 (2 H^{maj}, m, H-1 + H-11), 7.01 – 6.78 (4 H^{maj}, m, H-9 + H-10 + H-2), 6.35 (1 H^{maj}, d, *J* = 7.7 Hz, H-11), 3.17 (3 H^{maj}, s, H-12), 3.09 (3 H^{min}, br. s, H-12), 2.96 (3 H^{maj}, s, H-13), 2.91 (2 H^{maj} + 2 H^{min}, sept., *J* = 7.1 Hz, H-14), 2.64 (3 H^{min}, br. s, H-13), 1.36 – 0.86 (12 H^{min + maj}, m, H-15). **¹³C (101 MHz, CDCl₃)** 162.0 (C-5^{maj}), 146.8 (C-3^{maj}), 144.3 (C-6^{maj}), 140.0 (C-4^{maj}), 133.9 (C-8^{maj}), 130.2 (C-11^{maj}), 128.3 (C-9^{maj}), 127.9 (C-10^{maj}), 127.8 (C-1^{maj}), 124.1 (C-2^{maj}), 123.5 (C-7^{maj}), 40.2 (C-13^{maj}), 40.0 (C-12^{maj}), 27.9 (C-14^{maj}), 26.5 (C-15^{maj}), 22.9 (C-15^{maj}). **IR (film, cm⁻¹)** *v*_{max}

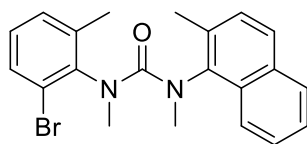
2963 (C–H), 1649 (C=O), 1351 (C–N). **HRMS (ESI⁺)** m/z calcd for $C_{21}H_{27}N_2OBrNa^+$ $[M+Na]^+$ 425.1199; found: 425.1191.

1-(2-Bromophenyl)-3-(2-(tert-butyl)-6-methylphenyl)-1,3-dimethylurea – 2.41m



Following **GP2.1 (Part 1)** 2-bromoaniline (0.50 mL, 4.4 mmol, 1 eq.), 1-(tert-butyl)-2-isocyanato-3-methylbenzene (1.0 g, 5.3 mmol, 1.2 eq.) in CH_2Cl_2 (8.0 mL, 0.55 M) were heated to reflux for 72 h. Volatiles were evaporated *in vacuo*, and the residue was suspended in Et_2O . Filtration yielded the urea as a white solid (1.41 g, 89%) which was used directly in the next step. Following **GP2.1 (Part 2)** the required urea (1.35 g, 3.73 mmol, 1 eq.), NaH (0.60 g, 15 mmol, 4.0 eq., 60% in mineral oil), MeI (1.4 mL, 22 mmol, 6.0 eq) in THF (7.4 mL, 0.5 M) were stirred at rt overnight. Purification by flash column chromatography eluting with (10% to 75% Et_2O /Petrol) yielded the *title compound* as a colourless oil (1.22 g, 84%). R_f 0.46 (25% $EtOAc$ /Petrol). Mixture of conformers in a 1.0:1.0 ratio. Integration are given relative to one conformer. δ^1H (400 MHz, $CDCl_3$) 7.71 (1 H, dd, J = 8.0, 1.4 Hz, ArH), 7.49 – 7.34 (3 H, m, ArH), 7.27 (2 H, d, J = 7.1 Hz, ArH), 7.19 (1 H, td, J = 7.6, 1.8 Hz, ArH), 7.15 – 7.08 (2 H, m, ArH), 6.89 (2 H, br. s, ArH), 6.73 (1 H, br. s, ArH), 6.50 (1 H, br. s, ArH), 6.28 (1 H, br. s, ArH), 3.16 (3 H, s, NCH_3), 3.15 (3 H, s, NCH_3), 3.05 – 2.80 (3 H, m, NCH_3), 2.60 (3 H, s, NCH_3), 2.13 – 1.85 (3 H, s, CCH_3), 1.96 (3 H, m, CCH_3) 1.44 (9 H, br. s, $C(CH_3)_3$), 1.35 (9 H, s, $C(CH_3)_3$). $\delta^{13}C$ (101 MHz, $CDCl_3$) 160.3 (C=O), 159.7 (C=O), 147.4 (ArC), 146.4 (ArC), 144.6 (ArC), 143.8 (ArC), 140.5 (ArC), 138.8 (ArC), 137.9 (ArC), 134.3 (ArCH), 133.1 (ArCH), 130.4 (ArCH), 130.4 (ArC), 129.9 (ArCH), 129.7 (ArCH), 128.7 (ArCH), 128.62 (ArCH), 128.60 (ArCH), 128.2 (ArCH), 127.6 (ArCH), 127.4 (ArCH), 127.1 (ArCH), 126.9 (ArCH), 125.5 (ArCH), 124.0 (ArC), 123.6 (ArC), 40.5 (NCH_3), 39.9 (NCH_3), 39.8 (NCH_3), 39.6 (NCH_3), 36.7 ($C(CH_3)_3$), 35.6 ($C(CH_3)_3$), 32.8 ($C(CH_3)_3$), 31.8 ($C(CH_3)_3$), 19.2 (CCH_3), 18.8 (CCH_3). IR (film, cm^{-1}) ν_{max} 2961 (C–H), 1648 (C=O), 1476, 1350 (C–N). **HRMS (ESI⁺)** m/z calcd for $C_{20}H_{25}N_2OBrNa^+$ $[M+Na]^+$ 411.1042; found: 411.1052.

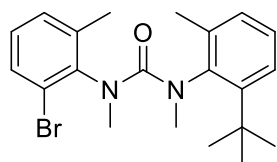
1-(2-Bromo-6-methylphenyl)-1,3-dimethyl-3-(2-methylnaphthalen-1-yl)urea – 2.41n



Following **GP2.1 (Part 1)** 2-methyl-1-naphthylamine (0.30 mL, 2.1 mmol, 1 eq.), 2-bromo-6-methylphenyl isocyanate (2.5 mmol, 1.2 eq.) in CH_2Cl_2 (3.9 mL, 0.55 M) were stirred at rt overnight. Filtration yielded the *title compound* as a white solid which was used directly in the next step. Following **GP2.1 (Part 2)** the required urea (2.1 mmol, 1 eq.), NaH (0.43 g, 8.5 mmol, 4.0 eq., 60% in mineral oil), MeI (0.79 mL, 13 mmol, 6.0 eq.) in THF (8.0 mL, 0.27 M reaction run more dilute because of solubility) were stirred at rt for 2.5 h. Purification by flash column chromatography eluting with (5% to 60% $EtOAc$ /Petrol) yielded the *title compound* as a colourless oil (0.77 g, 91%). R_f 0.24 (25% $EtOAc$ /Petrol). Mixture of conformers in a 1.0:1.0 ratio. δ^1H (400 MHz, $CDCl_3$) 7.72 (1 H, d, J = 7.6 Hz, ArH), 7.69 – 7.60 (2 H, m,

ArH), 7.55 (1 H, d, $J = 5.9$ Hz, ArH), 7.47 (2 H, dd, $J = 8.4, 5.7$ Hz, ArH), 7.36 – 7.29 (2 H, m, ArH), 7.28 – 7.16 (2 H, m, ArH), 7.11 (1 H, d, $J = 8.4$ Hz, ArH), 7.02 (1 H, d, $J = 8.4$ Hz, ArH), 6.95 (1 H, dd, $J = 7.1, 2.3$ Hz, ArH), 6.84 (1 H, d, $J = 7.8$ Hz, ArH), 6.56 – 6.45 (2 H, m, ArH), 6.34 (1 H, d, $J = 7.5$ Hz, ArH), 6.26 (1 H, t, $J = 7.7$ Hz, ArH), 3.25 (3 H, s, NCH₃), 3.24 (3 H, s, NCH₃), 3.06 (3 H, s, NCH₃), 3.04 (3 H, s, NCH₃), 2.32 (3 H, s, ArCH₃), 2.17 (3 H, s, ArCH₃), 1.70 (3 H, s, ArCH₃), 1.41 (3 H, s, ArCH₃). $\delta^{13}\text{C}$ (101 MHz, CDCl₃) 162.3 (C=O), 162.3 (C=O), 141.5 (ArC), 141.3 (ArC), 138.48 (ArC), 138.46 (ArC), 138.4 (ArC), 137.9 (ArC), 134.3 (ArC), 133.2 (ArC), 133.11 (ArC), 133.08 (ArC), 131.7 (ArCH), 130.8 (ArCH), 130.7 (ArC), 130.4 (ArC), 130.3 (ArCH), 129.6 (ArCH), 129.2 (ArCH), 129.1 (ArCH), 128.0 (ArCH), 127.4 (ArCH), 127.0 (ArCH), 126.92 (ArCH), 126.88 (ArCH), 126.6 (ArCH), 126.3 (ArCH), 126.0 (ArCH), 125.10 (ArCH), 125.05 (ArCH), 124.0 (ArC), 123.9 (ArC), 123.5 (ArCH), 122.7 (ArCH), 38.4 (NCH₃), 38.1 (NCH₃), 37.1 (NCH₃), 37.0 (NCH₃), 18.50 (CCH₃), 18.48 (CCH₃), 18.2 (CCH₃), 17.6 (CCH₃). IR (film, cm⁻¹) ν_{max} 1652 (C=O), 1347 (C–N). HRMS (ESI⁺) m/z calcd for C₂₁H₂₁N₂OBrNa⁺ [M+Na]⁺ 419.0729; found 419.0732.

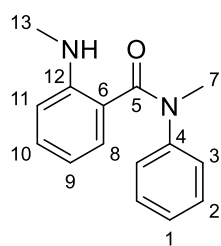
1-(2-Bromo-6-methylphenyl)-3-(2-(tert-butyl)-6-methylphenyl)-1,3-dimethylurea– 2.41o



Following **GP2.1 (Part 1)** 2-bromo-6-methylaniline (1.0 g, 5.3 mmol, 1 eq.), 1-(tert-butyl)-2-isocyanato-3-methylbenzene (1.0 g, 5.7 mmol, 1.1 eq.) in 1,4-dioxane (5.5 mL, 1.0 M) were heated in a microwave to 200 °C for 2 h.

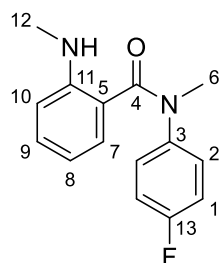
Volatiles were removed *in vacuo* and the crude mixture was used directly in the next step. Following **GP2.1 (Part 2)** the required urea (5.3 mmol, 1 eq.), NaH (0.85 g, 21 mmol, 4.0 eq., 60% in mineral oil), MeI (2.0 mL, 32 mmol, 6.0 eq.) in THF (10.6 mL, 0.5 M) were stirred at rt for 24 h. Purification by flash column chromatography eluting with (5% to 30% EtOAc/Petrol) yielded the *title compound* as a colourless oil (0.79 g, 37%). R_f 0.39 (25% EtOAc/Petrol). Mixture of conformers slowly interconverting giving rise to broad peaks. Peaks of the ¹³C NMR spectrum could not be assigned. $\delta^1\text{H}$ (400 MHz, CDCl₃) 7.66 – 6.62 (6 H, m, ArH), 3.36 – 3.06 (3 H, m, NCH₃), 2.93 – 2.11 (6 H, m, CCH₃ + NCH₃), 1.87 – 1.13 (12 H, m, CCH₃ + C(CH₃)₃). $\delta^{13}\text{C}$ (101 MHz, CDCl₃) 159.1 (C=O), 147.1, 146.8, 143.0, 137.8, 131.44, 131.42, 131.2, 130.8, 130.5, 130.3, 129.9, 129.2, 128.9, 128.6, 128.03, 128.00, 127.0, 126.9, 126.8, 125.6, 40.5, 38.9, 38.4, 38.3, 37.7, 36.9, 36.7, 35.8, 32.9, 32.8, 32.1, 32.0, 29.9, 19.30, 19.26, 19.21, 19.0, 18.1. IR (film, cm⁻¹) ν_{max} 2958, 2924 (C–H), 1644 (C=O), 1453, 1348 (C–N). HRMS (ESI⁺) m/z calcd for C₂₁H₂₈N₂OBr⁺ [M+H]⁺ 403.1380; found: 403.1382.

N-Methyl-2-(methylamino)-*N*-phenylbenzamide - 2.42a



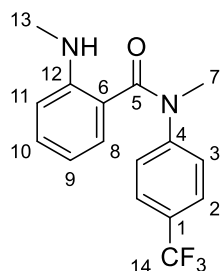
Following **GP2.2** on a 5.5 mmol scale, the *title compound* was obtained as a colourless oil (1.20 g, 91%). R_f 0.31 (25% EtOAc/Petrol). $\delta^1\text{H}$ (400 MHz, CDCl_3) 7.21 (2 H, t, $J = 7.5$ Hz, H-2), 7.14 – 7.05 (2 H, m, H-1 + H-10), 7.04 (2 H, d, $J = 7.5$ Hz, H-3), 6.73 (1 H, dd, $J = 7.6, 1.6$ Hz, H-8), 6.59 (1 H, d, $J = 8.3$ Hz, H-11), 6.26 (1 H, td, $J = 7.6, 1.1$, H-9), 5.76 (1 H, br. s, NH), 3.47 (3 H, s, H-7), 2.85 (3 H, s, H-13). $\delta^{13}\text{C}$ (101 MHz, CDCl_3) 171.7 (C-5), 149.2 (C-12), 145.3 (C-4), 131.0 (C-10), 130.0 (C-8), 129.2 (C-2), 126.4 (C-1), 126.3 (C-3), 119.0 (C-6), 114.9 (C-9), 110.6 (C-11), 38.1 (C-7), 30.3 (C-13). IR (film, cm^{-1}) ν_{max} 3393 (N–H), 1631 (C=O). HRMS (ESI^+) m/z calcd for $\text{C}_{15}\text{H}_{17}\text{N}_2\text{O}^+$ $[\text{M}+\text{H}]^+$ 241.1335; found: 241.1330.

N-(4-Fluorophenyl)-*N*-methyl-2-(methylamino)benzamide – 2.42b



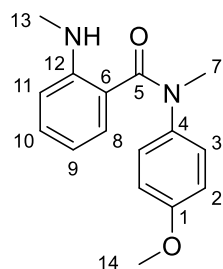
Following **GP2.2** on a 1.5 mmol scale, the *title compound* was obtained as a yellow solid (320 mg, 84%). R_f 0.30 (25% EtOAc/Petrol). **m.p.:** 81 – 82 °C. $\delta^1\text{H}$ (400 MHz, CDCl_3) 7.09 (1 H, ddd, $J = 8.3, 7.5, 1.6$ Hz, H-9), 7.06 – 6.96 (2 H, m, H-1), 6.93 – 6.86 (2 H, m, H-2), 6.71 (1 H, dd, $J = 7.5, 1.6$ Hz, H-7), 6.59 (1 H, dd, $J = 8.3, 1.1$, H-10), 6.30 (1 H, td, $J = 7.5, 1.1$ Hz, H-8), 5.68 (1 H, br. s, NH), 3.44 (3 H, s, H-6), 2.84 (3 H, s, H-12). $\delta^{13}\text{C}$ (101 MHz, CDCl_3) 171.7 (C-4), 160.8 (d, $J = 246$ Hz, C-13), 149.1 (C-11), 141.3 (d, $J = 3.2$ Hz, C-1), 131.1 (C-9), 129.8 (C-10), 127.9 (d, $J = 8.4$ Hz, C-2), 118.8 (C-5), 116.1 (d, $J = 23$ Hz, C-1), 115.1 (C-8), 110.7 (C-10), 38.3 (d, $J = 2.7$ Hz, C-6), 30.3 (C-12). $\delta^{19}\text{F}$ NMR (376 MHz, CDCl_3) -116.44 (dq, $J = 13.6, 5.4$ Hz, C–F). IR (film, cm^{-1}) ν_{max} 3388 (N–H), 1633 (C=O), 1507. HRMS (ESI^+) $\text{C}_{15}\text{H}_{15}\text{FN}_2\text{O}^+$ 281.1061; found: 281.1050.

N-Methyl-2-(methylamino)-*N*-(4-(trifluoromethyl)phenyl)benzamide – 2.42c



Following **GP2.2** on a 0.3 mmol scale, the *title compound* was obtained as a yellow solid (71 mg, 77%). R_f 0.34 (25% EtOAc/Petrol). **m.p.:** 76 – 77 °C. $\delta^1\text{H}$ (400 MHz, CDCl_3) 7.46 (2 H, dt, $J = 8.4, 0.7$ Hz, H-2), 7.18 – 7.08 (3 H, m, H-3 + H-10), 6.71 (1 H, dd, $J = 7.6, 1.6$ Hz, H-8), 6.61 (1 H, br. d, $J = 8.4$ Hz, H-11), 6.29 (1 H, td, $J = 7.6, 1.1$ Hz, H-9), 5.81 (1 H, br. s, NH), 2.48 (3 H, s, H-7), 2.85 (3 H, s, H-13). $\delta^{13}\text{C}$ (101 MHz, CDCl_3) 171.8 (C-5), 149.4 (C-12), 148.5 (q, $J = 1.5$ Hz, C-4), 131.6 (C-10), 130.0 (C-8), 128.0 (q, $J = 33$ Hz, C-1), 126.3 (q, $J = 3.8$ Hz, C-2), 126.2 (C-3), 123.9 (q, $J = 272$ Hz, C-14), 118.1 (C-6), 115.1 (C-9), 110.8 (C-11), 37.9 (C-7), 30.2 (C-13). $\delta^{19}\text{F}$ NMR (376 MHz, CDCl_3) -62.5 (s, CF_3). IR (film, cm^{-1}) ν_{max} 3404 (N–H), 1639 (C=O), 1325 (C–F). HRMS (ESI^+) $\text{C}_{16}\text{H}_{15}\text{F}_3\text{N}_2\text{O}^+$ 331.1029; found: 331.1028.

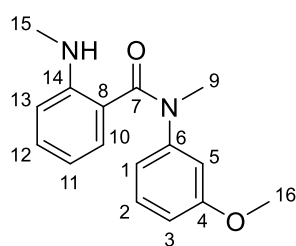
N-Methyl-2-(methylamino)-*N*-(4-(methoxy)phenyl)benzamide – 2.42e



Following **GP2.2** on a 1.2 mmol scale, the *title compound* was obtained as a yellow oil (275 mg, 88%). *R_f* 0.61 (40% EtOAc/Petrol). **$\delta^1\text{H}$ (400 MHz, CDCl_3)** 7.07 (1 H, ddd, $J = 8.3, 7.3, 1.6$ Hz, H-10), 6.96 (2 H, m, H-3), 6.74 (3 H, m, H-2 + H-8), 6.58 (1 H, d, $J = 8.3$ Hz, H-11), 6.29 (1 H, td, $J = 7.5, 1.1$ Hz, H-9), 5.69 (1 H, br. s, NH), 3.73 (3 H, s, H-14), 3.43 (3 H, s, H-13), 2.84 (3 H, s, H-13).

$\delta^{13}\text{C}$ (101 MHz, CDCl_3) 171.6 (C-5), 157.9 (C-1), 149.0 (C-12), 138.2 (C-4), 130.8 (C-10), 129.8 (C-8), 127.4 (C-3), 119.2 (C-6), 115.0 (C-9), 114.3 (C-2), 110.6 (C-11), 55.5 (d, $J = 2.6$ Hz, C-14), 38.4 (C-7), 30.3 (C-13). **IR (film, cm^{-1})** ν_{max} 3390 (N–H), 1627 (C=O), 1507, 1245 (C–O). **HRMS (ESI⁺)** $\text{C}_{16}\text{H}_{19}\text{N}_2\text{O}_2^+$ 271.1441; found: 271.1430.

N-(3-Methoxyphenyl)-*N*-methyl-2-(methylamino)benzamide – 2.42g

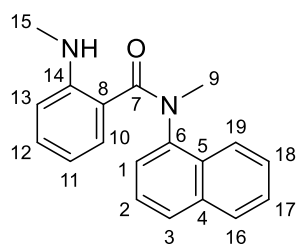


Following **GP2.2** on a 1.5 mmol scale, the *title compound* was obtained as a colourless oil (0.25 g, 62%). *R_f* 0.22 (25% EtOAc/Petrol).

$\delta^1\text{H}$ (400 MHz, CDCl_3) 7.10 (1 H, t, $J = 8.1$ Hz, H-2), 7.13 – 7.04 (1 H, m, H-12), 6.77 (1 H, dd, $J = 7.7, 1.6$ Hz, H-10), 6.68 – 6.64 (1 H, m, H-1), 6.64 – 6.61 (1 H, m, H-13), 6.60 – 6.56 (2 H, m, H-3 + H-5),

6.29 (1 H, td, $J = 7.5, 1.0$ Hz, H-11), 5.71 (1 H, br. s, NH), 3.66 (3 H, s, H-16), 3.46 (3 H, s, H-9), 2.84 (3 H, s, H-15). **$\delta^{13}\text{C}$ (101 MHz, CDCl_3)** 171.7 (C-7), 160.1 (C-4), 149.1 (C-14), 146.4 (C-6), 131.0 (C-12), 129.8 (C-2), 129.7 (C-10), 119.2 (C-8), 118.5 (C-13), 115.1 (C-11), 112.11 (C-1, C-3 or C-5), 112.05 (C-1 Hz, C-3 or C-5), 110.5 (C-1 Hz, C-3 or C-5), 55.4 (C-16), 38.0 (C-9), 30.3 (C-15). **IR (film, cm^{-1})** ν_{max} 3395 (N–H), 2921 (C–H), 1632 (C=O), 1582, 1042 (C–O). **HRMS (ESI⁺)** m/z calcd for $\text{C}_{16}\text{H}_{19}\text{N}_2\text{O}_2^+$ [M+H]⁺ 271.1441; found: 271.1445.

N-Methyl-2-(methylamino)-*N*-(naphthalen-1-yl)benzamide – 2.42j

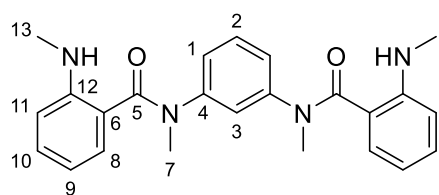


Following **GP2.2** on a 0.3 mmol scale, the *title compound* was obtained as a white solid (57 mg, 65%). *R_f* 0.38 (25% EtOAc/Petrol). **m.p.:** 166 – 167 °C.

$\delta^1\text{H}$ (400 MHz, CDCl_3) 8.01 (1 H, d, $J = 8.5$ Hz, H-19), 7.85 (1 H, d, $J = 8.2$ Hz, H-16), 7.69 (1 H, d, $J = 8.3$ Hz, H-3), 7.60 (1 H, ddd, $J = 8.4, 6.8, 1.3$ Hz, H-18), 7.52 (1 H, ddd, $J = 8.1, 6.8, 1.2$ Hz, H-17), 7.26 (1 H, br. s, H-2),

7.12 (1 H, br. s, H-1), 6.97 (1 H, br. s, H-12), 6.67 (1 H, s, H-10), 6.52 (1 H, d, $J = 8.3$ Hz, H-13), 5.99 (1 H, br. s, H-11), 5.95 (1 H, br. s, NH), 3.51 (3 H, s, H-9), 2.85 (3 H, s, H-15). **$\delta^{13}\text{C}$ (101 MHz, CDCl_3)** 172.8 (C-7), 148.9 (C-14), 141.7 (C-6), 134.6 (C-4), 131.1 (C-12), 129.8 (C-5), 128.8 (C-16), 128.3 (C-10), 127.9 (C-3), 127.2 (C-18), 126.4 (C-17), 125.7 (C-2), 125.5 (C-1), 122.8 (C-19), 118.8 (C-8), 114.7 (C-11), 110.6 (C-13), 38.4 (C-9), 30.2 (C-15). **IR (film, cm^{-1})** ν_{max} 3392 (N–H), 1632 (C=O), 1513. **HRMS (ESI⁺)** $\text{C}_{19}\text{H}_{19}\text{N}_2\text{O}^+$ 291.1492; found: 291.1499.

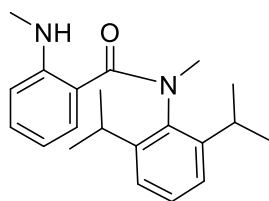
N,N'-(1,3-Phenylene)bis(*N*-methyl-2-(methylamino)benzamide) - 2.42k



Following **GP2.2** on a 0.45 mmol scale, the *title compound* was obtained as a white solid (0.15 g, 85%). *R_f* 0.37 (50% EtOAc/Petrol). **m.p.:** 70 – 72 °C. Mixture of conformers in a 1:0.15 ratio. **$\delta^1\text{H}$** (400 MHz, CDCl_3)

7.11 (2 $\text{H}^{\text{maj} + \text{min}}$, ddd, $J = 8.2, 7.3, 1.6$ Hz, H-10), 6.99 (1 $\text{H}^{\text{maj} + \text{min}}$, t, $J = 7.6$ Hz, H-2), 6.86 (3 H^{min} , m), 6.74 (1 H^{maj} , t, $J = 1.8$ Hz, H-3), 6.72 (2 H^{maj} , dd, $J = 7.9, 2.0$ Hz, H-1), 6.60 (2 H^{maj} , dd, $J = 8.3, 1.0$ Hz, H-11), 6.53 (2 H^{maj} , dd, $J = 7.7, 1.6$ Hz, H-8), 6.30 (2 H^{maj} , td, $J = 7.5, 1.1$ Hz, H-9), 6.19 (2 H^{min} , dddd, $J = 13.9, 7.8, 2.2, 0.9$), 6.01 (1 H^{min} , t, $J = 2.2$), 5.67 (2 H^{maj} , br. s, NH), 3.30 (6 H^{maj} , s, H-7), 3.17 (6 H^{min} , d, $J = 3.5$), 2.84 (6 H^{maj} , br. s, H-13), 2.69 (6 H^{min} , s). **$\delta^{13}\text{C}$** (101 MHz, CDCl_3) 171.4 (C-5), 149.0 (C-12), 145.7 (C-4), 131.0 (C-10), 129.7 (C-8), 129.3 (C-2), 123.7 (C-1), 123.6 (C-3), 118.6 (C-6), 115.0 (C-9), 110.6 (C-11), 37.5 (C-7), 30.1 (C-13). **IR (film, cm^{-1})** ν_{max} 3390 (N–H), 1633 (C=O), 1579. **HRMS (ESI⁺)** m/z calcd for $\text{C}_{24}\text{H}_{26}\text{N}_2\text{O}_2\text{Na}^+$ [$\text{M}+\text{Na}$]⁺ 425.1948; found: 425.1949.

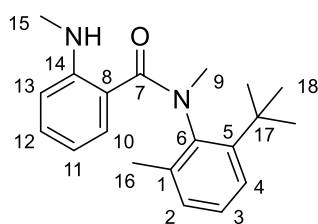
N-(2,6-Diisopropylphenyl)-*N*-methyl-2-(methylamino)benzamide – 2.42l



Following **GP2.2** on a 1.2 mmol scale, the *title compound* was obtained as a white solid (0.33 g, 83%). *R_f* 0.64 (25% EtOAc/Petrol). **m.p.:** 111 – 112 °C. Mixture of conformers in a 1:0.33 ratio. **$\delta^1\text{H}$** (400 MHz, CDCl_3)

7.39 – 7.28 (2 H^{min} , m, ArCH), 7.24 (1 H^{min} , s, ArCH), 7.20 (1 H^{maj} , t, $J = 7.7$ Hz, ArCH), 7.05 (2 H^{maj} , d, $J = 7.6$ Hz, ArCH), 7.03 (1 H^{maj} , td, $J = 7.8, 1.2$ Hz, ArCH), 6.74 (2 H^{min} , dd, $J = 8.2, 5.9$ Hz, ArCH), 6.62 (1 H^{maj} , dd, $J = 7.8, 1.6$ Hz, ArCH), 6.53 (1 H^{maj} , d, $J = 8.4$ Hz, ArCH), 6.31 (1 H^{maj} , br. s, NH), 6.12 (1 H^{maj} , t, $J = 7.3$ Hz, ArCH), 5.38 (1 H^{min} , br. s, NH), 3.31 (3 H^{maj} , s, NCH_3), 3.22 (3 H^{min} , s, NCH_3), 3.08 (2 H^{min} , hept, $J = 5.8$ Hz, $\text{CH}(\text{CH}_3)_2$), 3.01 (2 H^{maj} , hept, $J = 5.8$ Hz, $\text{CH}(\text{CH}_3)_2$), 2.84 (3 H^{min} , s, NHCH_3), 2.83 (3 H^{maj} , s, NHCH_3), 1.29 ($\text{CH}_\text{A}\text{H}_\text{B}$, 6 H^{min} , d, $J = 5.8$ Hz, $\text{CH}(\text{CH}_3)_2$), 1.27 ($\text{CH}_\text{A}\text{H}_\text{B}$, 6 H^{min} , d, $J = 5.8$ Hz, $\text{CH}(\text{CH}_3)_2$), 1.19 ($\text{CH}_\text{A}\text{H}_\text{B}$, 6 H^{maj} , d, $J = 5.8$ Hz, $\text{CH}(\text{CH}_3)_2$), 1.00 ($\text{CH}_\text{A}\text{H}_\text{B}$, 6 H^{maj} , d, $J = 5.8$ Hz, $\text{CH}(\text{CH}_3)_2$). **$\delta^{13}\text{C}$** (101 MHz, CDCl_3) 171.9 (C=O), 171.5 (C=O), 149.4 (ArC^{maj}), 148.7 (ArC^{min}), 145.7 (ArC^{maj}), 145.5 (ArC^{min}), 140.3 (ArC^{maj}), 137.9 (ArC^{min}), 131.3 (ArCH^{min}), 131.2 (ArCH^{maj}), 129.3 (ArCH^{maj}), 128.7 (ArCH^{min}), 128.3 (ArCH^{maj}), 127.7 (ArCH^{min}), 124.4 (ArCH^{maj}), 119.5 (ArC^{min}), 117.0 (ArCH^{maj}), 115.6 (ArCH^{min}), 113.6 (ArCH^{maj}), 111.3 (ArCH^{min}), 110.5 (ArCH^{maj}), 41.6 ($\text{NCH}_3^{\text{min}}$), 38.9 ($\text{NCH}_3^{\text{maj}}$), 30.5 ($\text{NHCH}_3^{\text{min}}$), 30.1 ($\text{NHCH}_3^{\text{maj}}$), 28.8 ($\text{CH}(\text{CH}_3)_2^{\text{min}}$), 28.4 ($\text{CH}(\text{CH}_3)_2^{\text{maj}}$), 26.0 ($\text{CH}(\text{CH}_3)_2^{\text{maj}}$), 24.5 ($\text{CH}(\text{CH}_3)_2^{\text{min}}$), 24.3 ($\text{CH}(\text{CH}_3)_2^{\text{min}}$), 22.9 ($\text{CH}(\text{CH}_3)_2^{\text{maj}}$). **IR (film, cm^{-1})** ν_{max} 3394 (N–H), 2963, 2927 (C–H), 1628 (C=O), 1516, 1358. **HRMS (ESI⁺)** m/z calcd for $\text{C}_{21}\text{H}_{29}\text{N}_2\text{O}^+$ [$\text{M}+\text{H}$]⁺ 325.2274; found: 325.2268.

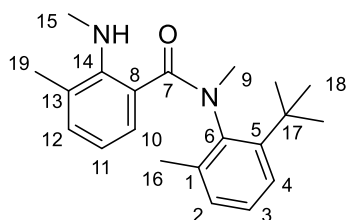
N-(2-(*tert*-Butyl)-6-methylphenyl)-*N*-methyl-2-(methylamino)benzamide - 2.42m



Following **GP2.2** on a 1.3 mmol scale, the *title compound* was obtained as a white solid (195 mg, 47%). *R_f* 0.52 and 0.63 (two conformers) (25% EtOAc/Petrol). *m.p.*: 129 – 130 °C. Mixture of conformers in a 1:0.07 ratio. Only major peaks were assigned in the ¹H NMR spectrum.

¹H (400 MHz, CDCl₃) 7.40 (1 H^{min}, t, *J* = 4.8), 7.35 (1 H^{min}, dd, *J* = 7.7, 1.4), 7.31 (1 H^{maj} + 1 H^{min}, d, *J* = 8.0 Hz, H-4), 7.20 (2 H^{min}, d, *J* = 5.0), 7.13 (1 H^{maj}, t, *J* = 7.7 Hz, H-12), 7.08 – 7.04 (1 H^{maj}, m, H-3), 7.02 (1 H^{maj}, d, *J* = 7.2 Hz, H-2), 6.83 (1 H^{maj}, br. s, NH), 6.75 – 6.67 (2 H^{min}, m), 6.60 – 6.53 (2 H^{maj}, m, H-13 + H-10), 6.09 (1 H^{maj}, t, *J* = 7.6 Hz, H-11), 3.29 (3 H^{maj}, s, H-9), 3.27 (3 H^{min}, s), 2.84 (3 H^{maj}, s, H-15), 2.81 (3 H^{min}, s), 2.26 (3 H^{min}, s), 2.18 (3 H^{maj}, s, H-16), 1.48 (9 H^{min}, s), 1.27 (9 H^{maj}, s, H-18). **¹³C (101 MHz, CDCl₃)** 172.5 (C-7^{min}), 170.2 (C-7^{maj}), 150.3 (C-14^{maj}), 149.6 (C-14^{min}), 146.9 (C-5^{min}), 146.1 (C-5^{maj}), 141.3 (C-6^{maj}), 137.2 (C-1^{maj}), 136.1 (C-1^{min}), 131.6 (C-3^{min}), 131.3 (C-3^{maj}), 130.0 (C-10^{min}), 129.11 (C-10^{maj}), 129.05 (C-2^{maj}), 128.5 (C-4^{maj}), 128.0 (C-4^{min}), 127.8 (C-12^{maj}), 126.6 (C-12^{min}), 116.7 (C-8^{maj}), 115.2 (C-8^{min}), 113.4 (C-11^{maj}), 111.4 (C-13^{min}), 110.8 (C-13^{maj}), 42.3 (C-9^{min}), 39.8 (C-9^{maj}), 36.6 (C-17^{maj}), 32.4 (C-18^{maj}), 32.2 (C-18^{min}), 30.3 (C-15^{min}), 30.1 (C-15^{maj}), 18.7 (C-16^{maj}). **IR (film, cm⁻¹)** *v*_{max} 3383 (N–H), 2958 (C–H), 1627 (C=O), 1516, 1359. **HRMS (ESI⁺)** *m/z* calcd for C₂₀H₂₇N₂O⁺ [M+H]⁺ 311.2118; found: 311.2117.

N-(2-(*tert*-Butyl)-6-methylphenyl)-*N*,3-dimethyl-2-(methylamino)benzamide - 2.42n

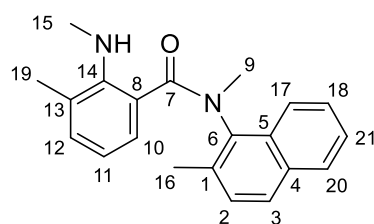


Following **GP2.2** 1-(2-bromo-6-methylphenyl)-3-(2-(*tert*-butyl)-6-methylphenyl)-1,3-dimethylurea **2.41n** (790 mg, 1.96 mmol, 1 eq.), *sec*-BuLi (1.80 mL, 2.16 mmol, 1.1 eq., 1.20 M in cyclohexane, added over 30 min), in THF (9.8 mL, 0.2 M) were stirred at –78 °C for 24 h. Purification by flash column chromatography eluting with (2% to 30%

EtOAc/Petrol) yielded a residue which was dissolved in Et₂O (10 mL). HCl (2.0 mL, 2.0 mmol, 1.0 M in Et₂O) was added and the resultant off-white precipitate filtered. The solid was Partitioned between CH₂Cl₂ and a saturated solution of aqueous NaHCO₃ and extracted with CH₂Cl₂. The combined organic phases were washed with brine, dried over MgSO₄, filtered and concentrated *in vacuo* to yield the *title compound* as a yellow oil (191 mg, 30%). *R_f* 0.33 (30% EtOAc/Petrol). Mixture of conformers in a 1.0:0.15 ratio. Only major peaks were assigned in the ¹³C spectrum. **¹H (400 MHz, CDCl₃)** 7.41 (1 H^{maj}, m, H-3), 7.30 (2 H^{min}, dd, *J* = 8.3, 1.4 Hz), 7.24 (1 H^{maj}, dd, *J* = 7.5, 1.4 Hz, H-10), 7.21 (3 H^{maj}, m, H-2 + H-4 + H-12), 7.14 (2 H^{min}, t, *J* = 7.7 Hz), 7.06 – 6.97 (2 H^{min}, m), 6.94 (1 H^{maj} + 1 H^{min}, t, *J* = 7.5 Hz, H-11), 6.48 (1 H^{min}, dd, *J* = 7.8, 1.6 Hz), 6.28 (1 H^{min}, t, *J* = 7.7 Hz), 4.69 (1 H^{maj}, br. s, NH), 3.32 (3 H^{min}, s, H-9), 3.18 (3 H^{maj}, s, H-9), 2.85 (3 H^{min}, s, H-15), 2.83 (3 H^{maj}, s,

H-15), 2.37 (3 H^{maj}, s, H-19), 2.33 (3 H^{maj}, s, H-16), 2.29 (3 H^{min}, s, H-19), 2.21 (3 H^{min}, s, H-16), 1.50 (9 H^{maj}, s, H-18), 1.28 (9 H^{min}, s, H-18). **$\delta^{13}\text{C}$ (101 MHz, CDCl_3)** 172.0 (C-7^{maj}), 170.1 (C^{min}), 148.1 (C-14^{maj}), 146.9 (C-5^{maj}), 146.0 (C^{min}), 141.10 (C-6^{maj}), 141.05 (C^{min}), 136.9 (C^{min}), 136.3 (C-1^{maj}), 133.7 (C^{min}), 133.0 (C-12^{maj}), 131.6 (C-13^{maj}), 129.9 (C-2^{maj}), 129.0 (C^{min}), 128.5 (C^{min}), 127.9 (C-4^{maj}), 127.84 (C^{min}), 127.77 (C-8^{maj}), 126.75 (C-3^{maj}), 126.3 (C^{min}), 125.1 (C^{min}), 125.0 (C-10^{maj}), 123.6 (C^{min}), 121.0 (C-11^{maj}), 117.9 (C^{min}), 42.0 (C-9^{maj}), 39.9 (C^{min}), 36.6 (C^{min}), 36.2 (C-17^{maj}), 36.1 (C-15^{maj}), 35.2 (C^{min}), 32.5 (C^{min}), 32.2 (C-18^{maj}), 20.4 (C^{min}), 19.1 (C-19^{maj}), 18.8 (C^{min}), 18.6 (C-16^{maj}). **IR (film, cm^{-1})** ν_{max} 3367 (N–H), 2958 (C–H), 1644 (C=O), 1449, 1352. **HRMS (ESI⁺)** m/z calcd for $\text{C}_{21}\text{H}_{29}\text{N}_2\text{O}^+$ [M+H]⁺ 325.2274; found: 325.2277.

N,3-Dimethyl-2-(methylamino)-N-(2-methylnaphthalen-1-yl)benzamide 2.42o



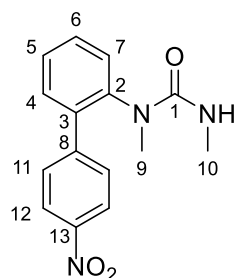
Following **GP2.2** 1-(2-bromo-6-methylphenyl)-1,3-dimethyl-3-(2-methylnaphthalen-1-yl)urea **2.41o** (646 mg, 1.62 mmol, 1 eq.), *s*-BuLi (1.37 mL, 1.78 mmol, 1.1 eq., 1.30 M in cyclohexane) in THF (8.1 mL, 0.2 M) were stirred at -78°C for 24 h. The compound was

purified by flash column chromatography eluting with (10% to 70% Et_2O /Petrol). The residue was dissolved in Et_2O and HCl 2 M in Et_2O was added. The white precipitate was filtered, dissolved in CH_2Cl_2 , and the organic phase was washed with a saturated solution of aqueous NaHCO_3 . Evaporation of the volatiles yielded the *title compound* as a yellow oil (161 mg, 32%). *R_f* 0.20 (30% EtOAc /Petrol). Mixture of conformers A:B:C in a 1.0:0.4:0.1 ratio. Only major peaks were assigned in the ^1H and ^{13}C spectra.

$\delta^1\text{H}$ (400 MHz, CDCl_3) 8.00 (1 H^C, dd, J = 8.4, 1.0 Hz), 7.96 (1 H^B, ddd, J = 8.4, 1.9, 1.0 Hz), 7.93 (1 H^A, dd, J = 8.5, 1.0 Hz, H-17), 7.87 (1 H^B, dt, J = 8.1, 0.7 Hz), 7.82 – 7.79 (1 H^C, m), 7.78 (1 H^A, dd, J = 8.2, 0.6 Hz, H-20), 7.78 (1 H^C, d, J = 8.2 Hz), 7.61 (1 H^A, d, J = 8.4 Hz, H-3), 7.61 – 7.54 (1 H^A + 2 H^B, m, H-18^A), 7.50 – 7.42 (1 H^A + 2 H^B + 2 H^C, m, H-21^A), 7.37 (1 H^B, ddd, J = 7.5, 1.6, 0.6 Hz), 7.22 (1 H^B, ddd, J = 7.5, 1.6, 0.8 Hz), 7.17 (1 H^A, d, J = 8.5 Hz, H-2), 7.15 – 7.12 (1 H^C, m), 6.99 (1 H^B, t, J = 7.5 Hz), 6.80 (1 H^A, ddd, J = 7.5, 1.7, 0.9 Hz, H-10), 6.75 (1 H^C, ddd, J = 7.3, 1.6, 0.8 Hz), 6.57 (1 H^A, ddd, J = 7.8, 1.6, 0.6 Hz, H-12), 6.48 (1 H^C, ddd, J = 7.8, 1.4, 0.5 Hz), 6.11 (1 H^A, t, J = 7.6 Hz, H-11), 5.91 (1 H^C, t, J = 7.6 Hz), 5.08 (1 H^A, s), 4.97 (1 H^B, s), 3.46 (3 H^A, s, H-9), 3.45 (3 H^C, s), 3.25 (3 H^B, s), 3.00 (3 H^B, s), 2.91 (3 H^A, s, H-16), 2.54 (3 H^B, s), 2.37 (3 H^B, s), 2.30 (3 H^A, s, H-16), 2.25 (3 H^C, s), 2.23 (3 H^A, s, H-19), 2.06 (3 H^C, s). **$\delta^{13}\text{C}$ (101 MHz, CDCl_3)** 172.7 (C^C), 172.4 (C-7^A), 171.4 (C^B), 149.1 (C-14^A), 146.5 (C^B), 145.3 (C^C), 138.7 (C^C), 138.6 (C-6^A), 136.8 (C^B), 133.5 (C^B), 132.48 (C-10^A), 133.4 (C^C), 133.03 (C-4^A), 132.99 (C^B), 132.6 (C-1^A), 132.1 (C^B), 131.8 (C^C), 130.6 (C^C), 130.5 (C-5^A), 129.9 (C^B), 129.6 (C^B), 129.3 (C-13^A), 129.1 (C^B), 128.9 (C^C), 128.8 (C-2^A), 128.54 (C^B), 128.49 (C-20^A), 128.47 (C^C), 127.9 (C^B), 127.7 (C-3^A), 127.5 (C^C), 127.43 (C^C), 127.36 (C-18^A), 127.3 (C^C), 126.9 (C^B), 126.0 (C^C), 125.7 (C^B),

125.53 (C-12^A), 125.49 (C-21^A), 125.4 (C^C), 125.3 (C^B), 124.2 (C-8^A), 122.7 (C^C), 122.6 (C-17^A), 122.0 (C^B), 120.8 (C^B), 118.2 (C-11^A), 117.8 (C^C), 115.2 (C^B), 39.4 (C^B), 37.0 (C-9^A), 36.8 (C^C), 36.1 (C^B), 35.4 (C-16^A), 19.8 (C-19^A), 18.4 (C^B), 18.2 (C-15^A), 18.01 (C^C), 17.96 (C^B), 17.5 (C^C). IR (film, cm⁻¹) ν_{\max} 2925 (C-H), 1652 (C=O), 1596, 1494, 1351. HRMS (ESI⁺) m/z calcd for C₂₁H₂₃N₂O⁺ [M+H]⁺ 319.1805; found: 319.1801.

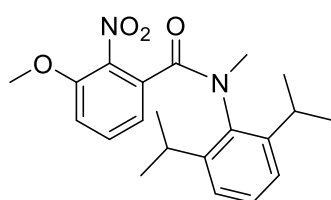
1,3-dimethyl-1-(4'-nitro-[1,1'-biphenyl]-2-yl)urea – 2.43



Following **GP2.2** on a 1.4 mmol scale, the *title compound* was obtained as a yellow oil (166 mg, 39%). R_f 0.14 (80% EtOAc/Petrol). $\delta^1\text{H}$ (400 MHz, CDCl₃) 8.27 (2 H, d, J = 7.7 Hz, H-12), 7.50 (2 H, d, J = 9.0 Hz, H-11), 7.46 (3 H, m, H-4 + H-5 + H-6), 7.35 (1 H, dt, J = 7.6, 1.0 Hz, H-7), 4.28 (1 H, q, J = 5.0 Hz, NH), 2.91 (3 H, s, H-9), 2.70 (3 H, d, J = 4.7 Hz, H-10). $\delta^{13}\text{C}$ (101 MHz, CDCl₃) 157.7 (C-1), 147.4 (C-13), 145.5 (C-8), 140.7 (C-2), 138.5 (C-3), 131.5 (C-6),

130.65 (C-5), 129.55 (C-4), 129.4 (C-11), 128.7 (C-7), 124.0 (C-12), 36.8 (C-9), 27.6 (C-10). IR (film, cm⁻¹) ν_{\max} 3446, 3346 (N-H), 1651 (C=O), 1515 (N=O), 1349 (C-N). HRMS (ESI⁺) m/z calcd for C₁₅H₁₅N₃O₃Na⁺ [M+Na]⁺ 308.1011; found 308.0971.

N-(2,6-diisopropylphenyl)-3-methoxy-N-methyl-2-nitrobenzamide – 2.45

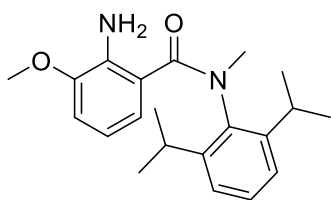


To a solution of 3-methoxy-2-nitrobenzoic acid (2.0 g, 10.1 mmol, 1 eq.) in toluene (10 mL, 1 M) under nitrogen was added thionyl chloride (2.2 mL, 30.3 mmol, 3.0 eq.) before heating to reflux for 2 h. The reaction mixture was concentrated *in vacuo*, before adding toluene (20 mL) to

azeotropically remove traces of thionyl chloride. The resulting residue was dissolved in MeCN (20 mL, 0.5 M) and, Et₃N (2.3 mL, 16.2 mmol, 1.6 eq.) followed by *N*-methyl-2,6-diisopropylaniline^[3] (2.1 g, 11.2 mmol, 1.1 eq.) were added at 0 °C before warming to rt and stirring for 16 h. The reaction mixture was quenched with sat. NH₄Cl (aq.) and extracted with EtOAc, dried over MgSO₄, filtered and concentrated *in vacuo*. Purification by flash column chromatography eluting with (5% to 60% EtOAc/Petrol) followed by trituration in Et₂O yielded the *title compound* (2.6 g, 71%) as a white solid. R_f 0.14 & 0.22 (30% EtOAc/Petrol). **m.p.:** 152 – 154 °C. Mixture of conformers in a 1.0:0.4 ratio $\delta^1\text{H}$ (400 MHz, CDCl₃) 7.56 (1 H^{maj}, dd, J = 8.5, 7.6 Hz, ArCH), 7.35 (1 H^{maj}, dd, J = 8.4, 7.0 Hz, ArCH), 7.32 – 7.28 (1 H^{min}, m, ArCH), 7.25 – 7.22 (2 H^{maj}, d, J = 7.3 Hz, ArCH), 7.15 (1 H^{maj}, dd, J = 8.7, 1.1 Hz, ArCH), 7.13 (2 H^{min}, d, J = 7.8 Hz, ArCH), 7.08 (1 H^{maj}, dd, J = 7.6, 1.1 Hz, ArCH), 6.98 – 6.89 (2 H^{min}, m, ArCH), 6.30 (1 H^{min}, dd, J = 5.9, 2.1 Hz, ArCH), 3.94 (3 H^{maj}, s, OCH₃), 3.83 (3 H^{min}, s, OCH₃), 3.33 (3 H^{min}, s, CH₃), 3.23 (2 H^{min}, hept, J = 5.9 Hz, CH(CH₃)₂), 3.17 (3 H^{maj}, s, CH₃), 3.10 (2 H^{maj}, hept, J = 5.9 Hz, CH(CH₃)₂), 1.30 (CH_AH_B, 6 H^{maj}, d, J = 5.9 Hz, CH(CH₃)₂), 1.25 (CH_AH_B, 6 H^{maj}, d, J = 5.8 Hz, CH(CH₃)₂), 1.21 (CH_AH_B, 6 H^{min}, d, J = 5.8 Hz, CH(CH₃)₂),

1.02 (CH_AH_B, 6 H^{min}, d, *J* = 5.8 Hz, CH(CH₃)₂). **δ¹³C (101 MHz, CDCl₃)** 166.4 (C^{maj}), 165.0 (C^{min}), 152.1 (C^{maj}), 151.5 (C^{min}), 146.3 (C^{min}), 146.1 (C^{maj}), 138.8 (C^{min}), 138.6 (C^{min}), 136.9 (C^{maj}), 133.0 (C^{maj}), 132.5 (CH^{maj}), 129.4 (CH^{min}), 129.3 (CH^{min}), 129.0 (CH^{maj}), 124.9 (CH^{min}), 124.5 (CH^{maj}), 120.2 (CH^{min}), 118.6 (CH^{maj}), 114.4 (CH^{min}), 114.0 (CH^{maj}), 56.96 (CH₃^{maj}), 56.94 (CH₃^{min}), 40.9 (CH₃^{maj}), 39.5 (CH₃^{min}), 28.7 (CH^{maj}), 28.2 (CH^{min}), (CH₃^{min}), 24.7 (CH₃^{maj}), 24.3 (CH₃^{maj}), 23.3 (CH₃^{min}). **IR (film, cm⁻¹)** ν_{max} 2966 (C–H), 1643 (C=O), 1537 (N=O), 1457, 1363 (C–N), 1285; **HRMS (MALDI⁺)** C₂₁H₂₆N₂O₄Na⁺ [M+Na]⁺ 393.1785; found: 393.1778.

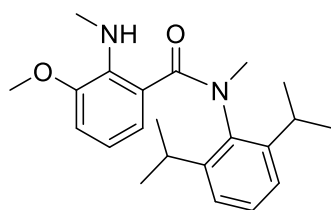
2-amino-N-(2,6-diisopropylphenyl)-3-methoxy-N-methylbenzamide



Pd/C (10 wt. % loading, 0.16 g, 1 mol% Pd) was suspended in a solution of *N*-(2,6-diisopropylphenyl)-3-methoxy-*N*-methyl-2-nitrobenzamide **2.45** (1.6 g, 4.7 mmol, 1 eq.) in EtOH (19 mL, 0.25 M) under nitrogen. Nitrogen was bubbled through the solution for 15 mins. The contents of the flask

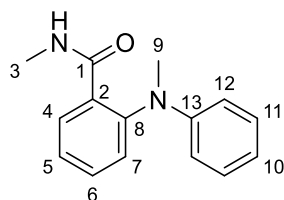
were placed under a hydrogen atmosphere using a two-way three-necked tap with a balloon of hydrogen attached. The solution was saturated with hydrogen three times using a vacuum/hydrogen cycle. The reaction was stirred under a hydrogen atmosphere for 16 h. The contents of the flask were placed under a nitrogen atmosphere and the hydrogen balloon removed. The crude reaction solution was filtered through a pad of Celite and washed with MeOH and was concentrated *in vacuo*. Purification by flash column chromatography eluting with (5% to 35% EtOAc/Petrol) to give the *title compound* (1.45 g, 99%) as a white solid. **R_f** 0.29 (20% EtOAc/Petrol). **m.p.:** 126 – 127 °C. Mixture of conformers in a 1.0:0.5 ratio. **δ¹H (400 MHz, CDCl₃)** 7.37 (1 H^{min}, dd, *J* = 8.4, 7.0 Hz, ArCH), 7.27 (2 H^{min}, d, *J* = 8.0 Hz, ArCH), 7.23 (1 H^{maj}, dd, *J* = 8.2, 7.3 Hz, ArCH), 7.09 (2 H^{maj}, d, *J* = 7.7 Hz, ArCH), 6.99 (1 H^{min}, dd, *J* = 7.6, 1.4 Hz, ArCH), 6.85 (1 H^{min}, dd, *J* = 8.1, 1.4 Hz, ArCH), 6.78 (1 H^{min}, t, *J* = 7.8 Hz, ArCH), 6.58 (1 H^{maj}, dd, *J* = 7.9, 1.3 Hz, ArCH), 6.26 (1 H^{maj}, dd, *J* = 8.1, 1.3 Hz, ArCH), 6.14 (1 H^{maj}, t, *J* = 8.0 Hz, ArCH), 5.25 (2 H^{maj}, s, NH₂), 4.65 (1 H^{min}, s, NH₂), 3.90 (3 H^{min}, s, OCH₃), 3.79 (3 H^{maj}, s, OCH₃), 3.35 (3 H^{maj}, s, CH₃), 3.24 (3 H^{min}, s, CH₃), 3.13 (2 H^{min}, hept, *J* = 5.9 Hz, CH(CH₃)₂), 3.05 (2 H^{maj}, hept, *J* = 5.8 Hz, CH(CH₃)₂), 1.32 (CH_AH_B, 6 H^{min}, d, *J* = 2.8 Hz, CH(CH₃)₂), 1.30 (CH_AH_B, 6 H^{min}, d, *J* = 2.7 Hz, CH(CH₃)₂), 1.22 (CH_AH_B, 6 H^{maj}, d, *J* = 5.8 Hz, CH(CH₃)₂), 1.04 (CH_AH_B, 6 H^{maj}, 6 H, d, *J* = 5.8 Hz, CH(CH₃)₂). **δ¹³C (101 MHz, CDCl₃)** 171.2 (C^{maj}), 171.0 (C^{min}), 148.2 (C^{min}), 147.5 (C^{maj}), 145.7 (2 * C^{maj}), 145.6 (2 * C^{min}), 140.2 (C^{min}), 138.7 (C^{maj}), 138.0 (C^{min}), 136.6 (C^{maj}), 128.6 (CH^{min}), 128.3 (CH^{maj}), 124.4 (2 * CH^{maj} + 2 * CH^{min}), 121.2 (CH^{maj}), 120.1 (C^{min}), 119.5 (CH^{min}), 117.4 (C^{maj}), 116.8 (CH^{min}), 114.1 (CH^{maj}), 111.2 (CH^{min}), 111.1 (CH^{maj}), 55.9 (CH₃^{maj}), 55.8 (CH₃^{min}), 41.3 (CH₃^{min}), 39.0 (CH₃^{maj}), 28.7 (CH^{min}), 28.3 (CH^{maj}), 25.9 (CH₃^{maj}), 24.5 (CH₃^{min}), 24.2 (CH₃^{min}), 22.9 (CH₃^{maj}). **IR (film, cm⁻¹)** ν_{max} 3480 (N–H), 3373 (N–H), 2963 (C–H), 1626 (C=O), 1553, 1464, 1361, 1230, 1046 (C–O); **HRMS (MALDI⁺)** C₂₁H₂₈N₂O₂Na⁺ [M+Na]⁺ 363.2043; found: 363.2053.

N-(2,6-diisopropylphenyl)-3-methoxy-*N*-methyl-2-(methylamino)benzamide – 2.46



To a solution of 2-amino-*N*-(2,6-diisopropylphenyl)-3-methoxy-*N*-methylbenzamide **2.45** (0.56 g, 1.6 mmol, 1 eq.) in 1,4-dioxane (16 mL, 0.1 M) was added Cu(OAc)₂ (0.75 g, 11 mmol, 2.5 eq.) and pyridine (0.45 mL, 15.6 mmol, 3.5 eq.) at rt under an atmosphere of air. The reaction mixture was stirred for 15 min before methylboronic acid (0.25 g, 11 mmol, 2.5 eq.) was added and the reaction mixture heated to reflux until consumption of the aniline was observed by LC-MS. After 4 h the reaction was cooled to rt and filtered through a plug of Celite, washing with EtOAc, and was concentrated *in vacuo*. Purification by flash column chromatography eluting with (5% to 40% EtOAc/Petrol) yielded the *title compound* (0.51 g, 90%) as a yellow oil. *R*_f 0.31 (30% EtOAc/Petrol). Mixture of conformers in a 1.0:0.3 ratio. **¹H (400 MHz, CDCl₃)** 7.34 (1 H^{maj}, dd, *J* = 8.4, 7.0 Hz, ArCH), 7.24 (2 H^{maj}, d, *J* = 7.3 Hz, ArCH), 7.21 (1 H^{min}, d, *J* = 7.8 Hz, ArCH), 7.06 (2 H^{min}, d, *J* = 7.7 Hz, ArCH), 6.93 (1 H^{maj}, dd, *J* = 7.3, 2.0 Hz, ArCH), 6.89 (1 H^{maj}, t, *J* = 7.6 Hz, ArCH), 6.86 (1 H^{maj}, dd, *J* = 7.8, 2.1 Hz, ArCH), 6.64 (1 H^{min}, dd, *J* = 7.8, 1.6 Hz, ArCH), 6.31 (1 H^{min}, dd, *J* = 8.0, 1.6 Hz, ArCH), 6.25 (1 H^{min}, t, *J* = 7.9 Hz, ArCH), 4.59 (1 H^{maj}, br. s, NH), 3.88 (3 H^{maj}, s, OCH₃), 3.75 (3 H^{min}, s, OCH₃), 3.34 (3 H^{min}, s, NCH₃), 3.16 (2 H^{maj}, hept, *J* = 5.9 Hz, CH(CH₃)₂), 3.12 (3 H^{maj}, s, NCH₃), 3.05 – 2.98 (2 H^{min}, m, CH(CH₃)₂), 3.01 (3 H^{min}, s, CH₃), 2.96 (3 H^{maj}, s, CH₃), 1.30 (CH_AH_B, 6 H^{maj}, d, *J* = 3.5 Hz, CH(CH₃)₂), 1.28 (CH_AH_B, 6 H^{maj}, d, *J* = 3.6 Hz, CH(CH₃)₂), 1.19 (CH_AH_B, 6 H^{min}, d, *J* = 5.8 Hz, CH(CH₃)₂), 1.05 (CH_AH_B, 6 H^{min}, d, *J* = 5.8 Hz, CH(CH₃)₂). **¹³C (101 MHz, CDCl₃)** 171.2 (C^{maj}), 171.1 (C^{min}), 151.2 (C^{min}), 150.7 (C^{maj}), 145.9 (C^{maj}), 145.6 (C^{min}), 141.0 (C^{min}), 140.1 (C^{min}), 138.0 (C^{maj}), 137.8 (C^{maj}), 128.6 (CH^{maj}), 128.5 (CH^{min}), 125.8 (C^{maj}), 124.5 (CH^{maj}), 124.4 (CH^{min}), 122.0 (C^{min}), 121.9 (CH^{min}), 120.0 (CH^{maj}), 119.7 (CH^{maj}), 116.6 (CH^{min}), 114.05 (CH^{min}), 111.2 (CH^{maj}), 56.2 (CH₃^{min}), 55.9 (CH₃^{maj}), 40.7 (CH₃^{maj}), 39.3 (CH₃^{min}), 35.2 (CH₃^{maj}), 34.3 (CH₃^{min}), 28.6 (CH^{maj}), 28.5 (CH^{min}), 25.9 (CH₃^{min}), 24.5 (CH₃^{maj}), 24.4 (CH₃^{maj}), 23.2 (CH₃^{min}). **IR (film, cm⁻¹)** *v*_{max} 3376 (N–H), 2963 (C–H), 1645 (C=O), 1467, 1374, 1361, 1257, 1046 (C–O). **HRMS** (MALDI⁺) C₂₂H₃₀N₂O₂Na⁺ [M+Na]⁺ 377.2199; found: 377.2192.

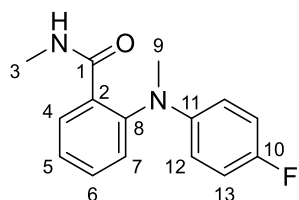
N-Methyl-2-(methyl(phenyl)amino)benzamide - 2.48a



Following **GP2.3** on a 6.0 mmol scale, the *title compound* was obtained as a colourless oil (1.4 g, 83%). *R*_f 0.13 (25% EtOAc/Petrol). **¹H (400 MHz, CDCl₃)** 8.22 (1 H, dd, *J* = 7.9, 1.7 Hz, H-4), 8.17 (1 H, br. s, NH), 7.43 (1 H, ddd, *J* = 7.9, 7.3, 1.7 Hz, H-6), 7.33 (1 H, ddd, *J* = 7.9, 7.3, 1.4 Hz, H-5), 7.28 – 7.19 (2 H, m, H-11), 7.08 (1 H, dd, *J* = 7.9, 1.4 Hz, H-7), 6.90 (1 H, tt, *J* = 7.4, 1.1 Hz, H-10), 6.78 (2 H, dd, *J* = 8.8, 1.1 Hz, H-12), 3.16 (3 H, s, H-9), 2.89 (3 H, d, *J* = 4.9 Hz, H-3). **¹³C (101 MHz, CDCl₃)** 166.6 (C-1), 149.3 (C-13), 148.2 (C-8), 132.6 (C-6), 131.6 (C-4), 131.0 (C-2),

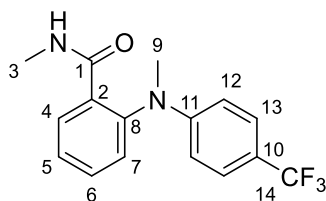
129.3 (C-11), 127.9 (C-7), 126.7 (C-5), 120.2 (C-10), 116.3 (C-12), 40.9 (C-9), 26.7 (C-3). **IR (film, cm⁻¹)** ν_{\max} 3340 (N–H), 1591 (C=O). **HRMS (ESI⁺)** m/z calcd for C₁₅H₁₇N₂O⁺ [M+H]⁺ 241.1335; found: 241.1334.

2-((4-Fluorophenyl)(methyl)amino)-N-methylbenzamide – 2.48b



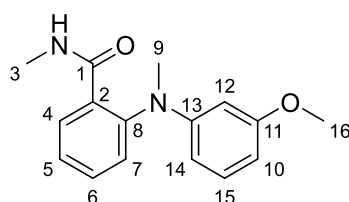
Following **GP2.3** on a 0.42 mmol scale, the *title compound* was obtained as a yellow oil (108 mg, 99%). R_f 0.35 (40% EtOAc/Petrol). **$\delta^1\text{H}$ (400 MHz, CDCl₃)** 8.23 (1 H, br. s, NH), 8.21 (1 H, dd, J = 7.8, 1.5 Hz, H-4), 7.43 (1 H, td, J = 7.8, 1.5 Hz, H-5), 7.33 (1 H, td, J = 7.8, 1.5 Hz, H-6), 7.05 (1 H, dd, J = 7.8, 1.5 Hz, H-7), 6.99 – 6.90 (2 H, m, H-13), 6.77 – 6.66 (2 H, m, H-12), 3.15 (3 H, s, H-9), 2.90 (3 H, d, J = 4.9 Hz, H-3). **$\delta^{13}\text{C}$ (101 MHz, CDCl₃)** 166.6 (C-1), 157.5 (d, J = 240 Hz, C-10), 148.5 (C-8), 145.8 (d, J = 2 Hz, C-11), 132.7 (C-5), 131.7 (C-4), 130.7 (C-2), 127.3 (C-7), 126.7 (C-6), 117.9 (d, J = 8 Hz, C-12), 115.9 (d, J = 23 Hz, C-13), 41.5 (C-9), 26.8 (C-3). **$\delta^{19}\text{F}$ NMR (376 MHz, CDCl₃)** -124.0 (dp, J = 8.6, 4.6 Hz, C–F). **IR (film, cm⁻¹)** ν_{\max} 3303 (N–H), 1644 (C=O), 1504, 1223 (C–F). **HRMS (ESI⁺)** m/z calcd for C₁₅H₁₅FN₂ONa⁺ [M+Na]⁺ 281.1061; found: 281.1065.

N-Methyl-2-(methyl(4-(trifluoromethyl)phenyl)amino)benzamide – 2.48c



Following **GP2.3** on a 0.33 mmol scale, the *title compound* was obtained as a colourless oil (94 mg, 92%). R_f 0.45 (40% EtOAc/Petrol). **$\delta^1\text{H}$ (400 MHz, CDCl₃)** 8.10 (1 H, dd, J = 7.7, 1.8 Hz, H-4), 7.49 (1 H, td, J = 7.7, 1.8 Hz, H-6), 7.46 (2 H, d, J = 9.1 Hz, H-13), 7.40 (1 H, td, J = 7.7, 1.3 Hz, H-5), 7.23 (1 H, br. s, NH), 7.12 (1 H, dd, J = 7.7, 1.3 Hz, H-7), 6.76 (2 H, d, J = 9.1 Hz, H-12), 3.23 (3 H, s, H-9), 2.86 (3 H, d, J = 4.9 Hz, H-3). **$\delta^{13}\text{C}$ (101 MHz, CDCl₃)** 166.8 (C-1), 151.6 (q, J = 1 Hz, C-11), 146.1 (C-8), 132.8 (C-6), 132.3 (C-2), 131.5 (C-4), 128.4 (C-7), 127.6 (C-5), 126.6 (q, J = 4 Hz, C-13), 125.6 (q, J = 271 Hz, C-14), 120.9 (q, J = 33 Hz, C-10), 114.5 (C-12), 40.6 (C-9), 26.9 (C-3). **$\delta^{19}\text{F}$ NMR (376 MHz, CDCl₃)** -61.74 (s, CF₃). **IR (film, cm⁻¹)** ν_{\max} 3383 (N–H), 2958, 1636 (C=O), 1516, 1359 (C–F). **HRMS (ESI⁺)** m/z calcd for C₁₆H₁₅F₃N₂ONa⁺ [M+Na]⁺ 331.1029; found: 331.1044.

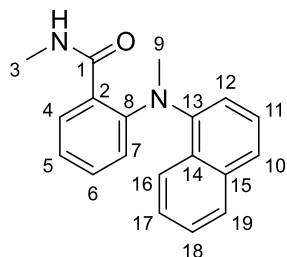
2-((3-Methoxyphenyl)(methyl)amino)-N-methylbenzamide – 2.48g



Following **GP2.3** on a 0.40 mmol scale, the *title compound* was obtained as a yellow oil (87 mg, 80%). R_f 0.23 (50% EtOAc/Petrol). **$\delta^1\text{H}$ (400 MHz, CDCl₃)** 8.21 (1 H, ddd, J = 7.9, 1.8, 0.4 Hz, H-4), 8.01 (1 H, br. s, NH), 7.43 (1 H, ddd, J = 7.9, 7.3, 1.8 Hz, H-6), 7.34 (1 H, ddd, J = 7.9, 7.3, 1.3 Hz, H-5), 7.14 (1 H, td, J = 8.2, 0.4 Hz, H-15), 7.10 (1 H, ddd, J = 7.9, 1.3, 0.4 Hz, H-7), 6.45 (1 H, ddd, J = 8.2, 2.3, 0.8 Hz, H-14),

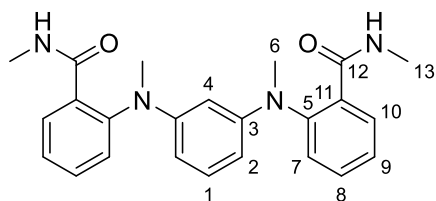
6.35 (1 H, ddd, $J = 8.2, 2.3, 0.8$ Hz, H-10), 6.32 (1 H, t, $J = 2.3$ Hz, H-12), 3.74 (3 H, s, H-16), 3.15 (3 H, s, H-9), 2.90 (3 H, d, $J = 4.9$ Hz, H-3). $\delta^{13}\text{C}$ (101 MHz, CDCl_3) 166.7 (C-1), 160.7 (C-11), 150.6 (C-13), 147.8 (C-8), 132.6 (C-6), 131.6 (C-4), 131.2 (C-2), 130.1 (C-15), 128.1 (C-7), 126.9 (C-5), 109.0 (C-10), 104.7 (C-14), 102.7 (C-12), 55.3 (C-16), 40.9 (C-9), 26.8 (C-3). IR (film, cm^{-1}) ν_{max} 3318 (N-H), 2939, 2477, 1645, 1594 (C=O), 1489, 1048 (O-CH₃). HRMS (ESI⁺) m/z calcd for $\text{C}_{16}\text{H}_{18}\text{N}_2\text{O}_2\text{Na}^+ [\text{M}+\text{Na}]^+$ 293.1260; found: 293.1263.

N-Methyl-2-(methyl(naphthalen-1-yl)amino)benzamide 2.48j



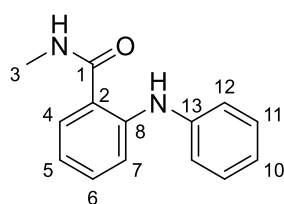
Following **GP2.3** on a 0.34 mmol scale, the *title compound* was obtained as a yellow oil (100 mg, quant.). R_f 0.19 (40% EtOAc/Petrol). $\delta^1\text{H}$ (400 MHz, CDCl_3) 8.15 (1 H, br. s, NH), 8.04 (1 H, dd, $J = 7.8, 1.8$ Hz, H-4), 7.85 (1 H, dd, $J = 8.3, 1.3$ Hz, H-19), 7.82 (1 H, d, $J = 8.4$ Hz, H-16), 7.64 (1 H, dt, $J = 8.2, 1.1$ Hz, H-10), 7.46 – 7.41 (2 H, m, H-11 + H-18), 7.38 (1 H, ddd, $J = 8.4, 6.8, 1.3$ Hz, H-17), 7.28 (1 H, td, $J = 7.8, 1.8$ Hz, H-6), 7.19 (1 H, dd, $J = 7.5, 1.1$ Hz, H-12), 7.15 (1 H, td, $J = 7.8, 1.2$ Hz, H-5), 6.92 (1 H, dd, $J = 7.8, 1.2$ Hz, H-7), 3.32 (3 H, s, H-9), 2.59 (3 H, d, $J = 4.9$ Hz, H-3). $\delta^{13}\text{C}$ (101 MHz, CDCl_3) 167.5 (C-1), 150.1 (C-8), 146.5 (C-13), 135.1 (C-15), 132.0 (C-6), 131.7 (C-4), 129.0 (C-19), 128.5 (C-14), 128.1 (C-2), 126.3 (C-17), 126.0 (C-11 + C-18), 125.1 (C-10), 124.1 (C-5), 123.3 (C-16), 122.2 (C-7), 118.6 (C-12), 43.7 (C-9), 26.3 (C-3). IR (film, cm^{-1}) ν_{max} 3304 (N-H), 3050, 1645 (C=O). HRMS (ESI⁺) m/z calcd for $\text{C}_{19}\text{H}_{18}\text{N}_2\text{ONa}^+ [\text{M}+\text{Na}]^+$ requires 313.1311; found 313.1304.

2,2'-(1,3-Phenylenebis(methylazanediyl))bis(*N*-methylbenzamide) - 2.48k



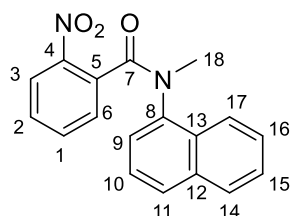
Following **GP2.3** on a 0.31 mmol scale, the *title compound* was obtained as a yellow oil (60 mg, 48%). R_f 0.38 (EtOAc). $\delta^1\text{H}$ (400 MHz, CDCl_3) 8.11 (2 H, dd, $J = 7.8, 1.8$ Hz, H-10), 7.91 (2 H, br. s, NH), 7.40 (2 H, td, $J = 7.8, 1.8$ Hz, H-8), 7.30 (2 H, td, $J = 7.8, 1.4$ Hz, H-9), 7.08 (2 H, dd, $J = 7.8, 1.4$ Hz, H-7), 7.06 (1 H, t, $J = 8.3$, overlaps, H-1), 6.28 (2 H, dd, $J = 8.3, 2.3$ Hz, H-2), 6.10 (1 H, t, $J = 2.3$ Hz, H-4), 3.09 (6 H, s, H-6), 2.88 (6 H, d, $J = 4.9$ Hz, H-13). $\delta^{13}\text{C}$ (101 MHz, CDCl_3) 166.8 (C-12), 150.4 (C-3), 147.6 (C-5), 132.4 (C-8), 131.4 (C-10), 131.3 (C-11), 129.9 (C-1), 127.7 (C-7), 126.7 (C-9), 108.3 (C-2), 103.8 (C-4), 40.8 (C-6), 26.8 (C-13). IR (film, cm^{-1}) ν_{max} 3304 (N-H), 1645 (C=O), 1594, 1482. HRMS (ESI⁺) m/z calcd for $\text{C}_{24}\text{H}_{26}\text{N}_4\text{O}_2\text{Na}^+ [\text{M}+\text{Na}]^+$ 425.1948; found: 425.1964.

N-Methyl-2-(phenylamino)benzamide 2.49



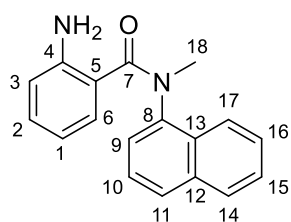
A solution of **2.48a** (51 mg, 0.21 mmol, 1.0 eq.), CuBr (3.1 mg, 0.021 mmol, 10 mol%) and *tert*-butyl hydroperoxide (5.0–6.0 M in decane, 86 μ L, 0.43–0.51 mmol, 2.0 to 2.4 eq.) in acetonitrile (0.86 mL, 0.25 M) was kept under air at 60 °C for 4 h. The reaction mixture was quenched with ethyl acetate, volatiles were removed *in vacuo*. Purification by flash column chromatography yielded the *title compound* as a yellow oil (17 mg, 35%). $\delta^1\text{H}$ (400 MHz, CDCl_3) 9.21 (1 H, br. s, NH), 7.32 (1 H, dd, J = 7.9, 1.6 Hz, ArCH), 7.27 (1 H, dd, J = 8.4, 1.2 Hz, ArCH), 7.24 – 7.15 (3 H, m, ArCH), 7.15 – 7.07 (2 H, m, ArCH), 6.92 (1 H, tt, J = 7.4, 1.2 Hz, ArCH), 6.68 (1 H, ddd, J = 7.8, 7.1, 1.2 Hz, ArCH), 6.12 (1 H, br. s, NH), 2.90 (3 H, d, J = 4.9 Hz, CH_3). $\delta^{13}\text{C}$ (101 MHz, CDCl_3) 170.3 (C=O), 145.4 (ArC), 141.7 (ArC), 132.2 (ArCH), 129.4 (2* ArCH), 127.5 (ArCH), 122.4 (ArCH), 120.8 (2* ArCH), 118.7 (ArC), 118.1 (ArCH), 115.6 (ArCH), 26.8 (CH_3). Data consistent with that reported in the literature.^[311]

N-Methyl-*N*-(naphthalen-1-yl)-2-nitrobenzamide



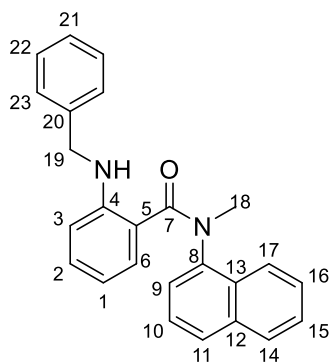
To a solution of anthranilic acid (0.5 g, 3.0 mmol, 1 eq.) in toluene (3 mL, 1 M) under nitrogen was added thionyl chloride (0.55 mL, 7.5 mmol, 2.5 eq.) before heating to reflux for 2 h. The reaction mixture was concentrated *in vacuo*, before adding toluene (10 mL) to azeotropically remove traces of thionyl chloride. The resulting residue was dissolved in CH_2Cl_2 (12 mL, 0.25 M) and pyridine (0.51 mL, 6.3 mmol, 2.1 eq.) followed by *N*-methyl-1-naphthylamine hydrochloride (0.64 g, 3.3 mmol, 1.1 eq.) were added at 0 °C before warming to rt and stirring for 16 h. The reaction mixture was quenched with sat. NH_4Cl (aq.) and extracted with EtOAc, dried over MgSO_4 , filtered and concentrated *in vacuo*. Purification by flash column chromatography eluting with (10% to 70% EtOAc/Petrol) yielded the *title compound* (0.61 g, 67%) as a brown solid. R_f 0.37 (50% EtOAc/Petrol). **m.p.**: 183 – 184 °C. Mixture of conformers in a 1:0.1 ratio. $\delta^1\text{H}$ (400 MHz, CDCl_3) 8.31 (1 H^{min} , dd, J = 8.3, 1.2), 7.99 (1 H^{maj} , dd, J = 8.5, 1.0 Hz, H-17), 7.94 – 7.89 (2 H^{min} , m), 7.85 (1 H^{maj} , d, J = 7.6 Hz, H-3), 7.80 (1 H^{maj} , d, J = 8.3 Hz, H-14), 7.74 (1 H^{min} , dd, J = 7.6, 1.4), 7.71 – 7.63 (1 H^{maj} , m, H-16), 7.66 – 7.59 (1 H^{maj} , m, H-11), 7.60 – 7.55 (2 H^{min} , m), 7.52 (1 H^{maj} , ddd, J = 8.2, 6.9, 1.2 Hz, H-15), 7.41 (1 H^{maj} , dd, J = 7.3, 1.2 Hz, H-10), 7.27 – 7.20 (1 H^{maj} , m, H-9), 7.20 – 7.15 (1 H^{maj} , m, H-1), 7.15 – 7.12 (2 H^{maj} , m, H-6 + H-2), 3.59 (3 H^{maj} , s, H-18), 3.25 (3 H^{min} , s, H-18). $\delta^{13}\text{C}$ (101 MHz, CDCl_3) 168.0 (C-7), 145.7 (C-4), 139.3 (C-8), 134.5 (C-12), 133.3 (C-2), 133.1 (C-5), 129.9 (C-13), 129.5 (C-1), 129.1 (C-16), 128.8 (C-14), 127.6 (C-6 and C-11), 126.7 (C-15), 125.7 (C-9), 125.6 (C-10), 124.3 (C-3), 122.5 (C-17), 37.5 (C-18). **IR (film, cm^{-1})** ν_{max} 1650 (C=O), 1526 (N–O), 1346 (N–O). **HRMS (ESI⁺)** m/z calcd for $\text{C}_{18}\text{H}_{14}\text{N}_2\text{O}_3\text{Na}^+$ $[\text{M}+\text{Na}]^+$ 329.0897; found: 329.0888.

2-Amino-N-methyl-N-(naphthalen-1-yl)benzamide – 2.51



Pd/C (10 wt. % loading, 58 mg, 1 mol% Pd) was suspended in a solution of *N*-Methyl-N-(naphthalen-1-yl)-2-nitrobenzamide (0.58 g, 1.9 mmol, 1 eq.) in EtOH (4.0 mL, 0.5 M) under nitrogen. Nitrogen was bubbled through the solution for 15 mins. The contents of the flask were placed under a hydrogen atmosphere using a two-way three-necked tap with a balloon of hydrogen attached. The solution was saturated with hydrogen three times using a vacuum/hydrogen cycle. The reaction was stirred under a hydrogen atmosphere for 16 h. The contents of the flask were placed under a nitrogen atmosphere and the hydrogen balloon removed. The crude reaction solution was filtered through a pad of Celite and washed with MeOH and was concentrated *in vacuo*. Purification by flash column chromatography eluting with (10% to 50% EtOAc/Petrol) yielded the *title compound* (0.45 g, 86%) as a yellow solid. R_f 0.33 (50% EtOAc/Petrol). **m.p.:** 189 – 190 °C. $\delta^1\text{H}$ (400 MHz, CDCl_3) 8.02 (1 H, d, J = 7.9 Hz, H-17), 7.85 (1 H, d, J = 7.9 Hz, H-14), 7.69 (1 H, d, J = 8.2 Hz, H-11), 7.61 (1 H, t, J = 7.9 Hz, H-16), 7.52 (1 H, t, J = 7.9 Hz, H-15), 7.26 (1 H, br. s, H-10), 7.17 (1 H, br. s, H-9), 6.84 (1 H, br. s, H-2), 6.63 (1 H, br. s, H-6), 6.53 (1 H, d, J = 8.1 Hz, H-1), 6.03 (1 H, br. s, H-3), 4.78 (2 H, br. s, NH_2), 3.52 (3 H, s, H-18). $\delta^{13}\text{C}$ (101 MHz, CDCl_3) 172.3 (C-7), 146.8 (C-4), 141.5 (C-8), 134.6 (C-12), 130.6 (C-2), 129.8 (C-13), 128.8 (C-14), 128.1 (C-6), 128.0 (C-11), 127.2 (C-16), 126.4 (C-15), 125.7 (C-10), 125.5 (C-9), 122.8 (C-17), 119.6 (C-5), 116.4 (C-1 and C-3), 38.3 (C-18). **IR (film, cm^{-1})** ν_{max} 3452 (N–H), 3352 (N–H), 1616 (C=O), 1586 (N–H), 1362 (C–N). **HRMS (ESI⁺)** m/z calcd for $\text{C}_{18}\text{H}_{17}\text{N}_2\text{O}^+$ $[\text{M}+\text{H}]^+$ 277.1335; found: 277.1341.

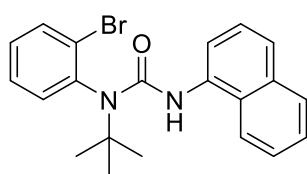
2-(Benzylamino)-N-methyl-N-(naphthalen-1-yl)benzamide – 2.52



A flame-dried round bottom flask was allowed to cool to rt *in vacuo*. To this was added 2-Amino-N-methyl-N-(naphthalen-1-yl)benzamide **2.51** (0.10 g, 0.37 mmol, 1 eq.), anhydrous toluene (3.7 mL, 1 M), molecular sieves 4 Å, and benzaldehyde (42 μL , 0.41 mmol, 1.1 eq.). The reaction mixture was allowed to stir at rt for 6 h. Extra benzaldehyde (84 μL , 0.82 mmol, 2.0 eq.) was added and the reaction mixture was stirred for 16 h. The reaction mixture was filtered and concentrated *in vacuo*. This residue was dissolved in MeOH (1.8 mL, 0.2 M), and NaBH_4 (83 mg, 2.2 mmol, 6.0 eq.) was added portion wise at 0 °C. The reaction mixture was allowed to stir at rt for 1 h. The reaction mixture was quenched with H_2O and extracted with EtOAc. The combined organic phases were washed with brine, dried over MgSO_4 , filtered and concentrated *in vacuo*. Purification by flash column chromatography eluting with (2% to 30% EtOAc/Petrol) yielded the *title compound* (97 mg, 72%) as a white solid R_f 0.46 (40% EtOAc/Petrol). **m.p.:** 145 – 146 °C. $\delta^1\text{H}$ (400 MHz, CDCl_3) 8.03 (1 H, d, J = 8.4 Hz, H-17),

7.86 (1 H, d, J = 8.1 Hz, H-14), 7.71 (1 H, d, J = 8.2, H-11), 7.61 (1 H, t, J = 7.6 Hz, H-16), 7.53 (1 H, t, J = 7.5 Hz, H-15), 7.43 (2 H, d, J = 7.1 Hz, H-23), 7.38 (2 H, t, J = 7.5 Hz, H-22), 7.34 – 7.27 (2 H, m, H-21 + H-10), 7.24 – 7.15 (1 H, m, H-9), 6.89 (1 H, br. s, H-2), 6.76 (1 H, br. s, H-6), 6.50 (2 H, d, J = 9.3 Hz, NH + H-3), 6.03 (1 H, br. s, H-1), 4.41 (2 H, s, H-19), 3.54 (3 H, s, H-18). $\delta^{13}\text{C}$ (101 MHz, CDCl_3) 172.7 (C-7), 147.6 (C-4), 141.7 (C-8), 139.5 (C-20), 134.6 (C-12), 129.8 (C-13), 128.78 (C-14), 128.75 (C-2), 128.7 (C-22), 128.5 (C-6), 128.0 (C-11), 127.30 (C-23), 127.25 (C-16), 127.1 (C-21), 126.4 (C-15), 125.7 (C-10), 125.5 (C-9), 122.7 (C-17), 119.1 (C-5), 115.1 (C-1), 111.6 (C-3), 47.6 (C-19), 38.4 (C-18). IR (film, cm^{-1}) ν_{max} 3380 (N–H), 2927 (C–H), 1629 (C=O), 1510, 1357 (C–N). HRMS (ESI⁺) m/z calcd for $\text{C}_{25}\text{H}_{22}\text{N}_2\text{ONa}^+$ $[\text{M}+\text{Na}]^+$ 389.1624; found: 389.1609.

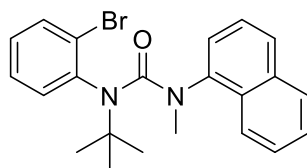
1-(2-Bromophenyl)-1-(tert-butyl)-3-(naphthalen-1-yl)urea – 2.55



To a solution of triphosgene (0.58 g, 2.0 mmol, 0.45 eq.) in CH_2Cl_2 (11.0 mL, 0.4 M) at -78°C was added 2,6-lutidine (0.61 mL, 5.3 mmol, 1.2 eq.) and 2-bromo-*N*-(*tert*-butyl)aniline^[312] (1.0 g, 4.4 mmol, 1.0 eq.).

The reaction mixture was kept at rt for 2 h. The reaction mixture was diluted in CH_2Cl_2 , washed with HCl (aq. 1 M), sat. NaHCO_3 (aq.), and brine. The combined organic phases were dried over Na_2SO_4 , filtered and concentrated *in vacuo* to give (*2-bromophenyl*)(*tert-butyl*)carbamoyl chloride as a yellow solid (1.0 g, 78%) which was used directly in the next step. This crude carbamoyl chloride (0.77 g, 2.6 mmol, 1.2 eq.), 1-naphthylamine (0.42 g, 2.2 mmol, 1.0 eq.), Et_3N (0.46 mL, 3.3 mmol, 1.5 eq.) in toluene (2.2 mL, 1 M) were heated to reflux for 48 h. The reaction mixture was diluted in ethyl acetate, washed with HCl (aq. 1 M), brine, and the combined organic phases were dried over MgSO_4 . Purification by flash column chromatography eluting with (5% to 75% Et_2O /Petrol) yielded the *title compound* as a yellow oil (0.73 g, 82%). $\delta^1\text{H}$ (400 MHz, CDCl_3) 7.86 (1 H, dd, J = 7.6, 1.0 Hz, ArCH), 7.83 (1 H, dd, J = 8.3, 1.4 Hz, ArCH), 7.78 (1 H, dd, J = 7.3, 1.4 Hz, ArCH), 7.57 (1 H, d, J = 8.2 Hz, ArCH), 7.54 – 7.47 (2 H, m, ArCH), 7.44 (1 H, d, J = 7.8 Hz, ArCH), 7.42 – 7.30 (4 H, m, ArCH) 6.05 (1H, br. s, NH), 1.55 (9 H, s, $\text{C}(\text{CH}_3)_3$). $\delta^{13}\text{C}$ (101 MHz, CDCl_3) 154.0 (C=O), 141.0 (ArC), 134.5 (ArCH), 134.2 (ArC), 133.8 (ArC), 132.5 (ArCH), 130.4 (ArCH), 129.2 (ArCH), 128.7 (ArCH), 127.6 (ArC), 127.1 (ArC), 126.0 (ArCH), 125.9 (ArCH), 125.7 (ArCH), 124.4 (ArCH), 120.6 (ArCH), 120.1 (ArCH), 59.1 (CCH_3), 29.7 (CCH_3). IR (film, cm^{-1}) ν_{max} 1783, 1731 1504, 1478, 1247, 1210, 1167.

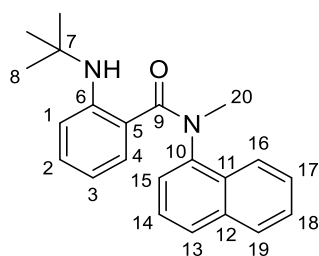
1-(2-Bromophenyl)-1-(tert-butyl)-3-methyl-3-(naphthalen-1-yl)urea – 2.56



Following **GP2.1 (Part 2)** 1-(2-bromophenyl)-1-(*tert*-butyl)-3-(naphthalen-1-yl)urea **2.55** (0.53 g, 1.3 mmol, 1 eq.), NaH (0.11 g, 2.7 mmol, 2.0 eq., 60% in mineral oil), MeI (0.25 mL, 4.0 mmol, 3.0 eq) in THF (2.7 mL, 0.5 M) were stirred at rt for 1 h. Purification by flash column

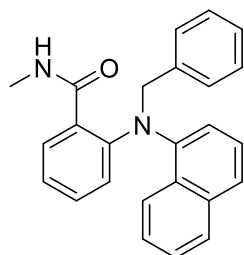
chromatography yielded the *title compound* as a white solid (0.49 g, 92%). R_f 0.52 (30% EtOAc/Petrol). **m.p.:** 95 – 96 °C. $\delta^1\text{H}$ (400 MHz, CDCl_3) 7.78 – 7.38 (4 H, m, ArCH) 7.31 (1 H, br. s, ArCH), 7.21 (2 H, br. s, ArCH), 7.00 (1 H, s, ArCH), 6.36 (1 H, br. s, ArCH), 6.16 (1 H, br. s, ArCH), 5.65 (1 H, br. s, ArCH), 3.21 (3 H, s, CH_3), 1.39 (9 H, s, $\text{C}(\text{CH}_3)_3$). $\delta^{13}\text{C}$ (101 MHz, CDCl_3) 161.4 (C=O), 143.4 (ArC), 140.1 (ArC), 134.4 (ArC), 134.2 (ArCH), 133.4 (ArCH), 129.9 (ArC), 127.8 (ArCH), 126.8 (ArCH), 126.5 (ArCH), 125.9 (ArCH), 125.73 (ArCH), 125.67 (ArCH), 125.57 (ArCH), 125.2 (ArCH), 123.5 (ArC), 123.2 (ArCH), 59.3 (CCH_3), 40.3 (CH_3), 30.2 (CCH_3). IR (film, cm^{-1}) ν_{max} 2973 (C–H), 1656 (C=O), 1323 (C–N). HRMS (ESI⁺) m/z calcd for $\text{C}_{22}\text{H}_{23}\text{N}_2\text{OBrNa}^+$ $[\text{M}+\text{Na}]^+$ 433.0886; found 433.0870.

2-(Tert-butylamino)-N-methyl-N-(naphthalen-1-yl)benzamide – 2.57



Following **GP2.2** 1-(2-bromophenyl)-1-(tert-butyl)-3-methyl-3-(naphthalen-1-yl)urea **2.56** (0.41 g, 0.95 mmol, 1 eq.), *n*-BuLi (0.79 mL, 1.1 mmol, 1.1 eq., 1.4 M in hexanes) in THF (5.0 mL, 0.2 M) were stirred at –78 °C for 2 h. Purification by flash column chromatography yielded the *title compound* as a white solid (0.28 g, 85%). R_f 0.41 (30% EtOAc/Petrol). **m.p.:** 148 – 149 °C. $\delta^1\text{H}$ (400 MHz, CDCl_3) 7.97 (1 H, m, H-16), 7.84 (1 H, d, J = 8.1 Hz, H-19), 7.69 (1 H, d, J = 8.3 Hz, H-13), 7.57 (1 H, ddd, J = 8.4, 6.8, 1.4 Hz, H-17), 7.50 (1 H, ddd, J = 8.1, 6.8, 1.3 Hz, H-18), 7.29 (1 H, s, H-14), 7.17 (1 H, s, H-15), 6.86 (1 H, br. s, H-2), 6.78 (1 H, br. s, H-1), 6.73 (1 H, br. s, H-4), 5.95 (2 H, br. s, NH + H-3), 3.50 (3 H, s, H-20), 1.44 (9 H, s, H-8). $\delta^{13}\text{C}$ (101 MHz, CDCl_3) 173.1 (C-9), 146.5 (C-6), 141.7 (C-10), 134.6 (C-12), 130.2 (C-2), 129.8 (C-11), 128.81 (C-4), 128.76 (C-19), 127.9 (C-13), 127.1 (C-17), 126.4 (C-18), 125.7 (C-14), 125.3 (C-15), 122.9 (C-16), 120.4 (C-5), 114.3 (C-1 + C-3), 50.8 (C-7), 38.5 (C-20), 30.2 (C-8). IR (film, cm^{-1}) ν_{max} 3373 (N–H), 2976 (C–H), 1633 (C=O). HRMS (ESI⁺) m/z calcd for $\text{C}_{22}\text{H}_{25}\text{N}_2\text{O}^+$ $[\text{M}+\text{H}]^+$ 333.1961; found 333.1963.

2-(Benzyl(naphthalen-1-yl)amino)-N-methylbenzamide – 2.58



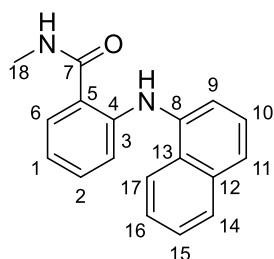
Following **GP2.3** on an 87 μmol scale (16 h reaction time), the *title compound* was obtained as a yellow solid (26 mg, 80%). R_f 0.18 (50% EtOAc/Petrol).

m.p.: 175 – 177 °C. $\delta^1\text{H}$ (400 MHz, CDCl_3) 8.07 (1 H, dd, J = 8.1, 1.5 Hz, ArCH), 7.97 – 7.83 (2 H, m, ArCH), 7.66 (1 H, d, J = 8.2 Hz, ArCH), 7.54 – 7.42 (3 H, m, ArCH + NH), 7.42 – 7.30 (4 H, m, ArCH), 7.30 – 7.22 (2 H, m, ArCH),

7.19 – 7.10 (2 H, m, ArCH), 7.03 (1 H, dd, J = 8.2, 1.1 Hz, ArCH), 5.03 (2 H, s, NCH_2), 2.36 (3 H, d, J = 4.9 Hz, NHCH_3). $\delta^{13}\text{C}$ (101 MHz, CDCl_3) 167.8 (C=O), 148.2 (ArC), 145.5 (ArC), 137.8 (ArC), 135.2 (ArC), 131.36 (ArCH), 131.34 (ArCH), 129.24 (ArC), 129.17 (ArC), 129.1 (ArCH), 128.8 (ArCH), 127.1 (ArCH), 126.60 (ArCH), 126.57 (ArCH), 126.1 (ArCH), 125.9 (ArCH), 125.4 (ArCH),

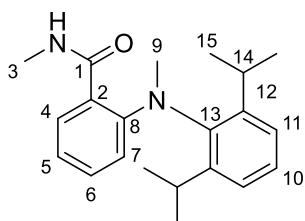
123.7 (ArCH), 123.0 (ArCH), 122.9 (ArCH), 121.1 (ArCH), 58.8 (NCH₂), 26.1 (NHCH₃). IR (film, cm⁻¹) ν_{\max} 3314 (N–H), 3060, 1651 (C=O), 1531. HRMS (ESI⁺) m/z calcd for C₂₅H₂₂N₂ONa⁺ [M+Na]⁺ 389.1624; found: 389.1630.

N-Methyl-2-(naphthalen-1-ylamino)benzamide – 2.59



Pd/C (10 wt. % loading, 15 mg, 2 mol% Pd) was suspended in a solution of 5-methoxy-*N*-methyl-2-nitro-*N*-phenylbenzamide **2.58** (75 mg, 0.21 mmol, 1 eq.) in EtOH (1.0 mL, 0.2 M) under nitrogen. Nitrogen was bubbled through the solution for 15 mins. The contents of the flask were placed under a hydrogen atmosphere using a two-way three-necked tap with a balloon of hydrogen attached. The solution was saturated with hydrogen three times using a vacuum/hydrogen cycle. The reaction was stirred under a hydrogen atmosphere for 24 h. The contents of the flask were placed under a nitrogen atmosphere and the hydrogen balloon removed. The crude reaction solution was filtered through a pad of Celite and washed with MeOH and was concentrated *in vacuo*. Purification by flash column chromatography eluting with (5% to 40% EtOAc/Petrol) yielded the *title compound* (47 mg, 83%) white solid. **m.p.:** 143 – 144 °C. **R_f** 0.18 (30% EtOAc/Petrol). **¹H (400 MHz, CDCl₃)** 9.92 (1 H, br. s, NH), 8.23 – 8.13 (1 H, m, H-17), 7.92 – 7.82 (1 H, m, H-14), 7.63 (1 H, d, J = 8.0 Hz, H-11), 7.55 – 7.47 (3 H, m, H-15 + H-16 + H-9), 7.47 – 7.39 (2 H, m, H-10 + H-3), 7.21 (1 H, ddd, J = 8.5, 7.0, 1.6 Hz, H-2), 7.14 (1 H, dd, J = 8.5, 1.2 Hz, H-6), 6.73 (1 H, ddd, J = 8.1, 7.1, 1.3 Hz, H-1), 6.31 (1 H, br. s, NH), 3.01 (3 H, d, J = 4.9 Hz, H-18). **¹³C (101 MHz, CDCl₃)** 170.6 (C-7), 147.0 (C-8), 137.6 (C-8), 134.9 (C-12), 132.3 (C-2), 129.0 (C-13), 128.4 (C-14), 127.4 (C-3), 126.3 (C-15 or C-16), 126.1 (C-15 or C-16), 125.9 (C-10), 123.9 (C-11), 122.7 (C-17), 118.1 (C-9), 117.7 (C-5), 117.6 (C-1), 115.6 (C-6), 26.8 (C-18). IR (film, cm⁻¹) ν_{\max} 3317 (N–H), 1633 (C=O), 1578 (N–H), 1521, 1450, 1406, 1282 (C–N). HRMS (ESI⁺) m/z calcd for C₁₈H₁₆N₂ONa⁺ [M+Na]⁺ 299.1155; found 299.1157.

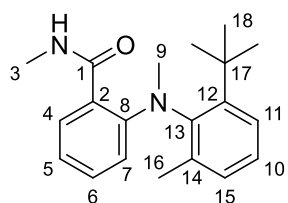
2-((2,6-Diisopropylphenyl)(methylamino)-*N*-methylbenzamide – 2.48l



Following **GP2.3** on a 0.4 mmol scale (16 h reaction time, reflux temperature), the *title compound* was obtained as a white solid (129 mg, 98%). **R_f** 0.61 (40% EtOAc/Petrol). **m.p.:** 134 – 135 °C. **¹H (400 MHz, CDCl₃)** 7.33 (1 H, t, J = 7.7 Hz, H-10), 7.29 (1 H, d, J = 8.0 Hz, H-4), 7.24 (2 H, d, J = 7.5 Hz, H-11), 7.00 (1 H, t, J = 8.0 Hz, H-5), 6.64 (1 H, t, J = 8.0 Hz, H-6), 6.16 (1 H, d, J = 8.0 Hz, H-7), 5.97 (1 H, br. s, NH), 3.23 (3 H, s, H-9), 3.09 (2 H, sept., J = 5.9, H-14), 3.04 (3 H, d, J = 4.9 Hz, H-3), 1.22 (CH_AH_B, 6 H, d, J = 5.9 Hz, H-15), 1.06 (CH_AH_B, 6 H, d, J = 5.9 Hz, H-15). **¹³C (101 MHz, CDCl₃)** 172.2 (C-1), 147.9 (C-12), 147.7 (C-8), 142.4 (C-13), 130.0 (C-6), 129.6 (C-4), 128.0 (C-10), 125.0 (C-11), 121.3 (C-2), 117.0 (C-7), 116.3 (C-5), 42.5 (C-9), 28.2 (C-14),

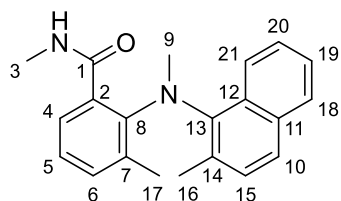
27.1 (C-3), 24.7 (C-11), 24.1 (C-11). **IR (film, cm⁻¹)** ν_{\max} 3296 (N–H), 2960 (C–H), 1633 (C=O), 1493. **HRMS (ESI⁺)** m/z calcd for C₂₁H₂₈N₂ONa⁺ [M+Na]⁺ 347.2094; found: 347.2088.

2-((2-(Tert-butyl)-6-methylphenyl)(methyl)amino)-N-methylbenzamide -2.48m



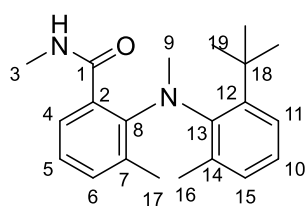
Following **GP2.3** on a 0.34 mmol scale (16 h reaction time, reflux temperature), the *title compound* was obtained as a white solid (91 mg, 77%). **R_f** 0.59 (40% EtOAc/Petrol). **m.p.:** 205 – 206 °C. **$\delta^1\text{H}$ (400 MHz, CDCl₃)** 7.41 – 7.37 (1 H, m, H-10), 7.31 (1 H, dd, J = 7.5, 1.7 Hz, H-4), 7.22 – 7.18 (2 H, m, H-11 + H-15), 7.00 (1 H, ddd, J = 8.7, 7.5, 1.7 Hz, H-6), 6.66 (1 H, td, J = 7.5, 1.0 Hz, H-5), 6.08 (1 H, dd, J = 8.7, 1.0 Hz, H-7), 5.95 (1 H, br. q, J = 5.0 Hz, NH), 3.22 (3 H, s, H-9), 3.03 (3 H, d, J = 4.9 Hz, H-3), 2.01 (3 H, s, H-16), 1.34 (9 H, s, H-18). **$\delta^{13}\text{C}$ (101 MHz, CDCl₃)** 172.1 (C-1), 148.7 (C-12), 148.0 (C-8), 145.3 (C-13), 139.0 (C-14), 130.4 (C-15), 129.8 (C-6), 129.6 (C-4), 127.2 (C-11), 126.2 (C-10), 121.9 (C-2), 116.8 (C-7), 116.6 (C-5), 43.8 (C-9), 35.7 (C-17), 31.7 (C-18), 26.8 (C-3), 18.9 (C-16). **IR (film, cm⁻¹)** ν_{\max} 3282 (N–H), 2954 (C–H), 1634 (C=O), 1490. **HRMS (ESI⁺)** m/z calcd for C₂₀H₂₆N₂ONa⁺ [M+Na]⁺ 333.1937; found: 333.1929. Supplementary crystallographic data can be obtained free of charge from The Cambridge Crystallographic Data Centre (CCDC 1557197).

N,3-Dimethyl-2-(methyl(2-methylnaphthalen-1-yl)amino)benzamide – 2.48n



Following **GP2.3** on a 0.49 mmol scale (16 h reaction time, reflux temperature), the *title compound* was obtained off-white solid (108 mg, 70%). **R_f** 0.40 (75% EtOAc/Petrol). **m.p.:** 204 – 206 °C. **$\delta^1\text{H}$ (400 MHz, CDCl₃)** 8.19 – 8.12 (1 H, m, H-21), 7.80 (1 H, dd, J = 8.0, 1.5 Hz, H-18), 7.57 (1 H, d, J = 8.3 Hz, H-10), 7.45 (1 H, ddd, J = 8.5, 6.8, 1.5 Hz, H-20), 7.39 (1 H, ddd, J = 8.0, 6.8, 1.3, H-19), 7.23 (1 H, d, J = 8.3 Hz, H-15), 7.17 (1 H, dd, J = 7.5, 1.8 Hz, H-4), 7.03 (1 H, dd, J = 7.5, 1.8 Hz, H-6), 6.83 (1 H, t, J = 7.5 Hz, H-5), 5.74 (1 H, q, J = 5.3 Hz, NH), 3.45 (3 H, s, H-9), 2.84 (3 H, d, J = 4.9 Hz, H-3), 2.32 (3 H, s, H-16), 1.64 (3 H, s, H-17). **$\delta^{13}\text{C}$ (101 MHz, CDCl₃)** 172.5 (C-1), 146.7 (C-8), 142.7 (C-13), 134.0 (C-6), 133.9 (C-11), 132.9 (C-14), 131.3 (C-7), 131.0 (C-12), 130.3 (C-15), 128.5 (C-18), 128.0 (C-2), 127.5 (C-4), 125.9 (C-20), 125.6 (C-10), 124.9 (C-19 or C-21), 124.8 (C-19 or C-21), 120.3 (C-5), 42.6 (C-9), 27.1 (C-3), 21.3 (C-17), 19.7 (C-16). **IR (film, cm⁻¹)** ν_{\max} 3303 (N–H), 2957, 2921 (C–H), 1635 (C=O), 1411. **HRMS (ESI⁺)** m/z calcd for C₂₁H₂₂N₂ONa⁺ [M+Na]⁺ 341.1624; found: 341.1622. Supplementary crystallographic data can be obtained free of charge from The Cambridge Crystallographic Data Centre (CCDC 1557204).

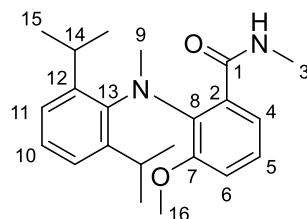
2-((2-(*Tert*-Butyl)-6-methylphenyl)(methylamino)-*N*,3-dimethylbenzamide – 2.48o



Following **GP2.3** on a 0.42 mmol scale (96 h reaction time, reflux temperature) yielded the unreacted starting material (40 mg, 29%) and the *title compound* as a yellow solid (77 mg, 57%, 80% brsm). R_f 0.26 (50% EtOAc/Petrol). **m.p.:** 203 – 205 °C. $\delta^1\text{H}$ (400 MHz, CDCl_3)

7.31 (1 H, dd, $J = 7.7, 1.6$ Hz, H-11), 7.18 (1 H, br. s, H-4), 7.13 (1 H, t, $J = 7.7$ Hz, H-10), 7.02 (1 H, dd, $J = 7.7, 1.6$ Hz, H-15), 6.91 (1 H, d, $J = 7.4$ Hz, H-6), 6.61 (1 H, t, $J = 7.4$ Hz, H-5), 5.91 (1 H, br. s, NH), 3.26 (3 H, s, H-9), 2.98 (3 H, br. s, H-3), 2.14 (3 H, s, H-16), 1.54 (3 H, br. s, H-17), 1.42 (9 H, s, H-19). $\delta^{13}\text{C}$ (101 MHz, CDCl_3) 173.1 (C-1), 147.8 (C-13), 147.7 (C-12), 146.4 (C-8), 139.5 (C-14), 135.2 (C-6), 128.8 (C-15), 128.6 (C-4), 126.8 (C-10), 126.3 (C-11), 125.0 (C-2 or C-7), 124.6 (C-2 or C-7), 117.0 (C-5), 47.2 (C-9), 36.2 (C-18), 31.9 (C-19), 26.9 (C-3), 22.7 (C-17), 19.1 (C-16). **IR (film, cm^{-1})** ν_{max} 3302 (N–H), 2957 (C–H), 1634 (C=O), 1467, 1404. **HRMS (ESI⁺)** m/z calcd for $\text{C}_{21}\text{H}_{28}\text{N}_2\text{ONa}^+ [\text{M}+\text{Na}]^+$ 347.2094; found: 347.2102.

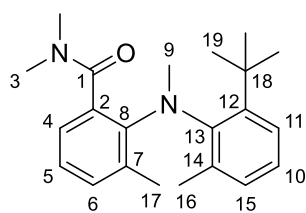
2-((2,6-Diisopropylphenyl)(methylamino)-3-methoxy-*N*-methylbenzamide 2.48p



A flame-dried Biotage microwave vial was allowed to cool to rt *in vacuo*. To this was added *N*-(2,6-diisopropylphenyl)-3-methoxy-*N*-methyl-2-(methylamino)benzamide **2.42p** (141 mg, 0.4 mmol, 1 eq.), and anhydrous THF (2.0 mL, 0.2 M). NaHMDS (0.44 mL, 0.44 mmol, 1.1 eq.,

1.0 M in THF) was added dropwise and the vial was sealed. The reaction was allowed to stir at 150 °C for 16 h under microwave irradiation, then quenched with MeOH, and the subsequent solution concentrated *in vacuo* to yield the crude diarylamine. Purification by flash column chromatography eluting with (10% to 90% Et₂O/Petrol) yielded the *title compound* as a white solid (101 mg, 72%). R_f 0.42 (75% Et₂O/Petrol). **m.p.:** 174 – 176 °C. $\delta^1\text{H}$ (500 MHz, CDCl_3) 7.16 (1 H, dd, $J = 8.4, 6.8$ Hz, H-10), 7.12 – 7.02 (2 H, dd, $J = 7.6, 0.8$ Hz, H-11), 6.89 (1 H, br. s, H-4), 6.77 – 6.65 (2 H, m, H-5 + H-6), 5.89 (1 H, br. s, NH), 3.55 – 3.37 (2 H, m, H-14), 3.21 (3 H, br. s, H-16), 3.20 – 3.08 (3 H, m, H-9), 2.99 (3 H, br. s, H-3), 1.48 – 1.12 ($\text{CH}_\text{A}\text{H}_\text{B}$, 6 H, br. d, $J = 3.5$), 1.00 – 0.76 ($\text{CH}_\text{A}\text{H}_\text{B}$, 6 H, br. d, $J = 3.5$ Hz, H-15). $\delta^{13}\text{C}$ (101 MHz, CDCl_3) 172.1 (C-1), 151.8 (C-7), 146.5 (C-12), 145.8 (C-13), 138.8 (C-8), 126.0 (C-10), 125.3 (C-2), 124.0 (C-11), 122.0 (C-4), 118.5 (C-6), 114.4 (C-5), 55.4 (C-16), 43.5 (C-9), 27.7 (C-14), 27.3 (C-3), 25.2 (C-15), 23.7 (C-15). **IR (film, cm^{-1})** ν_{max} 3291 (N–H), 2961 (C–H), 1638 (C=O), 1520, 1463, 1446, 1250 (C–O), 1084 (C–O). **HRMS (ESI⁺)** m/z calcd for $\text{C}_{22}\text{H}_{31}\text{N}_2\text{O}_2^+ [\text{M}+\text{H}]^+$ 354.2307; found: 354.2306.

2-((2-(*Tert*-Butyl)-6-methylphenyl)(methyl)amino)-*N,N*,3-trimethylbenzamide – 2.61



A flame-dried round bottom flask was allowed to cool to rt *in vacuo*. To this was added 2-((2-(*tert*-Butyl)-6-methylphenyl)(methyl) amino)-*N,N*,3-dimethylbenzamide **2.48o** (30.1 mg, 0.0928 mmol, 1.0 eq.) and anhydrous THF (0.4 mL, 0.23 M) and the reaction mixture was cooled to 0 °C. NaH (7.4 mg, 0.18 mmol, 2.0 eq.) was added portion wise, followed by dropwise addition of MeI (17 µL, 0.28 mmol, 3.0 eq.). The reaction mixture was allowed to stir at rt for 20 h. The reaction mixture was quenched with sat. Na₂S₂O₃ (aq.) and extracted with Et₂O. The combined organic phases were washed with brine, dried over MgSO₄, filtered and concentrated *in vacuo* to yield the crude methylated urea. Purification by flash column chromatography eluting with (5% to 50% EtOAc/Petrol) yielded the *title compound* **10** (23.6 mg, 75%) as a colourless oil. *R*_f 0.26 (50% EtOAc/Petrol). Mixture of conformers in a 1.0:0.8 ratio. Only major peaks were assigned in the ¹H NMR spectrum. **δ¹H (400 MHz, CDCl₃)** 7.35 (1 H^{maj}, dd, *J* = 8.1, 1.6 Hz, H-11), 7.30 (1 H^{min}, dd, *J* = 8.1, 1.6), 7.14 (1 H^{min}, t, *J* = 7.7), 7.09 (1 H^{maj}, t, *J* = 7.7 Hz, H-10), 7.05 (1 H^{min}, dd, *J* = 7.5, 1.6), 6.97 – 6.87 (3 H^{maj} + 1 H^{min}, m, H-4 + H-6 + H-15), 6.84 (1 H^{min}, dd, *J* = 7.5, 1.8), 6.64 (1 H^{maj}, t, *J* = 7.4 Hz, H-5), 6.58 (1 H^{min}, t, *J* = 7.4 Hz), 3.17 (3 H^{min}, s), 3.14 (3 H^{min}, s), 3.12 (3 H^{min}, s), 3.11 (3 H^{maj}, s, H-3), 3.10 (3 H^{maj}, s, H-9), 3.07 (3 H^{maj}, s, H-3), 2.16 (3 H^{min}, s), 2.11 (3 H^{maj}, s, H-16), 1.62 (3 H^{maj}, s, H-17), 1.47 (3 H^{min}, s), 1.46 (9 H^{maj}, s, H-19), 1.39 (9 H^{min}, s). **δ¹³C (101 MHz, CDCl₃)** 173.8 (C-1^{maj}), 173.5 (C-1^{min}), 149.7 (C-12^{min}), 148.8 (C-13^{min}), 146.5 (C-13^{maj}), 146.2 (C-8^{min}), 145.6 (C-12^{maj}), 144.7 (C-8^{maj}), 139.6 (C-14^{min}), 139.0 (C-14^{maj}), 135.0 (C-6^{min}), 134.3 (C-6^{maj}), 128.7 (C-15^{min}), 128.4 (C-15^{maj}), 128.3 (C-11^{maj}), 127.9 (C-4^{min}), 127.8 (C-4^{maj}), 127.0 (C-10^{min}), 126.3 (C-10^{maj}), 125.7 (C-11^{min}), 125.6 (C-7^{maj}), 124.8 (C-7^{min}), 122.5 (C-2^{maj}), 122.4 (C-2^{min}), 117.4 (C-5^{maj}), 116.6 (C-5^{min}), 46.0 (C-3^{min}), 45.1 (C-3^{maj}), 40.4 (C-3^{min}), 40.0 (C-3^{maj}), 36.7 (C-18^{maj}), 36.2 (C-18^{min}), 35.3 (C-9^{min}), 35.2 (C-9^{maj}), 32.6 (C-19^{maj}), 31.8 (C-19^{min}), 23.2 (C-17^{maj}), 22.8 (C-17^{min}), 19.3 (C-16^{min}), 18.9 (C-16^{maj}). **IR (film, cm⁻¹)** ν_{max} 2958 (C–H), 2925 (C–H), 1638 (C=O). **HRMS (ESI⁺)** *m/z* calcd for C₂₂H₃₁N₂O⁺ [M+H]⁺ 339.2431; found: 339.2446.

General Procedure 2.4 (GP2.4): One-pot anionic Fries-Smiles rearrangement: A flame-dried round bottom flask was allowed to cool to rt *in vacuo* and refilled with nitrogen. To this was added the required urea **2.41** (1.0 eq.) and anhydrous THF (0.2 M) and the reaction mixture was cooled to –78 °C. *n*-BuLi (1.4 M in hexanes, 1.1 eq.) was added dropwise and the reaction was allowed to stir at –78 °C for 2 h. DMPU (5.0 eq.) was added, and the reaction mixture was allowed to warm up to rt and stir for 4 h. The reaction was quenched with MeOH, and the subsequent solution concentrated *in vacuo*. Purification by flash column chromatography yielded the desired product

N-Methyl-2-(methyl(phenyl)amino)benzamide - 2.48a

Following **GP2.4** on a 0.4 mmol scale, the *title compound* was only observed as trace amounts by ^1H NMR of the crude reaction mixture after quench.

2-((4-Fluorophenyl)(methyl)amino)-N-methylbenzamide - 2.48b

Following **GP2.4** on a 0.75 mmol scale, the *title compound* was isolated as a yellow oil (48 mg, 25%).

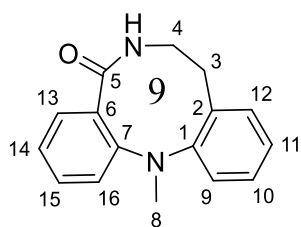
N-Methyl-2-(methyl(naphthalen-1-yl)amino)benzamide – 2.48j

Following **GP2.4** on a 0.4 mmol scale, the *title compound* was isolated as a colourless oil (67 mg, 58%).

Chapter 3

General Procedure 3.1 (GP3.1), Ring opening of anthranilamides: In a flame-dried microwave vial under nitrogen, anthranilamides **3.17** (1 eq.) was added. The vial was capped with a septum, evacuated *in vacuo* and refilled with nitrogen. Dry THF (0.2 M) was added and NaHMDS (1 M in THF, 1.1 eq.) was added dropwise at rt. The vial was sealed, and the reaction mixture was heated to 100 °C under microwave irradiation for 15 min and was quenched with MeOH. The organic phase was evaporated under reduced pressure and the residue was purified by silica gel column chromatography eluting with a gradient of petroleum ether /EtOAc.

13-Methyl-6,7,8,13-tetrahydro-5H-dibenzo[b,h][1,5]diazonin-5-one – 3.18a



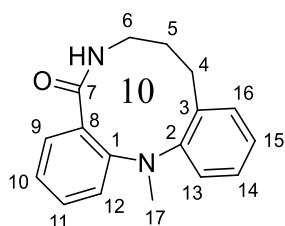
Prepared with modification to **GP3.1** (4 h reaction time at 120 °C) on a 0.4 mmol scale, the *title product* was obtained as a colourless solid (70 mg, 70%). 1:0.15 mixture of conformers. Crystals suitable for X-ray analysis were obtained by vapour diffusion of n-hexane in a saturated solution of the *title compound* in CH_2Cl_2 . **m.p.:** 163 – 164 °C (degradation).

$\delta^1\text{H}$ (400 MHz, CDCl_3) 7.43 (1 H^{maj} + 1 H^{min} , td, J = 7.8, 1.7 Hz, H-15), 7.36 (1 H^{maj} + 1 H^{min} , dd, J = 7.4, 1.7 Hz, H-13), 7.25 (1 H^{maj} + 1 H^{min} , d, J = 7.3 Hz, H-16), 7.22 (1 H^{maj} + 1 H^{min} , td, J = 5.2, 1.5 Hz, H-12), 7.18 (1 H^{maj} , dd, J = 7.3, 1.5 Hz, H-11), 7.14 (1 H^{maj} + 1 H^{min} , td, J = 7.4, 2.1 Hz, H-10), 7.00 (1 H^{maj} + 2 H^{min} , td, J = 7.5, 1.0 Hz, H-14), 6.87 (1 H^{min} , td, J = 7.5, 1.1 Hz), 6.78 (1 H^{maj} , dd, J = 7.6, 1.6 Hz, H-9), 5.87 (1 H^{maj} , d, J = 11.9 Hz, NH), 5.14 (1 H^{min} , d, J = 12.8 Hz, NH), 3.85 ($\text{CH}_\text{A}\text{H}_\text{B}$, 1 H^{maj} + 1 H^{min} , tdd, J = 12.8, 11.8, 2.5 Hz, H-4), 2.41 – 3.34 ($\text{CH}_\text{A}\text{H}_\text{B}$, 1 H^{maj} + 1 H^{min} , m, H-4), 3.29 ($\text{CH}_\text{A}\text{H}_\text{B}$, 1 H^{maj} + 1 H^{min} , td, J = 13.0, 3.8 Hz, H-3), 3.13 (3 H^{min} , s, H-8), 3.05 (3 H^{maj} , s, H-8), 2.72 ($\text{CH}_\text{A}\text{H}_\text{B}$, 1 H^{maj} + 1 H^{min} , dt, J = 13.2, 2.4 Hz, H-3).

$\delta^{13}\text{C}$ (101 MHz, CDCl_3) 173.3 (C-5 $^{\text{min}}$), 173.0 (C-5 $^{\text{maj}}$), 152.2 (C-1 $^{\text{maj}}$), 151.0 (C-7 $^{\text{maj}}$), 148.0 (ArC $^{\text{min}}$), 146.6 (ArC $^{\text{min}}$), 137.9 (ArC $^{\text{min}}$), 136.8 (C-2 $^{\text{maj}}$), 132.5 (ArCH $^{\text{min}}$), 131.9 (ArCH $^{\text{min}}$), 131.3 (C-12 $^{\text{maj}}$), 131.1 (C-15 $^{\text{maj}}$), 131.0 (ArCH $^{\text{min}}$), 129.9 (C-6 $^{\text{maj}}$), 129.3 (ArCH $^{\text{min}}$), 129.2 (C-10 $^{\text{maj}}$), 128.9 (C-13 $^{\text{maj}}$),

128.7 (ArCH^{min}), 128.6 (C-9^{maj}), 128.1 (ArCH^{min}), 128.0 (C-11^{maj}), 124.3 (ArC^{min}), 121.6 (C-14^{maj}), 119.1 (ArCH^{min}), 116.9 (C-16^{maj}), 114.3 (ArCH^{min}), 44.9 (C-4^{maj}), 41.9 (C-8^{maj}), 40.9 (C-4^{min}), 40.3 (C-8^{min}), 35.5 (C-3^{maj}), 34.7 (C-3^{min}). **IR (film, cm⁻¹)** ν_{\max} 3321 (N–H), 3063, 2933 (C–H), 1674 (C=O), 1451, 1308. **HRMS (ESI⁺)** m/z calcd for C₁₇H₁₉N₂O⁺ [M+H]⁺ 267.1492; found 267.1498. Supplementary crystallographic data can be obtained free of charge from The Cambridge Crystallographic Data Centre (CCDC 1571681).

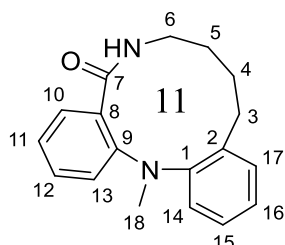
14-Methyl-7,8,9,14-tetrahydrodibenzo[b,i][1,5]diazecin-5(6H)-one – 3.18



Following **GP3.1** on a 0.4 mmol scale, the title product was obtained as a white solid (77 mg, 72%). Following **GP3.1** on a 3.0 mmol scale, the title product was obtained as a white solid (0.63 g, 79%). Following **GP3.1** on a 0.4 mmol scale in 2-Methyltetrahydrofuran, the title product was obtained as an off-white solid (71 mg, 67%). Crystals suitable for X-ray analysis were

obtained by vapour diffusion of n-hexane in a saturated solution of the *title compound* in CH₂Cl₂. **m.p.:** 162 – 164 °C. **$\delta^1\text{H}$ (400 MHz, CDCl₃)** 7.45 – 7.39 (2 H, m, H-9 + H-11), 7.32 (1 H, dd, J = 7.7, 1.7 Hz, H-16), 7.20 (1 H, dd, J = 8.2, 1.0 Hz, H-12), 7.16 (1 H, td, J = 7.7, 1.3 Hz, H-15), 7.09 (1 H, td, J = 7.7, 1.7 Hz, H-14), 7.00 (1 H, td, J = 7.5, 1.0 Hz, H-10), 6.72 (1 H, dd, J = 7.7, 1.3 Hz, H-13), 6.46 (1 H, br. t, J = 7.6 Hz, NH), 3.28 – 3.17 (CH_AH_B, 2 H, m, H-4 + H-6), 3.07 (3 H, s, H-17), 3.05 – 2.99 (CH_AH_B, 1 H, m, H-6), 2.69 (CH_AH_B, 1 H, ddd, J = 14.1, 6.6, 2.3 Hz, H-4), 2.25 – 2.08 (2 H, m, H-5). **$\delta^{13}\text{C}$ (101 MHz, CDCl₃)** 169.7 (C-7), 151.1 (C-2), 149.0 (C-1), 137.2 (C-3), 131.0 (C-11), 130.4 (C-9), 130.3 (C-16), 128.5 (C-8), 128.0 (C-14), 127.1 (C-13), 126.6 (C-15), 121.4 (C-10), 116.9 (C-12), 42.7 (C-17), 37.0 (C-6), 26.3 (C-5), 24.1 (C-4). **IR (film, cm⁻¹)** ν_{\max} 3303 (N–H), 2926 (C–H), 1658 (C=O). **HRMS (ESI⁺)** m/z calcd for C₁₆H₁₆N₂ONa⁺ [M+Na]⁺ 275.115; found: 275.115. Supplementary crystallographic data can be obtained free of charge from The Cambridge Crystallographic Data Centre (CCDC 1571682).

15-Methyl-6,7,8,9,10,15-hexahydro-5H-dibenzo[b,j][1,5]diazacycloundecin-5-one – 3.18c

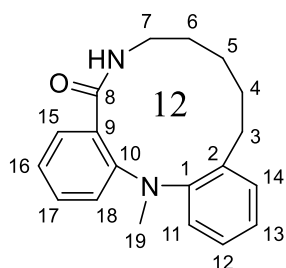


Following **GP3.1** on a 0.4 mmol scale, the title product was obtained as a white solid (92 mg, 82%). Crystals suitable for X-ray analysis were obtained by vapour diffusion of n-hexane in a saturated solution of the *title compound* in CH₂Cl₂. **m.p.:** 171 – 173 °C. **$\delta^1\text{H}$ (400 MHz, CDCl₃)** 7.72 (2 H, dd, J = 7.6, 1.8 Hz, NH + H-10), 7.46 (1 H, td, J = 7.7, 1.7 Hz, H-12),

7.33 (1 H, dd, J = 8.1, 1.1 Hz, H-13), 7.29 (1 H, dt, J = 7.8, 1.2 Hz, H-17), 7.12 (1 H, td, J = 7.5, 1.2 Hz, H-11), 7.08 (1 H, td, J = 7.5, 1.4 Hz, H-16), 6.99 (1 H, td, J = 7.7, 1.6 Hz, H-15), 6.54 (1 H, dd, J = 8.0, 1.3 Hz, H-14), 3.89 – 3.77 (CH_AH_B, 1 H, m, H-6), 3.12 (CH_AH_B, 1 H, ddd, J = 14.9, 13.4, 4.4 Hz, H-3), 3.05 (3 H, s, H-18), 2.89 – 2.79 (CH_AH_B, 1 H, m, H-3),

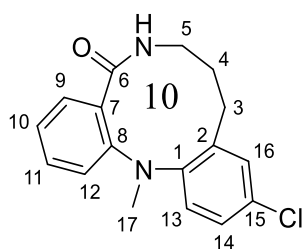
2.80 – 2.71 (CH_AH_B, 1 H, m, H-6), 2.27 – 2.12 (CH_AH_B, 1 H, m, H-4), 2.02 – 1.91 (CH_AH_B, 1 H, m, H-4), 1.62 – 1.40 (2 H, m, H-5). $\delta^{13}\text{C}$ (101 MHz, CDCl₃) 166.8 (C-7), 151.2 (C-1), 148.7 (C-9), 136.1 (C-2), 131.05 (C-10 or C-12), 131.01 (C-10 or C-12), 129.4 (C-8), 129.2 (C-17), 127.4 (C-15), 125.7 (C-14 or C-16), 125.6 (C-14 or C-16), 123.0 (C-11), 119.2 (C-13), 42.6 (C-18), 40.3 (C-7), 28.7 (C-6), 27.1 (C-3), 25.5 (C-5). IR (film, cm⁻¹) ν_{max} 3323 (N–H), 2925 (C–H), 1644 (C=O), 1586, 1483, 1449, 1306 (C–N). HRMS (ESI⁺) m/z calcd for C₁₈H₂₁N₂O⁺ [M+H]⁺ 281.1648; found: 281.1659. Supplementary crystallographic data can be obtained free of charge from The Cambridge Crystallographic Data Centre (CCDC 1571683).

16-Methyl-7,8,9,10,11,16-hexahydrodibenzo[b,k][1,5]diazacyclododecin-5(6H)-one– 3.18d



Following **GP3.1** on a 0.4 mmol scale, the title product was obtained as a white solid (quant.). Crystals suitable for X-ray analysis were obtained in a saturated solution of the *title compound* in toluene. **m.p.:** 137 – 138 °C. $\delta^1\text{H}$ (400 MHz, CDCl₃) 9.10 (1 H, br. s, NH), 8.18 (1 H, dd, J = 7.8, 1.8 Hz, H-15), 7.43 (1 H, ddd, J = 8.2, 7.3, 1.8 Hz, H-17), 7.29 – 7.21 (3 H, m, H-14 + H-16 + H-18), 7.12 (2 H, pd, J = 7.3, 1.8 Hz, H-12 + H-13), 6.96 (1 H, d, J = 7.4 Hz, H-11), 3.85 (CH_AH_B, 1 H, q, J = 9.8 Hz, H-7), 3.13 (3 H, s, H-19), 3.06 – 2.94 (CH_AH_B, 1 H, m, H-7), 2.81 – 2.69 (CH_AH_B, 1 H, m, H-3), 2.69 – 2.57 (CH_AH_B, 1 H, m, H-3), 2.02 – 1.90 (CH_AH_B, 1 H, m, H-4), 1.88 – 1.78 (CH_AH_B, 1 H, m, H-6), 1.77 – 1.66 (CH_AH_B, 2 H, m, H-4 + H-5), 1.62 – 1.46 (CH_AH_B, 1 H, m, H-6), 1.44 – 1.31 (CH_AH_B, 1 H, m, H-5). $\delta^{13}\text{C}$ (101 MHz, CDCl₃) 166.4 (C-8), 149.7 (C-1), 149.3 (C-10), 137.4 (C-2), 132.0 (C-15), 131.7 (C-17), 130.1 (C-14), 129.1 (C-9), 126.9 (C-13), 125.4 (C-12), 124.7 (C-17), 123.9 (C-11), 123.7 (C-16), 44.4 (C-19), 40.3 (C-7), 29.9 (C-4), 28.7 (C-3), 26.5 (C-6), 25.4 (C-5). IR (film, cm⁻¹) ν_{max} 3312 (N–H), 2930, 2864 (C–H), 1650 (C=O), 1532, 1486, 1449, 1290 (C–N). HRMS (ESI⁺) m/z calcd for C₁₉H₂₂N₂O⁺ [M+H]⁺ 317.1624; found: 317.1638. Supplementary crystallographic data can be obtained free of charge from The Cambridge Crystallographic Data Centre (CCDC 1571684).

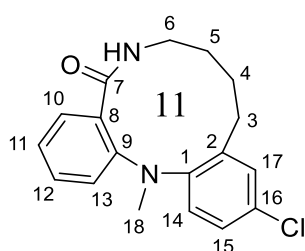
11-Chloro-14-methyl-7,8,9,14-tetrahydrodibenzo[b,i][1,5]diazecin-5(6H)-one –3.18e



Following **GP3.1** on a 0.4 mmol scale, the title product was obtained as a yellow solid (53 mg, 44%), together with recovered starting material (20 mg, 17%). **m.p.:** 217 – 218 °C Mixture of conformers in a 1:0.08 ratio. Only the major conformer is reported. $\delta^1\text{H}$ (400 MHz, CDCl₃) 7.43 – 7.38 (2 H, m, H-9 + H-11), 7.27 (1 H, dd, J = 2.5, 0.7 Hz, H-16), 7.18 (1 H, dd, J = 8.6, 1.0 Hz, H-12), 7.02 (1 H, dd, J = 8.5, 2.6 Hz, H-14), 6.99 (1 H, td, J = 7.5, 1.0 Hz, H-10), 6.64 (1 H, d, J = 8.5 Hz, H-13), 6.44 (1 H, d, J = 8.0 Hz, NH), 3.34 – 3.12 (CH_AH_B, 2 H, m, H-3 + H-5), 3.02 (3 H, s, H-17), 3.02 – 2.96 (CH_AH_B, 1 H, m, H-5),

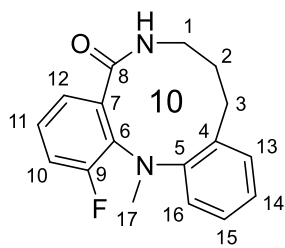
2.63 (CH_AH_B 1 H, ddd, J = 14.1, 6.6, 2.3 Hz, H-3), 2.24 – 2.04 (2 H, m, H-4). $\delta^{13}\text{C}$ (101 MHz, CDCl₃) 169.4 (C-6), 149.6 (C-1), 148.5 (C-8), 139.4 (C-2) 131.8 (C-7), 131.1 (C-9 or C-11), 130.4 (C-9 or C-11), 130.2 (C-16), 128.51 (C-15), 128.46 (C-13), 128.1 (C-14), 121.7 (C-11), 116.9 (C-12), 42.6 (C-17), 36.8 (C-5), 26.2 (C-4), 24.1 (C-3). IR (film, cm⁻¹) ν_{max} 3297 (N–H), 2932, 2874 (C–H), 1648 (C=O), 1600, 1520, 1477, 1321 (C–N), 1108. HRMS (ESI⁺) m/z calcd for C₁₇H₁₇ClN₂ONa⁺ [M+Na]⁺ 323.0927; found: 323.0922.

12-Chloro-15-methyl-6,7,8,9,10,15-hexahydro-5H-dibenzo[b,j][1,5]diazacycloundecin-5-one – 3.18f



Following **GP3.1** on a 0.4 mmol scale, the title product was obtained as a white solid (106 mg, 84%). **m.p.:** 207 – 208 °C. $\delta^1\text{H}$ (400 MHz, CDCl₃) 7.67 (1 H, d, J = 7.6 Hz, H-10), 7.48 (1 H, br. s, NH), 7.45 (1 H, t, J = 7.7 Hz, H-12), 7.30 (1 H, d, J = 8.2 Hz, H-13), 7.24 (1 H, d, J = 2.5 Hz, H-17), 7.12 (1 H, t, J = 7.5 Hz, H-11), 6.94 (1 H, dd, J = 8.6, 2.5 Hz, H-15), 6.48 (1 H, d, J = 8.6 Hz, H-14), 3.83 (CH_AH_B, 1 H, p, J = 5.7 Hz, H-6), 3.16 – 3.04 (CH_AH_B, 1 H, m, H-3), 3.01 (3 H, s, H-18), 2.85 – 2.69 (CH_AH_B, 2 H, m, H-3 + H-6), 2.13 (CH_AH_B, 1 H, dtd, J = 13.6, 8.6, 4.0 Hz, H-4), 1.96 (CH_AH_B, 1 H, tt, J = 11.0, 3.9 Hz, H-4), 1.67 – 1.39 (2 H, m, H-5). $\delta^{13}\text{C}$ (101 MHz, CDCl₃) 166.8 (C-7), 149.8 (C-1), 148.3 (C-9), 138.3 (C-2), 131.14 (C-8), 131.10 (C-12), 131.0 (C-10), 129.4 (C-16), 129.0 (C-17), 127.6 (C-15), 127.2 (C-14), 123.2 (C-11), 119.0 (C-13), 42.7 (C-18), 40.3 (C-6), 28.4 (C-5), 27.1 (C-3), 25.2 (C-5). IR (film, cm⁻¹) ν_{max} 3311 (N–H), 2926 (C–H), 1640 (C=O), 1534, 1476, 1308 (C–N), 1109. HRMS (ESI⁺) m/z calcd for C₁₈H₁₉ClN₂ONa⁺ [M+Na]⁺ 337.1078; found: 337.1067.

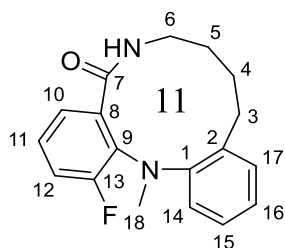
1-Fluoro-14-methyl-7,8,9,14-tetrahydrodibenzo[b,i][1,5]diazecin-5(6H)-one – 3.18g



Prepared with slight modification to **GP3.1** (45 minutes reaction time) on a 0.4 mmol scale, the title product was obtained as a yellow solid (51 mg, 45%), together with recovered starting material (50 mg, 44%). **m.p.:** 197 – 199 °C. $\delta^1\text{H}$ (400 MHz, CDCl₃) 7.28 – 7.23 (2 H, m, H-13 + H-12), 7.20 – 7.11 (2 H, m, H-10 + H-14), 7.08 (1 H, td, J = 7.5, 1.8 Hz, H-15), 7.03 (1 H, tdd, J = 8.1, 4.5, 0.6 Hz, H-11), 6.92 (1 H, dd, J = 7.8, 1.2 Hz, H-16), 6.82 (1 H, br. s, NH), 2.48 – 3.36 (CH_AH_B, 1 H, m, H-1), 3.32 (3 H, d, J = 5.6 Hz, H-17), 3.25 – 3.14 (CH_AH_B, 1 H, m, H-1), 3.06 (CH_AH_B, 1 H, ddd, J = 14.1, 11.5, 4.9 Hz, H-3), 2.73 (CH_AH_B, 1 H, dt, J = 14.2, 4.7 Hz, H-3), 2.30 – 2.16 (CH_AH_B, 1 H, m, H-2), 2.14 – 2.06 (CH_AH_B, 1 H, m, H-2). $\delta^{13}\text{C}$ (101 MHz, CDCl₃) 168.2 (d, J = 3.6 Hz, C-8), 158.2 (d, J = 247.5 Hz, C-9), 149.7 (C-5), 138.3 (C-4), 135.8 (d, J = 9.7 Hz,

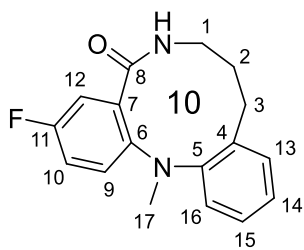
C-6), 134.1 (d, $J = 3.2$ Hz, C-7), 130.9 (C-13), 127.9 (C-15), 127.7 (d, $J = 1.4$ Hz, C-16), 126.5 (C-14), 125.7 (d, $J = 3.0$ Hz, C-12), 124.2 (d, $J = 8.3$ Hz, C-11), 119.1 (d, $J = 22.4$ Hz, C-10), 44.7 (d, $J = 11.6$ Hz, C-17), 37.5 (C-1), 27.7 (C-2), 25.3 (C-3). IR (film, cm^{-1}) ν_{max} 3292 (N-H), 2928 (C-H), 1644 (C=O), 1541, 1455, 1308 (C-N), 1236. HRMS (ESI⁺) m/z calcd for $\text{C}_{17}\text{H}_{17}\text{FN}_2\text{O}^+$ $[\text{M}+\text{Na}]^+$ 307.1217; found: 307.1229.

1-Fluoro-15-methyl-6,7,8,9,10,15-hexahydro-5H-dibenzo[b,j][1,5]diazacycloundecin-5-one – 3.18h



Following **GP3.1** on a 0.4 mmol scale, the title product was obtained as a white solid (93 mg, 78%). **m.p.:** 164 – 166 °C. $\delta^1\text{H}$ (400 MHz, CDCl_3) 8.17 (1 H, br. s, NH), 7.64 (1 H, ddd, $J = 7.5, 1.9, 0.9$ Hz, H-10), 7.31 (1 H, dt, $J = 7.6, 1.1$ Hz, H-17), 7.29 – 7.17 (2 H, m, H-11 + H-12), 7.10 (1 H, td, $J = 7.4, 1.5$ Hz, H-16), 7.04 (1 H, td, $J = 7.6, 1.8$ Hz, H-15), 6.78 (1 H, dt, $J = 7.9, 1.6$ Hz, H-14), 4.05 – 3.90 ($\text{CH}_\text{A}\text{H}_\text{B}$, 1 H, m, H-6), 3.30 (3 H, d, $J = 5.4$ Hz, H-18), 3.11 ($\text{CH}_\text{A}\text{H}_\text{B}$, 1 H, td, $J = 14.5, 14.1, 4.5$ Hz, H-3), 2.94 – 2.89 ($\text{CH}_\text{A}\text{H}_\text{B}$, 1 H, m, H-6), 2.89 – 2.81 ($\text{CH}_\text{A}\text{H}_\text{B}$, 1 H, m, H-3), 1.28 – 2.14 ($\text{CH}_\text{A}\text{H}_\text{B}$, 1 H, m, H-4), 2.02 – 1.89 ($\text{CH}_\text{A}\text{H}_\text{B}$, 1 H, m, H-4), 1.63 – 1.51 ($\text{CH}_\text{A}\text{H}_\text{B}$, 1 H, m, H-5), 1.44 – 1.30 ($\text{CH}_\text{A}\text{H}_\text{B}$, 1 H, m, H-5). $\delta^{13}\text{C}$ (101 MHz, CDCl_3) 165.5 (d, $J = 3.5$ Hz, C-7), 160.3 (d, $J = 249.2$ Hz, C-13), 149.2 (d, $J = 0.9$ Hz, C-1), 135.3 (d, $J = 10.7$ Hz, C-9), 135.1 (C-2), 134.1 (d, $J = 2.9$ Hz, C-8), 129.4 (C-17), 127.3 (C-15), 126.6 (d, $J = 2.9$ Hz, C-10), 126.0 (d, $J = 8.7$ Hz, C-11), 125.5 (d, $J = 1.3$ Hz, C-14), 125.4 (C-16), 119.2 (d, $J = 22.0$ Hz, C-12), 44.4 (d, $J = 11.1$ Hz, C-18), 40.2 (C-6), 29.1 (C-4), 27.5 (C-3), 25.3 (C-5). IR (film, cm^{-1}) ν_{max} 3312 (N-H), 2920 (C-H), 1641 (C=O), 1539, 1457, 1307 (C-N), 1237. HRMS (ESI⁺) m/z calcd for $\text{C}_{18}\text{H}_{19}\text{FN}_2\text{O}^+$ $[\text{M}+\text{H}]^+$ 321.1374; found: 321.1381.

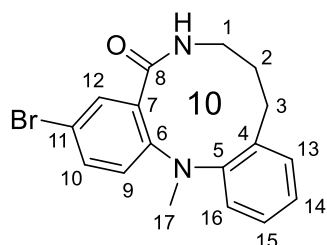
3-Fluoro-14-methyl-7,8,9,14-tetrahydrodibenzo[b,i][1,5]diazecin-5(6H)-one – 3.18i



Following **GP3.1** on a 0.4 mmol scale, the title product was obtained as a white solid (89 mg, 78%). **m.p.:** 159 – 161 °C. $\delta^1\text{H}$ (400 MHz, CDCl_3) 7.30 (1 H, dd, $J = 7.6, 1.6$ Hz, H-13), 7.19 – 7.13 (3 H, m, H-9 + H-12 + H-14), 7.12 – 7.05 (2 H, m, H-10 + H-15), 6.70 (1 H, br. s, NH), 6.68 (1 H, dd, $J = 7.9, 1.4$ Hz, H-16), 3.28 – 3.15 ($\text{CH}_\text{A}\text{H}_\text{B}$, 2 H, m, H-1 + H-3), 3.04 (3 H, s, H-17), 3.04 – 2.99 ($\text{CH}_\text{A}\text{H}_\text{B}$, 1 H, m, H-1), 2.69 ($\text{CH}_\text{A}\text{H}_\text{B}$, 1 H, ddd, $J = 14.1, 6.5, 2.4$ Hz, H-3), 2.26 – 2.06 (2 H, m, H-2). $\delta^{13}\text{C}$ (101 MHz, CDCl_3) 168.1 (d, $J = 1.9$ Hz, C-8), 157.9 (d, $J = 241.8$ Hz, C-11), 150.9 (C-5), 145.3 (d, $J = 2.5$ Hz, C-6), 137.2 (C-4), 130.4 (C-13), 130.0 (d, $J = 5.7$ Hz, C-7), 128.0 (C-15), 126.8 (C-16), 126.6 (C-14), 118.4 (d, $J = 7.5$ Hz, C-9), 117.4 (d, $J = 10.5$ Hz, C-12), 117.2 (d, $J = 9.0$ Hz, C-10), 43.1 (C-17), 37.1 (C-1), 26.3 (C-2), 24.1 (C-3). IR (film, cm^{-1}) ν_{max} 3306 (N-H), 2934, 2870 (C-H),

1650 (C=O), 1522, 1482. **HRMS (ESI⁺)** m/z calcd for C₁₇H₁₇FN₂ONa⁺ [M+Na]⁺ 307.1217; found: 307.1209.

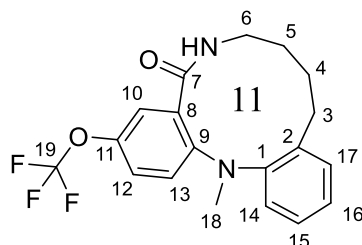
3-Bromo-14-methyl-7,8,9,14-tetrahydrodibenzo[b,i][1,5]diazecin-5(6H)-one – 3.18j



Following **GP3.1** on a 0.4 mmol scale, the title product was obtained as a yellow solid (72 mg, 52%) together with recovered starting material (31 mg, 22%). **m.p.:** 184 – 185 °C. **$\delta^1\text{H}$ (400 MHz, CDCl₃)** 7.54 – 7.46 (2 H, m, H-10 + H-12), 7.31 (1 H, dd, J = 8.0, 1.4 Hz, H-13), 7.18 (1 H, td, J = 7.5, 1.4, H-14), 7.10 (1 H, td, J = 7.7, 1.7 Hz, H-15),

7.06 (1 H, d, J = 8.3 Hz, H-9), 6.70 (1 H, dd, J = 7.9, 1.4 Hz, H-16), 6.36 (1 H, d, J = 7.9 Hz, NH), 3.25 – 3.14 (CH_AH_B, 2 H, m, H-1 + H-3), 3.04 (3 H, s, H-17), 3.03 – 2.96 (CH_AH_B, 1 H, m, H-1), 2.68 (CH_AH_B, 1 H, ddd, J = 14.1, 6.5, 2.5 Hz, H-3), 2.24 – 2.07 (2 H, m, H-2). **$\delta^{13}\text{C}$ (101 MHz, CDCl₃)** 168.0 (C-8), 150.5, 148.1, 137.2 (C-4), 133.6 (C-12), 133.1 (C-10), 130.4 (C-13), 130.2 (C-7), 128.1 (C-15), 127.0 (C-16), 126.9 (C-14), 118.6 (C-9), 114.0 (C-11), 42.8 (C-17), 37.0 (C-1), 26.1 (C-2), 24.0 (C-3). **IR (film, cm⁻¹)** ν_{max} 3300 (N–H), 2928 (C–H), 1649 (C=O), 1477, 1321 (C–N), 1104. **HRMS (ESI⁺)** m/z calcd for C₁₇H₁₇N₂OBrNa⁺ [M+Na]⁺ 367.0416; found: 367.0425.

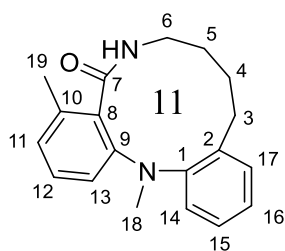
15-Methyl-3-(trifluoromethoxy)-6,7,8,9,10,15-hexahydro-5H-dibenzo[b,j][1,5]diazacycloundecin-5-one – 3.18k



Following **GP3.1** on a 0.4 mmol scale, the title product was obtained as a white solid (120 mg, 82%). **m.p.:** 192 – 193 °C. **$\delta^1\text{H}$ (400 MHz, CDCl₃)** 7.70 (1 H, br. d, J = 8.7 Hz, NH), 7.58 (1 H, d, J = 2.6 Hz, H-10), 7.37 – 7.20 (3 H, m, H-12 + H-13 + H-17), 7.10 (1 H, td, J = 7.5, 1.4, H-16), 7.01 (1 H, td, J = 7.7, 1.6 Hz, H-15),

6.53 (1 H, dd, J = 8.0, 1.4 Hz, H-14), 3.89 – 3.72 (CH_AH_B, 1 H, m, H-6), 3.18 – 2.97 (4 H, m, H-3 + H-18), 2.83 (CH_AH_B, 1 H, dt, J = 15.0, 4.5, H-3), 2.76 (CH_AH_B, 1 H, ddt, J = 10.5, 6.2, 3.6 Hz, H-6), 2.19 (CH_AH_B, 1 H, tq, J = 13.9, 4.9 Hz, H-4), 2.04 – 1.91 (CH_AH_B, 1 H, m, H-4), 1.59 – 1.41 (2 H, m, J = 12.5, 9.6, 5.5, 2.6 Hz, H-5). **$\delta^{13}\text{C}$ (101 MHz, CDCl₃)** 165.7 (C-7), 150.7 (C-1), 147.4 (C-9), 144.64 (q, J_F 2.1 Hz, C-11), 136.2 (C-2), 130.8 (C-8), 129.3 (C-17), 127.6 (C-15), 126.0 (C-16), 125.6 (C-14), 123.8 (C-10), 123.4 (C-12), 120.6 (q, J_F 257.1 Hz, C-19), 120.3 (C-13), 43.1 (C-18), 40.4 (C-6), 28.5 (C-4), 27.1 (C-3), 25.4 (C-5). **IR (film, cm⁻¹)** ν_{max} 3247 (N–H), 3082, 2938 (C–H), 1631 (C=O), 1256, 1218, 1158, 1151. **HRMS (ESI⁺)** m/z calcd for C₁₉H₁₉N₂O₂F₃Na⁺ [M+Na]⁺ 387.1291; found: 387.1293.

4,15-Dimethyl-6,7,8,9,10,15-hexahydro-5H-dibenzo[b,j][1,5]diazacycloundecan-5-one-3.18l



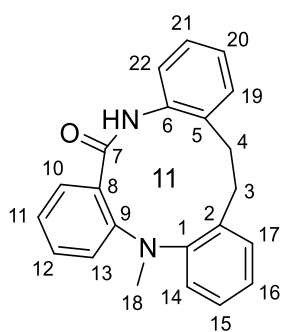
Following **GP3.1** on a 0.4 mmol scale, the title product was obtained as a white solid (67 mg, 57%), together with recovered starting material (27 mg, 23%). Crystals suitable for X-ray analysis were obtained by vapour diffusion of n-hexane in a saturated solution of the *title compound* in CH₂Cl₂.

m.p.: 203 – 204 °C. **$\delta^1\text{H}$ (400 MHz, CD₃OD)** 7.29 (1 H, d, J = 7.9 Hz, H-17),

7.26 (1 H, t, J = 7.8 Hz, H-12), 7.13 (1 H, d, J = 8.1 Hz, H-13), 7.08 (1 H, td, J = 7.5, 1.4 Hz, H-16), 6.99 (1 H, tdd, J = 7.3, 1.7, 0.8 Hz, H-15), 6.83 (1 H, dt, J = 7.5, 0.9 Hz, H-11), 6.68 (1 H, dd, J = 7.9, 1.4 Hz, H-14), 3.50 (CH_AH_B, 1 H, ddd, J = 13.7, 5.0, 2.0 Hz, H-6), 2.41 (CH_AH_B, 1 H, ddd, J = 14.7, 13.5, 4.4 Hz, H-3), 2.99 (3 H, s, H-18), 2.81 (CH_AH_B, 1 H, ddd, J = 13.4, 11.3, 1.8 Hz, H-6), 2.66 (CH_AH_B, 1 H, dt, J = 14.7, 4.4, H-3), 2.29 – 2.19 (CH_AH_B, 1 H, m, H-4), 2.18 (3 H, s, H-19), 1.98 – 1.88 (CH_AH_B, 1 H, m, H-4), 1.82 (CH_AH_B, 1 H, dtt, J = 14.1, 11.5, 2.4 Hz, H-5), 1.42 – 1.25 (CH_AH_B, 1 H, m, H-5).

$\delta^{13}\text{C}$ (101 MHz, CD₃OD) 170.7 (C-7), 152.4 (C-1), 150.0 (C-9), 138.8 (C-2), 138.3 (C-10), 131.3 (C-8), 130.5 (C-12), 129.9 (C-17), 128.0 (C-15), 127.6 (C-14), 126.3 (C-16), 124.4 (C-11), 116.9 (C-13), 42.9 (C-18), 42.4 (C-6), 29.1 (C-4), 27.4 (C-3), 24.2 (C-5), 20.0 (C-19). **IR (film, cm⁻¹)** ν_{max} 3319 (N–H), 2920, 2856 (C–H), 1641 (C=O), 1521, 1464, 1317 (C–N). **HRMS (ESI⁺)** m/z calcd for C₁₉H₂₂N₂ONa⁺ [M+Na]⁺ 317.1624; found: 317.1630. Supplementary crystallographic data can be obtained free of charge from The Cambridge Crystallographic Data Centre (CCDC 1571685).

5-Methyl-5,11,16,17-tetrahydro-10H-tribenzo[b,f,j][1,5]diazacycloundecin-10-one – 3.18m

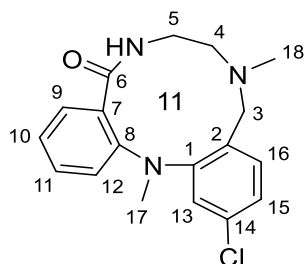


Following **GP3.1** on a 0.4 mmol scale, the title product was obtained as an off-white solid (129 mg, 98%). **m.p.:** 189 – 191 °C. **$\delta^1\text{H}$ (400 MHz, CDCl₃)**

10.19 (1 H, br. s, NH), 8.06 (1 H, dd, J = 8.1, 1.3 Hz, ArCH), 7.97 (1 H, dd, J = 7.7, 1.8 Hz, ArCH), 7.54 (1 H, ddd, J = 8.1, 7.3, 1.8 Hz, ArCH), 7.40 (1 H, dd, J = 8.2, 1.0 Hz, ArCH), 7.26 – 7.21 (2 H, m, ArCH), 7.20 – 7.14 (1 H, m, ArCH), 7.02 (2 H, qd, J = 7.5, 1.8 Hz, ArCH), 6.86 – 6.77 (3 H, m, ArCH), 3.57 – 2.42 (CH_AH_B, 2 H, m, CH₂), 3.35 (3 H, s, CH₃), 2.99 – 2.84 (CH_AH_B, 2 H, m, CH₂).

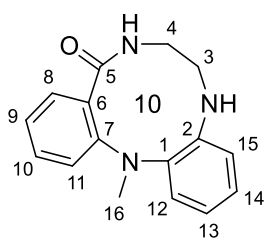
$\delta^{13}\text{C}$ (101 MHz, CDCl₃) 164.3 (C=O), 150.8 (ArC), 148.5 (ArC), 136.6 (ArC), 134.4 (ArC), 133.9 (ArCH), 132.1 (ArCH), 132.0 (ArCH), 129.5 (ArC), 129.4 (ArCH), 128.4 (ArC), 128.3 (ArCH), 127.6 (ArCH), 125.5 (ArCH), 124.5 (ArCH), 123.6 (ArCH), 123.4 (ArCH), 120.3 (ArCH), 119.9 (ArCH), 41.5 (CH₃), 36.5 (CH₂), 29.4 (CH₂). **IR (film, cm⁻¹)** ν_{max} 3345 (N–H), 3064 (C–H), 2944 (C–H), 1678 (C=O), 1592, 1539, 1455, 1327 (C–N), 1303. **HRMS (ESI⁺)** m/z calcd for C₂₂H₂₁N₂O⁺ [M+H]⁺ 329.1648; found: 329.1654. Supplementary crystallographic data can be obtained free of charge from The Cambridge Crystallographic Data Centre (CCDC 1576821).

13-Chloro-9,15-dimethyl-6,7,8,9,10,15-hexahydro-5H-dibenzo[f,i][1,4,8]triazacycloundecin-5-one – 3.18n



Following **GP3.1** on a 0.4 mmol scale, the title product was obtained as an off-white solid (119 mg, 91%). **m.p.:** 191 – 193 °C. **$\delta^1\text{H}$ (400 MHz, CDCl_3)** 7.66 (1 H, dd, J = 7.6, 1.7 Hz, H-9), 7.55 (1 H, br. s, NH), 7.49 – 7.45 (1 H, m, H-11), 7.44 (1 H, d, J = 8.1 Hz, H-16), 7.31 (1 H, dd, J = 8.1, 1.0 Hz, H-12), 7.15 (1 H, td, J = 7.5, 1.1 Hz, H-10), 7.05 (1 H, dd, J = 8.3, 2.2 Hz, H-15), 6.50 (1 H, d, J = 2.2 Hz, H-13), 3.99 ($\text{CH}_\text{A}\text{H}_\text{B}$, 1 H, d, J = 13.3 Hz, H-3), 3.63 ($\text{CH}_\text{A}\text{H}_\text{B}$, 1 H, d, J = 13.3 Hz, H-3), 3.58 – 3.50 ($\text{CH}_\text{A}\text{H}_\text{B}$, 1 H, m, H-5), 3.14 – 3.07 ($\text{CH}_\text{A}\text{H}_\text{B}$, 1 H, m, H-5), 3.05 (3 H, s, H-17), 2.77 ($\text{CH}_\text{A}\text{H}_\text{B}$, 1 H, ddd, J = 13.4, 10.7, 2.4 Hz, H-4), 2.61 (3 H, s, H-18), 2.44 ($\text{CH}_\text{A}\text{H}_\text{B}$, 1 H, ddd, J = 14.6, 4.1, 2.0 Hz, H-4). **$\delta^{13}\text{C}$ (101 MHz, CDCl_3)** 166.9 (C-6), 151.9 (C-1), 147.6 (C-8), 133.8 (C-14), 132.5 (C-16), 131.9 (C-2), 131.3 (C-12), 131.1 (C-9), 129.9 (C-7), 125.84 (C-13 or C-15), 125.78 (C-13 or C-15), 123.8 (C-10), 119.9 (C-12), 55.4 (C-3), 51.4 (C-4), 43.5 (C-18), 42.8 (C-17), 35.1 (C-5). **IR (film, cm^{-1})** ν_{max} 3300 (N–H), 2926 (C–H), 1637 (C=O), 1537, 1472, 1306 (C–N). **HRMS (ESI⁺)** m/z calcd for $\text{C}_{18}\text{H}_{21}\text{ClN}_2\text{O}^+$ $[\text{M}+\text{H}]^+$ 330.1368; found: 330.1373.

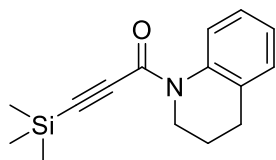
14-Methyl-5,7,8,14-tetrahydrodibenzo[b,i][1,4,7]triazecin-9(6H)-one - 3.18o



In a flame-dried microwave vial under nitrogen, *tert*-butyl 4-(2-(methyl amino)benzoyl)-3,4-dihydroquinoxaline-1(2H)-carboxylate **4.17o** (147 mg, 0.4 mmol, 1 eq.) was added. The vial was capped with a septum, evacuated *in vacuo* and refilled with nitrogen. Dry THF (2 mL) was added and NaHMDS (1 M in THF, 0.8 mmol, 2.0 eq., 0.8 mL) was added dropwise at rt. The vial was sealed, and the reaction mixture was heated to 100 °C under microwave irradiation for 60 min. The vial was opened to air and hydrochloric acid (aq. 6 N, 2 mL) was added. The vial was sealed and stirred vigorously at 80 °C in an oil bath for 30 min. The reaction mixture was poured onto aqueous sodium bicarbonate (20 mL) and extracted with EtOAc (2 × 20 mL). The combined organic phases were washed with brine, evaporated under reduced pressure and the residue was purified by silica gel column chromatography eluting with a gradient of $\text{CH}_2\text{Cl}_2/\text{MeOH}$ 20:1 to 10:1. The fractions containing the product were evaporated under reduced pressure to give the title product as a yellow oil (58 mg, 54%). **$\delta^1\text{H}$ (400 MHz, CDCl_3)** 7.73 (1 H, dd, J = 8.0, 1.7 Hz, H-8), 7.38 – 7.29 (1 H, m, H-10), 7.23 – 7.18 (1 H, m, H-15), 7.13 (2 H, d, J = 3.8 Hz, H-12 + H-13), 7.11 – 7.04 (1 H, m, H-14), 7.01 (2 H, d, J = 7.9 Hz, H-9 + H-11), 4.61 ($\text{CH}_\text{A}\text{H}_\text{B}$, 1 H, ddd, J = 13.5, 7.5, 5.6 Hz, H-4), 3.82 ($\text{CH}_\text{A}\text{H}_\text{B}$, 1 H, dt, J = 13.9, 5.4 Hz, H-4), 3.71 (2 H, br. s, 2 * NH), 3.29 (3 H, s, H-16), 3.17 – 3.03 ($\text{CH}_\text{A}\text{H}_\text{B}$, 1 H, m, H-3), 2.99 – 2.85 ($\text{CH}_\text{A}\text{H}_\text{B}$, 1 H, m, H-3). **$\delta^{13}\text{C}$ (101 MHz, CDCl_3)** 169.7 (C-5), 154.1 (C-7), 149.3 (C-1), 135.6 (C-2), 132.2 (C-10), 131.9 (C-8), 127.8 (C-6), 126.4 (C-12), 124.8 (C-14),

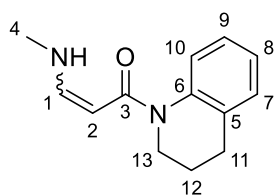
124.3 (C-15), 123.3 (C-9), 118.7 (C-13), 115.9 (C-11), 51.9 (C-4), 40.0 (C-3), 36.8 (C-16). IR (film, cm^{-1}) ν_{max} 2927 (C–H), 1627 (C=O), 1456, 1394, 1248. HRMS (ESI⁺) m/z calcd for $\text{C}_{16}\text{H}_{18}\text{N}_3\text{O}^+$ $[\text{M}+\text{H}]^+$ 268.1444; found: 268.1454.

1-(3,4-Dihydroquinolin-1(2H)-yl)-3-(trimethylsilyl)prop-2-yn-1-one - 3.23



To a solution of 3-(trimethylsilyl)propynoic acid (0.59 g, 4.1 mmol, 1.0 eq.) and tetrahydroisoquinoline (0.61 mL, 5.0 mmol, 1.2 eq.) in CH_2Cl_2 (8.2 mL, 0.5 M) at 0 °C was added DCC (0.93 g, 4.5 mmol, 1.1 eq.) and DMAP (50 mg, 0.41 mmol, 0.1 eq.) and the reaction mixture was stirred at rt for 3 h. The slurry was filtered over Celite and rinsed with ethyl acetate. The combined organic phases were washed with HCl (1 M aq.), brine, dried over MgSO_4 , filtered and concentrated under reduced pressure and the residue was purified by silica gel column chromatography to give the title product as a colourless oil (0.60 g, 60%). Mixture of slowly interconverting rotamers in a 1:0.8 ratio. Major/minor ^{13}C peaks could not be distinguished. $\delta^1\text{H}$ (400 MHz, CDCl_3) δ 7.98 (1 H^{min} , d, J = 8.1 Hz, ArCH), 7.65 (1 H^{maj} , br. s, ArCH), 7.14 (3 $\text{H}^{\text{maj+min}}$, br. s, ArCH), 4.06 (2 H^{min} , br. s, NCH_2), 3.84 (2 H^{maj} , br. t, J = 5.6 Hz, NCH_2), 2.85 (2 H^{min} , br. s, NCH_2CH_2), 2.76 (2 H^{maj} , br. t, J = 7.0 Hz, NCH_2CH_2), 2.05 (2 H^{min} , br. s, CCH_2), 1.97 (2 H^{maj} , br. s, CCH_2), 0.27 (9 H^{min} , br. s, $\text{Si}(\text{CH}_3)_3$), 0.15 (9 H^{maj} , br. s, $\text{Si}(\text{CH}_3)_3$). $\delta^{13}\text{C}$ (101 MHz, CDCl_3) . 152.8 ($\text{C}=\text{O}^{\text{maj+min}}$), 137.6 (ArC^{maj}), 137.0 (ArC^{min}), 132.8 ($\text{ArC}^{\text{maj+min}}$), 129.1 (ArCH^{min}), 128.3 (ArCH^{maj}), 126.1 (ArCH^{min}), 125.9 (ArCH^{maj}), 125.5 (ArCH^{maj}), 125.1 (ArCH^{min}), 124.9 (ArCH^{maj}), 124.4 (ArCH^{min}), 98.7 ($\text{C}\equiv\text{C}^{\text{maj}}$), 97.7 ($\text{C}\equiv\text{C}^{\text{min}}$), 97.4 ($\text{C}\equiv\text{C}^{\text{maj}}$), 96.9 ($\text{C}\equiv\text{C}^{\text{min}}$), 47.5 ($\text{NCH}_2^{\text{min}}$), 42.8 ($\text{NCH}_2^{\text{maj}}$), 27.0 ($\text{CCH}_2^{\text{maj+min}}$), 23.6 ($\text{NCH}_2\text{CH}_2^{\text{maj+min}}$), -0.5 ($\text{Si}(\text{CH}_3)_3^{\text{min}}$), -0.8 ($\text{Si}(\text{CH}_3)_3$).

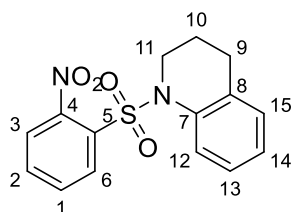
1-(3,4-Dihydroquinolin-1(2H)-yl)-3-(methylamino)prop-2-en-1-one – 3.24



To a solution of 1-(3,4-dihydroquinolin-1(2H)-yl)-3-(trimethylsilyl)prop-2-yn-1-one **3.23** (0.47 g, 1.9 mmol, 1.0 eq.) in MeOH (18 mL, 0.1 M) was added MeNH_2 (8 M in ethanol, 0.46 mL, 3.7 mmol, 2.0 eq.) and the reaction mixture was stirred at rt for 18 h. The reaction mixture was concentrated under reduced pressure and the residue was purified by silica gel column chromatography to give the title product as a yellow oil (0.40 g, 99%). Mixture of Z/E isomers in a 1:0.3 ratio. $\delta^1\text{H}$ (400 MHz, CDCl_3) 8.42 (1 H^{Z} , br. s, NH), 7.63 (1 H^{E} , dd, J = 12.8, 7.5 Hz, H-2), 7.36 (1 H^{Z} , dd, J = 8.3, 1.1 Hz, H-10), 7.33 (1 H^{E} , dd, J = 8.4, 1.3 Hz, H-10), 7.20 – 7.07 (2 H^{Z} + 2 H^{E} m, H-7 + H-9), 7.01 (1 H^{Z} + 1 H^{E} , qd, J = 7.6, 7.0, 1.3 Hz, H-8), 6.49 (1 H^{Z} , dd, J = 12.7, 8.2 Hz, H-1), 5.19 (1 H^{E} , d, J = 12.8 Hz, H-2), 4.88 (1 H^{Z} , d, J = 8.2 Hz, H-2), 4.58 (1 H^{E} , s, NH), 3.82 (2 H^{E} , t, J = 5.5 Hz, H-13), 3.75 (2 H^{Z} , t, J = 5.5 Hz, H-13), 2.93 (3 H^{Z} , d, J = 5.0 Hz, H-4), 2.74 – 2.63 (2 H^{Z} + 2 H^{E} , m, H-11), 2.02 – 1.87 (2 H^{Z} + 2 H^{E} , m, H-12). $\delta^{13}\text{C}$ (101 MHz, CDCl_3) 170.8 (C-3^Z), 168.9 (C-3^E), 152.0 (C-2^Z), 148.9 (C-2^E), 140.2 (C-6^E), 140.0 (C-6^Z), 132.7 (C-5^E),

132.4 (C-5^Z), 128.4 (C-9^{Z+E}), 125.7 (C-7^Z), 125.6 (C-7^E), 125.3 (C-10^E), 125.1 (C-10^Z), 124.0 (C-8^E), 123.9 (C-8^Z), 88.2 (C-1^E), 83.6 (C-1^Z), 42.9 (C-13^E), 42.6 (C-13^Z), 34.9 (C-4^{Z+E}), 27.22 (C-11^E), 27.20 (C-11^Z), 24.43 (C-12^E), 24.38 (C-12^Z).

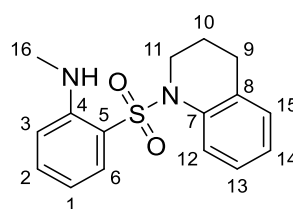
1-((2-Nitrophenyl)sulfonyl)-1,2,3,4-tetrahydroquinoline – 3.27



To a solution of 2-nitrobenzenesulfonyl chloride (1.0 g, 4.7 mmol, 1.0 eq.) in CH₂Cl₂ (12 mL, 0.4 M) was sequentially added pyridine (0.76 mL, 9.4 mmol, 2.0 eq.) and 1,2,3,4-Tetrahydroquinoline (0.70 mL, 5.6 mmol, 1.2 eq.) at 0 °C before warming to rt and stirring for 20 h. The reaction mixture was diluted in CH₂Cl₂ and washed with HCl (1 M aq.), sat. NaHCO₃

(aq.) and brine. The combined organic phases were dried over MgSO₄, filtered and concentrated *in vacuo*. The crude residue obtained was purified by flash column chromatography to give the *title compound* (0.88 g, 59%) as a light brown solid. **¹H (400 MHz, CDCl₃)** 7.73 – 7.65 (2 H, m, H-2 + H-3), 7.60 (1 H, dd, *J* = 8.0, 1.4 Hz, H-6), 7.56 (1 H, td, *J* = 7.7, 1.4 Hz, H-1), 7.52 (1 H, dd, *J* = 8.0, 1.3 Hz, H-12), 7.16 (1 H, td, *J* = 8.2, 7.6, 2.4 Hz, H-13), 7.13 – 7.06 (2 H, m, H-14 + H-15), 3.86 (2 H, t, *J* = 5.1 Hz, H-11), 2.63 (2 H, t, *J* = 5.8 Hz, H-9), 1.92 – 1.83 (2 H, m, H-10). **¹³C (101 MHz, CDCl₃)** 148.1 (C-4), 136.5 (C-7), 133.9 (C-2), 133.2 (C-5), 131.7 (C-1), 131.2 (C-8), 130.6 (C-3), 129.4 (C-15), 126.7 (C-13), 125.6 (C-14), 124.20 (C-6 or C-12), 124.19 (C-6 or C-12), 46.7 (C-11), 26.6 (C-9), 22.6 (C-10). **HRMS *m/z* (ESI⁺)** *m/z* calcd for C₁₅H₁₅N₂O₂S⁺ [M+H]⁺ requires: 319.0747; found: 319.0756.

1-((2-Nitrophenyl)sulfonyl)-2,3,4,5-tetrahydro-1H-benzo[b]azepine– 3.28

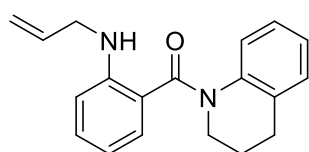


Pd/C (10 wt. % loading, 0.08 gm 1 mol%) was suspended in a solution of **3.27** (0.84 g, 2.6 mmol, 1.0 eq.) in EtOH (13 mL, 0.2 M) under nitrogen.

Nitrogen was bubbled through the solution for 15 mins. The contents of the flask were placed under a hydrogen atmosphere using a two-way three-necked tap with a balloon of hydrogen attached. The solution was saturated with hydrogen three times using a vacuum/hydrogen cycle. The reaction was stirred under a hydrogen atmosphere for 20 h. The crude reaction solution was filtered through a pad of Celite and washed with MeOH. The resulting filtrate was concentrated *in vacuo* to give the aniline which was taken onto the next step (0.75 g, quant.). To a solution of the aniline (0.75 g, 2.6 mmol, 1.0 eq.) in 1,4-dioxane (26 mL, 0.1 M) was added Cu(OAc)₂ (1.2 g, 6.5 mmol, 2.5 eq.) and pyridine (0.75 mL, 9.1 mmol, 3.5 eq.) at rt under an atmosphere of air. The reaction mixture was stirred for 15 min before methylboronic acid (0.39 g, 6.5 mmol, 2.5 eq.) was added and the reaction mixture heated to reflux for 4 h. The reaction was cooled to rt and filtered through a plug of Celite, washing with EtOAc. The resulting filtrate was concentrated *in vacuo* to give a crude residue, which was purified by flash column chromatography to give the *title compound* (0.36 g, 46%) as a yellow solid. **m.p.:** 105 – 107 °C. **¹H (400 MHz, CDCl₃)**

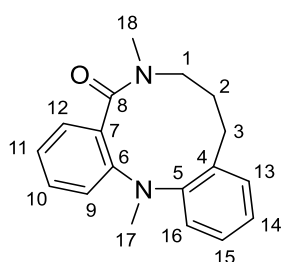
7.64 (1 H, dd, $J = 8.1, 1.2$ Hz, H-15), 7.52 (1 H, dd, $J = 8.0, 1.6$ Hz, H-6), 7.44 – 7.29 (1 H, m, H-3), 7.17 (1 H, tdt, $J = 7.1, 1.7, 0.9$ Hz, H-14), 7.06 (1 H, td, $J = 7.3, 1.2$ Hz, H-13), 7.04 – 6.99 (1 H, m, H-12), 6.60 (1 H, td, $J = 7.3, 1.2$ Hz, H-1), 6.57 (1 H, d, $J = 8.5$ Hz, H-2), 5.64 (1 H, br. s, NH), 3.75 – 3.68 (2 H, m, H-11), 2.56 (3 H, d, $J = 5.0$ Hz, H-16), 2.50 (2 H, t, $J = 5.8$ Hz, H-9), 1.70 – 1.60 (2 H, m, H-10). $\delta^{13}\text{C}$ (101 MHz, CDCl_3) 147.5 (C-4), 137.6 (C-7), 134.6 (C-3), 131.4 (C-8), 130.5 (C-6), 129.0 (C-12), 126.3 (C-14), 125.4 (C-15), 125.2 (C-13), 120.8 (C-5), 115.2 (C-1), 111.5 (C-2), 46.1 (C-11), 29.9 (C-16), 26.4 (C-9), 21.5 (C-10).

(2-(Allylamino)phenyl)(3,4-dihydroquinolin-1(2H)-yl)methanone – 3.31



To a solution of (2-aminophenyl)(3,4-dihydroquinolin-1(2H)-yl)methanone **3.30**^[178] (0.50 g, 2.0 mmol, 1.0 eq.) and allyl bromide (0.21 mL, 2.4 mmol, 1.2 eq.) in MeCN (4.0 mL, 0.5 M) at 0 °C was added K_2CO_3 (0.28 g, 2.0 mmol, 1.0 eq.). The reaction mixture was heated to 60 °C for 20 h, cooled to rt and filtered through a plug of Celite, washing with EtOAc. The resulting filtrate was concentrated *in vacuo* to give a crude residue, which was purified by flash column chromatography to give the *title compound* (0.35 g, 60%) as a colourless oil. Mixture of rotamers in a 1:0.4 ratio. ^1H NMR of the minor rotamer is broad and overlaps with the major species. $\delta^1\text{H}$ (400 MHz, CDCl_3) 7.19 – 7.14 (1 H, m, ArCH), 7.14 – 7.11 (1 H, m, ArCH), 7.05 (1 H, td, $J = 7.5, 1.1$ Hz, ArCH), 6.99 (1 H, td, $J = 7.4, 1.5$ Hz, ArCH), 6.92 (1 H, td, $J = 7.6, 7.1, 1.6$ Hz, ArCH), 6.88 – 6.85 (1 H, m, ArCH), 6.84 (1 H, dd, $J = 7.7, 1.7$ Hz, ArCH), 6.66 (1 H, dd, $J = 8.4, 1.0$ Hz, ArCH), 6.41 (1 H, td, $J = 7.5, 1.1$ Hz, ArCH), 6.05 – 5.88 (1 H, m, NHCH_2CH), 5.30 (1 H, ddd, $J = 17.2, 3.5, 1.7$ Hz, $\text{CH}=\text{CH}_2$), 5.17 (1 H, ddd, $J = 17.2, 3.5, 1.7$ Hz, $\text{CH}=\text{CH}_2$), 3.94 – 3.84 (2 H, m, NCH_2CH_2), 3.81 (2 H, br. s, NHCH_2), 2.83 (2 H, t, $J = 5.7$ Hz, CCH_2), 2.04 (2 H, p, $J = 5.6$ Hz, NCH_2CH_2). $\delta^{13}\text{C}$ (101 MHz, CDCl_3) 171.3 ($\text{C}=\text{O}^{\text{maj}}$), 170.8 ($\text{C}=\text{O}^{\text{min}}$), 148.3 (ArC^{maj}), 147.7 (ArC^{min}), 139.5 (ArC), 135.1 ($\text{CH}=\text{CH}_2$), 134.3 (ArC), 131.5 (ArCH), 131.1 (ArC), 129.9 (ArCH), 128.5 (ArCH), 125.9 (ArCH), 125.1 (ArCH), 124.6 (ArCH), 119.1 (ArC), 116.3 ($\text{CH}=\text{CH}_2$), 115.5 (ArCH), 111.8 (ArCH), 55.5 ($\text{NHCH}_2^{\text{maj+min}}$), 46.0 ($\text{NCH}_2\text{CH}_2^{\text{maj}}$), 44.7 ($\text{NCH}_2\text{CH}_2^{\text{min}}$), 27.0 ($\text{CCH}_2^{\text{maj+min}}$), 24.4 ($\text{NCH}_2\text{CH}_2^{\text{maj}}$), 23.8 ($\text{NCH}_2\text{CH}_2^{\text{min}}$). IR (film, cm^{-1}) $\nu_{\text{max}} = 3380$ (N-H), 1629 (C=O), 1491, 1375 (C-N).

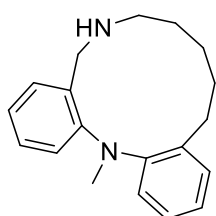
6,14-Dimethyl-7,8,9,14-tetrahydrodibenzo[b,i][1,5]diazecin-5(6H)-one – 3.36



To a solution of 14-Methyl-7,8,9,14-tetrahydrodibenzo[b,i][1,5]diazecin-5(6H)-one **3.18b** (50 mg, 0.19 mmol, 1 eq.) in THF (0.6 mL, 0.3 M) was added NaHMDS (1 M in THF, 0.21 mL, 0.21 mmol, 1.1 eq.) at 0 °C, followed by methyl iodide (24 μL , 0.38 mmol, 2.0 eq.). The reaction mixture was stirred at rt for 2 h, quenched with MeOH and evaporated under reduced pressure. The residue was purified by silica gel column chromatography eluting with a gradient of $\text{CH}_2\text{Cl}_2/\text{MeOH}$ 99.5:0.5 to 97:3 to give the corresponding product as a colourless oil (41 mg, 77%).

$\delta^1\text{H}$ (400 MHz, CD_3OD) 7.41 – 7.29 (2 H, m, H-10 + H-13), 7.20 (1 H, td, $J = 7.5, 1.5$ Hz, H-16), 7.10 (1 H, td, $J = 7.6, 1.6$ Hz, H-15), 7.03 (2 H, d, $J = 8.0$ Hz, H-9 + H-14), 6.90 (1 H, dd, $J = 7.6, 1.8$ Hz, H-12), 6.77 (1 H, td, $J = 7.4, 1.0$ Hz, H-11), 3.62 ($\text{CH}_\text{A}\text{H}_\text{B}$, 1 H, ddd, $J = 14.7, 12.9, 2.0$ Hz, H-1), 3.23 (3 H, s, H-17), 3.14 – 3.03 ($\text{CH}_\text{A}\text{H}_\text{B}$, 1 H, m, H-1), 2.95 ($\text{CH}_\text{A}\text{H}_\text{B}$, 1 H, td, $J = 13.2, 4.1$ Hz, H-3), 2.65 ($\text{CH}_\text{A}\text{H}_\text{B}$, 1 H, dt, $J = 13.5, 3.9$ Hz, H-3), 2.41 (3 H, s, H-18), 2.20 – 2.04 ($\text{CH}_\text{A}\text{H}_\text{B}$, 1 H, m, H-2), 1.64 ($\text{CH}_\text{A}\text{H}_\text{B}$, 1 H, dqd, $J = 14.9, 3.8, 2.0$ Hz, H-2). **$\delta^{13}\text{C}$ (101 MHz, CD_3OD)** 173.2 (C-8), 147.0 (C-5), 146.4 (C-6), 141.3 (C-4), 131.4 (C-10), 130.5 (C-12), 130.2 (C-13), 130.0 (C-16), 128.9 (C-14), 128.6 (C-15), 123.6 (C-7), 118.2 (C-11), 114.2 (C-9), 52.2 (C-1), 42.5 (C-17), 31.9 (C-18), 30.0 (C-3), 25.7 (C-2). **IR (film, cm^{-1})** ν_{max} 2922 (C–H), 1620 (C=O), 1597, 1486, 1342 (C–N). **HRMS (MALDI⁺)** m/z calcd for $\text{C}_{18}\text{H}_{20}\text{N}_2\text{ONa}^+$ $[\text{M}+\text{Na}]^+$ 303.1468; found: 303.1479.

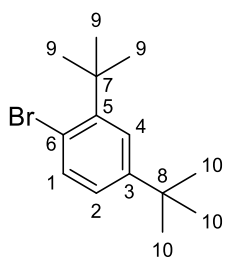
16-Methyl-5,6,7,8,9,10,11,16-octahydrodibenzo[b,k][1,5]diazacyclododecine – 3.38



In a microwave vial, to a solution of 16-methyl-7,8,9,10,11,16-hexahydrodibenzo[b,k][1,5]diazacyclododecin-5(6H)-one **3.18d** (44 mg, 0.15 mmol, 1 eq.) in THF (1.5 mL, 0.1 M) was added $\text{BH}_3\cdot\text{SMe}_2$ (2 M in THF, 0.15 mL, 0.3 mmol, 2.0 eq.) dropwise. The tube was sealed and the reaction mixture was stirred at 80 °C for 18 h. The reaction mixture was cooled down to rt, quenched with aqueous sodium hydroxide (2 M, 1 mL) and the biphasic mixture was vigorously stirred at rt for 15 min. The reaction mixture was diluted with 10 mL water and extracted with 10 mL ethyl acetate three times. The combined organic phases were washed with brine and evaporated under reduced pressure. The residue was purified by silica gel column chromatography eluting with a gradient of Pentane/EtOAc 20:1 to 10:1 to give the corresponding product as a colourless oil (21 mg, 50%). **$\delta^1\text{H}$ (400 MHz, CDCl_3)** 7.28 – 7.27 (2 H, m, ArCH), 7.21 – 7.07 (5 H, m, ArCH), 6.73 (1 H, dd, $J = 7.9, 1.3$ Hz, ArCH), 6.11 (1 H, br s, NH), 4.68 ($\text{CH}_\text{A}\text{H}_\text{B}$, 1 H, dd, $J = 15.4$ Hz, CH_2), 3.69 ($\text{CH}_\text{A}\text{H}_\text{B}$, 1 H, dd, $J = 15.4, 9.2$ Hz, CH_2), 3.22 (3 H, s, CH_3), 2.86 ($\text{CH}_\text{A}\text{H}_\text{B}$, 1 H, t, $J = 11.80$ Hz, CH_2), 2.76 – 2.68 ($\text{CH}_\text{A}\text{H}_\text{B}$, 1 H, m, CH_2), 2.41 – 2.32 ($\text{CH}_\text{A}\text{H}_\text{B}$, 1 H, m, CH_2), 2.24 – 2.07 (2 H, m, CH_2), 1.69 – 1.59 ($\text{CH}_\text{A}\text{H}_\text{B}$, 1 H, m, CH_2), 1.55 – 1.45 (2 H, m, CH_2), 1.33 – 1.26 (2 H, m, CH_2). **$\delta^{13}\text{C}$ (101 MHz, CDCl_3)** 152.0 (ArC), 148.0 (ArC), 135.4 (ArC), 132.3 (ArCH), 131.7 (ArCH), 129.9 (ArCH), 127.5 (ArC), 127.1 (ArCH), 124.7 (ArCH), 124.4 (ArCH), 124.3 (ArCH), 121.0 (ArCH), 61.3 (CH_2), 54.5 (CH_2), 41.0 (CH_3), 31.2 (CH_2), 30.7 (CH_2), 26.3 (CH_2), 22.6 (CH_2). **IR (film, cm^{-1})** ν_{max} 3168, 2923, 1487, 1450, 1166. **HRMS (MALDI⁺)** m/z calcd for $\text{C}_{19}\text{H}_{24}\text{N}_2\text{Na}^+$ $[\text{M}+\text{Na}]^+$ 303.1832; found: 303.1838.

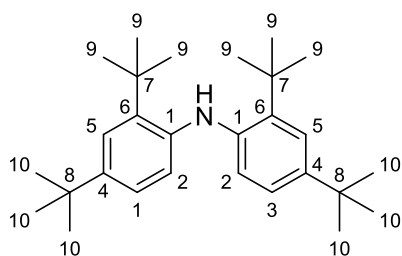
Chapter 4

2,4-Di-*tert*-butyl-1-bromobenzene – 4.25



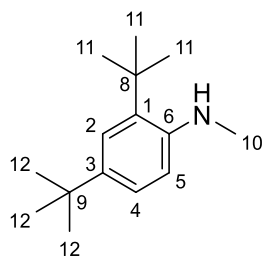
To a solution of 1,3-di-*tert*-butylbenzene (2.48 g, 13.0 mmol, 1.0 eq.) in TMPO (26 mL) at 70 °C was added dropwise a solution of bromine (0.84 mL, 16.4 mmol, 1.25 eq) in TMPO (14 mL). The reaction mixture was stirred at this temperature for 20 h and extracted with petroleum ether. The combined extraction layers were washed with a saturated aqueous solution of Na₂SO₃, brine, dried over MgSO₄ and concentrated *in vacuo* to yield to the title compound as a colourless oil (3.50 g, 13.0 mmol, quant.) **$\delta^1\text{H}$ (400 MHz, CDCl₃)** 7.49 (1 H, d, *J* = 8.3 Hz, H-1), 7.46 (1 H, d, *J* = 2.4 Hz, H-4), 7.05 (1 H, dd, *J* = 8.3, 2.5 Hz, H-2), 1.51 (9 H, s, H-9), 1.30 (9 H, s, H-10). **$\delta^{13}\text{C}$ (101 MHz, CDCl₃)** 150.1 (C-5), 146.9 (C-3), 135.3 (C-1), 125.3 (C-4), 124.7 (C-2), 119.5 (C-6), 36.9 (C-7), 34.9 (C-8), 31.4 (C-10), 29.8 (C-9). Data consistent with that reported in the literature.^[310]

Bis(2,4-di-*tert*-butylphenyl)amine – 4.26



Distilled toluene was added to a mixture of compound **4.24** (0.99 mg, 4.84 mmol, 1.0 eq.), compound **4.25** (1.57 g, 5.83 mmol, 1.2 eq.), NaOtBu (0.59 mg, 6.13 mmol, 1.25 eq.), Pd₂(dba)₃ (89 mg, 0.097 mmol, 2 mol%) and dppf (81 mg, 0.146 mmol, 3 mol%). The reaction mixture was degassed by sonication under vacuum, and heated under reflux under an argon atmosphere for 16 h. Filtration on a plug of silica (SiO₂, petroleum ether) yield the title compound as a white solid (1.21 g, 3.1 mmol, 65%), **m.p.:** 158 – 159 °C. **$\delta^1\text{H}$ (500 MHz, CDCl₃)** 7.41 (2 H, d, *J* = 2.3 Hz, H-5), 7.09 (2 H, dd, *J* = 8.4, 2.3 Hz, H-3), 6.87 (2 H, d, *J* = 8.4 Hz, H-2), 5.27 (1 H, br. s, NH), 1.50 (18 H, s, H-9), 1.33 (18 H, s, H-10). **$\delta^{13}\text{C}$ (126 MHz, CDCl₃)** 143.7 (C-4), 141.5 (C-1), 139.5 (C-6), 123.7 (C-3), 123.6 (C-5), 122.6 (C-2), 34.9 (C-7), 34.5 (C-8), 31.8 (C-10), 30.8 (C-9). **IR (film, cm⁻¹)** ν_{max} 2956 (C–H), 2904 (C–H), 2867 (C–H), 1499 (N–H), 1394; **HRMS (ESI⁺)** *m/z* calcd for C₂₈H₄₄N [M+H]⁺ 394.3474, found 394.3473.

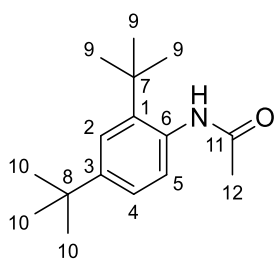
2,4-Di-*tert*-butyl-*N*-methylaniline – 4.28



To a solution of compound **4.24** (300 mg, 1.56 mmol, 1.0 eq.) and succinimide (168 mg, 1.70 mmol, 1.1 eq.) in ethanol (1 mL) was added formaldehyde 37% in water (137 μL , 1.70 mmol, 1.1 eq.). The reaction mixture was heated under reflux for 4 h, concentrated *in vacuo*, and dry DMSO (1 mL) and NaBH₄ (65 mg, 1.72 mmol, 1.1 eq.) were added. The reaction mixture was reflux for 1 h and an aqueous solution of LiCl was added. The solution was

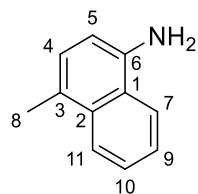
extracted with CH₂Cl₂, dried over Na₂SO₄ and concentrated *in vacuo*. Purification by flash column chromatography (SiO₂, petroleum ether/CH₂Cl₂, 70:30) yielded the title compound as a yellow oil (115 mg, 0.56 mmol, 36%). **¹H (400 MHz, CDCl₃)** 7.33 (1 H, d, *J* = 2.4 Hz, H-2), 7.21 (1 H, dd, *J* = 8.4, 2.4 Hz, H-4), 6.65 (1 H, d, *J* = 8.4 Hz, H-5), 3.87 (1 H, br. s, NH), 2.92 (3 H, s, H-10), 1.45 (9 H, s, H-11), 1.32 (9 H, s, H-12). **¹³C (101 MHz, CDCl₃)** 145.2 (C-6), 139.3 (C-3), 132.9 (C-1), 123.7 (C-4), 123.5 (C-2), 111.1 (C-5), 34.6 (C-9), 34.2 (C-8), 31.8 (C-12), 31.5 (C-10), 30.1 (C-11). Data consistent with that reported in the literature.^[308]

N-(2,4-Di-*tert*-butylphenyl)acetamide – 4.29



To a solution of compound **4.24** (219 mg, 1.14 mmol, 1.0 eq.) and Et₃N (0.17 mL, 1.21 mmol, 1.1 eq.) in CH₂Cl₂ (2.3 mL) at 0 °C was added acetyl chloride (89 µL, 1.25 mmol, 1.1 eq.). The reaction mixture was allowed to warm up to rt and stirred for 16 h. Water was added to the reaction mixture, and the aqueous phase was extracted with CH₂Cl₂. The organic phases were combined, washed with brine, dried over Na₂SO₄ and concentrated *in vacuo*. Purification by flash column chromatography (SiO₂, petroleum ether) yielded the title compound as a white solid (249 mg, 1.06 mmol, 96%), **m.p.**: 153 – 154 °C, Mixture of rotamers in a 1:0.4 ratio. **¹H (400 MHz, CDCl₃)** 7.47 (1 H^{min}, d, *J* = 1.8 Hz, H-2), 7.41 (1 H^{maj+min}, d, *J* = 2.2 Hz, H-2), 7.38 (1 H^{maj}, d, *J* = 8.3 Hz, H-5), 7.25 (1 H, dd, *J* = 8.3, 2.1 Hz, H-4), 7.04 (1 H^{maj}, br. s, NH), 7.01 (1 H^{min}, d, *J* = 8.1 Hz, H-5), 6.92 (1 H^{min}, br. s, NH), 2.20 (3 H^{maj}, s, H-12), 1.89 (3 H^{min}, s, H-12), 1.41 (9 H^{maj}, s, H-9), 1.39 (9 H^{min}, s, H-9), 1.33 (9 H^{min}, s, H-10), 1.30 (9 H^{maj}, s, H-10). **¹³C (101 MHz, CDCl₃)** 172.9 (C-11^{min}), 168.7 (C-11^{maj}), 151.0 (C-3^{min}), 149.2 (C-3^{maj}), 145.6 (C-1^{min}), 142.7 (C-1^{maj}), 133.4 (C-6^{min}), 132.4 (C-6^{maj}), 130.6 (C-5^{min}), 128.4 (C-5^{maj}), 124.3 (C-4^{min}), 124.0 (C-2^{min}), 123.9 (C-4^{maj}), 123.8 (C-2^{maj}), 35.5 (C-7^{min}), 35.0 (C-7^{maj}), 35.0 (C-8^{min}), 34.8 (C-8^{maj}), 31.5 (C-10^{maj+min}), 30.9 (C-9^{maj}), 30.7 (C-9^{min}), 24.5 (C-12^{maj}), 21.2 (C-12^{min}). Data consistent with that reported in the literature.^[58]

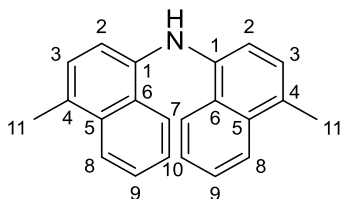
4-Methylnaphthalen-1-amine – 4.32



To a solution of 1-bromo-4-methylnaphthalene **4.31** (2.0 mL, 12.8 mmol, 1 eq.) in formamide (60 mL) was added K₂CO₃ (4.4 g, 31.8 mmol, 2.5 eq) and CuSO₄·5H₂O (3.9 g, 15.6 mmol, 1.2 eq.). The reaction mixture was heated to 150 °C for 2 h. Water was added, and the reaction mixture was extracted with CH₂Cl₂. The organic phases were combined, washed with brine, dried over MgSO₄ and concentrated *in vacuo*. The resulting brown solid was taken in ethanol (125 mL) and an aqueous solution of 0.5 M NaOH (30 mL, 15.0 mmol, 1.2 eq.) was added. The reaction mixture was heated under reflux for 2 h, concentrated *in vacuo*, and extracted with CH₂Cl₂. The organic phases were combined, washed with brine, dried over Na₂SO₄ and concentrated *in vacuo*. Purification by flash column chromatography (SiO₂, petroleum ether/EtOAc,

8515) yielded the title compound as a brown oil (1.6 g, 10.1 mmol, 79%). $\delta^1\text{H}$ (400 MHz, CDCl_3) 7.98 (1 H, d, $J = 7.9$ Hz, H-7), 7.87 (1 H, d, $J = 7.7$ Hz, H-11), 7.54 (1 H, dt, $J = 5.8, 1.3$, H-9), 7.50 (1 H, dt, $J = 5.8, 1.3$ Hz, H-10), 7.15 (1 H, d, $J = 7.4$ Hz, H-5), 6.72 (1 H, d, $J = 7.4$ Hz, H-4), 4.04 (2 H, br. s, NH_2), 2.61 (3 H, s, H-8). $\delta^{13}\text{C}$ (101 MHz, CDCl_3) 140.5 (C-6), 133.3 (C-2), 126.9 (C-11), 125.8 (C-10), 125.04 (C-3), 124.99 (C-9), 124.7 (C-4), 124.2 (C-1), 121.5 (C-7), 109.7 (C-5), 19.1 (C-8). Data consistent with that reported in the literature.^[313]

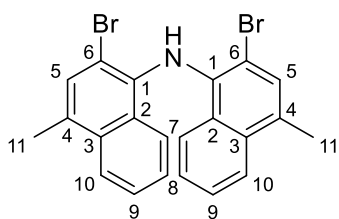
Bis(4-methylnaphthalen-1-yl)amine – 4.30



Distilled toluene was added to a mixture of compound **4.32** (1.0 g, 6.3 mmol, 1.0 eq.), **4.31** (1.2 mL, 7.7 mmol, 1.2 eq.), NaOtBu (0.77 g, 8.0 mmol, 1.25 eq.), $\text{Pd}_2(\text{dba})_3$ (116 mg, 0.127 mmol, 2 mol%) and dppf (105 mg, 0.189 mmol, 3 mol%). The reaction mixture was degassed by

sonication *in vacuo*, and heated under reflux under an argon atmosphere for 16 h. Filtration on a plug of silica (SiO_2 , petroleum ether) yield the title compound as a yellow solid (1.83 g, 6.1 mmol, 96%), **m.p.:** 98 – 99 °C. $\delta^1\text{H}$ (400 MHz, CDCl_3) 8.16 (2 H, d, $J = 8.4$ Hz, H-7), 8.07 (2 H, d, $J = 8.4$ Hz, H-8), 7.60 (2 H, t, $J = 7.5$ Hz, H-10), 7.51 (2 H, t, $J = 7.5$ Hz, H-9), 7.20 (2 H, d, $J = 7.5$ Hz, H-3), 6.89 (2 H, d, $J = 7.5$ Hz, H-2), 6.19 (1 H, br. s, NH), 2.70 (6 H, s, H-11). $\delta^{13}\text{C}$ (101 MHz, CDCl_3) 139.4 (C-1), 133.7 (C-6), 128.6 (C-7), 127.4 (C-5), 127.0 (C-3), 126.1 (C-10), 125.5 (C-9), 125.1 (C-8), 122.7 (C-7), 115.6 (C-2), 19.4 (C-2). IR (film, cm^{-1}) ν_{max} 3385 (N–H), 3067 (C–H), 2924 (C–H), 2854 (C–H), 1582 (N–H); HRMS (ESI⁺) m/z calcd for $\text{C}_{22}\text{H}_{20}\text{N}$ $[\text{M}+\text{H}]^+$ 298.1596, found 298.1593.

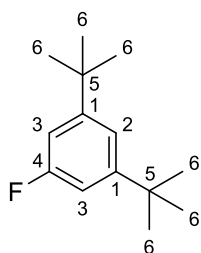
Bis(2-bromo-4-methylnaphthalen-1-yl)amine – 4.19



To a solution of compound **4.30** (600 mg, 2.0 mmol, 1 eq.) in AcOH (10 mL) was added dropwise bromine (205 μL , 4.0 mmol, 2.0 eq.). The reaction mixture was stirred for 3 h, and an aqueous solution of 3% $\text{Na}_2\text{S}_2\text{O}_4$ was added. The precipitate was filtered, rinsed with water, taken up in CH_2Cl_2 , washed with brine, dried over MgSO_4 and

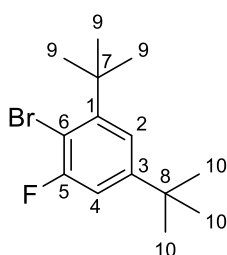
concentrated *in vacuo*. Purification by flash column chromatography (SiO_2 , petroleum ether/EtOAc, 99:1) followed by trituration in Et_2O yielded the title compound as an off-white solid (673 g, 1.5 mmol, 73%), **m.p.:** 165 °C (degradation). $\delta^1\text{H}$ (400 MHz, CDCl_3) 7.93 (2 H, d, $J = 8.4$ Hz, H-7), 7.81 (2 H, d, $J = 8.5$, H-10), 7.48 (2 H, s, H-5), 7.45 (2 H, t, $J = 7.2$ Hz, H-8), 7.24 (2 H, t, $J = 7.3$ Hz, H-9), 6.23 (1 H, s, NH), 2.65 (6 H, s, H-11). $\delta^{13}\text{C}$ (101 MHz, CDCl_3) 137.1 (C-1), 132.8 (C-4), 130.8 (C-5 + C-3), 129.4 (C-2), 126.1 (C-9 + C-8), 124.9 (C-7), 123.7 (C-10), 113.7 (C-6), 19.1 (C-4). IR (film, cm^{-1}) ν_{max} 3363 (N–H), 3069 (C–H), 2922 (C–H), 2856 (C–H), 1571 (N–H), 1391; HRMS (ESI⁺) m/z calcd for $\text{C}_{22}\text{H}_{18}\text{NBr}_2$ $[\text{M}+\text{H}]^+$ 453.9806, found 453.9815.

1,3-Di-tert-butyl-5-fluorobenzene – 4.38



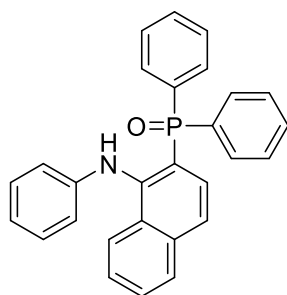
To NaOH (675 mg, 16.9 mmol, 1.2 eq.) in MeOH (30 mL) was added **4.37** (3.3 g, 14.1 mmol, 1.0 eq.). After stirring for 15 min, the reaction mixture was cooled to 0 °C and AgOTf (10.8 g, 42 mmol, 3.0 eq.) was added. After stirring for 30 min at 0 °C, the solvent was removed under reduced pressure at 0 °C and azeotroped with acetone. To the residue was added acetone (70 mL), 3 Å molecular sieves (7 g), Selectfluor® (5.2 g, 14.8 mmol, 1.05 eq.) and the reaction mixture was stirred for 1 h. The reaction mixture was concentrated *in vacuo*, taken up in CH₂Cl₂, filtered over Celite and concentrated *in vacuo*. Purification by flash column chromatography (SiO₂, petroleum ether) yielded the title compound as a colourless oil (1.75 g, 60%). $\delta^1\text{H}$ (400 MHz, CDCl₃) 7.19 (1 H, t, J = 1.7 Hz, H-2), 6.90 (2 H, dd, J = 10.7, 1.7 Hz, H-3), 1.32 (18 H, s, H-6). $\delta^{13}\text{C}$ (101 MHz, CDCl₃) 162.9 (d, J = 242.3 Hz, C-4), 153.3 (d, J = 5.7 Hz, C-1), 117.9 (d, J = 2.2 Hz, C-2), 109.6 (d, J = 21.7 Hz, C-3), 35.1 (d, J = 1.9 Hz, C-5), 31.5 (C-6). Data consistent with that reported in the literature.^[314]

2-Bromo-1,5-di-tert-butyl-3-fluorobenzene – 4.36a



To a solution of **4.38** (1.0 g, 4.8 mmol, 1.0 eq.) in TFA (10 mL) at 0 °C was added Br₂ (0.33 mL, 6.4 mmol, 1.2 eq.) dropwise. The reaction mixture was allowed to warm up to rt and stirred overnight. The reaction mixture was poured on ice and Na₂S₂O₃ was added. The aqueous phase was extracted with CH₂Cl₂, organic phases were combined, washed with brine, dried over MgSO₄ and concentrated *in vacuo*. Purification by flash column chromatography (SiO₂, petroleum ether) yielded the title compound as a yellow oil (1.1 g, 80%). NMR contains around 12% of the non-fluorinated analogue as an unseparable impurity. $\delta^1\text{H}$ (400 MHz, CDCl₃) 7.26 (1 H, dd, J = 2.3, 1.3 Hz, H-2), 7.02 (1 H, dd, J = 10.3, 2.3 Hz, H-4), 1.53 (9 H, s, H-9), 1.31 (9 H, s, H-10). $\delta^{13}\text{C}$ (101 MHz, CDCl₃) 159.5 (d, J = 241.5 Hz, C-5), 151.8 (d, J = 5.9 Hz, C-3), 149.4 (d, J = 0.7 Hz, C-1), 120.2 (d, J = 2.3 Hz, C-2), 111.3 (d, J = 25.2 Hz, C-4), 106.7 (d, J = 20.7 Hz, C-6), 37.5 (d, J = 1.9 Hz, H-7), 35.1 (d, J = 1.8 Hz, C-8), 31.3 (C-6), 30.0 (C-9). IR (film, cm⁻¹) ν_{max} 2964 (C–H), 1401 (C–F); HRMS (EI⁺) m/z calcd for C₁₄H₂₀BrF [M]⁺ 286.0732, found 286.0729.

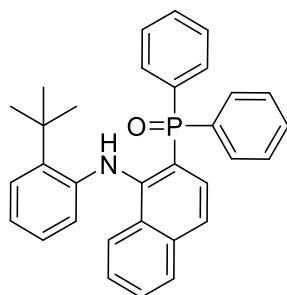
Diphenyl(1-(phenylamino)naphthalen-2-yl)phosphine oxide – 4.43a



To a solution of aniline (28 μ L, 0.30 mmol, 1.1 eq.) in THF (0.5 mL) at -78 °C was added *n*-BuLi (1.4 M in hexanes, 0.2 mL, 0.28 mmol, 1.0 eq.). The reaction mixture was stirred for 30 min and allowed to warm up to rt for 30 min. The reaction mixture was cooled to 0 °C and **4.41** (100 mg, 0.28 mmol, 1.0 eq.) was added. The reaction mixture was heated to 60 °C overnight and quenched with sat. NH₄Cl (aq.) and extracted with Et₂O. The

organic phases were combined, washed with brine, dried over Na₂SO₄ and concentrated *in vacuo*. Purification by flash column chromatography (SiO₂, petroleum ether/EtOAc, 70:30) yielded the title compound as a light brown solid (35 mg, 30%), **m.p.**: 195 °C. **$\delta^1\text{H}$ (400 MHz, CDCl₃)** 8.54 (1 H, s, NH), 7.93 (1 H, d, *J* = 8.6 Hz, ArCH), 7.82 (1 H, d, *J* = 8.2 Hz, ArCH), 7.65 (4 H, dd, *J* = 12.2, 7.0 Hz, ArCH), 7.52 (2 H, t, *J* = 8.7 Hz, ArCH), 7.44 (2 H, t, *J* = 7.3 Hz, ArCH), 7.35 (5 H, m, ArCH), 7.03 (1 H, dd, *J* = 12.1, 8.5 Hz, ArCH), 6.89 (2 H, t, *J* = 7.8 Hz, ArCH), 6.64 (1 H, t, *J* = 7.3 Hz, ArCH), 6.42 (2 H, d, *J* = 7.9 Hz, ArCH). **$\delta^{13}\text{C}$ (101 MHz, CDCl₃)** 146.5 (d, *J* = 3.9 Hz, ArC), 145.6 (ArC), 136.4 (d, *J* = 1.9 Hz, ArC), 132.1 (d, *J* = 9.9 Hz, ArCH), 131.99 (d, *J* = 104.9 Hz, ArC), 131.98 (d, *J* = 2.8 Hz, ArCH), 129.2 (d, *J* = 8.7 Hz, ArC), 128.6 (ArCH), 128.50 (ArCH), 128.48 (ArCH), 128.3 (d, *J* = 7.0 Hz, ArCH), 127.9 (d, *J* = 11.5 Hz, ArCH), 126.3 (ArCH), 126.1 (ArCH), 123.3 (d, *J* = 12.6 Hz, ArCH), 121.0 (d, *J* = 103.7 Hz, ArC), 119.7 (ArCH), 116.4 (ArCH). **IR (film, cm⁻¹)** ν_{max} 3267 (N–H), 3056 (C–H), 1601 (N–H), 1118 (P=O); **HRMS (ESI⁺)** *m/z* calcd for C₂₈H₂₃NOP [M+H]⁺ 420.1512, found 420.1492.

(1-((2-(*Tert*-butyl)phenyl)amino)naphthalen-2-yl)diphenylphosphine oxide – 4.43b

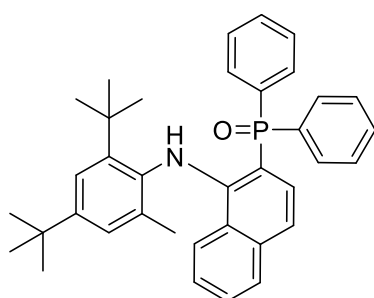


To a solution of 2-*tert*-butylaniline (47 μ L, 0.30 mmol, 1.1 eq.) in THF (0.5 mL) at -78 °C was added *n*-BuLi (1.4 M in hexanes, 0.2 mL, 0.28 mmol, 1.0 eq.). The reaction mixture was stirred for 30 min and allowed to warm up to rt for 30 min. The reaction mixture was cooled to 0 °C and **4.41** (100 mg, 0.28 mmol, 1.0 eq.) was added. The reaction mixture was heated to 60 °C overnight and quenched with sat. NH₄Cl (aq.) and extracted with Et₂O.

The organic phases were combined, washed with brine, dried over Na₂SO₄ and concentrated *in vacuo*. Purification by flash column chromatography (SiO₂, petroleum ether/EtOAc, 80:20) yielded the title compound as an orange oil (63 mg, 47%), **$\delta^1\text{H}$ (400 MHz, CDCl₃)** 8.63 (1 H, s, NH), 7.77 (3 H, m, ArCH), 7.66 (3 H, m, ArCH), 7.59 (1 H, *J* = 7.4, 1.3 Hz, ArCH), 7.53 (2 H, m, ArCH), 7.41 (2 H, m, ArCH), 7.34 (1 H, *J* = 7.6, 1.1 Hz, ArCH), 7.27 (3 H, m, ArCH), 7.20 (1 H, t, *J* = 8.6 Hz, ArCH), 7.04 (1 H, td, *J* = 12.4, 8.5 Hz, ArCH), 6.73 (1 H, td, *J* = 7.6, 1.1 Hz, ArCH), 6.55 (1 H, td, *J* = 7.6, 1.1 Hz, ArCH), 5.97 (1 H, d, *J* = 8.0 Hz, ArCH), 1.63 (9 H, s, CCH₃). **$\delta^{13}\text{C}$ (126 MHz, CDCl₃)** 148.2 (d, *J* = 4.1 Hz, ArC), 143.9 (ArC), 138.8 (ArC), 136.9 (d, *J* = 1.9 Hz, ArC),

132.5 (d, J = 9.8 Hz, ArCH), 132.4 (d, J = 50.5 Hz, ArC), 132.2 (d, J = 2.8 Hz, ArCH), 131.9 (d, J = 10.0 Hz, ArCH), 131.8 (d, J = 2.8 Hz, ArCH), 131.6 (d, J = 51.5 Hz, ArC), 128.7 (d, J = 12.2 Hz, ArCH), 128.4 (ArCH), 128.3 (d, J = 12.2 Hz, ArCH), 128.01 (ArCH), 127.99 (d, J = 8.8 Hz, ArC), 127.9 (ArCH), 126.49 (ArCH), 126.48 (ArCH), 125.9 (ArCH), 125.6 (d, J = 1.1 Hz, ArCH), 121.8 (d, J = 12.9 Hz, ArCH), 121.4 (ArCH), 121.2 (ArCH), 118.6 (d, J = 105.1 Hz, ArC), 35.0 (CCH₃), 30.2 (CCH₃). IR (film, cm⁻¹) ν_{\max} 3267 (N–H), 3056 (C–H), 1601 (N–H), 1118 (P=O); HRMS (ESI⁺) m/z calcd for C₃₂H₃₁NOP [M+H]⁺ 476.2138, found 476.2131.

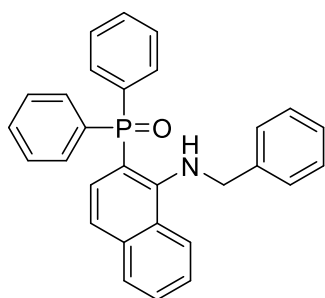
(1-((2,4-Di-tert-butyl-6-methylphenyl)amino)naphthalen-2-yl)diphenylphosphine oxide – 4.43c



To a solution of aniline **1.27** (66 mg, 0.30 mmol, 1.1 eq.) in THF (0.5 mL) at -78 °C was added *n*-BuLi (1.4 M in hexanes, 0.2 mL, 0.28 mmol, 1.0 eq.). The reaction mixture was stirred for 30 min and allowed to warm up to rt for 30 min. The reaction mixture was cooled to 0 °C and **4.41** (100 mg, 0.28 mmol, 1.0 eq.) was added. The reaction mixture was heated to 60 °C overnight and quenched with

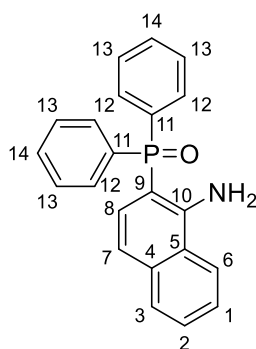
sat. NH₄Cl (aq.) and extracted with Et₂O. The organic phases were combined, washed with brine, dried over Na₂SO₄ and concentrated *in vacuo*. Purification by flash column chromatography (SiO₂, petroleum ether /EtOAc, 80:20) yielded the title compound as a light brown solid (70 mg, 53%), **m.p.**: > 200 °C. **¹H (400 MHz, CDCl₃)** 9.86 (1 H, s, NH), 7.78 (2 H, dd, J = 11.3, 8.0 Hz, ArCH), 7.71 (2 H, dd, J = 11.3, 8.0 Hz, ArCH), 7.64 (1 H, d, J = 8.2 Hz, ArCH), 7.55 (2 H, m, ArCH), 7.47 (4 H, m, ArCH), 7.39 (1 H, d, J = 1.8 Hz, ArCH), 7.33 (1 H, t, J = 7.8 Hz, ArCH), 7.26 (1 H, d, J = 5.8 Hz, ArCH), 7.06 (1 H, dd, J = 8.1, 1.9 Hz, ArCH), 6.91 (3 H, m, ArCH), 1.53 (9 H, s, CCH₃), 1.36 (3 H, s, CH₃), 1.32 (9 H, s, CCH₃). **¹³C (126 MHz, CDCl₃)** 151.8 (d, J = 4.4 Hz, ArC), 147.8 (ArC), 144.5 (ArC), 138.3 (ArC), 137.2 (d, J = 1.8 Hz, ArC), 134.5 (d, J = 134.4 Hz, ArC), 132.9 (d, J = 39.4 Hz, ArC), 132.5 (d, J = 2.5 Hz, ArCH), 132.4 (d, J = 2.7 Hz, ArCH), 132.02 (d, J = 2.7 Hz, ArCH), 131.98 (ArC), 131.96 (d, J = 2.7 Hz, ArCH), 129.0 (d, J = 11.9 Hz, ArCH), 128.6 (d, J = 5.2 Hz, ArCH), 128.5 (d, J = 5.2 Hz, ArCH), 128.2 (ArCH), 127.8 (ArCH), 126.1 (ArCH), 125.1 (ArCH), 124.9 (d, J = 8.9 Hz, ArC), 124.0 (ArCH), 122.0 (ArCH), 116.5 (d, J = 13.7 Hz, ArCH), 105.7 (d, J = 107.0 Hz, ArC), 36.0 (CCH₃), 34.7 (CCH₃), 31.6 (CCH₃), 31.0 (CCH₃), 19.6 (CH₃). IR (film, cm⁻¹) ν_{\max} 3244 (N–H), 3055 (C–H), 1118 (P=O); HRMS (ESI⁺) m/z calcd for C₃₇H₄₁NOP [M+H]⁺ 546.2920, found 546.2900.

(1-(Benzylamino)naphthalen-2-yl)diphenylphosphine oxide – 4.44



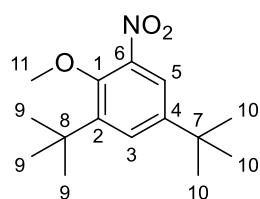
To a solution of benzylamine (163 μ L, 1.5 mmol, 2.2 eq.) in THF (3.0 mL) at -78°C was added *n*-BuLi (1.4 M in hexanes, 1.1 mL, 1.5 mmol, 2.2 eq.). The reaction mixture was stirred for 10 min and allowed to warm up to 0°C for 1 h. The reaction mixture was cooled to -20°C and **4.41** (250 mg, 0.7 mmol, 1.0 eq.) was added. The reaction mixture was allowed to warm up to rt and stirred for 2 h, quenched with sat. NH_4Cl (aq.) and extracted with Et_2O . The organic phases were combined, washed with brine, dried over Na_2SO_4 and concentrated *in vacuo*. Purification by flash column chromatography (SiO_2 , petroleum ether/ EtOAc , 80:20) yielded the title compound as a white solid (249 mg, 83%), **m.p.**: $142 - 143^{\circ}\text{C}$. **$\delta^1\text{H}$ (400 MHz, CDCl_3)** 8.26 (1 H, d, $J = 8.5$ Hz, ArCH), 7.78 (1 H, d, $J = 8.1$ Hz, ArCH), 7.66 (4 H, dd, $J = 12.0, 7.5$ Hz, ArCH), 7.54 (3 H, q, $J = 7.7$ Hz, ArCH), 7.45 (5 H, tt, $J = 9.4, 4.9$ Hz, ArCH), 7.36 – 7.18 (6 H, m, ArCH), 7.12 (1 H, t, $J = 7.3$ Hz, NH), 6.91 (1 H, dd, $J = 12.5, 8.5$ Hz, ArCH), 4.24 (2 H, d, $J = 5.9$ Hz, NCH_2). **$\delta^{13}\text{C}$ (101 MHz, CDCl_3)** 155.1 (d, $J = 4.7$ Hz, ArC), 139.9 (ArC), 136.8 (d, $J = 2.1$ Hz, ArC), 133.3 (d, $J = 104.0$ Hz, ArC), 132.2 (d, $J = 10.1$ Hz, ArCH), 132.0 (d, $J = 2.9$ Hz, ArCH), 128.6 (d, $J = 12.1$ Hz, ArCH), 128.4 (2*ArCH), 128.3 (d, $J = 9.2$ Hz, ArC), 128.2 (ArCH), 128.0 (d, $J = 12.4$ Hz, ArCH), 127.5 (ArCH), 127.0 (ArCH), 125.7 (ArCH), 125.4 (ArCH), 120.5 (d, $J = 13.0$ Hz, ArCH), 115.1 (d, $J = 105.5$ Hz, ArC), 54.4 (NCH_2). **IR (film, cm^{-1})** ν_{max} 3271 (N–H), 3054 (C–H), 1116 (P=O); **HRMS (ESI⁺)** m/z calcd for $\text{C}_{29}\text{H}_{24}\text{NOPNa}$ $[\text{M}+\text{Na}]^+$ 456.1488, found 456.1479.

(1-Aminonaphthalen-2-yl)diphenylphosphine oxide – 4.42



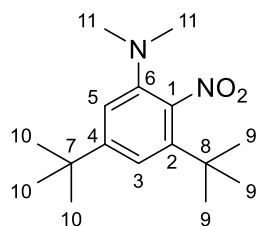
To a solution of **4.44** (110 mg, 0.25 mmol, 1.0 eq.) in MeOH (1.5 mL) and HCl (1 M in MeOH, 0.5 mL) was added Pd/C (10%, 20 mg) and the reaction mixture was placed under an atmosphere of hydrogen. The reaction mixture was stirred overnight, filtered over Celite and concentrated *in vacuo*. Purification by flash column chromatography (SiO_2 , petroleum ether/ EtOAc , 25:75) yielded the title compound as a light brown oil (83 mg, 95%). **$\delta^1\text{H}$ (400 MHz, CDCl_3)** 7.87 (1 H, d, $J = 8.4$ Hz, H-3), 7.77 – 7.64 (5 H, m, H-13 + H-6), 7.53 (3 H, qd, $J = 5.7, 6.3, 1.3$ Hz, H-14 + H-2), 7.46 (5 H, m, H-1 + H-12), 7.05 (1 H, dd, $J = 8.6, 2.6$ Hz, H-7), 6.84 (1 H, dd, $J = 12.7, 8.5$ Hz, H-8), 6.40 (2 H, s, NH). **$\delta^{13}\text{C}$ (101 MHz, CDCl_3)** 151.1 (d, $J = 4.4$ Hz, C-10), 136.0 (d, $J = 1.9$ Hz, C-4), 133.0 (d, $J = 104.1$ Hz, C-11), 132.2 (d, $J = 10.1$ Hz, C-13), 132.0 (d, $J = 2.7$ Hz, C-14), 128.61 (d, $J = 12.1$ Hz, C-12), 128.60 (C-2), 128.4 (d, $J = 11.9$ Hz, C-8), 128.3 (C-6), 125.6 (C-1), 123.4 (d, $J = 9.6$ Hz, C-5), 121.2 (C-3), 116.2 (d, $J = 13.2$ Hz, C-7), 103.0 (d, $J = 107.7$ Hz, C-9). **IR (film, cm^{-1})** ν_{max} 3397 (N–H), 3328 (N–H), 3234 (N–H), 1117 (P=O); **HRMS (ESI⁺)** m/z calcd for $\text{C}_{22}\text{H}_{19}\text{NOP}$ $[\text{M}+\text{H}]^+$ 344.1199, found 344.1202.

1,5-Di-*tert*-butyl-2-methoxy-3-nitrobenzene – 4.47



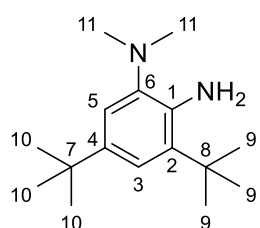
To a suspension of NaH (150 mg, 3.7 mmol, 1.1 eq. 60% in mineral oil) in THF (1.5 mL) at 0 °C was added dropwise a solution of 2,4-di-*tert*-butyl-6-nitrophenol (840 mg, 3.3 mmol, 1.0 eq.) in THF (1.5 mL). The suspension was diluted with 5 mL of THF and stirred for 2 h at rt. The reaction mixture was cooled to 0 °C and MeI (0.41 mL, 6.6 mmol, 2.0 eq.) was added dropwise, followed by DMF (3.5 mL). The reaction mixture was allowed to warm up to rt, stirred overnight and quenched with MeOH. The reaction mixture was filtered, concentrated *in vacuo* and purification by flash column chromatography (SiO₂, petroleum ether/Et₂O, 90/10) yielded the title compound as a yellow solid (484 mg, 55%), **m.p.**: 55 – 56 °C **$\delta^1\text{H}$ (400 MHz, CDCl₃)** 7.59 (1 H, d, *J* = 2.5 Hz, H-5), 7.55 (1 H, d, *J* = 2.5 Hz, H-3), 3.78 (3 H, s, H-11), 1.41 (9 H, s, H_{tBu}), 1.32 (9 H, s, H_{tBu}). **$\delta^{13}\text{C}$ (101 MHz, CDCl₃)** 151.0 (C-1), 145.9 (ArC), 144.5 (ArC), 143.9 (C-6), 128.6 (C-3), 120.5 (C-5), 61.4 (C-11), 35.9 (ArC), 34.9 (ArC), 31.3 (CH₃), 30.7 (CH₃). **IR (film, cm⁻¹)** ν_{max} 2962 (C–H), 1527 (N–O), 1353 (C–N), 1245 (C–O); **HRMS (ESI⁺)** *m/z* calcd for C₁₅H₂₃NONa [M+Na]⁺ 288.1570, found 288.1576

3,5-Di-*tert*-butyl-*N,N*-dimethyl-2-nitroaniline – 4.49



To a solution of **4.48** (418 mg, 1.67 mmol, 1.0 eq.) in anhydrous THF (2.0 mL) at 0 °C was added NaH (98 mg, 4.1 mmol, 2.5 eq., 60% in mineral oil) and the reaction mixture was stirred for 30 min. MeI (0.25 mL, 4.0 mmol, 2.4 eq.) was added and the reaction mixture was stirred at 0 °C for 30 min, after which it was allowed to warm up to rt and stir 20 h. The reaction mixture was quenched with water, diluted in sat. NaHCO₃ (aq.) and extracted with CH₂Cl₂. Organic phases were combined, washed with brine, dried over MgSO₄ and concentrated *in vacuo* to yield **60** as a yellow solid (451 mg, 97%), **m.p.**: 123 – 124 °C. **$\delta^1\text{H}$ (400 MHz, CDCl₃)** 7.30 (1 H, d, *J* = 1.9 Hz, H-3), 7.22 (1 H, d, *J* = 1.9 Hz, H-5), 2.66 (6 H, s, H-11), 1.37 (9 H, s, C-9), 1.32 (9 H, s, C-10). **$\delta^{13}\text{C}$ (101 MHz, CDCl₃)** 152.9 (C-4), 146.9 (C-6), 146.7 (C-1), 140.3 (C-2), 121.4 (C-3), 117.9 (C-5), 46.2 (C-11), 36.0 (C-8), 35.4 (C-7), 31.4 (C-10), 31.1 (C-9). **IR (film, cm⁻¹)** ν_{max} 2959 (C–H), 1532 (N–O), 1378 (C–N); **HRMS (ESI⁺)** *m/z* calcd for C₁₆H₂₇N₂O₂ [M+H]⁺ 279.2067, found 279.2065.

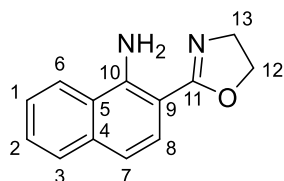
3,5-Di-*tert*-butyl-*N,N*-dimethyl-2-nitroaniline – 4.46



To a solution of **4.49** (394 mg, 1.4 mmol, 1.0 eq.) in anhydrous THF (12 mL) was added LiAlH₄ (266 mg, 7.0 mmol, 5.0 eq.) portionwise. THF mixture was heated under reflux overnight, quenched with water and extracted with ethyl acetate. Organic phases were combined, washed with brine, dried over Na₂SO₄ and concentrated *in vacuo*. Purification by flash column

chromatography (SiO₂, petroleum ether/Et₂O, 85:15) yielded the title compound as a white solid (286 mg, 81%), **¹H (400 MHz, CDCl₃)** 7.11 (1 H, d, *J* = 2.2 Hz, H-3), 7.04 (1 H, d, *J* = 2.2 Hz, H-5), 4.34 (2 H, br. s, NH), 2.68 (6 H, s, H-11), 1.46 (9 H, s, H-9), 1.32 (9 H, s, H-10). **¹³C (101 MHz, CDCl₃)** 141.1 (C-6), 139.7 (C-4), 137.6 (C-1), 133.1 (C-2), 119.2 (C-3), 114.6 (C-5), 44.5 (C-11), 35.0 (C-8), 34.6 (C-7), 31.9 (C-10), 29.9 (C-9). **IR (film, cm⁻¹)** *v*_{max} 3478, 3331 (N–H), 2955 (C–H), 1575 (N–H), 1478, 1449; **HRMS (ESI⁺)** *m/z* calcd for C₁₆H₂₇N₂O₂ [M+H]⁺ 279.2067, found 279.2065

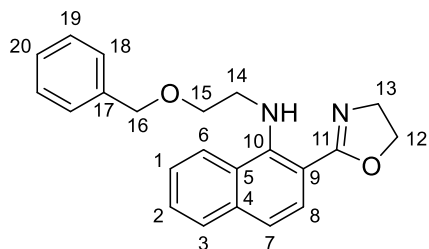
2-(4,5-Dihydrooxazol-2-yl)naphthalen-1-amine – 4.56



To a suspension of **4.55**^[257] (0.40 g, 2.4 mmol, 1.0 eq.) and ZnCl₂ (32 mg, 0.24 mmol, 0.1 eq.) in chlorobenzene (3.4 mL, 0.7 M), was added ethanolamine (0.43 mL, 7.2 mmol, 3.0 eq.) and the reaction mixture was slowly heated to 130 °C for 24 h. After cooling back to rt, ethyl acetate was

added, and the organic phase was washed with HCl (1 M aq.), brine, dried over Na₂SO₄ and concentrated *in vacuo*. Trituration in Et₂O yielded the title compound as an off-white solid (0.39 g, 77%). **m.p.:** 124 – 125 °C. **¹H (400 MHz, CDCl₃)** 7.90 (1 H, dd, *J* = 8.6, 1.0 Hz, H-6), 7.79 (1 H, d, *J* = 8.7 Hz, H-8), 7.76 (1 H, dd, *J* = 7.9, 1.4 Hz, H-3), 7.51 (1 H, ddd, *J* = 8.1, 6.8, 1.3 Hz, H-2), 7.45 (1 H, ddd, *J* = 8.3, 6.8, 1.5 Hz, H-1), 7.14 (1 H, d, *J* = 8.8 Hz, H-7), 7.11 (2 H, br. s, NH₂), 4.36 (2 H, td, *J* = 9.2, 1.1 Hz, H-12), 4.16 (2 H, td, *J* = 9.2, 1.1, H-13). **¹³C (101 MHz, CDCl₃)** 165.8 (C-11), 146.2 (C-10), 135.6 (C-5), 128.6 (C-3), 127.6 (C-2), 126.0 (C-8), 125.1 (C-1), 123.0 (C-4), 121.6 (C-6), 115.8 (C-7), 102.8 (C-9), 65.9 (C-12), 55.1 (C-13). **IR (film, cm⁻¹)** *v*_{max} 3474 (C–H), 3243 (C–H), 3185, 1607 (C=N), 1246 (C–N), 1057 (C–O). **HRMS (ESI⁺)**: *m/z* calcd for C₁₃H₁₃N₂O [M+H]⁺ 213.122, found 213.1028.

N-(2-(Benzyloxy)ethyl)-2-(4,5-dihydrooxazol-2-yl)naphthalen-1-amine - 4.57



A solution of **4.54** (50 mg, 0.23 mmol, 1.0 eq.), BnOCH₂CH₂I (78 μL, 0.46 mmol, 2.0 eq.), DIPEA (55 μL, 0.35 mmol, 1.5 eq.) in DMF (0.5 mL, 0.5 M), was heated to 150 °C for 4 h in a microwave oven. After cooling back to rt, ethyl acetate was added and the organic phase was washed with LiCl (5% aq.),

brine, dried over MgSO₄ and concentrated *in vacuo*. Purification by flash column chromatography yielded the title compound as a brown oil (16 mg, 20%). Mixture of conformers in a 4:1 ratio. Only the major conformer is reported. **¹H (400 MHz, CDCl₃)** 8.39 (1 H, dd, *J* = 8.1, 1.5 Hz, H-6), 7.86 (1 H, dd, *J* = 7.8, 1.6 Hz, H-3), 7.80 – 7.71 (2 H, m, H-7 + H-8), 7.59 – 7.50 (1 H, m, H-2), 7.53 – 7.47 (1 H, m, H-1), 7.34 – 7.27 (4 H, m, H-18 + H-19 + H-20), 7.11 (1 H, t, *J* = 5.9 Hz, NH), 4.43 (2 H, s, H-16), 3.69 (2 H, t, *J* = 5.8 Hz, H-15), 3.54 (4 H, dd, *J* = 9.5, 4.1 Hz, H-12 + H-13), 3.30 (2 H, q, *J* = 5.9 Hz, H-14). **¹³C (101 MHz, CDCl₃)** 173.5 (C-11), 145.0 (C-10), 138.5 (C-17),

136.5 (C-5), 132.4 (C-4), 131.2 (C-9), 128.4 (C-19), 128.3 (C-3), 127.7 (C-18), 127.6 (C-20), 127.5 (C-2), 126.4 (C-1), 126.2 (C-7), 126.0 (C-8), 125.3 (C-6), 73.3 (C-16), 69.7 (C-12), 57.9, (C-13) 57.6 (C-15), 41.4 (C-14). IR (film, cm^{-1}) ν_{max} 3295 (N–H), 2927 (C–H), 2856 (C–H), 1646 (C=N), 1102 (C–O). HRMS (ESI⁺): m/z calcd for $\text{C}_{22}\text{H}_{23}\text{N}_2\text{O}_2$ $[\text{M}+\text{H}]^+$ 347.1754, found 347.1763.

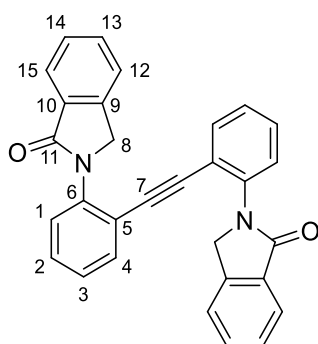
Chapter 5

General procedure 5.1 (GP5.1) : formation of the isoxindole ring: To a solution of aniline (1 eq.) in CH_2Cl_2 (0.1 M) was added 2-(chloromethyl)benzoyl chloride and Et_3N at 0 °C under an atmosphere of nitrogen. The reaction mixture was stirred at rt until consumption of the aniline was observed by TLC. DBU was added and the reaction mixture was stirred at rt until consumption of the intermediate amide was observed by TLC. The reaction mixture was diluted in ethyl acetate and washed with 1M HCl (aq.), brine, dried over MgSO_4 , filtered, and concentrated *in vacuo*. The crude residue obtained was purified by flash column chromatography.

General procedure 5.2 (GP5.2) – deprotection of the TMS group: To a solution of the required TMS-protected alkyne (1.0 eq.) in MeOH (0.5 M) was added K_2CO_3 (1.5 eq.) at rt. The reaction mixture was stirred at rt until consumption of the aniline was observed by TLC, quenched with water, and extracted with CH_2Cl_2 . The combined organic phases were washed with brine, dried over MgSO_4 , filtered and concentrated *in vacuo*. Purification by flash column chromatography yielded the desired product.

General procedure 5.3 (GP5.3) – Sonogashira coupling: A microwave vial was filled with nitrogen. To this was added the required iodo anilide (1.0 eq.), $\text{PdCl}_2(\text{PPh}_3)_2$ (2 mol%), CuI (5 mol%), and Et_3N of a mixture of Et_3N /DMF (1:1, 0.3 M). The reaction mixture was degassed by sonication *in vacuo* followed refill with nitrogen. The required alkyne (1.0 eq.) was added and the reaction allowed to stir at 90 °C until consumption of the starting materials was observed by TLC. The reaction mixture was diluted in ethyl acetate and washed with 1M HCl (aq.), brine, dried over MgSO_4 , filtered, and concentrated *in vacuo*. The crude residue obtained was purified by flash column chromatography.

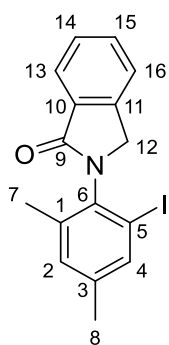
2,2'-(Ethyne-1,2-diylbis(2,1-phenylene))bis(isoindolin-1-one) – 5.20



Following **GP5.1** using 2,2'-(ethyne-1,2-diyl)dianiline **5.22**^[315] (75 mg, 0.36 mmol, 1 eq.), 2-(chloromethyl)benzoyl chloride **5.21** (0.11 mL, 0.76 mmol, 2.1 eq.) and Et₃N (0.16 mL, 1.1 mmol, 3.1 eq.) in CH₂Cl₂ (3.6 mL, 0.1 M) for 1 h, followed by DBU (0.16 mL, 1.1 mmol, 3.1 eq.) for 2 h. Purification by flash column chromatography yielded the title compound (31 mg, 20%) as a yellow solid. **m.p.**: 220 °C (degradation).

¹H (400 MHz, CDCl₃) 7.73 (2 H, d, *J* = 7.5 Hz, H-15), 7.57 (2 H, t, *J* = 7.5 Hz, H-13), 7.48 – 7.41 (6 H, m, H-1 + H-12 + H-14), 7.39 (1 H, d, *J* = 7.7 Hz, H-2), 7.32 (2 H, d, *J* = 7.7 Hz, H-4), 7.21 (2 H, t, *J* = 7.6 Hz, H-3), 4.89 (4 H, s, H-8). **¹³C** (101 MHz, CDCl₃) 168.2 (C-11), 141.6 (C-9), 139.8 (C-6), 133.6 (C-4), 132.1 (C-14 or C-16), 131.9 (C-10), 129.7 (C-2), 128.2 (C-14 or C-16), 127.9 (C-1), 127.3 (C-3), 124.2 (C-15), 123.0 (C-13), 120.5 (C-5), 91.5 (C-7), 52.4 (C-8). **IR** (film, cm⁻¹) *v*_{max} 2923 (C–H), 1689 (C=O), 1450, 1383. **HRMS** (ESI⁺): *m/z* calcd for C₃₀H₂₀N₂O₂Na⁺ [M+Na]⁺ 463.1417, found 463.1407

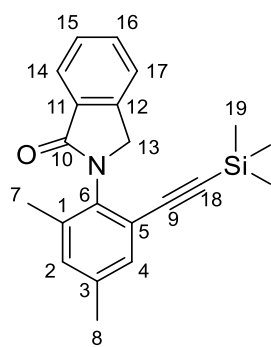
2-(2-Iodo-4,6-dimethylphenyl)isoindolin-1-one – 5.23



Following **GP5.1** using 2-iodo-4,6-dimethylaniline^[316] (0.25 g, 1.0 mmol, 1 eq.), 2-(chloromethyl)benzoyl chloride (0.16 mL, 1.1 mmol, 1.1 eq.) and Et₃N (0.29 mL, 2.1 mmol, 2.1 eq.) in CH₂Cl₂ (10 mL, 0.1 M) for 3 h, followed by DBU (0.33 mL, 2.2 mmol, 2.2 eq.) for 20 h. Purification by flash column chromatography yielded the title compound (0.26 g, 71%) as an off-white solid. **m.p.**: 146 – 148 °C.

¹H (400 MHz, CDCl₃) 7.96 (1 H, d, *J* = 8.1 Hz, H-13), 7.64 – 7.59 (2 H, m, H-4 + H-16), 7.56 – 7.48 (2 H, m, H-14 + H-15), 7.10 (1 H, s, H-2), 4.87 (CH_AH_B, 1 H, d, *J* = 16.7 Hz, H-12), 4.48 (CH_AH_B, 1 H, d, *J* = 16.4 Hz, H-12), 2.31 (3 H, s, H-8), 2.21 (3 H, s, H-7). **¹³C** (101 MHz, CDCl₃) 167.7 (C-9), 141.7 (C-11), 140.6 (C-3), 138.5 (C-1), 137.8 (C-4), 136.6 (C-6), 132.4 (C-10), 132.0 (C-2 + C-16), 128.3 (C-14), 124.6 (C-13), 123.1 (C-15), 99.6 (C-5), 50.9 (C-12), 20.7 (C-8), 19.2 (C-7). **IR** (film, cm⁻¹) *v*_{max} 1690 (C=O), 1469, 1385, 732 (C–I). **HRMS** (ESI⁺) *m/z* calcd for C₁₆H₁₄NOINa⁺ [M+Na]⁺ 386.0012, found 386.0020.

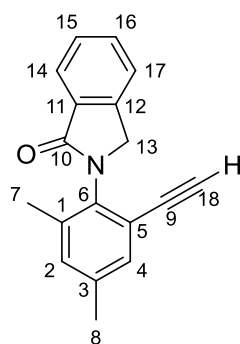
2-(2,4-Dimethyl-6-((trimethylsilyl)ethynyl)phenyl)isoindolin-1-one - 5.24



Following **GP5.3** using 2-(2-iodo-4,6-dimethylphenyl)isoindolin-1-one **5.23** (0.15 g, 0.41 mmol, 1 eq.), $\text{PdCl}_2(\text{PPh}_3)_2$ (6.0 mg, 0.0085 mmol, 2 mol%) and CuI (4.0 mg, 0.021 mmol, 5 mol%) in Et_3N (1.2 mL, 0.3 M), followed by ethynyltrimethylsilane (0.12 mL, 0.87 mmol, 2.1 eq.) at 90 °C for 16 h. Purification by flash column chromatography yielded the *title compound* (0.13 g, quant) as a yellow oil. $\delta^1\text{H}$ (400 MHz, CDCl_3) 7.95 (1 H, d, $J = 7.3$ Hz, H-14), 7.58 (1 H, d, $J = 7.8$ Hz, H-16), 7.49 (2 H, d, $J = 7.7$ Hz, H-15 + H-17),

7.21 (1 H, br. s, H-4), 7.11 (1 H, br. s, H-2), 5.01 ($\text{CH}_\text{A}\text{H}_\text{B}$, 1 H, d, $J = 16.5$ Hz, H-13), 4.51 ($\text{CH}_\text{A}\text{H}_\text{B}$, 1 H, d, $J = 16.6$ Hz, H-13), 2.31 (3 H, s, H-8), 2.22 (3 H, s, H-7), -0.12 (9 H, s, H-19). $\delta^{13}\text{C}$ (101 MHz, CDCl_3) 168.1 (C-10), 142.2 (C-12), 138.1 (C-3), 137.5 (C-6), 136.8 (C-1), 132.6 (C-11), 132.2 (C-2), 131.7 (C-16), 131.1 (C-4), 128.1 (C-15), 124.3 (C-14), 122.7 (C-17), 122.6 (C-5), 101.7 (C-9), 98.6 (C-18), 51.3 (C-13), 21.0 (C-8), 18.2 (C-7), -0.5 (C-19). IR (film, cm^{-1}): ν_{max} 2154 ($\text{C}\equiv\text{C}$), 1694 ($\text{C}=\text{O}$), 1469, 1384, 1249 (C-Si), 839. HRMS (ESI⁺): m/z calcd for $\text{C}_{21}\text{H}_{23}\text{NOSiNa}^+$ [$\text{M}+\text{Na}$]⁺ 356.1441, found 356.1442

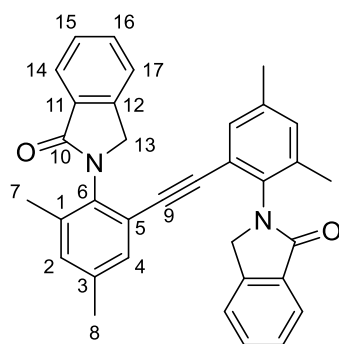
2-(2-Ethynyl-4,6-dimethylphenyl)isoindolin-1-one – 5.25



Following **GP5.2** using 2-(2,4-dimethyl-6-((trimethylsilyl)ethynyl)phenyl)isoindolin-1-one **5.24** (1.1 g, 3.3 mmol, 1.0 eq.) and K_2CO_3 (0.69 g, 5.0 mmol, 1.5 eq.) in MeOH (6.6 mL, 0.5M) for 2 h. Purification by flash column chromatography yielded the *title compound* (0.75 g, 87%) as a pink solid. **m.p.:** 138 °C (degradation). $\delta^1\text{H}$ (400 MHz, CDCl_3) 7.96 (1 H, dd, $J = 8.2, 1.1$ Hz, H-14), 7.60 (1 H, td, $J = 7.3, 1.2$ Hz, H-16), 7.55 – 7.44 (2 H, m, H-15 + H-17), 7.27 (1 H, d, $J = 2.1$ Hz, H-4), 7.14 (1 H, dd, $J = 1.9, 1.1$ Hz, H-2),

5.01 ($\text{CH}_\text{A}\text{H}_\text{B}$, 1 H, d, $J = 16.7$ Hz, H-13), 4.51 ($\text{CH}_\text{A}\text{H}_\text{B}$, 1 H, d, $J = 16.7$ Hz, H-13), 2.99 (1 H, s, H-18), 2.33 (3 H, s, H-8), 2.20 (3 H, s, H-7). $\delta^{13}\text{C}$ (101 MHz, CDCl_3) 168.0 (C-10), 142.1 (C-12), 138.3 (C-3), 137.5 (C-1), 136.4 (C-6), 132.6 (C-11), 132.4 (C-2), 132.0 (C-4), 131.7 (C-16), 128.2 (C-15), 124.5 (C-14), 122.9 (C-17), 121.8 (C-5), 81.1 (C-18), 80.5 (C-9), 51.5 (C-13), 21.0 (C-8), 18.2 (C-7). IR (film, cm^{-1}): ν_{max} 3218 ($\text{C}\equiv\text{C}-\text{H}$), 1690 ($\text{C}=\text{O}$), 1469, 1389. HRMS (ESI⁺): m/z calcd for $\text{C}_{18}\text{H}_{15}\text{NONa}^+$ [$\text{M}+\text{Na}$]⁺ 284.1046, found 284.1047.

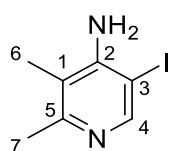
2,2'-(Ethyne-1,2-diylbis(4,6-dimethyl-2,1-phenylene))bis(isoindolin-1-one) – 5.26



Following **GP5.3** using 2-(2-iodo-4,6-dimethylphenyl)isoindolin-1-one **5.23** (0.14 g, 0.39 mmol, 1 eq.), PdCl₂(PPh₃)₂ (5.5 mg, 0.0078 mmol, 2 mol%) and CuI (3.7 mg, 0.02 mmol, 5 mol%) in Et₃N (1.2 mL, 0.3 M), followed by 2-(2-ethynyl-4,6-dimethylphenyl)isoindolin-1-one **5.25** (0.10 g, 0.39 mmol, 1 eq.) at 90 °C for 18 h. Purification by flash column chromatography yielded the *title compound* (0.13 g, 70%) as a white solid. **m.p.:** 205 °C (degradation). Mixture of conformers in a 1:0.3 ratio

in CDCl₃. **¹H (400 MHz, CDCl₃)** 7.99 (1 H^{maj}, dt, *J* = 7.6, 1.0 Hz, H-14), 7.84 (1 H^{min}, dt, *J* = 7.5, 1.1 Hz, H-14), 7.65 (1 H^{maj}, td, *J* = 7.5, 1.2 Hz, H-16), 7.61 (1 H^{min}, td, *J* = 7.5, 1.3 Hz, H-16), 7.61 – 7.51 (2 H^{maj}, m, H-15 + H-17), 7.53 – 7.50 (1 H^{min}, m, H-15), 7.46 (1 H^{min}, dt, *J* = 7.5, 0.9 Hz, H-17), 7.02 (1 H^{min}, dd, *J* = 1.4, 0.7 Hz, H-4), 6.99 (1 H^{maj}, dt, *J* = 2.1, 0.7 Hz, H-4), 6.56 (1 H^{min}, dt, *J* = 2.1, 0.7 Hz, H-2), 6.14 (1 H^{min}, dt, *J* = 2.1, 0.7 Hz, H-2), 4.94 (CH_AH_B, 1 H^{maj + min}, d, *J* = 16.6 Hz, H-13), 4.52 (CH_AH_B, 1 H^{maj}, d, *J* = 16.8 Hz, H-13), 4.43 (CH_AH_B, 1 H^{min}, d, *J* = 16.6 Hz, H-13), 2.18 (3 H^{maj}, s, H-7), 2.13 (6 H^{min}, br. s, H-7 + H-8), 2.04 (3 H^{maj}, s, H-8). **¹³C (101 MHz, CDCl₃)** 168.6 (C-10^{maj}), 167.9 (C-10^{min}), 142.4 (C-12^{maj}), 142.0 (C-12^{min}), 138.0 (C-3^{maj+min}), 137.4 (C-1^{min}), 137.3 (C-1^{maj}), 136.0 (C-6^{maj}), 135.7 (C-6^{min}), 132.5 (C-11^{maj}), 132.3 (C-11^{min}), 132.2 (C-4^{min}), 132.0 (C-4^{maj}), 131.8 (C-16^{maj}), 131.7 (C-16^{min}), 131.4 (C-2^{min}), 130.9 (C-2^{maj}), 128.14 (C-2^{min}), 128.1 (C-15^{maj}), 124.6 (C-15^{min}), 124.5 (C-14^{maj}), 123.2 (C-17^{maj}), 123.0 (C-17^{min}), 122.32 (C-5^{min}), 122.30 (C-5^{maj}), 90.3 (C-9^{min}), 90.1 (C-9^{maj}), 51.9 (C-13^{maj}), 51.7 (C-13^{min}), 20.85 (C-8^{min}), 20.82 (C-8^{maj}), 18.2 (C-7^{min}), 18.0 (C-7^{maj}). **IR (film, cm⁻¹)** ν_{max} 1693 (C=O), 1468, 1385. **HRMS (ESI⁺)** *m/z* calcd for C₃₄H₂₈N₂ONa⁺ [M+Na]⁺ 519.2043; found: 519.2044. Supplementary crystallographic data can be obtained free of charge from The Cambridge Crystallographic Data Centre (CCDC 1861805).

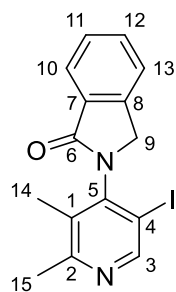
5-Iodo-2,3-dimethylpyridin-4-amine – 5.27



To a refluxing solution of 2,3-dimethylpyridin-4-amine^[317] (0.60 g, 4.9 mmol, 1.0 eq.) in conc. H₂SO₄ (0.45 mL), H₂O (2.4 mL) and AcOH (8.4 mL) was added H₅IO₆ (0.44 g, 1.9 mmol, 0.4 eq) and I₂ (0.88 g, 2.5 mmol, 0.5 eq.) and the reaction mixture was stirred at reflux for 3 h. The reaction mixture was allowed to cool down to rt and Na₂SO₃ sat was added until the colour changed to a clear solution. The reaction mixture was extracted with CH₂Cl₂, organic phases were combined, dried with MgSO₄, filtered, and concentrated *in vacuo* to give the title compound (0.92 g, 63%) as a white solid which was used without further purification. **m.p.:** 101 – 103 °C (degradation). **¹H (400 MHz, CDCl₃)** 8.33 (1 H, s, H-4), 4.52 (2 H, br. s, NH₂), 2.42 (3 H, s, H-7), 2.12 (3 H, s, H-6). **¹³C (101 MHz, CDCl₃)** 156.0 (C-5), 153.2 (C-4), 150.6 (C-2), 115.3 (C-1), 80.5 (C-3),

22.6 (C-7), 13.5 (C-6). **IR (film, cm⁻¹)** ν_{\max} 2958 (C–H), 1479, 1272, 1044 (C–I). **HRMS (ESI⁺)** m/z calcd for C₇H₁₀N₂I⁺ [M+H]⁺ 248.9889, found 248.9892.

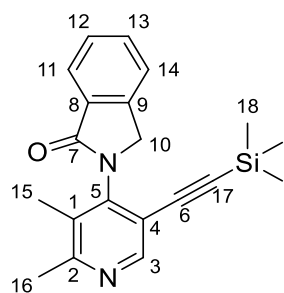
2-(5-Iodo-2,3-dimethylpyridin-4-yl)isoindolin-1-one – 5.28



To a solution of 5-iodo-2,3-dimethylpyridin-4-amine **5.27** (0.92 g, 3.7 mmol, 1.0 eq.) in CH₂Cl₂ (37 mL, 0.1 M) was added 2-(chloromethyl)benzoyl chloride **5.21** (0.58 mL, 4.1 mmol, 1.1 eq.) and Et₃N (0.61 mL, 4.4 mmol, 1.2 eq.) at 0 °C under an atmosphere of nitrogen. The reaction mixture was stirred at rt for 6 h, washed with sat. NaHCO₃ (aq.), water, brine, dried over MgSO₄, filtered, and concentrated *in vacuo*. The crude mixture was diluted in CH₂Cl₂ (37 mL, 0.1 M), DBU (0.61 mL, 4.4 mmol, 1.2 eq.) was

added and the reaction mixture was stirred at rt for 22 h. The reaction mixture was washed with sat. NaHCO₃ (aq.), water, brine, dried over MgSO₄, filtered, and concentrated *in vacuo*. Purification by flash column chromatography yielded the title compound (0.30 g, 22%) as a pink solid. **m.p.:** 192 °C (degradation) **$\delta^1\text{H}$ (400 MHz, CDCl₃)** 8.75 (1 H, s, H-3), 8.07 – 7.88 (1 H, m, H-10), 7.65 (1 H, td, J = 7.2, 6.8, 1.2 Hz, H-12), 7.56 (2 H, t, J = 7.2 Hz, H-11 + H-13), 4.90 (CH_AH_B, 1 H, d, J = 16.4 Hz, H-9), 4.48 (CH_AH_B, 1 H, d, J = 16.4 Hz, H-9), 2.54 (3 H, s, H-15), 2.20 (3 H, s, H-14). **$\delta^{13}\text{C}$ (101 MHz, CDCl₃)** 167.3 (C-6), 159.2 (C-2), 154.5 (C-3), 146.8 (C-5), 141.6 (C-7), 133.5 (C-1), 132.4 (C-12), 131.8 (C-7), 128.6 (C-11), 124.8 (C-10), 123.3 (C-13), 94.9 (C-4), 50.6 (C-9), 23.0 (C-15), 15.2 (C-14). **IR (film, cm⁻¹)** ν_{\max} 1694 (C=O), 1455. **HRMS (ESI⁺)** m/z calcd for C₁₅H₁₃N₂OINa⁺ [M+Na]⁺ 386.9970, found 386.9977.

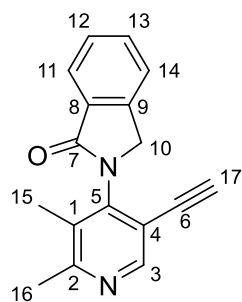
2-(2,3-Dimethyl-5-((trimethylsilyl)ethynyl)pyridin-4-yl)isoindolin-1-one – 5.29



Following **GP5.3** using 2-(5-iodo-2,3-dimethylpyridin-4-yl)isoindolin-1-one **5.28** (0.36 g, 1.0 mmol, 1 eq.), PdCl₂(PPh₃)₂ (14 mg, 0.02 mmol, 2 mol%) and CuI (9.5 mg, 0.05 mmol, 5 mol%) in Et₃N (3.5 mL, 0.3 M), followed by ethynyltrimethylsilane (0.29 mL, 2.1 mmol, 2.1 eq.) at 90 °C for 2 h. Purification by flash column chromatography yielded the title compound (0.26 g, 78%) as a yellow oil. **$\delta^1\text{H}$ (400 MHz, CDCl₃)** 8.50 (1 H, s, H-3),

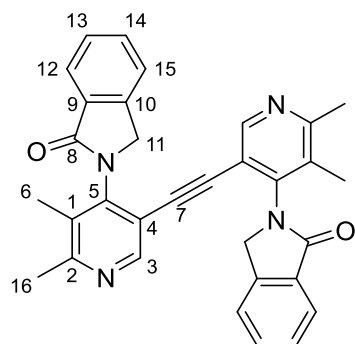
7.95 (1 H, dt, J = 7.7, 1.2 Hz, H-11), 7.62 (1 H, td, J = 7.6, 1.2 Hz, H-13), 7.57 – 7.48 (2 H, m, H-12 + H-14), 5.14 (CH_AH_B, 1 H, d, J = 16.4 Hz, H-10), 4.50 (CH_AH_B, 1 H, d, J = 16.4 Hz, H-10), 2.59 (3 H, s, H-16), 2.19 (3 H, s, H-15), -0.07 (9 H, s, H-18). **$\delta^{13}\text{C}$ (101 MHz, CDCl₃)** 167.7 (C-7), 159.2 (C-2), 150.1 (C-3), 146.5 (C-5), 142.1 (C-9), 132.2 (C-13), 131.9 (C-8), 131.0 (C-1), 128.4 (C-12), 124.6 (C-11), 122.9 (C-14), 117.0 (C-4), 102.3 (C-17), 98.8 (C-6), 51.0 (C-10), 23.6 (C-16), 14.3 (C-15), -0.5 (C-18). **IR (film, cm⁻¹):** ν_{\max} 2958 (C–H), 2156 (C≡C), 1700 (C=O), 1378, 1250 (C–Si), 843. **HRMS (ESI⁺):** m/z calcd for C₂₀H₂₂N₂OSiNa⁺ [M+Na]⁺ 357.1399, found 357.1403.

2-(5-Ethynyl-2,3-dimethylpyridin-4-yl)isoindolin-1-one



Following **GP5.2** using 2-(2,3-dimethyl-5-((trimethylsilyl)ethynyl)pyridin-4-yl)isoindolin-1-one **5.29** (0.23 g, 0.69 mmol, 1.0 eq.) and K_2CO_3 (0.14 g, 1.0 mmol, 1.5 eq.) in MeOH (2.3 mL, 0.3M) for 45 minutes. Purification by flash column chromatography yielded the *title compound* (0.16 g, 89%) as a white solid. **m.p.:** 151 °C (degradation). **δ^1H (400 MHz, $CDCl_3$)** 8.55 (1 H, s, H-3), 7.95 (1 H, dd, $J = 7.8, 1.5$ Hz, H-11), 7.63 (1 H, td, $J = 7.0, 1.1$ Hz, H-13), 7.56 – 7.50 (2 H, m, H-12 + H-14), 5.14 (CH_AH_B , 1 H, d, $J = 16.4$ Hz, H-10), 4.50 (CH_AH_B , 1 H, d, $J = 16.5$ Hz, H-10), 3.17 (1 H, s, H-17), 2.59 (3 H, s, H-16), 2.15 (3 H, s, H-15). **$\delta^{13}C$ (101 MHz, $CDCl_3$)** 167.5 (C-7), 159.7 (C-2), 150.9 (C-3), 146.1 (C-5), 142.0 (C-9), 132.2 (C-13), 131.7 (C-8), 130.9 (C-1), 128.4 (C-12), 124.6 (C-11), 123.1 (C-14), 116.1 (C-4), 84.1 (C-6), 77.9 (C-17), 51.1 (C-10), 23.7 (C-16), 14.4 (C-15). **IR (film, cm^{-1}):** ν_{max} 3291 (C \equiv C–H), 3221, 1692 (C=O), 1470, 1142. **HRMS (ESI⁺)** m/z calcd for $C_{17}H_{14}N_2ONa$ $[M+Na]^+$ 285.1004, found 285.1010

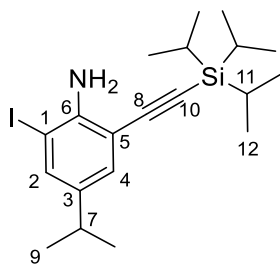
2,2'-(Ethyne-1,2-diylbis(5,6-dimethylpyridine-3,4-diyl))bis(isoindolin-1-one) 5.30



Following **GP5.3** using 2-(5-iodo-2,3-dimethylpyridin-4-yl)isoindolin-1-one (0.17 g, 0.48 mmol, 1 eq.), $PdCl_2(PPh_3)_2$ (6.7 mg, 9.5 μ mol, 2 mol%) and CuI (4.6 mg, 0.024 mmol, 5 mol%) in Et_3N /DMF (1:1, 1.6 mL, 0.3 M), followed by 2-(5-ethynyl-2,3-dimethylpyridin-4-yl)isoindolin-1-one (0.10 g, 0.39 mmol, 1 eq.) at 90 °C for 18 h. Purification by flash column chromatography yielded the *title compound* (5 mg, 2%) as a colourless oil. Mixture of conformers in a

1:0.4 ratio in $CDCl_3$. **δ^1H (500 MHz, $CDCl_3$)** 8.24 (2 H^{min} , s, H-3), 7.97 (2 H^{maj} , d, $J = 7.6$ Hz, H-12), 7.77 (2 H^{maj} , s, H-3), 7.70 – 7.65 (2 $H^{maj} + 2H^{min}$, m, H-13^{maj} + H-12^{min}), 7.62 (1 H^{min} , t, $J = 7.3$ Hz, H-13), 7.60 – 7.53 (4 H^{maj} , m, H-14 + H-15), 7.50 (1 H^{min} , t, $J = 7.5$ Hz, H-14), 7.45 (1 H^{min} , d, $J = 7.6$ Hz, H-15), 5.10 (CH_AH_B , 2 H^{min} , d, $J = 16.4$ Hz, H-11), 5.04 (CH_AH_B , 2 H^{maj} , d, $J = 16.5$ Hz, H-11), 4.51 (CH_AH_B , 2 H^{maj} , d, $J = 16.5$ Hz, H-11), 4.39 (CH_AH_B , 2 H^{min} , d, $J = 16.4$ Hz, H-11), 2.55 (6 H^{min} , s, H-16), 2.53 (6 H^{maj} , s, H-16), 2.16 (6 H^{maj} , s, H-6), 2.07 (6 H^{min} , s, H-6). **$\delta^{13}C$ (126 MHz, $CDCl_3$)** 168.1 (C-8^{maj}), 167.4 (C-8^{min}), 159.73 (C-1^{min}), 159.69 (C-1^{maj}), 150.3 (C-3^{min}), 149.7 (C-3^{maj}), 145.7 (C-5^{maj}), 145.3 (C-5^{min}), 141.9 (C-10^{maj}), 141.7 (C-10^{min}), 132.7 (C-14^{maj}), 132.5 (C-14^{min}), 131.5 (C-9^{maj}), 131.14 (C-1^{maj}), 131.08 (C-9^{min}), 130.8 (C-1^{min}), 128.8 (C-13^{maj}), 128.5 (C-13^{min}), 124.7 (C-12^{min}), 124.6 (C-12^{maj}), 123.3 (C-15^{maj}), 123.1 (C-15^{min}), 116.5 (C-4^{maj}), 116.2 (C-4^{min}), 90.2 (C-7^{min}), 90.0 (C-7^{maj}), 51.5 (C-11^{maj}), 51.3 (C-11^{min}), 23.7 (C-16^{min}), 23.6 (C-16^{maj}), 14.6 (C-6^{min}), 14.3 (C-6^{maj}). **IR (film, cm^{-1})** ν_{max} 2924 (C–H), 1701 (C=O), 1468, 1409, 1378, 1143. **HRMS (ESI⁺)** m/z calcd for $C_{32}H_{26}N_4O_2$ $[M+H]^+$ 499.2128; found: 499.2141.

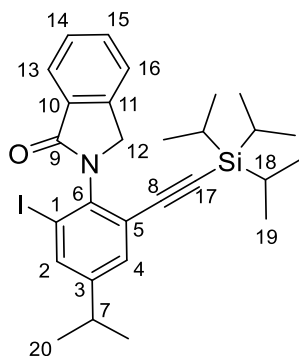
2-Iodo-4-isopropyl-6-((triisopropylsilyl)ethynyl)aniline – 5.32



Following **GP5.3** using 2,6-diiodo-4-isopropylaniline **5.31**^[318] (0.80 g, 2.1 mmol, 1 eq.), PdCl₂(PPh₃)₂ (29 mg, 0.042 mmol, 2 mol%) and CuI (20 mg, 0.11 mmol, 5 mol%) in Et₃N (7.0 mL, 0.3 M), followed by (triisopropylsilyl)acetylene (0.46 mL, 2.1 mmol, 1.0 eq.) at 90 °C for 15 h.

Purification by flash column chromatography yielded the title compound (0.26 g, 28%) as a yellow oil. **¹H (400 MHz, CDCl₃)** 7.47 (1 H, d, *J* = 2.0 Hz, H-2), 7.15 (1 H, d, *J* = 2.0 Hz, H-4), 4.59 (2 H, br. s, NH₂), 2.73 (1 H, hept, *J* = 5.9 Hz, H-7), 1.19 (6 H, d, *J* = 5.9 Hz, H-9), 1.14 (21 H, br. s, H-11 + H-12). **¹³C (101 MHz, CDCl₃)** 146.5 (C-6), 139.8 (C-3), 137.72 (C-2), 130.5 (C-4), 108.1 (C-5), 103.8 (C-8), 96.4 (C-10), 83.2 (C-1), 33.0 (C-7), 24.1 (C-9), 18.9 (C-12), 11.4 (C-11). **IR (film, cm⁻¹):** ν_{max} 3475 (N–H), 3376 (N–H), 2967 (C–H), 2941 (C–H), 2864 (C–H), 2143 (C≡C), 1609, 1583, 1464. **HRMS (ESI⁺):** *m/z* calcd for C₂₀H₃₃NOiSi [M+H]⁺ 442.1422, found 442.1406.

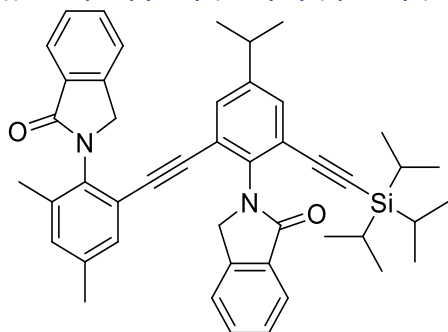
2-(2-Iodo-4-isopropyl-6-((triisopropylsilyl)ethynyl)phenyl)isoindolin-1-one – 5.33



To a solution of 2-iodo-4-isopropyl-6-((triisopropylsilyl)ethynyl)aniline **5.32** (0.23 g, 0.5 mmol, 1 eq.) in CH₂Cl₂ (2.6, 0.1 M) was added 2-(chloromethyl)benzoyl chloride **5.21** (0.15 mL, 1.0 mmol, 2.1 eq.) and Et₃N (0.22 mL, 1.6 mmol, 3.1 eq.) at rt under an atmosphere of nitrogen. The reaction mixture was stirred at rt for 24h. The reaction mixture was diluted in ethyl acetate and washed with 1M HCl (aq.), brine, dried over MgSO₄, filtered, and concentrated *in vacuo*. The crude residue obtained was

dissolved in CH₂Cl₂ (2.6 mL, 0.1 M) and DBU (0.24 mL, 1.6 mmol, 3.1 eq.) was added. The reaction mixture was heated under reflux for 24 h, diluted in ethyl acetate and washed with 1M HCl (aq.), brine, dried over MgSO₄, filtered, and concentrated *in vacuo*. Purification by flash column chromatography yielded the *title compound* (0.13 g, 45%) as a yellow oil. **¹H (400 MHz, CDCl₃)** 7.93 (1 H, dt, *J* = 7.5, 1.0 Hz, H-13), 7.74 (1 H, d, *J* = 2.0 Hz, H-2), 7.58 (1 H, td, *J* = 7.5, 1.2 Hz, H-15), 7.52 – 7.44 (2 H, m, H-14 + H-16), 7.39 (1 H, d, *J* = 1.9 Hz, H-4), 4.83 (CH_AH_B, 1 H, d, *J* = 16.2 Hz, H-12), 4.73 (CH_AH_B, 1 H, d, *J* = 16.2 Hz, H-12), 2.87 (1 H, hept, *J* = 5.9 Hz, H-7), 1.26 (6 H, d, *J* = 5.9 Hz, H-20), 0.90 – 0.82 (21 H, m, H-18 + H-19). **¹³C (101 MHz, CDCl₃)** 167.5 (C-9), 151.0 (C-3), 142.0 (C-11), 140.3 (C-6), 137.8 (C-2), 132.6 (C-10), 131.9 (C-15 or C-4), 131.8 (C-15 or C-4), 128.1 (C-14), 124.6 (C-13), 124.4 (C-5), 122.9 (C-16), 102.6 (C-1), 99.9 (C-8), 96.2 (C-17), 50.9 (C-12), 33.7 (C-7), 23.8 (C-20), 18.4 (C-19), 11.2 (C-18). **IR (film, cm⁻¹):** ν_{max} 2942 (C–H), 2863 (C–H), 1705 (C=O), 1460. **HRMS (ESI⁺):** *m/z* calcd for C₂₈H₃₇NOSiNa [M+Na]⁺ 558.1684, found 558.1687.

2-(2-((3,5-Dimethyl-2-(1-oxoisindolin-2-yl)phenyl)ethynyl)-4-isopropyl-6-
((triisopropylsilyl)ethynyl)phenyl)isoindolin-1-one – 5.34

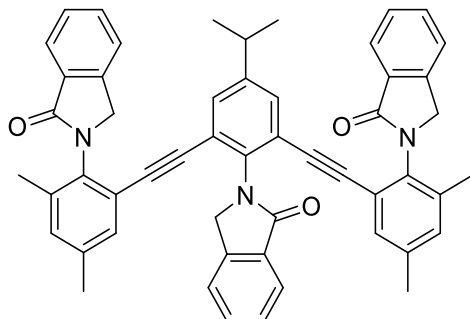


Following **GP5.3** using 2-(2-iodo-4-isopropyl-6-((triisopropylsilyl)ethynyl)phenyl)isoindolin-1-one **533** (0.13 g, 0.23 mmol, 1.0 eq.), PdCl₂(PPh₃)₂ (6.5 mg, 0.0092 mmol, 4 mol%) and CuI (4.4 mg, 0.023 mmol, 10 mol%) in Et₃N/DMF (1:1, 0.77 mL, 0.3 M), followed by 2-(2-ethynyl-4,6-dimethylphenyl)isoindolin-1-one **5.25** (0.12 g, 0.46 mmol, 2.0 eq.) at 90 °C for 18 h.

Purification by flash column chromatography yielded the *title compound* (0.12 g, 75%) as an off-white solid. **m.p.**: 107 – 111 °C. Mixture of conformers in a 1:0.3 ratio in CDCl₃. **¹H (500 MHz, CDCl₃)** 7.99 (1 H^{maj}, d, *J* = 7.6 Hz, ArCH), 7.96 (1 H^{maj}, d, *J* = 7.6 Hz, ArCH), 7.86 (1 H^{min}, d, *J* = 7.5 Hz, ArCH), 7.81 (1 H^{min}, d, *J* = 7.6 Hz, ArCH), 7.67 – 7.58 (2 H^{maj} + 1 H^{min}, m, ArCH), 7.57 – 7.44 (4 H^{maj} + 3 H^{min}, m, ArCH), 7.38 (1 H^{min}, d, *J* = 7.6 Hz, ArCH), 7.33 (1 H^{min}, d, *J* = 7.6 Hz, ArCH), 7.29 (1 H^{min}, d, *J* = 2.1 Hz, ArCH), 7.26 (1 H^{maj}, s, ArCH), 7.05 (1 H^{min}, s, ArCH), 7.02 (1 H^{maj}, s, ArCH), 6.93 – 6.87 (2 H^{min}, m, ArCH), 6.41 (2 H^{maj}, dd, *J* = 13.4, 2.0 Hz, ArCH), 5.01 (1 H^{maj}, d, *J* = 16.8 Hz, NCH₂), 4.85 (1 H^{maj}, d, *J* = 16.3 Hz, NCH₂), 4.82 (1 H^{min}, d, *J* = 16.8 Hz, NCH₂), 4.76 (1 H^{min}, d, *J* = 16.2 Hz, NCH₂), 4.73 (1 H^{maj}, d, *J* = 16.3 Hz, NCH₂), 4.54 (1 H^{maj} + 1 H^{min}, d, *J* = 16.9 Hz, NCH₂), 4.36 (1 H^{min}, d, *J* = 16.7 Hz, NCH₂), 2.72 (1 H^{min}, hept, *J* = 5.9 Hz, CCH(CH₃)₂), 2.58 (1 H^{maj}, hept, *J* = 7.0 Hz, CCH(CH₃)₂), 2.20 (3 H^{min}, s, CCH₃), 2.19 (3 H^{maj}, s, CCH₃), 2.12 (3 H^{min}, s, CCH₃), 2.09 (3 H^{maj}, s, CCH₃), 1.13 (6 H^{min}, dd, *J* = 7.0, 3.6 Hz, CCH(CH₃)₂), 1.01 (6 H^{maj}, dd, *J* = 5.9, 2.5 Hz, CCH(CH₃)₂), 0.89 (21 H^{maj}, s, SiCH(CH₃)₂ + CCH(CH₃)₂), 0.85 (21 H^{min}, d, *J* = 3.5, SiCH(CH₃)₂ + SiCH(CH₃)₂). **¹³C (126 MHz, CDCl₃)** 168.5 (C=O^{maj}), 168.1 (C=O^{min}), 167.8 (C=O^{min}), 167.6 (C=O^{min}), 148.8 (ArC^{maj} + ^{min}), 142.4 (ArC^{maj}), 142.3 (ArC^{maj}), 142.00 (ArC^{min}), 141.96 (ArC^{min}), 139.4 (ArC^{maj}), 138.9 (ArC^{min}), 138.12 (ArC^{min}), 138.10 (ArC^{maj}), 137.31 (ArC^{maj}), 137.26 (ArC^{min}), 136.1 (ArC^{maj}), 135.5 (ArC^{min}), 132.6 (ArC^{maj}), 132.48 (ArC^{maj}), 132.46 (ArC^{min}), 132.34 (ArCH^{min}), 132.30 (ArC^{min}), 132.2 (ArCH^{maj}), 132.0 (ArCH^{min}), 131.89 (ArCH^{maj}), 131.87 (ArCH^{min}), 131.7 (2 ArCH^{maj} + 1 ArCH^{min}), 131.6 (ArCH^{min}), 131.5 (ArCH^{min}), 131.1 (ArCH^{maj}), 130.7 (ArCH^{maj}), 128.2 (ArCH^{maj}), 128.17 (ArCH^{min}), 127.93 (ArCH^{min}), 127.91 (ArCH^{maj}), 124.6 (ArCH^{min}), 124.5 (ArCH^{min}), 124.41 (ArCH^{maj}), 124.40 (ArCH^{maj}), 123.8 (ArC^{maj}), 123.7 (ArC^{min}), 123.6 (ArC^{min}), 123.4 (ArC^{maj}), 123.2 (ArCH^{maj}), 123.0 (ArCH^{maj}), 122.92 (ArCH^{min}), 122.91 (ArCH^{min}), 122.3 (ArC^{min}), 122.2 (ArC^{maj}), 102.8 (C≡C^{min}), 102.7 (C≡C^{maj}), 95.81 (C≡C^{min}), 95.76 (C≡C^{maj}), 90.5 (C≡C^{min}), 90.4 (C≡C^{maj}), 89.8 (C≡C^{min}), 89.6 (C≡C^{maj}), 51.9 (NCH₂^{maj}), 51.7 (NCH₂^{maj}), 51.6 (NCH₂^{min}), 51.5 (NCH₂^{min}), 33.7 (CCH(CH₃)₂^{min}), 33.6 (CCH(CH₃)₂^{maj}), 23.64 (CCH(CH₃)₂^{min}), 23.56 (CCH(CH₃)₂^{maj}), 23.52 (CCH(CH₃)₂^{maj}), 20.90 (CCH₃^{min}), 20.87 (CCH₃^{maj}), 18.50 (SiCH(CH₃)₂^{maj}), 18.47 (SiCH(CH₃)₂^{min}), 18.2 (CCH₃^{min}), 18.1 (CCH₃^{maj}).

11.19 (SiCH(CH₃)₂^{maj}), 11.16 (SiCH(CH₃)₂^{min}). IR (film, cm⁻¹) ν_{\max} 2943 (C–H), 2864 (C–H), 1702 (C=O), 1468, 1384. HRMS (ESI⁺) m/z calcd for C₄₆H₅₀N₂O₂SiNa⁺ [M+Na]⁺ 713.3534; found: 713.3563.

2,2'-(((5-Isopropyl-2-(1-oxoisindolin-2-yl)-1,3-phenylene)bis(ethyne-2,1-diyl))bis(4,6-dimethyl-2,1-phenylene))bis(isoindolin-1-one) – 5.35

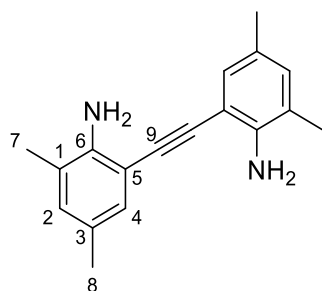


To a solution of 2-(2-((3,5-dimethyl-2-(1-oxoisindolin-2-yl)phenyl)ethynyl)-4-isopropyl-6-((triisopropylsilyl)ethynyl)phenyl)isoindolin-1-one **5.34** (110 mg, 0.16 mmol, 1.0 eq.) in THF (1.0 mL, 0.15M) was added TBAF (1.0M in THF, 0.24 mL, 0.24 mmol, 1.5 eq.) and the reaction mixture was stirred at rt for 30 min. Brine was added and the reaction

mixture was extracted with CH₂Cl₂. The combined organic phases were dried over MgSO₄, filtered and concentrated *in vacuo*. The crude deprotected alkyne was used without further purification. Following **GP5.3** using 2-(2-iodo-4,6-dimethylphenyl)isoindolin-1-one **5.23** (110 g, 0.32 mmol, 2.0 eq.), PdCl₂(PPh₃)₂ (4.5 mg, 0.0064 mmol, 4 mol%) and CuI (3.0 mg, 0.016 mmol, 10 mol%) in Et₃N/DMF (1:2, 0.8 mL, 0.2 M), followed by the previously deprotected alkyne (0.16 mmol, 1.0 eq.) at 90 °C for 20 h. Purification by flash column chromatography yielded the *title compound* (91 mg, 74%) as a yellow solid. **m.p.**: 204 °C (degradation). Mixture of conformers in CDCl₃: **A**(*syn, syn*): 8% ; **B**(*anti, anti*): 49% ; **C**(*anti, syn*) 43%. Not every signal for isomer A were visible by NMR. **$\delta^1\text{H}$ (400 MHz, CDCl₃)** 8.01 (1 H^B, dt, J = 7.6, 1.0 Hz, ArCH), 7.96 (2 H^B + 1 H^C, dt, J = 7.5, 0.9 Hz, ArCH), 7.88 (1 H^C, dt, J = 7.5, 1.0 Hz, ArCH), 7.77 (1 H^B, d, J = 7.6 Hz, ArCH), 7.70 – 7.66 (1 H^C, m, ArCH), 7.65 (1 H^B, td, J = 4.5, 1.2 Hz, ArH ArCH), 7.63 – 7.48 (6 H^B + 7 H^C, m, ArCH), 7.47 – 7.43 (2 H^B, m, ArCH), 7.32 (1 H^C, d, J = 7.5 Hz, ArCH), 7.05 (1 H^C, d, J = 2.0 Hz, ArCH), 7.02 (2 H^B, d, J = 2.0 Hz, ArCH), 6.99 (1 H^C, d, J = 1.7 Hz, ArCH), 6.94 (1 H^C, d, J = 2.0 Hz, ArCH), 6.79 (1 H^C, d, J = 2.1 Hz, ArCH), 6.47 (1 H^B + 1 H^C, d, J = 2.0 Hz, ArCH), 6.32 (2 H^B, s, ArH), 6.23 (1 H^C, d, J = 2.1 Hz, ArCH), 6.16 (1 H^C, d, J = 2.0 Hz, ArCH), 4.97 (CH_AH_B, 2 H^B, d, J = 16.6 Hz, NCH₂), 4.94 (CH_AH_B, 1 H^C, d, J = 16.9 Hz, NCH₂), 4.86 (CH_AH_B, 1 H^C, d, J = 16.7 Hz, NCH₂), 4.78 (CH_AH_B, 2 H^A, d, J = 16.7), 4.73 (2 H^B, br. s, NCH₂), 4.60 (2 H^C, br. s, NCH₂), 4.54 (CH_AH_B, 1 H^C, d, J = 16.9 Hz, NCH₂), 4.50 (CH_AH_B, 2 H^B, d, J = 16.8 Hz, NCH₂), 4.37 (CH_AH_B, 1 H^C, d, J = 16.7 Hz, NCH₂), 4.31 (CH_AH_B, 2 H^A, d, J = 16.9 Hz, NCH₂), 2.53 (1H^A, br. s, CH(CH₃)₂), 2.38 (1 H^C, hept, J = 7.0 Hz, CH(CH₃)₂), 2.31 – 2.24 (1 H^B, m, CH(CH₃)₂), 2.22 (3 H^C, s, CCH₃), 2.21 – 2.17 (6 H^A + 6 H^B + 3 H^C, m, CCH₃), 2.14 – 2.09 (6 H^A + 6 H^B + 3 H^C, m, CCH₃), 2.06 (3 H^C, s, CCH₃), 0.99 (6 H^A, d, J = 5.9 Hz, CH(CH₃)₂), 0.87 (6 H^C, d, J = 5.9 Hz, CH(CH₃)₂), 0.80 (6 H^B, d, J = 5.9 Hz, CH(CH₃)₂). **$\delta^{13}\text{C}$ (126 MHz, CDCl₃)** 168.8 (C^B=O), 168.6 (C^C=O), 168.5 (C^C=O), 168.4 (C^B=O), 167.83 (C^C=O), 167.81 (C^A=O), 148.65 (ArC^B), 148.62 (ArC^C), 148.59 (ArC^A), 142.6 (ArC^B), 142.5 (ArC^C), 142.4 (ArC^C),

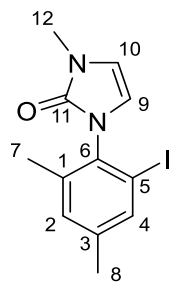
142.3 (ArC^B), 141.9 (ArC^B), 138.8 (ArC^B), 138.7 (ArC^C), 138.16 (ArC^B), 138.14 (ArC^B), 138.10 (ArC^A), 138.08 (ArC^C), 137.37 (ArC^B), 137.34 (ArC^C), 137.30 (ArC^C), 136.12 (ArC^B), 136.10 (ArC^C), 135.7 (ArC^C), 135.6 (ArC^A), 132.46 (ArCH^{B+C}), 132.44 (ArCH^C), 132.38 (ArCH^A), 132.32 (ArCH^B), 132.23 (ArCH^C), 132.17 (ArCH^C), 132.16 (ArCH^A), 132.0 (ArCH^C), 131.90 (ArCH^A), (ArCH^C) 131.86 (ArCH^B), 131.83 (ArCH^C), 131.76 (ArCH^A), 131.71 (ArCH^B), 131.69 (ArCH^A), 131.66 (ArCH^C), 131.04 (ArCH^C), 130.96 (ArCH^B), 130.87 (ArCH^A), 128.22 (ArCH^B), 128.19 (ArCH^C), 128.18 (ArCH^C), 128.16 (ArCH^A), 128.03 (ArCH^B), 128.00 (ArCH^A), 127.96 (ArCH^C), 124.82 (ArCH^A), 124.67 (ArCH^C), 124.46 (ArCH^C), 124.44 (ArCH^B), 124.41 (ArCH^C), 123.54 (ArCH^B), 123.47 (ArCH^C), 123.35 (ArCH^A), 123.23 (ArCH^C), 123.16 (ArC^B), 123.14 (ArCH^C), 123.13 (ArCH^B), 123.04 (ArC^C), 122.92 (ArCH^B), 122.90 (ArCH^A), 122.25 (ArC^C), 122.18 (ArC^A), 122.16 (ArC^B), 122.12 (ArC^C), 90.75 (C^A≡C), 90.65 (C^C≡C), 90.63 (C^C≡C), 90.53 (C^B≡C), 89.67 (C^A≡C), 89.63 (C^C≡C), 89.51 (C^C≡C), 89.45 (C^B≡C), 52.1 (NC^BH₂), 52.0 (NC^CH₂), 51.9 (NC^CH₂), 51.8 (NC^BH₂), 51.7 (NC^AH₂), 51.61 (NC^CH₂), 51.56 (NC^AH₂), 33.5 (C^AH(CH₃)₂), 33.4 (C^CH(CH₃)₂), 33.3 (C^BH(CH₃)₂), 23.5 (CH(C^AH₃)₂), 23.39 (CH(C^CH₃)₂), 23.38 (CH(C^CH₃)₂), 23.3 (CH(C^BH₃)₂), 20.94 (C^CH₃), 20.90 (C^BH₃), 20.86 (C^CH₃), 18.20 (C^CH₃), 18.18 (C^AH₃), 18.09 (C^BH₃), 18.04 (C^CH₃). IR (film, cm⁻¹) ν_{max} 1698 (C=O), 1468, 1384. HRMS (ESI⁺) *m/z* calcd for C₅₃H₄₄N₃O₃⁺ [M+H]⁺ 770.3377; found: 770.3408.

6,6'-(Ethyne-1,2-diyl)bis(2,4-dimethylaniline) -5.42



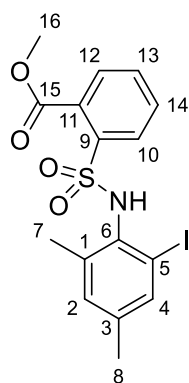
Following **GP5.2** using 2,4-dimethyl-6-((trimethylsilyl)ethynyl)aniline **5.41**^[319] (0.72 g, 3.3 mmol, 1.0 eq.) and K₂CO₃ (0.69 g, 5.0 mmol, 1.5 eq.) in MeOH (6.6 mL, 0.5M) to yield 2-ethynyl-4,6-dimethylaniline which was used without further purification. Following **GP5.3** using 2-iodo-4,6-dimethyl aniline^[316] (0.81 g, 3.3 mmol, 1 eq.), PdCl₂(PPh₃)₂ (46 mg, 0.066 mmol, 2 mol%) and CuI (31 mg, 0.16 mmol, 5 mol%) in Et₃N (11 mL, 0.3 M), followed by 2-ethynyl-4,6-dimethylaniline (3.3 mmol, 1.0 eq.) at 90 °C for 18 h. Purification by flash column chromatography yielded the title compound (0.38 g, 43%) as a brown oil. **^δ1H (400 MHz, CDCl₃)** 7.08 (2 H, br. s, H-4), 6.87 (2 H, br. s, H-2), 4.12 (4 H, br. s, NH), 2.22 (6 H, s, H-8), 2.17 (6 H, s, H-7). **^δ13C (101 MHz, CDCl₃)** 143.6 (C-6), 131.9 (C-2), 129.9 (C-4), 127.0 (C-8), 122.0 (C-1), 108.1 (C-5), 91.3 (C-9), 20.4 (C-8), 17.7 (C-7). IR (film, cm⁻¹) ν_{max} 3415 (N–H), 3329 (N–H), 1625, 1479, 1307, 1245. HRMS (ESI⁺) *m/z* calcd for C₁₈H₂₀N₂Na⁺ [M+Na]⁺ 287.1519; found: 187.1527.

1-(2-Iodo-4,6-dimethylphenyl)-3-methyl-1,3-dihydro-2H-imidazol-2-one – 5.44a



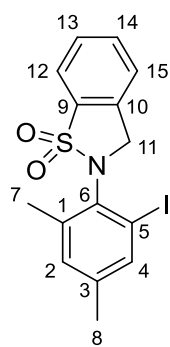
To a solution of 2-iodo-4,6-dimethylaniline^[316] (0.60 g, 2.4 mmol, 1 eq.) in CH₂Cl₂ (6 mL, 0.4 M) at -78 °C was added pyridine (0.23 mL, 2.9 mmol, 1.2 eq.), followed by triphosgene (0.33 g, 1.1 mmol, 0.45 eq.). The reaction mixture was allowed to warm up to rt and stirred for 2 h. The reaction mixture was concentrated *in vacuo*, dissolved in CH₂Cl₂ (24 mL, 0.1 M) and (methylamino)acetaldehyde dimethyl acetal (0.46 mL, 1.5 eq.). The reaction mixture was heated under reflux for 24 h, concentrated *in vacuo*, diluted in ethyl acetate, and washed with sat. NaHCO₃ (aq.), sat. NH₄Cl (aq.) and brine. The organic phase was dried over MgSO₄, filtered, and concentrated *in vacuo*. The crude residue was dissolved in chloroform (8 mL, 0.25 M) with TFA (0.38 mL, 5.1 mmol, 2.1 eq.), heated to 60 °C for 4 h and concentrated *in vacuo*. Purification by flash column chromatography yielded the title compound (0.63 g, 80%) as an off-white solid. **m.p.:** 136 – 138 °C. **$\delta^1\text{H}$ (400 MHz, CDCl₃)** 7.67 – 7.53 (1 H, m, H-4), 7.14 – 6.87 (1 H, m, H-2), 6.33 (1 H, d, *J* = 2.9 Hz, H-10), 6.14 (1 H, d, *J* = 2.9 Hz, H-9), 3.34 (3 H, s, H-12), 2.29 (3 H, s, H-8), 2.16 (3 H, s, H-7). **$\delta^{13}\text{C}$ (101 MHz, CDCl₃)** 151.8 (C-11), 140.9 (C-3), 138.4 (C-1), 137.7 (C-4), 135.7 (C-6), 131.8 (C-2), 112.6 (C-10), 111.0 (C-9), 99.3 (C-5), 30.9 (C-12), 20.7 (C-8), 19.1 (C-7). **IR (film, cm⁻¹)** ν_{max} 1682 (C=O), 1481. **HRMS (ESI⁺)** *m/z* calcd for C₁₂H₁₃N₂OINa⁺ [M+Na]⁺ 350.9965; found: 350.9981.

Methyl 2-(N-(2-iodo-4,6-dimethylphenyl)sulfamoyl)benzoate – 5.45



To a solution of 2-iodo-4,6-dimethylaniline^[316] (0.60 g, 2.4 mmol, 1.0 eq.) in pyridine (12 mL, 0.2 M) was added methyl 2-(chlorosulfonyl)benzoate (0.63 g, 2.7 mmol, 1.1 eq.) under an atmosphere of nitrogen. The reaction mixture was stirred at 60 °C for 72 h and concentrated *in vacuo*. The reaction mixture was diluted in ethyl acetate and washed with 1M HCl (aq.), brine, dried over MgSO₄, filtered, and concentrated *in vacuo*. Purification by flash column chromatography yielded the title compound (0.40 g, 37%) as an off-white solid. **m.p.:** 136 – 138 °C. **$\delta^1\text{H}$ (400 MHz, CDCl₃)** 7.96 (1 H, br. s, NH), 7.93 – 7.85 (2 H, m, H-12 + H-13), 7.64 (1 H, td, *J* = 7.7, 1.6 Hz, H-10), 7.59 (1 H, td, *J* = 7.6, 1.5 Hz, H-14), 7.43 (1 H, br. s, H-4), 7.04 (1 H, br. s, H-2), 4.05 (3 H, s, H-16), 2.42 (3 H, s, H-7), 2.24 (3 H, s, H-8). **$\delta^{13}\text{C}$ (101 MHz, CDCl₃)** 168.3 (C-15), 142.2 (C-9), 140.2 (C-6), 139.5 (C-3), 137.9 (H-4), 134.9 (C-1), 132.5 (C-10), 132.3 (C-2), 132.2 (C-14), 130.7 (C-12), 130.4 (C-11), 129.1 (C-13), 99.4 (C-5), 53.6 (C-16), 20.7 (C-7), 20.5 (C-8). **IR (film, cm⁻¹)** ν_{max} 3268 (N–H), 1717 (C=O), 1459, 1294, 1170 (S=O). **HRMS (ESI⁺)** *m/z* calcd for C₁₆H₁₆N₂OSNa⁺ [M+Na]⁺ 467.9737; found: 467.9744.

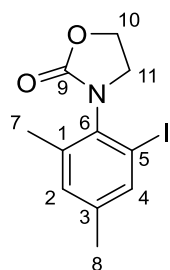
2-(2-Iodo-4,6-dimethylphenyl)-2,3-dihydrobenzo[d]isothiazole 1,1-dioxide - 5.44b



To a suspension of LiAlH_4 (70 mg, 1.8 mmol, 2.1 eq.) in THF (14 mL), at 0 °C under a nitrogen atmosphere was added dropwise a solution of *methyl 2-(N-(2-iodo-4,6-dimethylphenyl)sulfamoyl) benzoate* **5.45** (0.39 g, 0.88 mmol, 1.0 eq.) in THF (9 mL, 0.1 M). The reaction was stirred for 2 h at 0 °C and then quenched with water. The reaction was filtered through Celite, diluted in ethyl acetate and washed with 1M NaOH (aq.), brine, dried over Na_2SO_4 , filtered, and concentrated *in vacuo*. The crude product was dissolved in THF (11 mL, 0.08 M), and PBr_3 (0.42 mL, 4.4 mmol, 5.0 eq.)

was added dropwise at 0 °C under a nitrogen atmosphere. The reaction was stirred for 5 min at 0 °C and 1 h at rt, and then quenched with sat. Na_2CO_3 (aq.) and stirred overnight. The aqueous phase was extracted with EtOAc. The combined organic phases were washed with brine, dried with Na_2SO_4 and concentrated *in vacuo*. Purification by flash column chromatography yielded the *title compound* (0.16 g, 45%) as a brown solid. **m.p.:** 180 °C (degradation). **$\delta^1\text{H}$ (400 MHz, CDCl_3)** 7.87 (1 H, dt, $J = 7.7$, 0.9 Hz, H-12), 7.65 (1 H, td, $J = 7.6$, 1.3 Hz, H-14), 7.63 – 7.62 (1 H, m, H-4), 7.58 (1 H, td, $J = 7.6$, 1.0 Hz, H-13), 7.46 (1 H, dt, $J = 7.8$, 0.9 Hz, H-15), 7.12 – 7.08 (1 H, m, H-2), 4.94 ($\text{CH}_\text{AH}_\text{B}$, 1 H, d, $J = 13.9$ Hz, H-11), 4.69 ($\text{CH}_\text{AH}_\text{B}$, 1 H, d, $J = 13.9$ Hz, H-11), 2.47 (3 H, s, H-7), 2.29 (3 H, s, H-8). **$\delta^{13}\text{C}$ (101 MHz, CDCl_3)** 142.4 (C-6), 141.5 (C-3), 138.9 (C-4), 135.8 (C-9), 133.4 (C-10), 133.0 (C-1), 132.7 (C-14), 132.5 (C-2), 129.3 (C-13), 124.5 (C-15), 121.6 (C-12), 102.5 (C-5), 51.2 (C-11), 20.7 (C-8), 20.0 (C-7). **IR (film, cm^{-1})** ν_{max} 1458, 1292 (S=O), 1170 (S=O). **HRMS (ESI⁺)** m/z calcd for $\text{C}_{15}\text{H}_{14}\text{NO}_2\text{IS}^+$ $[\text{M}+\text{Na}]^+$ 421.9682; found: 421.9686.

3-(2-Iodo-4,6-dimethylphenyl)oxazolidin-2-one – 5.44c



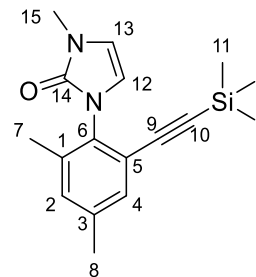
To a solution of 2-iodo-4,6-dimethylaniline^[316] (0.60 g, 2.4 mmol, 1.0 eq.) in CH_2Cl_2 (12 mL, 0.2 M) was added 2-chloroethyl chloroformate (0.30 mL, 2.9 mmol, 1.2 eq.) and pyridine (0.58 mL, 7.2 mmol, 3.0 eq.) under an atmosphere of nitrogen. The reaction mixture was stirred at rt for 20 h, and DBU (1.1 mL, 7.2 mmol, 3.0 eq.) was added dropwise. The reaction mixture was stirred at rt for 3 h and concentrated *in vacuo*. The crude mixture was diluted in ethyl acetate and washed with 1M NaOH

(aq.), brine, dried over MgSO_4 , filtered, and concentrated *in vacuo*. Purification by flash column chromatography yielded the title compound (0.70 g, 92%) as an off-white solid. **m.p.:** 150 – 151 °C. **$\delta^1\text{H}$ (400 MHz, CDCl_3)** 7.67 – 7.46 (1 H, m, H-4), 7.17 – 6.89 (1 H, m, H-2), 4.62 – 4.44 (2 H, m, H-10), 4.04 ($\text{CH}_\text{AH}_\text{B}$, 1 H, ddd, $J = 9.0$, 8.4, 6.0 Hz, H-11), 3.76 ($\text{CH}_\text{AH}_\text{B}$, 1 H, dt, $J = 9.1$, 8.2 Hz, H-11), 2.30 (3 H, s, H-7), 2.26 (3 H, s, H-8). **$\delta^{13}\text{C}$ (101 MHz, CDCl_3)** 156.2 (C-9), 140.9 (C-3), 138.4 (C-1), 137.9 (C-6), 134.8 (C-4), 132.2 (C-2), 99.6 (C-5), 62.8 (C-10), 45.8 (C-11), 20.6 (C-8), 18.9 (C-7).

IR (film, cm⁻¹) ν_{\max} 1745 (C=O), 1477, 1406, 1225 (C–N), 1106. **HRMS (ESI⁺)** m/z calcd for C₁₁H₁₂NO₂Na⁺ [M+Na]⁺ 339.9805; found: 339.9815.

1-(2,4-Dimethyl-6-((trimethylsilyl)ethynyl)phenyl)-3-methyl-1,3-dihydro-2H-imidazol-2-one

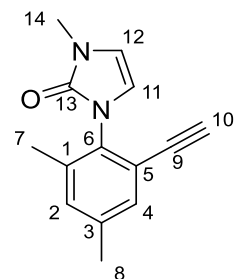
5.46a



Following **GP5.3** using 1-(2-iodo-4,6-dimethylphenyl)-3-methyl-1,3-dihydro-2H-imidazol-2-one **5.44a** (0.29 g, 0.88 mmol, 1.0 eq.), PdCl₂(PPh₃)₂ (12.3 mg, 0.018 mmol, 2 mol%) and CuI (8.4 mg, 0.044 mmol, 5 mol%) in Et₃N (3.0 mL, 0.3 M), followed by ethynyltrimethylsilane (0.24 mL, 1.8 mmol, 2.0 eq.) at 90 °C for 20 h. Purification by flash column chromatography yielded the *title compound* (0.17 g, 65%) as a yellow oil.

$\delta^1\text{H}$ (400 MHz, CDCl₃) 7.18 (1 H, dt, J = 2.0, 0.6 Hz, H-4), 7.06 (1 H, dt, J = 2.1, 0.7 Hz, H-2), 6.28 (1 H, d, J = 2.9 Hz, H-13), 6.26 (1 H, d, J = 3.0 Hz, H-12), 3.33 (3 H, s, H-15), 2.29 (3 H, s, H-8), 2.17 (3 H, s, H-7), 0.13 (9 H, s, H-11). **$\delta^{13}\text{C}$ (101 MHz, CDCl₃)** 152.2 (C-14), 138.3 (C-3), 137.0 (C-1), 135.2 (C-6), 132.1 (C-2), 131.1 (C-4), 122.7 (C-5), 112.1 (C-12 or C-13), 111.7 (C-12 or C-13), 101.5 (C-9), 98.9 (C-10), 30.7 (C-15), 21.0 (C-8), 18.1 (C-7), -0.1 (C-11). **IR (film, cm⁻¹)** ν_{\max} 2957 (C–H), 1689 (C=O), 1483, 1249 (C–Si). **HRMS (ESI⁺)** m/z calcd for C₁₇H₂₂N₂OSiNa⁺ [M+Na]⁺ 321.1394; found: 321.1398.

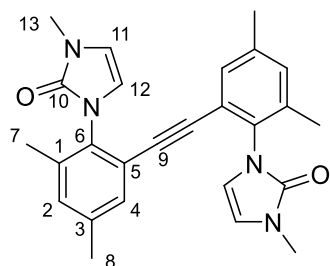
1-(2-Ethynyl-4,6-dimethylphenyl)-3-methyl-1,3-dihydro-2H-imidazol-2-one



Following **GP5.2** using 1-(2,4-dimethyl-6-((trimethylsilyl)ethynyl)phenyl)-3-methyl-1,3-dihydro-2H-imidazol-2-one **5.46a** (0.17 g, 0.57 mmol, 1.0 eq.) and K₂CO₃ (0.12 g, 0.85 mmol, 1.5 eq.) in MeOH (1.2 mL, 0.5M) for 2.5 h. Purification by flash column chromatography yielded the *title compound* (0.11 g, 82%) as a yellow oil.

$\delta^1\text{H}$ (400 MHz, CDCl₃) 7.23 – 7.19 (1 H, d, J = 2.2 Hz, H-4), 7.09 – 7.05 (1 H, d, J = 2.2 Hz, H-2), 6.30 (1 H, d, J = 3.0 Hz, H-12), 6.24 (1 H, d, J = 2.9 Hz, H-11), 3.31 (3 H, s, H-14), 3.04 (1 H, s, H-10), 2.29 (3 H, s, H-8), 2.14 (3 H, s, H-7). **$\delta^{13}\text{C}$ (101 MHz, CDCl₃)** 152.2 (C-13), 138.4 (C-3), 137.0 (C-1), 135.0 (C-6), 132.4 (C-2), 131.8 (C-4), 121.6 (C-5), 112.1 (C-12), 111.7 (C-11), 81.2 (C-10), 80.2 (C-9), 30.7 (C-14), 20.9 (C-8), 18.0 (C-7). **IR (film, cm⁻¹)** ν_{\max} 3287 (C≡C–H), 3203 (C=C–H), 2924 (C–H), 1681 (C=O), 1485, 1457, 1406, 1258. **HRMS (ESI⁺)** m/z calcd for C₁₄H₁₄N₂ONa⁺ [M+Na]⁺ 249.0998; found: 249.1010.

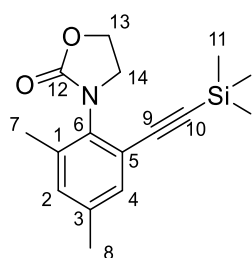
3,3'-(Ethyne-1,2-diylbis(4,6-dimethyl-2,1-phenylene))bis(1-methyl-1,3-dihydro-2H-imidazol-2-one) – 5.47a



Following **GP5.3** using 1-(2-iodo-4,6-dimethylphenyl)-3-methyl-1,3-dihydro-2H-imidazol-2-one (0.14 g, 0.44 mmol, 1 eq.), PdCl₂(PPh₃)₂ (6.2 mg, 0.0088 mmol, 2 mol%) and CuI (4.2 mg, 0.022 mmol, 5 mol%) in Et₃N (1.5 mL, 0.3 M), followed by 1-(2-ethynyl-4,6-dimethylphenyl)-3-methyl-1,3-dihydro-2H-imidazol-2-one (0.10 g, 0.44 mmol, 1 eq.) at 90

°C for 24 h. Purification by flash column chromatography yielded the *title compound* (31 mg, 16%) as a light brown solid. **m.p.:** 205 °C (degradation). Mixture of conformer in a 1:0.45 ratio in CDCl₃. **$\delta^1\text{H}$ (400 MHz, CDCl₃)** 7.11 – 7.07 (2 H^{min}, m, H-4^{min}), 7.05 (2 H^{maj} + 2 H^{min}, dt, *J* = 2.2, 0.7 Hz, H-2), 7.03 – 6.98 (2 H^{maj}, m, H-4), 6.31 (2 H^{maj}, d, *J* = 3.0 Hz, H-11), 6.26 (2 H^{min}, d, *J* = 3.0 Hz, H-11), 6.24 (2 H^{min}, d, *J* = 3.0 Hz, H-12), 6.23 (2 H^{maj}, d, *J* = 3.0 Hz, H-12), 3.33 (6 H^{min}, s, H-13), 3.32 (6 H^{maj}, s, H-13), 2.29 (6 H^{maj} + 6 H^{maj}, s, H-8), 2.18 (6 H^{maj}, s, H-7), 2.16 (6 H^{min}, s, H-7). **$\delta^{13}\text{C}$ (101 MHz, CDCl₃)** 152.2 (C-10^{maj}), 152.1 (C-10^{min}), 138.1 (C-3^{min}), 138.0 (C-3^{maj}), 137.0 (C-1^{min}), 136.9 (C-1^{maj}), 134.4 (C-6^{maj}), 134.3 (C-6^{min}), 132.1 (C-2^{maj} + C-2^{min}), 131.2 (C-4^{min}), 131.0 (C-4^{maj}), 122.4 (C-5^{min}), 122.3 (C-5^{maj}), 112.3 (C-12^{maj}), 112.0 (C-12^{min}), 111.9 (C-11^{min}), 111.8 (C-11^{maj}), 90.2 (C-9^{maj}), 89.9 (C-9^{min}), 30.84 (C-13^{maj}), 30.76 (C-13^{min}), 21.01 (C-8^{maj}), 20.99 (C-8^{min}), 18.20 (C-7^{maj}), 18.18 (C-7^{min}). **IR (film, cm⁻¹)** ν_{max} 1683 (C=O), 1486, 1456. **HRMS (ESI⁺)** *m/z* calcd for C₂₆H₂₆N₄O₂Na⁺ [M+Na]⁺ 449.1948; found: 449.1948.

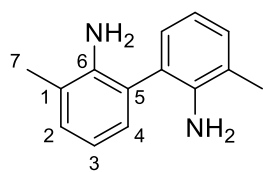
3-(2,4-Dimethyl-6-((trimethylsilyl)ethynyl)phenyl)oxazolidin-2-one – 5.46b



Following **GP5.3** using 3-(2-iodo-4,6-dimethylphenyl)oxazolidin-2-one **5.44c** (0.35 g, 1.1 mmol, 1.0 eq.), PdCl₂(PPh₃)₂ (15.4 mg, 0.022 mmol, 2 mol%) and CuI (10.5 mg, 0.055 mmol, 5 mol%) in Et₃N (3.7 mL, 0.3 M), followed by ethynyltrimethylsilane (0.30 mL, 2.2 mmol, 2.0 eq.) at 90 °C for 24 h.

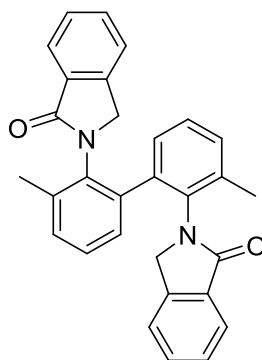
Purification by flash column chromatography yielded the *title compound* (0.21 g, 66%) as a yellow oil. **$\delta^1\text{H}$ (400 MHz, CDCl₃)** 7.20 – 7.13 (1 H, m, H-4), 7.06 – 6.97 (1 H, m, H-2), 4.57 – 4.35 (2 H, m, H-13), 4.15 (CH_AH_B, 1 H, ddd, *J* = 9.1, 8.3, 7.3 Hz, H-14), 3.73 (CH_AH_B, 1 H, ddd, *J* = 8.9, 8.3, 6.6 Hz, H-14), 2.26 (3 H, s, H-8), 2.24 (3 H, s, H-7), 0.23 (9 H, s, H-11). **$\delta^{13}\text{C}$ (101 MHz, CDCl₃)** 156.8 (C-12), 138.4 (C-3), 137.3 (C-1 or C-6), 134.9 (C-1 or C-6), 132.4 (C-2), 131.6 (C-4), 122.5 (C-5), 101.4 (C-9), 99.2 (C-10), 62.8 (C-13), 46.3 (C-14), 20.9 (C-8), 17.8 (C-7), 0.01 (C-11). **IR (film, cm⁻¹)** ν_{max} 2155 (C≡C), 1750 (C=O), 1479, 1405, 1248, 1221 (C–N). **HRMS (ESI⁺)** *m/z* calcd for C₁₆H₂₁NO₂SiNa⁺ [M+Na]⁺ 310.1234; found: 310.1246.

3,3'-Dimethyl-[1,1'-biphenyl]-2,2'-diamine – 5.49



Pd/C (10 wt. % loading, 35 mg, 1 mol%/Pd) was suspended in a solution of 3,3'-dimethyl-2,2'-dinitro-1,1'-biphenyl **5.48**^[299] (0.35 g, 1.3 mmol, 1.0 eq.) in MeOH (13 mL, 0.1 M) under nitrogen. Nitrogen was bubbled through the solution for 15 mins. The contents of the flask were placed under a hydrogen atmosphere using a two-way three-necked tap with a balloon of hydrogen attached. The solution was saturated with hydrogen three times using a vacuum/hydrogen cycle and was stirred under a hydrogen atmosphere for 20 h. The crude reaction solution was filtered through a pad of Celite and washed with MeOH. The resulting filtrate was concentrated *in vacuo* and purified by flash column chromatography to give the title product (96 mg, 35%) as an off-white solid **m.p.**: 245 – 247 °C. **$\delta^1\text{H}$ (400 MHz, CDCl_3)** 7.09 (2 H, dd, J = 7.4, 1.7 Hz, H-2), 7.01 (2 H, dd, J = 7.6, 1.6 Hz, H-4), 6.77 (2 H, t, J = 7.5 Hz, H-3), 3.62 (4 H, br. s, NH_2), 2.24 (6 H, s, H-7). **$\delta^{13}\text{C}$ (101 MHz, CDCl_3)** 142.6 (C-6), 130.0 (C-2), 128.8 (C-4), 124.5 (C-5), 122.6 (C-1), 118.4 (C-3), 18.0 (C-7). **IR (film, cm^{-1})** ν_{max} 3484 (N–H), 3393 (N–H), 1525, 1364. **HRMS (ESI⁺)** m/z calcd for $\text{C}_{14}\text{H}_{17}\text{N}_2^+$ $[\text{M}+\text{H}]^+$ 213.1386; found: 213.1382.

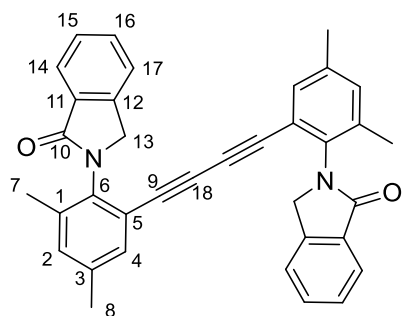
2,2'-(3,3'-Dimethyl-[1,1'-biphenyl]-2,2'-diyl)bis(isoindolin-1-one) – 5.50



To a solution of 3,3'-dimethyl-[1,1'-biphenyl]-2,2'-diamine **5.49** (0.85 mg, 0.4 mmol, 1 eq.) in CH_2Cl_2 (4.0 mL, 0.1 M) was added 2-(chloromethyl)benzoyl chloride **5.21** (0.14 mL, 1.0 mmol, 2.5 eq.) and Et_3N (0.17 mL, 1.2 mmol, 3.1 eq.) at rt under an atmosphere of nitrogen. The reaction mixture was stirred at rt for 18h. The reaction mixture was washed with 1M HCl (aq.), brine, dried over MgSO_4 , filtered, and concentrated *in vacuo*. The crude residue obtained was dissolved in CH_2Cl_2 (4.0 mL, 0.1 M) and DBU (0.18 mL, 1.2 mmol, 3.1 eq.) was added. The reaction mixture stirred at rt for 20 h, diluted in ethyl acetate and washed with 1M HCl (aq.), brine, dried over MgSO_4 , filtered, and concentrated *in vacuo*. Purification by flash column chromatography yielded the *title compound* (90 mg, 51%) as a white solid. **m.p.**: 225 – 227 °C. Mixture of conformers in a 1:1 ratio. **$\delta^1\text{H}$ (500 MHz, CDCl_3)** 7.92 (1 H, d, J = 7.5 Hz, ArCH), 7.86 (1 H, d, J = 7.8 Hz, ArCH), 7.55 (1 H, t, J = 7.5 Hz, ArCH), 7.51 – 7.42 (3 H, m, ArCH), 7.41 – 7.36 (1 H, m, ArCH), 7.33 (1 H, d, J = 7.3 Hz, ArCH), 7.28 – 7.27 (1 H, m, ArCH), 7.14 (2 H, d, J = 7.5 Hz, ArCH), 7.09 – 7.02 (2 H, m, ArCH), 6.80 (1 H, t, J = 7.6 Hz, ArCH), 5.32 (CH_AHB , 1 H, d, J = 14.2 Hz, NCH_2), 5.17 (CH_AHB , 1 H, d, J = 14.6 Hz, NCH_2), 4.44 (CH_AHB , 1 H, d, J = 17.3 Hz, NCH_2), 4.28 (CH_AHB , 1 H, d, J = 17.3 Hz, NCH_2), 2.21 (3 H, s, CH_3), 2.17 (3 H, s, CH_3). **$\delta^{13}\text{C}$ (126 MHz, CDCl_3)** 168.7 (C=O), 157.9 (ArC), 144.3 (ArC), 143.5 (ArC), 142.4 (ArC), 139.7 (ArC), 137.0 (ArC), 134.7 (ArC), 132.4 (ArC), 132.0 (ArCH), 132.0 (ArCH), 131.3 (ArCH),

129.9 (ArC), 129.6 (ArCH), 128.9 (ArCH), 128.8 (ArCH), 127.9 (ArCH), 127.8 (ArCH), 127.3 (ArCH), 124.3 (ArCH), 124.2 (ArCH), 123.3 (ArCH), 122.8 (ArCH), 121.6 (ArCH), 72.4 (NCH₂), 51.3 (NCH₂), 18.6 (2*CH₃). **IR (film, cm⁻¹)** ν_{\max} 2971 (C–H), 1693 (C=O), 1468. **HRMS (ESI⁺)** m/z calcd for C₃₀H₂₅N₂O₂⁺ [M+H]⁺ 445.1910; found: 445.1919.

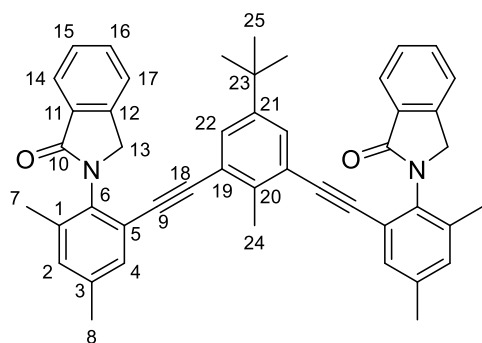
2,2'-(Buta-1,3-diyne-1,4-diylbis(4,6-dimethyl-2,1-phenylene))bis(isoindolin-1-one) – 5.51



A microwave vial was filled with nitrogen. To this was added 2-(2-ethynyl-4,6-dimethylphenyl)isoindolin-1-one (50 mg, 0.19 mmol, 1.0 eq.), CuI (3.6 mg, 0.019 mmol, 10 mol%), and pyrrolidine (16 μ L, 0.19 mmol, 1.0 eq.) in CH₂Cl₂ (0.4 mL, 0.5 M) and the reaction mixture was allowed to stir at rt for 2 h in an open vial. The reaction mixture was directly purified by flash column

chromatography to give the *title compound* (50 mg, quantitative) as a brown solid. **m.p.:** 113 – 115 °C. Mixture of conformer in a 1:0.7 ratio in CDCl₃. **$\delta^1\text{H}$ (400 MHz, CDCl₃)** 7.95 (2 H^{maj}, dt, J = 7.6, 1.0 Hz, H-14), 7.88 (2 H^{min}, dt, J = 7.4, 1.0 Hz, H-14), 7.61 (2 H^{maj}, td, J = 7.5, 1.2 Hz, H-16), 7.57 (2 H^{min}, td, J = 7.5, 1.2 Hz, H-16), 7.53 (2 H^{maj}, dd, J = 7.4, 1.1 Hz, H-17), 7.51 – 7.46 (2 H^{maj} + 2 H^{min}, m, H-15), 7.43 (2 H^{min}, dt, J = 7.5, 1.0 Hz, H-17), 7.20 (2 H^{min}, d, J = 2.0 Hz, H-4), 7.15 – 7.05 (4 H^{maj} + 2 H^{min}, m, H-2^{maj} + H-4^{maj} + H-2^{min}), 4.96 (CH_AH_B, 2 H^{maj}, d, J = 16.8 Hz, H-13), 4.89 (CH_AH_B, 2 H^{min}, d, J = 16.7 Hz, H-13), 4.44 (CH_AH_B, 2 H^{maj}, d, J = 16.7 Hz, H-13), 4.40 (CH_AH_B, 2 H^{min}, d, J = 16.7 Hz, H-13), 2.29 (6 H^{min}, s, H-8), 1.28 (6 H^{maj}, s, H-8), 2.14 (6 H^{maj}, s, H-7), 2.13 (6 H^{min}, s, H-7). **$\delta^{13}\text{C}$ (101 MHz, CDCl₃)** 168.0 (C-10^{maj}), 167.9 (C-10^{min}), 142.1 (C-12^{maj}), 142.0 (C-12^{min}), 138.2 (C-1^{maj} + C-1^{min}), 137.54 (C-3^{maj}), 137.52 (C-3^{min}), 136.7 (C-6^{maj}), 136.6 (C-6^{min}), 133.2 (C-2^{min}), 133.1 (C-2^{maj}), 132.8 (C-4^{min}), 132.5 (C-4^{maj}), 132.2 (C-11^{maj}), 132.1 (C-11^{min}), 131.84 (C-16^{maj}), 131.77 (C-16^{min}), 128.15 (C-15^{min}), 128.11 (C-15^{maj}), 124.4 (C-14^{min}), 124.3 (C-14^{maj}), 123.2 (C-17^{maj}), 122.9 (C-17^{min}), 121.27 (C-5^{min}), 121.26 (C-5^{maj}), 79.3 (C-9^{min}), 79.2 (C-9^{maj}), 77.4 (C-18^{min}), 77.3 (C-18^{maj}), 51.7 (C-13^{maj}), 51.6 (C-13^{min}), 20.9 (C-8^{maj} + C-8^{min}), 18.2 (C-7^{maj} + C-7^{min}). **IR (film, cm⁻¹)** ν_{\max} 3672, 2972 (C–H), 2922 (C–H), 1696 (C=O), 1468, 1384. **HRMS (ESI⁺)** m/z calcd for C₃₆H₂₈N₂O₂Na⁺ [M+Na]⁺ 543.2043; found: 543.2029. Supplementary crystallographic data can be obtained free of charge from The Cambridge Crystallographic Data Centre (CCDC 1861806).

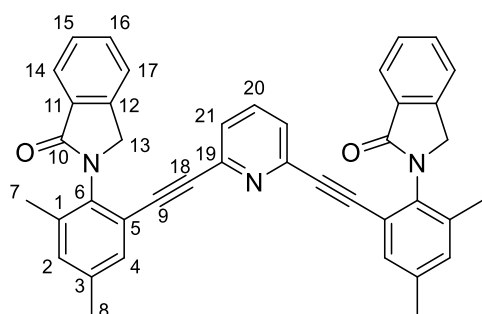
2,2'-(((5-(Tert-butyl)-2-methyl-1,3-phenylene)bis(ethyne-2,1-diyl))bis(4,6-dimethyl-2,1-phenylene)) bis(isoindolin-1-one) – 5.52



Following **GP5.3** using 4-(*tert*-butyl)-2,5-diiodo-toluene^[320] (73 mg, 0.18 mmol, 1 eq.), PdCl₂(PPh₃)₂ (2.5 mg, 3.6 μmol, 2 mol%) and CuI (1.7 mg, 8.9 μmol, 5 mol%) in Et₃N (0.6 mL, 0.3 M), followed by 2-(2-ethynyl-4,6-dimethylphenyl) isoindolin-1-one **5.25** (100 mg, 0.38 mmol, 2.1 eq.) at 90 °C for 19 h. Purification by flash column chromatography yielded the title compound (75 mg, 61%) as an off-white

solid. **m.p.:** 158 – 161 °C. Mixture of conformers in a 1:1 ratio in CDCl₃; consequently, some peaks of the ¹³C spectrum are doubled. **δ¹H (400 MHz, CDCl₃)** 7.97 (2 H, dd, *J* = 7.5, 1.0 Hz, H-14), 7.59 (2 H, tdd, *J* = 7.4, 4.8, 1.3 Hz, H-16), 7.54 – 7.51 (2 H, m, H-15), 7.53 – 7.44 (2 H, m, H-17), 7.31 – 7.28 (2 H, m, H-4), 7.17 – 7.11 (2 H, m, H-2), 6.85 (1 H, s, H-22), 6.79 (1 H, s, H-22), 5.05 (CH_AH_B, 2 H, d, *J* = 16.8 Hz, H-13), 4.54 (CH_AH_B, 2 H, d, *J* = 16.8 Hz, H-13), 2.36 (6 H, s, H-8), 2.23 (6 H, s, H-7), 2.04 (1.5 H, s, H-24), 1.94 (1.5 H, s, H-24), 0.93 (4.5 H, s, H-25), 0.89 (4.5 H, s, H-25). **δ¹³C (126 MHz, CDCl₃)** 168.0 (C-10), 148.25 (C-21), 148.23 (C-21), 142.09 (C-12), 142.06 (C-12), 138.54 (C-20), 138.52 (C-20), 138.3 (C-3), 137.5 (C-1), 135.68 (C-6), 135.64 (C-6), 132.53 (C-11), 132.52 (C-11), 132.1 (C-2), 131.90 (C-16), 131.86 (C-16), 131.25 (C-4), 131.21 (C-4), 129.5 (C-22), 128.33 (C-15), 128.28 (C-15), 124.5 (C-14), 124.4 (C-14), 122.98 (C-17), 122.94 (C-5 or C-19), 122.92 (C-17), 122.8 (C-5 or C-19), 92.32 (C-18), 92.29 (C-18), 89.6 (C-9), 51.6 (C-13), 33.94 (C-23), 33.89 (C-23), 30.92 (C-25), 30.89 (C-25), 21.1 (C-8), 18.2 (C-7), 18.0 (C-24), 17.9 (C-24). **IR (film, cm⁻¹)** ν_{max} 2956 (C–H), 2923 (C–H), 1698 (C=O), 1469, 1386. **HRMS (ESI⁺)** *m/z* calcd for C₄₇H₄₃N₂O₂Na⁺ [M+Na]⁺ 689.3138; found: 689.3133.

2,2'-((Pyridine-2,6-diylbis(ethyne-2,1-diyl))bis(4,6-dimethyl-2,1-phenylene))bis(isoindolin-1-one) – 5.53

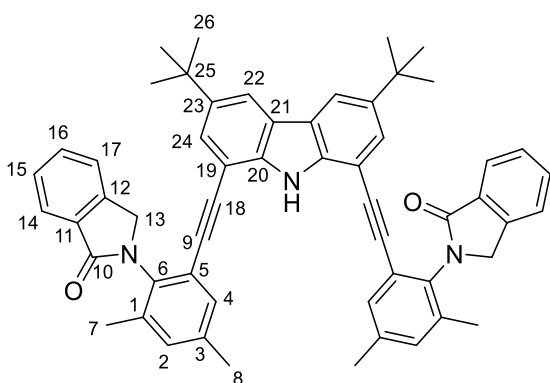


Following **GP5.3** using 2-(2-ethynyl-4,6-dimethylphenyl) isoindolin-1-one **5.25** (100 mg, 0.38 mmol, 2.1 eq.), PdCl₂(PPh₃)₂ (2.5 mg, 0.0036 mmol, 2 mol%) and CuI (1.7 mg, 8.9 μmol, 5 mol%) in Et₃N (0.6 mL, 0.3 M), followed by 2,5-dibromopyridine (43 mg, 0.18 mmol, 1 eq.) at 90 °C for 15 h. Purification by flash column chromatography

followed by trituration in Et₂O yielded the *title compound* (18 mg, 17%) as a yellow solid. Mixture of conformers in a 1:0.85 ratio in CDCl₃. **δ¹H (400 MHz, CDCl₃)** 7.97 (2 H^{min}, d, *J* = 3.9 Hz, H-14), 7.96 (2 H^{maj}, d, *J* = 3.9 Hz, H-14), 7.62 – 7.55 (2 H^{maj} + 2H^{min}, qd, *J* = 7.2, 1.2 Hz, H-16),

7.54 – 7.45 (4 H^{maj} + 4 H^{min} , m, H-15 + H-17), 7.35 (2 H^{maj} + 2 H^{min} , d, J = 2.1 Hz, H-4), 7.17 (2 H^{maj} + 2 H^{min} , d, J = 1.9 Hz, H-2), 7.12 (1 H^{min} , t, J = 7.9 Hz, H-20), 7.06 (1 H^{maj} , t, J = 7.8 Hz, H-20), 6.56 (2 H^{min} , d, J = 7.8 Hz, H-21), 6.44 (2 H^{maj} , d, J = 7.8 Hz, H-21), 5.05 ($\text{CH}_\text{A}\text{H}_\text{B}$, 2 H^{min} , d, J = 16.9 Hz, H-13), 5.02 ($\text{CH}_\text{A}\text{H}_\text{B}$, 2 H^{maj} , d, J = 16.9 Hz, H-13), 4.59 ($\text{CH}_\text{A}\text{H}_\text{B}$, 2 H^{maj} , d, J = 16.9 Hz, H-13), 4.55 ($\text{CH}_\text{A}\text{H}_\text{B}$, 2 H^{min} , d, J = 16.9 Hz, H-13), 2.35 (6 H^{maj} + 6 H^{min} , s, H-8), 2.24 (6 H^{maj} , s, H-7), 2.24 (6 H^{min} , s, H-7). $\delta^{13}\text{C}$ (126 MHz, CDCl_3) 168.3 (C-10 $^{\text{maj}}$), 168.2 (C-10 $^{\text{min}}$), 143.30 (C-19 $^{\text{min}}$), 143.26 (C-19 $^{\text{maj}}$), 142.24 (C-12 $^{\text{min}}$), 142.22 (C-12 $^{\text{maj}}$), 138.49 (C-3 $^{\text{maj}}$), 138.46 (C-3 $^{\text{min}}$), 137.6 (C-6 $^{\text{maj+min}}$), 136.6 (C-1 $^{\text{maj}}$), 136.5 (C-1 $^{\text{min}}$), 136.09 (C-20 $^{\text{maj}}$), 136.08 (C-20 $^{\text{min}}$), 133.02 (C-2 $^{\text{maj+min}}$), 132.42 (C-11 $^{\text{min}}$), 132.37 (C-11 $^{\text{maj}}$), 131.88 (C-16 $^{\text{min}}$), 131.80 (C-16 $^{\text{maj}}$), 131.79 (C-4 $^{\text{maj}}$), 131.75 (C-4 $^{\text{min}}$), 128.23 (C-15 $^{\text{maj}}$), 128.20 (C-18 $^{\text{min}}$), 126.3 (C-21 $^{\text{min}}$), 126.2 (C-21 $^{\text{maj}}$), 124.51 (C-14 $^{\text{min}}$), 124.46 (C-14 $^{\text{maj}}$), 123.2 (C-17 $^{\text{maj}}$), 123.1 (C-17 $^{\text{min}}$), 121.7 (C-5 $^{\text{maj+min}}$), 91.96 (C-18 $^{\text{min}}$), 91.93 (C-18 $^{\text{maj}}$), 86.49 (C-9 $^{\text{min}}$), 86.46 (C-9 $^{\text{maj}}$), 51.92 (C-13 $^{\text{maj}}$), 51.88 (C-13 $^{\text{min}}$), 21.13 (C-8 $^{\text{maj}}$), 21.11 (C-8 $^{\text{min}}$), 18.23 (C-7 $^{\text{min}}$), 18.20 (C-7 $^{\text{maj}}$). IR (film, cm^{-1}) ν_{max} 2923 (C–H), 1697 (C=O), 1469, 1449, 1385, 1066. HRMS (ESI $^+$) m/z calcd for $\text{C}_{41}\text{H}_{32}\text{N}_3\text{O}_2$ $^+$ [M+H] $^+$ 598.2489; found: 598.2481.

2,2'-(((3,6-Di-tert-butyl-9H-carbazole-1,8-diyl)bis(ethyne-2,1-diyl))bis(4,6-dimethyl-2,1-phenylene))bis(isoindolin-1-one)– 5.54a

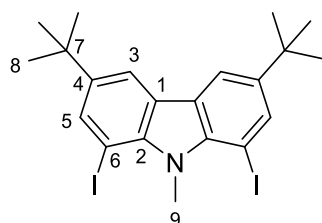


Following **GP5.3** using 3,6-di-*tert*-butyl-1,8-diiodo-9H-carbazole^[321] (69 mg, 0.13 mmol, 1.0 eq.), $\text{PdCl}_2(\text{PPh}_3)_2$ (3.6 mg, 5.2 μmol , 4 mol%) and CuI (2.5 mg, 0.013 mmol, 10 mol%) in Et_3N (0.45 mL, 0.3 M), followed by 2-(2-ethynyl-4,6-dimethylphenyl)isoindolin-1-one **5.25** (70 mg, 0.27 mmol, 2.1 eq.) at 90 °C for 16 h. Purification by flash column chromatography yielded the title compound (60 mg,

58%) as a yellow solid. **m.p.:** 213 °C (degradation). Mixture of conformers in a 1:0.35 ratio in CDCl_3 ; some peaks overlap in the ^{13}C spectrum. $\delta^1\text{H}$ (500 MHz, CDCl_3) 10.59 (1 H^{maj} , s, NH), 10.22 (1 H^{min} , s, NH), 8.15 (2 H^{maj} , d, J = 7.7 Hz, H-14), 8.10 (2 H^{min} , d, J = 7.6 Hz, H-14), 7.91 (2 H^{maj} + 2 H^{min} , d, J = 2.0 Hz, H-24), 7.64 (2 H^{maj} + 2 H^{min} , d, J = 1.9 Hz, H-4), 7.58 – 7.44 (2 H^{maj} + 4 H^{min} , m, H-16 + H-17 $^{\text{min}}$), 7.47 (2 H^{maj} , d, J = 7.4 Hz, H-17), 7.43 (2 H^{maj} + 2 H^{min} , t, J = 5.9 Hz, H-15), 7.13 (2 H^{min} , d, J = 1.9 Hz, H-2), 7.11 (2 H^{maj} , d, J = 1.9 Hz, H-2), 7.08 (2 H^{maj} , d, J = 2.0 Hz, H-22), 7.03 (2 H^{min} , d, J = 2.0 Hz, H-22), 5.03 ($\text{CH}_\text{A}\text{H}_\text{B}$, 2 H^{min} , d, J = 16.7 Hz, H-13), 4.95 ($\text{CH}_\text{A}\text{H}_\text{B}$, 2 H^{maj} , d, J = 16.8 Hz, H-13), 4.74 ($\text{CH}_\text{A}\text{H}_\text{B}$, 2 H^{min} , d, J = 16.8 Hz, H-13), 4.71 ($\text{CH}_\text{A}\text{H}_\text{B}$, 2 H^{maj} , d, J = 16.8 Hz, H-13), 2.31 (12 H^{maj} , s, H-7 + H-8), 2.29 (12 H^{min} , s, H-7 + H-8), 1.25 (18 H^{maj} , s, H-26), 1.24 (18 H^{min} , s, H-26). $\delta^{13}\text{C}$ (126 MHz, CDCl_3) 169.0 (C-10 $^{\text{maj}}$), 168.7 (C-10 $^{\text{min}}$),

142.2 (C-12^{min}), 142.1 (C-12^{maj}), 141.9 (C-23^{min}), 141.8 (C-23^{maj}), 139.3 (C-20^{maj}), 139.2 (C-20^{min}), 138.2 (C-1^{min} or C-3^{min}), 138.1 (C-1^{maj} or C-3^{maj}), 136.7 (C-1^{min} or C-3^{min}), 136.6 (C-1^{maj} or C-3^{maj}), 135.84 (C-6^{maj}), 135.82 (C-6^{min}), 132.7 (C-11^{min}), 132.5 (C-11^{maj}), 131.9 (C-2^{min} or C-16^{min}), 131.8 (C-2^{maj} or C-16^{maj}), 131.82 (C-2^{maj} or C-16^{maj}), 131.77 (C-2^{min} or C-16^{min}), 131.69 (C-4^{min}), 131.67 (C-4^{maj}), 128.7 (C-15^{maj}), 128.4 (C-15^{min}), 126.96 (C-22^{maj}), 126.95 (C-22^{min}), 125.0 (C-14^{maj}), 124.9 (C-14^{min}), 123.22 (C-5^{maj}), 123.19 (C-5^{min}), 123.16 (C-21^{maj+min}), 122.93 (C-17^{min}), 122.88 (C-17^{maj}), 117.4 (C-24^{min}), 117.3 (C-24^{maj}), 105.0 (C-19^{maj+min}), 91.1 (C-18^{maj}), 91.0 (C-18^{min}), 90.3 (C-9^{maj+min}), 52.2 (C-13^{maj}), 52.1 (C-13^{min}), 34.5 (C-25^{maj+min}), 31.9 (C-26^{maj+min}), 21.1 (C-8^{maj+min}), 18.24 (C-7^{min}), 18.22 (C-7^{maj}). IR (film, cm⁻¹) ν_{\max} 2959 (C–H), 1684 (C=O), 1479, 1389. HRMS (ESI⁺) m/z calcd for C₅₆H₅₂N₃O₂⁺ [M+H]⁺ 798.4054; found: 798.4053.

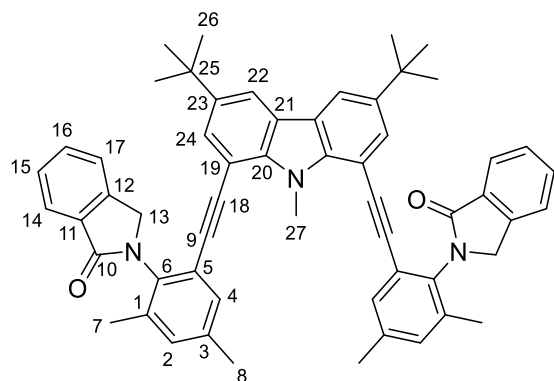
3,6-Di-*tert*-butyl-1,8-diiodo-9-methyl-9H-carbazole



To a solution of 3,6-di-*tert*-butyl-1,8-diiodo-9H-carbazole^[321] (0.30 g, 0.57 mmol, 1.0 eq.) in DMF (2.8 mL, 0.2 M) was added NaH (44 mg, 1.1 mmol, 2.0 eq., 60% in mineral oil) and the green solution was stirred at rt for 10 minutes. Methyl iodide (69 μ L, 1.1 mmol, 2.0 eq.) was added and the reaction mixture was stirred at 40 °C for 5 h, during which the

solution went from green to yellow to a white suspension. The reaction mixture was diluted in ethyl acetate, washed with LiCl (5% aq.), brine, dried over MgSO₄, filtered, and concentrated *in vacuo*. Purification by trituration in Et₂O yielded the title compound (0.31 g, quant.) as a white solid. **m.p.:** 191 – 193 °C. **$\delta^1\text{H}$ (500 MHz, CDCl₃)** 7.97 (1 H, d, J = 1.8 Hz, H-3), 7.95 (1 H, d, J = 1.8 Hz, H-5), 4.31 (3 H, s, H-9), 1.43 (18 H, s, H-8). **$\delta^{13}\text{C}$ (101 MHz, CDCl₃)** 145.4 (C-4), 142.4 (C-2), 137.0 (C-5), 126.0 (C-1), 116.2 (C-3), 74.4 (C-6), 37.1 (C-9), 34.6 (C-7), 31.9 (C-8). IR (film, cm⁻¹) ν_{\max} 1960, 1479, 1285, 1178. No major peak could be found by HRMS (ESI, EI, APCI).

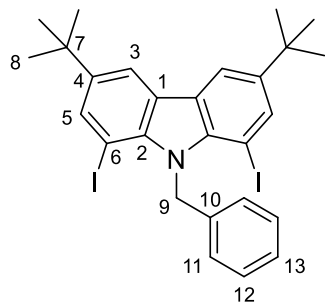
2,2'-(((3,6-Di-*tert*-butyl-9-methyl-9H-carbazole-1,8-diyl)bis(ethyne-2,1-diyl))bis(4,6-dimethyl-2,1-phenylene))bis(isoindolin-1-one) – 5.54b



Following **GP5.3** using 3,6-di-*tert*-butyl-1,8-diiodo-9-methyl-9H-carbazole (54 mg, 0.10 mmol, 1.0 eq.), PdCl₂(PPh₃)₂ (2.8 mg, 0.004 mmol, 4 mol%) and CuI (1.9 mg, 0.01 mmol, 10 mol%) in Et₃N/DMF (1:1, 0.5 mL, 0.2 M), followed by ethynyltrimethylsilane (65 mg, 0.25 mmol, 2.5 eq.) at 90 °C for 20 h. Purification by flash column chromatography yielded the *title compound* (49 mg, 60%) as a white solid.

m.p.: >250 °C. Mixture of conformers in a 1:0.80 ratio in CDCl₃. **$\delta^1\text{H}$ (400 MHz, CDCl₃)** 7.98 (2 H^{min}, dt, J = 7.6, 1.0 Hz, H-14), 7.93 (2 H^{maj}, dt, J = 7.5, 1.0 Hz, H-14), 7.88 (2 H^{maj}, d, J = 1.9 Hz, H-22), 7.87 (2 H^{min}, d, J = 2.0 Hz, H-22), 7.60 – 7.40 (6 H^{maj+min}, m, H-15 + H-16 + H-17), 7.49 (2 H^{maj+min}, m, H-4), 7.19 (2 H^{maj+min}, t, J = 2.5 Hz, H-2), 7.12 (2 H^{maj}, d, J = 1.9 Hz, H-24), 6.99 (2 H^{min}, d, J = 1.9 Hz, H-24), 5.25 (CH_AH_B, 2 H^{min}, d, J = 16.9 Hz, H-13), 5.22 (CH_AH_B, 2 H^{maj}, d, J = 16.9 Hz, H-13), 4.65 (CH_AH_B, 2 H^{min}, d, J = 16.9 Hz, H-13), 4.61 (CH_AH_B, 2 H^{maj}, d, J = 16.9 Hz, H-13), 4.48 (3 H^{min}, s, H-27), 4.24 (3 H^{maj}, s, H-27), 2.47 (3 H^{maj}, s, H-8), 2.45 (3 H^{min}, s, H-8), 2.29 (6 H^{maj+min}, s, H-7), 1.22 (18 H^{maj}, s, H-26), 1.17 (18 H^{min}, s, H-26). **$\delta^{13}\text{C}$ (101 MHz, CDCl₃)** 168.10 (C-10^{maj}), 168.09 (C-10^{min}), 142.13 (C_{Ar}^{min}), 142.08 (C_{Ar}^{maj}), 141.96 (C_{Ar}^{min}), 141.95 (C_{Ar}^{maj}), 138.69 (C_{Ar}^{min}), 138.68 (C_{Ar}^{maj}), 138.5 (C_{Ar}^{maj+min}), 137.61 (C_{Ar}^{min}), 137.60 (C_{Ar}^{maj}), 135.56 (C_{Ar}^{min}), 135.5 (C_{Ar}^{maj}), 132.6 (C_{Ar}^{min}), 132.5 (C_{Ar}^{maj}), 132.06 (C-2^{maj}), 132.03 (C-2^{min}), 131.96 (C-16^{maj}), 131.88 (C-16^{min}), 131.0 (C-4^{maj}), 130.7 (C-4^{min}), 129.88 (C-24^{maj}), 129.87 (C-24^{min}), 128.5 (C-15^{maj}), 128.4 (C-15^{min}), 124.5 (C-14^{min}), 124.4 (C-14^{maj}), 123.4 (C_{Ar}^{maj+min}), 123.26 (C_{Ar}^{maj}), 123.25 (C_{Ar}^{min}), 123.09 (C-17^{maj}), 123.07 (C-17^{min}), 117.2 (C-22^{maj+min}), 104.6 (C_{Ar}^{maj+min}), 92.4 (C-18^{min}), 92.2 (C-18^{maj}), 90.0 (C-9^{maj}), 89.9 (C-9^{min}), 51.9 (C-13^{maj}), 51.8 (C-13^{min}), 34.4 (C-25^{maj}), 34.3 (C-25^{min}), 33.1 (C-27^{maj}), 32.9 (C-27^{min}), 31.8 (C-26^{maj}), 31.7 (C-26^{min}), 21.16 (C-8^{min}), 21.14 (C-8^{maj}), 18.32 (C-7^{maj}), 18.30 (C-7^{min}). **IR (film, cm⁻¹)** ν_{max} 2957 (C–H), 2243 (C≡C), 2206 (C≡C), 1690 (C=O), 1468, 1286, 1274. **HRMS (ESI⁺)** m/z calcd for C₅₇H₅₄N₃O₂ [M+H]⁺ 812.4211, found 812.4236.

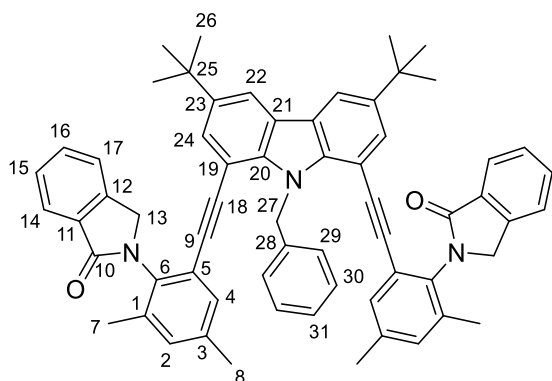
9-Benzyl-3,6-di-*tert*-butyl-1,8-diiodo-9H-carbazole



To a solution of 3,6-di-*tert*-butyl-1,8-diiodo-9H-carbazole^[321] (0.30 g, 0.57 mmol, 1.0 eq.) in DMF (2.8 mL, 0.2 M) was added NaH (44 mg, 1.1 mmol, 2.0 eq. 60% in mineral oil) and the green solution was stirred at rt for 10 minutes. Benzyl bromide (0.13 mL, 1.1 mmol, 2.0 eq.) was added and the reaction mixture was stirred at 40 °C for 4 h, during which the solution went from green to yellow to a white suspension. The

reaction mixture was diluted in ethyl acetate, washed with LiCl (5% aq.), brine, dried over MgSO₄, filtered, and concentrated *in vacuo*. Purification by flash column chromatography yielded the title compound (0.32 g, 91%) as a white foam. **m.p.:** 108 – 110 °C. **$\delta^1\text{H}$ (400 MHz, CDCl₃)** 8.04 (2 H, d, J = 1.9 Hz, H-3), 7.94 (2 H, d, J = 1.8 Hz, H-5), 7.24 – 7.16 (3 H, m, H-12 + H-13), 6.92 (2 H, dd, J = 8.0, 1.6 Hz, H-11), 6.46 (2 H, s, H-9), 1.42 (18 H, s, H-8). **$\delta^{13}\text{C}$ (101 MHz, CDCl₃)** 145.2 (C-4), 140.1 (C-10), 139.5 (C-2), 138.1 (C-5), 128.4 (C-12), 126.8 (C-13), 126.4 (C-11), 125.8 (C-1), 116.1 (C-3), 73.4 (C-6), 46.9 (C-9), 34.6 (C-7), 31.9 (C-8). **IR (film, cm⁻¹)** ν_{max} 2960 (C–H), 1479, 1285, 1178. No major peak could be found by **HRMS** (ESI, EI, APCI).

2,2'-(((9-Benzyl-3,6-di-tert-butyl-9H-carbazole-1,8-diyl)bis(ethyne-2,1-diyl))bis(4,6-dimethyl-2,1-phenylene))bis(isoindolin-1-one)– 5.54c



Following **GP5.3** using 9-benzyl-3,6-di-tert-butyl-1,8-diiodo-9H-carbazole (62 mg, 0.10 mmol, 1.0 eq.), PdCl₂(PPh₃)₂ (2.8 mg, 0.004 mmol, 4 mol%) and CuI (1.9 mg, 0.01 mmol, 10 mol%) in Et₃N/DMF (1:1, 0.5 mL, 0.2 M), followed by ethynyltrimethylsilane (65 mg, 0.25 mmol, 2.5 eq.) at 90 °C for 20 h. Purification by flash column chromatography yielded the *title compound* (52 mg, 58%) as an off-white

solid. **m.p.:** 192 – 195 °C (degradation). Broad signals in the ¹H NMR spectrum at rt due to slow blond rotation. Mixture of conformers A/B in a 1:1 ratio in CDCl₃. **δ¹H (400 MHz, CDCl₃)** 7.99 (2 H^A, br. s, H-14), 7.97 (2 H^B, br. s, H-14), 7.93 (2 H^{A+B}, t, *J* = 2.2 Hz, H-22), 7.60 – 7.53 (2 H^{A+B}, m, H-16), 7.52 – 7.40 (4 H^{A+B}, m, H-15 + H-17), 7.29 – 7.20 (4 H^{A+B}, m, H-29 + H-30), 7.18 – 7.13 (1 H^{A+B}, m, H-31), 7.12 – 7.06 (2 H^{A+B}, m, H-2), 6.97 (2 H^A, br. s, H-24), 6.93 (2 H^B, br. s, H-24), 6.71 (2 H^{A+B}, br. s, H-4), 6.43 (2 H^A, br. s, H-27), 6.38 (2 H^B, br. s, H-27), 5.21 (CH_AH_B, 2 H^A, br. s, H-27), 4.95 (CH_AH_B, 2 H^B, br. s, H-27), 4.47 (CH_AH_B, 2 H^{A+B}, br. s, H-27), 2.34 (6 H^A, s, H-8), 2.32 (6 H^B, s, H-8), 2.22 (6 H^{A+B}, s, H-7), 1.17 (18 H^B, br. s, H-26), 1.15 (18 H^A, br. s, H-26). **δ¹³C (101 MHz, CDCl₃)** 168.01 (C-10^A), 167.97 (C-10^B), 142.4 (broad, ArC^{A+B}), 142.14 (ArC^{A+B}), 142.08 (ArC^{A+B}), 140.9 (ArC^{A+B}), 138.4 (ArC^A), 138.3 (ArC^B), 138.1 (ArC^A), 138.0 (ArC^B), 137.3 (ArC^A), 137.2 (ArC^B), 135.5 (ArC^{A+B}), 132.56 (ArC^A), 132.54 (ArC^B), 131.84 (C-2^A), 131.83 (C-2^B), 131.80 (C-16^A), 131.79 (C-16^B), 130.98 (C-4^A), 130.97 (C-4^B), 130.2 (broad, C-24^{A+B}), 128.64 (C-29^A or C-30^A), 128.57 (C-29^B or C-30^B), 128.4 (C-15^A), 128.3 (C-15^B), 126.7 (C-29^{A+B} or C-30^{A+B}), 126.17 (C-21^A), 126.14 (C-21^B), 124.50 (C-14^A), 124.47 (C-14^B), 123.8 (broad, ArC^{A+B}), 123.1 (C-17^A), 123.0 (C-17^B), 122.88 (ArC^A), 122.85 (ArC^B), 117.24 (C-22^A), 117.23 (C-22^B), 104.7 (C-18^{A+B}), 91.7 (C-9^{A+B}), 51.71 (C-13^A), 51.68 (C-13^B), 48.5 (C-27^{A+B}), 34.32 (C-25^A), 34.29 (C-25^B), 31.71 (C-26^A), 31.69 (C-26^B), 21.06 (C-8^A), 21.05 (C-8^B), 18.25 (C-7^A), 18.22 (C-7^B). **IR (film, cm⁻¹)** ν_{max} 2958 (C–H), 1697 (C=O), 1478, 1386, 1207. **HRMS (ESI⁺)** *m/z* calcd for C₅₃H₅₈N₃O₂⁺ [M+H]⁺ 888.4524, found 888.4521.

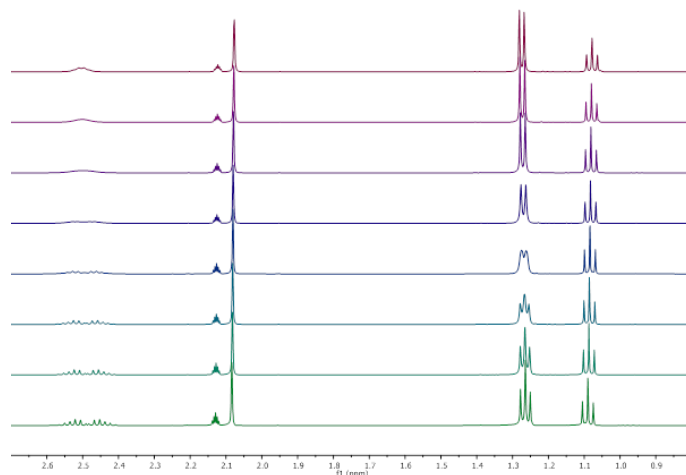
Appendix

Chapter 1 - VT ^1H NMR experiments

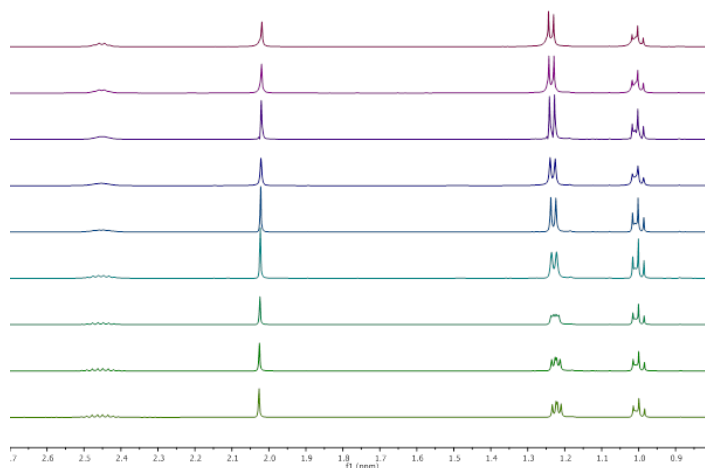
^1H NMR spectra of a solution of the corresponding diarylamine in deuterated solvent were recorded at different temperatures until coalescence was reached. Their slow exchange spectra were simulated using the Spinworks 4 (available at <ftp://davinci.chem.umanitoba.ca/pub/marat/SpinWorks/>), and for each temperature, the corresponding rate of enantiomerisation k_{enant} was calculated using the DNMR simulation module MEXICO. From an Eyring plot, their enthalpy ΔH^\ddagger and entropy ΔS^\ddagger were calculated, and their corresponding Gibbs free energy ΔG^\ddagger were found at 25 °C. Using the following equations, their rate of enantiomerisation and half-life to enantiomerisation at 25 °C were calculated:

$$\Delta G_T^\ddagger = R * T * \ln\left(\frac{k_B * T}{h * k_{\text{enant}}}\right) ; t_{1/2} = \frac{\ln(2)}{2 * k_{\text{enant}}}$$

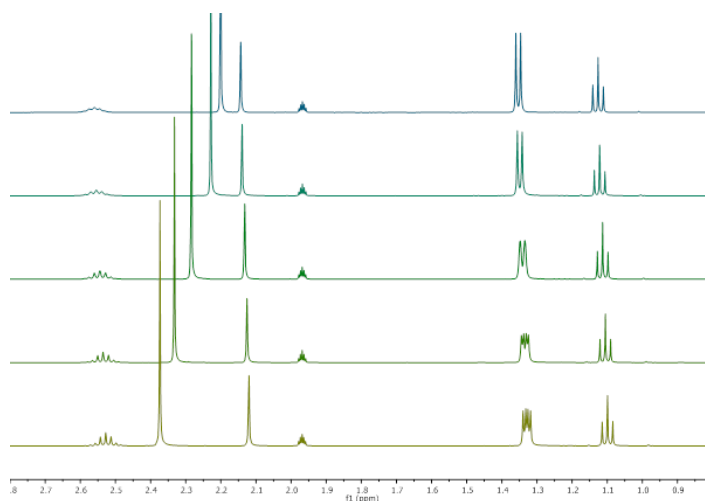
Diarylamine 1.28e



Alkyl region (2.7 – 0.8 ppm) of 1.28e in toluene- d_8 (top to bottom: 60 °C to -10 °C, 10 °C step)



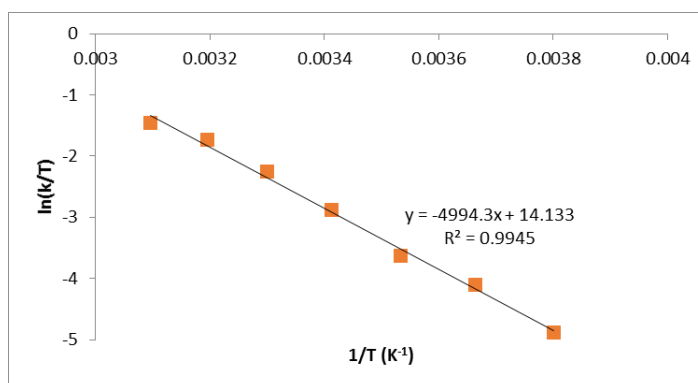
Alkyl region (2.7 – 0.8 ppm) of 1.28e in $\text{C}_2\text{D}_5\text{OD}$ (top to bottom: 70 °C, to -10 °C, 10 °C step)



Alkyl region (2.7 – 0.8 ppm) of 1.28e in CD_3CN (top to bottom: 30 °C, to -10 °C, 10 °C step)

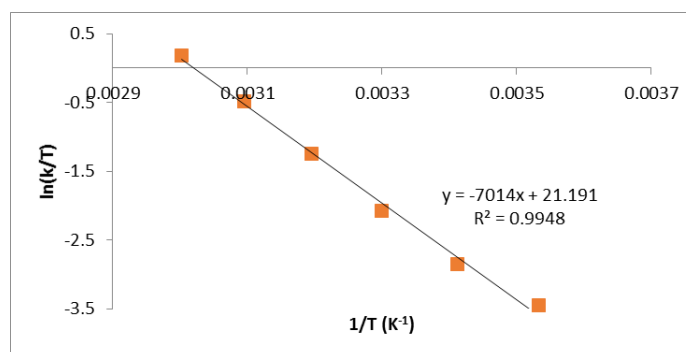
Calculation in $\text{tol-}d_8$ with coalescence of the signal centred around 1.28 ppm for the CHMe_2 protons.

Temperature (K)	k (Hz)
263	2
273	4.5
283	7.5
293	16.5
303	32
313	55
323	75



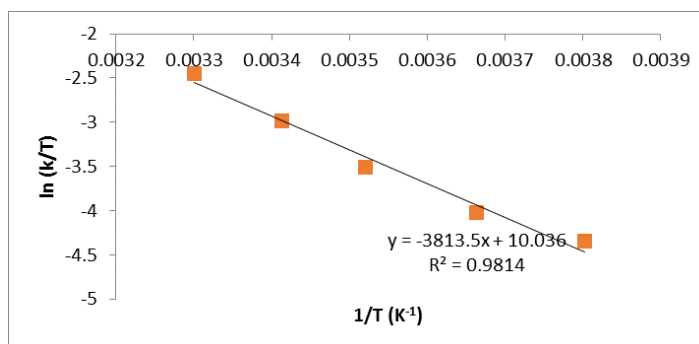
Calculation in $\text{tol-}d_8$ with coalescence of the signal centred around 2.49 ppm for the CH_2CH_3 protons.

Temperature (K)	k (Hz)
283	9
293	17
303	38
313	90
323	200
333	400



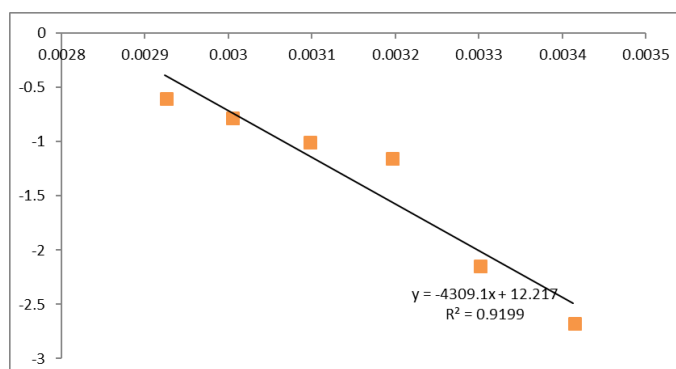
Calculation in C₂D₅OD with coalescence of the signal centred around 1.23 ppm for the CHMe₂ proton

Temperature (K)	k (Hz)
263	3.4
273	4.9
284	8.5
293	14.8
303	26



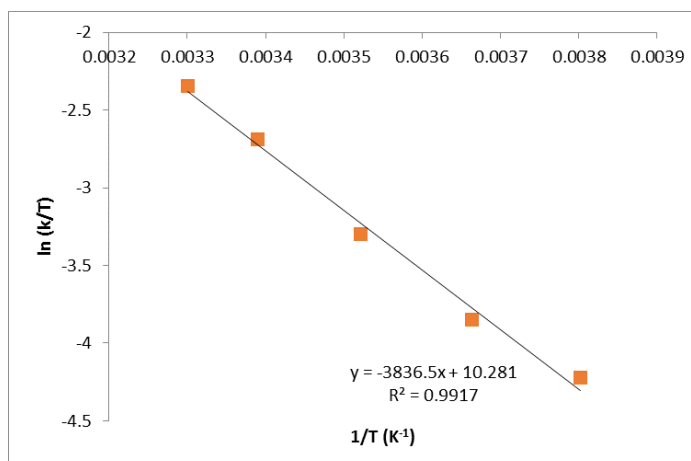
Calculation in C₂D₅OD with coalescence of the signal centred around 2.45 ppm for the CH₂CH₃ proton

Temperature (K)	k (Hz)
293	20.5
303	36
313	100
323	120
333	155
342	190

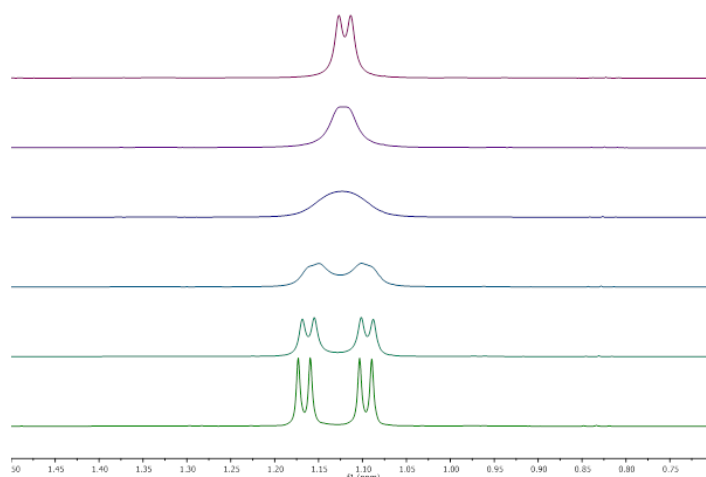


Calculation in CD₃CN with coalescence of the signal centred around 1.33 ppm for the CHMe₂ protons

Temperature (K)	k (Hz)
263	3.85
273	5.8
284	10.5
295	20
303	29



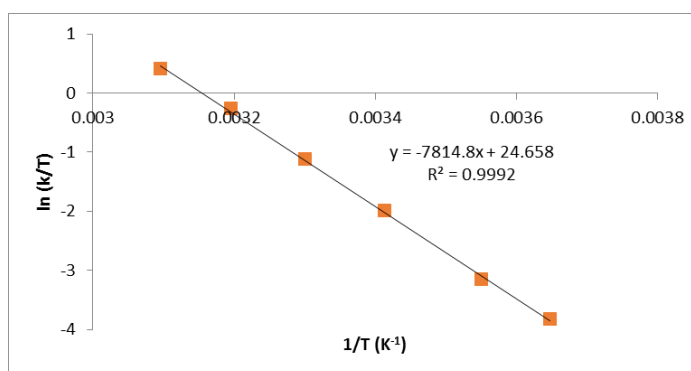
Diarylamine 1.28g



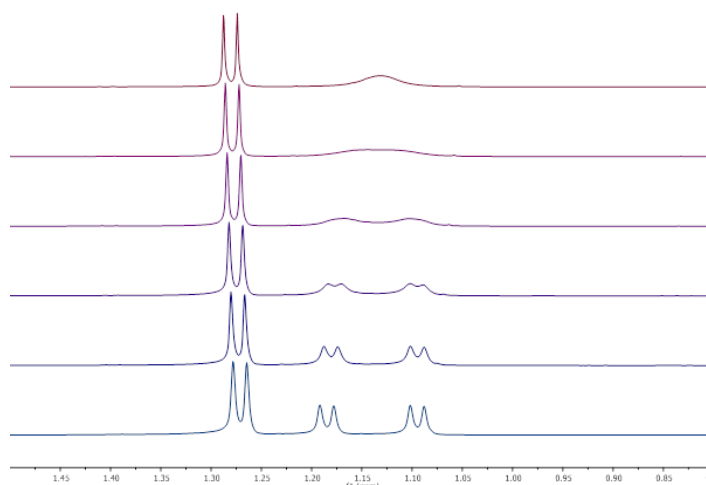
CHMe₂ region (1.5 – 0.7 ppm) of 1.28g in toluene-*d*₈ (top to bottom: 50 °C, to 1 °C, 10 °C step)

Calculation in tol-*d*₈ with coalescence of the signal centred around 1.13 ppm for the CHMe₂ protons.

Temperature (K)	K (Hz)
274	6
282	12
293	40
303	100
313	240
323	490



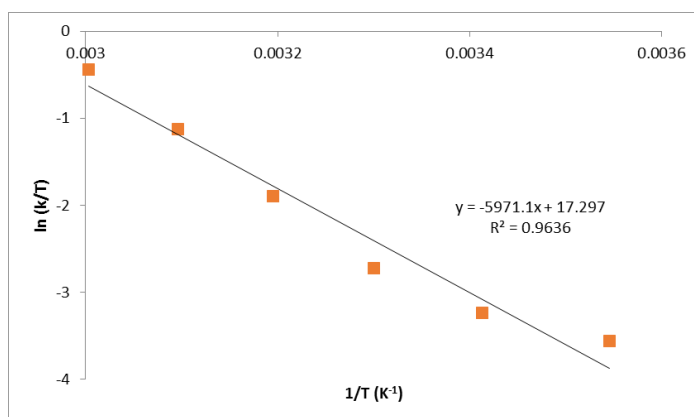
Diarylamine 1.28h



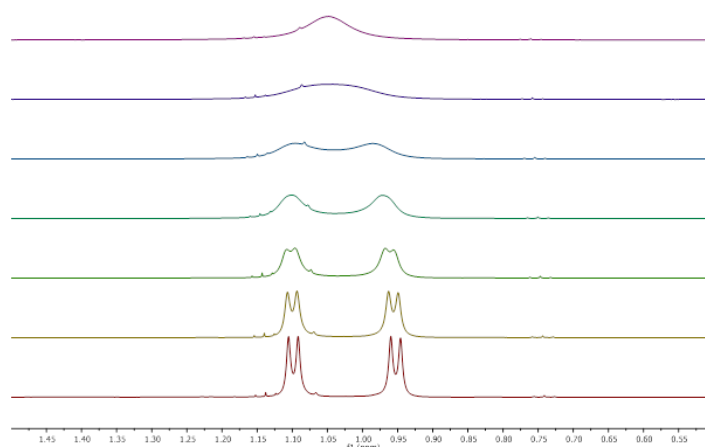
CHMe₂ region (1.5 – 0.8 ppm) of 1.28h in tol-*d*₈ (top to bottom: 60 °C, to 9 °C, 10 °C step)

Calculation in $\text{tol-}d_8$ with coalescence of the signal centred around 1.14 ppm for the CHMe_2 protons.

Temperature (K)	k (Hz)
282	8
293	11.5
303	20
313	47
323	105
333	215



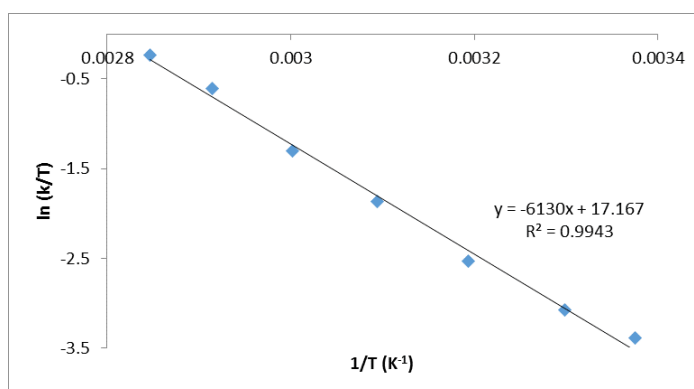
Diarylamine 1.28j



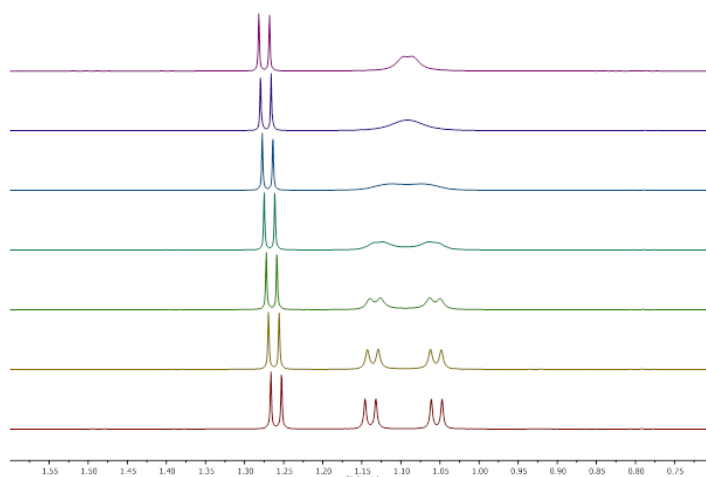
CHMe_2 region (1.5 – 0.8 ppm) of 1.28j in $\text{DMSO-}d_6$ (top to bottom: 80 °C, to 23 °C, 10 °C step)

Calculation in $\text{DMSO-}d_6$ with coalescence of the signal centred at 1.02 ppm for the CHMe_2 protons.

Temperature (K)	k (Hz)
296	10
303	14
313	25
323	50
333	91
343	186
351	278



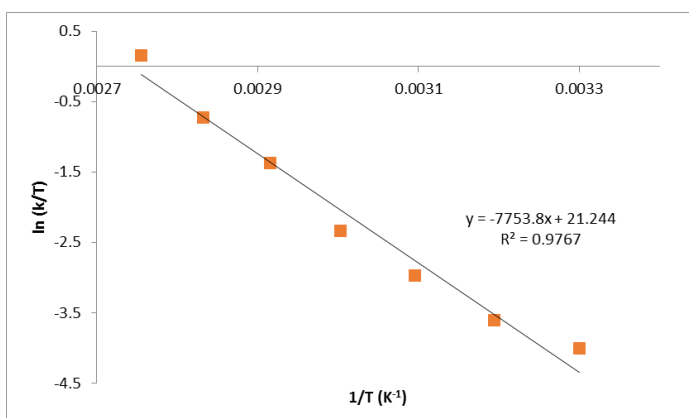
Diarylamine 1.28k



CHMe₂ region (1.6 – 0.7 ppm) of 1.28k in toluene-*d*₈ (top to bottom: 90 °C to 30 °C, 10 °C step)

Calculation in tol-*d*₈ with coalescence of the signal centred around 1.10 ppm for the CHMe₂ protons.

Temperature (K)	K (Hz)
303	5.5
313	8.5
323	16.5
333	32
343	87
353	170
363	425



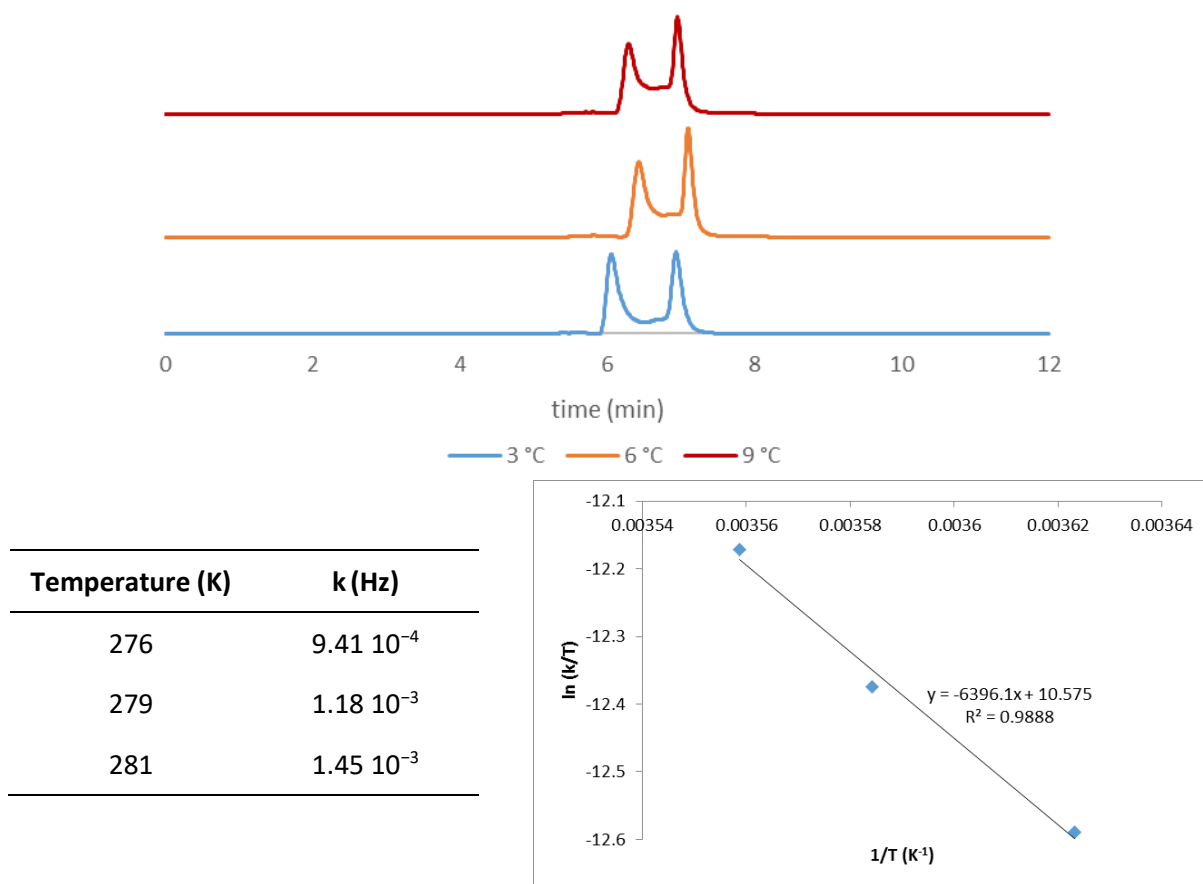
Chapter 1 - Chiral VT-HPLC experiments

Separation of both enantiomers of the corresponding compound by chiral HPLC was performed on an Agilent 1260 Infinity. Temperature of the eluent and of the column was controlled with a ± 0.3 °C error margin. For each temperature, the corresponding rate of enantiomerisation was calculated using the Trapp equation.^[51] From an Eyring plot, their enthalpy ΔH^\ddagger and entropy ΔS^\ddagger were calculated, and their corresponding Gibbs free energy ΔG^\ddagger were found at 25 °C. Using the following equations, their rate of enantiomerisation and half-life to enantiomerisation at 25 °C were calculated:

$$\Delta G_T^\ddagger = R * T * \ln\left(\frac{k_B * T}{h * k_{\text{enant}}}\right) ; t_{1/2} = \frac{\ln(2)}{2 * k_{\text{enant}}}$$

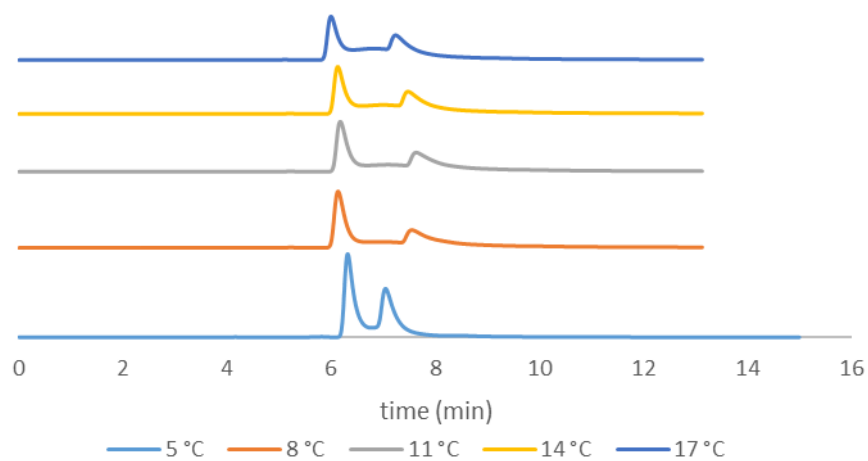
Diarylamine 1.28f

Conditions: Daicel OD-H, n-hexane/2-propanol (98:2), flow: 0.8 mL/min.

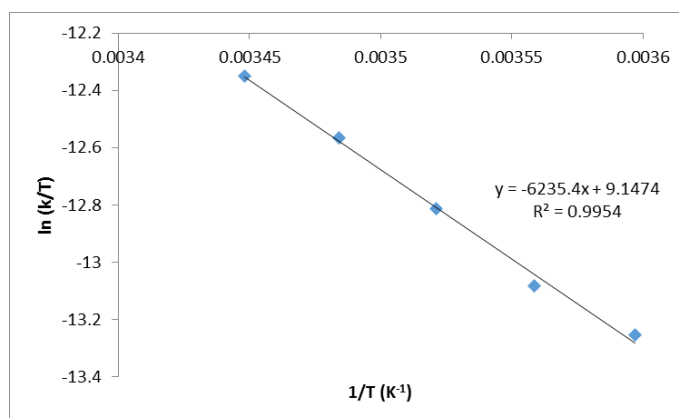


Diarylamine 1.28i

Conditions: Daicel OD-H, n-hexane/2-propanol (99.8:0.2), flow: 0.8 mL/min.

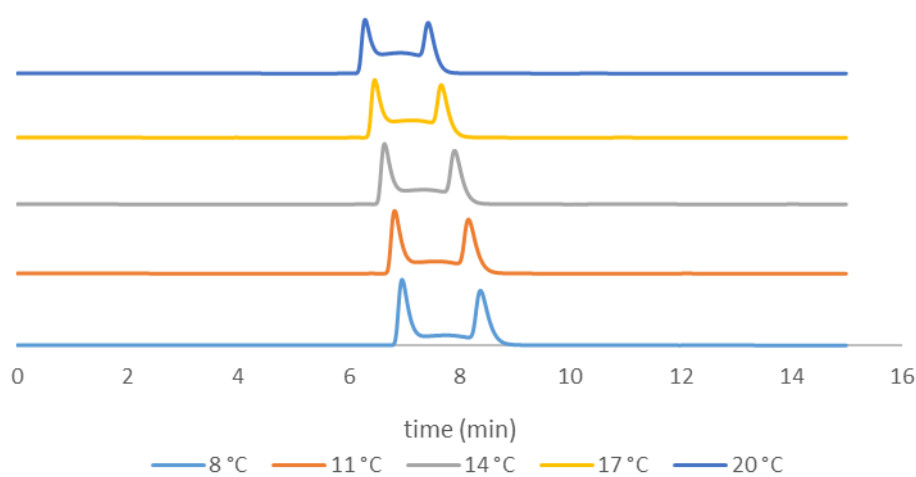


Temperature (K)	k (Hz)
278	$4.87 \cdot 10^{-4}$
281	$5.86 \cdot 10^{-4}$
284	$7.74 \cdot 10^{-4}$
287	$1.00 \cdot 10^{-3}$
290	$1.25 \cdot 10^{-3}$

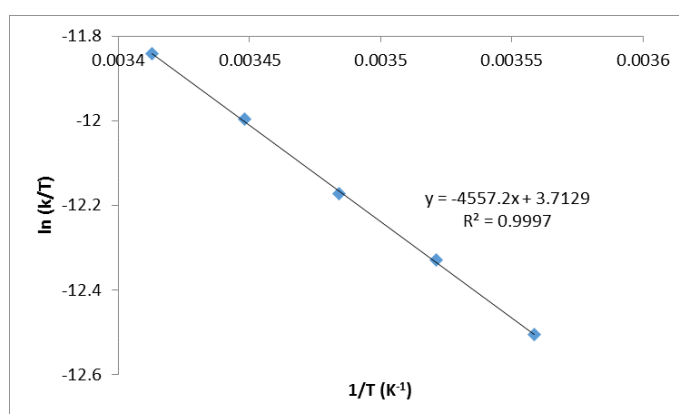


Diarylamine 1.28m

Conditions: Daicel OD-H, *n*-hexane, flow: 0.8 mL/min.

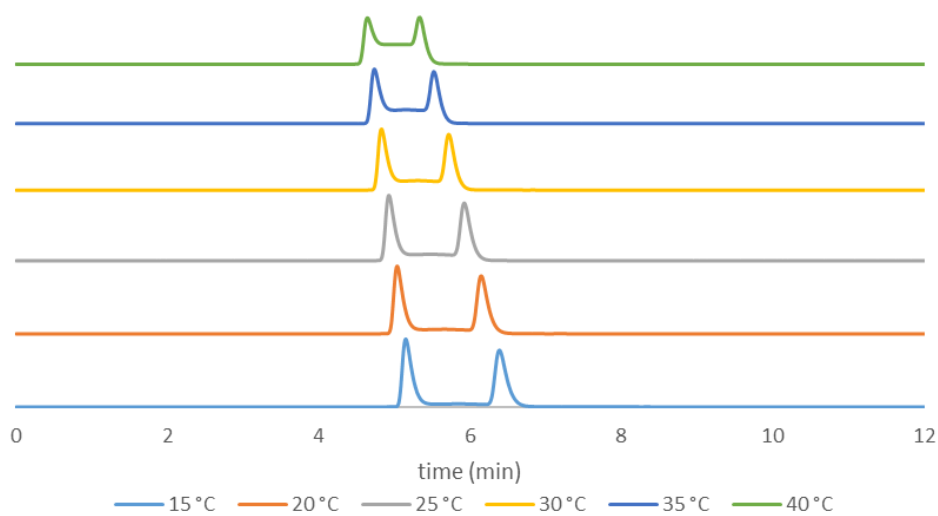


Temperature (K)	k (Hz)
281	$1.04 \cdot 10^{-3}$
284	$1.25 \cdot 10^{-3}$
287	$1.48 \cdot 10^{-3}$
290	$1.79 \cdot 10^{-3}$
293	$2.11 \cdot 10^{-3}$

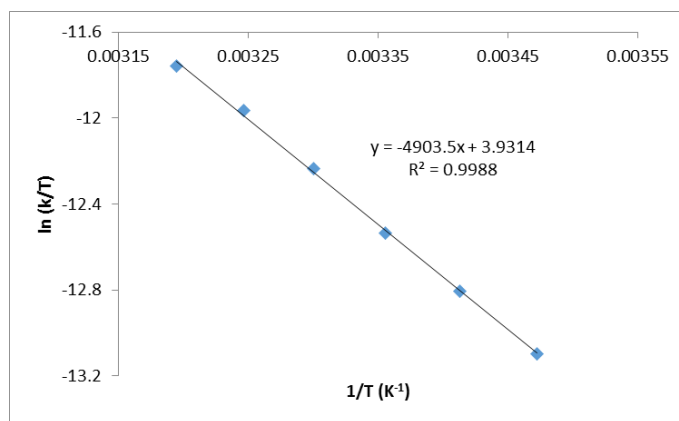


Diarylamine 1.28o

Conditions: Daicel OD-H, n-hexane/2-propanol (99:1), flow: 0.8 mL/min.

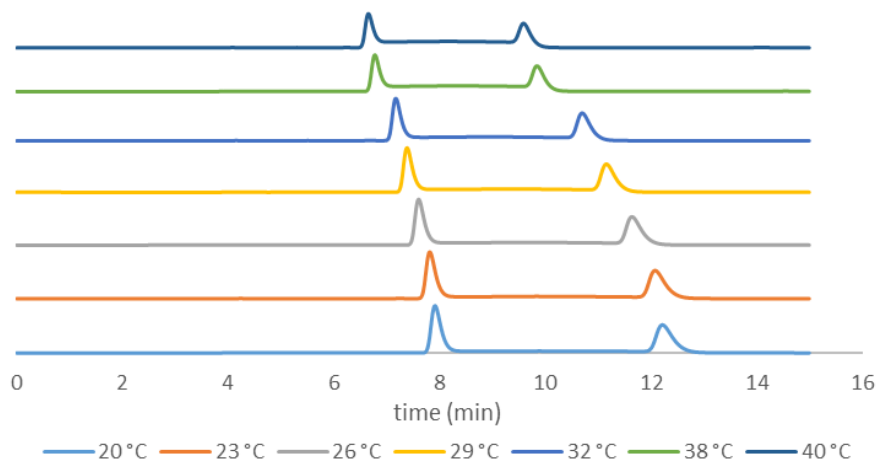


Temperature (K)	k (Hz)
288	$5.91 \cdot 10^{-4}$
293	$8.05 \cdot 10^{-4}$
298	$1.07 \cdot 10^{-3}$
303	$1.47 \cdot 10^{-3}$
308	$1.96 \cdot 10^{-3}$
313	$2.45 \cdot 10^{-3}$

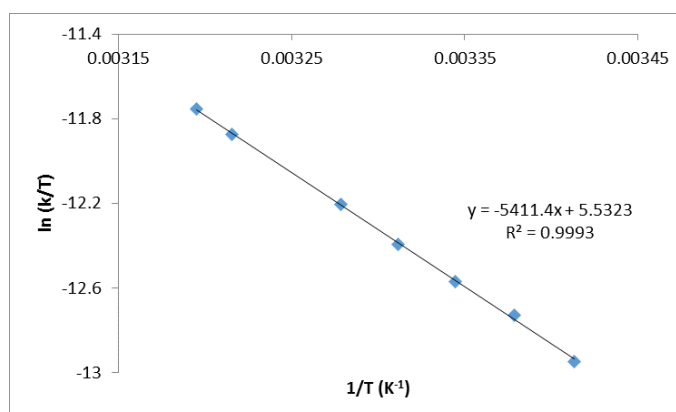


Diarylamine 1.28q

Conditions: Daicel OD-H, n-hexane/2-propanol (99:1), flow: 0.8 mL/min.



Temperature (K)	k (Hz)
293	$6.98 \cdot 10^{-4}$
296	$8.77 \cdot 10^{-4}$
299	$1.04 \cdot 10^{-3}$
302	$1.25 \cdot 10^{-3}$
305	$1.53 \cdot 10^{-3}$
311	$2.17 \cdot 10^{-3}$
313	$2.46 \cdot 10^{-3}$



Chapter 1 - Decay of enantiomeric excess

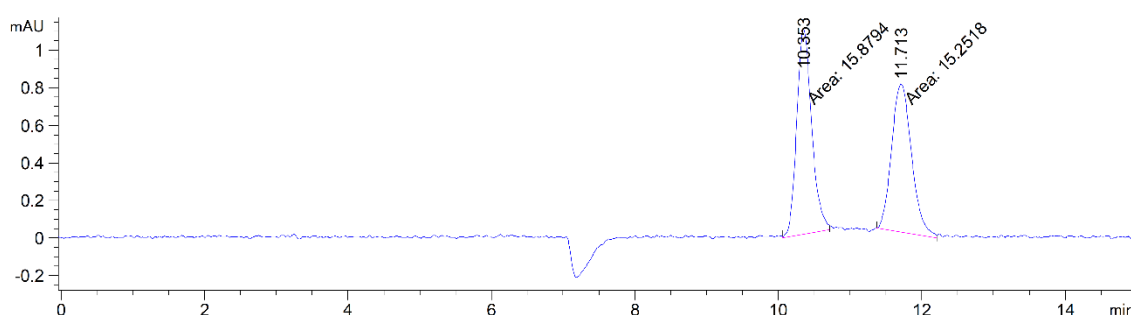
Separation of both enantiomers of the respective compounds by chiral HPLC was performed on an Agilent 1260 Infinity. The pure fractions of each enantiomer were combined, diluted and toluene and left at room temperature or heated to 100 °C for **1.28u** and **1.28x** respectively. Aliquots of the solution were taken, diluted in n-hexane and ran on HPLC using the conditions stated below.

The ln of the enantiomeric excess was plotted against time, and their rate of racemisation k_{rac} was obtained with the slope of the trendline. (Caution!: $k_{rac} = 2 * k_{enant}$). Their Gibbs free energy and half-life to enantiomerisation were calculated at 25 °C and 100 °C, respectively, using:

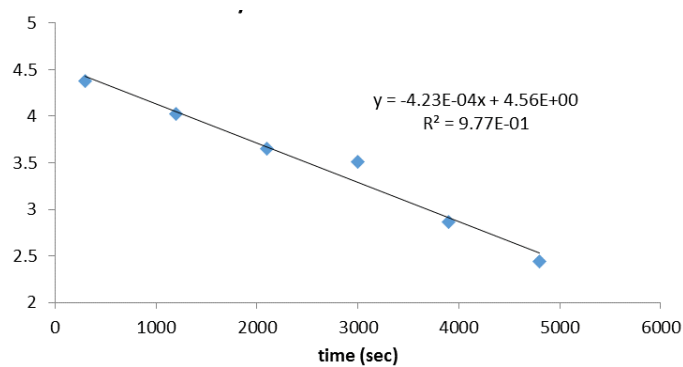
$$\Delta G_T^\ddagger = R * T * \ln\left(\frac{k_B * T}{h * k_{enant}}\right) ; t_{1/2} = \frac{\ln(2)}{2 * k_{enant}}$$

Diarylamine 1.28u

Conditions: Daicel OD-H, n-hexane/2-propanol (99.5:0.5), 1.0 mL/min, $t_R = 11.2$ and 12.3 min.

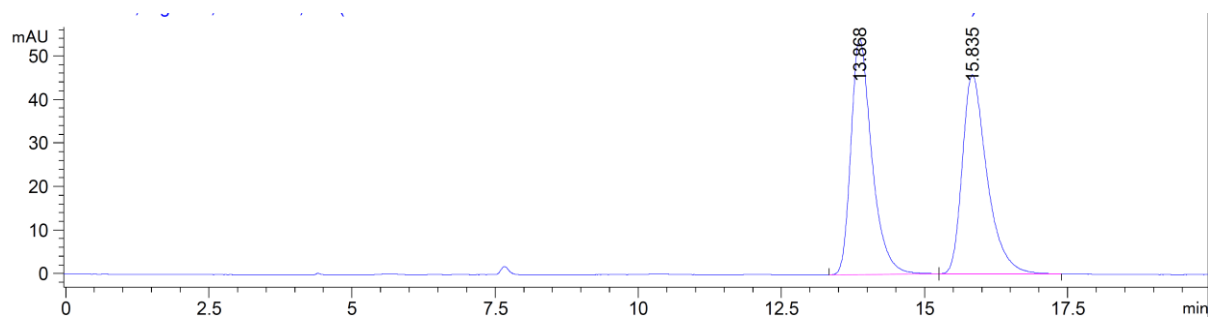


Time (min)	ee (%)
5	79.8
20	56.0
35	38.6
50	33.4
65	17.5
80	11.5

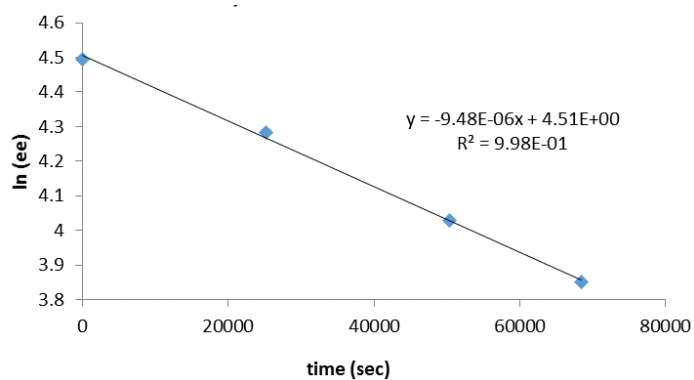


Diarylamine 1.28x

Conditions: Daicel OD-H, n-hexane, flow: 1.0 mL/min, $t_R = 13.9$ and 15.8 min.



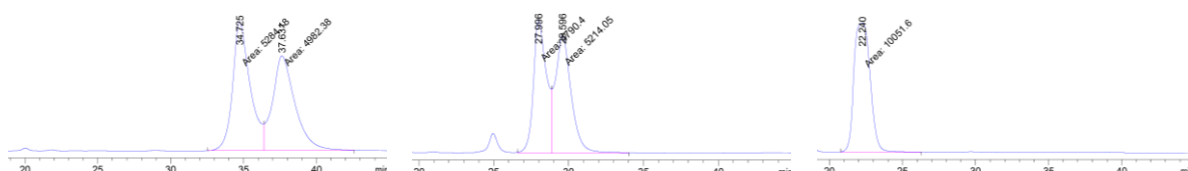
Time (h)	ee (%)
0	98.6
7	72.4
14	56.2
19	47.0



Chapter 2 - Decay of enantiomeric excess

Separation of both enantiomers of compound **2.48m** by chiral HPLC was possible at low temperature (273 K). However, the absence of observable plateau due to moderate separation as well as temperature-dependant retention time precluded calculation of the barrier to rotation.

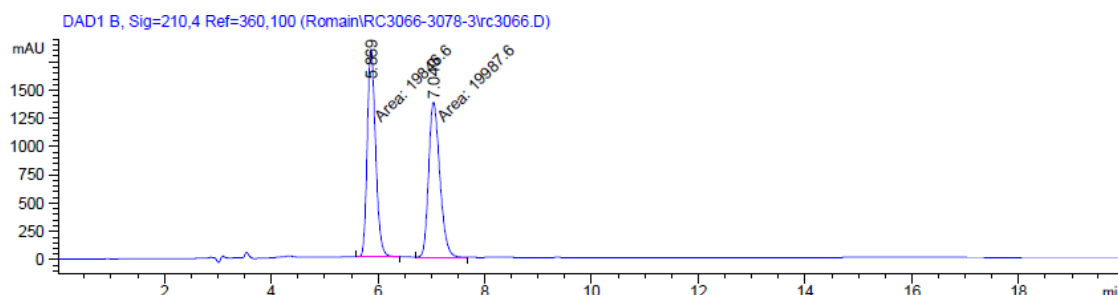
2.48m: RegisTech Alpha Burke 2, *n*-hexane/2-propanol (99:1), flow: 0.8 mL/min. The following traces were run at 5 °C, 20 °C and 35 °C respectively.



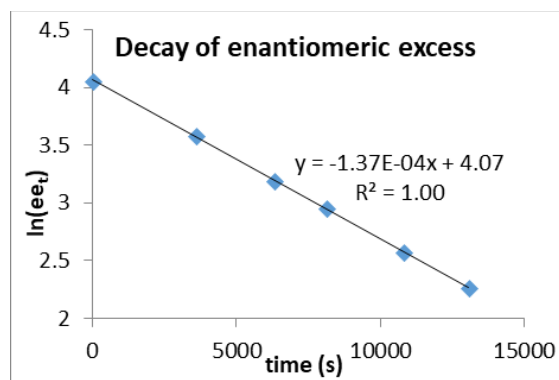
Following time-dependent decrease in the enantiomeric purity of the enantioenriched samples by chiral stationary phase HPLC. Time-dependent decrease in the enantiomeric purity of **2.48o** and **2.61** at 60 °C in toluene was monitored by HPLC analysis. The slope of the plot of the decay of enantiomeric excess *versus* time indicates the barrier to racemisation.

Barrier to racemisation of 2.48o

2.48o: Daicel Chiralpak OD-H, *n*-hexane/2-propanol (90:10), flow: 1.0 mL/min, t_R = 5.9, 7.0 min.



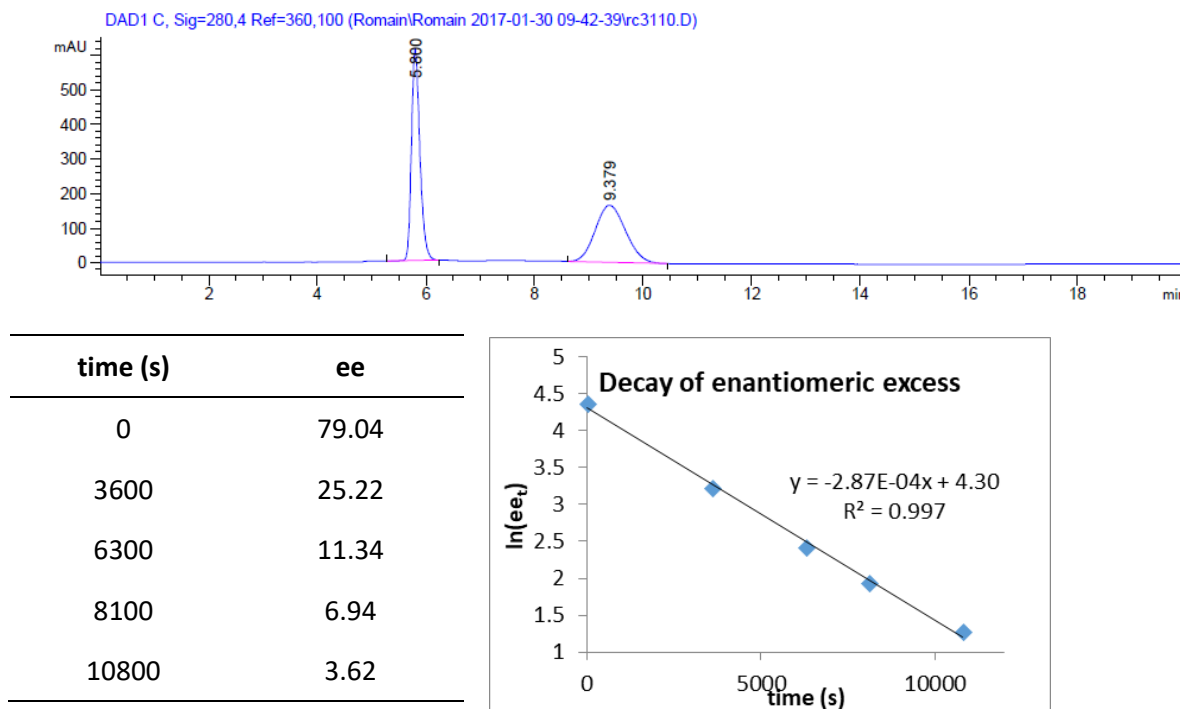
time (s)	ee
0	58.1
3600	35.8
6300	24.5
8100	19.3
10800	13.1
13080	9.7



$$k = 1.37 \times 10^{-4} \text{ s}^{-1}; t_{1/2} = 84 \text{ min}; \Delta G^\ddagger_{333 \text{ K}} = 106.5 \text{ kJ.mol}^{-1}$$

Barrier to racemisation of 2.61

2.61: Daicel Chiralpak OD-H, *n*-hexane/2-propanol (90:10), flow: 1.0 mL/min, t_R = 5.8, 9.4 min.

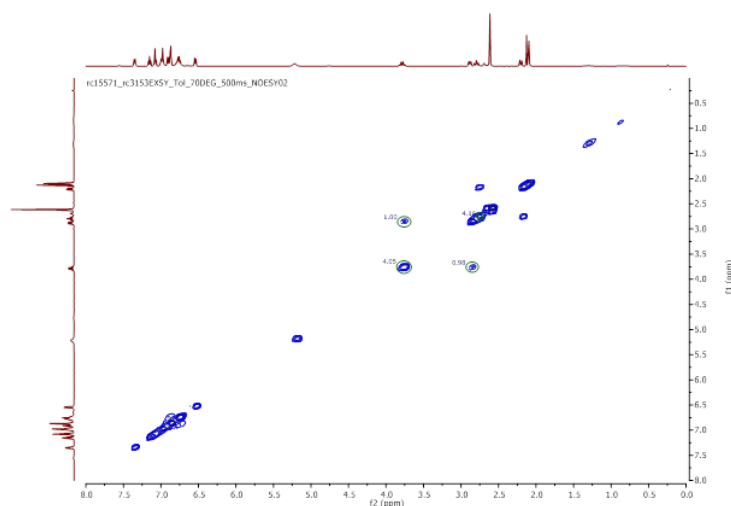


$$k = 2.87 \times 10^{-4} \text{ s}^{-1}; t_{1/2} = 40 \text{ min}; \Delta G_{333\text{K}}^\ddagger = 104.4 \text{ kJ.mol}^{-1}$$

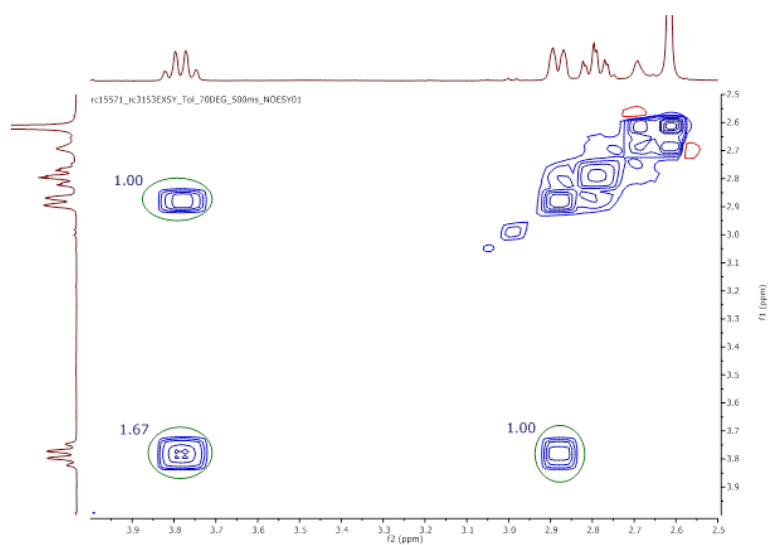
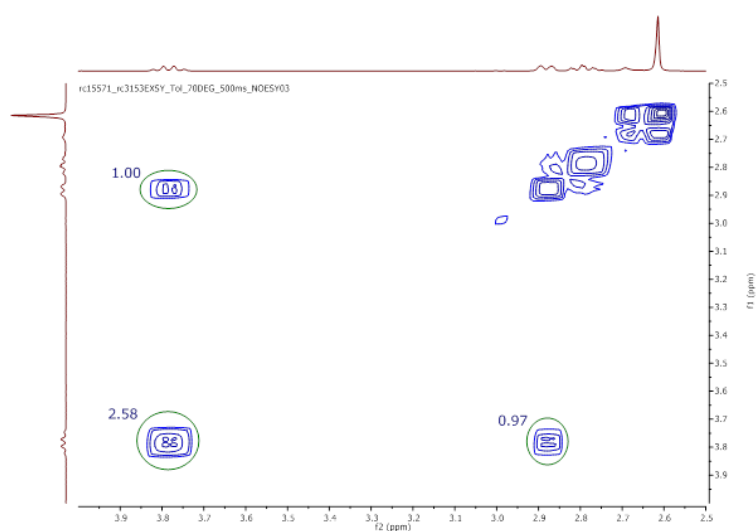
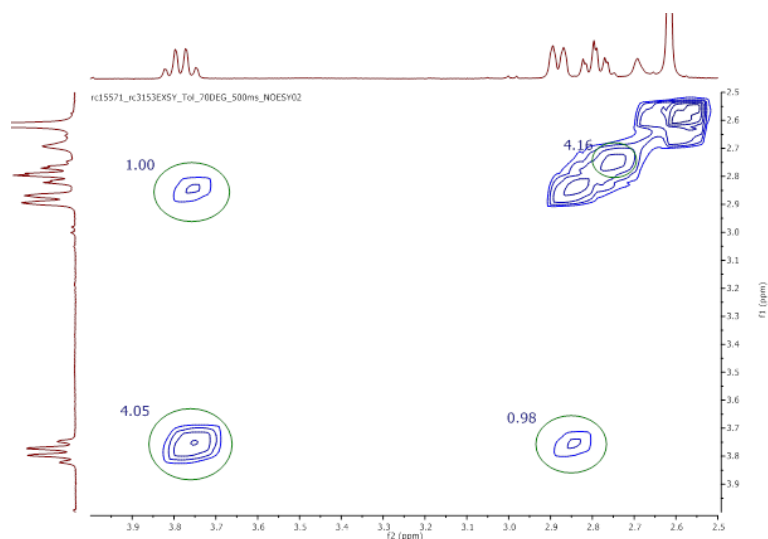
Chapter 3 - EXSY experiments

The EXSY experiments were performed on a Varian 500 MHz spectrometer using the standard noesygpph pulse program. The acquired data points were zero-filled to 1K x 1K. The data were processed using MestReNova and the integration of the various signals was analysed using the EXSYCalc program from MestReC to obtain the rate constant.

Enantiomerisation of 3.18a

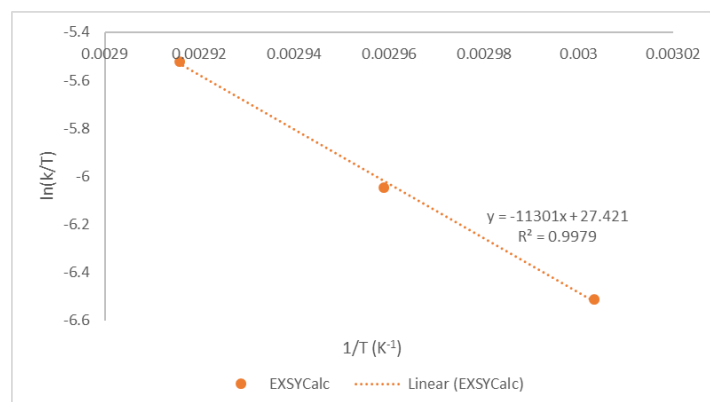


EXSY spectrum of 3.18a in toluene- d_8 , at 60 °C, 500 ms mixing time.



Solvent	Temperature	Mixing time	$k_{\text{enant}} \text{ (s}^{-1}\text{)}$
toluene- d_8	60 °C	500 ms	0.499
	65 °C	500 ms	0.804
	70 °C	500 ms	1.383

Enantiomerisation of 3.18a in toluene- d_8



Eyring plot for the enantiomerisation of 3.18a in toluene- d_8

Enantiomerisation of 3.18b

Solvent	Temperature	Mixing time	$k_{\text{enant}} \text{ (s}^{-1}\text{)}$
DMSO- d_6	40 °C	800 ms	0.162
	45 °C	500 ms	0.509
	50 °C	500 ms	1.126
CDCl ₃	40 °C	2000 ms	0.0525
	45 °C	1000 ms	0.216
	50 °C	1000 ms	0.430

Enantiomerisation of 3.18c

Solvent	Temperature	Mixing time	$k_{\text{enant}} \text{ (s}^{-1}\text{)}$
DMSO- d_6	25 °C	400 ms	0.164
CDCl ₃	40 °C	1000 ms	0.184
	45 °C	700 ms	0.410
	50 °C	500 ms	0.751

Enantiomerisation of 3.18d

Solvent	Temperature	Mixing time	$k_{\text{enant}} (\text{s}^{-1})$
CD ₃ OD	3 °C	100 ms	1.780
	8 °C	100 ms	4.279
	13 °C	100 ms	6.613
CDCl ₃	25 °C	150 ms	4.582

Enantiomerisation of 3.18l

Solvent	Temperature	Mixing time	$k_{\text{enant}} (\text{s}^{-1})$
DMSO- <i>d</i> ₆	40 °C	1000 ms	0.435
	45 °C	1000 ms	1.019
	50 °C	600 ms	1.711
CDCl ₃	40 °C	1000 ms	0.260
	45 °C	1000 ms	0.527
	50 °C	600 ms	0.967

Diastereomerisation of 3.18a

Solvent	Temperature	Mixing time (no exchange)	Mixing time (with exchange)	$k_1 (\text{s}^{-1})$	$k_{-1} (\text{s}^{-1})$
CD ₃ OD	25 °C	30 ms	1000 ms	0.326	0.099
toluene- <i>d</i> ₈	25 °C	30 ms	600 ms	0.306	0.035

Diastereomerisation of 3.18l

Solvent	Temperature	Mixing time (no exchange)	Mixing time (with exchange)	$k_1 (\text{s}^{-1})$	$k_{-1} (\text{s}^{-1})$
DMSO- <i>d</i> ₆	80 °C	30 ms	500 ms	0.409	0.098
	85 °C	30 ms	500 ms	0.680	0.166
	90 °C	30 ms	500 ms	1.11	0.245
CDCl ₃	40 °C	30 ms	1000 ms	0.071	0.020
	45 °C	30 ms	1000 ms	0.156	0.036
	50 °C	30 ms	600 ms	0.271	0.070

Chapter 4 - Chiral VT-HPLC experiments

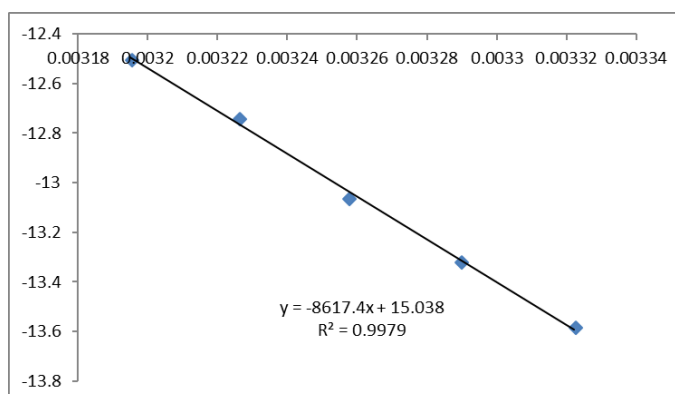
Barrier to enantiomerisation of 4.43b

Separation of both enantiomers of the corresponding compound by chiral HPLC was performed on an Agilent 1260 Infinity. Temperature of the eluent and of the column was controlled with a ± 0.3 °C error margin. For each temperature, the corresponding rate of enantiomerisation was calculated using the Trapp equation.^[51] From an Eyring plot, their enthalpy ΔH^\ddagger and entropy ΔS^\ddagger were calculated, and their corresponding Gibbs free energy ΔG^\ddagger were found at 25 °C. Using the following equations, their rate of enantiomerisation and half-life to enantiomerisation at 25 °C were calculated:

$$\Delta G_T^\ddagger = R * T * \ln\left(\frac{k_B * T}{h * k_{\text{enant}}}\right) ; t_{1/2} = \frac{\ln(2)}{2 * k_{\text{enant}}}$$

Conditions: Daicel OD-H, n-hexane, flow: 1.0 mL/min.

Temperature (K)	k (Hz)
301	$3.81 \cdot 10^{-4}$
304	$5.01 \cdot 10^{-4}$
307	$6.54 \cdot 10^{-4}$
310	$9.13 \cdot 10^{-4}$
313	$11.7 \cdot 10^{-4}$



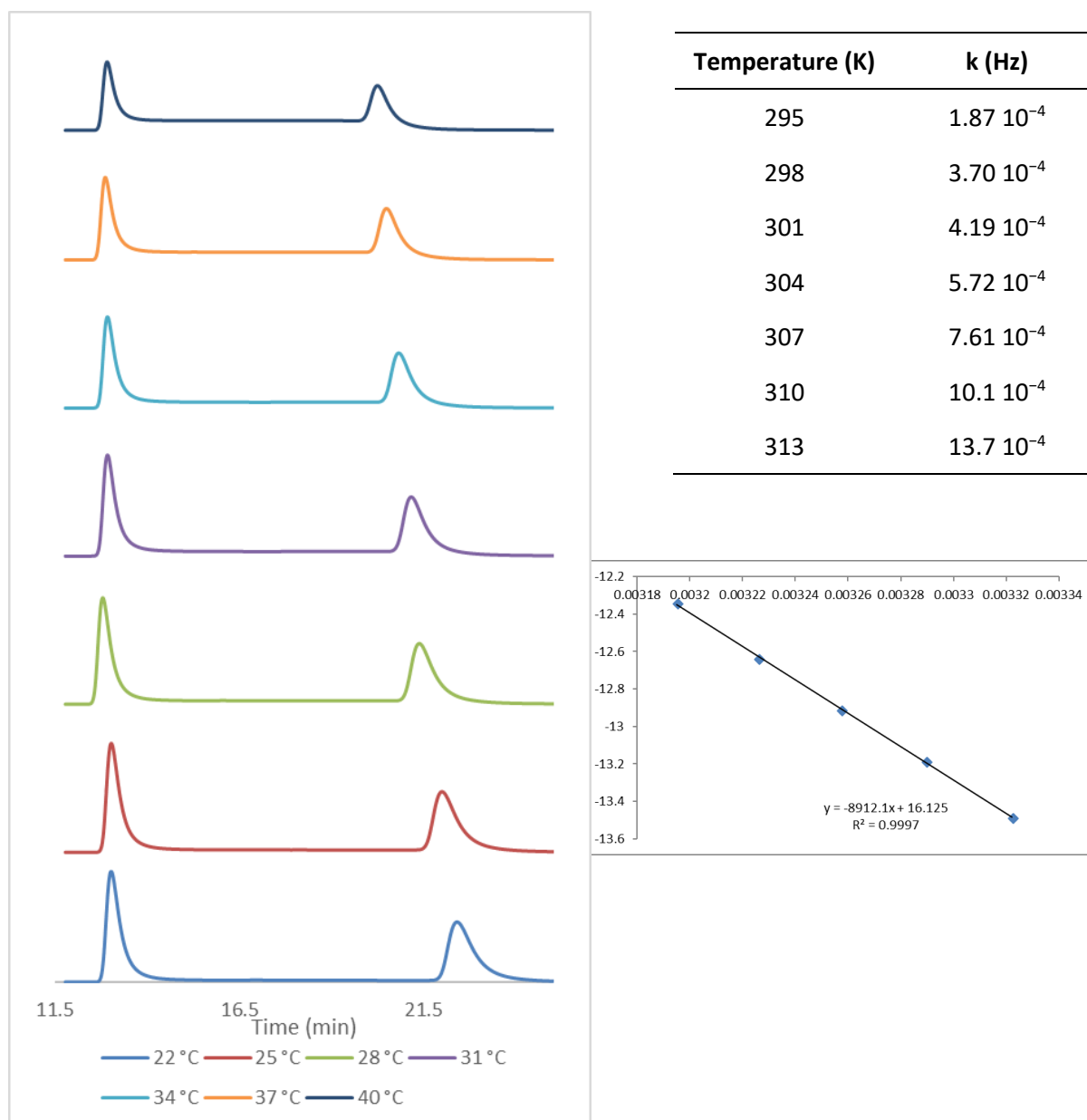
Chapter 5 - Chiral VT-HPLC experiments

Barrier to enantiomerisation of **5.24**

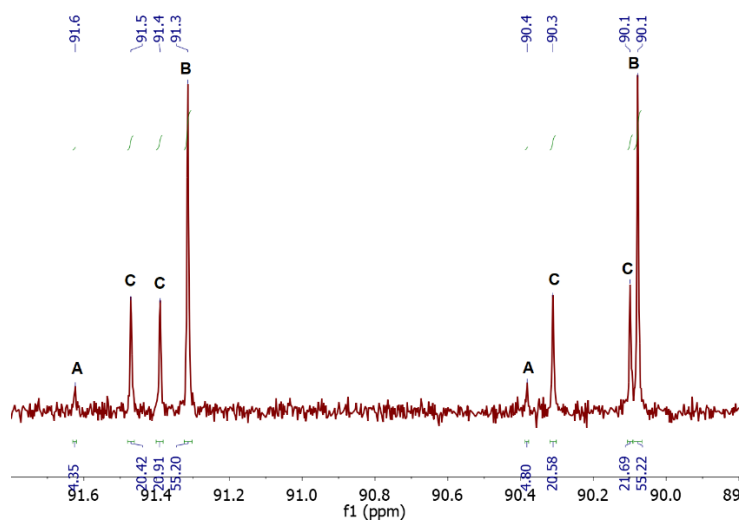
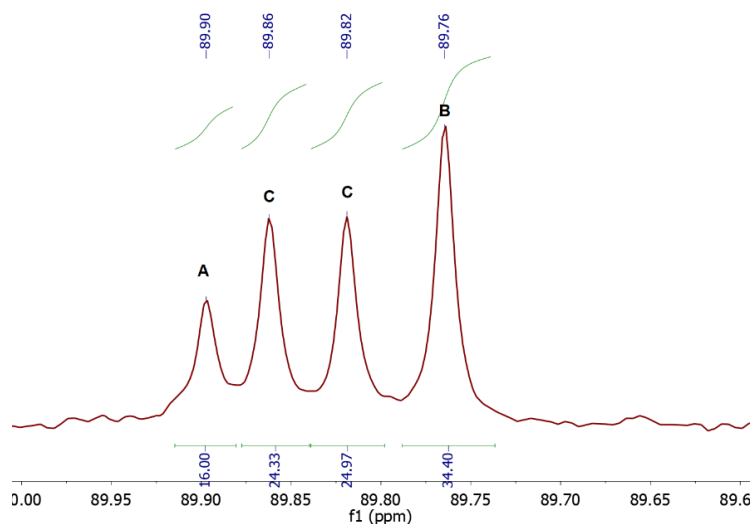
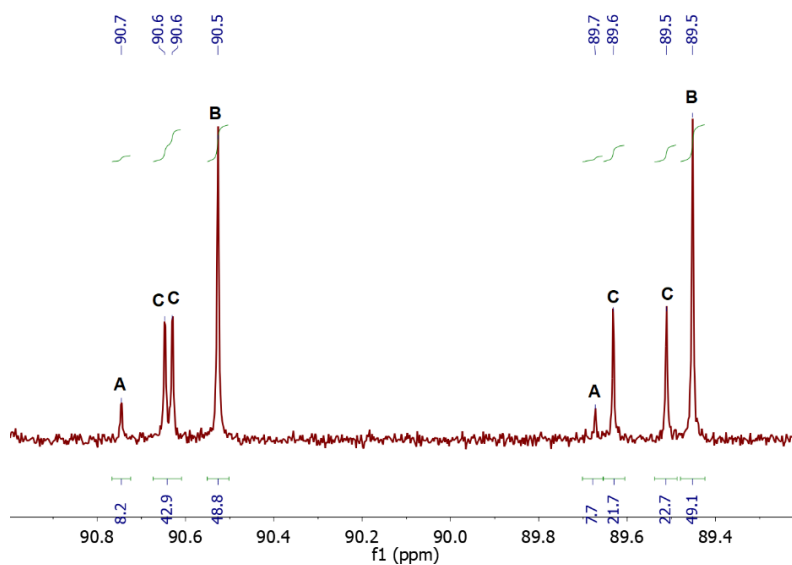
Separation of both enantiomers of **5.24** by chiral HPLC was performed on an Agilent 1260 Infinity. Temperature of the eluent and column was controlled with a ± 0.3 °C margin. For each temperature, the corresponding rate of enantiomerisation was calculated using the Trapp equation.^[51] From an Eyring plot, the enthalpy ΔH^\ddagger and entropy ΔS^\ddagger were calculated, and the Gibbs free energy ΔG^\ddagger was found at 25 °C. Using the following equations, the rate of enantiomerisation and half-life to enantiomerisation at 25 °C were calculated:

$$\Delta G_T^\ddagger = R * T * \ln\left(\frac{k_B * T}{h * k_{\text{enant}}}\right) ; t_{1/2} = \frac{\ln(2)}{2 * k_{\text{enant}}}$$

Conditions: Daicel AD-H, *n*-hexane/2-propanol (98:2), flow: 1.0 mL/min.



Chapter 5 - Determination of conformers distribution of 5.35



References

- [1] G. H. Christie, J. Kenner, *J. Chem. Soc. Trans.* **1922**, 121, 614–620.
- [2] R. Kuhn, in *Stereochemie* (Ed.: H. Freudenberg), Franz Deutike, Leipzig-Wien, **1933**, pp. 803–824.
- [3] M. Ōki, in *Top. Stereochem.*, **1983**, pp. 1–81.
- [4] R. Noyori, *Nobel Lecture* **2001**, 186–215.
- [5] J. Wencel-Delord, A. Panossian, F. R. Leroux, F. Colobert, *Chem. Soc. Rev.* **2015**, 44, 3418–3430.
- [6] G. Bringmann, A. J. Price Mortimer, P. A. Keller, M. J. Gresser, J. Garner, M. Breuning, *Angew. Chemie Int. Ed.* **2005**, 44, 5384–5427.
- [7] M. P. Johansson, J. Olsen, *J. Chem. Theory Comput.* **2008**, 4, 1460–1471.
- [8] G. Bott, L. D. Field, S. Sternhell, *J. Am. Chem. Soc.* **1980**, 102, 5618–5626.
- [9] M. Rieger, F. H. Westheimer, *J. Am. Chem. Soc.* **1950**, 72, 19–28.
- [10] C. Wolf, W. A. König, C. Roussel, *Liebigs Ann.* **1995**, 1995, 781–786.
- [11] J. Clayden, *Angew. Chemie Int. Ed.* **1997**, 36, 949–951.
- [12] M. S. Betson, J. Clayden, C. P. Worrall, S. Peace, P. General, *Angew. Chem. Int. Ed.* **2006**, 45, 5803–5807.
- [13] T. Mino, H. Yamada, S. Komatsu, M. Kasai, M. Sakamoto, T. Fujita, *Eur. J. Org. Chem.* **2011**, 4540–4542.
- [14] J. Clayden, J. Senior, M. Helliwell, *Angew. Chemie Int. Ed.* **2009**, 48, 6270–6273.
- [15] E. Kumarasamy, R. Raghunathan, M. P. Sibi, J. Sivaguru, *Chem. Rev.* **2015**, 150928132717005.
- [16] R. C. Moellering, *Clin. Infect. Dis.* **2006**, 42, S3–S4.
- [17] D. A. Evans, M. R. Wood, B. W. Trotter, T. I. Richardson, J. C. Barrow, J. L. Katz, *Angew. Chemie Int. Ed.* **1998**, 37, 2700–2704.
- [18] J. Clayden, S. P. Fletcher, J. Senior, C. P. Worrall, *Tetrahedron: Asymmetry* **2010**, 21, 1355–1360.
- [19] G. Bringmann, T. Gulder, M. Reichert, F. Meyer, *Org. Lett.* **2006**, 8, 1037–1040.
- [20] G. Bringmann, S. Tasler, H. Endress, K. Messer, M. Wohlfarth, W. Lobin, D.-Wu, *J. Am. Chem. Soc.* **2001**, 123, 2703–2712.
- [21] Y. Chen, M. D. Smith, K. D. Shimizu, *Tetrahedron Lett.* **2001**, 42, 7185–7187.
- [22] Y. Suzuki, M. Kageyama, R. Morisawa, Y. Dobashi, H. Hasegawa, S. Yokojima, O. Kitagawa, *Chem. Commun.* **2015**, 51, 11229–11232.
- [23] B. J. Price, J. a. Eggleston, I. O. Sutherland, *J. Chem. Soc. B Phys. Org.* **1966**, 88, 922–925.
- [24] T. H. Siddall, W. E. Stewart, *J. Phys. Chem.* **1968**, 15, 40–45.
- [25] D. P. Curran, H. Qi, S. J. Geib, N. C. Demello, *J. Am. Chem. Soc.* **1994**, 116, 3131–3132.
- [26] D. P. Curran, G. R. Hale, S. J. Geib, A. Balog, Q. B. Cass, A. L. G. Degani, M. Z. Hernandez, L. C. G. Freitas, *Tetrahedron: Asymmetry* **1997**, 8, 3955–3975.
- [27] S. Davalli, L. Lunazzi, D. Macciantelli, *J. Org. Chem.* **1991**, 56, 1739–1747.
- [28] D. Casarini, L. Lunazzi, D. Macciantelli, *J. Org. Chem.* **1988**, 53, 182–185.
- [29] T. Kawabata, C. Jiang, K. Hayashi, K. Tsubaki, T. Yoshimura, S. Majumdar, T. Sasamori, N. Tokitoh, *J. Am. Chem. Soc.* **2009**, 131, 54–55.
- [30] K. Hayashi, N. Matubayasi, C. Jiang, T. Yoshimura, S. Majumdar, T. Sasamori, N. Tokitoh, T. Kawabata, *J. Org. Chem.* **2010**, 75, 5031–5036.
- [31] Y. Iwasaki, R. Morisawa, S. Yokojima, H. Hasegawa, C. Roussel, N. Vanthuyne, E. Caytan, O. Kitagawa, *Chem. Eur. J.* **2018**, 24, 4453–4458.
- [32] S. M. Raders, J. N. Moore, J. K. Parks, A. D. Miller, T. M. Leißing, S. P. Kelley, R. D. Rogers, K. H. Shaughnessy, *J. Org. Chem.* **2013**, 78, 4649–4664.
- [33] P. Ruiz-Castillo, S. L. Buchwald, *Chem. Rev.* **2016**, 116, 12564–12649.
- [34] D. S. Surry, S. L. Buchwald, *Chem. Sci.* **2011**, 2, 27–50.
- [35] G. Bauer, X. Hu, *Inorg. Chem. Front.* **2016**, 3, 741–765.
- [36] F. Casaluce, A. Sgambato, P. Maione, P. C. Sacco, G. Santabarbara, C. Gridelli, *Expert Opin. Investig. Drugs* **2017**, 26, 973–984.

- [37] W. G. Whittingham, in *Mod. Crop Prot. Compd.* (Eds.: W. Kramer, U. Schirmer), Wiley-VCH, Weinheim, **2007**, pp. 520–522.
- [38] O. A. Bell, G. Wu, J. S. Haataja, F. Brömmel, N. Fey, A. M. Seddon, R. L. Harniman, R. M. Richardson, O. Ikkala, X. Zhang, et al., *J. Am. Chem. Soc.* **2015**, *137*, 14288–14294.
- [39] H. Hu, F. Qu, D. L. Gerlach, K. H. Shaughnessy, *ACS Catal.* **2017**, *7*, 2516–2527.
- [40] J. Yu, P. Zhang, J. Wu, Z. Shang, *Tetrahedron Lett.* **2013**, *54*, 3167–3170.
- [41] J. Yu, Y. Wang, P. Zhang, J. Wu, *Synlett* **2013**, *24*, 1448–1454.
- [42] T. Piou, A. Bunesco, Q. Wang, L. Neuville, J. Zhu, *Angew. Chemie Int. Ed.* **2013**, *52*, 12385–12389.
- [43] P. Beak, S. T. Kerrick, D. J. Gallagher, *J. Am. Chem. Soc.* **1993**, *115*, 10628–10636.
- [44] M. Arisawa, M. Kuwajima, M. Yamaguchi, *Tetrahedron Lett.* **2010**, *51*, 3116–3118.
- [45] K. Yang, R. J. Lachicotte, R. Eisenberg, *Organometallics* **1997**, *16*, 5234–5243.
- [46] R. R. Schrock, J. D. Fellmann, *J. Am. Chem. Soc.* **1978**, *100*, 3359–3370.
- [47] P. K. Freeman, L. L. Hutchinson, *J. Org. Chem.* **1983**, *48*, 879–881.
- [48] R. B. King, J. C. Cloyd, R. H. Reimann, *J. Org. Chem.* **1976**, *41*, 972–977.
- [49] C. Wolf, in *Dynamic Stereochemistry of Chiral Compounds*, Royal Society Of Chemistry, Cambridge, **2007**, pp. 136–179.
- [50] G. Binsch, *J. Am. Chem. Soc.* **1969**, *91*, 1304–1309.
- [51] O. Trapp, *Anal. Chem.* **2006**, *78*, 189–198.
- [52] O. Trapp, V. Schurig, *Chirality* **2002**, *14*, 465–470.
- [53] M. Watanabe, H. Suzuki, Y. Tanaka, T. Ishida, T. Oshikawa, A. Tori-i, *J. Org. Chem.* **2004**, *69*, 7794–7801.
- [54] C. Wolf, *Chem. Soc. Rev.* **2005**, *34*, 595–608.
- [55] K. C. Gross, P. G. Seybold, *Int. J. Quantum Chem.* **2000**, *80*, 1107–1115.
- [56] B. M. Graybill, J. E. Leffler, *J. Phys. Chem.* **1959**, *63*, 1461–1463.
- [57] E. Masson, *Org. Biomol. Chem.* **2013**, *11*, 2859–2871.
- [58] J. Burgers, W. Van Hartingsveldt, J. Van Keulen, P. E. Verkade, H. Visser, B. M. Wepster, *Recl. Trav. Chim. Pays-Bas* **1956**, *75*, 1327–1342.
- [59] R. J. Tang, T. Milcent, B. Crousse, *Eur. J. Org. Chem.* **2017**, 4753–4757.
- [60] I. Goldberg, *Berichte der Dtsch. Chem. Gesellschaft* **1906**, *39*, 1691–1692.
- [61] Z. Rappoport, in *The Chemistry of Anilines*, John Wiley & Sons, Ltd, Chichester, **2007**, p. 1180.
- [62] S. Chakrabarty, D. Monlish, P. Flaherty, J. E. Cavanaugh, S. Potdar, *PCT Int. Appl. WO 2014/078669*, **2014**.
- [63] D. M. T. Chan, K. L. Monaco, R.-P. Wang, M. P. Winters, *Tetrahedron Lett.* **1998**, *39*, 2933–2936.
- [64] P. Y. S. Lam, C. G. Clark, S. Saubern, J. Adams, M. P. Winters, D. M. T. Chan, A. Combs, *Tetrahedron Lett.* **1998**, *39*, 2941–2944.
- [65] S. Rasheed, D. N. Rao, K. R. Reddy, S. Aravinda, R. A. Vishwakarma, P. Das, *RSC Adv.* **2014**, *4*, 4960.
- [66] J. X. Qiao, P. Y. S. Lam, in *Boronic Acids Preparation and Application in Organic Synthesis, Medicine and Materials* (Ed.: D.G. Hall), Wiley-VCH, Weinheim, **2011**, pp. 315–361.
- [67] J. C. Vantourout, H. N. Miras, A. Isidro-Llobet, S. Sproules, A. J. B. Watson, *J. Am. Chem. Soc.* **2017**, *139*, 4769–4779.
- [68] M. T. Wentzel, J. B. Hewgley, R. M. Kamble, P. D. Wall, M. C. Kozlowski, *Adv. Synth. Catal.* **2009**, *351*, 931–937.
- [69] J. Louie, J. F. Hartwig, *Tetrahedron Lett.* **1995**, *36*, 3609–3612.
- [70] A. S. Guram, R. A. Rennels, S. L. Buchwald, *Angew. Chemie Int. Ed. English* **1995**, *34*, 1348–1350.
- [71] J. P. Wolfe, S. L. Buchwald, *J. Org. Chem.* **1996**, *61*, 1133–1135.
- [72] L. L. Hill, L. R. Moore, R. Huang, R. Craciun, A. J. Vincent, D. A. Dixon, J. Chou, C. J. Woltermann, K. H. Shaughnessy, T. Uni, *J. Org. Chem.* **2006**, *71*, 5117–5125.
- [73] L. L. Hill, J. M. Smith, W. S. Brown, L. R. Moore, P. Guevera, E. S. Pair, J. Porter, J. Chou, C. J. Wolterman, R. Craciun, et al., *Tetrahedron* **2008**, *64*, 6920–6934.

- [74] G. Bastug, S. P. Nolan, *Organometallics* **2014**, *33*, 1253–1258.
- [75] Q. Shen, T. Ogata, J. F. Hartwig, *J. Am. Chem. Soc.* **2008**, *130*, 6586–6596.
- [76] F. Brotzel, C. C. Ying, H. Mayr, *J. Org. Chem.* **2007**, *72*, 3679–3688.
- [77] A. Ehrentraut, A. Zapf, M. Beller, *J. Mol. Catal. A Chem.* **2002**, *182–183*, 515–523.
- [78] N. Marion, O. Navarro, J. Mei, E. D. Stevens, N. M. Scott, S. P. Nolan, *J. Am. Chem. Soc.* **2006**, *128*, 4101–4111.
- [79] D. H. Lee, A. Taher, S. Hossain, M. J. Jin, *Org. Lett.* **2011**, *13*, 5540–5543.
- [80] X. Tian, R. Goddard, K. R. Pörschke, *Organometallics* **2006**, *25*, 5854–5862.
- [81] C. V. Reddy, J. V. Kingston, J. G. Verkade, *J. Org. Chem.* **2008**, *73*, 3047–3062.
- [82] J. M. Dennis, N. A. White, R. Y. Liu, S. L. Buchwald, *J. Am. Chem. Soc.* **2018**, *140*, 4721–4725.
- [83] F. Barrios-Landeros, J. F. Hartwig, *J. Am. Chem. Soc.* **2005**, *127*, 6944–6945.
- [84] E. Galardon, S. Ramdeehul, J. M. Brown, A. Cowley, K. K. Hii, A. Jutand, *Angew. Chemie Int. Ed.* **2002**, *41*, 1760–1763.
- [85] F. Terrier, in *Modern Nucleophilic Aromatic Substitution*, Wiley-VCH, Weinheim, **2013**, pp. 1–94.
- [86] E. E. Kwan, Y. Zeng, H. A. Besser, E. N. Jacobsen, *Nat. Chem.* **2018**, 1–7.
- [87] W. Eggimann, H. Zollinger, *Helv. Chim. Acta* **1975**, *58*, 257–268.
- [88] J. S. Sawyer, E. A. Schmittling, J. A. Palkowitz, W. J. Smith, *J. Org. Chem.* **1998**, *63*, 6338–6343.
- [89] J. P. Henichart, J. L. Bernier, C. Vaccher, R. Houssin, V. Warin, F. Baert, *Tetrahedron* **1980**, *36*, 3535–3541.
- [90] E. M. Davis, T. N. Nanninga, H. I. Tjong, D. D. Winkle, *Org. Process Res. Dev.* **2005**, *9*, 843–846.
- [91] T. Mino, Y. Tanaka, Y. Hattori, T. Yabusaki, H. Saotome, M. Sakamoto, T. Fujita, *J. Org. Chem.* **2006**, *71*, 7346–53.
- [92] C. Isanbor, T. A. Emokpae, M. R. Crampton, *J. Chem. Soc. Perkin Trans. 2* **2002**, 2019–2024.
- [93] M. R. Crampton, T. A. Emokpae, C. Isanbo, *J. Phys. Org. Chem.* **2006**, *19*, 75–80.
- [94] C. Isanbor, *J. Phys. Org. Chem.* **2017**, *30*, e3687.
- [95] W. E. Truce, E. M. Kreider, W. W. Brand, in *Org. React.*, **1970**, pp. 99–215.
- [96] C. M. Holden, M. F. Greaney, *Chem. Eur. J.* **2017**, *23*, 8992–9008.
- [97] W. J. Evans, S. Smiles, *J. Chem. Soc.* **1935**, 181–188.
- [98] Y. Mettey, J. Vierfond, *Heterocycles* **1993**, *36*, 987–993.
- [99] A. Moritomo, H. Yamada, T. Watanabe, H. Itahana, S. Akuzawa, M. Okada, M. Ohta, *Bioorg. Med. Chem.* **2013**, *21*, 7841–7852.
- [100] M. S. Wadia, D. V. Patil, *Synth. Commun.* **2003**, *33*, 2725–2736.
- [101] Y. S. Xie, B. V.D. Vijaykumar, K. Jang, H. H. Shin, H. Zuo, D. S. Shin, *Tetrahedron Lett.* **2013**, *54*, 5151–5154.
- [102] H. Yang, Z. B. Li, D. S. Shin, L. Y. Wang, J. Z. Zhou, H. B. Qiao, X. Tian, X. Y. Ma, H. Zuo, *Synlett* **2010**, 483–487.
- [103] X. Tian, R. M. Wu, G. Liu, Z. B. Li, H. L. Wei, H. Yang, D. S. Shin, L. Y. Wang, H. Zuo, *ARKIVOC* **2011**, *2011*, 118–126.
- [104] J. F. Bunnett, T. Okamoto, *J. Am. Chem. Soc.* **1956**, *78*, 5363–5367.
- [105] R. Bayles, M. C. Johnson, R. F. Maissey, R. W. Turner, *Synthesis* **1977**, *1*, 33–34.
- [106] J. Clayden, J. Dufour, D. M. Grainger, M. Helliwell, *J. Am. Chem. Soc.* **2007**, *129*, 7488–7489.
- [107] S. L. MacNeil, B. J. Wilson, V. Snieckus, *Org. Lett.* **2006**, *8*, 1133–1136.
- [108] D. Sriram, P. Yogeewari, *Medicinal Chemistry*, Pearson Education India, **2010**.
- [109] J. S. Sebolt-Leopold, D. T. Dudley, R. Herrera, K. Van Becelaere, A. Wiland, R. C. Gowan, H. Tecle, S. D. Barrett, A. Bridges, S. Przybranowski, et al., *Nat. Med.* **1999**, *5*, 810–816.
- [110] C. E. Augelli-Szafran, M. R. Barvian, C. F. Bigge, S. A. Glase, T. Hachiya, Y. Lai, A. T. Sakkab, M. J. Suto, W. L. Craswell, T. Yasunaga, et al., *PCT Int. Appl. WO 00/76489*, **2000**.
- [111] J. Clayden, L. Lemiègre, M. Helliwell, *J. Org. Chem.* **2007**, *72*, 2302–2308.
- [112] A. Mannschreck, *Tetrahedron Lett.* **1965**, *19*, 1341–1347.
- [113] A. Ahmed, R. A. Bragg, J. Clayden, L. W. Lai, C. McCarthy, J. H. Pink, N. Westlund, S. A. Yasin,

- Tetrahedron* **1998**, *54*, 13277–13294.
- [114] L. Chabaud, J. Clayden, M. Helliwell, A. Page, J. Raftery, L. Vallverdú, *Tetrahedron* **2010**, *66*, 6936–6957.
- [115] S. Lal, T. J. Snape, *Med. Hypotheses* **2014**, *83*, 751–754.
- [116] K. Yamaguchi, G. Matsumura, H. Kagechika, I. Azumaya, Y. Ito, A. Itai, K. Shudo, *J. Am. Chem. Soc.* **1991**, *113*, 5474–5475.
- [117] R. Szostak, G. Meng, M. Szostak, *J. Org. Chem.* **2017**, *82*, 6373–6378.
- [118] J. Wu, X. Yu, J. Liu, Y. Lin, Y. Gao, L. Jia, H. Chen, *RSC Adv.* **2016**, *6*, 7195–7197.
- [119] V. Botla, C. Barreddi, R. V. Daggupati, C. Malapaka, *J. Chem. Sci.* **2016**, *128*, 1469–1473.
- [120] M. Periasamy, K. N. Jayakumar, *J. o* **2000**, *65*, 3548–3550.
- [121] C. Tang, N. Jiao, *J. Am. Chem. Soc.* **2012**, *134*, 18924–18927.
- [122] J. R. Kosowan, Z. W'Giorgis, R. Grewal, T. E. Wood, *Org. Biomol. Chem.* **2015**, *13*, 6754–6765.
- [123] F. Lovering, J. Bikker, C. Humblet, *J. Med. Chem.* **2009**, *52*, 6752–6756.
- [124] F. Lovering, *MedChemComm* **2013**, *4*, 515–519.
- [125] D. C. Kombo, K. Tallapragada, R. Jain, J. Chewning, A. A. Mazurov, J. D. Speake, T. A. Hauser, S. Toler, *J. Chem. Inf. Model.* **2013**, *53*, 327–342.
- [126] P. A. Clemons, J. A. Wilson, V. Dancik, S. Muller, H. A. Carrinski, B. K. Wagner, A. N. Koehler, S. L. Schreiber, *Proc. Natl. Acad. Sci.* **2011**, *108*, 6817–6822.
- [127] C. A. Lipinski, F. Lombardo, B. W. Dominy, P. J. Feeney, *Adv. Drug Deliv. Rev.* **1997**, *23*, 3–25.
- [128] C. A. Lipinski, *Drug Discov. Today Technol.* **2004**, *1*, 337–341.
- [129] D. F. Veber, S. R. Johnson, H. Y. Cheng, B. R. Smith, K. W. Ward, K. D. Kopple, *J. Med. Chem.* **2002**, *45*, 2615–2623.
- [130] J. Magano, J. R. Dunetz, Eds. , *Transition Metal-Catalyzed Couplings in Process Chemistry: Case Studies From the Pharmaceutical Industry*, Wiley-VCH, Weinheim, **2013**.
- [131] W. H. B. Sauer, M. K. Schwarz, *J. Chem. Inf. Comput. Sci.* **2003**, *43*, 987–1003.
- [132] T. Rezai, J. E. Bock, M. V. Zhou, C. Kalyanaraman, R. S. Lokey, M. P. Jacobson, *J. Am. Chem. Soc.* **2006**, *128*, 14073–14080.
- [133] J. Meyers, M. Carter, N. Y. Mok, N. Brown, *Future Med. Chem.* **2016**, *8*, 1753–1767.
- [134] U. Nubbemeyer, *Top. Curr. Chem.* **2001**, *216*, 125–196.
- [135] A. Hussain, S. K. Yousuf, D. Mukherjee, *RSC Adv.* **2014**, *4*, 43241–43257.
- [136] A. Sharma, P. Appukkuttan, E. Van der Eycken, *Chem. Commun.* **2012**, *48*, 1623–1637.
- [137] M. Rossi Sebastiano, B. C. Doak, M. Backlund, V. Poongavanam, B. Over, G. Ermondi, G. Caron, P. Matsson, J. Kihlberg, *J. Med. Chem.* **2018**, *61*, 4189–4202.
- [138] P. Matsson, B. C. Doak, B. Over, J. Kihlberg, *Adv. Drug Deliv. Rev.* **2016**, *101*, 42–61.
- [139] G. Illuminati, L. Mandolini, *Acc. Chem. Res.* **1981**, *14*, 95–102.
- [140] E. Vitaku, D. T. Smith, J. T. Njardarson, *J. Med. Chem.* **2014**, *57*, 10257–10274.
- [141] R. D. Taylor, M. Maccoss, A. D. G. Lawson, *J. Med. Chem.* **2014**, *57*, 5845–5859.
- [142] J. Elleraas, J. Ewanicki, T. W. Johnson, N. W. Sach, M. R. Collins, P. F. Richardson, *Angew. Chemie Int. Ed.* **2016**, *55*, 3590–3595.
- [143] R. Mancuso, D. S. Raut, N. Marino, G. De Luca, C. Giordano, S. Catalano, I. Barone, S. Andò, B. Gabriele, *Chem. Eur. J.* **2016**, *22*, 3053–3064.
- [144] P. A. N. V Harita, P. S. Kumar, S. Krishna, R. Guduru, P. Ravula, J. N. N. S. Chandra, *EXCLI J.* **2017**, *16*, 1090–1098.
- [145] G. Ding, F. Liu, T. Yang, Y. Jiang, H. Fu, Y. Zhao, *Bioorganic Med. Chem.* **2006**, *14*, 3766–3774.
- [146] V. Magné, C. Lorton, A. Marinetti, X. Guinchard, A. Voituriez, *Org. Lett.* **2017**, *19*, 4794–4797.
- [147] S. B. Singh, H. Jayasuriya, D. L. Zink, J. D. Polishook, A. W. Dombrowski, H. Zweerink, *Tetrahedron Lett.* **2004**, *45*, 7605–7608.
- [148] P. Imming, B. Klar, D. Dix, *J. Med. Chem.* **2000**, *43*, 4328–4331.
- [149] J. R. Donald, W. P. Unsworth, *Chem. Eur. J.* **2017**, *23*, 8780–8799.
- [150] L. G. Baud, M. A. Manning, H. L. Arkless, T. C. Stephens, W. P. Unsworth, *Chem. Eur. J.* **2017**, *23*, 2225–2230.

- [151] R. Mendoza-Sanchez, V. B. Corless, Q. N. N. Nguyen, M. Bergeron-Brlek, J. Frost, S. Adachi, D. J. Tantillo, A. K. Yudin, *Chem. Eur. J.* **2017**, *23*, 13319–13322.
- [152] A. Klapars, S. Parris, K. W. Anderson, S. L. Buchwald, *J. Am. Chem. Soc.* **2004**, *126*, 3529–3533.
- [153] A. Sapegin, A. Osipyan, M. Krasavin, *Org. Biomol. Chem.* **2017**, *15*, 2906–2909.
- [154] A. Borchardt, W. C. Still, *Synlett* **1995**, 539–540.
- [155] J. E. Hall, J. V. Matlock, J. W. Ward, K. V. Gray, J. Clayden, *Angew. Chemie Int. Ed.* **2016**, *55*, 11153–11157.
- [156] R. E. Hubbard, M. Kamran Haider, *Encyclopedia of Life Science (ELS)* **2010**, DOI 10.1002/9780470015902.a0003011.pub2.
- [157] R. L. Panek, G. H. Lu, S. R. Klutchko, B. L. Batley, T. K. Dahring, J. M. Hamby, H. Hallak, A. M. Doherty, J. A. Keiser, *J. Pharmacol. Exp. Ther.* **1997**, *283*, 1433–1444.
- [158] P. Furet, G. Caravatti, V. Guagnano, M. Lang, T. Meyer, J. Schoepfer, *Bioorganic Med. Chem. Lett.* **2008**, *18*, 897–900.
- [159] G. Caron, G. Ermondi, *Future Med. Chem.* **2017**, *9*, 1–5.
- [160] M. Kijima, M. Yoshida, K. Sugita, S. Horinouchi, T. Beppu, *J. Biol. Chem.* **1993**, *268*, 22429–22435.
- [161] S. B. Singh, D. L. Zink, J. M. Liesch, R. T. Mosley, A. W. Dombrowski, G. F. Bills, S. J. Darkin-Rattray, D. M. Schmatz, M. A. Goetz, *J. Org. Chem.* **2002**, *67*, 815–825.
- [162] M. P. Glenn, M. J. Kelso, J. D. A. Tyndall, D. P. Fairlie, *J. Am. Chem. Soc.* **2003**, *125*, 640–641.
- [163] T. Rezai, B. Yu, G. L. Millhauser, M. P. Jacobson, R. S. Lokey, *J. Am. Chem. Soc.* **2006**, *128*, 2510–2511.
- [164] S. Z. Ferreira, H. C. Carneiro, H. A. Lara, R. B. Alves, J. M. Resende, H. M. Oliveira, L. M. Silva, D. A. Santos, R. P. Freitas, *ACS Med. Chem. Lett.* **2015**, *6*, 271–275.
- [165] F. Francisco Hilário, M. D. M. Traoré, V. Zwick, L. Berry, C. A. Simões-Pires, M. Cuendet, N. Fantozzi, R. Pereira De Freitas, M. Maynadier, S. Wein, et al., *Org. Lett.* **2017**, *19*, 612–615.
- [166] S. Boyle, S. Guard, M. Higginbottom, D. C. Horwell, W. Howson, A. T. McKnight, K. Martin, M. C. Pritchard, J. O'Toole, J. Raphy, et al., *Bioorganic Med. Chem.* **1994**, *2*, 357–370.
- [167] M. Muñoz, R. Coveñas, F. Esteban, M. Redondo, *J. Biosci.* **2015**, *40*, 441–463.
- [168] V. A. Ashwood, M. J. Field, D. C. Horwell, C. Julien-Larose, R. A. Lewthwaite, S. McCleary, M. C. Pritchard, J. Raphy, L. Singh, *J. Med. Chem.* **2001**, *44*, 2276–2285.
- [169] A. Whitty, M. Zhong, L. Viarengo, D. Beglov, D. R. Hall, S. Vajda, *Drug Discov. Today* **2016**, *21*, 712–717.
- [170] R. H. Minham, in *Drugs in Psychiatric Practice* (Ed.: P.J. Tyrer), Butterworth-Heinemann, Oxford, **1982**, p. 177.
- [171] M. Rehavi, S. Maayani, L. Goldstein, M. Assael, M. Sokolovsky, *Psychopharmacology* **1977**, *54*, 35–38.
- [172] K. Ramig, *Tetrahedron* **2013**, *69*, 10783–10795.
- [173] M. Simonyi, *Adv. Drug Res.* **1997**, *30*, 73–110.
- [174] J. Clayden, W. J. Moran, P. J. Edwards, S. R. Laplante, *Angew. Chemie Int. Ed.* **2009**, *48*, 6398–6401.
- [175] S. M. Bromidge, B. S. Orlek, D. A. Entwistle, J. Goldstein, *Synth. Commun.* **1993**, *23*, 487–494.
- [176] M. V Andreev, A. S. Medvedeva, L. P. Safronova, *Russ. J. Org. Chem.* **2013**, *49*, 822–827.
- [177] K. A. Brameld, B. Kuhn, D. C. Reuter, M. Stahl, *J. Chem. Inf. Model.* **2008**, *48*, 1–24.
- [178] S. Shang, D. Zhang-Negrerie, Y. Du, K. Zhao, *Angew. Chemie Int. Ed.* **2014**, *53*, 6216–6219.
- [179] I. Colomer, C. J. Empson, P. Craven, Z. Owen, R. G. Doveston, I. Churcher, S. P. Marsden, A. Nelson, *Chem. Commun.* **2016**, *52*, 7209–7212.
- [180] F. K. Winkler, J. D. Dunitz, *J. Mol. Biol.* **1971**, *59*, 169–182.
- [181] Y. Otani, O. Nagae, Y. Naruse, S. Inagaki, M. Ohno, K. Yamaguchi, G. Yamamoto, M. Uchiyama, T. Ohwada, *J. Am. Chem. Soc.* **2003**, *125*, 15191–15199.
- [182] C. L. Perrin, T. J. Dwyer, *Chem. Rev.* **1990**, *90*, 935–967.
- [183] D. Morales-Morales, C. M. Jensen, Eds., *The Chemistry of Pincer Compounds*, Elsevier B.V.,

- Amsterdam, **2007**.
- [184] B. C. J. Moulton, B. L. Shaw, *J. Chem. Soc., Dalton Trans.* **1976**, 0, 1020–1024.
 - [185] E. Peris, R. H. Crabtree, *Chem. Soc. Rev.* **2018**, 47, 1959–1968.
 - [186] K. J. Szabó, O. F. Wendt, Eds., *Pincer and Pincer-Type Compounds*, Wiley-VCH, Weinheim, **2014**.
 - [187] J. Choi, A. H. R. MacArthur, M. Brookhart, A. S. Goldman, *Chem. Rev.* **2011**, 111, 1761–1779.
 - [188] F. E. Wood, M. M. Olmstead, A. L. Balch, *J. Am. Chem. Soc.* **1983**, 105, 6332–6334.
 - [189] A. A. Danopoulos, P. G. Edwards, *Polyhedron* **1989**, 8, 1339–1344.
 - [190] A. M. Winter, K. Eichele, H. G. Mack, S. Potuznik, H. A. Mayer, W. C. Kaska, *J. Organomet. Chem.* **2003**, 682, 149–154.
 - [191] L. C. Liang, J. M. Lin, C. H. Hung, *Organometallics* **2003**, 22, 3007–3009.
 - [192] K. J. Szabo, in *Pincer Pincer-Type Complexes: Applications in Organic Synthesis and Catalysis* (Eds.: K.J. Szabo, O.F. Wendt), Wiley-VCH, Weinheim, **2014**, pp. 95–116.
 - [193] C. J. Richards, J. S. Fossey, in *The Chemistry of Pincer Compounds* (Eds.: D. Morales-Morales, C.M. Jensen), Elsevier B.V., Amsterdam, **2007**, pp. 45–77.
 - [194] R. Çelenligil-Çetin, L. A. Watson, C. Guo, B. M. Foxman, O. V. Ozerov, *Organometallics* **2005**, 24, 186–189.
 - [195] H. Zhao, X. Li, S. Zhang, H. Sun, *Z. Anorg. Allg. Chem.* **2015**, 641, 2435–2439.
 - [196] O. V. Ozerov, C. Guo, V. A. Papkov, B. M. Foxman, *J. Am. Chem. Soc.* **2004**, 126, 4792–4793.
 - [197] E. Calimano, T. D. Tilley, *J. Am. Chem. Soc.* **2009**, 131, 11161–11173.
 - [198] L. Fan, B. M. Foxman, O. V. Ozerov, *Organometallics* **2004**, 23, 326–328.
 - [199] L. C. Liang, J. M. Lin, W. Y. Lee, *Chem. Commun.* **2005**, 2462–2464.
 - [200] D. E. Herbert, A. D. Miller, O. V. Ozerov, *Chem. Eur. J.* **2012**, 18, 7696–7704.
 - [201] C. M. Brammell, E. J. Pelton, C. H. Chen, A. A. Yakovenko, W. Weng, B. M. Foxman, O. V. Ozerov, *J. Organomet. Chem.* **2011**, 696, 4132–4137.
 - [202] A. R. Fout, B. C. Bailey, D. M. Buck, H. Fan, J. C. Huffman, M. H. Baik, D. J. Mindiola, *Organometallics* **2010**, 29, 5409–5422.
 - [203] W. Weng, L. Yang, B. M. Foxman, O. V. Ozerov, *Organometallics* **2004**, 23, 4700–4705.
 - [204] B. C. Bailey, H. Fan, J. C. Huffman, M. H. Baik, D. J. Mindiola, *J. Am. Chem. Soc.* **2006**, 128, 6798–6799.
 - [205] E. Calimano, T. D. Tilley, *J. Am. Chem. Soc.* **2008**, 130, 9226–9227.
 - [206] E. Calimano, T. D. Tilley, *Organometallics* **2010**, 29, 1680–1692.
 - [207] M.-H. Huang, L.-C. Liang, *Organometallics* **2004**, 35, 2813–2816.
 - [208] D. Roy, Y. Uozumi, *Adv. Synth. Catal.* **2018**, 360, 602–625.
 - [209] L. C. Liang, P. S. Chien, P. Y. Lee, *Organometallics* **2008**, 27, 3082–3093.
 - [210] J. Breitenfeld, O. Vechorkin, C. Corminboeuf, R. Scopelliti, X. Hu, *Organometallics* **2010**, 29, 3686–3689.
 - [211] L. C. Liang, P. S. Chien, J. M. Lin, M. H. Huang, Y. L. Huang, J. H. Liao, *Organometallics* **2006**, 25, 1399–1411.
 - [212] X. Hu, *Chem. Sci.* **2011**, 2, 1867–1886.
 - [213] O. Vechorkin, V. Proust, X. Hu, *J. Am. Chem. Soc.* **2009**, 131, 9756–9766.
 - [214] O. Vechorkin, X. Hu, *Angew. Chemie Int. Ed.* **2009**, 48, 2937–2940.
 - [215] P. Knochel, Ed., *Handbook of Functionalized Organometallics*, Wiley-VCH, Weinheim, **2005**.
 - [216] O. Vechorkin, D. Barmaz, *Synfacts* **2009**, 2009, 1383–1383.
 - [217] O. Vechorkin, A. Godinat, R. Scopelliti, X. Hu, *Angew. Chemie Int. Ed.* **2011**, 50, 11777–11781.
 - [218] O. Vechorkin, V. Proust, X. Hu, *Angew. Chemie Int. Ed.* **2010**, 49, 3061–3064.
 - [219] I. Buslov, J. Becouse, S. Mazza, M. Montandon-Clerc, X. Hu, *Angew. Chemie Int. Ed.* **2015**, 54, 14523–14526.
 - [220] J. Lu, J. Ye, W. L. Duan, *Org. Lett.* **2013**, 15, 5016–5019.
 - [221] Z. Yang, C. Xia, D. Liu, Y. Liu, M. Sugiya, T. Imamoto, W. Zhang, *Org. Biomol. Chem.* **2015**, 13, 2694–2702.
 - [222] H. Liu, J. Xu, D. M. Du, *Org. Lett.* **2007**, 9, 4725–4728.

- [223] Q. H. Deng, R. L. Melen, L. H. Gade, *Acc. Chem. Res.* **2014**, *47*, 3162–3173.
- [224] H. A. McManus, P. J. Guiry, *J. Org. Chem.* **2002**, *67*, 8566–8573.
- [225] S. F. Lu, D. M. Du, S. W. Zhang, J. Xu, *Tetrahedron Asymmetry* **2004**, *15*, 3433–3441.
- [226] H. Liu, S. F. Lu, J. Xu, D. M. Du, *Chem. - An Asian J.* **2008**, *3*, 1111–1121.
- [227] S. Lu, D. Du, J. Xu, *Org. Lett.* **2006**, *8*, 2115–2118.
- [228] H. Liu, D. M. Du, *Eur. J. Org. Chem.* **2010**, 2121–2131.
- [229] C. Despotopoulou, S. C. McKeon, R. Connon, V. Coeffard, H. Müller-Bunz, P. J. Guiry, *Eur. J. Org. Chem.* **2017**, 6734–6738.
- [230] T. Inagaki, L. T. Phong, A. Furuta, J. I. Ito, H. Nishiyama, *Chem. Eur. J.* **2010**, *16*, 3090–3096.
- [231] T. D. Nixon, B. D. Ward, *Chem. Commun.* **2012**, *48*, 11790–11792.
- [232] V. Coeffard, M. Aylward, P. J. Guiry, *Angew. Chemie Int. Ed.* **2009**, *48*, 9152–9155.
- [233] S. Gru, M. Albrecht, J. A. Loch, J. W. Faller, R. H. Crabtree, *Organometallics* **2001**, *20*, 5485–5488.
- [234] C. J. Pell, O. V Ozerov, *ACS Catal.* **2014**, *4*, 3470–3480.
- [235] W. Weng, C. Guo, C. Remle, B. M. Foxman, O. V Ozerov, *Chem. Commun.* **2006**, 197–199.
- [236] J. R. Miecznikowski, S. Gründemann, M. Albrecht, C. Mégret, E. Clot, J. W. Faller, R. H. Crabtree, *Dalton Trans.* **2003**, *0*, 831–838.
- [237] K. R. Pichaandi, L. Kabalan, S. Kais, M. M. Abu-Omar, *J. Organomet. Chem.* **2017**, *843*, 62–65.
- [238] M. C. Lipke, R. A. Woloszynek, L. Ma, J. D. Protasiewicz, *Organometallics* **2009**, *28*, 188–196.
- [239] J. S. Hewage, S. Wanniarachchi, T. J. Morin, B. J. Liddle, M. Banaszynski, S. V Lindeman, B. Bennett, J. R. Gardinier, *Inorg. Chem.* **2014**, *53*, 10070–10084.
- [240] K. R. Seipel, Z. H. Platt, M. Nguyen, A. W. Holland, *J. Org. Chem.* **2008**, *73*, 4291–4294.
- [241] T. Hattori, J. Sakamoto, N. Hayashizaka, S. Miyano, *Synthesis* **1994**, *2*, 199–202.
- [242] M. H. Huang, L. C. Liang, *Organometallics* **2004**, *23*, 2813–2816.
- [243] M. E. O. Reilly, I. Ghiviriga, K. A. Abboud, A. S. Veige, *J. Am. Chem. Soc.* **2012**, *134*, 11185–11195.
- [244] Y. N. Polivin, R. A. Karakhanov, V. I. Kelarev, A. A. Bratkov, B. I. Ugrald, G. K. Anashki, M. E. Panina, *Russ. Chem. Bull.* **1993**, *42*, 214.
- [245] J. J. Kulagowski, C. J. Moody, C. W. Rees, *J. Chem. Soc. Perkin Trans. 1* **1985**, *0*, 2725–2732.
- [246] M. A. Buden, V. A. Vaillard, S. E. Martin, R. A. Rossi, *J. Org. Chem.* **2009**, *74*, 4490–4498.
- [247] A. C. Kung, S. P. McIlroy, D. E. Falvey, *J. Org. Chem.* **2005**, *70*, 5283–5290.
- [248] D. L. Dodds, M. D. K. Boele, G. P. F. van Strijdonck, J. G. de Vries, P. W. N. M. van Leeuwen, P. C. J. Kamer, *Eur. J. Inorg. Chem.* **2012**, *2012*, 1660–1671.
- [249] T. Furuya, T. Ritter, *Org. Lett.* **2009**, *11*, 2860–2863.
- [250] A. Schöbel, E. Herdtweck, M. Parkinson, B. Rieger, *Chem. Eur. J.* **2012**, *18*, 4174–4178.
- [251] T. Mino, Y. Tanaka, T. Yabusaki, D. Okumura, M. Sakamoto, T. Fujita, *Tetrahedron: Asymmetry* **2003**, *14*, 2503–2506.
- [252] T. Mino, M. Asakawa, Y. Shima, H. Yamada, F. Yagishita, M. Sakamoto, *Tetrahedron* **2015**, *71*, 5985–5993.
- [253] E. Bappert, G. Helmchen, *Synlett* **2004**, *10*, 1789–1793.
- [254] D. Hellwinkel, F. Lammerzahl, G. Hofmann, *Chem. Ber.* **1983**, *116*, 3375–3405.
- [255] M. S. Carpenter, W. M. Easter, T. F. Wood, *J. Org. Chem.* **1951**, *16*, 586–617.
- [256] L. Qiu, X. Zhuang, N. Zhao, X. Wang, Z. An, Z. Lan, X. Wan, *Chem. Commun.* **2014**, *50*, 3324–3327.
- [257] Y. L. Yang, F. R. Chang, Y. C. Wu, *Tetrahedron Lett.* **2003**, *44*, 319–322.
- [258] A. Leonardi, D. Barlocco, F. Montesano, G. Cignarella, G. Motta, R. Testa, E. Poggesi, M. Seeber, P. G. De Benedetti, F. Fanelli, *J. Med. Chem.* **2004**, *47*, 1900–1918.
- [259] P. J. Llabres-Campaner, R. Ballesteros-Garrido, R. Ballesteros, B. Abarca, *Tetrahedron* **2017**, *73*, 5552–5561.
- [260] T. Itoh, K. Nagata, M. Miyazaki, H. Ishikawa, A. Kurihara, A. Ohsawa, *Tetrahedron* **2004**, *60*, 6649–6655.
- [261] E. D. Bergmann, *Chem. Rev.* **1953**, *53*, 309–352.

- [262] J. M. Schomaker, S. Bhattacharjee, J. Yan, B. Borhan, *J. Am. Chem. Soc.* **2007**, *129*, 1996–2003.
- [263] P. J. Garegg, T. Regberg, J. Stawinski, R. Stromberg, *J. Chem. Soc. Perkin Trans. 2* **1987**, *0*, 271–274.
- [264] E. R. Kay, D. A. Leigh, *Angew. Chemie Int. Ed.* **2015**, *54*, 10080–10088.
- [265] V. Balzani, M. Venturi, A. Credi, Eds., *Molecular Devices and Machines, Concepts and Perspectives for the Nanoworld*, Wiley-VCH, Weinheim, **2008**.
- [266] K. Fuji, T. Oka, T. Kawabata, T. Kinoshita, *Tetrahedron Lett.* **1998**, *39*, 1373–1376.
- [267] R. Katoono, H. Kawai, K. Fujiwara, T. Suzuki, *J. Am. Chem. Soc.* **2009**, *131*, 16896–16904.
- [268] J. Chen, F. K. C. Leung, M. C. A. Stuart, T. Kajitani, T. Fukushima, E. Van Der Giessen, B. L. Feringa, *Nat. Chem.* **2018**, *10*, 132–138.
- [269] C. Wolf, in *Dynamic Stereochemistry of Chiral Compounds: Principle and Applications*, Royal Society Of Chemistry, Cambridge, **2007**.
- [270] J. Clayden, *Chem. Soc. Rev.* **2009**, *38*, 817–829.
- [271] J. Clayden, N. Vassiliou, *Org. Biomol. Chem.* **2006**, *4*, 2667–2678.
- [272] J. Clayden, A. Lund, L. Vallverdú, M. Helliwell, *Nature* **2004**, *431*, 966–971.
- [273] J. Venkatraman, S. C. Shankaramma, P. Balaram, *Chem. Rev.* **2001**, *101*, 3131–3152.
- [274] B. A. F. Le Bailly, J. Clayden, *Chem. Commun.* **2016**, *52*, 4852–4863.
- [275] F. H. Allen, C. A. Baalham, J. P. M. Lommerse, P. R. Raithby, *Acta Crystallogr. Sect. B Struct. Sci.* **1998**, *54*, 320–329.
- [276] K. Kahn, K. W. Plaxco, in *Recognition Receptors in Biosensors* (Ed.: M. Zourob), Springer Verlag, New York, **2010**, pp. 3–46.
- [277] S. Terdale, A. Tantray, *J. Mol. Liq.* **2017**, *225*, 662–671.
- [278] E. A. German, J. E. Ross, P. C. Knipe, M. F. Don, S. Thompson, A. D. Hamilton, *Angew. Chemie Int. Ed.* **2015**, *54*, 2649–2652.
- [279] H. Kawai, R. Katoono, K. Fujiwara, T. Tsuji, T. Suzuki, *Chem. Eur. J.* **2005**, *11*, 815–824.
- [280] C. L. Sutherell, S. Thompson, R. T. W. Scott, A. D. Hamilton, *Chem. Commun.* **2012**, *48*, 9834–9836.
- [281] T. Yamashita, P. C. Knipe, N. Busschaert, S. Thompson, A. D. Hamilton, *Chemistry* **2015**, *21*, 14657.
- [282] W. A. Loughlin, J. D. A. Tyndall, M. P. Glenn, T. A. Hill, D. P. Fairlie, *Chem. Rev.* **2010**, *110*, 6085–6117.
- [283] M. S. Betson, J. Clayden, H. K. Lam, M. Helliwell, *Angew. Chemie Int. Ed.* **2005**, *44*, 1241–1244.
- [284] R. Katoono, H. Kawai, K. Fujiwara, T. Suzuki, *Tetrahedron Lett.* **2006**, *47*, 1513–1518.
- [285] J. Clayden, A. Lund, L. H. Youssef, *Org. Lett.* **2001**, *3*, 4133–4136.
- [286] J. Clayden, L. W. Lai, M. Helliwell, *Tetrahedron Asymmetry* **2001**, *12*, 695–698.
- [287] J. Clayden, L. Vallverdú, M. Helliwell, *Chem. Commun.* **2007**, 2357–2359.
- [288] J. Clayden, M. N. Kenworthy, L. H. Youssef, M. Helliwell, *Tetrahedron Lett.* **2000**, *41*, 5171–5175.
- [289] M. B. Robin, F. A. Bovey, H. Basch, in *The Chemistry of AMides* (Ed.: J. Zabicky), Interscience, London, **1970**, pp. 1–72.
- [290] A. Itai, Y. Toriumi, S. Saito, H. Kagechika, K. Shudo, *J. Am. Chem. Soc.* **1992**, *114*, 10649–10650.
- [291] D. J. Bennett, A. J. Blake, P. A. Cooke, C. R. A. Godfrey, P. L. Pickering, N. S. Simpkins, M. D. Walker, C. Wilson, *Tetrahedron* **2004**, *60*, 4491–4511.
- [292] P. V. Jog, R. E. Brown, D. K. Bates, *J. Org. Chem.* **2003**, *68*, 8240–8243.
- [293] A. Mazzanti, M. Chiarucci, L. Prati, K. W. Bentley, C. Wolf, *J. Org. Chem.* **2016**, *81*, 89–99.
- [294] J. Clayden, L. Vallverdú, J. Clayton, M. Helliwell, *Chem. Commun.* **2008**, *8*, 561–563.
- [295] R. Chinchilla, C. Nájera, *Chem. Rev.* **2007**, *107*, 874–922.
- [296] T. Katsura, T. Hayashi, M. Tanaka, *EP2072507*, **2009**.
- [297] A. R. Burirov, M. S. Khakimov, A. S. Gazizov, M. A. Pudovik, V. V. Syakaev, D. B. Krivolapov, A. I. Konovalov, *Mendeleev Commun.* **2008**, *18*, 54–55.
- [298] C. M. G. Azevedo, K. R. Watterson, E. T. Wargent, S. V. F. Hansen, B. D. Hudson, M. A.

- Kępczyńska, J. Dunlop, B. Shimpukade, E. Christiansen, G. Milligan, et al., *J. Med. Chem.* **2016**, *59*, 8868–8878.
- [299] K. Xie, S. Wang, Z. Yang, J. Liu, A. Wang, X. Li, Z. Tan, C. C. Guo, W. Deng, *Eur. J. Org. Chem.* **2011**, 5787–5790.
- [300] M. Lorentzen, I. Kalvet, F. Sauriol, T. Rantanen, K. B. Jørgensen, V. Snieckus, *J. Org. Chem.* **2017**, *82*, 7300–7308.
- [301] M. C. Sicilia, A. Niño, C. Muñoz-Caro, *J. Phys. Chem. A* **2005**, *109*, 8341–8347.
- [302] R. J. Abraham, M. Reid, *J. Chem. Soc. Perkin Trans. 2* **2002**, 1081–1091.
- [303] H. Frej, W. Wacławek, J. B. Kyzioł, I. Chemii, W. S. Pedagogiczna, I. Chemii, W. S. Pedagogiczna, *Chem. Pap.* **1988**, *42*, 213–221.
- [304] M. T. Stone, J. M. Heemstra, J. S. Moore, *Acc. Chem. Res.* **2006**, *39*, 11–20.
- [305] G. R. Fulmer, A. J. M. Miller, N. H. Sherden, H. E. Gottlieb, A. Nudelman, B. M. Stoltz, J. E. Bercaw, K. I. Goldberg, *Organometallics* **2010**, *29*, 2176–2179.
- [306] G. J. Ellames, J. S. Gibson, J. M. Herbert, A. H. McNeill, *Tetrahedron* **2001**, *57*, 9487–9497.
- [307] J. J. Neumann, S. Rakshit, T. Dröge, F. Glorius, *Angew. Chem. Int. Ed.* **2009**, *48*, 6892–6895.
- [308] J. Burgers, M. A. Hoefnagel, P. E. Verkade, H. Visser, B. M. Wepster, *Recl. Trav. Chim. Pays-Bas* **1958**, *77*, 491–530.
- [309] Y. Hou, C. Y. Meyers, *J. Org. Chem.* **2004**, *69*, 1186–1195.
- [310] C. M. D. Komen, F. Bickelhaupt, *Synth. Commun.* **1996**, *26*, 1693–1697.
- [311] E. Sawatzky, A. Drakopoulos, M. Rolz, C. Sottriffer, B. Engels, M. Decker, *Beilstein J. Org. Chem.* **2016**, *12*, 2280–2292.
- [312] A. R. Chianese, S. E. Shaner, J. A. Tendler, D. M. Pudalov, D. Y. Shopov, D. Kim, S. L. Rogers, A. Mo, *Organometallics* **2012**, *31*, 7359–7367.
- [313] W. P. Hong, A. V Iosub, S. S. Stahl, *J. Am. Chem. Soc.* **2013**, *135*, 13664–13667.
- [314] T. Ikawa, C. S. Masuda, B. T. Nishiyama, A. Takagi, S. Akai, *Aust. J. Chem.* **2014**, *67*, 475–480.
- [315] H. E. Ho, K. Oniwa, Y. Yamamoto, T. Jin, *Org. Lett.* **2016**, *18*, 2487–2490.
- [316] R. Adepu, A. Rajitha, D. Ahuja, A. K. Sharma, B. Ramudu, R. Kapavarapu, K. V. L. Parsa, M. Pal, *Org. Biomol. Chem.* **2014**, *12*, 2514–2518.
- [317] F. Hirayama, K. Konno, H. Shirahama, M. Matsumoto, *Phytochemistry* **1989**, *28*, 1133–1135.
- [318] J. Tang, B. Xu, X. Mao, H. Yang, X. Wang, X. Lv, *J. Org. Chem.* **2015**, *80*, 11108–11114.
- [319] J. Ezquerro, C. Pedregal, C. Lamas, J. Barluenga, M. Perez, M. A. Garcia-Martin, J. M. Gonzalez, *J. Org. Chem.* **1996**, *61*, 5804–5812.
- [320] S. Stavber, P. Kralj, M. Zupan, *Synthesis* **2002**, *11*, 1513–1518.
- [321] E. Jürgens, K. N. Buys, A. T. Schmidt, S. K. Furfari, M. L. Cole, M. Moser, F. Rominger, D. Kunz, *New J. Chem.* **2016**, *40*, 9160–9169.